

# In-Vivo Assessment of Coronary Atherosclerosis

Gastón A. Rodríguez-Granillo

ISBN 90-8559-144-9

Cover Design: Isabel Usandivaras, for @design

Printed by OPTIMA

© 2006 G.A. Rodriguez-Granillo

# In Vivo Assessment of Coronary Atherosclerosis

## In vivo beoordeling van coronaire atherosclerose

Thesis

to obtain the degree of Doctor from the  
Erasmus University Rotterdam  
by command of the  
rector magnificus

Prof.dr. S.W.J. Lamberts

and in accordance with the decision of the Doctorate Board.

The public defence shall be held on

Wednesday, 14th June 2006 at 13:45 hrs

by

Gastón Alfredo Rodríguez-Granillo

born at Buenos Aires, Argentina

## **Doctoral Committee**

Promotors:            Prof.dr. P.W. Serruys  
                             Prof.dr. P.J. de Feyter

Other members:     Prof.dr.ir. A.F.W. van der Steen  
                             Dr. R. Krams  
                             Prof.dr. D. Poldermans

Financial support from the Netherlands Heart Foundation for the publication of this thesis is gratefully acknowledged.

“Para Ines”



# Table of contents:

## General Introduction and Outline of the Thesis

### PART I: TECHNICAL BACKGROUND

#### Chapter 1. *Intravascular ultrasound and vulnerable plaque imaging*

- 1.1) **Intravascular Ultrasound. Chapter Atheroma book (Cambridge University Press). In press.**  
**Rodriguez-Granillo GA, Serruys PW.** 21
- 1.2) **New insights towards catheter-based identification of vulnerable plaque.**  
Rev Esp Cardiol 2005; 58: 1197 - 1206.  
**Rodriguez Granillo GA, Regar E, Schaar J et al** 49

#### Chapter 2. *Internal validation and approach to cross-correlation*

- 2.1) **In vivo variability in quantitative coronary ultrasound and tissue characterization with mechanical and phased-array catheters.** Int J Cardiovasc Imaging. 2006 Feb;22(1):47-53.  
**Rodriguez Granillo GA, McFadden EP, Aoki J, et al.** 61
- 2.2) **Geometrical validation of intravascular ultrasound radiofrequency data analysis (Virtual Histology<sup>TM</sup>) acquired with a 30 MHz Boston Scientific Corporation imaging catheter.** Catheter Cardiovasc Interv. 66:514-518 (2005)  
**Rodriguez Granillo GA, Bruining N, McFadden E, et al.** 71
- 2.3) **Reproducibility of Intravascular Ultrasound Radiofrequency Data Analysis: Implications for the Design and Conduction of Longitudinal Studies.** Int J Cardiovasc Imag. 2006 Mar 31; (Epub ahead of print)  
**Rodriguez Granillo GA, Vaina S, García-García HM, et al.** 79

- 2.4) **Methodological Considerations and Approach to Cross-Technique Comparisons using In Vivo Coronary Plaque Characterization Based on Intravascular Ultrasound Radiofrequency Data Analysis: Insights From the Integrated Biomarker and Imaging Study (IBIS).** Int J Cardiovasc Interv. 2005;7(1):52-8.

Rodriguez Granillo GA, Aoki J, Ong ATL, et al

93

**PART II: ASSESSMENT OF THE EXTENT, DISTRIBUTION, MORPHOLOGY AND COMPOSITION OF CORONARY ATHEROSCLEROSIS USING INTRAVASCULAR ULTRASOUND.**

**Chapter 3. *Non-uniform distribution of plaque composition along coronary vessels.***

- 3.1) **Distance from the Ostium as an Independent Determinant of Coronary Plaque Composition In Vivo An Intravascular Ultrasound Study Based Radiofrequency Data Analysis In Humans.** Eur Heart J. 2006 Mar; 27(6):655-63. Epub 2006 Jan 13.

Valgimigli M, Rodriguez-Granillo GA, Garcia-Garcia HM, et al.

105

- 3.2) **Plaque composition in the left main Stem mimics the distal but not the proximal tract of left coronary artery. Influence of clinical presentation, length of the left main trunk, lipid profile and systemic inflammatory status.** J Am Coll Cardiol. In press.

Valgimigli M, Rodriguez-Granillo GA, Garcia-Garcia HM, et al.

117

**Chapter 4. *Effect of shear stress on plaque composition.***

- 4.1) **Plaque Composition and its Relationship with Acknowledged Shear Stress Patterns in Coronary Arteries.** J Am Coll Cardiol. 2006 Feb 21;47(4):884-5.

Rodriguez Granillo GA, García-García HM, Wentzel JJ, et al.

147

- 4.2) **Distribution of Necrotic Core in Human Coronary Arteries is Related to the Blood Stream: An in vivo Assessment by Intravascular Ultrasound – Virtual Histology.** Submitted.

García-García HM, Rodríguez Granillo G-A, Valgimigli M, et al. 151

**Chapter 5. *Tissue characterization of non-target atherosclerotic coronary plaques. Relationship with demographical data.***

- 5.1) **Coronary plaque composition of non-culprit lesions by in vivo intravascular ultrasound radiofrequency data analysis is related to clinical presentation.** Am Heart Journal. 2006 May;151(5):1027-31.

Rodríguez Granillo GA, McFadden EP, Valgimigli M, et al. 179

**PART III: EXPLORING HISTOLOGICAL SURROGATES AND PLAQUE VULNERABILITY CRITERIA USING INTRAVASCULAR ULTRASOUND RADIOFREQUENCY DATA ANALYSIS.**

**Chapter 6. *Plaque rupture***

- 6.1) **Global characterization of coronary plaque rupture phenotype using 3-vessel intravascular ultrasound radiofrequency data analysis.** Eur Heart J. Accepted.

Rodríguez Granillo GA, García-García HM, Valgimigli M, et al. 191

**Chapter 7. *Thin-cap fibroatheroma***

7.1)	<b>In vivo intravascular ultrasound derived thin-cap fibroatheroma detection using ultrasound radiofrequency data analysis.</b> J Am Coll Cardiol. 2005 Dec 6;46(11):2038-42.	
	<b>Rodriguez Granillo GA, García-García HM, McFadden EP, et al.</b>	217
7.2)	<b>Characterization of IVUS-Derived Thin-Cap Fibroatheroma, Plaque Rupture and Healed Rupture Plaques in Patients with Acute Coronary Syndrome: An in vivo Three-Vessel Assessment Using Intravascular Ultrasound Radiofrequency Data Analysis.</b> Submitted.	
	García-García HM, <b>Rodriguez-Granillo GA</b> , Valgimigli, et al.	225
<b>Chapter 8.</b>	<b><i>Coronary remodelling.</i></b>	
8.1)	<b>Coronary artery remodelling is related to plaque composition.</b> Heart 2006;92:388-391.	
	<b>Rodriguez Granillo GA, Serruys PW, García-García HM, et al.</b>	259
8.2)	<b>Protective Effect of Perindopril on Coronary Remodelling: Insights from a multicenter, randomized study.</b> Submitted	
	<b>Rodriguez-Granillo GA, de Winter SA, Bruining N, et al</b>	265
<b>PART IV</b>	<b>EXPLORING A COMBINED IMAGING APPROACH</b>	
<b>Chapter 9.</b>	<b><i>Combining different IVUS techniques to assess plaque vulnerability.</i></b>	
9.1)	<b>Detection of a lipid-rich, highly deformable plaque in an angiographically non-diseased proximal LAD.</b> Eurointervention. 2005;3	
	<b>Rodriguez Granillo GA, del Valle R, Ligthart J, et al.</b>	287

- 9.2) **In vivo relationship between compositional and mechanical imaging of coronary arteries: insights from intravascular ultrasound radiofrequency data analysis.** Am Heart Journal. 2006 May;151(5):1032-6.

**Rodriguez Granillo GA, García-García HM, Valgimigli M, et al.** 291

- 9.3) **In vivo, cardiac-cycle related intimal displacement of coronary plaques assessed by 3-D ECG-gated intravascular ultrasound: exploring its correlate with tissue deformability identified by palpography.** Int J Cardiovasc Imaging. 2006 Apr;22(2):147-52.

**Rodriguez Granillo GA, Agostoni P, García-García HM, et al.** 299

**Chapter 10. *Plaque Characterization using IVUS-VH and Optical Coherence Tomography.***

- 10.1) **Optical coherence tomography plaque characterization. Comparison with IVUS-VH. Handbook of optical coherence tomography.** Taylor & Francis. 2006.

**Rodriguez Granillo GA, Regar E, Serruys PW.** 307

**PART V. IN VIVO EVALUATION OF THE EFFECT OF MEDICAL THERAPIES ON CORONARY PLAQUE PROGRESSION**

- 11.1) **Statin therapy promotes plaque regression: a meta-analysis of the studies assessing temporal changes in coronary plaque volume using intravascular ultrasound.** Submitted

**Rodriguez Granillo GA, Agostoni P, García-García HM et al.** 337

- 11.2) **Long-term effect of perindopril on coronary atherosclerosis progression: Results from the multicenter, randomized PERindopril's Prospective Effect on Coronary aTherosclerosis by**

<b>angiography and IntraVascular ultrasound Evaluation (PERSPECTIVE) study, an EUROPA substudy. Submitted</b>	
<b>Rodriguez-Granillo GA, Bruining N, de Winter SA, et al.</b>	<b>369</b>
<b>11.3) First-In-Man Prospective Evaluation of Temporal Changes in Coronary Plaque Composition By In Vivo Ultrasound Radio Frequency Data Analysis: An Integrated Biomarker and Imaging Study (IBIS) Substudy. Eurointervention. 2005;3:282-288.</b>	
<b>Rodriguez Granillo GA, Serruys PW, McFadden, et al.</b>	<b>391</b>
Summary and conclusions	401
Samenvatting en conclusies	407
Acknowledgements	413
Curriculum vitae	419
List of publications	420
Colour figures	441

## Introduction

It has been established that unheralded acute coronary syndromes are common initial manifestations of coronary atherosclerosis and that most such events arise from sites with non-flow limiting coronary atherosclerosis<sup>1,2</sup>. Histopathological studies have retrospectively suggested that plaque composition is a crucial determinant of the propensity of atherosclerotic lesions to rupture. Recently, a study including a large series of victims of sudden cardiac death showed that 60 % of acute coronary thrombi had ruptured thin-cap fibroatheroma (TCFA) lesions as a substrate. Furthermore, 70 % of those patients had additional TCFA in their coronary tree that had not ruptured<sup>5</sup>. A large (avascular, hypocellular, lipid-rich) necrotic core, a thin fibrous cap with inflammatory infiltration and paucity of smooth muscle cells, and the presence of expansive (positive) remodeling have been identified as the major criteria to define TCFA lesions<sup>6,7-10</sup>. Detection of these non-obstructive, lipid rich, high-risk plaques may have an important impact on the prevention of acute myocardial infarction and sudden death.

Angiography has been for decades the gold standard to assess the morphology and severity of atherosclerotic lesions in the coronary tree. Nevertheless, quantitative angiographic measurements can be deceptive since this technique only allows the assessment of the shape of the lumen<sup>3</sup>. In turn, atherosclerosis is a disease of the vessel wall and, due to the compensatory expansive remodelling effect, the lumen area remains unaffected until final stages of the disease<sup>4</sup>.

Intravascular Ultrasound (IVUS) is a safe catheter-based diagnostic tool that provides a real-time, high-resolution, tomographic view of coronary arteries<sup>5</sup>. It thereby enables the assessment of morphology, severity and extension of coronary plaque.

There are basically two types of commercially available IVUS imaging catheters: a single-element mechanically rotational transducer and a phased-array electronical system. Differences between these catheters regarding plaque size and composition are explored in chapter 2.1.

In vivo plaque characterization through visual interpretation of gray-scale IVUS is sub-optimal, especially when assessing heterogeneous, lipid-rich plaques<sup>6</sup>. Low echo-reflectance plaques are considered “soft” or lipid-rich. The accuracy of gray-scale IVUS for discriminating lipid from fibrous tissue is limited since in addition to large amounts of extracellular lipids (low echo-reflective areas), the lipid core contains cholesterol crystals, necrotic debris and microcalcifications (highly echoreflective areas)<sup>6</sup>.

On the contrary, spectral analysis of IVUS RF data (IVUS-VH) has demonstrated its potential to provide an objective and accurate assessment of coronary plaque composition<sup>8,9,10</sup>.

By means of the frequency domain analysis of the RF data, tissue maps that classify plaque into four major components were constructed<sup>8</sup>. In preliminary *in vitro* studies, four histological plaque components were correlated with a specific spectrum of the radiofrequency signal<sup>8,10</sup>. These different plaque components were assigned colour codes. Calcified, fibrous, fibrolipidic and necrotic core regions were labelled white, green, greenish-yellow and red respectively. IVUS RF data analysis may follow the progression of the disease not only with regards to its volume, but to its composition as well<sup>11,12</sup>. In addition, this novel IVUS application may potentially refine risk stratification strategies, and allow a more comprehensive pathophysiologic approach towards natural history studies.

In the present thesis, work has been done to explore the in vivo accuracy of intravascular ultrasound radiofrequency data analysis (IVUS-VH) for the assessment of plaque composition. To accomplish this, we have investigated the geometrical accuracy of the technique (chapter 2.2) and its reproducibility (chapter 2.3). In addition, we have carried out an extensive program to help enlighten its potential clinical value. For that purpose, we have confronted our results to previous histo-pathological and clinical knowledge as an indirect validation of the technique. IVUS-VH was therefore used to describe the extent, distribution, morphology and composition of coronary atherosclerosis in non-intervened coronary arteries (chapter 3). Chapter 4 explores the association between flow dynamics and plaque composition.

The correlation between composition and demographical data is evaluated in chapter 5.

Since IVUS-VH is a tool able to detect 2 major components of the plaque vulnerability criteria, this thesis would not be complete without exploring this area. The global characteristics of plaque rupture are discussed in chapter 6.1, whereas chapter 8.1 explores the relationship between coronary remodeling and plaque composition. Chapters 7.1 and 7.2 explore the prevalence and distribution of a histological surrogate of TCFA in vivo.

Since IVUS-VH and palpography (mechanical strain imaging) utilize the same source data (radiofrequency data analysis), information regarding both techniques might be obtained using the same pullback, potentially increasing the prognostic value of certain seemingly pejorative plaque characteristics assessed in prospective natural history studies. We therefore explored the agreement between compositional and mechanical imaging in vivo on chapter 9.2. Other attempts to correlate other different invasive imaging techniques are discussed on chapters 9.3 and 10.1.

A second very important piece of the thesis is part V, where the effect of statins and ACE-inhibitors on coronary atherosclerosis is explored.

To conclude, the aim of this thesis was threefold: 1) to explore in vivo the size, morphology, distribution and composition of coronary atherosclerosis; 2) to explore potential histological surrogates of plaque vulnerability as well as to help find a role for the technique in the clinical setting; 3) to assess in vivo the effect of conventional medical interventions on plaque size and composition.

## References

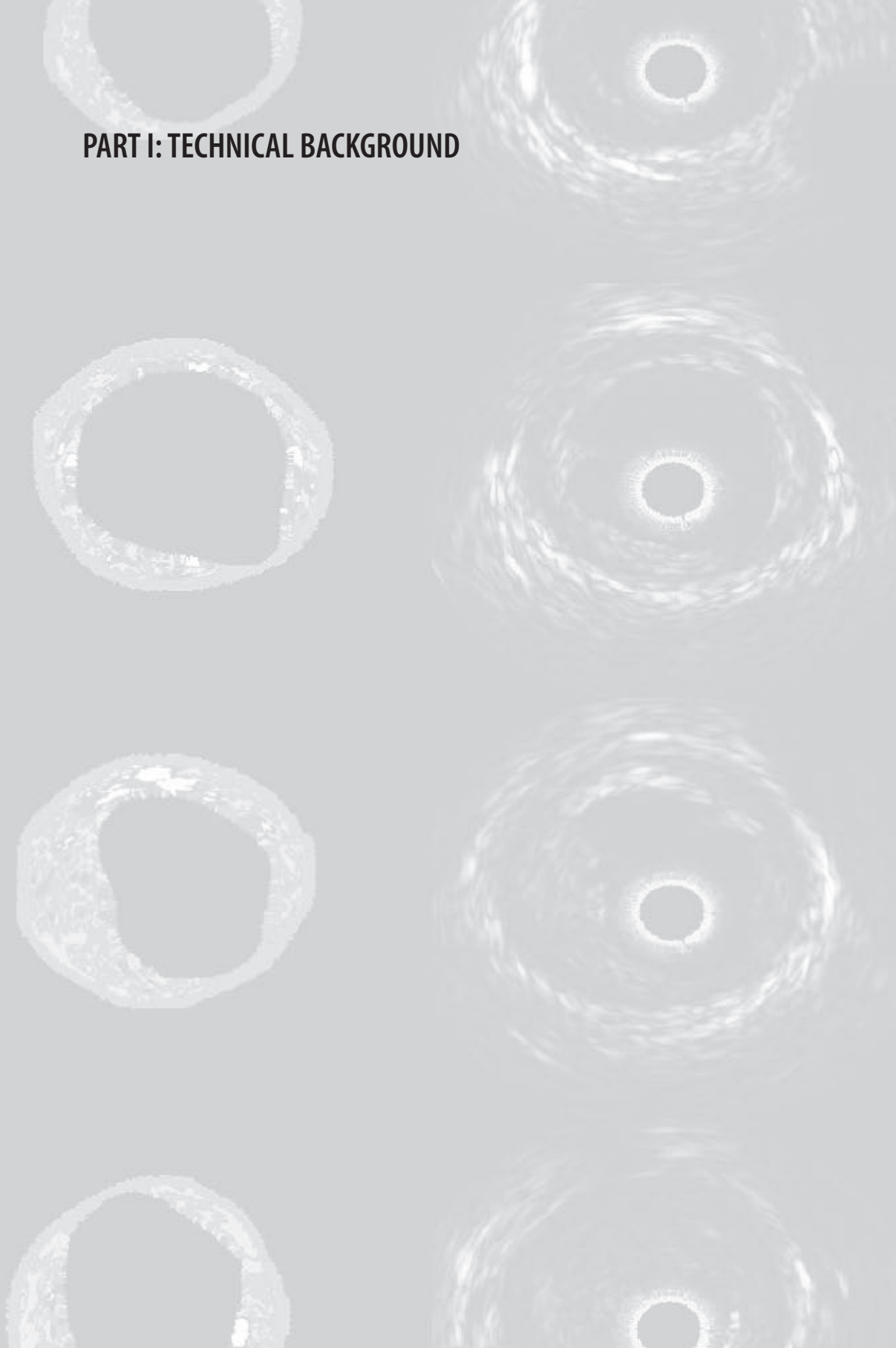
1. Ambrose JA, Tannenbaum MA, Alexopoulos D, Hjemdahl-Monsen CE, Leavy J, Weiss M, Borrico S, Gorlin R, Fuster V. Angiographic progression of coronary artery disease and the development of myocardial infarction. *J Am Coll Cardiol* 1988;12:56-62.
2. Little WC, Constantinescu M, Applegate RJ, Kutcher MA, Burrows MT, Kahl FR, Santamore WP. Can coronary angiography predict the site of a subsequent myocardial infarction in patients with mild-to-moderate coronary artery disease? *Circulation* 1988;78:1157-66.

3. Topol EJ, Nissen SE. Our preoccupation with coronary luminology. The dissociation between clinical and angiographic findings in ischemic heart disease. *Circulation* 1995;92:2333-42.
4. Glagov S, Weisenberg E, Zarins CK, Stankunavicius R, Kolettis GJ. Compensatory enlargement of human atherosclerotic coronary arteries. *N Engl J Med* 1987;316:1371-5.
5. Guedes A, Keller PF, L'Allier PL, Lesperance J, Gregoire J, Tardif JC. Long-term safety of intravascular ultrasound in nontransplant, nonintervened, atherosclerotic coronary arteries. *J Am Coll Cardiol* 2005;45:559-64.
6. Peters RJ, Kok WE, Havenith MG, Rijsterborgh H, van der Wal AC, Visser CA. Histopathologic validation of intracoronary ultrasound imaging. *J Am Soc Echocardiogr* 1994;7:230-41.
7. Virmani R, Kolodgie FD, Burke AP, Farb A, Schwartz SM. Lessons from sudden coronary death: a comprehensive morphological classification scheme for atherosclerotic lesions. *Arterioscler Thromb Vasc Biol* 2000;20:1262-75.
8. Nair A, Kuban BD, Tuzcu EM, Schoenhagen P, Nissen SE, Vince DG. Coronary plaque classification with intravascular ultrasound radiofrequency data analysis. *Circulation* 2002;106:2200-6.
9. Kawasaki M, Sano K, Okubo M, et al. Volumetric quantitative analysis of tissue characteristics of coronary plaques after statin therapy using three-dimensional integrated backscatter intravascular ultrasound. *J Am Coll Cardiol* 2005;45:1946-53.
10. Moore MP, Spencer T, Salter DM, et al. Characterisation of coronary atherosclerotic morphology by spectral analysis of radiofrequency signal: in vitro

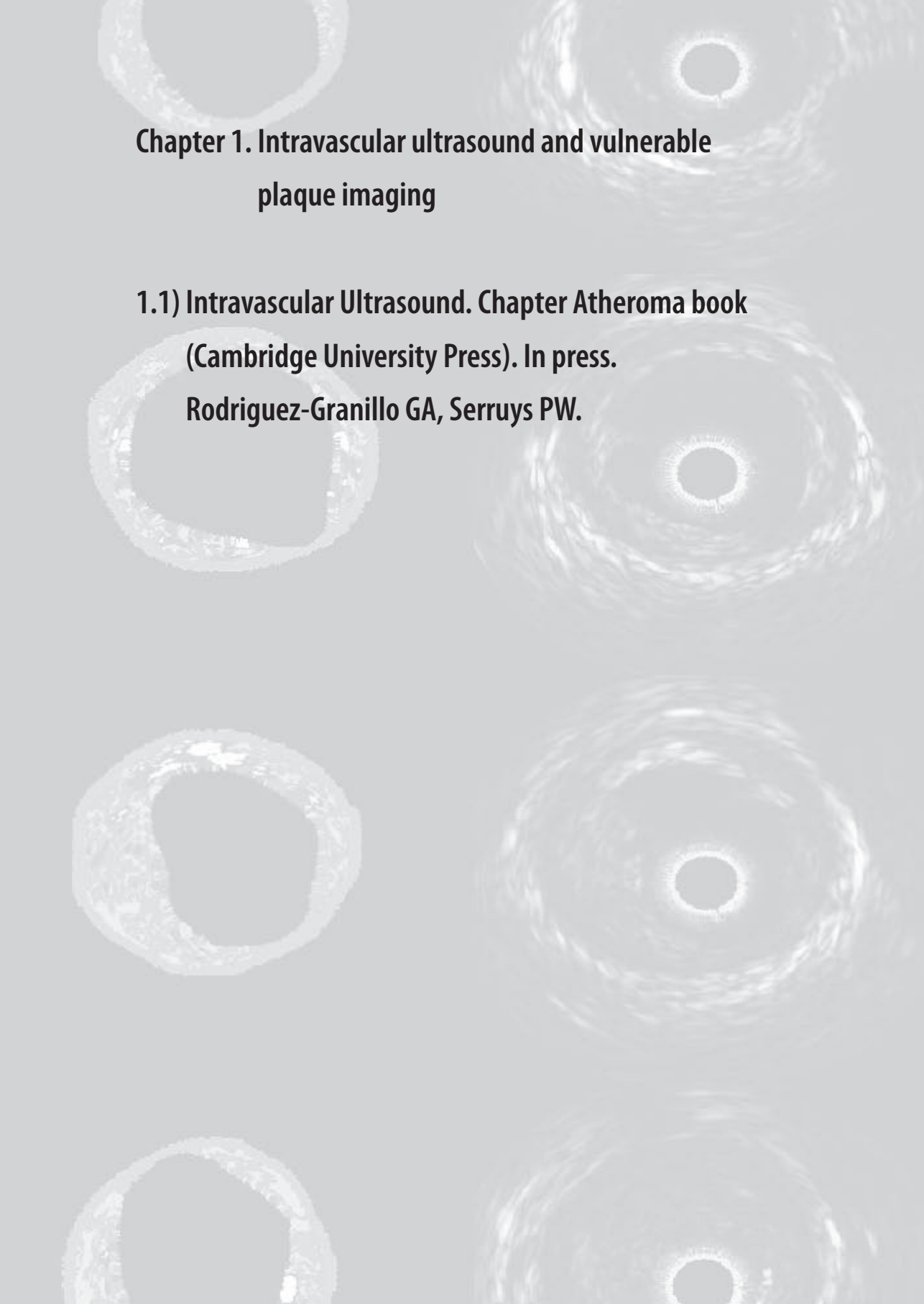
intravascular ultrasound study with histological and radiological validation. *Heart* 1998;79:459-67.

11. Kawasaki M, Sano K, Okubo M, et al. Volumetric quantitative analysis of tissue characteristics of coronary plaques after statin therapy using three-dimensional integrated backscatter intravascular ultrasound. *J Am Coll Cardiol* 2005;45:1946-53.
12. Rodriguez Granillo GA SP, Mc Fadden E, van Mieghem C, Goedhart D, Bruining N , Sianos G, van der Giessen W, van der Steen A, Vince DG, Kaplow J, Zalewski A, , de Feyter P,. First-In-Man Prospective Evaluation of Temporal Changes in Coronary Plaque Composition By In Vivo Ultrasound Radio Frequency Data Analysis: An Integrated Biomarker and Imaging Study (IBIS) Substudy. *Eurointervention* 2005;In press.

# PART I: TECHNICAL BACKGROUND







**Chapter 1. Intravascular ultrasound and vulnerable  
plaque imaging**

**1.1) Intravascular Ultrasound. Chapter Atheroma book  
(Cambridge University Press). In press.  
Rodriguez-Granillo GA, Serruys PW.**



## HISTORY

Intravascular ultrasound (IVUS) has a relatively short yet highly prolific history that started in the late 80's. Early studies already demonstrated that the extension and severity of coronary atherosclerosis might be greatly underestimated with angiography, whereas highly accurate measurements could be obtained using IVUS (1-3). Later, plaque characterization by means of the visual assessment was attempted and correlation with histopathology offered questionable results (4-6). Moving forward to the core of the past decade, interventional cardiologists sought to find an application of IVUS in the catheterization laboratory. As a result, several studies evaluated the potential of IVUS as an adjunctive tool for guiding percutaneous coronary interventions. IVUS has thereafter aided the evolution of angioplasty providing insights about the morphology of atherosclerotic plaque (7), the mechanisms involved in the restenotic process (8-11), the assessment of lesion severity (12-15) and complications (9,16) and the guidance of percutaneous coronary interventions (17-21).

More recently, IVUS has emerged as a highly accurate tool for the serial assessment of the natural history of coronary atherosclerosis and to evaluate the effect of different conventional and emerging drug therapies in the progression of atherosclerosis (22-27). Finally, the contemporary and future application of IVUS is linked to the study of different applications of the analysis of radiofrequency data, both for the improvement of plaque characterization (28,29) and for the assessment of mechanical properties of plaques (30,31). Overall, such insightful analysis of the radiofrequency data might potentially aid the detection of plaques with certain allegedly high-risk characteristics (32,33) and monitor their natural history in prospective natural history studies.

## THE TECHNOLOGY

Intravascular Ultrasound (IVUS) is a catheter-based diagnostic tool that provides a real-time, high-resolution, tomographic view of coronary arteries. It thereby enables the assessment of morphology, severity and extension of coronary plaque. There are basically two types of commercially available IVUS imaging catheters: a single-element mechanically rotational transducer and a phased-array electrical system. Mechanical systems comprise flexible cable with a single rotation transducer that revolves at 30 revolutions per second emitting and receiving ultrasound signals every 1° increment. Such catheters are covered with an echolucent outer sheath to prevent direct contact of the ultrasound element with the vessel wall. Phased-array catheters contain a 64-element annular array that enables a coordinated emission of the ultrasound signal.

Mechanical and phased-array catheters have relative advantages and disadvantages. Mechanical catheters have higher resolution but display specific artifacts such as non-uniform rotational distortion. In addition, far field imaging can be more problematic with mechanical catheters due to amplified attenuation and enhanced blood backscatter. On the other hand, phased-array catheters have lower resolution resulting in inferior near-field imaging and as they are not pulled-back within a sheath, are more susceptible to non-uniform pullback speed particularly in tortuous vessels.

Currently, the use of automated pullbacks has overcome the manual interrogation of the vessels, in particular since the former allows volumetrical determination of direct (lumen and vessel) and indirect (e.g. plaque, neointima) measurements.

## **SAFETY**

IVUS has been widely performed over the past 2 decades without significant or frequent adverse effects. In a recent large study who evaluated the long-term safety of IVUS, coronary spasm (easily reversed with intracoronary administration of nitrates) occurred in 1.9% of procedures and IVUS was not found to accelerate atherosclerosis.(34)

## **LIMITATIONS OF ANGIOGRAPHY**

Quantitative angiographic measurements can be misleading since this technique only allows the evaluation of the profile of the lumen (35). Compensatory expansive remodelled coronaries may present a significant increase in the burden of atherosclerotic plaque without evident changes in the degree of stenosis (2). Such phenomenon may impair the visual interpretation of this technique, yielding to significant inter-observer variability and poor *in vitro* correlation (36). Coronary atherosclerosis is commonly a diffuse disease of the vessel wall, involving long segments of the coronaries, rarely sparing segments. The diffuse distribution of plaque has lead to misinterpretation of angiography, eventually having the appearance of small reference vessels with minimal disease (35). Such masking of the true severity and extension of the disease has been clearly depicted by Mintz et al, who showed that reference segments of treated lesions had a mean plaque burden of 51% (37).

Vessel foreshortening, irregular plaque distribution and irregular lumen geometry are all additional factors that further impair the accuracy of angiographic measurements.

## QUANTITATIVE and QUALITATIVE IVUS

Contour detection at the leading edge of both the lumen and the media-adventitia interface (external elastic membrane, EEM) allows the assessment of 2 direct measurements (lumen and vessel area). From these contours, plaque volume [ $\sum_{m=1}^n (\text{Vessel}_{\text{area}} - \text{Lumen}_{\text{area}}) * d$ ]; where n refers to number of images, m to image and d to distance between images] and plaque burden  $[(\text{Vessel}_{\text{area}} - \text{Lumen}_{\text{area}} / \text{Vessel}_{\text{area}}) \times 100]$  can be estimated.

Several other area measurements can be obtained with IVUS. Minimum and maximum lumen diameter, minimum and maximal and plaque thickness and lumen and plaque eccentricity (38). It is noteworthy that since the leading edge of the media is not well defined, IVUS measurements cannot determine the real (histological) plaque area delineated by the internal elastic membrane. Hence, the area enclosed within the EEM and lumen contours is solely a surrogate of the plaque area, comprising the media as well. However, the inclusion of the media into the plaque area does not affect the measurements, since it represents a negligible fraction of the “plaque plus media”.

In addition to its precise quantitative measurements, IVUS has been used as a tool to characterize in-vivo the composition of coronary plaques. Initially, this was attempted by means of the visual judgement of the images (5). Using this approach, plaques were qualitatively defined as soft (echolucent), fibrous (plaques with intermediate echogenicity between soft and highly echogenic plaques), mixed (plaques containing more than one acoustical subtype) or calcified (38).

It has been recognized that its value for identification of specific plaque components, particularly of lipid rich plaques, is limited (6). Nevertheless, IVUS remains a highly accurate tool regarding calcium detection (39). Dense calcium deposits reflect the entire ultrasound energy, thus causing a phenomenon called acoustic shadowing.

Coronary plaque characterization has currently evolved to a more automated approach, leading to more accurate results (40,41). More recently, spectral analysis of IVUS radiofrequency (RF) data has emerged as a promising tool to accurately and quantitatively assess the individual components of plaques (28). Accurate characterization in vivo using IVUS RF data analysis has the potential to allow the assessment of the effects of pharmacological therapies on the coronary arteries, thereby enabling a better understanding of the disease and further development of new pharmacologic interventions (42).

## PROGRESSION-REGRESSION

Several angiographic studies have extensively explored the efficacy of lipid-lowering therapies to slow coronary plaque progression. A meta-analysis of such studies has concluded that the magnitude of the antiatherosclerotic effects is small compared with the effects of statins on the prevention of cardiovascular events (43). Such clinical-angiographic discordance has been initially attributed to the aforementioned limitations of angiography, leading investigators to pursue the conductance of progression-regression studies with the aid of IVUS (44). Thereafter, several serial studies evaluated the impact of different medical strategies on the atherosclerotic burden over time with the aid of IVUS (26,40,45). However, results are still conflicting, showing no definitive differences in plaque volume over time thus reinforcing the discrepancies between the observed clinical benefit of medical therapies and the absence of a significant impact on plaque progression. Two major theories might explain such discrepancy. First, although IVUS provides accurate morphometric measurements, several factors such as intra and inter-observer variability, different position of the catheter, severely calcified vessels and artifacts can impair the reproducibility of serial measurements (46-48). Secondly, it has been established that the histological composition of coronary plaques can precipitate atherothrombotic events regardless of the hemodynamical compromise of the lesion (49,50).

Whether the striking discordance between the clinical effects of validated anti-atherosclerotic therapies and their effects on plaque volume is due to a significant change in plaque composition or to deficiencies in the methodology of IVUS studies remains unknown. Nevertheless, recent studies have shed some light by showing significant changes in plaque composition with no alteration in the plaque burden (29,40).

## VULNERABLE PLAQUE

Major improvements in the management and diagnosis of patients with coronary artery disease have been accomplished. Still, a large number of victims who are apparently healthy die suddenly without prior symptom (51,52). Most of these events are related to plaque rupture (PR) and subsequent thrombotic occlusion at the site of non-flow limiting atherosclerotic lesions in epicardial coronary arteries (50,53). In addition, silent PR and its subsequent wound healing accelerate plaque growth and are a more frequent feature in arteries with less severe luminal narrowing (54). These dire consequences of PR have brought about the development of several catheter-based techniques with the potential to detect *in vivo* vulnerability features of coronary atherosclerotic plaques (33,55-57).

The detection of ruptured plaques by IVUS has been recently reported by several investigators (58-61). In these studies, PR was found to be ubiquitous in culprit vessels of acute myocardial infarction patients (59,61). Nevertheless, though less frequent, PR was also a common finding in non-culprit vessels and even in stable patients (58,59). In addition, in agreement with angiographical findings, PR was non-uniformly distributed throughout the coronary tree, showing a clear clustering pattern involving particularly the proximal segments and sparing the distal segments and the left main coronary artery (60,62). Finally, the presence of PR has also been associated with high levels of CRP (61).

Although these studies have provided valuable data regarding morphologic features of already ruptured plaques, it is important to stress that they do not provide evidence about the prospective detection of rupture-prone plaques.

Histological characteristics of thin-cap fibroatheroma (TCFA), the major predecessor of plaque rupture, have been extensively described (52,63,64). Indeed, an expert consensus

document has established the major criteria for defining TCFA being: 1) the presence of a lipid-rich atheromatous core, 2) a thin fibrous cap with macrophage infiltration and decreased smooth muscle cell content and 3) expansive remodeling (65).

### ***IVUS RF data analysis: IVUS-VH and Palpography***

As aforementioned, plaque characterization through visual interpretation of gray-scale IVUS is sub-optimal, especially when assessing heterogeneous, lipid-rich plaques (6). Low echo-reflectance plaques are considered “soft” or lipid-rich. However, the accuracy of gray-scale IVUS for discriminating lipid from fibrous tissue is limited since in addition to large amounts of extracellular lipids (low echo-reflective areas), the lipid core contains cholesterol crystals, necrotic debris and microcalcifications (highly echoreflective areas) (66).

On the contrary, spectral analysis of IVUS RF data (IVUS-VH) has demonstrated its potential to provide an objective and accurate assessment of coronary plaque composition (28,29,67).

By means of the frequency domain analysis of the RF data, tissue maps that classify plaque into four major components were constructed (28). In preliminary *in vitro* studies, four histological plaque components were correlated with a specific spectrum of the radiofrequency signal (28,67). These different plaque components were assigned colour codes. Calcified, fibrous, fibrolipidic and necrotic core regions were labelled white, green, greenish-yellow and red respectively (figure 1). IVUS RF data analysis may follow the progression of the disease not only with regards to its volume, but to its composition as well (29,42). In addition, this novel IVUS application may potentially refine risk stratification strategies, and allow a more comprehensive pathophysiologic approach towards natural history studies. Recently, using this technique, we have identified *in vivo* a surrogate of TCFA (IVUS-derived thin-cap fibroatheroma, IDTCFA) as a more prevalent finding in ACS than in

stable angina patients. In addition, the distribution of IDTCFA lesions along the coronary vessels was clearly clustered (33).

Although the most accepted threshold to define a cap as “thin” has been set at 65  $\mu\text{m}$  (68), a number of important ex vivo studies have used a higher ( $> 200 \mu\text{m}$ ) thresholds (32,69,70). It is well established that significant tissue shrinkage occurs during tissue fixation (71). Furthermore, post-mortem contraction of arteries is an additional confounding factor (72). Since the axial resolution of IVUS RF data is between 100-150  $\mu\text{m}$ , we assumed that the absence of visible fibrous tissue overlying a necrotic core suggested a cap thickness of below 100-150  $\mu\text{m}$  and used the absence of such tissue to define a thin fibrous cap (73).

The eccentric accumulation of a lipid-rich necrotic core within the vessel wall is usually separated from the lumen by a thin fibrous cap. This observation led to the hypothesis that vulnerable lesions might have mechanical properties that differ from those of chronic stable lesions. Indeed, both plaque rupture and increased inflammatory markers have been reported to occur more frequently in regions and patients with increased mechanical stress (55,74,75).. The palpography rationale is that, at a defined pressure, soft tissue (lipid-rich) components will deform more than hard tissue components (fibrous-calcified) (30). Images obtained at different pressure levels and compared to determine the local tissue compression. The radial strain in the tissue is calculated by cross-correlation techniques on the radio frequency signal and can be displayed as a colour-coded image (figure 1) (30). The sensitivity and specificity to detect vulnerable plaques has recently been assessed in post-mortem human coronary arteries where vulnerable plaques were detected with a sensitivity of 88% and a specificity of 89% (32). In addition to ex-vivo studies, this technique has also been tested in-vivo, where palpography detected a high incidence of deformable plaques in ACS patients.

### ***Coronary remodelling***

Coronary artery remodelling was initially described by Glagov as a compensatory enlargement of the coronary arteries in response to an increase in plaque area (2). This concept has later evolved to a dynamic theory where vessels may also experience shrinkage in response to plaque growth (76). Several studies have associated positive (expansive) remodelling to an increase in inflammatory marker levels, larger necrotic cores, pronounced medial thinning and worse clinical presentation (77-80). IVUS has been utilized to assess the relationship between vascular remodelling and plaque composition (81-84). More recently, we have shown a significantly larger necrotic core content in positively remodelled lesions, whereas the fibrotic burden of plaques was inversely correlated with the remodelling index (85).

It is important though to stress that, ideally, the presence of coronary remodelling should be established by serial determinations (86).

### **SHEAR STRESS**

Carotid and coronary studies have used MRI and IVUS to show that atherosclerosis has a tendency to arise more frequently in low-oscillatory shear stress regions such as in inner curvature of non-branching segments and opposite to the flow-divider at bifurcations (87-90). The pathophysiology of such phenomenon can be explained by the fact that low-oscillatory shear stress induces a loss of the physiological flow-oriented alignment of the endothelial cells, thus causing an enhancement of the expression of adhesion molecules and a weakening of cell junctions, ultimately leading to an increase in permeability to lipids and macrophages (91-94). Shear stress can be calculated by a combined approach using IVUS and angiography (90). Indeed, the relation between shear stress and plaque vulnerability is currently subject of intensive research efforts (94).

## **FUTURE DIRECTIONS**

Since IVUS-VH and palpography utilize the same source data (radiofrequency data analysis), information regarding both techniques might be obtained using the same pullback (figure 1); potentially increasing the prognostic value of certain seemingly pejorative plaque characteristics assessed in prospective natural history studies. Other future avenue is the imaging of the vasa vasorum, which can now be achieved using micro bubble-contrast enhanced IVUS, thus enabling the measurement of activity and inflammation within plaques (95).

As pictured along the chapter, IVUS has numerous applications that have supported the development and progress of interventional cardiology through the past decades. Towards the future, we foresee a pivotal role of IVUS for the detection of vulnerable plaque and the assessment of the effect of emergent medical strategies both related to plaque volume and composition. The utility of IVUS for carotid imaging has been less exploited and limited to the guidance of percutaneous coronary interventions (96). This was driven by the excellent imaging quality provided by non-invasive B-mode carotid ultrasound.

However, the rising body of investigations using IVUS for the detection of vulnerable plaque might promote a more universal application of the technique potentially including imaging of mild carotid artery atherosclerosis (97).

## REFERENCES

1. McPherson DD, Hiratzka LF, Lamberth WC, et al. Delineation of the extent of coronary atherosclerosis by high-frequency epicardial echocardiography. *N Engl J Med* 1987;316:304-9.
2. Glagov S, Weisenberg E, Zarins CK, Stankunavicius R, Kolettis GJ. Compensatory enlargement of human atherosclerotic coronary arteries. *N Engl J Med* 1987;316:1371-5.
3. Gussenhoven WJ, Essed CE, Frietman P, et al. Intravascular echographic assessment of vessel wall characteristics: a correlation with histology. *Int J Card Imaging* 1989;4:105-16.
4. Gussenhoven EJ, Essed CE, Lancee CT, et al. Arterial wall characteristics determined by intravascular ultrasound imaging: an in vitro study. *J Am Coll Cardiol* 1989;14:947-52.
5. Gussenhoven EJ, Essed CE, Frietman P, et al. Intravascular ultrasonic imaging: histologic and echographic correlation. *Eur J Vasc Surg* 1989;3:571-6.
6. Peters RJ, Kok WE, Havenith MG, Rijsterborgh H, van der Wal AC, Visser CA. Histopathologic validation of intracoronary ultrasound imaging. *J Am Soc Echocardiogr* 1994;7:230-41.
7. Suzuki T, Hosokawa H, Katoh O, et al. Effects of adjunctive balloon angioplasty after intravascular ultrasound-guided optimal directional coronary atherectomy: the result of Adjunctive Balloon Angioplasty After Coronary Atherectomy Study (ABACAS). *J Am Coll Cardiol* 1999;34:1028-35.

8. de Feyter PJ, Kay P, Disco C, Serruys PW. Reference chart derived from post-stent-implantation intravascular ultrasound predictors of 6-month expected restenosis on quantitative coronary angiography. *Circulation* 1999;100:1777-83.
9. Sheris SJ, Canos MR, Weissman NJ. Natural history of intravascular ultrasound-detected edge dissections from coronary stent deployment. *Am Heart J* 2000;139:59-63.
10. Shiran A, Mintz GS, Waksman R, et al. Early lumen loss after treatment of in-stent restenosis: an intravascular ultrasound study. *Circulation* 1998;98:200-3.
11. Hoffmann R, Mintz GS, Dussailant GR, et al. Patterns and mechanisms of in-stent restenosis. A serial intravascular ultrasound study. *Circulation* 1996;94:1247-54.
12. Abizaid A, Mintz GS, Pichard AD, et al. Clinical, intravascular ultrasound, and quantitative angiographic determinants of the coronary flow reserve before and after percutaneous transluminal coronary angioplasty. *Am J Cardiol* 1998;82:423-8.
13. Nishioka T, Amanullah AM, Luo H, et al. Clinical validation of intravascular ultrasound imaging for assessment of coronary stenosis severity: comparison with stress myocardial perfusion imaging. *J Am Coll Cardiol* 1999;33:1870-8.
14. Takagi A, Tsurumi Y, Ishii Y, Suzuki K, Kawana M, Kasanuki H. Clinical potential of intravascular ultrasound for physiological assessment of coronary stenosis: relationship between quantitative ultrasound tomography and pressure-derived fractional flow reserve. *Circulation* 1999;100:250-5.
15. Abizaid AS, Mintz GS, Mehran R, et al. Long-term follow-up after percutaneous transluminal coronary angioplasty was not performed based on intravascular ultrasound findings: importance of lumen dimensions. *Circulation* 1999;100:256-61.

16. Degertekin M, Serruys PW, Tanabe K, et al. Long-term follow-up of incomplete stent apposition in patients who received sirolimus-eluting stent for de novo coronary lesions: an intravascular ultrasound analysis. *Circulation* 2003;108:2747-50.
17. Schiele F, Meneveau N, Vuilleminot A, et al. Impact of intravascular ultrasound guidance in stent deployment on 6-month restenosis rate: a multicenter, randomized study comparing two strategies--with and without intravascular ultrasound guidance. RESIST Study Group. REStenosis after Ivus guided STenting. *J Am Coll Cardiol* 1998;32:320-8.
18. Fitzgerald PJ, Oshima A, Hayase M, et al. Final results of the Can Routine Ultrasound Influence Stent Expansion (CRUISE) study. *Circulation* 2000;102:523-30.
19. Mudra H, di Mario C, de Jaegere P, et al. Randomized comparison of coronary stent implantation under ultrasound or angiographic guidance to reduce stent restenosis (OPTICUS Study). *Circulation* 2001;104:1343-9.
20. Frey AW, Hodgson JM, Muller C, Bestehorn HP, Roskamm H. Ultrasound-guided strategy for provisional stenting with focal balloon combination catheter: results from the randomized Strategy for Intracoronary Ultrasound-guided PTCA and Stenting (SIPS) trial. *Circulation* 2000;102:2497-502.
21. Oemrawsingh PV, Mintz GS, SchaliJ MJ, Zwinderman AH, Jukema JW, van der Wall EE. Intravascular ultrasound guidance improves angiographic and clinical outcome of stent implantation for long coronary artery stenoses: final results of a randomized comparison with angiographic guidance (TULIP Study). *Circulation* 2003;107:62-7.
22. Matsuzaki M, Hiramori K, Imaizumi T, et al. Intravascular ultrasound evaluation of coronary plaque regression by low density lipoprotein-apheresis in familial hypercholesterolemia: the Low Density Lipoprotein-Apheresis Coronary Morphology and Reserve Trial (LACMART). *J Am Coll Cardiol* 2002;40:220-7.

23. Nissen SE, Tsunoda T, Tuzcu EM, et al. Effect of recombinant ApoA-I Milano on coronary atherosclerosis in patients with acute coronary syndromes: a randomized controlled trial. *Jama* 2003;290:2292-300.
24. Fang JC, Kinlay S, Beltrame J, et al. Effect of vitamins C and E on progression of transplant-associated arteriosclerosis: a randomised trial. *Lancet* 2002;359:1108-13.
25. Nissen SE, Tuzcu EM, Schoenhagen P, et al. Effect of intensive compared with moderate lipid-lowering therapy on progression of coronary atherosclerosis: a randomized controlled trial. *Jama* 2004;291:1071-80.
26. Nissen SE, Tuzcu EM, Libby P, et al. Effect of antihypertensive agents on cardiovascular events in patients with coronary disease and normal blood pressure: the CAMELOT study: a randomized controlled trial. *Jama* 2004;292:2217-25.
27. Tardif JC, Gregoire J, L'Allier PL, et al. Effects of the acyl coenzyme A:cholesterol acyltransferase inhibitor avasimibe on human atherosclerotic lesions. *Circulation* 2004;110:3372-7.
28. Nair A, Kuban BD, Tuzcu EM, Schoenhagen P, Nissen SE, Vince DG. Coronary plaque classification with intravascular ultrasound radiofrequency data analysis. *Circulation* 2002;106:2200-6.
29. Kawasaki M, Sano K, Okubo M, et al. Volumetric quantitative analysis of tissue characteristics of coronary plaques after statin therapy using three-dimensional integrated backscatter intravascular ultrasound. *J Am Coll Cardiol* 2005;45:1946-53.
30. de Korte CL, van der Steen AF, Cespedes EI, Pasterkamp G. Intravascular ultrasound elastography in human arteries: initial experience in vitro. *Ultrasound Med Biol* 1998;24:401-8.

31. de Korte CL, Carlier SG, Mastik F, et al. Morphological and mechanical information of coronary arteries obtained with intravascular elastography; feasibility study in vivo. *Eur Heart J* 2002;23:405-13.
32. Schaar JA, De Korte CL, Mastik F, et al. Characterizing vulnerable plaque features with intravascular elastography. *Circulation* 2003;108:2636-41.
33. Rodriguez-Granillo GA G-GH, Mc Fadden E, Valgimigli M, Aoki J, de Feyter P, Serruys PW. In Vivo Intravascular Ultrasound-Derived Thin-Cap Fibroatheroma Detection Using Ultrasound Radio Frequency Data Analysis. *J Am Coll Cardiol* 2005;In press.
34. Guedes A, Keller PF, L'Allier PL, Lesperance J, Gregoire J, Tardif JC. Long-term safety of intravascular ultrasound in nontransplant, nonintervened, atherosclerotic coronary arteries. *J Am Coll Cardiol* 2005;45:559-64.
35. Topol EJ, Nissen SE. Our preoccupation with coronary luminology. The dissociation between clinical and angiographic findings in ischemic heart disease. *Circulation* 1995;92:2333-42.
36. Grodin CM DI, Pastgernac A, et al. Discrepancies between cineangiographic and post-mortem findings in patients with coronary artery disease and recent myocardial revascularization. *Circulation* 1974;49:703-709.
37. Mintz GS, Painter JA, Pichard AD, et al. Atherosclerosis in angiographically "normal" coronary artery reference segments: an intravascular ultrasound study with clinical correlations. *J Am Coll Cardiol* 1995;25:1479-85.
38. Mintz GS, Nissen SE, Anderson WD, et al. American College of Cardiology Clinical Expert Consensus Document on Standards for Acquisition, Measurement and Reporting of Intravascular Ultrasound Studies (IVUS). A report of the American

- College of Cardiology Task Force on Clinical Expert Consensus Documents. *J Am Coll Cardiol* 2001;37:1478-92.
39. Tuzcu EM, Berkalp B, De Franco AC, et al. The dilemma of diagnosing coronary calcification: angiography versus intravascular ultrasound. *J Am Coll Cardiol* 1996;27:832-8.
  40. Schartl M, Bocksch W, Koschyk DH, et al. Use of intravascular ultrasound to compare effects of different strategies of lipid-lowering therapy on plaque volume and composition in patients with coronary artery disease. *Circulation* 2001;104:387-92.
  41. de Winter SA HI, Hamers R, de Feyter PJ, Serruys PWC, Roelandt JRTC, Bruining N. Computer assisted three-dimensional plaque characterization in ultracoronary ultrasound studies. *Computers in Cardiology* 2003;30:73-76.
  42. Rodriguez Granillo GA SP, Mc Fadden E, van Mieghem C, Goedhart D, Bruining N, Sianos G, van der Giessen W, van der Steen A, Vince DG, Kaplow J, Zalewski A, de Feyter P. First-In-Man Prospective Evaluation of Temporal Changes in Coronary Plaque Composition By In Vivo Ultrasound Radio Frequency Data Analysis: An Integrated Biomarker and Imaging Study (IBIS) Substudy. *Eurointervention* 2005;In press.
  43. Balk EM, Karas RH, Jordan HS, Kupelnick B, Chew P, Lau J. Effects of statins on vascular structure and function: A systematic review. *Am J Med* 2004;117:775-90.
  44. Takagi T, Yoshida K, Akasaka T, Hozumi T, Morioka S, Yoshikawa J. Intravascular ultrasound analysis of reduction in progression of coronary narrowing by treatment with pravastatin. *Am J Cardiol* 1997;79:1673-6.
  45. Okazaki S, Yokoyama T, Miyauchi K, et al. Early statin treatment in patients with acute coronary syndrome: demonstration of the beneficial effect on atherosclerotic

- lesions by serial volumetric intravascular ultrasound analysis during half a year after coronary event: the ESTABLISH Study. *Circulation* 2004;110:1061-8.
46. Gaster AL, Korsholm L, Thayssen P, Pedersen KE, Haghfelt TH. Reproducibility of intravascular ultrasound and intracoronary Doppler measurements. *Catheter Cardiovasc Interv* 2001;53:449-58.
  47. Blessing E, Hausmann D, Sturm M, Wolpers HG, Amende I, Mugge A. Intravascular ultrasound and stent implantation: intraobserver and interobserver variability. *Am Heart J* 1999;137:368-71.
  48. Bekeredjian R, Hardt S, Just A, Hansen A, Kuecherer H. Influence of Catheter Position and Equipment-Related Factors on the Accuracy of Intravascular Ultrasound Measurements. *J Invasive Cardiol* 1999;11:207-212.
  49. Davies MJ, Richardson PD, Woolf N, Katz DR, Mann J. Risk of thrombosis in human atherosclerotic plaques: role of extracellular lipid, macrophage, and smooth muscle cell content. *Br Heart J* 1993;69:377-81.
  50. Ambrose JA, Tannenbaum MA, Alexopoulos D, et al. Angiographic progression of coronary artery disease and the development of myocardial infarction. *J Am Coll Cardiol* 1988;12:56-62.
  51. Kannel WB, Doyle JT, McNamara PM, Quickenton P, Gordon T. Precursors of sudden coronary death. Factors related to the incidence of sudden death. *Circulation* 1975;51:606-13.
  52. Falk E, Shah PK, Fuster V. Coronary plaque disruption. *Circulation* 1995;92:657-71.
  53. Little WC, Constantinescu M, Applegate RJ, et al. Can coronary angiography predict the site of a subsequent myocardial infarction in patients with mild-to-moderate coronary artery disease? *Circulation* 1988;78:1157-66.

54. Burke AP, Kolodgie FD, Farb A, et al. Healed plaque ruptures and sudden coronary death: evidence that subclinical rupture has a role in plaque progression. *Circulation* 2001;103:934-40.
55. Schaar JA, Regar E, Mastik F, et al. Incidence of high-strain patterns in human coronary arteries: assessment with three-dimensional intravascular palpography and correlation with clinical presentation. *Circulation* 2004;109:2716-9.
56. Regar E SJ, van der Giessen W, van der Steen, Serruys PW. Real-time, in-vivo optical coherence tomography of human coronary arteries using a dedicated imaging wire. *Am J Cardiol* 2002;90:129H.
57. Asakura M, Ueda Y, Yamaguchi O, et al. Extensive development of vulnerable plaques as a pan-coronary process in patients with myocardial infarction: an angioscopic study. *J Am Coll Cardiol* 2001;37:1284-8.
58. Maehara A, Mintz GS, Bui AB, et al. Morphologic and angiographic features of coronary plaque rupture detected by intravascular ultrasound. *J Am Coll Cardiol* 2002;40:904-10.
59. Rioufol G, Finet G, Ginon I, et al. Multiple atherosclerotic plaque rupture in acute coronary syndrome: a three-vessel intravascular ultrasound study. *Circulation* 2002;106:804-8.
60. Hong MK, Mintz GS, Lee CW, et al. The site of plaque rupture in native coronary arteries: a three-vessel intravascular ultrasound analysis. *J Am Coll Cardiol* 2005;46:261-5.
61. Hong MK, Mintz GS, Lee CW, et al. Comparison of coronary plaque rupture between stable angina and acute myocardial infarction: a three-vessel intravascular ultrasound study in 235 patients. *Circulation* 2004;110:928-33.

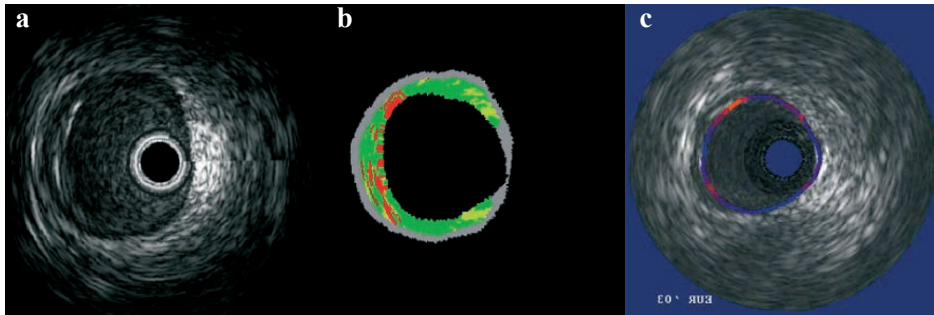
62. Wang JC, Normand SL, Mauri L, Kuntz RE. Coronary artery spatial distribution of acute myocardial infarction occlusions. *Circulation* 2004;110:278-84.
63. Kolodgie FD, Burke AP, Farb A, et al. The thin-cap fibroatheroma: a type of vulnerable plaque: the major precursor lesion to acute coronary syndromes. *Curr Opin Cardiol* 2001;16:285-92.
64. Naghavi M, Libby P, Falk E, et al. From vulnerable plaque to vulnerable patient: a call for new definitions and risk assessment strategies: Part I. *Circulation* 2003;108:1664-72.
65. Schaar JA, Muller JE, Falk E, et al. Terminology for high-risk and vulnerable coronary artery plaques. Report of a meeting on the vulnerable plaque, June 17 and 18, 2003, Santorini, Greece. *Eur Heart J* 2004;25:1077-82.
66. Virmani R, Kolodgie FD, Burke AP, Farb A, Schwartz SM. Lessons from sudden coronary death: a comprehensive morphological classification scheme for atherosclerotic lesions. *Arterioscler Thromb Vasc Biol* 2000;20:1262-75.
67. Moore MP, Spencer T, Salter DM, et al. Characterisation of coronary atherosclerotic morphology by spectral analysis of radiofrequency signal: in vitro intravascular ultrasound study with histological and radiological validation. *Heart* 1998;79:459-67.
68. Burke AP, Farb A, Malcom GT, Liang YH, Smialek J, Virmani R. Coronary risk factors and plaque morphology in men with coronary disease who died suddenly. *N Engl J Med* 1997;336:1276-82.
69. Mann JM, Davies MJ. Vulnerable plaque. Relation of characteristics to degree of stenosis in human coronary arteries. *Circulation* 1996;94:928-31.
70. Felton CV, Crook D, Davies MJ, Oliver MF. Relation of plaque lipid composition and morphology to the stability of human aortic plaques. *Arterioscler Thromb Vasc Biol* 1997;17:1337-45.

71. MKW L. A critical appraisal of the effects of fixation, dehydration and embedding of cell volume. In: *The Science of Biological Specimen Preparation for Microscopy and Microanalysis*. Revel JP, Barnard T, Haggis GH (eds). Scanning Electron Microscopy, AMF O'Hare, 1984;IL 60666:pp.61-70.
72. Fishbein MC, Siegel RJ. How big are coronary atherosclerotic plaques that rupture? *Circulation* 1996;94:2662-6.
73. Nair A CD, Vince DG. Regularized Autoregressive Analysis of Intravascular Ultrasound Data: Improvement in Spatial Accuracy of Plaque Tissue Maps. *IEEE Transactions on Ultrasonics, Ferroelectrics, and Frequency Control* 2004;51:420-431.
74. Burleigh MC, Briggs AD, Lendon CL, Davies MJ, Born GV, Richardson PD. Collagen types I and III, collagen content, GAGs and mechanical strength of human atherosclerotic plaque caps: span-wise variations. *Atherosclerosis* 1992;96:71-81.
75. Loree HM, Kamm RD, Stringfellow RG, Lee RT. Effects of fibrous cap thickness on peak circumferential stress in model atherosclerotic vessels. *Circ Res* 1992;71:850-8.
76. Pasterkamp G, Wensing PJ, Post MJ, Hillen B, Mali WP, Borst C. Paradoxical arterial wall shrinkage may contribute to luminal narrowing of human atherosclerotic femoral arteries. *Circulation* 1995;91:1444-9.
77. Pasterkamp G, Schoneveld AH, van der Wal AC, et al. Relation of arterial geometry to luminal narrowing and histologic markers for plaque vulnerability: the remodeling paradox. *J Am Coll Cardiol* 1998;32:655-62.
78. Burke AP, Kolodgie FD, Farb A, Weber D, Virmani R. Morphological predictors of arterial remodeling in coronary atherosclerosis. *Circulation* 2002;105:297-303.
79. Varnava AM, Mills PG, Davies MJ. Relationship between coronary artery remodeling and plaque vulnerability. *Circulation* 2002;105:939-43.

80. Smits PC, Pasterkamp G, Quarles van Ufford MA, et al. Coronary artery disease: arterial remodelling and clinical presentation. *Heart* 1999;82:461-4.
81. Mintz GS, Kent KM, Pichard AD, Satler LF, Popma JJ, Leon MB. Contribution of inadequate arterial remodeling to the development of focal coronary artery stenoses. An intravascular ultrasound study. *Circulation* 1997;95:1791-8.
82. Tauth J, Pinnow E, Sullebarger JT, et al. Predictors of coronary arterial remodeling patterns in patients with myocardial ischemia. *Am J Cardiol* 1997;80:1352-5.
83. Sabate M, Kay IP, de Feyter PJ, et al. Remodeling of atherosclerotic coronary arteries varies in relation to location and composition of plaque. *Am J Cardiol* 1999;84:135-40.
84. Fuesl RT, Kranenberg E, Kiausch U, Baer FM, Sechtem U, Hopp HW. Vascular remodeling in atherosclerotic coronary arteries is affected by plaque composition. *Coron Artery Dis* 2001;12:91-7.
85. Rodriguez-Granillo GA, Serruys PW, Garcia-Garcia HM, et al. Coronary artery remodelling is related to plaque composition. *Heart* 2005.
86. Hibi K, Ward MR, Honda Y, et al. Impact of different definitions on the interpretation of coronary remodeling determined by intravascular ultrasound. *Catheter Cardiovasc Interv* 2005;65:233-239.
87. Jeremias A, Huegel H, Lee DP, et al. Spatial orientation of atherosclerotic plaque in non-branching coronary artery segments. *Atherosclerosis* 2000;152:209-15.
88. Kimura BJ, Russo RJ, Bhargava V, McDaniel MB, Peterson KL, DeMaria AN. Atheroma morphology and distribution in proximal left anterior descending coronary artery: in vivo observations. *J Am Coll Cardiol* 1996;27:825-31.

89. Irace C, Cortese C, Fiaschi E, Carallo C, Farinaro E, Gnasso A. Wall shear stress is associated with intima-media thickness and carotid atherosclerosis in subjects at low coronary heart disease risk. *Stroke* 2004;35:464-8.
90. Krams R, Wentzel JJ, Oomen JA, et al. Evaluation of endothelial shear stress and 3D geometry as factors determining the development of atherosclerosis and remodeling in human coronary arteries in vivo. Combining 3D reconstruction from angiography and IVUS (ANGUS) with computational fluid dynamics. *Arterioscler Thromb Vasc Biol* 1997;17:2061-5.
91. Berceci SA, Warty VS, Sheppeck RA, Mandarino WA, Tanksale SK, Borovetz HS. Hemodynamics and low density lipoprotein metabolism. Rates of low density lipoprotein incorporation and degradation along medial and lateral walls of the rabbit aorto-iliac bifurcation. *Arteriosclerosis* 1990;10:686-94.
92. Kornet L, Hoeks AP, Lambregts J, Reneman RS. In the femoral artery bifurcation, differences in mean wall shear stress within subjects are associated with different intima-media thicknesses. *Arterioscler Thromb Vasc Biol* 1999;19:2933-9.
93. Kaazempur-Mofrad MR, Isasi AG, Younis HF, et al. Characterization of the atherosclerotic carotid bifurcation using MRI, finite element modeling, and histology. *Ann Biomed Eng* 2004;32:932-46.
94. Slager CJ WJ, Gijzen FJH, Schuurbiens JCH, van der Wal AC, van der Steen AFW, Serruys PW. The role of shear stress in the generation of rupture-prone vulnerable plaques. *Nature Clinical Practice* 2005;2:401-407.
95. Carlier S, Kakadiaris IA, Dib N, et al. Vasa vasorum imaging: a new window to the clinical detection of vulnerable atherosclerotic plaques. *Curr Atheroscler Rep* 2005;7:164-9.

96. Clark DJ, Lessio S, O'Donoghue M, Schainfeld R, Rosenfield K. Safety and utility of intravascular ultrasound-guided carotid artery stenting. *Catheter Cardiovasc Interv* 2004;63:355-62.
97. Rasanen HT, Manninen HI, Vanninen RL, Vainio P, Berg M, Saari T. Mild carotid artery atherosclerosis: assessment by 3-dimensional time-of-flight magnetic resonance angiography, with reference to intravascular ultrasound imaging and contrast angiography. *Stroke* 1999;30:827-33.

**FIGURES**

Colour figures on pages 441-449

**Figure 1**

Matched cross-section of a left anterior coronary artery imaged by conventional (gray-scale) IVUS (a), IVUS-VH (b) and palpography (c).

IVUS-VH colour-coding labels calcified, fibrous, fibrolipidic and necrotic core regions as white, green, greenish-yellow and red respectively. For palpography, the calculated local strain is also colour-coded, from blue (for 0% strain) through yellow (for 2% strain) via red.

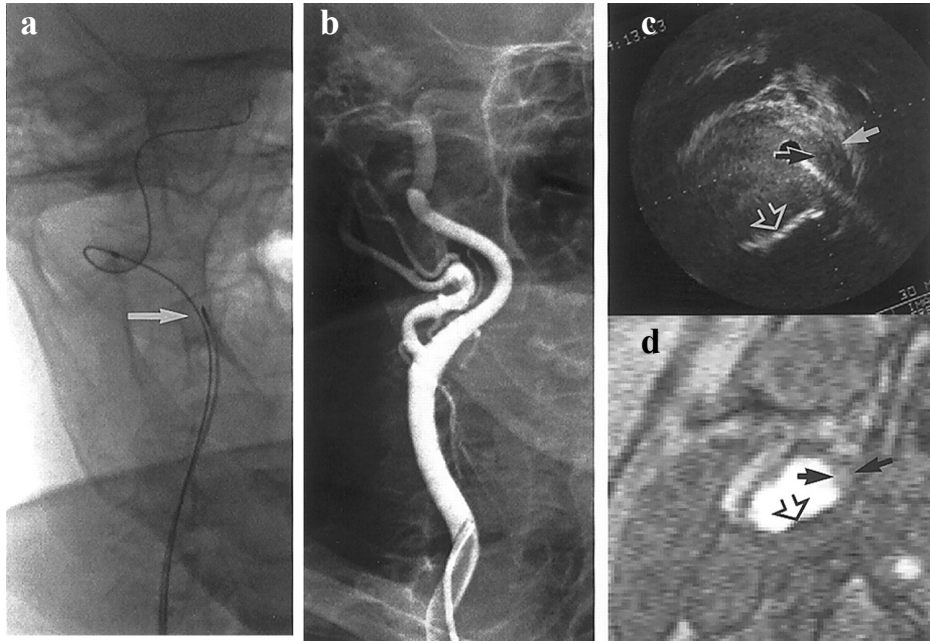


**Figure 2.**

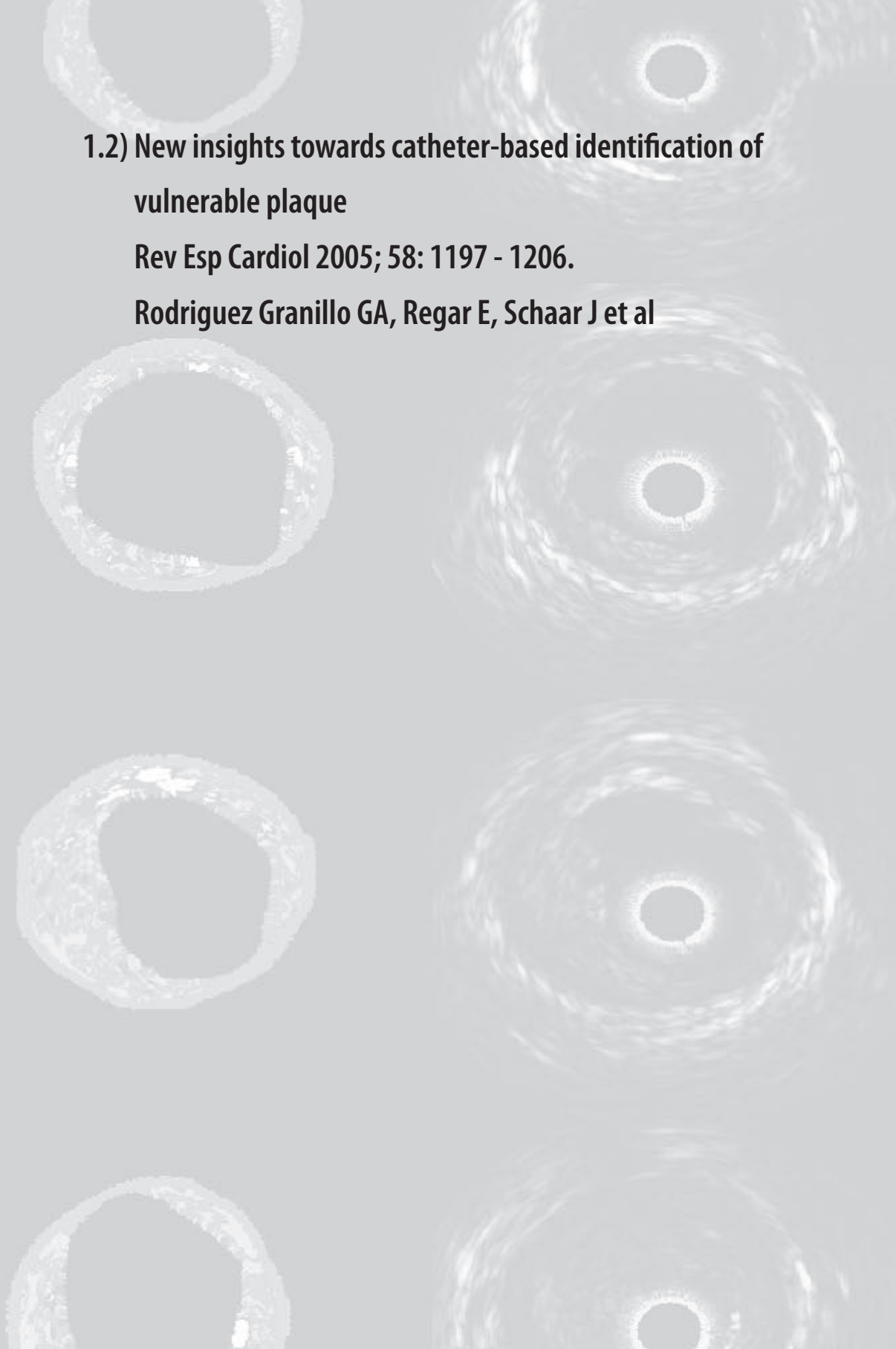
Intravascular ultrasound (IVUS) transducer at the internal carotid artery (a, arrow indicates transducer location). Panel b shows a seemingly normal contrast angiography. IVUS (c) and corresponding MRA (d) cross-sections of the carotid bifurcation are shown. Wide eccentric plaque (between arrows) is seen similarly on both IVUS and magnetic resonance angiography.

(Extracted with permission from Rasanen, H. T. et al. Stroke 1999;30:827-833)

**1.2) New insights towards catheter-based identification of vulnerable plaque**

**Rev Esp Cardiol 2005; 58: 1197 - 1206.**

**Rodriguez Granillo GA, Regar E, Schaar J et al**





## REVIEW ARTICLE

## New Insights Towards Catheter-Based Identification of Vulnerable Plaque

Gastón A. Rodríguez-Granillo, Evelyn Regar, Johanness A. Schaar, and Patrick W. Serruys

Interventional Cardiology, Thoraxcenter, Erasmus MC, Rotterdam, The Netherlands.

Sudden cardiac death or unheralded acute coronary syndromes are common initial manifestations of coronary atherosclerosis and most such events occur at sites of non-flow limiting coronary atherosclerosis. Autopsy data suggests that plaque composition is a key determinant of the propensity of atherosclerotic lesions to provoke clinical events. Most of these events are related to plaque rupture and subsequent thrombotic occlusion at the site of non-flow limiting atherosclerotic lesions in epicardial coronary arteries. Detection of these non-obstructive, lipid rich, high-risk plaques may have an important impact on the prevention of acute myocardial infarction and sudden death. Currently, there are several intravascular tools capable of locally evaluating determinants of plaque vulnerability such as the size of the lipid core, thickness of the fibrous cap, inflammation within the cap and positive remodeling. These new modalities have the potential to provide insights into the pathophysiology of the natural history of coronary plaque by means of prospective studies.

**Key words:** *Vulnerable plaque. Coronary artery disease. Intravascular techniques.*

### Nuevas tendencias en la evaluación de la placa vulnerable mediante técnicas de cateterismo

La muerte súbita y los síndromes coronarios agudos son, frecuentemente, manifestaciones iniciales de la cardiopatía isquémica. Estudios post mórtem han indicado que la composición de las placas ateromatosas es un factor determinante para la predisposición de las lesiones coronarias a la rotura y el subsiguiente evento clínico. La mayor parte de estos eventos está relacionada con la rotura de placas ateromatosas situadas en lesiones hemodinámicamente no significativas. La detección de estas placas no obstructivas, pero ricas en lípidos, podría tener un gran impacto en la prevención del infarto y la muerte súbita. Actualmente, hay diversas técnicas intravasculares capaces de evaluar distintos determinantes de vulnerabilidad coronaria localmente, tales como el tamaño del core lipídico, el grosor y la inflamación de la cápsula fibrosa y el remodelamiento positivo.

Mediante la conducción de estudios prospectivos, estas nuevas modalidades poseen el potencial para proveer *in vivo* información acerca de la fisiopatología de la historia natural de la aterosclerosis coronaria.

**Palabras clave:** *Placa vulnerable. Enfermedad coronaria. Técnicas intravasculares.*

## INTRODUCTION

Cardiovascular disease is a major cause of morbidity and mortality in the western hemisphere.<sup>1</sup> Despite major advances in the management and diagnosis of patients with coronary artery disease, a large number of victims who are apparently healthy die suddenly without prior symptoms.<sup>2,3</sup> Most of these events are re-

lated to plaque rupture and subsequent thrombotic occlusion at the site of non-flow limiting atherosclerotic lesions in epicardial coronary arteries.<sup>4,5</sup> In addition, silent plaque rupture and its subsequent wound healing accelerate plaque growth and are a more frequent feature in arteries with less severe luminal narrowing.<sup>6</sup>

According to histological studies, plaque composition plays a central role in the pathogenesis of epicardial occlusion, irrespective of the severity of the underlying stenosis.<sup>5</sup>

### THE IMAGING TARGET: THE THIN-CAP FIBROATHEROMA

Recently, retrospective studies have identified morphological and compositional characteristics of

Correspondence: Dr P.W Serruys.  
Prof. of Interventional Cardiology,  
Thoraxcenter, Bd 406, Erasmus MC,  
Dr Molewaterplein 40, 3015 GD Rotterdam, The Netherlands.  
E-mail: p.w.j.c.serruys@erasmusmc.nl

plaques prone to rupture.<sup>7,8</sup> This has led to a new classification of coronary lesions that depicts plaque progression in a more comprehensive manner.<sup>8</sup>

Thin-cap fibro atheroma (TCFA) lesions, the most prevalent predecessor of plaque rupture, are composed of a lipid-rich atheromatous core, a thin ( $\leq 65 \mu\text{m}$ ) fibrous cap with macrophage and lymphocyte infiltration, decreased smooth muscle cell content and expansive remodeling.<sup>8,9</sup>

Detection of these non-obstructive, lipid rich, high-risk plaques may have an important impact on the prevention of acute myocardial infarction and sudden death.

Although angiography can identify obstructive as well as complex lesions,<sup>10</sup> it is restricted to the visualization of the coronary lumen and is unable to visualize the coronary wall. Thus, features as vessel remodeling or plaque composition are missed. Recently, a post-mortem study evaluated the geometrical aspect of the vessel wall and showed a relationship between local alterations of vessel size and plaque stability.<sup>11</sup>

Currently, there are several intravascular tools capable of locally evaluating determinants of plaque vulnerability such as the size of the lipid core, thickness of the fibrous cap, inflammation within the cap and positive remodelling.

A recent study proposed a critical cap thickness of  $<65$  micron based on post mortem histomorphometry.<sup>12</sup> However, in vivo the threshold for defining a fibrous cap as thin should probably be higher than  $65 \mu\text{m}$  for several reasons. First, it is well established that general tissue shrinkage can not be avoided during histologic fixation which implies dehydration processes.<sup>13,14</sup> Furthermore, circumferential stress at the luminal border of the plaque increases critically when cap thickness is less than approximately  $150 \mu\text{m}$ .<sup>15</sup>

We summarize the current status of imaging techniques that have the potential to detect the vulnerable plaque features in vivo and may allow risk stratification in a specific individual and ultimately guide systemic and local preventive strategies.<sup>9,16-20</sup>

## INTRAVASCULAR ULTRASOUND

Gray scale IntraVascular UltraSound (IVUS) is an invasive diagnostic tool that provides a real-time, high-resolution, tomographic view of coronary arteries. It thereby enables the assessment of morphology, severity and extension of coronary plaque.

IVUS is currently the only imaging modality that can provide in vivo information regarding temporal changes in the atherosclerotic plaque size.<sup>21</sup>

Qualitative plaque characterization is based on the echogenicity of the received ultrasound signal, whereas echolucent zones reflect lipid-rich tissue and highly reflective structures with dorsal shadowing calcified tissue. Nevertheless, plaque characterization through visual interpretation of gray-scale IVUS is imprecise, specially when assessing heterogeneous, lipid-rich plaques.<sup>22</sup>

Axial resolution is limited to  $100\text{-}200 \mu\text{m}$  thus impairing the ability of detecting thin fibrous caps. Notwithstanding, for the aforementioned reasons, we believe that the threshold for defining a fibrous cap as thin should be higher than  $65 \mu\text{m}$ .

The detection of vulnerable plaques by IVUS is mainly based on a series of case reports.<sup>23-26</sup> These reports describe morphologic features of already ruptured plaques but not the prospective detection of rupture-prone plaques. Nevertheless, one prospective study showed that large eccentric plaques containing an echolucent zone by IVUS were found to be at increased risk of instability even though the lumen area was preserved at the time of initial study.<sup>27</sup>

## ROLE OF VESSEL REMODELING

Vascular remodeling was described by Glagov as a compensatory enlargement of the coronary arteries in response to an increase in plaque area.<sup>28</sup> Several studies showed an increase level of inflammatory marker levels, larger lipid cores and pronounced medial thinning in positive remodeled vessels.<sup>11,29,30</sup> This concept has further evolved to a dynamic theory

TABLE. Comparison of Catheter-Based Techniques for Detection of Individual Features of Vulnerable Plaque

Technique	Thin-Cap Detection	Inflammation	Lipid Core	Remodeling
Intravascular ultrasound	+	-	+	+++
Echogenicity	-	-	+	-
Palpography	++	++	+	-
Virtual histology	++	-	+++	+++
Optical coherence tomography	+++	+	+	-
Thermography	-	+++	-	-
Angioscopy	-	-	++	-
Intravascular MRI	-	-	++	-
Spectroscopy	-	++	++	-

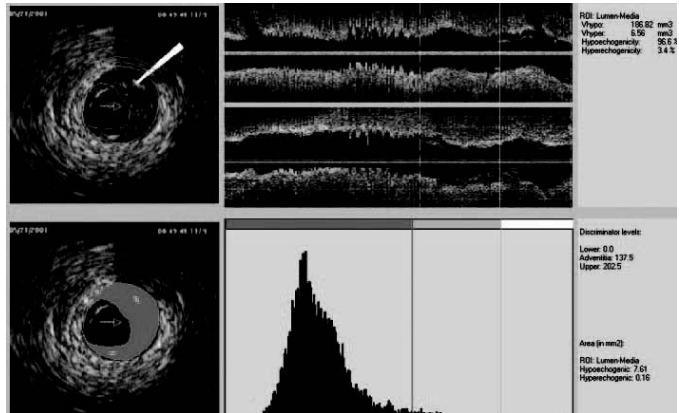


**Figure 1.** IVUS echogenicity: the adventitia is defined as tissue outside the external elastic membrane. For all non-shadowed adventitia pixels, the mean value and standard deviation are calculated. To observe the suitability, a normal distribution curve based on the same mean and standard deviation histogram is created. Hypoechoogenic areas are colored red and hyperechoic areas green.

where vessels may also shrink in response to plaque growth.<sup>31</sup> This remodeling modality has been related to a more stable phenotype and clinical presentation.<sup>11,29,32,33</sup> Recently, the relationship between vascular remodeling and plaque composition was assessed using IVUS.<sup>34-36</sup> In these studies, the remodeling index for soft lesions was significantly higher than those for fibrous/mixed and calcified lesions.<sup>34-36</sup> It is noteworthy though, that most studies evaluating this phenomenon are of cross sectional design. Since atherosclerosis is usually a diffuse disease, finding a fully non-diseased reference is not guaranteed. Therefore, the early presence of remodeling in the reference site can't be ruled out.

#### QUANTITATIVE IVUS ECHOGENICITY ASSESSMENT

We recently developed a computer-aided, gray-scale value, analysis program for plaque characterization.<sup>37</sup> Based on the mean gray level (brightness) of the adventitia, plaque is classified as more (hyperechoic) or less bright (hypoechoic) in relation to the adventitia (Figure 1). The percentage of hypoechoic plaque is calculated for the entire region of interest and for slices with significant plaque. In the carotid circulation, plaque echogenicity, measured noninvasively, has been related to the histological components of plaque.<sup>38-41</sup> Furthermore, carotid plaque echolucency (low echogenicity) was associated with future neurological events.<sup>42-44</sup> IVUS-based plaque characterization in the coronary circulation requires invasive assessment and has been less extensively studied. A recent study showed that treatment with atorvastatin resulted in quantifiable changes in coronary plaque echogenicity, compatible with changes in plaque composition.<sup>45</sup> These findings offered a potential explana-

tion for the clinical efficacy of statins despite only modest effects on plaque volume.<sup>21,46</sup> Both ex vivo and clinical studies that will provide validation data about the technique are currently in progress.

#### Intravascular Ultrasound Elastography and Palpography

An important patho-morphologic feature of vulnerable plaque is

the eccentric accumulation of a lipid-rich necrotic core within the vessel wall, separated from the lumen by a thin fibrous cap. This observation led to the hypothesis that vulnerable lesions might have mechanical properties that differ from those of chronic stable lesions. Intravascular ultrasound elastography and palpography are techniques that allow the assessment of local mechanical tissue properties.<sup>19,47</sup>

At a defined pressure, soft tissue (lipid-rich) components will deform more than hard tissue components (fibrous-calcified).<sup>48</sup> In coronaries, the tissue of interest is the vessel wall, whereas the blood pressure with its physiologic, systolic and diastolic changes during the heart cycle is used as the excitation force. Images obtained at different pressure levels are compared to determine the local tissue compression. The radial strain in the tissue is calculated by cross-correlation techniques on the radio frequency signal and can be displayed as a colour-coded image.<sup>48</sup> The sensitivity and specificity to detect vulnerable plaques has recently been assessed in post-mortem human coronary arteries where vulnerable plaques were detected with a sensitivity of 88% and a specificity of 89% (Figure 2).<sup>19</sup> In addition to ex-vivo studies, this technique has also been tested in vivo, where palpography detected a high incidence of deformable plaques in acute coronary syndrome (ACS) patients.

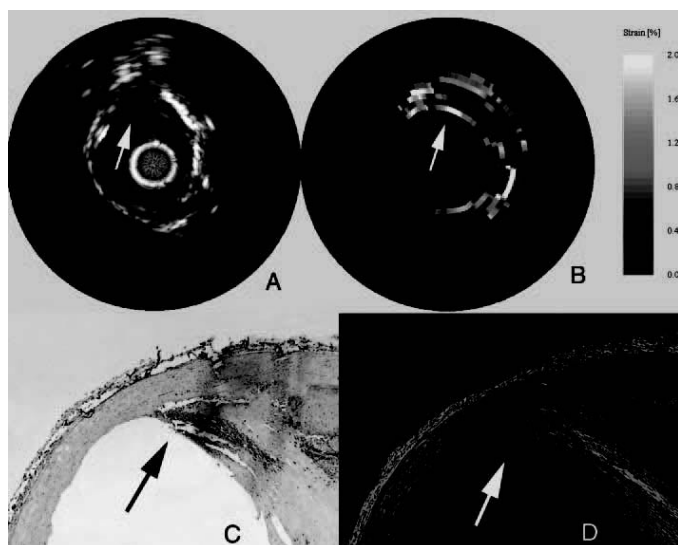


**Figure 2.** Vulnerable plaque marked in IVUS (A), elastogram (B), macrophage staining (C), and collagen staining (D). In the elastogram, a vulnerable plaque is indicated by a high strain on the surface. In the corresponding histology, a high amount of macrophages (C) is visible with a thin cap (D) and a lipid pool (LP). (Schaar et al. *Circulation*. 2003;108:2636.)

Furthermore, the number of highly deformable lesions was correlated to the clinical presentation and levels of C-reactive protein.<sup>47</sup>

The main limitation of the technique is that it depends on the quality and stability of the coronary pressure signal. Accordingly, it might be disturbed by high heart rates and rhythm disturbances.

### Virtual Histology

Gray-scale IVUS is of limited value for identification of specific plaque components.<sup>49</sup> Calcified and dense fibrous tissues usually are highly echo-reflective thus calcified areas are commonly overestimated. On the other hand, low echo-reflectance plaques are considered “soft” or lipid-rich. However, the accuracy of gray-scale IVUS for discriminating lipid from fibrous tissue is limited since in addition to large amounts of extracellular lipids (low echo-reflective areas), the lipid core contains cholesterol crystals, necrotic debris and microcalcifications (highly echo-reflective areas).<sup>8</sup>

A recently introduced technique (IVUS-Virtual Histology™ [IVUS-VH], Volcano Therapeutics, Rancho Cordova, CA) that uses the substrate (frequency domain analysis) of the IVUS radiofrequency (RF) data rather than the envelope (amplitude), has demonstrated its potential to provide an objective and accurate assessment of coronary plaque composition in studies of explanted human coronary segments.<sup>20</sup>

IVUS-VH uses spectral analysis of IVUS radiofrequency data to construct tissue maps that classify plaque into four major components. In preliminary *in vitro* studies, four histological plaque components (fibrous, fibrolipidic, lipid core, and calcium) were correlated with a specific spectrum of the radiofrequency signal.<sup>20,50</sup> These different plaque components were assigned color codes. Calcified, fibrous, fibrolipidic, and lipid core regions were labeled white, green, greenish-yellow, and red respectively (Figure 3).

IVUS studies have failed to conclusively demonstrate regression in plaque burden over time.<sup>21,51,52</sup> IVUS-VH has, though, the potential to follow the progression of the disease not only with regards to its volume, but to its composition as well.<sup>53</sup> Moreover, this tool could also be helpful in evaluating the effect of both conventional and emerging therapeutic interventions.

With regards to vulnerable plaque detection, IVUS-VH allows an accurate and quantitative assessment of 2 of the main features of the TCFA: lipid core and positive remodeling.

A main limitation of this technique is its inability to detect thin fibrous caps. However, as aforementioned we believe that the threshold for defining a thin fibrous cap should be higher than 65  $\mu\text{m}$ .

### Optical Coherence Tomography

Optical coherence tomography (OCT) is an imaging technique that allows high-resolution (axial re-

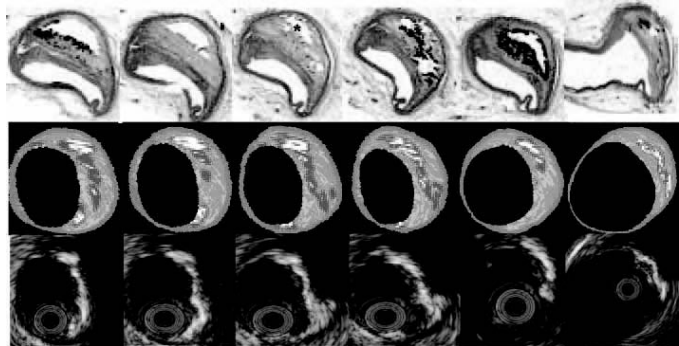


**Figure 3.** Serial histological sectioning of a coronary vessel. The middle and below panels depict the cross-correlation with Virtual Histology™ and gray-scale IVUS respectively. Calcified, fibrous, fibrolipidic and lipid core regions are labeled white, green, greenish-yellow and red respectively.

solution of 15  $\mu\text{m}$ ) imaging in biological systems.<sup>54</sup> Accordingly, OCT has the capacity to allow in vivo, real time visualization of a thin fibrous cap. OCT imaging is based on low coherence near infrared light that is emitted by a superluminescent diode. A center wave length around 1300 nm is used since it minimizes the energy absorption in the light beam caused by protein, water, haemoglobin, and lipids. The light waves are reflected by the internal microstructures within biological tissues as a result of their differing optical indices.

Animal and Post-mortem studies demonstrated the accuracy of OCT in comparison to histology.<sup>55-57</sup> These studies showed that OCT can detect both normal and pathologic artery structures (Figure 4).<sup>57</sup> Recent in vivo data have shown that OCT can differentiate different plaque types and suggested the possibility of detection of macrophages in atherosclerotic plaques.<sup>58,59</sup>

In our experience, TCFA with low-reflecting necrotic cores covered by highly reflecting thin (mean 50  $\mu\text{m}$ ) fibrous caps can be visualized in patients scheduled for percutaneous coronary intervention (PCI).<sup>60</sup>

The high resolution of OCT offers the potential to detect TCFA in living patients.<sup>59,60</sup> OCT imaging, however, is limited by the relative shallow penetration depth that hampers imaging of the entire vessel wall in medium and large vessels large vessels, and the need to clear the artery from blood during imaging causing transient ischemia of the studied region.

### Intravascular Thermography

The rationale to measure vascular temperature is based on the observation that atherosclerosis is accompanied by inflammation. Vulnerable plaques have been associated with increased macrophage activity, metabolism and inflammation.<sup>61</sup> Based on

these findings the hypothesis was generated that these “activated” macrophages produce thermal energy, which might be detected on the surface of these atherosclerotic lesions. Infrared and contact-sensor thermographies are the most important invasive methods (Figure 5). The contact thermographic methods seem to be the most feasible at the present time, mainly due to the difficulties of infrared radiation to penetrate the flowing blood to detect vessel wall temperature. A small study of 19 patients that included patients with stable angina, unstable angina, and with acute myocardial infarction reported temperature heterogeneity in human atherosclerotic coronary plaques.<sup>62</sup> Intracoronary temperature was assessed using a dedicated catheter. In most coronary segments with atherosclerotic plaques a rise in temperature was seen as compared to coronary segments with a normal vessel wall. Temperature differences between an atherosclerotic plaque and a normal vessel wall increased progressively from patients with stable angina to patients with acute myocardial infarction with a maximum temperature difference to the background temperature of  $1.5 \pm 0.7^\circ\text{C}$ . However, there are somewhat conflicting published and unpublished reports with other thermography devices (circular basket or self expanding arms) that have documented a much lower heterogeneity of temperature distribution. The most likely explanation for this discrepancy in temperature observations might be related to the difference in catheter design and the way coronary flow is affected.

These preliminary findings about the thermal status of atherosclerotic plaques seem promising. However, accurate temperature evaluation requires direct contact of the thermistors with the vessel wall, carrying the potential risk of endothelial damage. In addition, the cooling effect caused by blood flow may hamper data interpretation.<sup>63</sup>



**Figure 4.** Optical coherence tomography of a non-flow limiting lesion showing a “swiss-cheese” vessel wall suggestive of a thin-cap fibroatheroma.

### Angioscopy

This technique allows real-time direct visualization of coronary plaques (Figure 6). Ex vivo validation of angioscopy was performed by Thieme et al, who compared angioscopic observations with histologic samples obtained by coronary atherectomy. In this study, yellow plaques were related to atheromatous lesions.<sup>64</sup> These findings were confirmed in clinical studies, where lipid-rich, rupture-prone plaques were easily detected by angioscopy as yellow plaques, and found more commonly in acute coronary syndromes.<sup>65</sup> Furthermore, angioscopy has shown in-

triguing results in the prediction of acute coronary syndromes.<sup>65</sup>

Despite these encouraging findings, this technique examines solely the luminal surface of the intima. Thus, key TCFA features such as thickness of the cap, lipid core content, and remodelling can not be assessed. In addition, blood must be cleared away from the view causing transient ischemia of the studied region.

### RAMAN SPECTROSCOPY

Raman spectroscopy is a technique that can characterize the chemical composition by means of the Raman effect.<sup>66</sup> This effect is created when incident light excites molecules in a tissue sample, which scatter light in a different wave length. This change in wave length called the “Raman effect” is dependent on the chemical components of the tissue sample. Thus, Raman spectroscopy can provide quantitative information about molecular composition of a sample.<sup>67</sup> The spectra obtained require post-processing to differentiate between plaque components (Figure 7). In vitro studies have demonstrated that diagnostic algorithms allow the discrimination of coronary arterial tissue in 3 categories: non-atherosclerotic, non-calcified and calcified plaques.<sup>67</sup>

The main limitations of the technique are the inability to provide geometrical information, the narrow penetration depth (1.0 to 1.5 mm) and the absorbance of the laser light by the blood.

### INTRAVASCULAR MAGNETIC RESONANCE IMAGING

Intravascular magnetic resonance imaging (MRI) is another potential approach to determine plaque composition based on the diffusion properties of the

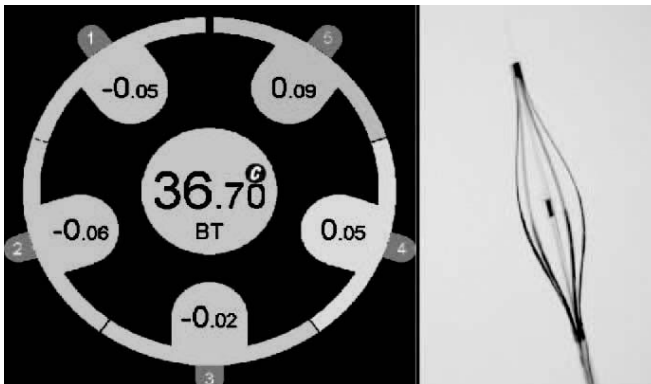


**Figure 5.** Dedicated thermography catheter with 5 thermistors in contact to the vessel wall showing significant heterogeneity in the measurements compatible with increased macrophage activity, metabolism, and inflammation.

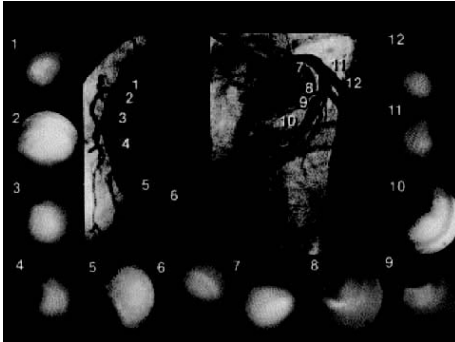


**Figure 6.** Patient with anterior myocardial infarction. Angioscopic images of the culprit lesion (8 and 9) and of all the yellow plaques in the non-culprit segments are presented. Thrombus was detected over the yellow plaque in the culprit segment. (Asakura et al. *J Am Coll Cardiol.* 2001;37:1284-8.)

analyzed tissue. MRI can determine the presence of lipid within the arterial wall. Current technology for intravascular MRI consists of a self-contained MRI probe that allows sequential scanning of different vessels sectors. The lipid-content within a sector is determined and the data is displayed color-coded (yellow corresponds to high lipid content within the region of interest, blue to low lipid-content [Figure 8]).

The intravascular MRI system has been evaluated in ex-vivo human carotid tissue, aortic tissue and coronary arteries to correlate MRI findings with histology. In ex vivo aortic studies the MRI correctly predicted the histologic results in 15 of 16 aortic cases, and in ex-vivo coronary arteries 16 of 18 lesions were correctly predicted, including the diagnosis of 3 thin cap fibroatheromas.<sup>68,69</sup> In vivo feasibility is currently under investigation in a multi-center trial.

## FUTURE PERSPECTIVES

It has previously been shown that a multifocal instability process is present in acute coronary syndromes.<sup>26,70</sup> Rioufol et al demonstrated in ACS patients that at least one plaque rupture is found away from the culprit lesion in 80% of the patients, away from the culprit artery in 71% and in the 2 non-culprit arteries in 12.5%.<sup>26</sup>

The large number of high-risk lesions found throughout the coronary tree by means of angiography,<sup>71</sup> angiography,<sup>70</sup> IVUS,<sup>26</sup> and palpography<sup>47</sup> in addition to the unpredictability of the natural history of such lesions and the uncertainty about if vulnerable plaque characteristics might subsequently lead to fatal or non-fatal is-

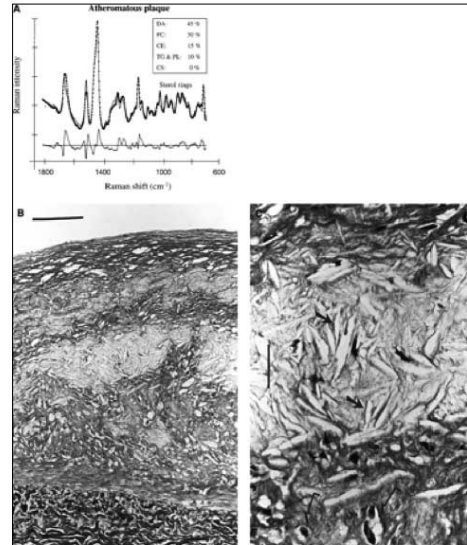


**Figure 7.** Raman spectrum from atheromatous plaque and model fit (A). The increase of the relative weights of the chemical components FC and CE, as compared with intimal fibroplasia, corresponds to the presence of an atheromatous core under a fibrous cap (B, bar indicates 100  $\mu\text{m}$ ). An abundance of lipid-laden foam cells (open arrows) and FC crystal clefts (solid arrows) is visible in the atheromatous core (C, bar indicates 25  $\mu\text{m}$ ). (Romer et al. *Circulation.* 1998;97:878-85.)

chemic events, suggests that potential local preventive strategies could not be cost-effective.

However, high-risk “yellow” plaques identified in stable patients by angiography have been found predictors of ischemic events.<sup>65</sup> Accordingly, a systemic approach including intensive statin therapy could be a reasonable approach to “cool-down” the inflammatory burden.

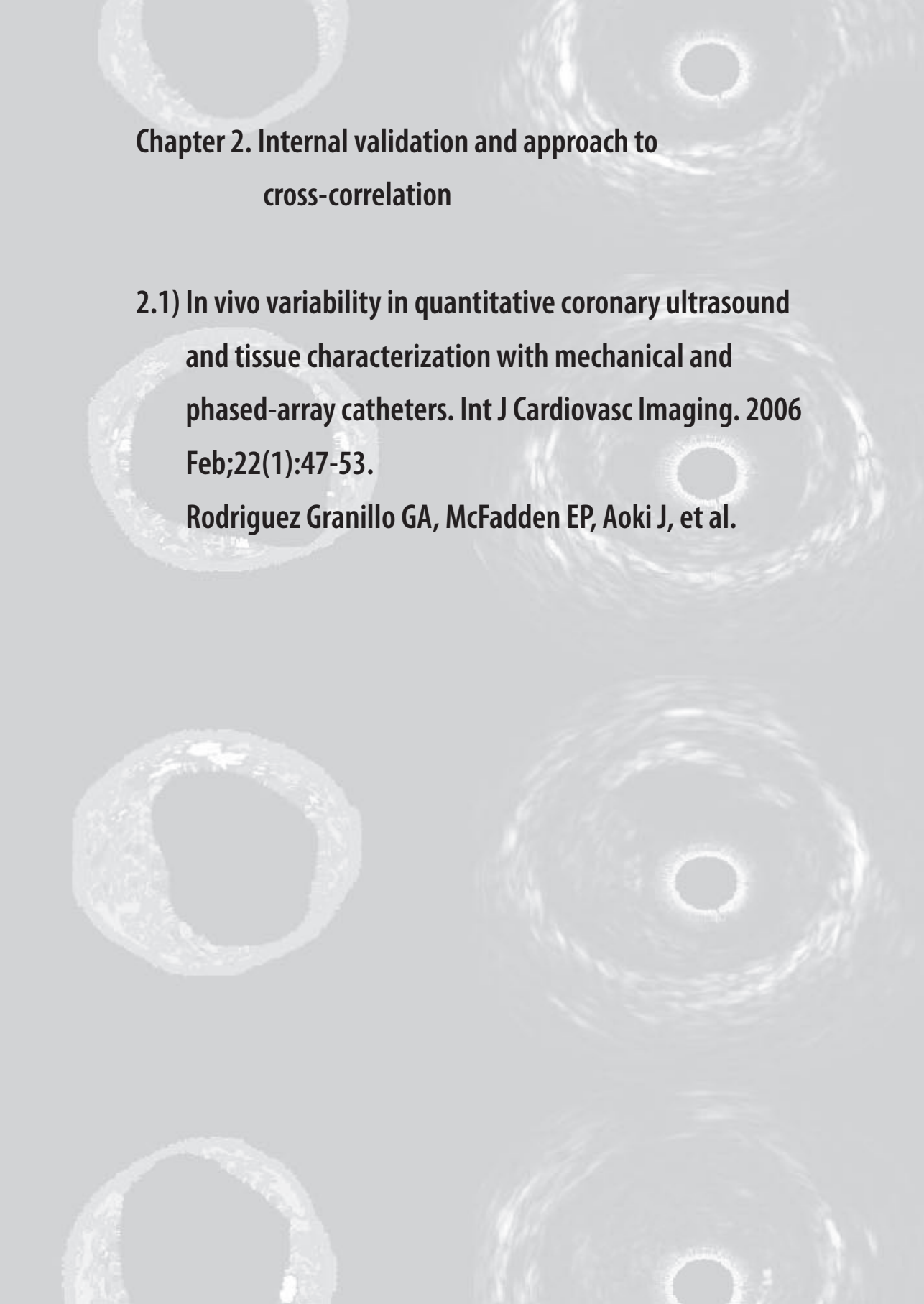
Although enormously promising, catheter-based techniques need more extensive validation and an appropriate vulnerable plaque model is yet to be developed. In addition, these techniques interrogate the coronary arteries in a localized manner, whereas inflammation is distributed throughout the whole coronary tree.<sup>72</sup>

These new modalities have the potential to provide insights into pathophysiology in studies of the natural history of coronary plaque. Furthermore, they may provide surrogate endpoints. Finally, the combination between novel imaging techniques and the assessment of circulating biomarkers could have a potential role in patient risk stratification and eventually offer the potential to allow the effect of conventional and emer-



29. Varnava AM, Mills PG, Davies MJ. Relationship between coronary artery remodeling and plaque vulnerability. *Circulation*. 2002;105:939-43.
30. Burke AP, Kolodgie FD, Farb A, Weber D, Virmani R. Morphological predictors of arterial remodeling in coronary atherosclerosis. *Circulation*. 2002;105:297-303.
31. Pasterkamp G, Wensing PJ, Post MJ, Hillen B, Mali WP, Borst C. Paradoxical arterial wall shrinkage may contribute to luminal narrowing of human atherosclerotic femoral arteries. *Circulation*. 1995;91:1444-9.
32. Smits PC, Pasterkamp G, Quarles van Ufford MA, Eefting FD, Stella PR, de Jaegere PP, et al. Coronary artery disease: arterial remodeling and clinical presentation. *Heart*. 1999;82:461-4.
33. Nakamura M, Nishikawa H, Mukai S, Setsuda M, Nakajima K, Tamada H, et al. Impact of coronary artery remodeling on clinical presentation of coronary artery disease: an intravascular ultrasound study. *J Am Coll Cardiol*. 2001;37:63-9.
34. Tauth J, Pinnow E, Sullebarger JT, Basta L, Gursoy S, Lindsay J Jr, et al. Predictors of coronary arterial remodeling patterns in patients with myocardial ischemia. *Am J Cardiol*. 1997;80:1352-5.
35. Sabate M, Kay IP, de Feyter PJ, van Domburg RT, Deshpande NV, Ligthart JM, et al. Remodeling of atherosclerotic coronary arteries varies in relation to location and composition of plaque. *Am J Cardiol*. 1999;84:135-40.
36. Fuessl RT, Kranenberg E, Kiausich U, Baer FM, Sechtem U, Hopp HW. Vascular remodeling in atherosclerotic coronary arteries is affected by plaque composition. *Coron Artery Dis*. 2001;12:91-7.
37. de Winter SA HI, Hamers R, de Feyter PJ, Serruys PWC, Roelandt JRTC, Bruining N. Computer assisted three-dimensional plaque characterization in ultracoronary ultrasound studies. *Comput Cardiol*. 2003;30:73-6.
38. el-Barghouty NM, Levine T, Ladva S, Flanagan A, Nicolaidis A. Histological verification of computerised carotid plaque characterisation. *Eur J Vasc Endovasc Surg*. 1996;11:414-6.
39. Gronholdt ML, Nordestgaard BG, Wiebe BM, Wilhelm JE, Sillesen H. Echo-lucency of computerized ultrasound images of carotid atherosclerotic plaques are associated with increased levels of triglyceride-rich lipoproteins as well as increased plaque lipid content. *Circulation* 1998;97:34-40.
40. Rasheed Q, Dhawale PJ, Anderson J, Hodgson JM. Intracoronary ultrasound-defined plaque composition: computer-aided plaque characterization and correlation with histologic samples obtained during directional coronary atherectomy. *Am Heart J*. 1995;129:631-7.
41. Prati F, Arbustini E, Labellarte A, dal Bello B, Sommariva L, Mallus MT, et al. Correlation between high frequency intravascular ultrasound and histomorphology in human coronary arteries. *Heart*. 2001;85:567-70.
42. Polak JF, Shemanski L, O'Leary DH, Lefkowitz D, Price TR, Savage PJ, et al. Hypoechoic plaque at US of the carotid artery: an independent risk factor for incident stroke in adults aged 65 years or older. *Cardiovascular Health Study*. *Radiology*. 1998;208:649-54.
43. Gronholdt ML, Nordestgaard BG, Schroeder TV, Vorstrup S, Sillesen H. Ultrasonic echolucent carotid plaques predict future strokes. *Circulation*. 2001;104:68-73.
44. Mathiesen EB, Bona KH, Joakimsen O. Echolucent plaques are associated with high risk of ischemic cerebrovascular events in carotid stenosis: the tromso study. *Circulation*. 2001;103:2171-5.
45. Schartl M, Bocksch W, Koschyk DH, Voelker W, Karsch KR, Kreuzer J, et al. Use of intravascular ultrasound to compare effects of different strategies of lipid-lowering therapy on plaque volume and composition in patients with coronary artery disease. *Circulation*. 2001;104:387-92.
46. Cannon CP, Braunwald E, McCabe CH, Rader DJ, Rouleau JL, Belder R, et al. Intensive versus moderate lipid lowering with statins after acute coronary syndromes. *N Engl J Med*. 2004;350:1495-504.
47. Schaar JA, Regar E, Mastik F, McFadden EP, Saia F, Disco C, et al. Incidence of high-strain patterns in human coronary arteries: assessment with three-dimensional intravascular palpography and correlation with clinical presentation. *Circulation*. 2004;109:2716-9.
48. de Korte CL, van der Steen AF, Cespedes EI, Pasterkamp G. Intravascular ultrasound elastography in human arteries: initial experience in vitro. *Ultrasound Med Biol*. 1998;24:401-8.
49. Peters RJ, Kok WE, Rijsterborgh H, van Dijk M, Koch KT, Piek JJ, et al. Reproducibility of quantitative measurements from intracoronary ultrasound images. Beat-to-beat variability and influence of the cardiac cycle. *Eur Heart J*. 1996;17:1593-9.
50. Moore MP, Spencer T, Salter DM, Kearney PP, Shaw TR, Starkey IR, et al. Characterisation of coronary atherosclerotic morphology by spectral analysis of radiofrequency signal: in vitro intravascular ultrasound study with histological and radiological validation. *Heart*. 1998;79:459-67.
51. von Birgelen C, Hartmann M, Mintz GS, Baumgart D, Schmermund A, Erbel R. Relation between progression and regression of atherosclerotic left main coronary artery disease and serum cholesterol levels as assessed with serial long-term ( $\geq 12$  months) follow-up intravascular ultrasound. *Circulation*. 2003;108:2757-62.
52. Takagi T, Yoshida K, Akasaka T, Hozumi T, Morioka S, Yoshikawa J. Intravascular ultrasound analysis of reduction in progression of coronary narrowing by treatment with pravastatin. *Am J Cardiol*. 1997;79:1673-6.
53. Rodriguez-Granillo GA, Aoki J, Ong ATL, Valgimigli M, van Mieghem CAG, Regar E, et al. Methodological considerations and approach to cross-technique comparisons using in vivo coronary plaque characterization based on intravascular ultrasound radiofrequency data analysis: insights from the Integrated Biomarker and Imaging Study (IBIS). *International Journal of Cardiovascular Interventions* 2005; In press.
54. Hrynchak P, Simpson T. Optical coherence tomography: an introduction to the technique and its use. *Optom Vis Sci*. 2000;77:347-56.
55. Brezinski ME, Tearney GJ, Bouma BE, Boppart SA, He MR, Swanson EA, et al. Imaging of coronary artery microstructure (in vitro) with optical coherence tomography. *Am J Cardiol*. 1996;77:92-3.
56. Patwari P, Weissman NJ, Boppart SA, Jesser C, Stamper D, Fujimoto JG, et al. Assessment of coronary plaque with optical coherence tomography and high-frequency ultrasound. *Am J Cardiol*. 2000;85:641-4.
57. Tearney GJ, Jang IK, Kang DH, Aretz HT, Houser SL, Brady TJ, et al. Porcine coronary imaging in vivo by optical coherence tomography. *Acta Cardiol*. 2000;55:233-7.
58. MacNeill BD, Jang IK, Bouma BE, Ifitima N, Takano M, Yabushita H, et al. Focal and multi-focal plaque macrophage distributions in patients with acute and stable presentations of coronary artery disease. *J Am Coll Cardiol*. 2004;44:972-9.
59. Jang IK, Tearney GJ, MacNeill B, Takano M, Moselewski F, Ifitima N, et al. In vivo characterization of coronary atherosclerotic plaque by use of optical coherence tomography. *Circulation*. 2005;111:1551-5.
60. Regar E SJ, van der Giessen W, van der Steen AF, Serruys PW. Real-time, in-vivo optical coherence tomography of human coronary arteries using a dedicated imaging wire. *Am J Cardiol*. 2002;90:129H.
61. Fuster V. Human lesion studies. *Ann N Y Acad Sci*. 1997;811:207-24; discussion 224-5.
62. Stefanadis C, Diamantopoulos V, Llachopoulos C, Tsiamis E, Dernellis J, Toutouzas K, et al. Thermal heterogeneity within human atherosclerotic coronary arteries detected in vivo: A new method of detection by application of a special thermography catheter. *Circulation*. 1999;99:1965-71.
63. Diamantopoulos L, Liu X, De Scheerder I, Krams R, Li S, Van Cleemput J, et al. The effect of reduced blood-flow on the coronary wall temperature. Are significant lesions suitable for intravascular thermography? *Eur Heart J*. 2003;24:1788-95.

64. Thieme T, Wernecke KD, Meyer R, Brandenstein E, Habedank D, Hinz A, et al. Angioscopic evaluation of atherosclerotic plaques: validation by histomorphologic analysis and association with stable and unstable coronary syndromes. *J Am Coll Cardiol.* 1996;28:1-6.
65. Uchida Y, Nakamura F, Tomaru T, Morita T, Oshima T, Sasaki T, et al. Prediction of acute coronary syndromes by percutaneous coronary angiography in patients with stable angina. *Am Heart J.* 1995;130:195-203.
66. Baraga JJ, Feld MS, Rava RP. In situ optical histochemistry of human artery using near infrared Fourier transform Raman spectroscopy. *Proc Natl Acad Sci U S A.* 1992;89:3473-7.
67. Romer TJ, Brennan JF 3rd, Fitzmaurice M, Feldstein ML, Deinum G, Myles JL, et al. Histopathology of human coronary atherosclerosis by quantifying its chemical composition with Raman spectroscopy. *Circulation.* 1998;97:878-85.
68. Schneiderman J WR, Weiss A, Smouha E, Muchnik L, Chen-Zion M, Golan E, et al. Detection of vulnerable plaques in ex-vivo human aortas with novel intravascular magnetic resonance catheter (abstract). *Circulation* 2002;Suppl.:657.
69. Schneiderman J WR, Weiss A, Smouha E, Muchnik L, Alexandrowicz G, Chen-Zion M, et al. Vulnerable plaque diagnosis by a self-contained intravascular magnetic resonance imaging probe in ex-vivo human in-situ coronary arteries. *J Am Coll Cardiol.* 2003;41.
70. Asakura M, Ueda Y, Yamaguchi O, Adachi T, Hirayama A, Hori M, et al. Extensive development of vulnerable plaques as a pan-coronary process in patients with myocardial infarction: an angioscopic study. *J Am Coll Cardiol.* 2001;37:1284-8.
71. Goldstein JA, Demetriou D, Grines CL, Pica M, Shoukfeh M, O'Neill WW. Multiple complex coronary plaques in patients with acute myocardial infarction. *N Engl J Med.* 2000;343:915-22.
72. Buffon A, Biasucci LM, Liuzzo G, D'Onofrio G, Crea F, Maseri A. Widespread coronary inflammation in unstable angina. *N Engl J Med.* 2002;347:5-12.



## **Chapter 2. Internal validation and approach to cross-correlation**

**2.1) In vivo variability in quantitative coronary ultrasound and tissue characterization with mechanical and phased-array catheters. Int J Cardiovasc Imaging. 2006 Feb;22(1):47-53.**

**Rodriguez Granillo GA, McFadden EP, Aoki J, et al.**



## In vivo variability in quantitative coronary ultrasound and tissue characterization measurements with mechanical and phased-array catheters

Gastón A. Rodríguez-Granillo, Eugène P. Mc Fadden, Jiro Aoki,  
Carlos A. G. van Mieghem, Evelyn Regar, Nico Bruining & Patrick W. Serruys  
*Thoraxcenter, Erasmus Medical Center, Bd406, Dr. Molewaterplein 40, 3015 GD Rotterdam,  
The Netherlands*

Received 3 March 2005; accepted in revised form 26 April 2005

*Key words:* atherosclerosis, imaging, plaque characterization, ultrasonography

### Abstract

*Background:* Both mechanical and phased-array catheters are used in clinical trials to assess quantitative parameters. Only limited evaluation of the in vivo agreement of volumetrical measurements between such systems has been performed, despite the fact that such information is essential for the conduction of atherosclerosis regression trials. *Methods and results:* We prospectively evaluated the agreement in morphometric measurements and intravascular ultrasound (IVUS)-based plaque characterization between a 40 MHz rotating transducer (3.2 F Atlantis, Boston Scientific Corp.) and a 20 MHz phased-array catheter (2.9 F Eagle Eye, Volcano Therapeutics, Rancho Cordova, California) in 16 patients. Lumen ( $7.3 \pm 2.0 \text{ mm}^2$  vs.  $6.7 \pm 1.8 \text{ mm}^2$ ,  $p = 0.001$ ) and vessel ( $11.8 \pm 3.3 \text{ mm}^2$  vs.  $11.0 \pm 2.9 \text{ mm}^2$ ,  $p = 0.02$ ) cross-sectional areas (CSA) were significantly greater with the 20 MHz system. Plaque CSA measurements showed no significant difference between systems ( $4.4 \pm 2.3 \text{ mm}^2$  vs.  $4.4 \pm 2.1$ ). The relative differences were less than 10% for the three variables. On IVUS-based tissue characterization (13 patients), calculated percentage hypoechogenic volume was significantly higher for the 20 MHz system ( $96.7 \pm 2.38$  vs.  $88.4 \pm 5.53$ ,  $p < 0.0001$ ). *Conclusions:* Quantitative IVUS analyses display significant catheter type-dependent variability. It is unclear whether the variability reflects overestimation of measurements with the phased-array or underestimation with the mechanical system. Although plaque burden measurements did not differ significantly between systems, it appears prudent to recommend the use of a single system for progression/regression studies.

### Introduction

Intravascular ultrasound (IVUS) allows a high resolution tomographic assessment of the coronary artery and provides accurate measurements of both lumen and vessel wall dimensions. Initially used in interventional cardiology for diagnostic and interventional procedures, IVUS has more recently been used as a tool to assess atherosclerosis progression/regression in single and

multicenter studies, given its ability to accurately quantify the presence and extent of plaque formation [1–3]. In addition, plaque characterization using gray-scale IVUS and the spectral analysis of the raw radiofrequency data is subject to intensive research [4–6]. Currently, a number of IVUS systems are commercially available and there is limited in vivo data regarding the agreement between mechanical and phased-array catheters although this information is valuable

for the conductance of multicenter progression/regression studies. Previous *in vitro* and *in vivo* data showed significant variability between different catheters in quantitative and tissue characterization data [7–9]. The purpose of this study was to compare *in vivo* the quantitative coronary ultrasound measurements and plaque characterization with mechanical and phased-array catheters.

## Materials and methods

### *Patient population*

Patients were eligible if they had a *de novo*, non-significant (angiographically <50%) stenosis in a native coronary artery. Patients were excluded from the study if any of the following conditions were present: (1) presentation with acute coronary syndrome, (2) vessel tortuosity (3) calcified vessels. The institutional ethics committee approved the study protocol and written informed consent was obtained from all patients.

### *IVUS imaging systems*

Two commercially available systems were used: a single-element, 40 MHz rotating transducer (3.2 F Atlantis, Boston Scientific Corp.), and a 20 MHz phased-array catheter (2.9 F Eagle Eye, Volcano Therapeutics, Rancho Cordova, California).

### *Vessel interrogation*

IVUS was performed after intracoronary administration of nitrates. Cine runs, before and during contrast injection, were performed to define the position of the IVUS catheter  $\geq 10$  mm distal to a clear anatomical landmark. Using an automated pullback device, the transducer of the phased array catheter was withdrawn at a continuous speed of 0.5 mm/s until the ostium of the study vessel was seen. Subsequently, the same procedure was performed with the other IVUS imaging catheter using a different automated pullback device (Boston Scientific Corp, Santa Clara, USA) at the same speed. IVUS data was stored on S-VHS videotape. The videotapes were digitized on a computer

system, transformed into the DICOM medical image standard and stored on an IVUS Picture Archiving and Communications System (PACS).

### *IVUS analysis*

Quantitative coronary ultrasound (QCU) analysis was performed by a core laboratory (Cardialysis BV, Rotterdam, The Netherlands) using validated software (Curad, version 3.1, Wijk bij Duurstede, The Netherlands). IVUS analysts were not aware of the purpose of the study. The regions of interest (ROI) were matched simultaneously for the two systems and selected by an independent observer who did not participate in the contour detection and subsequent analysis. The borders of the external elastic membrane (EEM) and the lumen-intima interface were determined with manual planimetry and enclosed a volume that was defined as the coronary plaque plus media volume. Lumen (LCSA), vessel (VCSA), and plaque (PCSA) cross sectional areas (CSA) were evaluated. Plaque CSA was calculated as:

$$PCSA = \text{Vessel}_{\text{area}} - \text{Lumen}_{\text{area}}$$

### *IVUS tissue characterization*

In addition to volumetric parameters, IVUS also provides information on plaque echogenicity, a potential source of information on plaque composition. The acoustic characterization of a coronary plaque has been investigated by *in vitro* and *in vivo* studies that support a role for echogenicity as a predictor of histological plaque composition [1, 6, 10–12]. In the present study, we used a computer-aided grey scale value analysis program for plaque characterization [13]. Using the mean grey level of the adventitia as a threshold, five main tissue types can be characterized (Figure 3): (1) hypoechogenic tissue has a mean grey level lower than that of the adventitia, (2) hyperechogenic tissue, defined as tissue with a mean grey value higher than that of the adventitia, (3) calcified tissue, defined as a tissue with a mean grey value higher than that of the adventitia with associated acoustic shadowing, (4) unknown

tissue, defined as tissue shadowed by calcification and (5) 'upper tissue', defined as tissue that has a mean grey value higher than the mean adventitial intensity plus two times its standard deviation but is not typical calcified tissue with acoustic shadowing. The percentage of hypoechoic plaque was calculated for the entire ROI, excluding 'upper tissue'.

#### Statistical analysis

Results are reported as mean  $\pm$  standard deviation. Bland–Altman plots were constructed in order to assess the agreement between measurements with both types of catheter [14]. This method plots the mean against the difference in measurements between catheters. Limits of agreement were set by adding two SDs to the mean difference for the upper limit and by subtracting two SDs from the mean difference for the lower limit. A  $p$  value of less than 0.05 indicated statistical significance.

#### Results

Sixteen patients were included in the analysis. The mean age was  $64 \pm 9$  years (range 49–82), 9 patients (56.3%) were males. The study vessel location was RCA 4 (25%), LCX 5 (31%) and LAD 7 (44%). Table 1 shows CSA measurements with the two systems. Lumen ( $7.3 \pm 2.0$  mm<sup>2</sup> vs  $6.7 \pm 1.8$  mm<sup>2</sup>,  $p = 0.001$ ) and vessel ( $11.8 \pm 3.3$  mm<sup>2</sup> vs.  $11.0 \pm 2.9$  mm<sup>2</sup>,  $p = 0.02$ ) CSAs were significantly larger with the 20 MHz. PCSA measurements showed no significant

Table 1. Cross-sectional area measurements for two different IVUS imaging catheter systems (n:16).

	Length	LCSA	VCSA	PCSA
20 MHz	37.1 $\pm$ 16.8	7.3 $\pm$ 2.0	11.8 $\pm$ 3.3	4.4 $\pm$ 2.3
40 MHz	35.7 $\pm$ 15.7	6.7 $\pm$ 1.8	11.0 $\pm$ 2.9	4.4 $\pm$ 2.1
Absolute $\Delta$	1.4 $\pm$ 2.2	0.6 $\pm$ 0.7	0.7 $\pm$ 0.9	0.1 $\pm$ 0.4
Relative $\Delta$	3.0 $\pm$ 5.8	9.3 $\pm$ 8.7	5.9 $\pm$ 6.7	-1.4 $\pm$ 13.4
p value	0.023	0.001	0.005	NS

LCSA, VCSA and PCSA refer to lumen, vessel and plaque cross-sectional areas.

difference between systems ( $4.4 \pm 2.3$  mm<sup>2</sup> vs  $4.4 \pm 2.1$ ,  $p = \text{NS}$ ). The relative differences were less than 10% for the 3 variables. Bland–Altman plots for LCSA, VCSA and PCSA are shown in Figure 1 (a, b, c).

#### Tissue characterization

Paired tissue characterization data was available for 13 patients. The percent hypoechoic volume was significantly higher with the 20 MHz system ( $96.7 \pm 2.38$  vs.  $88.4 \pm 5.53$ ,  $p < 0.0001$ ). Figure 2 shows the systematic difference between both systems.

#### Discussion

IVUS is currently been employed as a tool to assess atherosclerosis progression/regression in longitudinal studies [6, 15–17]. As the impact of drug therapies on the atherosclerotic plaque burden over time is relatively small, highly reproducible IVUS measurements are essential. A number of IVUS systems are commercially available and the potential impact of inter-catheter variability, in this setting, has not been extensively studied. Mechanical and phased-array catheters have relative advantages and disadvantages. Mechanical catheters have higher resolution but display specific artifacts such as non-uniform rotational distortion. In addition, far field imaging can be more problematic with mechanical catheters due to amplified attenuation and enhanced blood backscatter. On the other hand, phased-array catheters have lower resolution resulting in inferior near-field imaging and as they are not pulled-back within a sheath, are more susceptible to non-uniform pullback speed particularly in tortuous vessels.

Three studies explored the variability between such systems and results were not determinant [7, 18, 19].

In an *in vitro* study conducted by Schoenhagen et al., two mechanical and two phased-array catheters were compared. The largest difference in measurements compared to a phantom model was found with a 30 MHz mechanical catheter [18]. In the study of Hiro et al., the phased array system

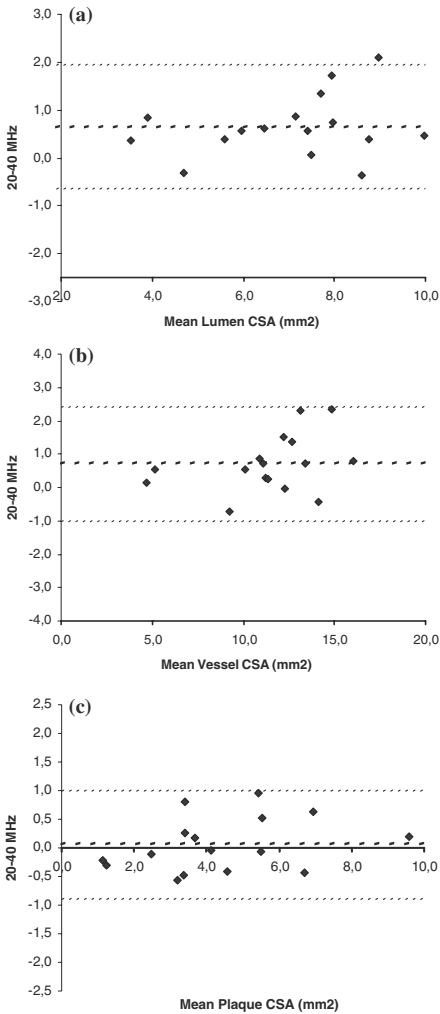


Figure 1. (a) Bland–Altman plot where the *X* axis shows the mean lumen cross sectional area (LCSA, mm<sup>2</sup>), and the *Y* axis shows the difference between the LCSA measurements by 20 and 40 MHz. Thin discontinuous lines show limits of agreement (upper limit 1.95 mm<sup>2</sup> and lower limit -0.65 mm<sup>2</sup>). (b) Bland–Altman plot where the *X* axis shows the mean vessel cross sectional area (VCSA, mm<sup>2</sup>), and the *Y* axis shows the difference between the VCSA measurements by 20 and 40 MHz. Thin discontinuous lines show limits of agreement (upper limit 2.42 mm<sup>2</sup> and lower limit -1.0 mm<sup>2</sup>). (c) Bland–Altman plot where the *X* axis shows the mean plaque cross sectional area (PCSA, mm<sup>2</sup>), and the *Y* axis shows the difference between the PCSA measurements by 20 and 40 MHz. Thin discontinuous lines show limits of agreement (upper limit 1.0 mm<sup>2</sup> and lower limit -0.88 mm<sup>2</sup>).

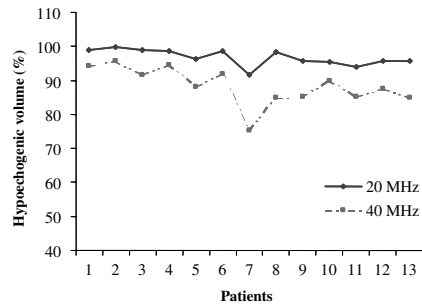


Figure 2. This plot shows the individual (n:13) hypoechoic volume (%) for the two systems. The percentage hypoechoic volume was significantly and systematically higher in the 20 MHz system ( $96.7 \pm 2.38$  vs.  $88.4 \pm 5.53$ ,  $p < 0.0001$ ).

showed a tendency towards a higher correlation with histology in comparison to mechanical systems [8].

The present in vivo study shows a slight systematic difference in lumen and vessel area measurements between the 20 MHz and the 40 MHz

catheters. These results are consistent with previously reported in vivo data [19]. It remains unclear whether such variability is caused by an overestimation of measurements with the phased-array system, or by an underestimation by the mechanical system. It is noteworthy, yet expected, that measurements in vessels with mild disease were subject to greater variability (Figure 1a).

Plaque burden measurements, a key endpoint for atherosclerosis progression/regression trials, showed no difference between the two systems [16]. Similar results have been shown between different mechanical catheters[9]. Notwithstanding, the variability shown in direct measurements, albeit low (<10%), is not insignificant when taking into

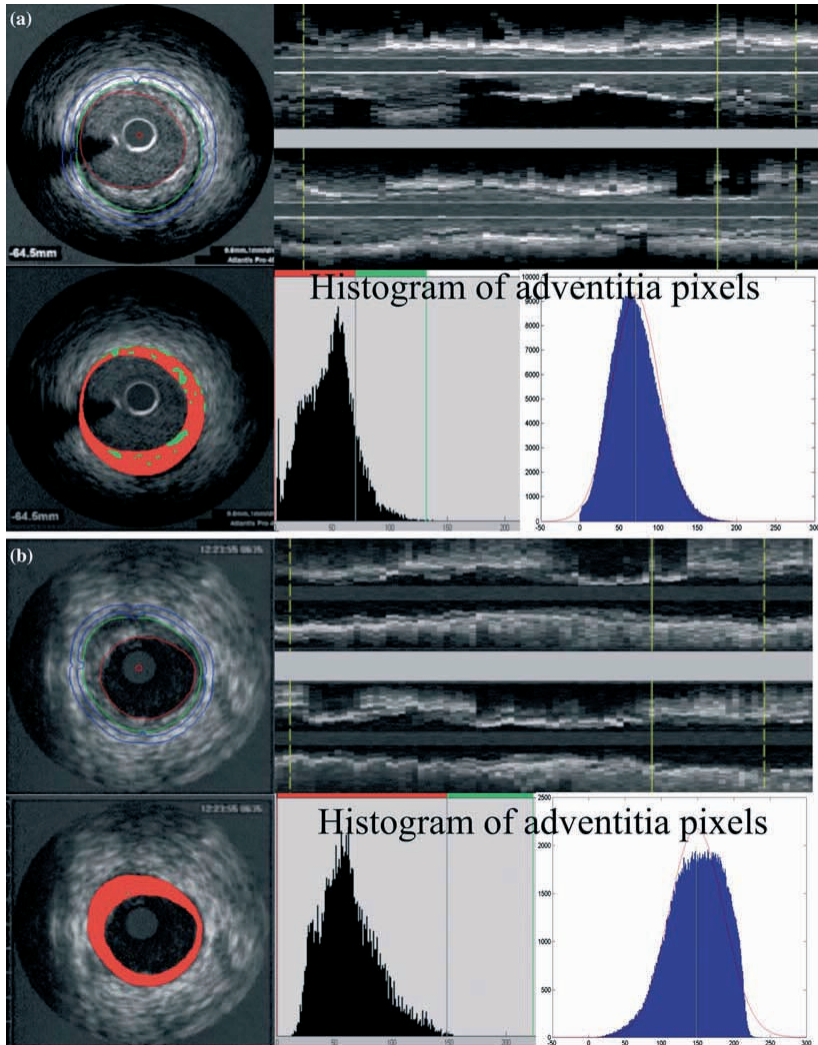


Figure 3. Cross-sectional and longitudinal views of a matched region of interest with 40 (a) and 20 (b) MHz. The adventitia is defined as tissue outside the external elastic membrane. For all non-shadowed adventitia pixels, the mean value and standard deviation are calculated. To observe the suitability, a normal distribution curve based on the same mean and standard deviation histogram is created. Hypoechoic areas are colored red (dark circle) and hyperechoic areas green (lighter spots).

Colour figures on pages 441-449

account the relatively small changes observed with drug therapies on plaque burden over time and therefore might contribute to a misinterpretation of their real biological effects.

Our results confirm that the precision required for accurate assessment of modest drug effects could be compromised when different IVUS systems are used in a single study.

Furthermore, the differences shown between catheters are comparable to those previously shown on intra and inter-observer variability [20]. We thus believe that the use of the same IVUS system for longitudinal assessments should be encouraged in order to achieve optimal quality standards [21].

However, the use of a single IVUS system for the conduction of multicenter studies is not easy in practice and it has been previously established that calibration equation methods can correct for differences between catheters.

In line with the morphometric measurements, tissue characterization data with the 20 MHz catheter showed systematically higher hypocholesteric volumes and percentages. It is well known that mechanical catheters have increased acoustic power since they send all the energy in the same direction. Conversely, phased-array catheters send the energy in multiple directions, attenuating their acoustic power. Accordingly, this could potentially be the source for such difference.

## Conclusions

In this *in vivo* study where we evaluated the agreement between two different catheter designs, plaque burden measurements, a key endpoint for atherosclerosis progression/regression trials, showed no difference between the two systems. However, a significant and systematic variability was detected in direct measurements. Tissue characterization yielded a similar systematic difference between catheters.

It remains unclear whether the difference is caused by an overestimation of measurements with the phased-array system, or by an underestimation by the mechanical system. Nevertheless, until this issue is further explored, we consider that the use

of a single IVUS system should be recommended for serial studies.

## Limitations

The number of patients included in this study was small. However, the conductance of large *in vivo* studies of this type is difficult due to obvious ethical issues. The relatively small amount of plaque in some patients influenced the results as clearly shown in the Bland–Altman plots. Finally, the present study data was processed as analog (video tape). Digital processing could have improved the results. However, we chose the former processing since it is the most commonly used.

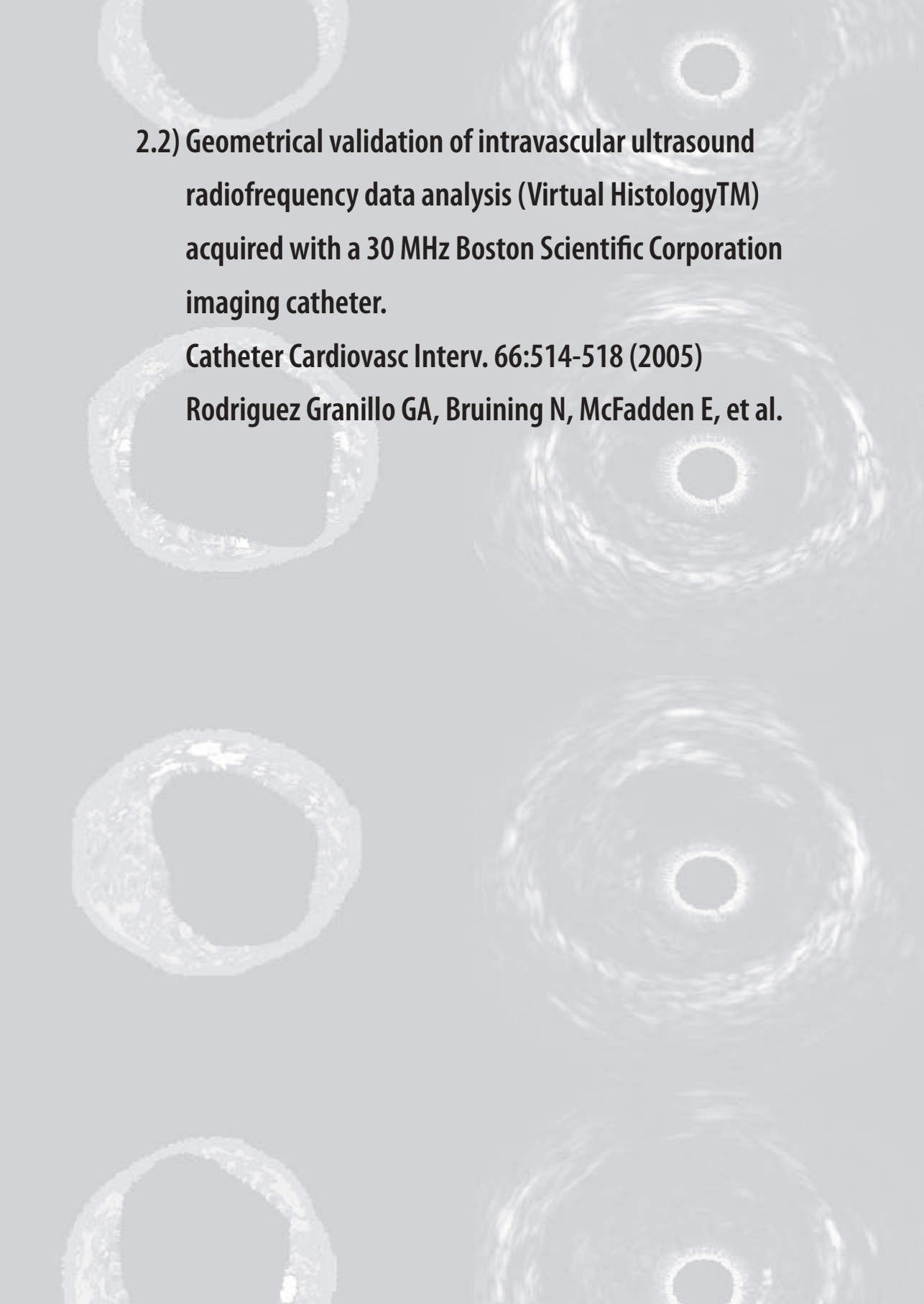
## References

1. Nishimura RA, Edwards WD, Warnes CA, et al. Intravascular ultrasound imaging: *in vitro* validation and pathologic correlation. *J Am Coll Cardiol* 1990; 16: 145–154.
2. Jaeger Pde, Mudra H, Figulla H, et al. Intravascular ultrasound-guided optimized stent deployment. Immediate and 6 months clinical and angiographic results from the Multicenter Ultrasound Stenting in Coronaries Study (MUSIC Study). *Eur Heart J* 1998; 19: 1214–1223.
3. Fitzgerald PJ, Oshima A, Hayase M, et al. Final results of the Can Routine Ultrasound Influence Stent Expansion (CRUISE) study. *Circulation* 2000; 102: 523–530.
4. Rasheed Q, Dhawale PJ, Anderson J, Hodgson JM. Intracoronary ultrasound-defined plaque composition: computer-aided plaque characterization and correlation with histologic samples obtained during directional coronary atherectomy. *Am Heart J* 1995; 129: 631–637.
5. Nair A, Kuban BD, Tuzcu EM, Schoenhagen P, Nissen SE, Vince DG. Coronary plaque classification with intravascular ultrasound radiofrequency data analysis. *Circulation* 2002; 106: 2200–2206.
6. Schartl M, Bocksch W, Koschyk DH, et al. Use of intravascular ultrasound to compare effects of different strategies of lipid-lowering therapy on plaque volume and composition in patients with coronary artery disease. *Circulation* 2001; 104: 387–392.
7. Hiro T, Leung CY, Russo RJ, Karimi H, Farvid AR, Tobis JM. Variability of a three-layered appearance in intravascular ultrasound coronary images: a comparison of morphometric measurements with four intravascular ultrasound systems. *Am J Card Imaging* 1996; 10: 219–227.
8. Hiro T, Leung CY, Russo RJ, et al. Variability in tissue characterization of atherosclerotic plaque by intravascular ultrasound: a comparison of four intravascular ultrasound systems. *Am J Card Imaging* 1996; 10: 209–218.

9. Li Y, Honye J, Saito S, et al. Variability in quantitative measurement of the same segment with two different intravascular ultrasound systems: in vivo and in vitro studies. *Catheter Cardiovasc Interv* 2004; 62: 175–180.
10. Nissen SE, Yock P. Intravascular ultrasound: novel pathophysiological insights and current clinical applications. *Circulation* 2001; 103: 604–616.
11. Prati F, Arbustini E, Labellarte A, et al. Correlation between high frequency intravascular ultrasound and histomorphology in human coronary arteries. *Heart* 2001; 85: 567–570.
12. Okimoto T, Imazu M, Hayashi Y, Fujiwara H, Ueda H, Kohno N. Atherosclerotic plaque characterization by quantitative analysis using intravascular ultrasound: correlation with histological and immunohistochemical findings. *Circ J* 2002; 66: 173–177.
13. Winter SAde, Heller I, Hamers R, et al. Computer assisted three-dimensional plaque characterization in ultracoronary ultrasound studies. *Computers in Cardiology* 2003; 30: 73–76.
14. Bland JM, Altman DG. Statistical methods for assessing agreement between two methods of clinical measurement. *Lancet* 1986; 1: 307–310.
15. Nissen SE, Tsunoda T, Tuzcu EM, et al. Effect of recombinant ApoA-I Milano on coronary atherosclerosis in patients with acute coronary syndromes: a randomized controlled trial. *Jama* 2003; 290: 2292–2300.
16. Nissen SE, Tuzcu EM, Schoenhagen P, et al. Effect of intensive compared with moderate lipid-lowering therapy on progression of coronary atherosclerosis: a randomized controlled trial. *Jama* 2004; 291: 1071–1080.
17. Jensen LO, Thayssen P, Pedersen KE, Stender S, Haghfelt T. Regression of coronary atherosclerosis by simvastatin: a serial intravascular ultrasound study. *Circulation* 2004; 110: 265–270.
18. Schoenhagen P, Sapp SK, Tuzcu EM, et al. Variability of area measurements obtained with different intravascular ultrasound catheter systems: Impact on clinical trials and a method for accurate calibration. *J Am Soc Echocardiogr* 2003; 16: 277–284.
19. Tardif JC, Bertrand OF, Mongrain R, et al. Reliability of mechanical and phased-array designs for serial intravascular ultrasound examinations – animal and clinical studies in stented and non-stented coronary arteries. *Int J Card Imaging* 2000; 16: 365–375.
20. Hausmann D, Lundkvist AJ, Friedrich GJ, Mullen WL, Fitzgerald PJ, Yock PG. Intracoronary ultrasound imaging: intraobserver and interobserver variability of morphometric measurements. *Am Heart J* 1994; 128: 674–680.
21. Von Birgelen C, Hartmann M, Mintz GS, et al. Spectrum of remodeling behavior observed with serial long-term ( $\geq 12$  months) follow-up intravascular ultrasound studies in left main coronary arteries. *Am J Cardiol* 2004; 93: 1107–1113.

*Address for correspondence:* P.W. Serruys, Thoraxcenter, Bd406, Dr. Molewaterplein 40, 3015 GD Rotterdam, The Netherlands  
Tel.: +31-10-4635260; Fax: +31-10-4369154  
E-mail: p.w.j.c.serruys@erasmusmc.nl





**2.2) Geometrical validation of intravascular ultrasound  
radiofrequency data analysis (Virtual Histology™)  
acquired with a 30 MHz Boston Scientific Corporation  
imaging catheter.**

**Catheter Cardiovasc Interv. 66:514-518 (2005)**

**Rodriguez Granillo GA, Bruining N, McFadden E, et al.**



# Geometrical Validation of Intravascular Ultrasound Radiofrequency Data Analysis (Virtual Histology) Acquired With a 30 MHz Boston Scientific Corporation Imaging Catheter

Gastón A. Rodriguez-Granillo, MD, Nico Bruining, PhD, Eugene Mc Fadden, MD, Jurgén M.R. Ligthart, Jiro Aoki, MD, Evelyn Regar, MD, PhD, Pim de Feyter, MD, PhD, and Patrick W. Serruys,\* MD, PhD

Recently, the plaque characterization field was explored with the use of the substrate (frequency domain analysis) rather than the envelope (amplitude or gray-scale imaging) of the intravascular ultrasound (IVUS) radiofrequency data. However, there is no data about the agreement of quantitative outcome between the two methods. The aim of this study was to assess the correlation and agreement between quantitative coronary ultrasound and the geometrical measurements provided by the spectral analysis of ultrasound radiofrequency data [IVUS-Virtual Histology (IVUS-VH), Volcano Therapeutics]. Twenty-five patients were included in this study. The IVUS catheter used was a commercially available mechanical sector scanner (Ultracross 2.9 Fr 30 MHz catheter, Boston Scientific) covered with an outer sheath. IVUS-VH significantly underestimated lumen [relative difference (RD) =  $14.8 \pm 5.6$ ;  $P < 0.001$ ], vessel (RD =  $14.1 \pm 4.8$ ;  $P < 0.001$ ), and plaque (RD =  $11.5 \pm 10.8$ ;  $P < 0.001$ ) cross-sectional areas (CSAs). Nevertheless, when adjusted for the ultrasound propagation delay caused by the sheath, relative differences of measurements were remarkably low ( $0.49\% \pm 6.3\%$ ,  $P = 0.64$  for lumen;  $2.33\% \pm 4.6\%$ ,  $P = 0.007$  for vessel; and  $4.2\% \pm 10.4\%$ ,  $P = 0.005$  for plaque CSA). These data suggest that the volumetric output of the IVUS-VH software underestimates measurements when acquired with a 30 MHz catheter. However, after applying a mathematical adjustment method for the ultrasound propagation delay caused by the outer sheath of the 30 MHz catheter, relative differences of direct measurements were negligible. These results suggest that ultrasound radiofrequency data analysis could provide, aside from precise compositional data, an accurate geometrical output. © 2005 Wiley-Liss, Inc.

**Key words:** ultrasonography; atherosclerosis; imaging

## INTRODUCTION

Intravascular ultrasound (IVUS) provides a tomographic view of coronary arteries, thereby facilitating the assessment of morphology, severity, and extension of a certain lesion. In addition, it enables the operator to choose more accurately the device size [1–3]. Several IVUS studies using different therapeutic strategies were recently conducted to assess progression/regression of plaque and showed a discordance between the clinical effects of validated therapies and their effects on plaque burden [4–6]. However, since stability of atherosclerotic plaques has been linked to their histological composition [7], precise plaque characterization could provide important additional information and become a target for future drug therapies. In vitro studies have shown that accurate visual interpretation

of IVUS gray-scale images for plaque composition is limited [8]. Recently, an ex vivo validation study showed that plaque characterization with the use of the substrate (frequency domain analysis) rather than the

Erasmus Medical Center, Thoraxcenter, Rotterdam, The Netherlands

\*Correspondence to: Dr. Patrick W. Serruys, Thoraxcenter, Bd406, Dr. Molewaterplein 40, 3015-GD Rotterdam, The Netherlands. E-mail: p.w.j.c.serruys@erasmusmc.nl

Received 14 February 2005; Revision accepted 24 March 2005

DOI 10.1002/ccd.20447

Published online 9 November 2005 in Wiley InterScience (www.interscience.wiley.com).

envelope (amplitude) of the IVUS radiofrequency data was feasible and four plaque types (fibrous, fibrolipidic, lipid-core, and calcium) as defined by histology could be correlated with a specific spectrum of the radiofrequency signal [9]. In the present study, we evaluated the agreement between the output of a validated (Curad, version 3.1; Wijk bij Duurstede, The Netherlands) standard gray-scale quantitative coronary ultrasound (QCU) software and the geometrical measurements (lumen, vessel, and plaque) provided by ultrasound radiofrequency data analysis (IVUS-Virtual Histology; Volcano Therapeutics, Rancho Cordova, CA) of the same region of interest (ROI).

## MATERIALS AND METHODS

### Patient Population

The study population consisted of a subset of 25 patients who were referred for percutaneous intervention and where IVUS-Virtual Histology (VH) was performed in addition to conventional IVUS in a nonculprit vessel. The study protocol was approved by the institutional ethics committee and a written informed consent was obtained from all patients.

### Intravascular Ultrasound

The IVUS catheter used was a commercially available mechanical sector scanner (Ultracross 2.9 Fr 30 MHz catheter; Boston Scientific, Santa Clara, CA) covered with a 127  $\mu\text{m}$  outer sheath to prevent direct contact of the ultrasound element to the vessel wall. IVUS was performed prior to any interventions. Using an automated pullback device, the transducer was withdrawn at a continuous speed of 0.5 mm/sec. Cine runs before and during contrast injection were performed to define the position of the IVUS catheter before the pullback was started. IVUS data were acquired after the intracoronary administration of isosorbide dinitrate and the data were stored on S-VHS videotape. The videotapes were digitized on a computer system, transformed into the DICOM medical image standard, and stored on an IVUS Picture Archiving and Communications System (PACS).

QCU analysis was performed by the core laboratory (Cardialysis, Rotterdam, The Netherlands) using validated semiautomatic contour detection software (Curad, version 3.1; Wijk bij Duurstede, The Netherlands). The IntelliGate image-based gating method was applied to eliminate catheter-induced image artifacts by retrospectively selecting end-diastolic frames [10]. Contour detection was performed using a longitudinal view and correcting each cross-sectional area (CSA) contours using a cross-sectional view. Whenever side branches were encountered throughout the ROI, the

semiautomatic contour detection software interpolated the contours. The borders of the external elastic membrane (EEM) and the lumen-intima interface enclosed a volume that was defined as the coronary plaque plus media volume.

### Virtual Histology

**In vivo experience.** Extensive methodological details about the technique have been described elsewhere [9]. Briefly, IVUS-VH is a catheter-based technique that uses the spectral analysis of the radiofrequency data to reconstruct tissue maps with the aim to provide classification of plaque composition.

IVUS-VH derives its data from the RF output of a conventional IVUS console and is ECG-gated for accurate data analysis. The RF and ECG signal were transferred from the Boston Scientific Galaxy ultrasound console to a dedicated IVUS-VH platform (Volcano Therapeutics).

The IVUS-VH data were stored on a CD-ROM and sent to the core laboratory (Cardialysis) for offline analysis. IVUS B-mode images were reconstructed from the RF data by custom software (IVUSLab; Volcano Therapeutics). Subsequently, manual contour detection of both the lumen and the media-adventitia interface was performed. Cross-sectional view was used for this purpose. Side branches were eliminated from the analysis drawing the lumen contour over the media. The IVUSLab software provides geometrical (Table I) and compositional information for each frame (cross-sectional area) of the pullback.

In preliminary *in vitro* studies, four plaque types (fibrous, fibrolipid, lipid-necrotic, and calcium) as defined by histology could be correlated with a specific spectrum of the radiofrequency signal [9,11]. The different plaque components are assigned color codes; fibrous, fibrolipidic, lipid-core, and calcified regions are labeled green, greenish-yellow, red, and white, respectively.

### Region of Interest Correlation

Once the ROI was visually matched with the QCU using identifiable anatomic landmarks (side branches and ostium of the vessel), volumetrical data were correlated.

**Ex vivo experience.** In addition, we measured a phantom model using conventional IVUS and IVUS-VH. The phantom model consisted of one 5 mm steel ring (deviation < 1%) mounted in a transparent synthetic housing. The outer sheath of the catheter was straightened in the opening of the phantom and the ultrasound element was positioned in the center of the steel ring. As a transporter of the ultrasound waves, we used a fluid mixture containing 90% degassed water

**TABLE I. Comparison of QCU With IVUS-VH Geometrical Measurements (n = 25)**

	LCSA (mm <sup>2</sup> )	VCSA (mm <sup>2</sup> )	PCSA (mm <sup>2</sup> )	Length
QCU	9.62 ± 3.5	16.09 ± 4.7	6.47 ± 2.6	32.76 ± 13.9
IVUS-VH	8.28 ± 2.9	13.99 ± 4.1	5.70 ± 2.2	31.89 ± 13.8
Absolute delta	1.34 ± 0.7	2.10 ± 0.9	0.77 ± 0.7	0.44 ± 0.7
Relative delta (%)	14.8 ± 5.6	14.1 ± 4.8	11.50 ± 10.8	2.76 ± 4.6
<i>P</i>	< 0.001	< 0.001	< 0.001	0.006

and 10% ethanol as the ex vivo substitute for blood. The room temperature was 22°C, resulting in an ultrasound propagation speed of approximately 1.548 mm/sec [12]. Gray-scale images and RF data were stored on CD-ROM and submitted for analysis using IVUSLab (for RF data) and Curad (QCU) softwares. Semiautomatic contour detection of the inner surface of the ring was independently performed in the three systems (Galaxy, Curad, and IVUSLab).

### Statistical Analysis

Measurements are expressed as mean ± standard deviation. A *P* value < 0.05 was considered statistically significant. In addition to Pearson correlation coefficient, the degree of agreement between both techniques was assessed using Bland-Altman analysis plots [13]. The limits of agreement were determined by the mean difference between both techniques ± 2 standard deviations.

## RESULTS

### In Vivo Results

The mean age was 59.1 ± 11.5; 20 (80%) were male. Twenty-five vessels were interrogated with IVUS: LAD 13 (52%), LCx 4 (16%), and RCA 8 (32%). The measured length was 32.76 ± 13.9 with the QCU software and 31.89 ± 13.8 with IVUS-VH (*P* = 0.006). There was a high correlation between measurements [Pearson correlation coefficient (*r*) for lumen *r* = 0.99; vessel *r* = 0.99; plaque *r* = 0.98]. Nevertheless, IVUS-VH software significantly underestimated lumen (8.28 ± 2.9 vs. 9.62 ± 3.25; *P* < 0.001), vessel (13.99 ± 4.1 vs. 16.09 ± 4.7; *P* < 0.001), and plaque (5.70 ± 2.2 vs. 6.47 ± 2.6; *P* < 0.001) cross-sectional areas. Moreover, the relative differences were 14.8% ± 5.6%, 14.1% ± 4.8%, and 11.50% ± 10.8% for lumen, vessel, and plaque CSAs, respectively.

**TABLE II. In Vitro Validation**

	Diameter (mm)	Areas (mm <sup>2</sup> )	Absolute difference		Relative difference (%)	
			mm	mm <sup>2</sup>	mm	mm <sup>2</sup>
Phantom	5	19.63				
Galaxy I	4.8	18.09	0.2	1.54	4	7.8
QCU	4.83	18.34	0.17	1.29	3.4	6.6
IVUS-VH	4.63	16.89	0.37	2.74	7.4	14.0

### Phantom Results

As depicted in Table II, the results of the in vitro study showed a significant underestimation of measurements using IVUS-VH with respect to the Galaxy and the Curad (QCU) software.

Such in vivo and in vitro underestimation of measurements with IVUS-VH software raised the presumption that the attenuation suffered by the ultrasound propagation speed while crossing the sheath was not accounted for in the IVUSLab software, thus delaying the ultrasound signal and potentially affecting the results [12]. Such suspicion was confirmed by the manufacturer. Accordingly, an adjustment method for 30 MHz Boston Scientific catheters described by Bruining et al. [12] was applied to the in vivo and in vitro results.

Adjusted for the ultrasound propagation delay caused by the sheath, relative differences of direct measurements (0.49% ± 6.3% for lumen, *P* = 0.64; 2.33 ± 4.6 for vessel, *P* = 0.007 CSAs) decreased up to less than 3%, while an indirect measurement such as plaque area decreased up to 4.2% ± 10.4% (*P* = 0.005) (Table III). Bland-Altman analysis plots of the adjusted measurements are depicted in Figure 1A, B, and C for lumen, vessel, and plaque CSA (expressed as mean), respectively.

## DISCUSSION

Previous in vitro validation of quantitative coronary ultrasound has shown a high correlation with histology samples [1,14,15]. Nevertheless, accurate plaque characterization with IVUS, particularly of lipid-rich plaques, remains an unresolved issue [15]. Ultrasound radiofrequency data analysis has the potential to characterize coronary plaque composition accurately, thereby enabling the physicians to follow the progression of coronary artery disease in a given patient not only in a quantitative but also in a qualitative manner.

The present study is the first where the geometrical output of ultrasound radiofrequency data analysis was compared with standard gray-scale QCU data. The out-

**TABLE III. Adjusted Measurements (n = 25)**

	LCSA (mm <sup>2</sup> )	VCSA (mm <sup>2</sup> )	PCSA (mm <sup>2</sup> )
QCU	9.62 ± 3.5	16.09 ± 4.7	6.47 ± 2.6
IVUS-VH	9.57 ± 3.1	15.66 ± 4.4	6.08 ± 2.3
Absolute delta	0.06 ± 0.6	0.44 ± 0.7	0.38 ± 0.6
Relative delta (%)	0.49 ± 6.3	2.33 ± 4.6	4.2 ± 10.4
<i>P</i>	0.64	0.007	0.005

come of both techniques are highly correlated. However, lumen, vessel, and plaque areas were systematically underestimated with IVUS-VH software.

The source of such variability was identified as the ultrasound propagation speed delay caused by the outer sheath of the 30 MHz catheter [12]. Accordingly, we applied a mathematical adjustment method previously developed by our group, achieving negligible relative differences of direct measurements. It is noteworthy that such algorithm is not applicable to plaque measurements. The adjusted plaque area is the difference between the adjusted vessel and lumen areas. As expected and previously described by Peters et al. [16], direct measurements (lumen and vessel area) are less subject to variability than derived measurements (plaque area).

IVUS-VH is a novel imaging technique with no intention to replace QCU. The purpose of this study was to demonstrate that ultrasound radiofrequency data analysis obtained with a 30 MHz catheter provides, aside from accurate compositional data [9] and with the aid of an adjustment algorithm, an accurate geometrical output.

### Study Limitations

The study included a small patient population. As earlier, acquisition and analysis were done using different methodologies. This could have had an impact on the final results. Moreover, gating was performed in a different manner. We cannot disregard this fact as a potential source of diversity between measurements. In addition, we cannot rule out an influence of the inter-observer variability in the results. Finally, the steel ring used in the phantom cause hard reflections, potentially leading to a blooming effect that could impair accurate measurements. Nevertheless, softer materials are more affected by temperature [12].

These data suggest that the volumetric output of the IVUS-VH software underestimates measurements when acquired with a 30 MHz catheter. However, after applying a mathematical adjustment method for the ultrasound propagation delay caused by the outer sheath of the 30 MHz catheter [12], relative differences of direct measurements were negligible. These results suggest that ultrasound radiofrequency data

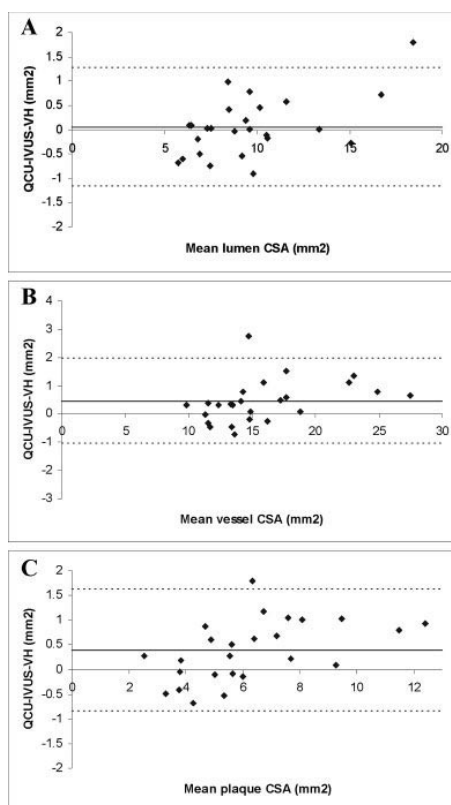


**Fig. 1.** Bland-Altman plots where the X-axis shows the mean CSAs for lumen (LCSA; A), vessel (VCSA; B), and plaque (PCSA; C), whereas the Y-axis shows the difference between measurements by QCU and IVUS-VH.

analysis could provide, aside from precise compositional data [9], an accurate geometrical output.

### REFERENCES

1. Nishimura RA, Edwards WD, Warnes CA, et al. Intravascular ultrasound imaging: in vitro validation and pathologic correlation. *J Am Coll Cardiol* 1990;16:145-154.
2. de Jaegere P, Mudra H, Figulla H, et al. Intravascular ultrasound-guided optimized stent deployment: immediate and 6 months clinical and angiographic results from the Multicenter Ultrasound Stenting in Coronaries Study (MUSIC study). *Eur Heart J* 1998;19:1214-1223.
3. Fitzgerald PJ, Oshima A, Hayase M, et al. Final results of the Can Routine Ultrasound Influence Stent Expansion (CRUISE) study. *Circulation* 2000;102:523-530.

4. Nissen SE, Tuzcu EM, Schoenhagen P, et al. Effect of intensive compared with moderate lipid-lowering therapy on progression of coronary atherosclerosis: a randomized controlled trial. *JAMA* 2004;291:1071–1080.
5. Scharl M, Bocksch W, Koschyk DH, et al. Use of intravascular ultrasound to compare effects of different strategies of lipid-lowering therapy on plaque volume and composition in patients with coronary artery disease. *Circulation* 2001;104:387–392.
6. Jensen LO, Thyssen P, Pedersen KE, Stender S, Hagfeldt T. Regression of coronary atherosclerosis by simvastatin: a serial intravascular ultrasound study. *Circulation* 2004;110:265–270.
7. Davies MJ, Richardson PD, Woolf N, Katz DR, Mann J. Risk of thrombosis in human atherosclerotic plaques: role of extracellular lipid, macrophage, and smooth muscle cell content. *Br Heart J* 1993;69:377–381.
8. Peters RJ, Kok WE, Havenith MG, Rijsterborgh H, van der Wal AC, Visser CA. Histopathologic validation of intracoronary ultrasound imaging. *J Am Soc Echocardiogr* 1994;7:230–241.
9. Nair A, Kuban BD, Tuzcu EM, Schoenhagen P, Nissen SE, Vince DG. Coronary plaque classification with intravascular ultrasound radiofrequency data analysis. *Circulation* 2002;106:2200–2206.
10. De Winter SA, Hamers R, Degertekin M, et al. Retrospective image-based gating of intracoronary ultrasound images for improved quantitative analysis: the intelligate method. *Catheter Cardiovasc Interv* 2004;61:84–94.
11. Moore MP, Spencer T, Salter DM, et al. Characterisation of coronary atherosclerotic morphology by spectral analysis of radiofrequency signal: in vitro intravascular ultrasound study with histological and radiological validation. *Heart* 1998;79:459–467.
12. Bruining N, Hamers R, Teo TJ, de Feijter PJ, Serruys PW, Roelandt JR. Adjustment method for mechanical Boston scientific corporation 30 MHz intravascular ultrasound catheters connected to a Clearview console: mechanical 30 MHz IVUS catheter adjustment. *Int J Cardiovasc Imaging* 2004;20:83–91.
13. Bland JM, Altman DG. Statistical methods for assessing agreement between two methods of clinical measurement. *Lancet* 1986;1:307–310.
14. Tobis JM, Mallery JA, Gessert J, et al. Intravascular ultrasound cross-sectional arterial imaging before and after balloon angioplasty in vitro. *Circulation* 1989;80:873–882.
15. Potkin BN, Bartorelli AL, Gessert JM, et al. Coronary artery imaging with intravascular high-frequency ultrasound. *Circulation* 1990;81:1575–1585.
16. Peters RJ, Kok WE, Rijsterborgh H, et al. Reproducibility of quantitative measurements from intracoronary ultrasound images: beat-to-beat variability and influence of the cardiac cycle. *Eur Heart J* 1996;17:1593–1599.





## **2.3) Reproducibility of Intravascular Ultrasound**

**Radiofrequency Data Analysis: Implications for the  
Design and Conduction of Longitudinal Studies**

**Int J Cardiovasc Imag. 2006 Mar 31; (Epub ahead of  
print)**

**Rodriguez Granillo GA, Vaina S, García-García HM, et al.**



## Reproducibility of intravascular ultrasound radiofrequency data analysis: implications for the design of longitudinal studies

Gastón A. Rodríguez-Granillo<sup>1</sup>, Sophia Vaina<sup>1</sup>, Héctor M. García-García<sup>1</sup>, Marco Valgimigli<sup>1</sup>, Eric Duckers<sup>1</sup>, Robert J. van Geuns<sup>1</sup>, Evelyn Regar<sup>1</sup>, William J. van der Giessen<sup>1</sup>, Marco Bressers<sup>2</sup>, Dick Goedhart<sup>2</sup>, Marie-Angele Morel<sup>2</sup>, Pim J. de Feyter<sup>1</sup> & Patrick W. Serruys<sup>1</sup>

<sup>1</sup>Department of Interventional Cardiology of the Erasmus Medical Center, Rotterdam, The Netherlands;

<sup>2</sup>Cardialysis BV, Rotterdam, The Netherlands

Received 24 November 2005; accepted in revised form 19 January 2006

**Key words:** agreement, atherosclerosis, plaque characterization, reproducibility, ultrasonography

### Abstract

**Objectives:** The purpose of this study was to assess in vivo the reproducibility of tissue characterization using spectral analysis of intravascular ultrasound (IVUS) radiofrequency data (IVUS-VH). **Background:** Despite the need for reproducibility data to design longitudinal studies, such information remains unexplored. **Methods and results:** IVUS-VH (Volcano Corp., Rancho Cordova, USA) was performed in patients referred for elective percutaneous intervention and in whom a non-intervened vessel was judged suitable for a safe IVUS interrogation. The IVUS catheters used were commercially available catheters (20 MHz, Volcano Corp., Rancho Cordova, USA). Following IVUS-VH acquisition, and after the disengagement and re-engagement of the guiding catheter, an additional acquisition was performed using a new IVUS catheter. Fifteen patients with 16 non-significant lesions were assessed by 2 independent observers. The relative inter-catheter differences regarding geometrical measurements were negligible for both observers. The inter-catheter relative difference in plaque cross-sectional area (CSA) was 3.2% for observer 1 and 0.5% for observer 2. The limits of agreement for (observer 1 measurements) lumen, vessel, plaque and plaque burden measurements were 0.82, -1.10 mm<sup>2</sup>; 0.80, -0.66 mm<sup>2</sup>; 1.08, -0.66 mm<sup>2</sup>; and 5.83, -3.89%; respectively. Limits of agreement for calcium, fibrous, fibrolipidic and necrotic core CSA measurements were 0.22, -0.25 mm<sup>2</sup>; 1.02, -0.71 mm<sup>2</sup>; 0.61, -0.65 mm<sup>2</sup>; and 0.43, -0.38 mm<sup>2</sup> respectively. Regarding the inter-observer agreement, the limits of agreement for lumen, vessel, plaque and plaque burden measurements were 2.61, -2.09 mm<sup>2</sup>; 2.20-3.03 mm<sup>2</sup>; 1.70, -3.04 mm<sup>2</sup>; and 9.16, -16.41%; respectively, and for calcium, fibrous, fibrolipidic and necrotic core measurements of 0.08, -0.09 mm<sup>2</sup>; 0.89, -1.28 mm<sup>2</sup>; 0.74, -1.06 mm<sup>2</sup>; and 0.16, -0.20 mm<sup>2</sup>; respectively. **Conclusions:** The present study demonstrates that the geometrical and compositional output of IVUS-VH is acceptably reproducible.

### Introduction

Intravascular ultrasound (IVUS) imaging has been shown to provide safe, accurate, real-time, tomographic measurements of coronary vessels in vivo

[1-4]. Over the past decade, IVUS has been used to describe the extent, severity, distribution, and morphology of coronary atherosclerosis [5-7]. Furthermore, several studies have evaluated the temporal effect of conventional and novel medical

therapies on plaque progression by means of IVUS [8–10].

Since the fate of coronary atherosclerotic plaques has been related to their histological composition [11], precise in-vivo tissue characterization could provide important additional information and become a target for future drug therapy studies.

In-vitro studies have shown that visual interpretation of IVUS gray-scale images for plaque characterization is imprecise, in particular when assessing heterogeneous, lipid-rich plaques [12]. This has led investigators to explore the radiofrequency data analysis, a potential source for in-vivo tissue characterization. Indeed, a recent ex-vivo study on explanted coronary segments showed that plaque characterization using spectral analysis of IVUS radiofrequency data (IVUS-VH) was feasible and provided a high predictive accuracy to estimate the composition of atherosclerotic plaques [13]. Several in-vivo studies have been conducted thereafter using this approach [14–17]. Nevertheless, although prior knowledge about the reproducibility of measurements are essential for the internal validity of any study using this technique, to date, only indirect evidence on the reproducibility of the technique is available [18]. Accordingly, we sought to study the inter-observer and inter-catheter agreement of IVUS-VH measurements at a single time-point.

## Methods

### *Patient population*

This was a single-center prospective, investigator-driven study that sought to explore in vivo the reproducibility of spectral analysis of IVUS radiofrequency data (IVUS-VH, Volcano Corp., Rancho Cordova, USA). The study population consisted of consecutive patients that were referred for elective percutaneous intervention and in whom a non-intervened vessel was judged suitable for a safe IVUS interrogation of a vessel segment of at least 30 mm.

Exclusion criteria included the presence of severe calcification, vessel tortuosity, and haemodynamic instability. The study protocol was approved by the

institutional ethics committee and a written informed consent was obtained from all patients.

### *IVUS-VH*

IVUS-VH evaluates different spectral parameters of the radiofrequency data (*Y*-intercept, minimum power, maximum power, mid-band power, frequency at minimum power, frequency at maximum power, slope, etc.) to construct tissue maps that classify plaque into four major components. In preliminary in vitro studies, four histological plaque components (fibrous, fibrolipidic, necrotic core and calcium) were correlated with a specific spectrum of the radiofrequency signal [13]. These different plaque components were assigned color codes. Calcified, fibrous, fibrolipidic and necrotic core regions were labeled white, green, greenish-yellow and red respectively.

### *IVUS-VH acquisition*

The IVUS catheters used were commercially available phased array catheters (Eagle Eye Gold™ 2.9 F 20 MHz, Volcano Corp., Rancho Cordova, USA). The catheter probe was advanced at least 10 mm distal to a clearly visible side-branch and angiographic cine runs, before and during contrast injection, were performed to define the position of the IVUS catheter before the pullback was started. Using an automated pullback device, the transducer was withdrawn at a continuous speed of 0.5 mm/s. IVUS-VH acquisition was ECG-gated and acquired using a dedicated console (Volcano Corporation, Rancho Cordova, USA). IVUS-VH data was acquired after intra-coronary administration of isosorbide dinitrate and data was stored on DVD. Subsequently, and after the disengagement and re-engagement of the guiding catheter, the same procedure was performed using a new catheter (Eagle Eye Gold™ 2.9 F 20 MHz, Volcano Corp., Rancho Cordova, USA) and with the same side-branches as landmarks.

### *IVUS-VH analysis*

IVUS-VH analysis was performed by an independent core laboratory (Cardialysis BV, Rotterdam,

The Netherlands) using a semi-automatic contour detection software (IVUSLab 4.4, Volcano Corp., Rancho Cordova, USA). A region of interest (ROI) was identified using the inner side of two clear side-branches as reference and avoiding the presence of large side-branches within the ROI. Subsequently, the same ROI was identified in the other catheter's acquisition using side-by-side longitudinal and cross-sectional, contour-free views.

Contour detection of the lumen and the media-adventitia interface was performed by 2 independent experienced IVUS analysts. The same 2 IVUS analysts re-analyzed the same cases, leading to the possibility of multiple comparisons: 2 sets (observers 1 and 2) of intra-catheter agreement, and 1 set of inter-observer agreement [observer 1 (catheters 1 and 2) vs. observer 2 (catheters 1 and 2)].

The contours of the external elastic membrane (EEM) and the lumen-intima interface enclosed an area that was defined as the coronary plaque plus media area. Geometrical and compositional data were obtained for each cross-sectional area (CSA) and an average was calculated for each ROI. Plaque burden was calculated as  $[(EEM_{\text{area}} - \text{Lumen}_{\text{area}}) / EEM_{\text{area}}] \times 100$ . The lumen and vessel eccentricity indexes were calculated dividing the minimum (lumen and vessel, respectively) diameter by the maximum diameter, whereas the plaque eccentricity index was calculated dividing the minimum plaque thickness by the maximum plaque thickness.

### Statistical analysis

Discrete variables are presented as counts and percentages. Continuous variables are presented as means  $\pm$  SD. The inter-observer and inter-catheter agreement were assessed using Bland-Altman plots [19]. This method plots the mean against the difference in measurements. Limits of agreement were determined by adding two standard deviations to the mean difference for the upper limit and by subtracting two standard deviations from the mean difference for the lower limit. A two-sided  $p$  value of less than 0.05 indicated statistical significance.

## Results

Fifteen consecutive patients with 16 non-significant lesions were included in the study. Baseline characteristics of the patients included are depicted in Table 1. The study vessel was the left anterior descending in 9 patients (60.0%), the left circumflex in 5 (33.3%), and the right coronary artery in 1 patient (6.7%). There were no peri-procedural complications.

### Inter-catheter agreement

The studied length determined by landmarks was  $19.71 \pm 10.5$  mm for catheter 1 and  $21.01 \pm 11.1$  mm for catheter 2 ( $p=0.32$ ). Geometrical and compositional data of matched ROIs interrogated with IVUS-VH using 2 subsequent 20 MHz catheters are extensively depicted in Tables 2 and 3. The relative inter-catheter differences regarding geometrical measurements were negligible for both observers. Of note, the inter-catheter relative difference in plaque CSA was 3.2% for observer 1 and 0.5% for observer 2. Only other less common indirect measurements such as plaque eccentricity and plaque minimal thickness showed relative differences  $> 5\%$ . Compositional measurements showed higher relative differences, although not

Table 1. Study population ( $n=15$ ).

	<i>n</i> (%)
Age (years $\pm$ SD)	63.1 $\pm$ 8.6
Male sex	8 (53.3)
Diabetes	2 (13.3)
Hypertension	11 (73.3)
Current smoking	1 (6.7)
Previous smoking	5 (33.3)
Hypercholesterolemia	8 (53.3)
Family history of coronary disease	9 (60.0)
Lipid lowering agents	11 (73.3)
Clinical presentation	
Stable angina	14 (93.3)
Unstable angina	1 (6.7)
Study vessel	
Left anterior descending	9 (60.0)
Left circumflex	5 (33.3)
Right coronary artery	1 (6.7)

Table 2. Mean CSA geometrical measurements of matched ROI with two subsequent 20 MHz IVUS imaging catheters ( $n:16$ ).

	Catheter 1	Catheter 2	Absolute $\Delta$	Relative $\Delta$ (%)
Observer 1				
Lumen CSA (mm <sup>2</sup> )	11.08 ± 3.5	10.94 ± 3.5	0.14 ± 0.5	1.3
Lumen max. diameter (mm)	4.03 ± 0.7	4.01 ± 0.6	0.02 ± 0.1	0.4
Lumen min. diameter (mm)	3.37 ± 0.6	3.34 ± 0.6	0.03 ± 0.1	0.9
Lumen mean diameter (mm)	3.69 ± 0.6	3.67 ± 0.6	0.02 ± 0.1	0.6
Lumen eccentricity	0.84 ± 0.0	0.83 ± 0.0	0.00 ± 0.0	0.5
Vessel CSA (mm <sup>2</sup> )	17.40 ± 4.0	17.46 ± 4.0	0.07 ± 0.4	0.4
Vessel max. diameter (mm)	4.92 ± 0.6	4.93 ± 0.6	0.01 ± 0.1	0.3
Vessel min. diameter (mm)	4.36 ± 0.6	4.37 ± 0.6	0.01 ± 0.1	0.2
Vessel mean diameter (mm)	4.63 ± 0.6	4.64 ± 0.6	0.01 ± 0.0	0.2
Vessel eccentricity	0.89 ± 0.0	0.89 ± 0.0	0.00 ± 0.0	0.1
Plaque CSA (mm <sup>2</sup> )	6.32 ± 2.0	6.53 ± 2.1	0.21 ± 0.4	3.2
Plaque max. thickness (mm)	1.01 ± 0.2	1.02 ± 0.2	0.01 ± 0.1	0.7
Plaque min. thickness (mm)	0.09 ± 0.1	0.09 ± 0.1	0.01 ± 0.0	8.2
Plaque eccentricity (mm)	0.09 ± 0.1	0.10 ± 0.1	0.01 ± 0.0	10.0
Plaque burden (%)	36.80 ± 9.9	37.77 ± 9.9	0.97 ± 2.4	2.6
Observer 2				
Lumen CSA (mm <sup>2</sup> )	10.66 ± 3.8	10.67 ± 3.8	0.01 ± 0.4	0.1
Lumen max. diameter (mm)	3.90 ± 0.7	3.91 ± 0.7	0.01 ± 0.1	0.2
Lumen min. diameter (mm)	3.34 ± 0.6	3.33 ± 0.6	0.01 ± 0.1	0.3
Lumen mean diameter (mm)	3.61 ± 0.6	3.61 ± 0.7	0.00 ± 0.1	0.0
Lumen eccentricity	0.86 ± 0.0	0.85 ± 0.0	0.01 ± 0.0	0.6
Vessel CSA (mm <sup>2</sup> )	17.76 ± 4.0	17.80 ± 4.0	0.05 ± 0.4	0.3
Vessel max. diameter (mm)	4.95 ± 0.6	4.96 ± 0.6	0.01 ± 0.1	0.3
Vessel min. diameter (mm)	4.41 ± 0.6	4.42 ± 0.6	0.01 ± 0.1	0.1
Vessel mean diameter (mm)	4.68 ± 0.6	4.69 ± 0.6	0.01 ± 0.0	0.1
Vessel eccentricity	0.89 ± 0.0	0.89 ± 0.0	0.00 ± 0.0	0.1
Plaque CSA (mm <sup>2</sup> )	7.10 ± 2.1	7.13 ± 2.2	0.03 ± 0.4	0.5
Plaque max. thickness (mm)	1.05 ± 0.2	1.04 ± 0.3	0.00 ± 0.1	0.2
Plaque min. thickness (mm)	0.16 ± 0.1	0.16 ± 0.1	0.01 ± 0.0	4.7
Plaque eccentricity (mm)	0.16 ± 0.1	0.17 ± 0.1	0.01 ± 0.0	6.7
Plaque burden (%)	40.75 ± 10.7	40.93 ± 11.2	0.19 ± 1.8	0.5

LCSA, VCSA and PCSA refer to lumen, vessel and plaque CSAs. Plaque burden was calculated as  $[(EEM_{\text{area}} - \text{Lumen}_{\text{area}}) / EEM_{\text{area}}] \times 100$ .

exceeding 10%, except from calcium (11%) for observer 1 and fibrolipidic tissue (13%) for observer 2 (Table 3). Indeed, Bland–Altman plots showed a good inter-catheter agreement for geometrical (Figure 1) and compositional (Figure 2) measurements. The limits of agreement for (observer 1 measurements) lumen, vessel, plaque and plaque burden measurements were 0.82,  $-1.10 \text{ mm}^2$ ; 0.80,  $-0.66 \text{ mm}^2$ ; 1.08,  $-0.66 \text{ mm}^2$ ; and 5.83,  $-3.89\%$ ; respectively. Limits of agreement for calcium, fibrous, fibrolipidic and necrotic core CSA measurements were 0.22,  $-0.25 \text{ mm}^2$ ; 1.02,  $-0.71 \text{ mm}^2$ ; 0.61,  $-0.65 \text{ mm}^2$ ; and 0.43,  $-0.38 \text{ mm}^2$  respectively.

#### Inter-observer agreement

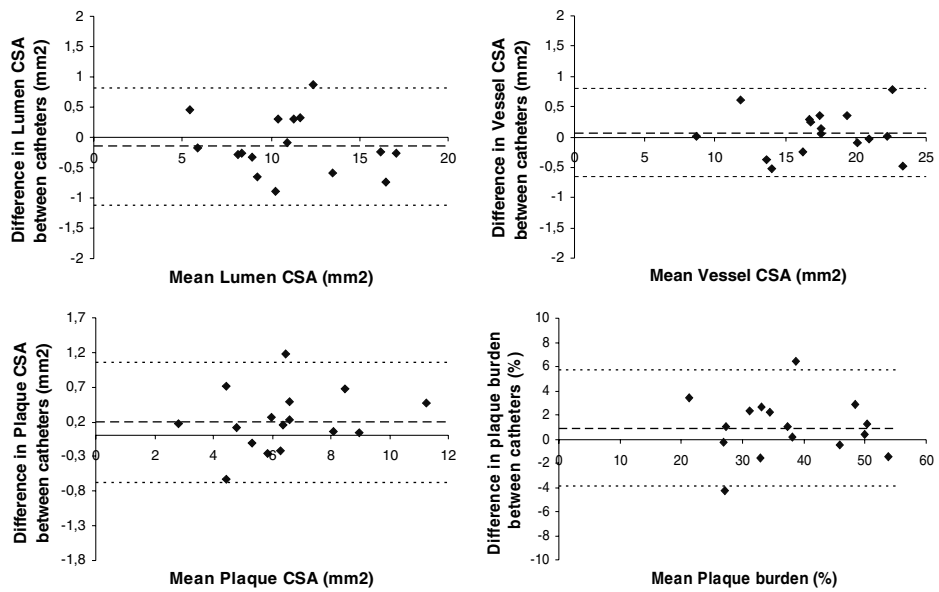
For the assessment of the inter-observer agreement, a comparison between the same matched cross-sections (653 frames for catheter 1 and 663 frames for catheter 2) were analyzed by 2 independent observers. These 2 datasets were merged resulting in a paired inter-observer agreement evaluation of 1316 frames.

Inter-observer differences were larger than the inter-catheter measurements (performed by the same observer). This was particularly noticed in indirect measurements such as plaque CSA (10%), plaque minimal thickness (53%) and plaque

Table 3. Mean CSA compositional measurements of matched ROI with two subsequent 20 MHz IVUS imaging catheters ( $n:16$ ).

	Catheter 1	Catheter 2	Absolute $\Delta$	Relative $\Delta$ (%)
<b>Observer 1</b>				
Calcium CSA (mm <sup>2</sup> )	0.17 ± 0.3	0.16 ± 0.2	0.01 ± 0.1	8.0
Calcium (%)	4.27 ± 5.2	3.82 ± 3.8	0.45 ± 2.6	11.1
Fibrous CSA (mm <sup>2</sup> )	1.96 ± 1.0	2.11 ± 1.1	0.16 ± 0.4	7.7
Fibrous (%)	60.37 ± 9.2	62.15 ± 8.7	1.78 ± 10.0	2.9
Fibrolipidic CSA (mm <sup>2</sup> )	0.66 ± 0.4	0.63 ± 0.3	0.02 ± 0.3	3.5
Fibrolipidic (%)	21.10 ± 9.8	19.58 ± 7.0	1.53 ± 8.3	7.5
Necrotic core CSA (mm <sup>2</sup> )	0.40 ± 0.4	0.43 ± 0.4	0.02 ± 0.2	5.7
Necrotic core (%)	11.27 ± 6.8	10.87 ± 6.6	0.40 ± 5.4	3.6
<b>Observer 2</b>				
Calcium CSA (mm <sup>2</sup> )	0.17 ± 0.3	0.16 ± 0.2	0.01 ± 0.1	8.7
Calcium (%)	4.08 ± 5.0	3.74 ± 3.4	0.34 ± 2.4	8.7
Fibrous CSA (mm <sup>2</sup> )	2.21 ± 1.1	2.28 ± 1.2	0.07 ± 0.4	3.1
Fibrous (%)	58.12 ± 10.5	60.63 ± 7.9	2.51 ± 10.1	4.2
Fibrolipidic CSA (mm <sup>2</sup> )	0.88 ± 0.6	0.77 ± 0.4	0.11 ± 0.4	13.1
Fibrolipidic (%)	22.97 ± 11.7	20.95 ± 10.8	2.01 ± 9.6	9.2
Necrotic core CSA (mm <sup>2</sup> )	0.42 ± 0.4	0.45 ± 0.5	0.03 ± 0.2	6.1
Necrotic core (%)	10.75 ± 6.9	11.02 ± 6.5	0.26 ± 5.5	2.4

LCSA, VCSA and PCSA refer to lumen, vessel and plaque CSAs. Plaque burden was calculated as  $[(EEM_{area} - Lumen_{area}) / EEM_{area}] \times 100$ .


 Figure 1. Bland–Altman plots depicting the (observer 1) agreement between catheters for geometrical measurements ( $n = 16$ ).

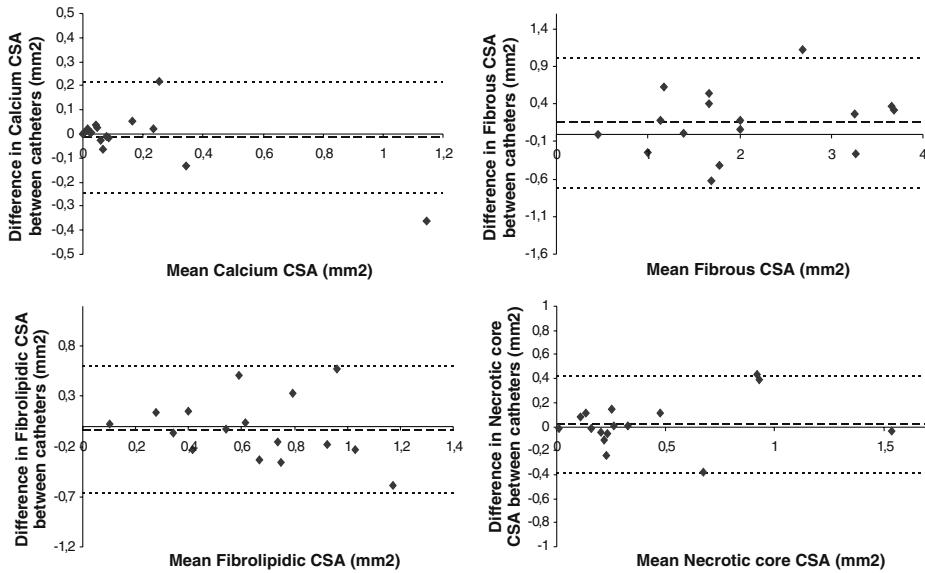


Figure 2. Bland–Altman plots depicting the (observer 1) agreement between catheters for compositional measurements ( $n = 16$ ).

eccentricity (54%). The largest relative difference was found in fibrolipidic measurements (Table 4).

Narrow limits of agreement and few outliers (Figures 3 and 4) were found between observers both for geometrical (limits of agreement for lumen, vessel, plaque and plaque burden measurements of 2.61,  $-2.09$  mm<sup>2</sup>; 2.20–3.03 mm<sup>2</sup>; 1.70,  $-3.04$  mm<sup>2</sup>; and 9.16,  $-16.41\%$ ; respectively) and compositional (limits of agreement for calcium, fibrous, fibrolipidic and necrotic core measurements of 0.08,  $-0.09$  mm<sup>2</sup>; 0.89,  $-1.28$  mm<sup>2</sup>; 0.74,  $-1.06$  mm<sup>2</sup>; and 0.16,  $-0.20$  mm<sup>2</sup>; respectively) measurements. It is noteworthy that the fibrous and fibrolipidic CSA measurements were highly accurate when assessing cross-sections with small fibrous or fibrolipidic content (Figure 4).

## Discussion

Over the past few years, IVUS has been employed as a tool to assess the temporal effect of conventional

and novel drug therapies on coronary plaque size in longitudinal studies [8, 20]. More recently, the discordance between the beneficial clinical effects of secondary prevention strategies and their effect on plaque volume had lead investigators to explore a potential significant effect on plaque composition [21].

Tissue characterization by means of IVUS radiofrequency (RF) data analysis is a potential tool to enable an accurate evaluation of the composition of coronary plaques [13]. Several investigators have explored the potential of RF data analysis in vivo and reported promising findings [15–17, 22, 23]. This technique has the potential to detect temporal changes in plaque composition and therefore studies have been conducted to assess the effect of conventional drug therapies on the phenotype of coronary atherosclerosis [18, 22, 23]. In addition, there are currently several large trials being conducted with the aim to assess the natural history of high-risk plaques by means of this technique.

Table 4. Geometrical and compositional measurements of matched CSAs between different observers ( $n$ :1316).

	Observer 1	Observer 2	Absolute $\Delta$	Relative $\Delta$ (%)
<b>Geometrical data</b>				
Lumen CSA (mm <sup>2</sup> )	10.83 ± 3.8	10.51 ± 4.0	0.26 ± 1.2	2.5
Lumen max. diameter (mm)	3.96 ± 0.7	3.86 ± 0.8	0.08 ± 0.4	2.1
Lumen min. diameter (mm)	3.34 ± 0.6	3.31 ± 0.7	0.01 ± 0.3	0.2
Lumen mean diameter (mm)	3.65 ± 0.7	3.58 ± 0.7	0.04 ± 0.3	1.1
Lumen eccentricity	0.84 ± 0.1	0.86 ± 0.1	0.02 ± 0.1	2.3
Vessel CSA (mm <sup>2</sup> )	16.90 ± 4.2	17.22 ± 4.3	0.41 ± 1.3	2.4
Vessel max. diameter (mm)	4.84 ± 0.6	4.87 ± 0.6	0.06 ± 0.4	1.1
Vessel min. diameter (mm)	4.30 ± 0.6	4.35 ± 0.6	0.08 ± 0.3	1.7
Vessel mean diameter (mm)	4.56 ± 0.6	4.61 ± 0.6	0.07 ± 0.3	1.5
Vessel eccentricity	0.89 ± 0.1	0.89 ± 0.1	0.01 ± 0.1	1.1
Plaque CSA (mm <sup>2</sup> )	6.07 ± 2.3	6.72 ± 2.3	0.67 ± 1.2	10.3
Plaque max. thickness (mm)	0.96 ± 0.3	1.01 ± 0.3	0.03 ± 0.2	3.4
Plaque min. thickness (mm)	0.09 ± 0.1	0.16 ± 0.1	0.07 ± 0.1	53.3
Plaque eccentricity (mm)	0.09 ± 0.1	0.16 ± 0.1	0.07 ± 0.1	53.6
Plaque burden (%)	36.62 ± 12.2	40.07 ± 12.5	3.63 ± 6.4	9.5
<b>Compositional data</b>				
Calcium CSA (mm <sup>2</sup> )	0.12 ± 0.2	0.12 ± 0.2	0.00 ± 0.0	2.9
Calcium (%)	3.66 ± 6.4	3.51 ± 6.0	0.13 ± 2.4	3.7
Fibrous CSA (mm <sup>2</sup> )	1.86 ± 1.3	2.05 ± 1.3	0.20 ± 0.5	10.2
Fibrous (%)	61.48 ± 18.2	60.05 ± 18.2	1.10 ± 14.3	1.8
Fibrolipidic CSA (mm <sup>2</sup> )	0.60 ± 0.5	0.75 ± 0.7	0.16 ± 0.5	23.5
Fibrolipidic (%)	22.34 ± 14.0	22.09 ± 15.3	1.86 ± 11.8	8.8
Necrotic core CSA (mm <sup>2</sup> )	0.35 ± 0.4	0.37 ± 0.4	0.02 ± 0.1	6.3
Necrotic core (%)	10.45 ± 10.1	10.22 ± 9.8	0.17 ± 5.7	1.6

LCSA, VCSA and PCSA refer to lumen, vessel and plaque CSAs. Plaque burden was calculated as  $[(EEM_{\text{area}} - \text{Lumen}_{\text{area}}) / EEM_{\text{area}}] \times 100$ .

As the impact of drug therapies on the atherosclerotic plaque burden and composition over time is relatively small, highly reproducible IVUS-VH measurements are essential. Despite such pivotal need for reproducibility data to address the stability of the technique, such studies are lacking. Only indirect evidence of reproducibility has been reported such as a study conducted by our group to assess the 6-month change in plaque composition with no controlled therapeutic intervention [18], and the study conducted by Kawasaki et al. who reported the intra and inter-observer variability of measurements performed using the same pullback [22].

The present study has a unique characteristic since we used two catheters of the same kind at the same time-point, thus simulating the scenario of a longitudinal study.

The main finding of the present study was that IVUS-VH measurements had an acceptable

reproducibility. As expected, compositional measurements were more variable than geometrical measurements. Nevertheless, it is noteworthy that inter-catheter differences were predominantly lower than 10%, highly correlated and showed a good agreement. Of note, necrotic core measurements, probably the most relevant component of coronary plaques and currently subject of intense research, showed an excellent inter-catheter and inter-observer agreement. This has a major importance since the temporal change of such component could potentially become an imaging endpoint of longitudinal studies. Similarly, calcium measurements, another important component of atherosclerotic plaques, showed good inter-catheter and inter-observer agreement. The relatively high inter-observer variability of some IVUS-VH variables raises some caution and should be taken into consideration when performing longitudinal studies analyzed by

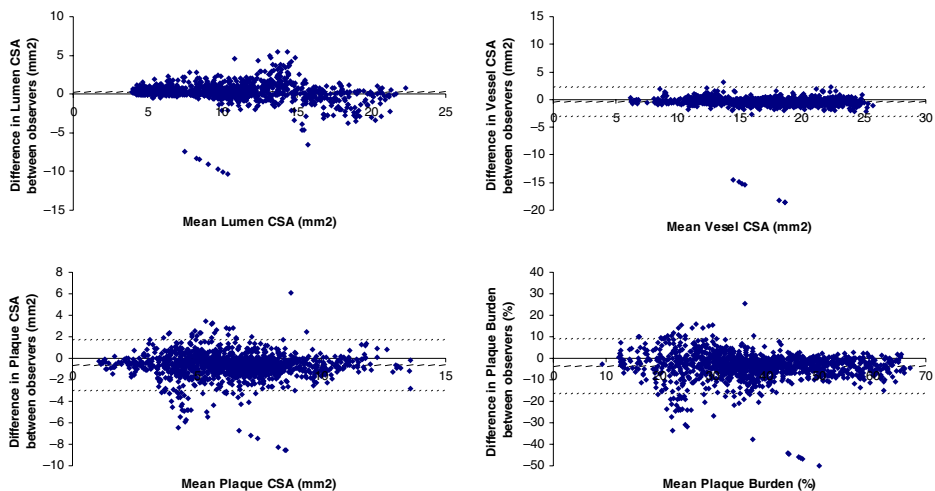


Figure 3. Bland-Altman plots showing the inter-observer agreement for geometrical measurements ( $n=1316$ ).

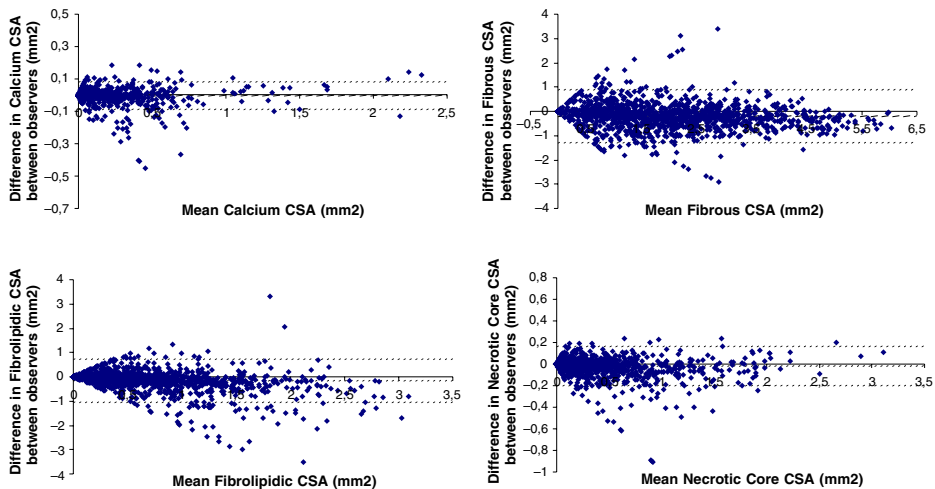


Figure 4. Bland-Altman plots showing the inter-observer agreement for compositional measurements ( $n=1316$ ).

core laboratories. Overall, the inter-catheter and inter-observer differences shown might provide boundaries over which changes are statistically significant.

It is evident yet worth mentioning that precise contour detection probably has an essential role in the reproducibility of IVUS-VH measurements. The inter-observer relative difference in plaque CSA measurements was 10%, the commonly accepted threshold. This gives an additive value to our study, since it provides a “real-world” scenario

that can aid investigators to perform precise power calculations for longitudinal studies.

Finally, although we aimed at studying non-tortuous and non-severely calcified vessels, phased-array IVUS imaging catheters are devoid from a covering sheath and pullbacks are therefore occasionally prone to be non-uniform. This clearly has an impact on determination of the size and composition of atherosclerotic plaques and needs to be taken into consideration for the design of longitudinal studies (Figure 5).

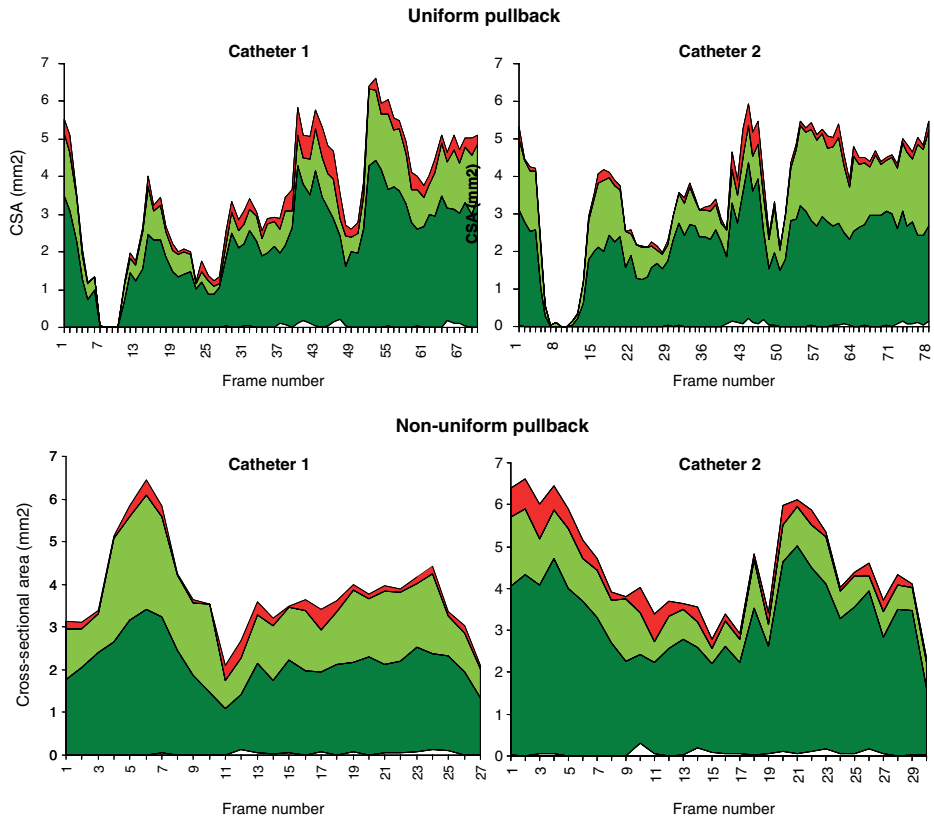


Figure 5. Sequential plotting of a matched ROI interrogated with two catheters. The mean CSA (y axis) of each plaque component is colour-coded (calcium: white, fibrous: green, fibrolipidic: greenish-yellow and necrotic core: red). This figure shows an example of the impact of non-uniform pullbacks on geometrical and compositional measurements.

Colour figures on pages 441-449

### Limitations

The studied population was relatively small. Nevertheless, the conductance of large *in vivo* studies of this nature is complicated due to obvious ethical issues. The selection of a population of patients with non-tortuous and non-severely calcified vessels was driven by the aim to study the reproducibility of the technique itself, not of the pullback device. Nevertheless, as shown in Figure 5, the impact of non-uniform pullback speed was not negligible potentially influencing the results.

### Conclusions

The present study demonstrates that the geometrical and compositional output of IVUS-VH is acceptably reproducible. In addition, by providing a “real-world” scenario, this study can aid investigators to perform precise power calculations for longitudinal studies.

### References

- Guedes A, Keller PF, L'Allier PL, Lesperance J, Gregoire J, Tardif JC. Long-term safety of intravascular ultrasound in nontransplant, nonintervened, atherosclerotic coronary arteries. *J Am Coll Cardiol* 2005; 45: 559–564.
- Wenguang L, Gussenhoven WJ, Zhong Y, et al. Validation of quantitative analysis of intravascular ultrasound images. *Int J Card Imaging* 1991; 6(3–4): 247–253.
- de Jaegere P, Mudra H, Figulla H, et al. Intravascular ultrasound-guided optimized stent deployment. Immediate and 6 months clinical and angiographic results from the Multicenter Ultrasound Stenting in Coronaries Study (MUSIC Study). *Eur Heart J* 1998; 19: 1214–1223.
- Fitzgerald PJ, Oshima A, Hayase M, et al. Final results of the Can Routine Ultrasound Influence Stent Expansion CRUISE study. *Circulation* 2000; 102: 523–530.
- Jeremias A, Huegel H, Lee DP, et al. Spatial orientation of atherosclerotic plaque in non-branching coronary artery segments. *Atherosclerosis* 2000; 152: 209–215.
- Kimura BJ, Russo RJ, Bhargava V, McDaniel MB, Peterson KL, DeMaria AN. Atheroma morphology and distribution in proximal left anterior descending coronary artery: *in vivo* observations. *J Am Coll Cardiol* 1996; 27: 825–831.
- Smits PC, Pasterkamp G, Quarles van Ufford MA, et al. Coronary artery disease: arterial remodelling and clinical presentation. *Heart* 1999; 82: 461–464.
- Nissen SE, Tsunoda T, Tuzcu EM, et al. Effect of recombinant ApoA-I Milano on coronary atherosclerosis in patients with acute coronary syndromes: a randomized controlled trial. *JAMA* 2003; 290: 2292–2300.
- Fang JC, Kinlay S, Beltrame J, et al. Effect of vitamins C and E on progression of transplant-associated arteriosclerosis: a randomised trial. *Lancet* 2002; 359: 1108–1113.
- Nissen SE, Tuzcu EM, Schoenhagen P, et al. Effect of intensive compared with moderate lipid-lowering therapy on progression of coronary atherosclerosis: a randomized controlled trial. *JAMA* 2004; 291: 1071–1080.
- Davies MJ, Richardson PD, Woolf N, Katz DR, Mann J. Risk of thrombosis in human atherosclerotic plaques: role of extracellular lipid, macrophage, and smooth muscle cell content. *Br Heart J* 1993; 69: 377–381.
- Peters RJ, Kok WE, Havenith MG, Rijsterborgh H, van der Wal AC, Visser CA. Histopathologic validation of intracoronary ultrasound imaging. *J Am Soc Echocardiogr* 1994; 7: 230–241.
- Nair A, Kuban BD, Tuzcu EM, Schoenhagen P, Nissen SE, Vince DG. Coronary plaque classification with intravascular ultrasound radiofrequency data analysis. *Circulation* 2002; 106: 2200–2206.
- Rodriguez-Granillo GA, Aoki J, Ong AT, et al. Methodological considerations and approach to cross-technique comparisons using *in vivo* coronary plaque characterization based on intravascular ultrasound radiofrequency data analysis: insights from the Integrated Biomarker and Imaging Study (IBIS). *Int J Cardiovasc Intervent* 2005; 7: 52–58.
- Rodriguez-Granillo GA, Serruys PW, Garcia-Garcia HM, et al. Coronary artery remodelling is related to plaque composition. *Heart* 2005 Jun 17; (Epub ahead of print).
- Rodriguez-Granillo GA, Garcia-Garcia H, Mc Fadden E, et al. *In vivo* intravascular ultrasound-derived thin-cap fibroatheroma detection using ultrasound radiofrequency data analysis. *J Am Coll Cardiol* 2005; 46(11): 2038–2042.
- Rodriguez-Granillo GA, McFadden E, Valgimigli M, et al. Coronary plaque composition of non-culprit lesions assessed by *in vivo* intracoronary ultrasound radio frequency data analysis, is related to clinical presentation. *Am Heart J* 2006; In press.
- Rodriguez-Granillo GA, Serruys PW, Mc Fadden E, et al. First-in-man prospective evaluation of temporal changes in coronary plaque composition by *in vivo* ultrasound radio frequency data analysis: an integrated biomarker and imaging study (IBIS) substudy. *Eurointervention* 2005; 3: 282–288.
- Bland JM, Altman DG. Statistical methods for assessing agreement between two methods of clinical measurement. *Lancet* 1986; 1: 307–310.
- Takagi T, Yoshida K, Akasaka T, Hozumi T, Morioka S, Yoshikawa J. Intravascular ultrasound analysis of reduction in progression of coronary narrowing by treatment with pravastatin. *Am J Cardiol* 1997; 79: 1673–1676.
- Schartl M, Bocksch W, Koschyk DH, et al. Use of intravascular ultrasound to compare effects of different strategies

- of lipid-lowering therapy on plaque volume and composition in patients with coronary artery disease. *Circulation* 2001; 104: 387–392.
22. Kawasaki M, Sano K, Okubo M, et al. Volumetric quantitative analysis of tissue characteristics of coronary plaques after statin therapy using three-dimensional integrated backscatter intravascular ultrasound. *J Am Coll Cardiol* 2005; 45: 1946–1953.
23. Yokoyama M, Komiyama N, Courtney BK, et al. Plasma low-density lipoprotein reduction and structural effects on coronary atherosclerotic plaques by atorvastatin as clinically assessed with intravascular ultrasound radio-frequency signal analysis: a randomized prospective study. *Am Heart J* 2005; 150: 287.

*Address for correspondence:* Patrick W. Serruys, Thoraxcenter, Bd 406, Dr Molewaterplein 40, 3015 GD, Rotterdam, The Netherlands

Tel.: +31-10-4635260; Fax: +31-10-4369154

E-mail: p.w.j.c.serruys@erasmusmc.nl





**2.4) Methodological Considerations and Approach to Cross-Technique Comparisons using In Vivo Coronary Plaque Characterization Based on Intravascular Ultrasound Radiofrequency Data Analysis: Insights From the Integrated Biomarker and Imaging Study (IBIS).**

**Int J Cardiovasc Interv. 2005;7(1):52-8.**

**Rodriguez Granillo GA, Aoki J, Ong ATL, et al**



## ORIGINAL ARTICLE

**Methodological considerations and approach to cross-technique comparisons using in vivo coronary plaque characterization based on intravascular ultrasound radiofrequency data analysis: insights from the Integrated Biomarker and Imaging Study (IBIS)**

G. A. RODRIGUEZ GRANILLO, J. AOKI, A. T. L. ONG, M. VALGIMIGLI, C. A. G. VAN MIEGHEM, E. REGAR, E. MCFADDEN, P. DE FEYTER & P. W. SERRUYS

*Erasmus Medical Center, Thoraxcenter, Rotterdam, Netherlands*

**Abstract**

Grey scale intravascular ultrasound (IVUS) is a valuable clinical tool to assess the extent and severity of coronary atheroma. However, it cannot reliably identify plaques with a high-risk of future clinical events. Serial IVUS studies to assess the progression and/or regression of atherosclerotic plaques demonstrated only modest effects, of pharmacological intervention on plaque burden, even when clinical efficacy is documented. Spectral analysis of radiofrequency ultrasound data (IVUS-virtual histology<sup>TM</sup> (IVUS-VH), Volcano Therapeutics, Rancho Cordova, CA) has the potential to characterize accurately plaque composition. The Integrated Biomarker and Imaging Study (IBIS) evaluated both invasive and non-invasive imaging techniques along with the assessment of novel biomarkers to characterize sub-clinical atherosclerosis. IVUS-VH was not included at the start of the IBIS protocol. The purpose of this paper is to describe the methodology we used to obtain and analyse IVUS-VH images and the approach to cross-correlations with the other techniques.

**Key Words:** *Intravascular ultrasound, imaging, atherosclerosis, biomarker*

**Introduction**

Atherosclerosis is a systemic disease whose clinical sequelae are unpredictable and only weakly related to its extent or severity. Atherosclerotic plaque stability appears to be influenced more by the histological composition of plaque than by stenosis severity and pathological studies have related specific coronary plaque characteristics such as the presence of a thin-cap fibroatheroma (TCFA) with a lipid-rich core, often associated with expansive remodelling, to fatal ischemic events [1–4]. However, conventional imaging techniques such as coronary angiography or intravascular ultrasonography (IVUS) cannot reliably identify such ‘high-risk’ plaques prospectively [5]. The potential of novel coronary imaging techniques to refine risk stratification is the subject of intensive research effort, reflecting the growing emphasis on preventing the ischemic consequences of coronary atherosclerosis.

A recently introduced technique (IVUS-virtual histology<sup>TM</sup> (IVUS-VH), Volcano Therapeutics, Rancho Cordova, CA) that uses the substrate (frequency domain analysis) of the IVUS radio-frequency (RF) data rather than the envelope (amplitude), has demonstrated its potential to provide an objective and accurate assessment of coronary plaque composition [6].

Serial-imaging studies, with use of IVUS, have become the preferred technique to assess the effects of pharmacological, and other, interventions designed to retard progression or induce regression of coronary atherosclerotic plaques. Such studies have shown a marked discordance between the clinical effects of validated therapies and their effects on plaque volume [7–11]. For statin therapy, it has been postulated, based on serial measurements of plaque echogenicity, that changes in plaque composition may provide an explanation for this paradox [8]. In this context, the advent of catheter-based technologies, such as IVUS-VH, that provide

the means to assess changes in plaque composition through time, are being explored in research settings.

The Integrated Biomarker and Imaging Study (IBIS) evaluated both invasive (angiography, quantitative intravascular ultrasound), IVUS based techniques (tissue echogenicity and palpography) and non-invasive (MSCT) imaging techniques in conjunction with the assessment of novel biomarkers to characterize sub-clinical atherosclerosis. IVUS-VH became available to us during the course of the IBIS protocol; the purpose of this paper is to describe the methodology we used to perform and interpret IVUS-VH, and to correlate reliably IVUS-VH findings in a predefined region of interest with findings on other imaging techniques. In addition, we tested the accuracy of the calibration of the technique.

## Methods

This pilot study was prospective, observational, single centre, and investigator-initiated. Patients with stable angina, unstable angina, non-ST segment elevation or ST segment elevation myocardial infarction, referred for percutaneous intervention, were eligible for inclusion. Major clinical exclusion criteria included significant renal dysfunction (creatinine more than 2 mg/dl), prior coronary intervention in the region of interest, life expectancy less than one year or factors that made follow-up difficult. Major imaging-related exclusion criteria included coronary anatomy that precluded safe intravascular ultrasonographic examination of a suitable region of interest or criteria that precluded acquisition of diagnostic non-invasive angiographic images (irregular heart rhythm or inability to hold breath for 20 seconds). The Medical Ethics Committee of the Erasmus University approved the study protocol and all patients gave written informed consent. The coronary study vessel, preferentially a vessel not targeted for intervention, was, in order of preference, the left anterior descending, right and circumflex coronary arteries. At the discretion of the operator, a second artery could be studied. The region of interest was defined on the basis of identifiable landmarks, such as branches or the vessel origin.

### *Intracoronary ultrasound*

The IVUS catheter used was a commercially available mechanical sector scanner (Ultracross<sup>TM</sup> 2.9F 30 MHz catheter or CVIS Atlantis<sup>TM</sup> SR Pro 2.5F 40 MHz catheter, Boston Scientific, Santa Clara, USA). Using an automated pullback device, the transducer was withdrawn at a continuous speed of 0.5 mm/second. Cine runs, before and during contrast injection, were performed to define the position of the IVUS catheter before the pullback

was started. IVUS data were acquired after the intracoronary administration of nitrates. Data were stored on S-VHS videotape. The videotapes were digitized on a computer system, transformed into the DICOM medical image standard and archived.

QCU analysis was performed by the core laboratory (Cardialysis BV, Rotterdam, The Netherlands) using validated software (Curad, version 3.1, Wijk bij Duurstede, The Netherlands). The IntelliGate<sup>TM</sup> image-based gating method was applied, to eliminate catheter-induced image artefacts, by retrospectively selecting end-diastolic frames [12]. After performing QCU, the borders of the external elastic membrane (EEM) and the lumen-intima interface enclose a volume that was defined as the coronary plaque plus media volume. Significant plaque was defined as a plaque plus media area  $\geq 50\%$  of the cross-sectional area circumscribed by the external elastic membrane (EEM).

### *Virtual histology: rationale and acquisition*

Extensive detail regarding the validation of the technique on explanted human coronary segments has previously been reported [6]. Briefly, IVUS-VH uses spectral analysis of IVUS radiofrequency data to construct tissue maps that classify plaque into four major components. In preliminary in vitro studies, four histological plaque components (fibrous, fibro-lipid, lipid-necrotic and calcium) were correlated with a specific spectrum of the radiofrequency signal [6,13]. These different plaque components were assigned colour codes. Calcified, fibrous, fibrolipidic and lipid-necrotic regions were labelled white, green, greenish-yellow and red respectively.

IVUS-VH data will be acquired using a continuous ECG-gated IVUS pullback (0.5 mm per second) with a commercially available mechanical sector scanner (Ultracross<sup>TM</sup> 2.9F 30 MHz catheter, Boston Scientific, Santa Clara, CA), by a dedicated IVUS-VH platform (Volcano Therapeutics, Rancho Cordova, CA). The IVUS VH data will be stored on a CD-ROM and sent to the imaging core laboratory for offline analysis by a single observer unaware of patient data. IVUS B-mode images will be reconstructed from the RF data by custom software (IVUSLab, Volcano Therapeutics, Rancho Cordova, CA). Subsequently, manual contour detection of both the lumen and the media-adventitia interface will be performed.

### *Calibration*

Manual calibration was performed after removal of the catheter by placing the transducer in a fluid container in the centre of a plexi-glass phantom to obtain a homogeneous echogenic radiofrequency

signal circumference around the catheter. We assessed the effect of different calibrations on the observed results for plaque composition results, within the same frozen ROIs, in 15 consecutive vessels.

#### Definitions

The tissue enclosed by the external elastic membrane and lumen-intima interface was defined as plaque+media for geometrical data and plaque. Plaque area refers to  $\text{Vessel}_{\text{area}} - \text{Lumen}_{\text{area}}$ .

#### Region of interest (ROI) identification

Ideally, we aim to study a common ROI  $\geq 30$  mm long determined by identifiable anatomic landmarks on IVUS. The IVUS-VH software (IVUSLab) allows simultaneous viewing of both the longitudinal and cross-sectional views. This facilitates accurate definition of the ROI and of specific spots within this region.

Using longitudinal (Figure 1) and cross-sectional (Figure 2) views to identify anatomical landmarks such as side branches, veins, the pericardium, and muscle strands, correlation between IVUS-VH and other technologies such as QCU and palpography can be readily accomplished.

## Correlations

### *IVUS-VH with quantitative coronary ultrasound (QCU)*

Once the ROI is visually matched with the QCU, geometrical data from both techniques can be correlated. Lumen, vessel and plaque CSA's will be assessed as well as percent area stenosis. In addition to Pearson correlation coefficients, the degree of agreement between both techniques was assessed using Bland Altman analysis plots [14].

### *IVUS-VH with palpography*

Palpography is a technique that allows the assessment of the mechanical properties (deformability) of coronary plaques by measuring the relative displacements of radiofrequency signals, recorded during IVUS acquisition, at 2 different pressure levels [15,16]. A recent in vitro study demonstrated the diagnostic potential of palpography to identify thin cap fibroatheromas [15].

We will explore the potential correlation between lipid core content and high strain pattern within matched ROIs. In addition, using the longitudinal and cross-sectional views, individual high and low strain spots can be located in the IVUS-VH software thereby allowing correlations with areas classified as predominantly ( $\geq 40\%$  of the CSA) consisting of

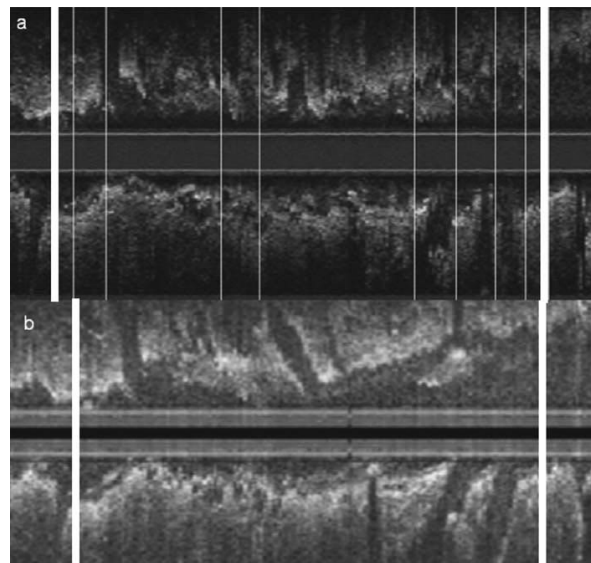


Figure 1. (a) Longitudinal view of the LAD obtained with an Ultracross™ 2.9F 30 MHz IVUS imaging catheter showing distal and proximal references of the Region of Interest (ROI) in strong lines. Thin lines correspond to sub-segmentation analysis of the ROI. (b) Longitudinal view of the same ROI displayed with the IVUS-VH software, with the same distal and proximal references.

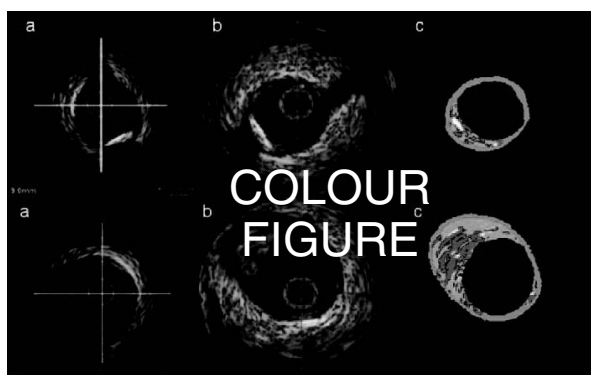


Figure 2. Upper panel: distal reference of the Region of Interest (ROI) showing the same cross-sectional area (CSA) with: (a) conventional ultrasound, (b) radiofrequency data, and (c) reconstruction of the Virtual Histology™ images, where green is fibrous tissue, greenish-yellow is fibrolipidic, red is lipid core and white is calcium. Lower panel: proximal reference of the ROI showing the same CSA with: (a) conventional ultrasound, (b) radiofrequency data, and (c) reconstruction of the Virtual Histology™ images.

fibrous or lipid core components respectively on IVUS-VH (Figure 3).

#### *IVUS-VH with blood analysis*

In addition to the correlation with novel imaging techniques, blood was obtained to perform detailed analysis of standard lipid profiles as well as classic and novel biomarkers and lipoproteins.

The mean CSA of the lipid core, a key compositional factor as it contains thrombogenic material rich in tissue factor [17], will be the main point of reference for correlation with HDL and LDL. In addition, the lipid core will also be correlated with novel pro-inflammatory markers high sensitive-C reactive protein, interleukin-6, tumour necrosis factor- $\alpha$ , and novel markers (lipoprotein phospholipase A<sub>2</sub> activity, soluble CD40 ligand, N-terminal pro-brain natriuretic peptide and matrix-metalloproteinase-9)

#### *Paired IVUS-VH*

Patients will be followed-up at six months with the same imaging and blood analysis as at baseline. Accordingly, geometrical (plaque progression/regression/remodelling index) and compositional (delta of the different components) assessments of the plaque at six-month follow-up could be performed. Changes in plaque composition will be presented in delta mean CSA for each one of the four different components.

Since the IBIS is an observational study, these results will provide some insights regarding in vivo reproducibility of the technique.

#### *IVUS-VH with multislice spiral computed tomography (MSCT)*

All scans will be performed on a 16-row detector scanner (Sensation 16, Straton, Siemens,

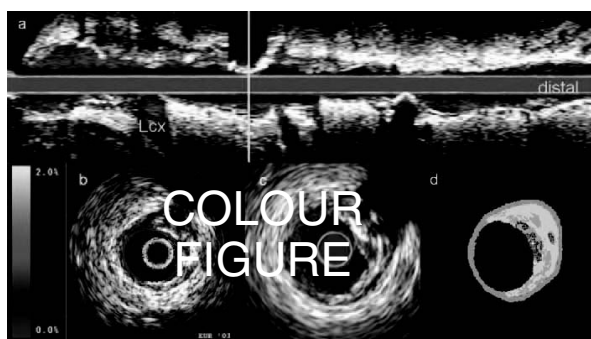


Figure 3. (a) Longitudinal view of a LAD obtained with an Ultracross™ 2.9F 30 MHz IVUS imaging catheter. The yellow line points out the cross-sectional area (CSA) of interest, and (b, c and d) respectively show palpography, conventional IVUS and Virtual Histology™ reconstruction of such CSA.

Forchheim, Germany). The region of interest will be identified on multi-planar reconstructions, based on anatomic landmarks and subdivided in 5 mm segments. The ability to detect calcium with MSCT and IVUS-VH will be assessed. Calcification in MSCT is defined by the presence of high-density components ( $> 130$  Hounsfield Unit).

#### *IVUS-VH with grey-scale tissue characterization*

With the aid of a computer-aided grey-scale value analysis program for plaque characterization [18], IVUS can also provide information on tissue characterization, therefore becoming a potential source of information on plaque composition. Accordingly, we will evaluate the correlation and agreement in the assessment of plaque characterization using RF data analysis and grey-scale IVUS.

#### *Additional correlations*

In a small subset of patients, a method based on a combination of IVUS and computational fluid dynamics that enables to calculate the regional shear stress was performed and will allow us to correlate the plaque composition with the regional shear stress [19]. IVUS-VH compositional results will also be correlated with patient's demographics.

## Results

#### *Manual calibration variability*

Manual calibration was performed after the procedure by an experienced IVUS technician. Two good quality calibrations (homogeneous echogenic radiofrequency signal circumference around the catheter) were obtained per pullback for 15 consecutive frozen (same contours) ROIs. The average difference in calcium, fibrous, fibrolipidic and lipid core volumes between calibrations for the same ROI is shown in Table 3. There were no significant difference in calcium, fibrous and fibrolipidic volumes, but there was a trend for the difference in lipid core volume.

#### *Interpretation of the results*

These results suggest that there is an imperceptible (for the naked eye) variability in the radiofrequency data between same quality calibrations. As this technology is aimed to assess changes in plaque composition, such differences could be amplified when applied to different catheters and it have a significant impact.

Therefore, to account for catheter-to-catheter variability manual calibration is currently being replaced by a technique known as 'Blind

Table 1. Geometrical output of the IVUS-VH software for:

(a) Region of interest:	
Mean lumen CSA	
Mean vessel CSA	
Mean plaque CSA	
Mean percent area obstruction	
Lumen volume	
Vessel volume	
Plaque volume	
(b) For each frame:	
Lumen CSA	
Lumen perimeter length	
Lumen maximum diameter	
Lumen minimum diameter	
Lumen eccentricity (min/max)	
Vessel CSA	
Plaque CSA	
Plaque maximum thickness	
Plaque minimum thickness	
Plaque eccentricity (min/max)	
Mean percent area obstruction	
CSA: cross-sectional area (mean). Plaque area refers to $Vessel_{area} - Lumen_{area}$ . Plaque area obstruction refers to $(Vessel_{area} - Lumen_{area}) / Vessel_{area} \times 100$ .	

Table 2. Compositional output of the IVUS-VH software for:

(a) Region of interest:	
Calcium volume ( $mm^3$ )	
Fibrous volume ( $mm^3$ )	
Fibrolipidic volume ( $mm^3$ )	
Lipid core volume ( $mm^3$ )	
(b) For each frame:	
Calcium CSA ( $mm^2$ )	
Calcium % CSA	
Fibrous CSA ( $mm^2$ )	
Fibrous % CSA	
Fibrolipidic CSA ( $mm^2$ )	
Fibro-Lipidic % CSA	
Lipid Core CSA ( $mm^2$ )	
Lipid Core % CSA	
CSA: cross-sectional area (mean).	

Table 3. Difference in plaque composition within the same frozen ROI with two same quality calibrations ( $n: 15$ ).

Volumes ( $mm^3$ ):	Mean $\Delta$ between calibrations	$p$ value
Calcium	$0.014 \pm 1.5$	NS
Fibrous	$-0.24 \pm 6.3$	NS
Fibrolipidic	$-1.24 \pm 7.73$	NS
Lipid core	$1.50 \pm 2.88$	0.06

Deconvolution'. Blind deconvolution is an iterative algorithm that deconvolves the catheter transfer function from the backscatter, thus enabling automated data normalization [20,21]. All upcoming IVUS-VH data will require such automated calibration. This algorithm will be incorporated in the IVUS-VH software and applied to the RF data for reconstruction.

## Discussion

Half of cardiac deaths in the western countries are sudden [22] and 73% of these deaths have clear evidence of plaque rupture and overlying thrombosis [23]. Non flow-limiting lesions are the most frequent substrate of culprit plaques [24]. Therefore, the detection of such plaques might have an important impact in the prevention of acute myocardial infarction and sudden cardiac death. Although angiography can identify obstructive lesions as well as complex lesions [25], this technique still only assesses the lumen of the coronaries and dismisses the significant impact of vessel remodelling as well as plaque composition. Recently, a post-mortem study evaluated the geometrical aspect of the vessel wall and showed a relationship between local alterations of vessel size and plaque stability [26]. In addition, new coming tissue characterization techniques and other catheter-based techniques with the potential of detecting features of TCFA [6,15,27,28], along with the measurement of blood biomarkers of inflammation and oxidation could aid us in the difficult task of having a multiple targeted approach for the assessment of a coronary artery. Nevertheless, there are many drawbacks for this kind of approach. Catheter-based techniques need more extensive validation and an appropriate vulnerable plaque model is yet to be developed. In addition, these techniques interrogate the coronary arteries in a localized manner, whereas inflammation is distributed throughout the whole coronary tree [29].

Plaque characterization through visual interpretation of grey-scale IVUS is poorly accurate, in particular when assessing heterogeneous, lipid-rich plaques [5]. Calcified and dense fibrous tissues usually are highly echo-reflective thus calcified areas are commonly overestimated. However, low echo-reflectance plaques are considered 'soft'. However, in addition to large amounts of extracellular lipids, the lipid core contains cholesterol crystals, necrotic debris and microcalcifications [30].

In contrast, spectral analysis of the RF data has shown potential to provide detailed quantitative information on plaque composition and it has been validated in studies of explanted human coronary segments [6].

IVUS studies have failed to conclusively demonstrate regression in plaque burden throughout time [7–11], although IVUS-VH has the potential of characterizing the vessel wall composition thereby allowing us to follow not only the progression of the disease not only in a quantitative, but also in a qualitative manner. Moreover, this tool could also be helpful in evaluating the effect of both conventional and future drug therapies.

Accordingly, a natural history study of these plaques is needed in order to understand the progression of the disease as well as the significance of the different components of the IBIS 'puzzle'.

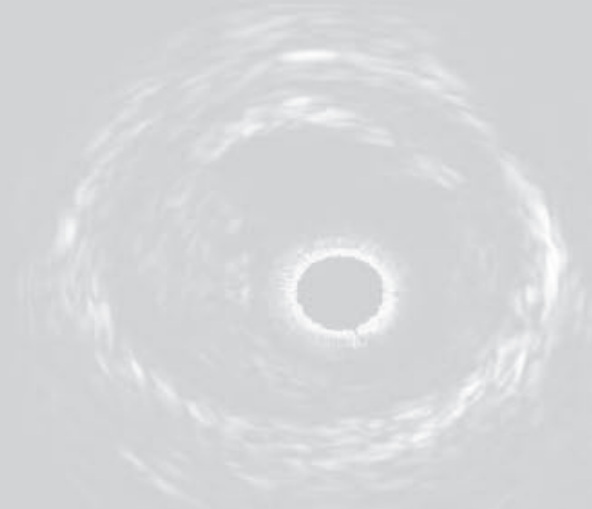
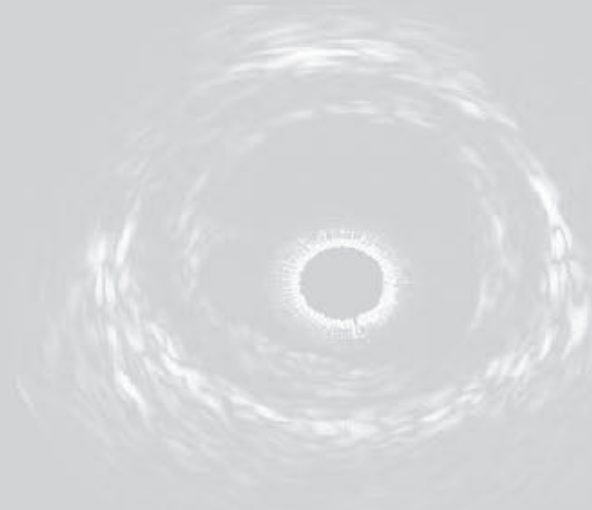
## References

- [1] Davies MJ, Richardson PD, Woolf N, et al. Risk of thrombosis in human atherosclerotic plaques: role of extracellular lipid, macrophage, and smooth muscle cell content. *Br Heart J* 1993;69:377–81.
- [2] Gertz SD, Roberts WC. Hemodynamic shear force in rupture of coronary arterial atherosclerotic plaques. *Am J Cardiol* 1990;66:1368–72.
- [3] Davies MJ, Woolf N, Rowles P, et al. Lipid and cellular constituents of unstable human aortic plaques. *Basic Res Cardiol* 1994;89(Suppl 1):33–9.
- [4] Kolodgie FD, Burke AP, Farb A, et al. The thin-cap fibroatheroma: a type of vulnerable plaque: the major precursor lesion to acute coronary syndromes. *Curr Opin Cardiol* 2001;16:285–92.
- [5] Peters RJ, Kok WE, Havenith MG, et al. Histopathologic validation of intracoronary ultrasound imaging. *J Am Soc Echocardiogr* 1994;7:230–41.
- [6] Nair A, Kuban BD, Tuzcu EM, et al. Coronary plaque classification with intravascular ultrasound radiofrequency data analysis. *Circulation* 2002;106:2200–6.
- [7] Nissen SE, Tuzcu EM, Schoenhagen P, et al. Effect of intensive compared with moderate lipid-lowering therapy on progression of coronary atherosclerosis: a randomized controlled trial. *JAMA* 2004;291:1071–80.
- [8] Schartl M, Bocksch W, Koschyk DH, et al. Use of intravascular ultrasound to compare effects of different strategies of lipid-lowering therapy on plaque volume and composition in patients with coronary artery disease. *Circulation* 2001;104:387–92.
- [9] Jensen LO, Thayssen P, Pedersen KE, et al. Regression of coronary atherosclerosis by simvastatin: a serial intravascular ultrasound study. *Circulation* 2004;110:265–70.
- [10] von Birgelen C, Hartmann M, Mintz GS, et al. Relation between progression and regression of atherosclerotic left main coronary artery disease and serum cholesterol levels as assessed with serial long-term (> or =12 months) follow-up intravascular ultrasound. *Circulation* 2003;108:2757–62.
- [11] Takagi T, Yoshida K, Akasaka T, et al. Intravascular ultrasound analysis of reduction in progression of coronary narrowing by treatment with pravastatin. *Am J Cardiol* 1997;79:1673–6.
- [12] De Winter SA, Hamers R, Degertekin M, et al. Retrospective image-based gating of intracoronary ultrasound images for improved quantitative analysis: the intelligate method. *Catheter Cardiovasc Interv* 2004;61:84–94.
- [13] Moore MP, Spencer T, Salter DM, et al. Characterisation of coronary atherosclerotic morphology by spectral analysis of radiofrequency signal: in vitro intravascular ultrasound study with histological and radiological validation. *Heart* 1998;79:459–67.
- [14] Bland JM, Altman DG. Statistical methods for assessing agreement between two methods of clinical measurement. *Lancet* 1986;1:307–10.
- [15] Schaar JA, De Korte CL, Mastik F, et al. Characterizing vulnerable plaque features with intravascular elastography. *Circulation* 2003;108:2636–41.
- [16] de Korte CL, Siervogel MJ, Mastik F, et al. Identification of atherosclerotic plaque components with intravascular ultrasound elastography in vivo: a Yucatan pig study. *Circulation* 2002;105:1627–30.
- [17] Wilcox JN, Smith KM, Schwartz SM, et al. Localization of tissue factor in the normal vessel wall and in the atherosclerotic plaque. *Proc Natl Acad Sci USA* 1989;86:2839–43.
- [18] de Winter SA, Heller I, Hamers R, et al. Computer assisted three-dimensional plaque characterization in ultracoronary ultrasound studies. *Computers in Cardiology* 2003;30:73–6.

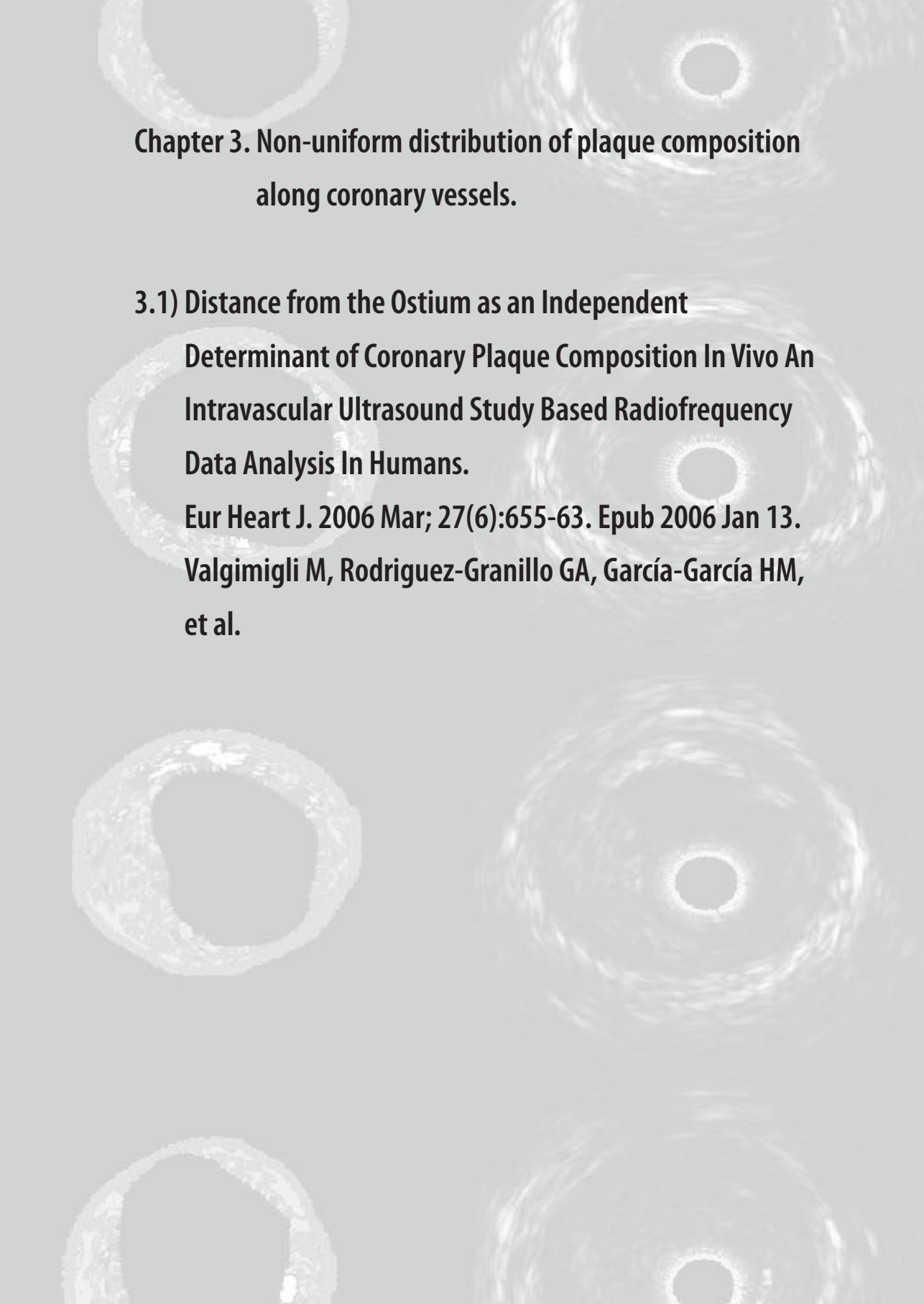
- [19] Slager CJ, Wentzel JJ, Schuurbiens JC, et al. True 3-dimensional reconstruction of coronary arteries in patients by fusion of angiography and IVUS (ANGUS) and its quantitative validation. *Circulation* 2000;102:511–6.
- [20] Kåresen K. Deconvolution of sparse spike trains by iterated window maximization. *IEEE Trans Signal Process* 1997;45:1173–83.
- [21] Kåresen KF BE. Blind deconvolution of ultrasonic traces accounting for pulse variance. *IEEE Trans Ultrason Ferroelectr Freq Control* 1999;46:564–573.
- [22] Yusuf S, Reddy S, Ounpuu S, et al. Global burden of cardiovascular diseases: part I: general considerations, the epidemiologic transition, risk factors, and impact of urbanization. *Circulation* 2001;104:2746–53.
- [23] Davies MJ. Anatomic features in victims of sudden coronary death *Coronary* 1992;85:119–24.
- [24] Ambrose JA, Tannenbaum MA, Alexopoulos D, et al. Angiographic progression of coronary artery disease and the development of myocardial infarction. *J Am Coll Cardiol* 1988;12:56–62.
- [25] Ambrose JA. Prognostic implications of lesion irregularity on coronary angiography. *J Am Coll Cardiol* 1991;18:675–6.
- [26] Pasterkamp G, Schoneveld AH, van der Wal AC, et al. Relation of arterial geometry to luminal narrowing and histologic markers for plaque vulnerability: the remodeling paradox. *J Am Coll Cardiol* 1998;32:655–62.
- [27] Moreno PR, Muller JE. Detection of high-risk atherosclerotic coronary plaques by intravascular spectroscopy. *J Interv Cardiol* 2003;16:243–52.
- [28] Jang IK, Bouma BE, Kang DH, et al. Visualization of coronary atherosclerotic plaques in patients using optical coherence tomography: comparison with intravascular ultrasound. *J Am Coll Cardiol* 2002;39:604–9.
- [29] Buffon A, Biasucci LM, Liuzzo G, et al. Widespread coronary inflammation in unstable angina. *N Engl J Med* 2002;347:5–12.
- [30] Virmani R, Kolodgie FD, Burke AP, et al. Lessons from sudden coronary death: a comprehensive morphological classification scheme for atherosclerotic lesions. *Arterioscler Thromb Vasc Biol* 2000;20:1262–75.



**PART II: ASSESSMENT OF THE EXTENT, DISTRIBUTION,  
MORPHOLOGY AND COMPOSITION OF CORONARY  
ATHEROSCLEROSIS USING INTRAVASCULAR ULTRASOUND**







**Chapter 3. Non-uniform distribution of plaque composition  
along coronary vessels.**

**3.1) Distance from the Ostium as an Independent  
Determinant of Coronary Plaque Composition In Vivo An  
Intravascular Ultrasound Study Based Radiofrequency  
Data Analysis In Humans.**

**Eur Heart J. 2006 Mar; 27(6):655-63. Epub 2006 Jan 13.  
Valgimigli M, Rodriguez-Granillo GA, García-García HM,  
et al.**



# Distance from the ostium as an independent determinant of coronary plaque composition *in vivo*: an intravascular ultrasound study based radiofrequency data analysis in humans

Marco Valgimigli, Gastón A. Rodriguez-Granillo, Héctor M. Garcia-Garcia, Patrizia Malagutti, Evelyn Regar, Peter De Jaegere, Pim De Feyter, and Patrick W. Serruys\*

Erasmus Medical Center, Thoraxcenter Bd-406, Dr Molewaterplein 40, 3015-GD Rotterdam, The Netherlands

Received 15 June 2005; revised 3 November 2005; accepted 15 December 2005

## KEYWORDS

Plaque;  
Lipid core;  
Imaging;  
Vulnerable plaque;  
Virtual histology

**Aims** Relative plaque composition, more than its morphology alone, is thought to play a pivotal role in determining propensity to vulnerability. Thus, we investigated *in vivo* whether the distance from coronary ostium to plaque location independently affects plaque composition in humans. This may help explaining the recently reported non-uniform distribution of culprit lesions along the vessel in acute coronary syndromes.

**Methods and results** In 51 consecutive patients (45 men), aged 38–76 years (mean age: 58 ± 10), a non-culprit vessel was investigated through spectral analysis of IVUS radiofrequency data (IVUS-Virtual Histology™). The study vessel was the left anterior descending artery in 23 (45%) patients; the circumflex artery in nine (18%), and right coronary artery in 19 (37%). The overall length of the region of interest, subsequently divided into 10 mm segments, was 41.5 ± 13 mm long (range: 30.2–78.4). No significant change was observed in terms of relative plaque composition along the vessel with respect to fibrous, fibrolipidic, and calcified tissue, whereas the percentage of lipid core resulted to be increased in the first (median: 8.75%; IQR: 5.7–18) vs. the third (median: 6.1%; IQR: 3.2–12) ( $P = 0.036$ ) and fourth (median: 4.5%; IQR: 2.4–7.9) ( $P = 0.006$ ) segment. At multivariable regression analysis, distance from the ostium resulted to be an independent predictor of relative lipid content [ $\beta = -0.28$  (95%CI: -0.15, -0.41)], together with older age, unstable presentation, no use of statin, and presence of diabetes mellitus.

**Conclusion** Plaque distance from the coronary ostium, as an independent determinant of relative lipid content, is potentially associated to plaque vulnerability in humans.

Coronary plaque rupture or erosion, by triggering local thrombosis is thought to play a pivotal role in the genesis of acute coronary syndromes (ACS) and sudden death.<sup>1,2</sup>

A series of landmark angiographic studies in the mid-1980s demonstrated that nearly two-thirds of all myocardial infarction originate from non-flow limiting atherosclerotic lesions and prior angiographic studies focusing on plaque morphology alone failed to identify quiescent plaques prone to rapidly progress or rupture.<sup>3–7</sup>

Consequently, the mechanical and biological properties of coronary plaques, which overall reflect plaque composition, along with systemic inflammation has mainly been targeted for the diagnosis and treatment of plaque instability.<sup>8</sup>

Epidemiological studies in patients with ST-segment elevation myocardial infarction (STEMI) report that sites of occlusion are not uniformly distributed throughout each of

the major epicardial coronary arteries but tended to cluster within the proximal third of each of the vessels.<sup>9,10</sup> Accordingly, despite the recognition that several factors involved in the pathogenesis of plaque vulnerability are widespread,<sup>11–14</sup> local trigger(s) should be also targeted to explain the presence of high-risk coronary spots.<sup>15</sup>

Plaque composition, favouring propensity to vulnerability, might also be non-uniformly distributed along each coronary vessel. This might explain the higher likelihood for plaque erosion or rupture to occur proximally in the coronary tree.

To investigate this hypothesis, the non-culprit, non-treated vessel containing angiographically non-obstructive (<50%) lesions was systematically investigated to assess plaque composition through spectral analysis of IVUS radiofrequency data [IVUS-Virtual Histology™ (IVUS-VH)] in consecutive patients referred to our institution for percutaneous coronary intervention (PCI).

Our findings support for the first time to the best of our knowledge *in vivo* the hypothesis that plaque composition

\* Corresponding author. Tel: +31 10 4635260; fax: +31 10 4369154.  
E-mail address: p.w.j.c.serruys@erasmusmc.nl

in humans may differ in relation to plaque localization along the coronary tree.

## Methods

### Study protocol and patients enrolment

This was a single-center, investigators-driven, observational prospective study aimed to evaluate the distribution of plaque composition along the coronary vessel in consecutive patients referred to our institution for elective or urgent PCI, in whom the non-culprit, non-treated vessel was judged suitable for a safe IVUS 30 mm-pullback or more, based on angiographic (absence of the following: >50% stenotic disease, extensive calcification, severe vessel tortuosity) and clinical (haemodynamic stability) findings. According to the protocol, not more than one vessel-per patient could be evaluated and the region of interest (ROI), subsequently divided into 10 mm segments, had to start from the coronary ostium. Thus, an analysable interrogated vessel length of at least 30 mm, starting from coronary ostium, was the main selection criterion, once the patient was included in the study.

In the group of patients presenting with an ACS, the culprit lesion has been categorized as complex or non-complex, based on angiographic findings as previously described.<sup>12</sup>

This protocol was approved by the Hospital Ethics Committee and is in accordance with the declaration of Helsinki. Written informed consent was obtained from every patient.

### IVUS-VH acquisition and analysis

Details regarding the validation of the technique, on explanted human coronary segments, have previously been reported.<sup>16</sup> Briefly, IVUS-VH uses spectral analysis of IVUS radiofrequency data to construct tissue maps that classify plaque into four major components. In preliminary *in vitro* studies, four histological plaque components (fibrous, fibro-lipid, lipid core, and calcium) were correlated with a specific spectrum of the radiofrequency signal.<sup>16</sup> These different plaque components were assigned colour codes. Calcified, fibrous, fibrolipidic, and lipid-necrotic regions were labelled white, green, greenish-yellow, and red, respectively.<sup>17</sup>

IVUS-VH data was acquired after intracoronary administration of nitrates using a continuous pullback (0.5 mm/s) with a commercially available mechanical sector scanner (Ultracross<sup>TM</sup> 2.9F 30 MHz catheter, Boston Scientific, Santa Clara, CA), by a dedicated IVUS-VH console (Volcano Therapeutics, Rancho Cordova, CA). The IVUS-VH data were stored on a CD-ROM and sent to the imaging core lab for offline analysis. IVUS B-mode images were reconstructed from the RF data by customized software (IVUSLab, Volcano Therapeutics, Rancho Cordova, CA).<sup>17</sup> Manual contour detection of both the lumen and the media-adventitia interface was performed and the RF data was normalized using a technique known as 'Blind Deconvolution', an iterative algorithm that deconvolves the catheter transfer function from the backscatter, thus accounting for catheter-to-catheter variability.<sup>18,19</sup>

### Statistical analysis

The sample size was calculated on the assumption that plaques located in the proximal segment of the coronary artery, defined as the first 10 mm coronary segment, would display a mean lipid content of around 40%, with a sigma of around 35% based on previous findings,<sup>20</sup> with a lipid content of 10% in the distal plaques, defined as those located beyond the first 20 mm from the coronary ostium. To detect this effect size with 80% power and a type-I error (alpha) of 0.05, 48 patients were required. Four main models were constructed based on the number of 10 mm segments that were included.

**Model 1** comprised three 10 mm segments available in all patients included.

**Model 2** comprised four 10 mm segments available in 43 patients.

**Models 3 and 4**, composed of five and six 10 mm segments in 20 and 11 patients, respectively, were considered as exploratory analysis because of limited sample size.

Values are expressed as mean  $\pm$  SD and median and inter-quartile range (IQR) as appropriate.

As all cross-sectional areas (CSA) provided by IVUS analysis, were shown to have a non-normal distribution at Kolmogorov-Smirnov goodness-of-fit test, they were log-transformed before analysis. Similarly, to all percentages relative to stenosis rate and plaque composition were applied an arcsin transformation.<sup>21</sup> Comparisons between the two groups were performed with the Student's *t*-test. Fisher's exact test was used for categorical variables. Comparisons among 10 mm segments were accomplished through a general linear mixed model with a compound symmetry correlation structure and the intercept as only random effect. Maximum likelihood method was adopted to estimate parameters in the models. Linear contrasts were applied to evaluate effects of distance, analysed as dummy variable, on the studied parameters. *Post hoc* comparisons were systematically performed by Turkey honest significance difference test.<sup>22</sup>

Because of limited statistical power in models 3 and 4, the multi-variable analysis regarding both clinical presentation and plaque location along the vessel, along with the interaction between the two was restricted to models 1 and 2.

In order to establish the determinants of lipid relative content in the plaques in our model and confirm distance from the coronary ostium as an independent predictor of relative lipid content, a univariate (including age, sex, history of hypertension, hypercholesterolaemia, cardiovascular disorders in the family, diabetes mellitus, levels of LDL, HDL, and triglycerides, use of statin, coronary vessel analysed, clinical presentation, and distance for the ostium stratified into 10 mm segments) and multivariable (with all variables showing a *P*-value of  $\leq 0.1$  at univariate analysis) linear mixed model using percentage of lipid content in all 10 mm segments, analysed as outcome variable, was also applied.

All statistical tests were two-tailed. Probability was significant at a level of  $< 0.05$ . Statistical analysis was performed using Statistica 6.1 Software (Statsoft Inc.) and R-language (R Foundation).

## Results

From 16 April 2003 to 10 September 2004, 67 patients were prospectively included in the protocol. Sixteen patients were subsequently excluded from the final analysis because of short ( $< 30$  mm) IVUS pullback in 10, poor IVUS quality in two and lack of coronary plaque at IVUS investigation in four patients. Thus, 51 patients (45 men), aged 38–76 years (mean age:  $58 \pm 10$ ) constituted the final patient population. Their baseline characteristics are provided in *Table 1*. Overall, 33 patients were affected by stable angina (SA), whereas the remaining 18 patients were admitted to hospital because of a non-ST-elevation ACS. In the SA group, the mean Cardiovascular Canadian Score was  $2 \pm 1$ , whereas the TIMI risk score, the percentage of patients with troponin T above upper limit of normal ( $0.02 \mu\text{g/L}$ ) and the delay from symptoms onset to PCI were  $4 \pm 2$ , 56% and  $4 \pm 3$  days in the ACS group, respectively. In the ACS group, the culprit lesion was located in the proximal coronary segments in 13 (72%) patients, including 6 (33%) in the left anterior descending artery (LAD), four (22%) in the circumflex artery (CFX), and three (17%) in the right coronary artery (RCA), while in the remaining five (28%) patients the culprit lesion was located in the mid or distal segment of the coronary vessels. Overall, 11 out of 18 identified culprit lesions in the ACS group satisfied the criteria for complex lesions

**Table 1** Study population

Variables	Patients		
	All (n = 51)	SA Group (n = 33)	ACS Group (n = 18)
Age (years)	58 ± 10	56 ± 12	59 ± 9
Males, no. (%)	45 (88)	28 (85)	16 (94)
Weight (kg)	80 ± 9	80 ± 8	81 ± 9
Height (cm)	174 ± 7	174 ± 7	175 ± 8
BMI (kg/m <sup>2</sup> )	27 ± 4	27 ± 3	28 ± 5
Diabetes, no. (%)	12 (23)	8 (24)	4 (22)
Hypertension, no. (%)	20 (39)	14 (42)	6 (33)
Current smokers, no. (%)	19 (37)	13 (39)	6 (33)
Previous smoker, no. (%)	16 (31)	9 (27)	7 (39)
Medical history, no. (%)			
CABG	3 (6)	2 (6)	1 (6)
PCI	11 (22)	8 (24)	3 (17)
ACS	23 (45)	18 (54)	5 (28)
Medical treatment at entry, no. (%) <sup>a</sup>			
Aspirin	51 (100)	33 (100)	18 (100)
Clopidogrel	51 (100)	51 (100)	18 (100)
Statin	38 (75)	25 (76)	13 (72)
ACE-inhibitor	40 (78)	30 (91)	10 (56)
β-Blocker	48 (94)	32 (97)	16 (89)

Plus-minus values are means ± SD. BMI, Body mass index; CABG, coronary artery bypass grafting; ACE, angiotensin converting enzyme.

The SA group was well matched (*P*-value >0.3) with the ACS group with respect to all variables reported earlier.

<sup>a</sup>For this analysis we considered all medications administered in the previous 4 or more days. At discharge all patients except one were taking statins.

based on angiographic findings. The study vessel was the LAD artery in 23 (45%) patients, the CFX in nine (18%), and RCA in 19 (37%). The overall length of the ROI was 41.5 ± 13 mm long [(range: 30.2–78.4) (41 ± 13 in SA group vs. 42 ± 13 in ACS group, *P* = 0.6)]. The results regarding quantitative coronary IVUS analysis in the whole population, stratified into 10 mm vessel length (paired-segment analysis), are reported in Table 2. Lumen CSA significantly decreased every 10 mm in model 1, whereas this happened starting from the third segment, as compared with first coronary tract, in model 2.

As compared with ostial 10 mm segment, vessel CSA resulted to be decreased in the third and fourth segment in models 1 and 2, respectively, whereas plaque CSA reduction reached statistical significance only in the fourth segment of model 2. Distance from the coronary ostium did not affect the percentage of stenosis. The third and fourth models, restricted to a progressively lower number of patients but based on a longer vessel length, mainly confirmed the trends observed in the first two models.

### Change in plaque composition along the study vessel

The results regarding quantitative coronary plaque composition analysis are reported in Table 3.

Fibrous tissue was the most prevalent component of plaque composition in each 10 mm segment throughout the four models considered, followed by fibrolipidic tissue, lipidic core, and calcium.

No significant change was observed in terms of relative plaque composition passing from the most proximal to those progressively more distally located segments along the vessel with respect to fibrous, fibrolipidic, and calcified tissue. Conversely, the percentage of lipid core resulted to be increased in the first [(mean: 13%; 95%CI: 10, 16), (median: 8.75%; IQR: 5.7, 18)] with respect to the third segment [(mean: 8.7%; 95%CI: 6.5, 11), (median: 6.2%; IQR: 2.6, 12.1)] in model 1 (*P* < 0.05; primary endpoint) and to third [(mean: 8.4%; 95%CI: 6, 11), (median: 6.1%; IQR: 3.2–12)] (*P* < 0.05) and fourth [(mean: 6.8%; 95%CI: 4, 9.6), (median: 4.5%; IQR: 2.4–7.9)] (*P* < 0.01) segment in model 2 (Figure 3). A similar shift in relative plaque composition along the vessel was observed in models 3 and 4. Interestingly, ACS patients presenting with the culprit lesion located in the proximal segment of the coronary artery did not differ in terms of relative plaque distribution along the vessel with respect to those with culprit lesion sited in the mid of distal tract.

### Clinical presentation and change in plaque composition along the study vessel

No significant change in calcium content with respect to clinical presentation (stable vs. unstable) was observed (data not shown). In model 1, fibrous plaque content was overall significantly increased in stable (68%) [95%CI: 65%, 71%] vs. unstable (63%) [95%CI: 59%, 64.7%] group, whereas a decrease in stable (17%) [95%CI: 16%, 19%] vs. unstable (22%) [95%CI: 20%, 24%] patients was observed for

**Table 2** Quantitative vessel analysis at IVUS

Coronary segments	Mean cross-sectional areas (mm <sup>2</sup> )			Stenosis (%)
	Lumen	Vessel	Plaque	
<b>Model 1; n = 51</b>				
1° (0–10 mm)	9.4 ± 3.6	17.1 ± 8.1	7.3 ± 3.7	41.4 ± 10.5
2° (10–20 mm)	7.8 ± 2.9 <sup>†</sup>	15.7 ± 7.8	7.2 ± 3.4	46 ± 12
3° (20–30 mm)	7.1 ± 2.8 <sup>‡</sup>	14.2 ± 8 <sup>‡</sup>	6.2 ± 2.7	45 ± 11
P-value	0.002	0.01	0.12	0.08
<b>Model 2; n = 43</b>				
1° (0–10 mm)	9.3 ± 3.6	17.4 ± 8.6	7.6 ± 3.9	42 ± 11
2° (10–20 mm)	7.7 ± 2.7	15.9 ± 8.2	7.3 ± 3.5	46 ± 12
3° (20–30 mm)	7 ± 2.6 <sup>*</sup>	14.5 ± 8.7	6.3 ± 2.8	45 ± 11.2
4° (30–40 mm)	6.4 ± 2.7 <sup>‡</sup>	13.5 ± 9.7 <sup>‡</sup>	6 ± 3.4 <sup>†</sup>	45.3 ± 12.4
P-value	0.0002	0.001	0.02	0.4
<b>Model 3; n = 20</b>				
1° (0–10 mm)	10.4 ± 4.3	20.5 ± 11.5	9 ± 5.2	39.8 ± 10.5
2° (10–20 mm)	8.8 ± 2.8	19 ± 11	8.2 ± 4.7	41.7 ± 12
3° (20–30 mm)	8 ± 2.9	17.4 ± 12	6.9 ± 3	42 ± 10
4° (30–40 mm)	7.3 ± 3.2	16.5 ± 13.3	6.8 ± 4.2	42 ± 12
5° (40–50 mm)	7 ± 2.9	16.2 ± 15	5.7 ± 2.3	41 ± 11.4
P-value	0.07	0.12	0.054	0.98
<b>Model 4; n = 11</b>				
1° (0–10 mm)	10.7 ± 2.8	19.3 ± 2.7	8.6 ± 2.1	45 ± 7.8
2° (10–20 mm)	9.3 ± 3.7	18 ± 4	8.6 ± 2.4	49 ± 10
3° (20–30 mm)	8.6 ± 2.3	16.8 ± 4.6	8.2 ± 2.4	48 ± 8.3
4° (30–40 mm)	8.3 ± 2.2	17.1 ± 5	8.8 ± 2.8	51 ± 5.7
5° (40–50 mm)	7.5 ± 2.5	15.3 ± 4.9	7.8 ± 2.6	51.3 ± 4.8
6° (50–60 mm)	6.7 ± 2.6 <sup>†</sup>	13 ± 4	6.2 ± 2	48.3 ± 9.7
P-value	0.023	0.06	0.063	0.4

<sup>\*</sup>P < 0.01; <sup>†</sup>P < 0.05; <sup>‡</sup>P < 0.001 as compared with segment 1 at *post hoc* analysis. Results are given as mean ± SD.

fibrolipid content when all 227 segments were pooled together ( $P = 0.03$  and  $P = 0.006$ , respectively). However, when distance from the ostium, stratified into 10 mm segments, was also inserted into the model, only trends towards increase in fibrous and decrease in fibrolipid content in stable vs. unstable patients were observed, which did not reach statistical significance. This was confirmed in model 2. In contrary, even when analysed simultaneously, both plaque location along the vessel ( $P = 0.044$  and  $P = 0.002$  for models 1 and 2, respectively) and clinical presentation (stable vs. unstable) ( $P = 0.01$  and  $P = 0.004$  for models 1 and 2, respectively) resulted to be independent predictors of lipid content (Figures 1B and 2B) after adjustment for age, sex, diabetic status, type of coronary artery analysed, and use of statin. Finally, in order to evaluate whether the shift in lipid content along the vessel was influenced by clinical presentation, the interplay between these two main determinants of lipid content was investigated, but no statistical interaction emerged between plaque location and lipid core content ( $P = 0.8$  and  $P = 0.49$  for models 1 and 2, respectively).

#### Distance from the ostium as an independent predictor of lipid content

In Table 4 the variables found to be associated to the relative lipid content along the vessel are shown. The lipid

core in the most distally located coronary segment (segment 3) in the model 1 was significantly lower compared with segment 1, taken as a reference, independently from all other identified predictors. When all 227 segments were included in the model, distance from the ostium, stratified into 10 mm segments, resulted to be an independent predictor of relative lipid content along vessel wall, together with older age, unstable presentation, no use of statin, and the presence of diabetes mellitus. In keeping with the results obtained at the *post hoc* analysis, after adjusting for clinical presentation, relative lipid content in segment 1 did not differ from segment 2 [ $\beta -0.08$  (95%CI:  $-0.28, 0.116$ )], while it did so starting from segment 3 [ $\beta -0.22$  (95%CI:  $\beta 0.39, \beta 0.05$ )], with a progressively lower  $\beta$ -value for segment 4 [ $\beta -0.34$  (95%CI:  $-0.39, -0.05$ )] and 5 [ $\beta -0.38$  (95%CI:  $-0.55, -0.21$ )].

#### Discussion

Several lines of research in the last decades have clearly pointed out how factors involved in pathogenesis and progression of atherosclerotic lesions are widespread throughout the circulatory bed.<sup>8,11,12,14,23,24</sup>

As a corollary to this, evidence that a single pharmacological or mechanical treatment, when applied locally, is able to affect progression of coronary atherosclerosis is weak and not conclusive.<sup>25</sup> On the other hand, systemic

**Table 3** Plaque composition stratified into 10 mm segments

Coronary segments	Plaque composition (%)			
	Calcium	Fibrous	Fibrolipidic	Lipid core
<b>Model 1; n = 51</b>				
1 <sup>†</sup> (0–10 mm)	0.69 (0.26–1.98)	67.1 (60–74.4)	16.86 (11.2–24)	8.8 (5.7–18)
2 <sup>†</sup> (10–20 mm)	0.67 (0.3–1.58)	68.3 (60–77)	18.1 (12.7–23.1)	9.6 (4.3–15.1)
3 <sup>†</sup> (20–30 mm)	0.79 (0.37–1.82)	69 (64–78)	18.7 (13.4–25.3)	6.2 (2.6–12.1)*
P-value	0.67	0.40	0.84	0.039
<b>Model 2; n = 43</b>				
1 <sup>†</sup> (0–10 mm)	0.76 (0.28–2.3)	64.7 (59.3–74)	17.7 (13.4–24.5)	8.01 (5.7–18)
2 <sup>†</sup> (10–20 mm)	0.70 (0.4–1.58)	66.9 (57.9–77)	18.6 (14–24.4)	10 (4.2–16.7)
3 <sup>†</sup> (20–30 mm)	0.75 (0.37–1.82)	69 (63.9–77.8)	19.8 (14.3–25.4)	6.1 (3.5–12)*
4 <sup>†</sup> (30–40 mm)	0.48 (0.09–1.5)	68.7 (60.8–75)	21.1 (17–28.2)	4.5 (2.4–8) <sup>†</sup>
P-value	0.36	0.55	0.63	0.0058
<b>Model 3; n = 20</b>				
1 <sup>†</sup> (0–10 mm)	0.77 (0.5–2.6)	71.4 (49.7–76.4)	17.3 (13.4–23.7)	8 (6–25)
2 <sup>†</sup> (10–20 mm)	0.49 (0.18–1.15)	72.3 (57.9–79.59)	17.2 (100–22.7)	9.3 (4.1–14.6)
3 <sup>†</sup> (20–30 mm)	0.87 (0.1–2.4)	69.3 (61.1–79.6)	17.4 (13.1–25.3)	6.8 (4.1–12)
4 <sup>†</sup> (30–40 mm)	0.9 (0.2–2.6)	67.8 (57.1–77.6)	19.1 (17.4–30)	6.1 (3–8.3)
5 <sup>†</sup> (40–50 mm)	0.65 (0–1)	75.3 (60.6–81.4)	16.4 (14.5–32.6)	3.5 (0.7–5.8)*
P-value	0.14	0.8	0.71	0.039
<b>Model 4; n = 11</b>				
1 <sup>†</sup> (0–10 mm)	0.3(0.2–1.6)	74.1 (61–79)	20.8 (16–28)	5.97 (2.25–12)
2 <sup>†</sup> (10–20 mm)	0.8 (0.4–1)	74 (64–79)	20.5 (18–22)	5.7 (3–13)
3 <sup>†</sup> (20–30 mm)	0.54 (0.13–1.6)	75.1 (70–80)	18.5 (16.8–22)	5 (2.8–6.5)
4 <sup>†</sup> (30–40 mm)	0.63 (0.1–1.8)	75.7 (66–77)	21 (20–27)	3.4 (92.4–5.7)
5 <sup>†</sup> (40–50 mm)	0.38 (0.1–1.3)	73.1 (67–81)	21.2 (15–27)	3.2 (2.7–5.3)
6 <sup>†</sup> (50–60 mm)	0.37 (0–0.8)	77.3 (66–79)	24 (19–28)	2.7 (1–4.3)*
P-value	0.65	0.78	0.78	0.036

\*  $P < 0.05$ ; <sup>†</sup> $P < 0.01$  as compared with segment 1 at *post hoc* analysis. Results are given as median (IQR).

therapy, such as an intensive lipid-lowering treatment, has been convincingly shown to be able to stop atherosclerotic disease progression and even induce coronary lesions regression in some studies.<sup>26–30</sup> The same paradigm is thought to be true for factors involved in atherosclerotic lesions vulnerability, albeit probably in a more elusive way.<sup>25</sup>

These findings should be combined, however, with the evidence provided by recent epidemiological studies, which corroborate the hypothesis according to which sites of occlusions are not uniformly distributed throughout the coronary tree, rather they show a tendency to cluster in partially predictable hot spots located within the proximal third of each coronary vessels.<sup>9,10</sup>

Thus, the interplay among systemic and local factors able to promote progression and vulnerability of atherosclerotic coronary lesions should be probably both targeted in the attempt to control the chronic and acute consequences of coronary atherosclerosis.<sup>15</sup>

Among local factors known to affect genesis and progression of coronary atherosclerotic lesions, shear stress (SS) has been extensively investigated.

Fluid SS, acting on genes 'sensitive' to local haemodynamic forces, is known to elicit a large number of humoral, metabolic, and structural responses in endothelial cells (EC).<sup>31</sup> Low SS on ECs partially explains the local arterial susceptibility to atherosclerosis, as low SS

enhances the oxidation of lipids and their accumulation in the intima.<sup>31,32</sup>

Moreover, fluid turbulence in itself is able to directly activate platelets, thus possibly playing a pivotal role in thrombogenesis as well.<sup>33</sup>

It is tempting to speculate that other local factors could play additional roles in modulating progression and instability of atherosclerotic lesions in coronary arteries. Among them, pathological studies have suggested that the distribution of thin-cap atheromas, which are lipid rich core plaques known to be at particularly high-risk for rupture, are not uniformly distributed along the coronary vessels in post-mortem examinations.<sup>34</sup> Rather, they cluster in the proximal segments of the three main coronary arteries, which is in keeping with the longitudinal distribution of both ruptured and healed plaques.<sup>34</sup>

This non-uniform distribution of vulnerable plaques in humans could partially explain the clustering of occlusive culprit lesion in the proximal or middle tract of coronary arteries. In this regard, we hypothesized that plaque composition was also not uniformly distributed *in vivo* in humans in patients with symptomatic coronary disease. Thanks to a recently developed technology based on spectral analysis of IVUS radiofrequency data (IVUS-VH),<sup>16,17</sup> we prospectively evaluated whether plaque composition is independently affected by the distance from coronary ostium in a

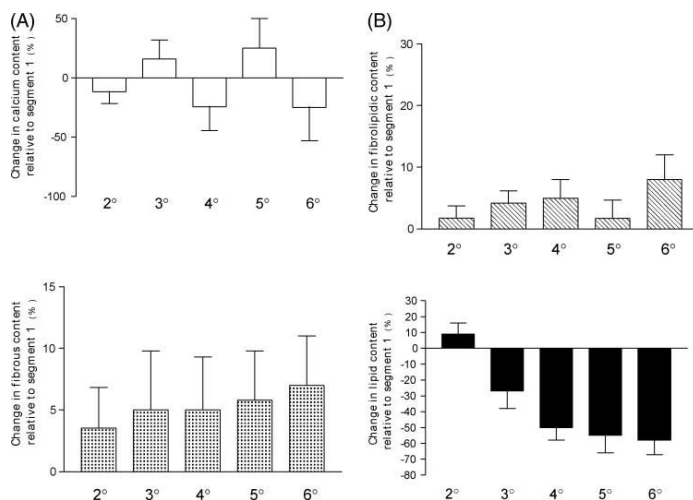


**Figure 1** Relative change in plaque composition with respect to segment 1. Starting from segment 3, relative lipid content showed a progressive decrease with respect to ostial segment (segment 1) taken as a reference. Relative changes in segments 2 and 3 were calculated using model 1, whereas for the relative change in segments 4, 5, and 6, models 2, 3, and 4 were employed, respectively. All relative changes are expressed as mean value and standard deviation.

consecutive series of patients. Our findings support the concept that coronary plaques located in the proximal tract ( $\approx 20$  mm) of coronary vessels are relatively richer in lipid content with respect to those more distally located, independently from clinical presentation. In this regard, the magnitude of lipid content appeared to be relatively higher in patients presenting with clinical instability but no interaction emerged in our model between clinical presentation and lipid content, suggesting that the relative change in plaque composition along the vessel is a well-preserved phenotype in both groups of patients. Moreover, distance from the coronary ostium resulted to be an independent predictor of relative lipid content along the vessel wall in our regression model, together with age, unstable presentation, presence of diabetes mellitus, and no use of statin.

Our current findings should be regarded as an attempt to extend the pathophysiological knowledge on plaque vulnerability, mainly because of the well-known linkage between plaque composition and risk of plaque rupture or erosion.<sup>34–36</sup> Thus, this might contribute to explain the higher likelihood for plaque erosion or rupture to occur proximally in the coronary tree. Moreover, the finding that coronary plaques show a relatively higher lipid content if proximally located along the longitudinal axis of the vessel with respect to those more distally located might elicit new methodological issues in future investigations. In particular, hypothesizing that plaque progression/regression studies accomplished through aggressive lipid-lowering regimen would mainly affect the lipid content in the plaque, it seems reasonable to believe that the relative effect of the tested medication observed at IVUS investigation in terms of overall plaque CSA, could differ in relation to the localization of ROI

with respect to the coronary ostium. This could bear special hazard particularly in those studies having limited ROI length.<sup>37</sup>

An interesting finding of our study was that the percentage of stenosis did not differ in relation to the distance from the ostium, whereas plaque area was progressively smaller moving from proximal to distal segments. This might be explained by the interplay between the physiological proximal–distal tapering of the coronary vessel and the higher propensity of the proximal segments to undergo positive remodelling with respect to those located more distally. This seems to be in keeping with our recent findings that positive remodelling is indeed more pronounced in lipid-rich coronary segments.<sup>38</sup>

### Limitations of the study

As exploratory-pilot investigation, our current findings should be regarded as provisional. In particular, to assess relatively minor changes in plaque composition along longitudinal vessel axis, such as that observed for fibrous tissue, or for highly dispersed data such as for relative calcium content, a bigger, properly powered, sample size is clearly needed. Similarly, the observed insignificant trends for fibrous tissue to be increased and fibrotipidic content to be decreased in stable vs. unstable patients may reflect a type-II error. Our results mainly apply to the first 40 mm of the three main coronary arteries, whereas the longitudinal pattern of shift in coronary plaque composition in coronary segments more distally located or in left main coronary artery should be evaluated in studies specifically designed for such an aim. In particular, in keeping with our primary endpoint, the only comparison for which this study was properly powered for is the one between the first and the

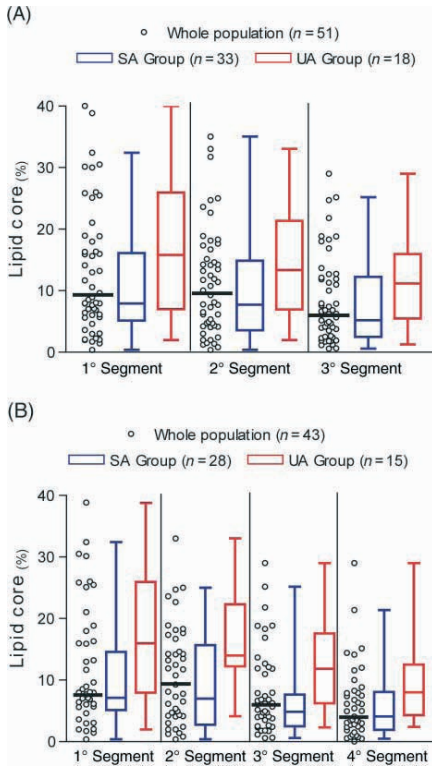


**Figure 2** Per-segment distribution of relative lipid content in the study population. Per-segment distribution of relative lipid contents both in the whole population and stable vs. unstable patients in model 1 (A) and 2 (B). Bars indicate median values in the whole population. As shown in Table 3, relative lipid content significantly decreased in the whole population in segment 3 in model 1 and in segments 3 and 4 in model 2 with respect to segment 1 at *post hoc* analysis.

third segment in model 1. All other analyses, including the tests for four models and all *post hoc* comparisons should be regarded as exploratory. Despite careful examination of all angiograms, we cannot completely rule out the possibility that patients with a higher number of IVUS interrogated 10 mm segments had a more favourable coronary anatomy as compared with those in whom a long pull-back could not be obtained.

Relevant to this point, it is the fact that: (i) plaque composition in the first three coronary segments did not differ in patients with 30 mm pull back length as compared with those in whom a longer IVUS pull back was obtained; and (ii) the change in plaque composition along the study vessel was remarkably consistent in all the four models analysed.

We failed to find sex-related differences in the proximal-distal pattern of plaque composition. However, the great majority (88%) of patients enrolled were males, which

**Table 4** Predictors of plaque lipid content at uni- and multivariate analysis in model 1

Variables	Beta-values (95% CI)	P-values
<b>Univariate analysis</b>		
Age (years)	-0.12 -0.25, 0.008	0.069
Sex (M vs. F)	0.029 -0.101, 0.16	0.66
Smoking status	0.022 -0.108, 0.15	0.7
<b>Previous history of</b>		
Hypertension	0.048 -0.08, 0.16	0.48
CVD in the family	-0.038 -0.16, 0.082	0.56
Hypercholesterolaemia	0.08 -0.032, 0.197	0.21
Diabetes mellitus	0.14 0.023, 0.257	0.041
ACS	0.044 -0.086, 0.174	0.50
Coronary revascularization	-0.15 -0.2, -0.028	0.02
Coronary vessel <sup>a</sup>	0.038 -1.93, 2.008	0.5
ACS at presentation	0.25 0.11, 0.39	0.0032
LDL (mg/dL)	0.09 -0.04, 0.22	0.42
HDL (mg/dL)	-0.12 -0.25, 0.01	0.067
Triglycerides (mg/dL)	0.04 -0.09, 0.17	0.78
Use of statin	-0.25 -0.37, -0.12	0.0001
Distance from ostium <sup>b</sup>	-0.32 -0.45, -0.30	<0.0001
<b>Multivariable analysis<sup>c</sup></b>		
Distance from ostium <sup>b</sup>	-0.28 -0.15, -0.41	<0.0001
Age (years)	-0.26 -0.12, -0.40	0.0004
ACS at presentation	0.16 0.03, 0.29	0.005
Use of statin	-0.18 -0.36, 0.004	0.057
Diabetes mellitus	0.21 0.07, 0.34	0.003
Coronary revascularization	-0.07 -0.02, 0.12	0.46
HDL (mg/dL)	-0.02 -0.05, 0.21	0.84

CVD, cardiovascular disease; LDL, low-density lipoprotein; HDL, high-density lipoprotein.

<sup>a</sup>Analysed as left anterior descending vs. circumflex vs. right coronary artery

<sup>b</sup>Analysed as segment 1 taken as a reference vs. segment 3.

<sup>c</sup>Adjusted R<sup>2</sup> = 0.36 for the model.

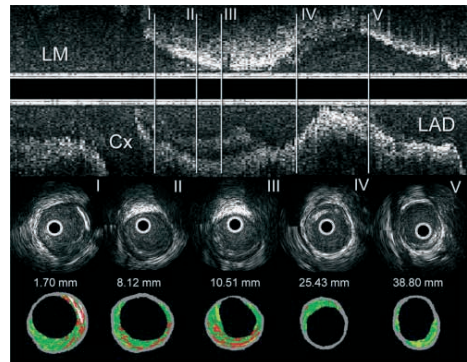


**Figure 3** IVUS-VH CSA along a coronary vessel. IVUS-VH cross-sectional areas in a representative patient showing the change in plaque composition (calcium: white; fibrous: green; fibrolipidic: greenish-yellow; and lipid core: red) along the longitudinal axis of the vessel. LM, left main coronary artery; CFX, circumflex artery; LAD, left anterior descending artery. The distance between the cross-sectional area and the ostium of the vessel is reported in millimetres (mm).

Colour figures on pages 441-449

calls for future studies with more balanced sex-distribution to properly address this gender issue.

Finally, it should not undergo unnoticed that the proportion of lipid core content predicted by our multi-variable regression model, despite highly significant, was far from being optimal. This means that future investigations should probably aim to increase the capability to predict relative lipid content in coronary plaques taking a broader set of possible independent predictors into account.

## Conclusion

Our study provides proof of concept for a non-uniform longitudinal distribution of plaque composition mainly in terms of lipid core content along the main coronary arteries *in vivo* in humans. The clinical and pathophysiological meaning of this observation and whether it could help explaining the non-uniform distribution of vulnerable plaques along the coronary vessel remains unclear. Future studies are needed to extend and possibly confirm our current findings.

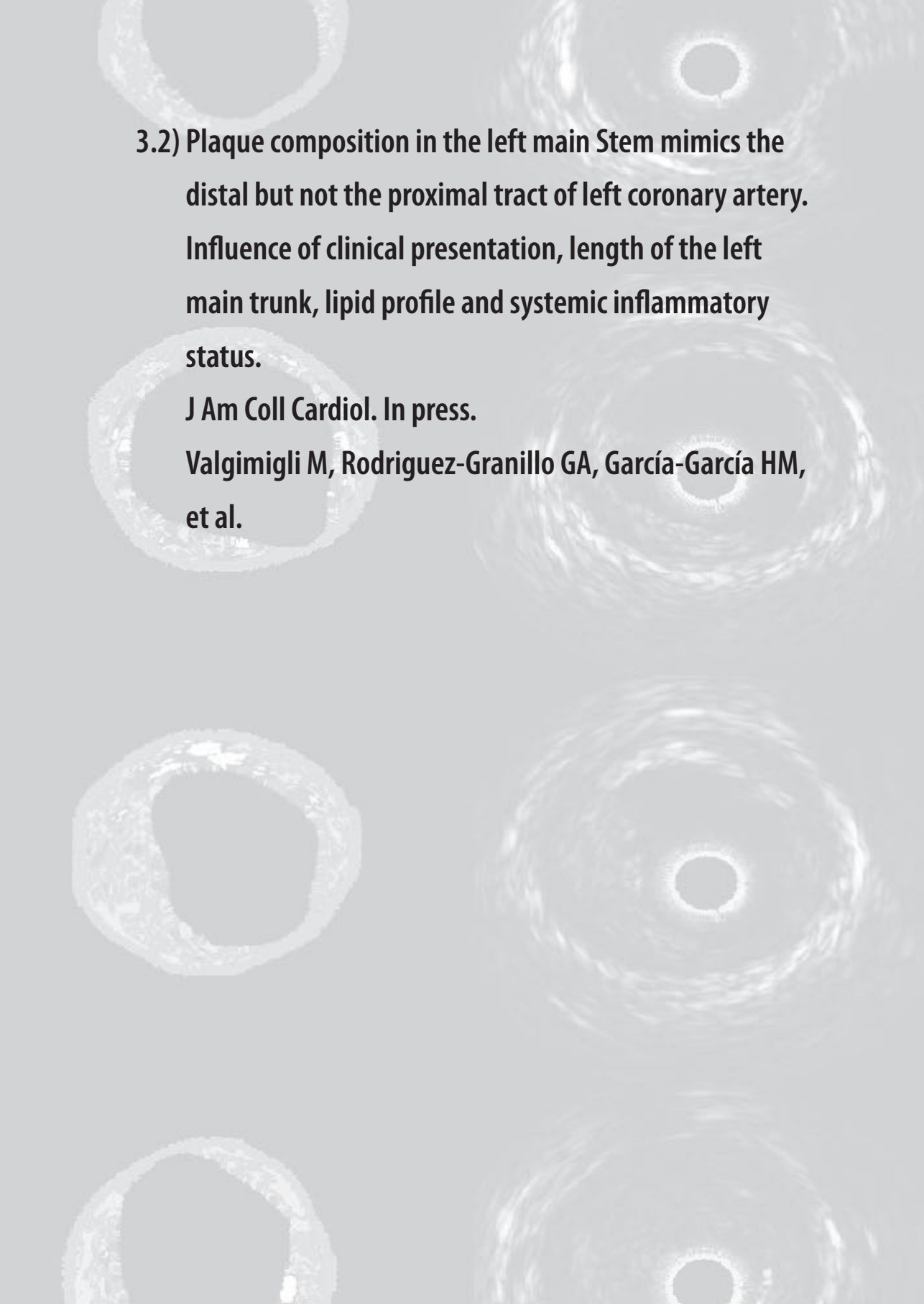
**Conflict of interest:** none declared.

## References

- Burke AP, Farb A, Pestaner J, Malcom GT, Zieske A, Kutys R, Smialek J, Virmani R. Traditional risk factors and the incidence of sudden coronary death with and without coronary thrombosis in blacks. *Circulation* 2002;105:419-424.
- Shah PK. Mechanisms of plaque vulnerability and rupture. *J Am Coll Cardiol* 2003;41:155-225.
- Ambrose JA, Tannenbaum MA, Alexopoulos D, Hjemedahl-Monsen CE, Leavy J, Weiss M, Borrico S, Gortin R, Fuster V. Angiographic progression of coronary artery disease and the development of myocardial infarction. *J Am Coll Cardiol* 1988;12:56-62.
- Giroud D, Li JM, Urban P, Meier B, Rutishauer W. Relation of the site of acute myocardial infarction to the most severe coronary arterial stenosis at prior angiography. *Am J Cardiol* 1992;69:729-732.
- Hackett D, Davies G, Maseri A. Pre-existing coronary stenoses in patients with first myocardial infarction are not necessarily severe. *Eur Heart J* 1988;9:1317-1323.
- Lichtlen PR, Nikutta P, Jost S, Deckers J, Wiese B, Rafflenbeul W. Anatomical progression of coronary artery disease in humans as seen by prospective, repeated, quantitated coronary angiography. Relation to clinical events and risk factors. The INTACT Study Group. *Circulation* 1992;86:828-838.
- Little WC, Constantinescu M, Applegate RJ, Kutcher MA, Burrows MT, Kahl FR, Santamore WP. Can coronary angiography predict the site of a subsequent myocardial infarction in patients with mild-to-moderate coronary artery disease? *Circulation* 1988;78:1157-1166.
- Naghavi M, Libby P, Falk E, Casscells SW, Litovsky S, Rumberger J, Badimon JJ, Stefanadis C, Moreno P, Pasterkamp G, Fayad Z, Stone PH, Waxman S, Raji P, Madjid M, Zarrabi A, Burke A, Yuan C, Fitzgerald PJ, Siscovick DS, de Korte CL, Aikawa M, Aikawa KE, Assmann G, Becker CR, Chesebro JH, Farb A, Galis ZS, Jackson C, Jang IK, Koenig W, Lodder RA, March K, Demirovic J, Navab M, Puri SG, Rehkter MD, Bahr R, Grundy SM, Mehran R, Colombo A, Boerwinkle E, Ballantyne C, Inahl W Jr, Schwartz RS, Vogel R, Serruys PW, Hansson GK, Faxon DP, Kaul S, Drexler H, Greenland P, Muller JE, Virmani R, Ridker PM, Zipes DP, Shah PK, Willerson JT. From vulnerable plaque to vulnerable patient: a call for new definitions and risk assessment strategies: Part II. *Circulation* 2003;108:1772-1778.
- Gibson CM, Kirtane AJ, Murphy SA, Karha J, Cannon CP, Giugliano RP, Roe MT, Harrington RA, Ohman EM, Antman EM. Distance from the coronary ostium to the culprit lesion in acute ST-elevation myocardial infarction and its implications regarding the potential prevention of proximal plaque rupture. *J Thromb Thrombolysis* 2003;15:189-196.
- Wang JC, Normand SL, Mauri L, Kuntz RE. Coronary artery spatial distribution of acute myocardial infarction occlusions. *Circulation* 2004;110:278-284.
- Buffon A, Biasucci LM, Liuzzo G, D'Onofrio G, Crea F, Maseri A. Widespread coronary inflammation in unstable angina. *N Engl J Med* 2002;347:5-12.
- Valgimigli M, Agnoletti L, Curello S, Comini L, Francolini G, Mastroianni F, Merli E, Pirani R, Guardigli G, Grigolato PG, Ferrari R. Serum from patients with acute coronary syndromes displays a proapoptotic effect on human endothelial cells: a possible link to pan-coronary syndromes. *Circulation* 2003;107:264-270.
- Madjid M, Zarrabi A, Litovsky S, Willerson JT, Casscells W. Finding vulnerable atherosclerotic plaques: is it worth the effort? *Arterioscler Thromb Vasc Biol* 2004;24:1775-1782.
- Maseri A, Fuster V. Is there a vulnerable plaque? *Circulation* 2003;107:2068-2071.
- VanderLaan PA, Reardon CA, Getz GS. Site specificity of atherosclerosis: site-selective responses to atherosclerotic modulators. *Arterioscler Thromb Vasc Biol* 2004;24:12-22.
- Nair A, Kuban BD, Tuzcu EM, Schoenhagen P, Nissen SE, Vince DG. Coronary plaque classification with intravascular ultrasound radio-frequency data analysis. *Circulation* 2002;106:2200-2206.
- Rodriguez-Granillo GA, Aoki J, Ong ATL, Valgimigli M, van Mieghem CAG, Regar E, McFadden E, de Feyter P, Serruys PW. Methodological considerations and approach to cross-technique comparisons using *in vivo* coronary plaque characterization based on intravascular radiofrequency data analysis: insights from the integrated Biomarker and Imaging Study (IBIS). *Int J Cardiovasc Interv* 2005;7:52-58.
- Käresen K. Deconvolution of sparse spike trains by iterated window maximization. *IEEE Trans Signal Process* 1997;45:1173-1183.
- Käresen KF BE. Blind deconvolution of ultrasonic traces accounting for pulse variance. *IEEE Trans Ultrason Ferroelectr Freq Contr* 1999;46:564-573.
- Mann JM, Davies MJ. Vulnerable plaque. Relation of characteristics to degree of stenosis in human coronary arteries. *Circulation* 1996;94:928-931.
- Draper NR, Smith H. *Applied Regression Analysis*. New York, NY: Wiley; 1981.
- Diggle PJ, Heagerty PJ, Liang KY, Zeger SL. *Analysis of Longitudinal Data*. New York, NY: Oxford University Press; 2002.
- Monroe VS, Kerensky RA, Rivera E, Smith KM, Pepine CJ. Pharmacologic plaque passivation for the reduction of recurrent cardiac events in acute coronary syndromes. *J Am Coll Cardiol* 2003;41:235-305.
- Casscells W, Naghavi M, Willerson JT. Vulnerable atherosclerotic plaque: a multifocal disease. *Circulation* 2003;107:2072-2075.
- Ambrose JA, D'Agate DJ. Classification of systemic therapies for potential stabilization of the vulnerable plaque to prevent acute myocardial infarction. *Am J Cardiol* 2005;95:379-382.
- Balk EM, Karas RH, Jordan HS, Kuelnick B, Chew P, Lau J. Effects of statins on vascular structure and function: a systematic review. *Am J Med* 2004;117:775-790.
- Nissen SE, Tsumoda T, Tuzcu EM, Schoenhagen P, Cooper CJ, Yasin M, Eaton GM, Lauer MA, Sheldon WS, Grines CL, Halpern S, Crowe T, Blankenship JC, Kerensky R. Effect of recombinant ApoA-I Milano on coronary atherosclerosis in patients with acute coronary syndromes: a randomized controlled trial. *JAMA* 2003;290:2292-2300.
- Nissen SE, Tuzcu EM, Schoenhagen P, Brown BG, Ganz P, Vogel RA, Crowe T, Howard G, Cooper CJ, Brodie B, Grines CL, DeMaria AN. Effect of intensive compared with moderate lipid-lowering therapy on progression of coronary atherosclerosis: a randomized controlled trial. *JAMA* 2004;291:1071-1080.
- Matsuzaki M, Hiramori K, Imaizumi T, Kitabatake A, Hishida H, Nomura M, Fujii T, Sakuma I, Fukami K, Honda T, Ogawa H, Yamagishi M. Intravascular ultrasound evaluation of coronary plaque regression by low density lipoprotein-apheresis in familial hypercholesterolemia: the Low Density Lipoprotein-Apheresis Coronary Morphology and Reserve Trial (LACMART). *J Am Coll Cardiol* 2002;40:220-227.
- Lima JA, Desai MY, Steen H, Warren WP, Gautam S, Lai S. Statin-induced cholesterol lowering and plaque regression after 6 months of magnetic resonance imaging-monitored therapy. *Circulation* 2004;110:2336-2341.
- Malek AM, Alper SL, Izumo S. Hemodynamic shear stress and its role in atherosclerosis. *JAMA* 1999;282:2035-2042.
- Kinlay S, Libby P, Ganz P. Endothelial function and coronary artery disease. *Curr Opin Lipidol* 2001;12:383-389.
- Einaev S, Bluestein D. Dynamics of blood flow and platelet transport in pathological vessels. *Ann NY Acad Sci* 2004;1015:351-366.

34. Kolodgie FD, Burke AP, Farb A, Gold HK, Yuan J, Narula J, Finn AV, Virmani R. The thin-cap fibroatheroma: a type of vulnerable plaque: the major precursor lesion to acute coronary syndromes. *Curr Opin Cardiol* 2001;16:285-292.
35. Fayad ZA, Fuster V. Clinical imaging of the high-risk or vulnerable atherosclerotic plaque. *Circ Res* 2001;89:305-316.
36. Kolodgie FD, Virmani R, Burke AP, Farb A, Weber DK, Kutys R, Finn AV, Gold HK. Pathologic assessment of the vulnerable human coronary plaque. *Heart* 2004;90:1385-1391.
37. Okazaki S, Yokoyama T, Miyauchi K, Shimada K, Kurata T, Sato H, Daida H. Early statin treatment in patients with acute coronary syndrome: demonstration of the beneficial effect on atherosclerotic lesions by serial volumetric intravascular ultrasound analysis during half a year after coronary event: the ESTABLISH Study. *Circulation* 2004;110: 1061-1068.
38. Rodriguez-Granillo GA, Serruys PW, Garcia-Garcia HM, Aoki J, Valgimigli M, van Mieghem CA, Mc Fadden E, de Jaegere PP, de Feyter P. Coronary artery remodelling is related to plaque composition. *Heart* 2005; doi:10.1136/hrt.2004.057810.





**3.2) Plaque composition in the left main Stem mimics the distal but not the proximal tract of left coronary artery. Influence of clinical presentation, length of the left main trunk, lipid profile and systemic inflammatory status.**

**J Am Coll Cardiol. In press.**

**Valgimigli M, Rodriguez-Granillo GA, García-García HM, et al.**



# **Plaque Composition in the Left Main Stem Mimics the Distal but not the Proximal Tract of the Left Coronary Artery**

**Influence of Clinical Presentation, Length of the Left Main Trunk,  
Lipid Profile and Systemic levels of C-Reactive Protein**

Marco Valgimigli, MD, Gastón A. Rodriguez-Granillo, MD, Héctor  
M. Garcia-Garcia, MD, Sophia Vaina, MD, Peter De Jaegere, MD,  
PhD, Pim De Feyter, MD, PhD, Patrick W Serruys, MD, PhD

Erasmus Medical Center, Thoraxcenter, Rotterdam, the Netherlands.

**ABSTRACT**

**Objective:** To investigate whether plaques located in the left main stem (LMS) differ in terms of necrotic core content from those sited in the proximal tract of the left coronary artery. **Background:** Plaque composition, favoring propensity to vulnerability, might be non-uniformly distributed along the vessel. This might explain the higher likelihood for plaque erosion or rupture to occur in the proximal but not in the distal tracts of the coronary artery or in LMS. **Methods:** 72 patients were prospectively included: 48 (32 men; mean age:  $57\pm 11$ ), [25 with stable angina (SA); 23 affected by acute coronary syndromes (ACS)] underwent a satisfactory non-culprit vessel investigation through spectral analysis of IVUS radiofrequency data (IVUS-Virtual Histology<sup>TM</sup>). The region of interest was subsequently divided into LMS and LMS carina, followed by six consecutive non-overlapping 6 mm-segments in left anterior descending (LAD) artery in 34 or in circumflex artery (CFX) in 14 patients. **Results:** Necrotic core content (%) i) was minimal in LMS [median (IQR): 4.6 (2-7)]; peaked in the first 6-mm coronary segment [11.8 (8-16);  $p < 0.01$ ], while it then progressively decreased distally; ii) was overall higher in ACS [11.4 (5.5-19.8) than SA patients [7.3 (3.2-12.9)]; ( $p < 0.001$ ); iii) was largely independent from plaque size and iv) did not correlate to systemic levels of CRP or lipid profile. **Conclusions:** Plaques located in the LMS carry minimal necrotic content. Thus, they mimic the distal but not the proximal tract of the left coronary artery where plaque rupture or vessel occlusion occurs more frequently.

**Key Words:** Plaque – necrotic core – Imaging – vulnerable plaque – Virtual histology

### **CONDENSED ABSTRACT**

In 48 patients [25 with stable angina; 23 affected by acute coronary syndromes] who underwent spectral analysis of IVUS radiofrequency data (IVUS-Virtual Histology<sup>TM</sup>), necrotic core content was minimal in left main stem (LMS), peaked in the first 6-mm coronary segment, while it then progressively decreased distally; suggesting that plaques located in the LMS, by carrying minimal necrotic content, mimic the distal but not the proximal tract of the left coronary artery where plaque rupture or vessel occlusion occurs more frequently.

## **ABBREVIATIONS LIST**

ACS: acute coronary syndrome

CRP: C-reactive protein

CFX: circumflex artery

HDL: high-density lipoprotein cholesterol

IVUS: Intravascular ultrasound

LMS: left main stem

LAD: left anterior descending artery

LDL: low-density lipoprotein cholesterol

STEMI: ST-segment elevation myocardial infarction

VH: virtual histology

## INTRODUCTION

The distribution of ruptured or prone to rupture plaques is known to be non-uniform throughout the coronary tree(1-5). Pathological studies have suggested the so called “thin-cap atheromas” –necrotic rich core plaques at high risk for rupture– are infrequent in the left main stem (LMS) and in the distal tracts of the coronary vessels, while they group together with ruptured and healed plaques in the proximal segments of the three main coronary arteries(1).

Similarly i) angiographic studies in patients with ST-segment elevation myocardial infarction (STEMI) have recently shown that sites of occlusion are clustered within the proximal third of each of the vessels(2,3) and ii) intravascular ultrasound (IVUS) analyses have observed that plaque rupture rarely occurs in the LMS or the distal part of the coronary arteries, whereas it is far more common in the proximal part of the coronary vessels(4), especially in the left anterior descending artery (5).

The reasons why vulnerable or ruptured plaques tend to spare the LMS and distal segments of the left coronary vessels remain poorly understood. Plaque composition, favoring propensity to vulnerability(6-8), might also be non-uniformly distributed along the coronary arteries.

We sought to investigate whether the plaques located in the LMS, which are known to be at low probability of rupture, differ in terms of composition from those sited in the proximal tract of left anterior descending or circumflex artery, where rupture or occlusion occurs more frequently. This may contribute establishing *in vivo* the role of plaque composition as key determinant of vulnerability in humans. In this context, the role of clinical presentation, length of LMS, lipid profile and systemic level of C-reactive protein were also investigated.

## **METHODS**

### **Study Protocol and Patients Enrolment**

This was a single-centre, investigators-driven, observational study aimed to evaluate the distribution of plaque composition along the left coronary artery in consecutive patients referred to our institution for elective or urgent PCI, in whom the non-culprit, non-treated vessel was judged suitable for a safe IVUS 35 mm-pullback or more, based on angiographic (absence of the following: >50% stenotic disease, extensive calcification, severe vessel tortuosity) and clinical (haemodynamic stability) findings.

According to the protocol, not more than one vessel-per patient could be evaluated and the region of interest (ROI) was subsequently divided into the following coronary segments: LMS and LMS carina, based on anatomical landmarks, followed by six consecutive non-overlapping 6 mm-segments, with the first one to be started at the coronary ostium of either left anterior descending or circumflex artery. The length chosen for those coronary segments located distally to the LMS carina was based on the median length of LMS in the study population.

To ensure that the ostial-proximal part of the LMS was included in the IVUS pullback and to rule out the occurrence of deep intubation by the guiding catheter, the last part of the pullback was filmed and each angiogram carefully inspected before patient inclusion. An analyzable interrogated vessel length of at least 35 mm beyond LMS carina, starting from coronary ostium, was the main selection criterion, once the patient was included in the study. This protocol was approved by the hospital ethics committee and is in accordance with the declaration of Helsinki. Written informed consent was obtained from every patient.

### **IVUS-VH Acquisition and Analysis**

Details regarding the validation of the technique, on explanted human coronary segments, have previously been reported (9). Briefly, IVUS radiofrequency data (IVUS-Virtual Histology<sup>TM</sup>)

uses spectral analysis of IVUS radiofrequency data to construct tissue maps that classify plaque into four major components. In preliminary *in vitro* studies, four histological plaque components (fibrous, fibro-lipid, necrotic core and calcium) were correlated with a specific spectrum of the radiofrequency signal (9). These different plaque components were assigned color codes. Calcified, fibrous, fibrolipidic and necrotic core regions were labeled white, green, greenish-yellow and red respectively(10).

IVUS-VH data was acquired after intracoronary administration of nitrates using a continuous pullback (0.5 mm per second) with commercially available mechanical sector scanners (Ultracross™ 30 MHz catheter, Boston Scientific, Santa Clara, CA-USA- or Eagle Eye™ 20 MHz catheter, Volcano Corporation, Rancho Cordova, USA), by a dedicated IVUS-VH console (Volcano Therapeutics, Rancho Cordova, CA). The IVUS VH data were stored on a CD-ROM/DVD and sent to the imaging core lab for offline analysis (Cardialysis). IVUS B-mode images were reconstructed from the RF data by customized software and contour detection was performed using cross-sectional views with a semi-automatic contour detection software to provide geometrical and compositional output (IvusLab 3.0 for 30 MHz acquisitions and IvusLab 4.4 for 20 MHz acquisitions respectively; Volcano Corporation, Rancho Cordova, USA)(10).

The contours of the external elastic membrane (EEM) and the lumen-intima interface enclosed an area that was defined as the coronary plaque plus media area. Plaque burden was calculated as  $[(EEM_{\text{area}} - \text{Lumen}_{\text{area}}) / EEM_{\text{area}}] \times 100$ . Plaque eccentricity was defined as minimum plaque thickness divided by maximum plaque thickness. Geometrical and compositional data were obtained for each cross-sectional area (CSA) and an average was calculated for each coronary and for the total coronary tree. RF data was normalized using a technique known as “Blind Deconvolution”, an iterative algorithm that deconvolves the catheter transfer function from the backscatter, thus accounting for catheter-to-catheter variability (11,12).

### **Biochemical measures**

Antecubital venous blood was collected from all patients at entry, left in ice for 45 min, centrifuged at 1700×g at 4°C for 15 min and serum obtained finally stored at -80°C. High-sensitive (hs) C-reactive protein (CRP) was measured in serum using a commercially available kit (N High Sensitivity CRP, Dade Behring, Marburg, Germany). Plasma concentrations of total cholesterol, high-density lipoprotein cholesterol (HDL), and triglycerides were measured in the local laboratory. The Friedewald formula was used to derive low-density lipoprotein cholesterol (LDL) levels.

### **Statistical Analysis**

The sample size was calculated on the assumption that plaques located in the most proximal 6-mm segment of the LAD or CFX, would display a mean necrotic core content of approximately 10% and a standard deviation of 10%, based on previous findings(13), with a relative necrotic core content of around 5% in plaques located in the LMS. To detect this effect size with 80% power and a type I error (alpha) of 0.05, at least 46 patients were required (model 1). Model 2 was also created to explore whether in patients with LMS length beyond median value (long LMS cohort) plaque composition differs in the proximal compared to the distal tract of the LMS. No formal sample size was calculated for model 2 as it was meant to be a hypothesis generating analysis.

Values are expressed as mean±SD and median and interquartile range (IQR) whenever appropriate. Since all cross sectional areas, provided by IVUS analysis, were shown to have a non-normal distribution at Kolmogorov-Smirnov goodness-of-fit test, they were log-transformed before analysis. Similarly, to all percentages relative to stenosis rate and plaque composition an arcsin transformation was applied (14). Assumptions for normality were checked after transformation based on a p-value >0.20 at Kolmogorov-Smirnov test and on visual assessment of Q-Q plots of residuals.

Comparisons between the two groups were performed with the Student's *t*-test. Fisher's exact test was used for categorical variables. Comparisons among coronary segments were accomplished through a general linear mixed model and *post hoc* comparisons by Tukey honest

significance difference test(15). Spearman's correlation coefficients were used to detect any association between variables. Probability was significant at a level of  $<0.05$ . Statistical analysis was performed using Statistica 6.1 Software (Statsoft Inc.) and R-language (R Foundation).

## RESULTS

From 11 December 2003 to 27 July 2005, seventy-two patients were prospectively included in the protocol. Twenty-four patients were subsequently excluded from the final analysis due to short (< 36 mm) IVUS pullback in 16, uncertainty regarding the true interface lumen-vessel wall based on IVUS grey-scale in 4 and occurrence of angiographically confirmed deep intubation of the guiding catheter during the pullback in 4 patients. Thus, 48 patients (32 men), aged 30 to 75 years (mean age:  $57\pm 11$ ) constituted the final patient population. Their baseline characteristics are provided in Table 1.

The study vessel was the LMS and left anterior descending (LAD) artery in 34 (71%) patients and LMS and circumflex artery (CFX) in 14 (29%). The overall LMS length was  $7.49\pm 4$  mm [median (IQR): 6 (4.8-9.3); range: 3.4-20]; ( $7.3\pm 4$  in SA group vs.  $7.8\pm 5$  in ACS group,  $p=0.64$ ). Lumen and vessel cross sectional area (CSA) decreased significantly starting from the first 6-mm segment of the coronary artery as compared to LMS (table 2). Plaque CSA in the LMS was significantly increased only compared to the most distal 6-mm segment. The degree of plaque eccentricity was relatively constant throughout the vessel except in the LMS carina, where it resulted to be higher compared to both the LMS and the coronary segments distal to the first one. Plaque burden did not change along the vessel in model 1, despite a trend being progressively increased from proximal to distal.

Model 2 (Table 2), in which LMS has been stratified into the proximal and distal segment after selection of those patients ( $n=24$ ) with long LMS (length >6 mm), mainly confirmed the trends observed along the vessels in model 1.

### Change in plaque composition along the study vessel

Fibrous tissue was the most prevalent component of plaque composition in each analyzed segment throughout the two models, followed by fibrolipidic tissue, necrotic core and calcium (table 3). No significant change was observed in terms of relative plaque composition throughout

the study vessel with respect to fibrous and calcified tissue content. The percentage of fibrolipidic tissue decreased in the second and third 6-mm segment when contrasted to the LMS. When compared to the 6<sup>th</sup> coronary segment, however, no difference emerged among the vessel tracts in terms of fibrolipidic content at post-hoc analysis.

The necrotic core increased significantly in the first, second and third 6-mm segment compared to the LMS. When the most distal segment of the study vessel was taken as reference, the necrotic core remained greater in both the first and second 6-mm segment at post-hoc analysis. As shown in figure 1, the necrotic core was the plaque component with the highest relative change along the vessel (Figure 1). Changes in terms of plaque composition in model 2 are shown in table 3.

### **Change in plaque composition according to clinical presentation**

No significant change in calcium, fibrous and fibrolipidic content with respect to clinical presentation (stable vs. unstable) was observed when all 384 coronary segments were pooled together (Figure 2). Necrotic core (%) was significantly increased in patients with [median (IQR): 11.4 (5.5-19.8)] as compared to those [median (IQR): 7.3 (3.2-12.9)] without ACS ( $p < 0.001$ ) (Figure 2). After introducing anatomical location stratified into eight coronary segments in the model, the increase in necrotic core in ACS patients was mainly confined to the LMS [6.9 (2.6-9.4) vs. 3.5 (1.4-6.2) in stable patients;  $p = 0.02$ ], in the first [14.9 (7.7-19.6) vs. 11.5 (4.9-17.3) in stable patients;  $p = 0.03$ ], second [12.2 (5.5-16.1) vs. 9.4 (5.1-20.6) in stable patients;  $p = 0.03$ ] and third 6-mm coronary segment [11.4 (5.4-15) vs. 8 (3.6-14.4) in stable patients;  $p = 0.04$ ]. However, the statistical interaction between necrotic core and the anatomical location of the segments did not reach the significance ( $p = 0.12$ ).

### **LMS length as a predictor of plaque composition along the study vessel**

Patients were stratified into two groups based on median LMS length (short LMS  $\leq 6$  mm and long LMS  $>6$  mm). These two groups did not differ in terms of baseline and procedural characteristics. When each coronary segment was separately analyzed, no difference emerged between the two groups for IVUS-derived quantitative vessel analysis. The same held true if all 384 coronary segments were cumulatively considered independently from their anatomical location. Calcium, fibrous and fibrolipid content did not differ between the two groups (data not shown). The pattern of necrotic distribution in relation to LMS length is shown in figure 3.

### **Correlations**

In a segment-based analysis, necrotic core was largely independent from plaque area ( $r=0.17$ ;  $p=0.06$ ;  $R^2=0.09$ ). Similarly, we failed to find an association between necrotic core content and C-reactive protein levels ( $r=0.09$ ,  $p=0.8$ ), level of LDL ( $p=0.11$ ,  $p=0.23$ ) or HDL ( $r=-0.2$ ,  $p=0.4$ ) at entry. However, there was a significant, although weak, direct correlation between necrotic core and cholesterol/HDL ratio ( $r=0.18$ ,  $p=0.01$ ;  $R^2=0.1$ ).

## DISCUSSION

There is increasing evidence that the distribution of ruptured or prone to ruptured plaques is not uniform along the coronary vessel: they cluster in the proximal tract of the three major coronary vessels while they tend to spare both the LMS and distal segments of coronary arteries(4,16). These findings have been recently confirmed by mapping the distribution of angiographic sites of occlusive or non-occlusive culprit lesions along the coronary arteries in patients with ST segment elevation acute coronary syndromes(2,3).

The reason why vulnerable plaques show a tendency to cluster in partially predictable *hot spots* located within the proximal tracts of coronary vessel is largely unknown. Atherosclerotic plaques also cluster within the proximal portions of the three major coronaries(17-20). Thus, the risk to undergo rupture may be identical for each coronary plaque independently from its anatomical location, being rupture simply more likely to occur where atherosclerotic plaques are more frequently clustered(21). This may easily explain the non-uniform distribution of ruptured or prone to rupture plaques without calling into question the idea that plaque rupture is partially a site-specific phenomenon.

Alternatively, plaques located within the proximal third of each coronary may harbour some specific hallmark of vulnerability which makes them *individually* more likely to undergo rupture. To gain some insights into this topic of debate, we hypothesized that plaque necrotic core content, which is a well-known determinant of vulnerability(7,8,22), may differ along the coronary vessel, being greater at the spots where plaque rupture is known to be more frequent.

Our main findings can be summarized as follows:

- 1) The plaque necrotic content was minimal in the LMS, particularly in the most proximal tract, while it peaked in the first 6-mm segments after the ostium of the two major left coronaries, progressively decreasing towards the more distal segments.

- 2) The plaque CSA was largely unrelated to necrotic core content throughout the left coronary vessel. This statement is supported by the absence of correlation between necrotic content in plaques and plaque CSA at the segment-based analysis and by the observation that plaque CSA showed a progressive increase in the distal-proximal direction along the vessel whereas plaque necrotic content did not.
- 3) The necrotic core was higher in patients with clinical instability, presenting with ACS compared to those affected by stable atherosclerotic disease.
- 4) The necrotic content was not related to systemic inflammatory status, as measured by a well recognized prognostic marker of inflammation such as C-reactive protein nor LDL or HDL alone, while it showed a significant although weak correlation to cholesterol/HDL ratio.
- 5) The length of left main trunk was shown to affect the distribution of necrotic core along the vessel. In patients with long LMS, necrotic core content peaked immediately in the first coronary segment after LMS and rapidly decreased distally. Conversely, the necrotic core content peaked in the second 6-mm segment in patients with short LMS and it resulted to be increased in the two most distally analyzed segments compared to the long LMS group.

It is tempting to speculate that the observed clustering of ruptured or prone to rupture plaques in the proximal segment of each coronary artery is not just a simple reflection of the non-uniform distribution of atherosclerosis along the coronary vessel. The necrotic content of those plaques located in these proximal segments, independent of their size, was higher, both compared to the LMS and to those segments which are more distally located. The plaques located within the proximal segments of the left coronary artery, being relatively richer in necrotic content, may undergo rupture more easily than those located in the LMS or in the distal tracts of the vessel.

Some preliminary unpublished findings by our group suggest that plaque necrotic core content, as assessed through IVUS-VH, may be the only independent predictor for mechanically deformable regions (high-strain spots)(23) throughout the coronary arteries in humans. Thus, when

our findings are put in perspective of current evidence, they support the idea that vulnerability may cluster in necro-lipid-rich regions throughout the vessel.

Necrotic core content in the present study was higher in patients with ACS, suggesting again that plaque composition in itself may play a pivotal role in determining vulnerability. Interestingly, it was recently reported that when rupture of coronary plaques occurs in the LMS, the distal half of LMS is more likely to be involved (24). Our findings that the distal LMS tends to harbour a greater necrotic core content compared to proximal half, together with the well established role of shear stress in bifurcated lesions(25), may contribute to explain the non-uniform distribution of plaque rupture even within the LMS.

The reasons why the plaque necrotic core seems to exceed in the proximal as compared to the distal tracts of the coronary vessel or the LMS remain speculative at the present time. Low-oscillatory shear stress is known to induce a loss of the physiological flow-oriented alignment of the endothelial cells, an enhancement of the expression of adhesion molecules and a weakening of cell junctions, ultimately leading to an increase in permeability to lipids and macrophages(25). The segments located in the first few centimetres of the coronary arteries, due to flow turbulence generated by high velocity blood impacting against anatomical flow dividers(26), may be more exposed to low-oscillatory shear stress compared to the most proximal (i.e. LMS) or more distal coronary segments, thus possibly explaining our present findings(27). Concomitant quantitative measurement of shear stress and plaque composition along coronary vessels in vivo would be pivotal in corroborating this working hypothesis.

### **Limitations of the Study**

Based on previous findings and the well known role of necrotic core content in determining vulnerability(6-8,22), our investigation was primarily focused on the distribution of necrotic core content along the left coronary artery. In order to assess relatively minor changes in plaque

composition along the longitudinal artery axis, such as that observed for fibrous tissue, a bigger properly powered sample size is clearly needed. In keeping with previous considerations, all other analyses and comparisons performed in the current manuscript should be regarded as exploratory and hypothesis-generating since we cannot rule out the possibility that inflation of type I error due to multiple comparisons may have confounded our results.

In our study the operators were left free to wire the most suitable vessel for the IVUS pullback, provided it was supplying a major left ventricle territory. This resulted in the predominance of LAD as region of interest, while the CFX artery was mainly investigated in those patients presenting with small or tortuous LAD. The distribution of necrotic core along the vessel did not differ in LAD as compared to CFX. The same held true for other studied plaque components. However, the applied selection process may have biased this comparison. Thus, whether the distribution of plaque composition may differ in relation to the studied vessel remains to be tested. Similarly, in order to maximize patients' safety and avoid potential IVUS-related complications, individuals with severe angiographic calcification were excluded. Despite this decision may have clearly contributed to generate some selection bias, the distribution of calcium along the coronary vessel intriguingly mirrored the one observed for the necrotic core. Further studies are needed to investigate the specific role of calcium content in determining plaque vulnerability.

Patients with proximal occlusions have bigger MI and thus they are more likely to present to hospital and be referred for angioplasty. Similarly, myocardial infarction due to LMS as culprit artery may often result in immediate death. Thus, it may be argued that a selection bias might have artificially increased the prevalence of patients with culprit lesions located in the proximal compared to distal tracts of coronaries or LMS. This is obviously theoretical possible. However, for the following reasons, we believe that this possibility is relatively unlikely:

- A. The Necrotic core in our series clustered in the same coronary spots where previous studies, based on post-mortem examination, found a higher prevalence of ruptured or healed plaques.
- B. Our results are based on the investigation of the non-culprit vessel. Thus, they are potentially less prone to suffer from clinical selection due to the location of the culprit lesion in the culprit vessel.
- C. Although it seems to be exacerbated in patients presenting with clinical instability, the non-uniform distribution of plaque composition along the vessel has been observed also in patients with stable coronary disease, in whom the selection bias due to the importance of the culprit lesion is less obvious, at least for the comparison LMS vs. proximal tracts of LAD or CFX.

Thus, based on these considerations, we think that our findings, especially when put in the context of previous evidence(1-5), may help reinforcing the notion that there may be some hot spots along the coronary vessel which are per se more prone to develop vulnerable plaque and as such undergo plaque rupture.

### **Summary and Conclusions**

Plaque composition was found to be not uniformly distributed along the left coronary artery with a progressive increase in necrotic core starting from the proximal half of the LMS to the most proximal segments of the LAD or CFX, followed by a steady decline towards those segments which are more distally located along the vessel. The necrotic core appeared to be increased in patients with ACS, especially in the LMS and in the three proximal coronary segments of LAD or CFX, while it did not correlate with the CRP or lipid profile. The relatively site-specificity of necrotic core content towards the proximal segment of the left coronary artery is in keeping with the increasing evidence that a clear clustering of ruptured or prone to rupture plaques occurs in humans within this region (2,3,5). Our findings i) reinforce the notion the plaque composition may be a

major determinant for and subsequently a potential target of plaque vulnerability in humans and ii) call for prospective evaluation of the independent role of plaque composition on long-term outcome in patients with established coronary artery disease.

## REFERENCES

1. Kolodgie FD, Burke AP, Farb A, et al. The thin-cap fibroatheroma: a type of vulnerable plaque: the major precursor lesion to acute coronary syndromes. *Curr Opin Cardiol* 2001;16:285-92.
2. Gibson CM, Kirtane AJ, Murphy SA, et al. Distance from the coronary ostium to the culprit lesion in acute ST-elevation myocardial infarction and its implications regarding the potential prevention of proximal plaque rupture. *J Thromb Thrombolysis* 2003;15:189-96.
3. Wang JC, Normand SL, Mauri L, Kuntz RE. Coronary artery spatial distribution of acute myocardial infarction occlusions. *Circulation* 2004;110:278-84.
4. von Birgelen C, Klinkhart W, Mintz GS, et al. Plaque distribution and vascular remodeling of ruptured and nonruptured coronary plaques in the same vessel: an intravascular ultrasound study in vivo. *J Am Coll Cardiol* 2001;37:1864-70.
5. Hong MK, Mintz GS, Lee CW, et al. The site of plaque rupture in native coronary arteries: a three-vessel intravascular ultrasound analysis. *J Am Coll Cardiol* 2005;46:261-5.
6. Shah PK. Mechanisms of plaque vulnerability and rupture. *J Am Coll Cardiol* 2003;41:15S-22S.
7. Naghavi M, Libby P, Falk E, et al. From vulnerable plaque to vulnerable patient: a call for new definitions and risk assessment strategies: Part II. *Circulation* 2003;108:1772-8.
8. Naghavi M, Libby P, Falk E, et al. From vulnerable plaque to vulnerable patient: a call for new definitions and risk assessment strategies: Part I. *Circulation* 2003;108:1664-72.
9. Nair A, Kuban BD, Tuzcu EM, Schoenhagen P, Nissen SE, Vince DG. Coronary plaque classification with intravascular ultrasound radiofrequency data analysis. *Circulation* 2002;106:2200-6.
10. Rodriguez-Granillo GA, Aoki J, Ong ATL, et al. Methodological considerations and approach to cross-technique comparisons using in vivo coronary plaque characterization based on intravascular radiogrequency data anlysis: insights from the integrated Biomarker and Imaging Study (IBIS). *Int J Cardiovasc Intervent.* 2005;7:52-58.
11. Kåresen K. Deconvolution of sparse spike trains by iterated window maximization. *IEEE Trans Signal Process* 1997;45:1173-1183.
12. Kåresen KF BE. Blind deconvolution of ultrasonic traces accounting for pulse variance. *IEEE Trans Ultrason Ferroelectr Freq Control* 1999;46:564-573.
13. Mann JM, Davies MJ. Vulnerable plaque. Relation of characteristics to degree of stenosis in human coronary arteries. *Circulation* 1996;94:928-31.
14. Draper NR, Smith H. *Applied regression analysis*. 2nd ed. New York, NY: Wiley, 1981.
15. Diggle PJ, Heagerty PJ, Liang KY, Zeger SL. *Analysis of longitudinal data*. 2nd ed. New York, NY: Oxford University Press, 2002.
16. Virmani R, Burke AP, Kolodgie FD, Farb A. Pathology of the thin-cap fibroatheroma: a type of vulnerable plaque. *J Interv Cardiol* 2003;16:267-72.
17. Vieweg WV, Warren SE, Alpert JS, Hagan AD. The distribution and severity of coronary artery disease and left ventricular dysfunction among patients with single coronary artery disease and angina pectoris. *Clin Cardiol* 1980;3:241-5.
18. Vieweg WV, Alpert JS, Johnson AD, et al. Distribution and severity of coronary artery disease in 500 patients with angina pectoris. *Cathet Cardiovasc Diagn* 1979;5:319-30.
19. Hochman JS, Phillips WJ, Ruggieri D, Ryan SF. The distribution of atherosclerotic lesions in the coronary arterial tree: relation to cardiac risk factors. *Am Heart J* 1988;116:1217-22.
20. Fox B, James K, Morgan B, Seed A. Distribution of fatty and fibrous plaques in young human coronary arteries. *Atherosclerosis* 1982;41:337-47.
21. Abaci A. Letter regarding article by Wang et al, "coronary artery spatial distribution of acute myocardial infarction occlusions". *Circulation* 2005;111:e369; author reply e369.

22. Shah PK. Pathophysiology of plaque rupture and the concept of plaque stabilization. *Cardiol Clin* 2003;21:303-14, v.
23. Schaar JA, Regar E, Mastik F, et al. Incidence of high-strain patterns in human coronary arteries: assessment with three-dimensional intravascular palpography and correlation with clinical presentation. *Circulation* 2004;109:2716-9.
24. Tyczynski P, Pregowski J, Mintz GS, et al. Intravascular ultrasound assessment of ruptured atherosclerotic plaques in left main coronary arteries. *Am J Cardiol* 2005;96:794-8.
25. McLenachan JM, Vita J, Fish DR, et al. Early evidence of endothelial vasodilator dysfunction at coronary branch points. *Circulation* 1990;82:1169-73.
26. Kimura BJ, Russo RJ, Bhargava V, McDaniel MB, Peterson KL, DeMaria AN. Atheroma morphology and distribution in proximal left anterior descending coronary artery: in vivo observations. *J Am Coll Cardiol* 1996;27:825-31.
27. Rodriguez-Granillo GA, Garcia-Garcia HM, Wentzel J, et al. Plaque composition and its relationship with acknowledged shear stress patterns in coronary arteries. *J Am Coll Cardiol* 2006;47:884-5.

## Figure Legends

### Figure 1. **Change in plaque composition along the left coronary artery**

A: plaque composition in terms of median necrotic, fibro-lipid, fibrous and calcium core content expressed in absolute values along the left coronary vessel. In B the percentage of each plaque components are reported with respect to left main coronary artery (LMS) taken as reference. All analyses are based on model 1.

### Figure 2. **Plaque composition in relation to clinical presentation**

Plaque composition on a per segment based analysis in patients with stable angina (stable pts) or with acute coronary syndromes (ACS) (unstable pts). The necrotic core (%) was significantly increased in patients with [median (IQR): 11.4 (5.5-19.8)] as compared to those [median (IQR): 7.3 (3.2-12.9)] without ACS.

\*:  $p < 0.001$  vs. stable pts.

### Figure 3. **Necrotic core distribution along the left coronary artery according to the length of LMS**

The necrotic core peaked in the first and in the second 6-mm segment in patients with long (above median value) and short left main coronary artery (LMS), respectively. After the peak, the necrotic core decrease was more pronounced in the long than in the short LMS group. As a consequence, the necrotic core content resulted to be significantly increased in the fifth and sixth 6-mm segments in the short as compared to the long LMS group.

\*:  $p < 0.05$  vs. short LMS.

### Figure 4. **Correlation between arcsin transformed plaque cross sectional area (CSA) and log transformed necrotic core content**

**Table 1. Study Population**

Variables	Patients			P-Value*
	All (N=48)	SA Group (N=25)	ACS Group (N=23)	
Age (ys)	57±11	58±11	57±12	0.81
Males, no. (%)	32 (67)	16 (64)	16 (65)	>0.99
Weight (kg)	82±12	81±12	84±12	0.36
Height (cm)	174±9	173±8	176±10	0.28
BMI (kg/m <sup>2</sup> )	27±3	27±4	27±2	0.81
Diabetes, no. (%)	11 (23)	5 (20)	6 (26)	0.75
Hypertension, no. (%)	37 (77)	20 (80)	17 (74)	>0.99
Current Smokers, no. (%)	19 (40)	8 (32)	11 (48)	0.32
Previous Smoker, no. (%)	16 (33)	9 (36)	7 (30)	0.50
C-reactive protein (mg/l)	29±48	12.7±15	38±58	0.19
Low density lipoprotein (mmol/l)	3.09±1.22	3.26±1.3	2.9±1.3	0.44
High density lipoprotein (mmol/l)	1.22±0.5	1.30±0.6	1.14±0.4	0.39
Cholesterol/HDL ratio	4.26±1.49	4.26±1.5	4.25±1.2	0.99
<b>Medical History, no. (%)</b>				
CABG	2(4)	2 (6)	0 (0)	0.29
PCI	11 (23)	8 (32)	3 (13)	0.32
Acute Coronary Syndrome	18 (37)	10 (40)	8 (35)	>0.99
<b>Medical Treatment, no. (%)</b>				
Aspirin	48 (100)	25 (100)	23 (100)	>0.99
Clopidogrel	48 (100)	25 (100)	23 (100)	>0.99
Statin	42 (88)	23(92)	19 (83)	0.84
ACE-inhibitor	40 (83)	25 (100)	15 (65)	0.39
β-Blocker	42 (88)	23 (92)	19 (83)	0.84

Plus-minus values are means±SD.

BMI: Body mass index, SA: Stable angina, ACS: acute coronary syndrome.

CABG: coronary artery bypass grafting, PCI: percutaneous coronary intervention, ACE: angiotensin converting enzyme

Table 2: Quantitative Vessel Analysis at IVUS stratified into coronary segments

	Cross Sectional Areas (mm <sup>2</sup> )			Plaque Burden (%)
	Lumen	Vessel	Plaque	
<b>MODEL 1 N=48</b>				
<b>CORONARY SEGMENTS</b>				
<b>LMS</b>				
<b>LMS Carina</b>				
<b>1°</b> (0-6 mm)	15.2 (12-17)	24.5 (19-26)	8 (6-9)	0.11 (0.05-0.18)
<b>2°</b> (6-12 mm)	12.2 (11-15)	20.4 (16-24)	6.7 (6-8)	0.03 (0.01-0.06)†
<b>3°</b> (12-18 mm)	9.9 (7-11) †	16.2 (14-18) †	6.4 (5-7)	0.09 (0.07-0.14)
<b>4°</b> (18-24 mm)	9.1 (7-10) †	16 (14-18) †	6.8 (5-8)	0.11 (0.06-0.16)
<b>5°</b> (24-30 mm)	8.6 (7-10) †	15 (13-17) †	6.9 (5-8)	0.10 (0.08-0.15)
<b>6°</b> (30-36 mm)	8.2 (7-10) †	14 (13-16) †	6.3 (5-7)	0.13 (0.06-0.17)
	7.5 (6-9) †	13.2 (12-15) †	5.6 (5-6)	0.16 (0.10-0.20)
	7.2 (6-8) †	12.3 (11-14) †	4.9 (4-6)†	0.12 (0.08-0.21)
<b>P-VALUE</b>	<0.0001	<0.0001	0.0006	0.0001
<b>MODEL 2 N=24</b>				
<b>CORONARY SEGMENTS</b>				
<b>PROX. LMS</b>				
<b>DIST. LMS</b>				
<b>LMS CARINA</b>				
<b>1°</b> (0-6 mm)	16.1 (13-19)	23.4 (21-27)	7.5 (5-9)	0.11 (0.07-0.15)
<b>2°</b> (6-12 mm)	14.6 (12-17)	25.8 (20-27)†	8.9 (7-10)	0.11 (0.07-0.25)
<b>3°</b> (12-18 mm)	13.1 (11-15)†	21.2 (18-25)	7.7 (7-8)	0.05 (0.02-0.08)
<b>4°</b> (18-24 mm)	9.9 (8-11)†	16.3 (15-19)†	7.1 (6-8)	0.13 (0.09-0.14)
<b>5°</b> (24-30 mm)	9.1 (7-11)†	16.6 (14-19)†	7.7 (6-9)	0.15 (0.08-0.17)
<b>6°</b> (30-36 mm)	8.6 (7-10)†	15.7 (14-18)†	7.4 (6-8)	0.11 (0.09-0.21)
	8.2 (7-10)†	14.5 (13-16)†	7.0 (5-8)	0.14 (0.09-0.17)
	8.2 (6-10)†	14.0 (12-17)†	5.7 (5-7)	0.19 (13-24)
	7.0 (6-8)†	12.0 (11-14)†	5.1 (4-7)*	0.19 (0.11-0.30)
<b>P-VALUE</b>	<0.001	<0.0001	0.002	0.019
				0.0093

P-values refer to results for the whole model at general linear analysis. \*: p<0.05; †: p<0.01 at adjusted-post-hoc comparison as compared to left main stem (LMS) in model 1 and to Prox. LMS in model 2. Results are given as median (IQR); Prox.: proximal; Dist.: distal.

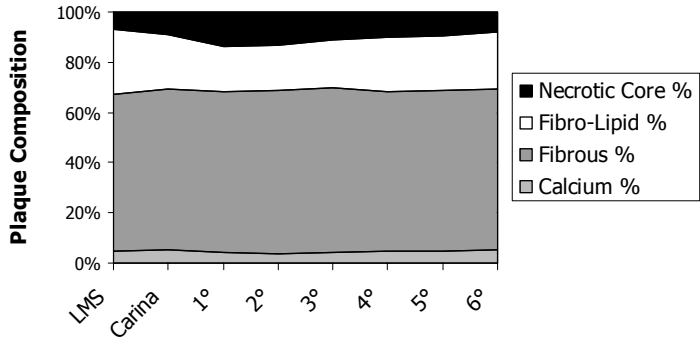
Table 3. Plaque Composition along the left coronary artery stratified into coronary segments

	Plaque Composition (%)			
	Calcium Core	Fibrous Core	Fibrolipidic Core	Necrotic core
<b>MODEL 1; N=48</b>				
<b>CORONARY SEGMENTS</b>				
<b>LMS</b>	0.65 (0.2-1.7)	63.5 (57-68)	24.9 (20-29)	4.6 (2-7)
<b>LMS CARINA</b>	1.1 (0.3-1.6)	63.6 (62-71)	23.0 (15-28)	7.2 (4-9)
<b>1° (0-6 mm)</b>	2.1 (0.8-3.8)	61.6 (59-70)	19.8 (8-24)	11.8 (7.8-16)†
<b>2° (6-12 mm)</b>	2.2 (1.1-3.3)	62.4 (59-68)	15 (10-24)*	10.8 (7-16)*
<b>3° (12-18 mm)</b>	1.9 (1.0-3)	64.4 (60-70)	17.4 (10-21)*	9.5 (6.5-13.3)*
<b>4° (18-24 mm)</b>	1.6 (1-3)	61.7 (57-70)	17.6 (11-23)	8.7 (6-10)
<b>5° (24-30 mm)</b>	1.2 (1-3)	63.4 (58-66)	18.7 (13-26)	7 (4-11)
<b>6° (30-36 mm)</b>	1.4(0.6-2.4)	61.5 (57-67)	18.4 (11-25)	6.1 (3-9)
<b>P-VALUE</b>	p=0.32	p=0.88	p=0.01	p=0.0001
<b>MODEL 2; N=24</b>				
<b>CORONARY SEGMENTS</b>				
<b>PROX. LMS</b>	0.85 (0.08-1.5)	62.8 (55-69)	24.6 (20-30)	3.8 (2.3-6.8)
<b>DIST. LMS</b>	1.0 (0.3-2.1)	64.1 (59-69)	25 (22-28)	6.5 (4.5-8.8)
<b>LMS CARINA</b>	1.3 (0.3-1.6)	64 (61-71)	28.8 (20-29)	7.3 (4.2-8)
<b>1° (0-6 mm)</b>	2.3 (1-3.4)	62.9 (60-71)	20.9 (13.1-25)	11.3 (8-16)†
<b>2° (6-12 mm)</b>	2.3 (1.2-5.0)	62.6 (55-69)	18.8 (13-27)	9.1 (7-13)*
<b>3° (12-18 mm)</b>	2.2 (0.98-4.3)	64.2 (60-70)	20 (16-23)	8.7 (6.7-13.3)*
<b>4° (18-24 mm)</b>	1.2 (0.9-4.5)	64.4 (57-71)	19.5 (11-26)	8.9 (8-10)*
<b>5° (24-30 mm)</b>	1.3 (0.3-4.8)	63.4 (58-68)	22.5 (13-27)	4.9 (4-8)
<b>6° (30-36 mm)</b>	1.2 (0.6-4)	59.9 (52-66)	22.2 (13-29)	3.5 (1.8-6)
<b>P-VALUE</b>	0.36	0.89	0.19	<0.0001

P-values refer to results for the whole model at general linear analysis. \*, p<0.05; †, p<0.01 at adjusted-post-hoc comparison as compared to left main stem (LMS) in model 1 and to Prox. LMS in model 2. Results are given as median (IQR). Prox.: proximal; Dist.: distal.

Figure 1

A



B

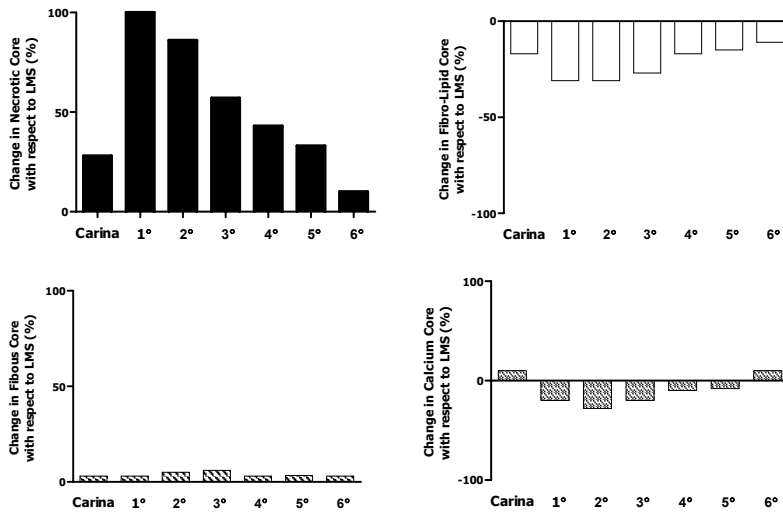


Figure 2

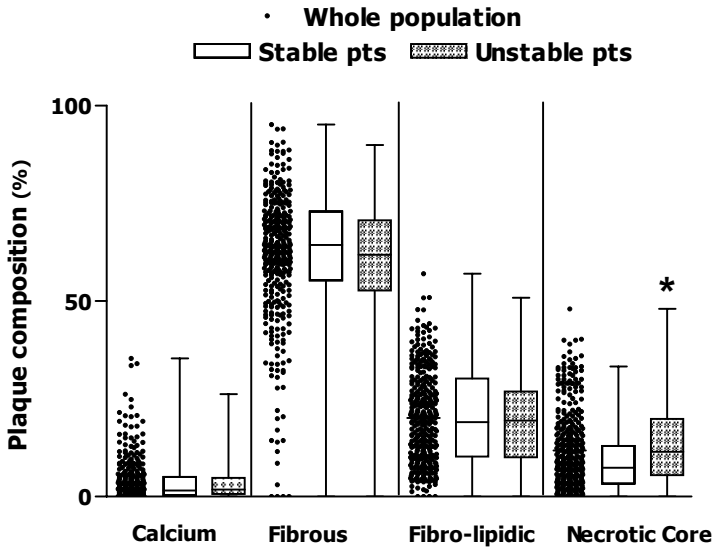


Figure 3

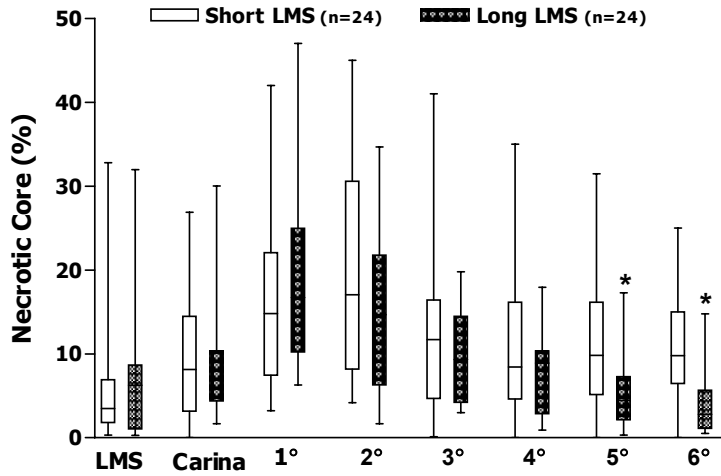
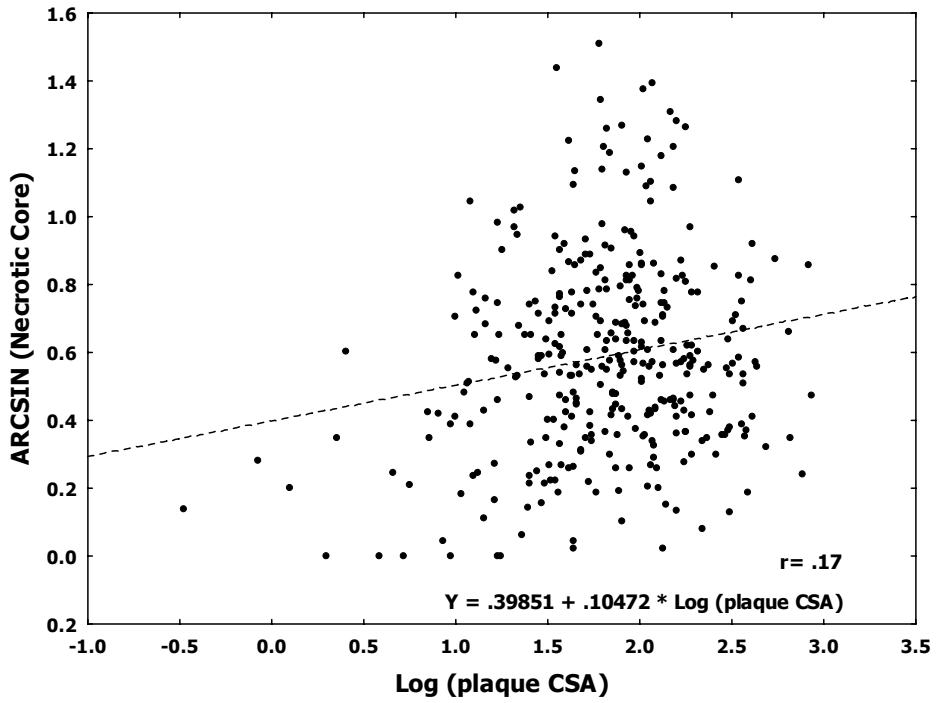
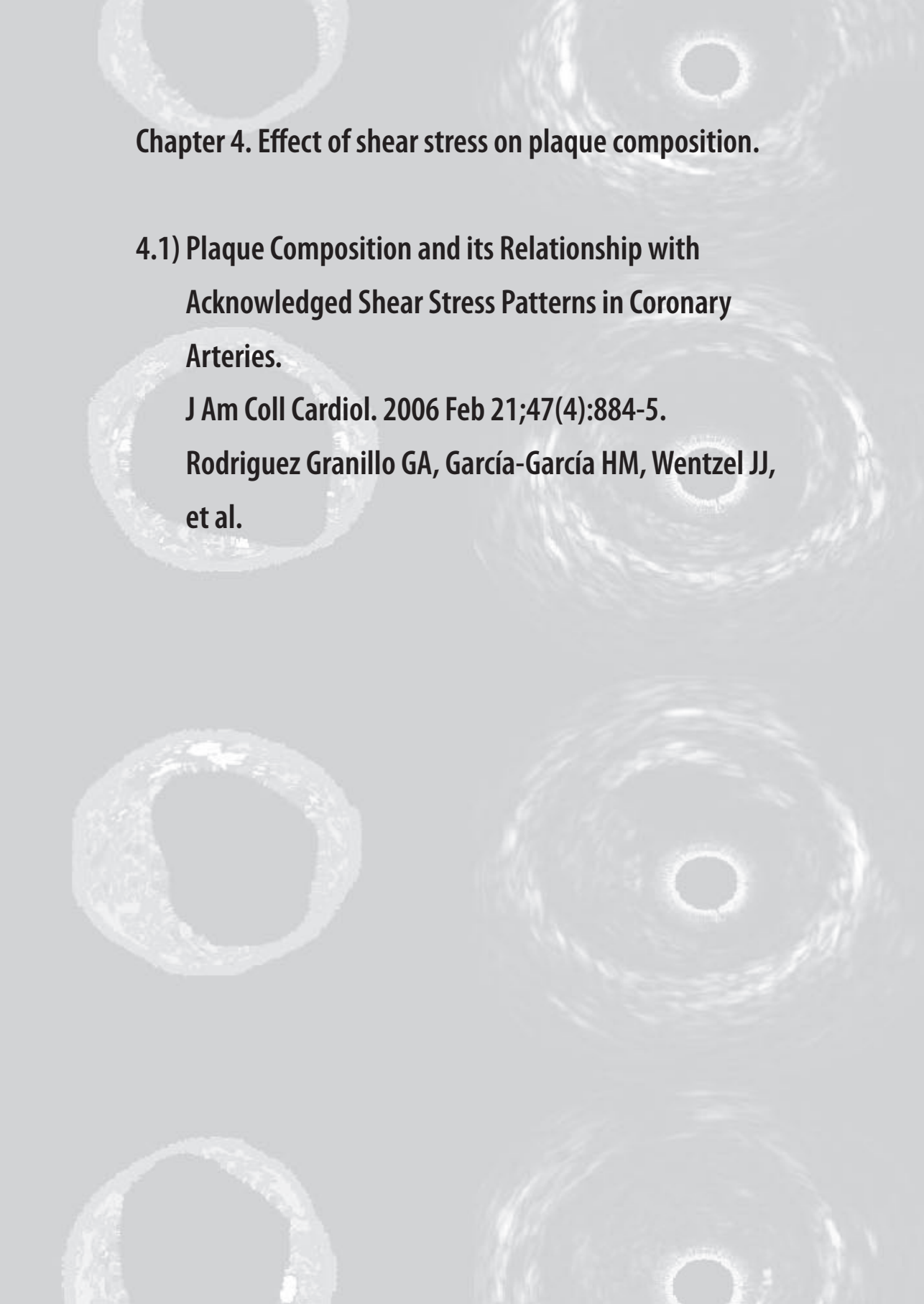


Figure 4







**Chapter 4. Effect of shear stress on plaque composition.**

**4.1) Plaque Composition and its Relationship with  
Acknowledged Shear Stress Patterns in Coronary  
Arteries.**

**J Am Coll Cardiol. 2006 Feb 21;47(4):884-5.**

**Rodriguez Granillo GA, García-García HM, Wentzel JJ,  
et al.**



## CORRESPONDENCE

## Research Correspondence

### Plaque Composition and its Relationship With Acknowledged Shear Stress Patterns in Coronary Arteries

**To the Editor:** Several studies in coronary and peripheral arteries have demonstrated that atherosclerosis has a tendency to arise more frequently in low-oscillatory shear stress (LOSS) regions such as in inner curvature of nonbranching segments and opposite to the flow divider (FD) at bifurcations (1–3). In particular, atherosclerotic disease has certain predilection for the outer wall of the left main coronary artery bifurcation, sparing the FD (2). Intravascular ultrasound (IVUS) has been used to describe the extent, distribution, and profile of plaques in the proximal left anterior descending coronary artery (LAD) (2). Nevertheless, in vivo data regarding tissue composition of this region remain unknown. Furthermore, to date, no study has explored the characteristics of plaques located in the proximal LAD compared to the left main coronary artery (LMCA). In the present study, we sought to explore the morphologic and compositional characteristics of plaque located at an acknowledged LOSS area (outer wall of the ostial LAD [OLAD]) and compare them to the characteristics of plaque located at an average shear stress region (distal LMCA [DLMCA]).

This prospective investigators-driven study included patients where the LAD was interrogated before any intervention using IVUS radiofrequency data (RFD) analysis (IVUS-VH; Volcano Therapeutics, Rancho Cordova, California). The IVUS-VH uses spectral analysis of IVUS RFD to construct tissue maps

that were correlated with a specific spectrum of the RFD and assigned color codes (Fig. 1) (4). The IVUS-VH was performed with 30-MHz (Ultracross; Boston Scientific, Santa Clara, California) and 20-MHz (Eagle Eye; Volcano Therapeutics) catheters, and contour detection was determined using previously reported methodology (5). Informed consent was obtained from all patients. Plaque eccentricity was defined as the ratio of maximal to minimal plaque thickness (1). Plaque burden was defined as  $([EEM_{area} - lumen_{area}]/EEM_{area}) \times 100$ . The carina of the bifurcation was identified as the frame immediately distal to the take-off of the circumflex.

The maximal plaque thickness (MPT) was calculated at this level and spatially located according to a circumference ranging from 0° to 360°, being the inner and opposite part of the carina at 0° and 180°, respectively. Lesions were therefore prospectively divided into two groups, according to their localization in the outer (from 91° to 271°) or inner (from 270° to 90°) hemisphere of the carina.

Two regions were prospectively identified and their morphology and composition compared. The OLAD was defined as the carina and the immediate 3-mm distal segment, because the flow in this area is still influenced by the bifurcation (6). Similarly, the DLMCA was identified as the 3-mm segment immediately

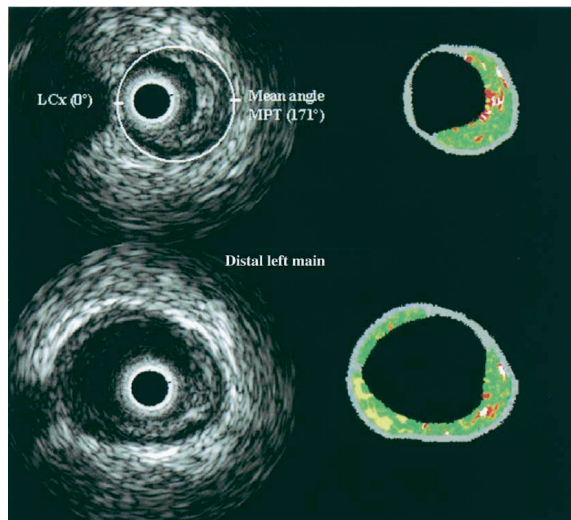


**Figure 1.** Intravascular ultrasound cross-section images from the carina of the left anterior descending coronary artery and of the left main coronary artery. The **left side** shows the reconstructed grayscale, and the **right side** shows the color-coded data (**green** = fibrous; **yellow-green** = fibrolipidic; **red** = necrotic core; **white** = calcium) provided by the IVUS-VH unit (Volcano Therapeutics, Rancho Cordova, California). LCx = left circumflex artery; MPT = maximal plaque thickness.

**Table 1.** Volumetrical and Compositional Comparative Results Between the Ostial Left Anterior Descending Coronary Artery (OLAD) and the Distal Left Main Coronary Artery (DLMCA)

	OLAD	DLMCA	p Value
Plaque burden (%)	45.5 ± 10.2	36.4 ± 10.8	<0.0001
Plaque eccentricity	14.5 ± 11.6	10.4 ± 7.6	0.05
Max. plaque thickness (mm)	1.24 ± 0.4	1.04 ± 0.3	0.002
Necrotic core (%)	12.4 ± 9.2	7.9 ± 8.6	<0.0001
Calcium (%)	4.1 ± 5.1	1.3 ± 2.0	<0.0001
Fibrous (%)	64.5 ± 13.6	64.9 ± 13.3	0.82
Fibrolytic (%)	18.4 ± 11.8	24.9 ± 12.8	0.005

Values are presented as mean ± SD. Plaque eccentricity was defined as the ratio of maximal to minimal plaque thickness. Plaque burden was defined as  $(\text{EEM}_{\text{area}} - \text{lumen}_{\text{area}}) / \text{EEM}_{\text{area}} \times 100$ .

proximal to the bifurcation. Compositional and geometrical data were expressed as mean percentages.

Discrete variables are presented as counts and percentages. Continuous variables are presented as mean ± SD. Differences in means among groups were analyzed by two-sample *t* test. A *p* value of <0.05 (two-sided) was considered to indicate statistical significance.

Forty-four patients were finally included in the analysis. The clinical presentation was stable angina in 23 patients (52.3%), unstable angina in 10 patients (22.7%) and acute myocardial infarction in 11 patients (5%); the mean age of the patients was 58.8 ± 11.5 years, and 33 patients (75%) were male. Geometric and compositional comparative results between the OLAD and the DLMCA are depicted in Table 1. Plaque burden was larger in the OLAD than in the DLMCA (45.5 ± 10.2% vs. 36.4 ± 10.8%; *p* < 0.0001). OLAD plaques presented more calcified (4.13 ± 5.1% vs. 1.28 ± 2.0%; *p* < 0.0001) and necrotic (12.36 ± 9.2% vs. 7.90 ± 8.6%, *p* < 0.0001) core content.

The MPT was located in the outer hemisphere of the carina in 77.3% (*n* = 34) of the cases and the mean angle was 170.7 ± 60.6°. Only one case presented the MPT at 0 degrees. Necrotic core content was larger in outer than in inner lesions (14.4 ± 10.0% vs. 6.3 ± 6.9%; *p* = 0.02).

The current investigation extends earlier findings on atheroma distribution in the LAD by comparing *in vivo* plaque burden and composition in acknowledged areas of low and average shear stress. It has been previously established that an inverse relationship exists between LOSS and thickness of the vessel wall (3). The pathophysiology of such phenomena can briefly be explained by the fact that LOSS induces a loss of the physiologic flow-oriented alignment of the endothelial cells, thus causing an enhancement of the expression of adhesion molecules and a weakening of cell junctions, ultimately leading to an increase in permeability to lipids and macrophages (3,7–9). The results of the present study are in line with histopathologic data, showing higher concentrations of necrotic core and calcium in an acknowledged area subject to LOSS. Such difference may be driven by the lipid leakage present in these areas (8). The high lipid load in addition to the eccentric characteristics of the atheroma would potentially render these plaques more susceptible to rupture (10). Conversely, the more stable phenotype observed in DLMCA lesions supports the low incidence of atherothrombotic events at this level (11). Finally, these results may provide another potential explanation for the higher risk of restenosis after percutaneous coronary intervention of bifurcation lesions.

In summary, we found that OLAD atherosclerotic plaques present larger plaque burden, eccentricity, and MPT than DLMCA plaques. In addition, a larger calcified and necrotic core content was found distal to the circumflex take-off. Lesions were predominantly located in the outer wall of the carina, and such location was associated with larger necrotic core content.

**Gastón A. Rodríguez-Granillo, MD**  
**Héctor M. García-García, MD**  
**Jolanda Wentzel, PhD**  
**Marco Valgimigli, MD**  
**Keiichi Tsuchida, MD**  
**Wim van der Giessen, MD, PhD**  
**Peter de Jaegere, MD, PhD**  
**Evelyn Regar, MD, PhD**  
**Pim J. de Feyter, MD, PhD**  
**\*Patrick W. Serruys, MD, PhD, FACC**

\*Thoraxcenter, Bld406

Dr. Molewaterplein 40

3015-GD Rotterdam

the Netherlands

E-mail: p.w.j.c.serruys@erasmusmc.nl

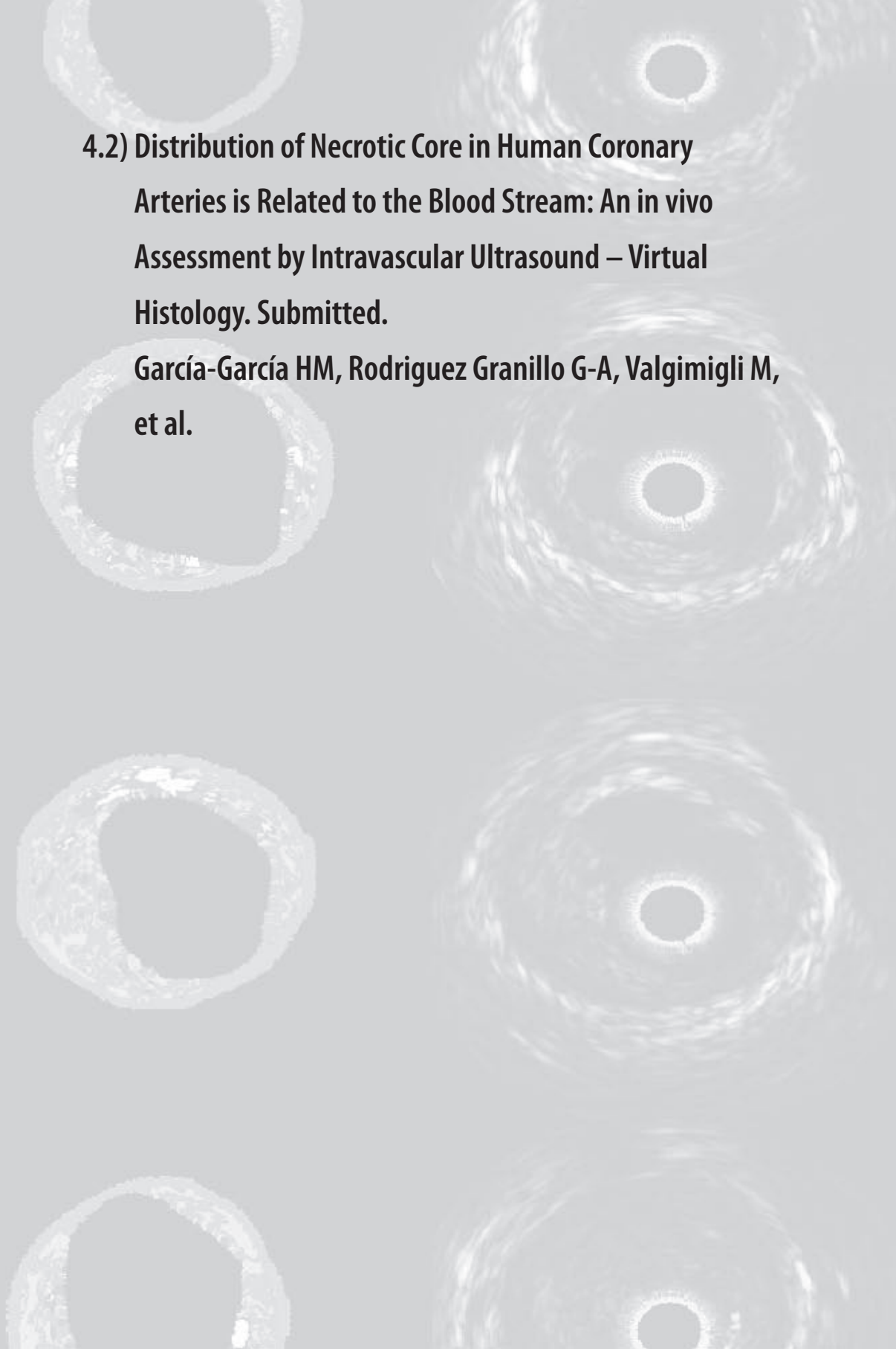
doi:10.1016/j.jacc.2005.11.027

## REFERENCES

- Jeremias A, Huegel H, Lee DP, et al. Spatial orientation of atherosclerotic plaque in nonbranching coronary artery segments. *Atherosclerosis* 2000;152:209–15.
- Kimura BJ, Russo RJ, Bhargava V, McDaniel MB, Peterson KL, DeMaria AN. Atheroma morphology and distribution in proximal left anterior descending coronary artery: *in vivo* observations. *J Am Coll Cardiol* 1996;27:825–31.
- Kornet L, Hoeks AP, Lambregts J, Reneman RS. In the femoral artery bifurcation, differences in mean wall shear stress within subjects are associated with different intima-media thicknesses. *Arterioscler Thromb Vasc Biol* 1999;19:2933–9.
- Nair A, Kuban BD, Tuzcu EM, Schoenhagen P, Nissen SE, Vince DG. Coronary plaque classification with intravascular ultrasound radiofrequency data analysis. *Circulation* 2002;106:2200–6.
- Rodríguez-Granillo GA, Serruys PW, García-García HM, et al. Coronary artery remodeling is related to plaque composition. *Heart* 2005 Jun 17; [Epub ahead of print].
- Gijssen F, Thury A, Lamers B, Wentzel JJ, Schuurbiens JCH, Serruys PW, Slager CJ. 3D plaque distribution and its relationship to shear stress in a human coronary artery bifurcation *in vivo*. Presented at: Summer Bioengineering Conference, June 22–26, 2005 Vail, Colorado.
- Berclé SA, Warty VS, Shepeck RA, Mandarino WA, Tanksale SK, Borovetz HS. Hemodynamics and low density lipoprotein metabolism. Rates of low density lipoprotein incorporation and degradation along medial and lateral walls of the rabbit aorto-iliac bifurcation. *Arteriosclerosis* 1990;10:686–94.
- Kaazempur-Mofrad MR, Isasi AG, Younis HF, et al. Characterization of the atherosclerotic carotid bifurcation using MRI, finite element modeling, and histology. *Ann Biomed Eng* 2004;32:932–46.
- Slager CJ, Wentzel J, Gijssen FJH, Schuurbiens JCH, van der Wal AC, van der Steen AFW, Serruys PW. The role of shear stress in the generation of rupture-prone vulnerable plaques. *Nat Clin Pract* 2005; 2:401–7.
- Falk E, Shah PK, Fuster V. Coronary plaque disruption. *Circulation* 1995;92:657–71.
- Wang JC, Normand SL, Mauri L, Kuntz RE. Coronary artery spatial distribution of acute myocardial infarction occlusions. *Circulation* 2004;110:278–84.

**4.2) Distribution of Necrotic Core in Human Coronary Arteries is Related to the Blood Stream: An in vivo Assessment by Intravascular Ultrasound – Virtual Histology. Submitted.**

**García-García HM, Rodríguez Granillo G-A, Valgimigli M, et al.**





**Necrotic Core is Distributed Predominantly in the  
Upstream Segments of the Human Coronary Plaques: An  
*in vivo* Assessment Using Intravascular Ultrasound  
Radiofrequency Data Analysis**

Héctor M. García-García MD; Gastón A. Rodríguez-Granillo MD;  
Marco Valgimigli MD; Jolanda J. Wentzel PhD; Frank Gijssen PhD; Johan  
C.H. Schuurbiers BSc; Marie-Angele M. Morel BSc<sup>1</sup>, Peter P.T. de Jaegere  
MD, PhD; Pim de Feyter MD, PhD; Rob Krams MD, PhD; Patrick W. Serruys  
MD, PhD.

Thoraxcenter, Erasmus Medical Center, Rotterdam, Netherlands.

<sup>1</sup>Cardialysis BV, Rotterdam, The Netherlands

## ABBREVIATIONS

ACS- Acute coronary syndrome

EEM- External elastic membrane

CSA – Cross sectional area

IVUS- Intravascular Ultrasound

NC – Necrotic core

NO - Nitric oxide

SMC- Smooth muscle cells

SS - Shear stress

VH- Virtual histology

## INTRODUCTION

Atherothrombosis in coronary arteries is the corollary of inflammation, deposit of cholesterol and thrombus formation. An encroaching atherosclerotic plaque has an impact on the pattern of the blood flow. Indeed, the upstream endothelium sites of the plaque is under high-shear stress (SS), whereas at the downstream endothelium low-SS prevails<sup>1</sup>. Furthermore, atherosclerotic plaque composition varies greatly<sup>2</sup>, being the macrophages concentration higher in the upstream part and the smooth muscle cells (SMCs) in the downstream part of the atherosclerotic plaque<sup>2,3</sup>. It has been shown that macrophages are a major source of metalloproteinases, which might lead to reduction of extracellular matrix<sup>4,5</sup> and the macrophages can also induce apoptosis of SMCs<sup>6,7</sup>, resulting in thinning of the fibrous cap in the upstream part of the plaque<sup>8</sup>. On the other hand, on the downstream part of the plaque, an intense synthesis of extracellular matrix is observed as a result of the SMCs function. Moreover, clinical presentation is related to both the tissue composition of the coronary tree<sup>9</sup> and the cell distribution in the coronary plaques. Thus, in patients with stable angina, the SMCs are the predominant cell type, whereas in unstable patients the macrophages are the most prevalent cell type<sup>10,11</sup>.

Lastly, it has been hypothesized that the differences in the shear stress may influence also the distribution of the necrotic core (NC) in the atherosclerotic plaques in the coronary arteries<sup>8,12</sup>. We sought to explore the potential presence of an uneven distribution of NC along focal coronary atherosclerotic plaques using intravascular ultrasound radiofrequency analysis data (IVUS-VH).

## **MATERIAL AND METHODS**

The present investigation was an investigators-driven study. Consecutive patients admitted for coronary catheterization and subsequent intervention were eligible for IVUS interrogation of at least 30 mm of length in a non-branching coronary segment with an angiographically nonobstructive (<50%) de novo lesion, in a non-target vessel suitable for IVUS interrogation. Patients with lesions located in proximal (but not ostial) and mid segments of a coronary artery were included. Patients with stable angina or acute coronary syndromes (ACS) were included. Acute coronary syndrome patients encompassed patients presenting with unstable angina, non-ST segment elevation MI, or ST segment elevation MI. Acute Myocardial infarction (MI) was diagnosed by an increase in the creatine kinase MB level to more than two-fold the normal limit.

Major exclusion criteria included hemodynamically unstable, coronary anatomy that precluded safe IVUS examination or severe angiographic calcification.

The institutional ethic committee approved the study protocol and informed written consent was obtained from all patients.

### **IVUS-VH Acquisition and Analysis**

Details regarding the validation of the technique, on explanted human coronary segments, have previously been reported<sup>13</sup>. Briefly, IVUS-VH uses spectral analysis of IVUS radiofrequency data to build tissue maps that are correlated with a specific spectrum of the radiofrequency signal and assigned colour codes [fibrous (labelled green), fibrolipidic (labelled greenish-yellow), necrotic core (labelled red) and calcium (labelled white)]<sup>13</sup>.

IVUS-VH data was acquired using a continuous pullback (Ultracross™ 30 MHz catheter, Boston Scientific, Santa Clara, USA and Eagle-Eye™ 20 MHz Volcano Therapeutics, Rancho Cordova, CA ), by a dedicated IVUS-VH console (Volcano Therapeutics, Rancho

Cordova, CA). The Ultracross™ 30 MHz catheter is covered with a 127 mm outer sheath to prevent direct contact of the ultrasound element with the vessel wall. The results of an in vitro study showed a significant underestimation of measurements using IVUS-VH with respect to the Galaxy and the Curad (QCU) software<sup>14</sup>. The attenuation suffered by the ultrasound propagation speed while crossing the sheath was not accounted for in the IVUSLab software (Volcano Therapeutics, Rancho Cordova, CA). Accordingly, an adjustment method for 30 MHz Boston Scientific catheters described by Bruining et al. was applied to the results<sup>15</sup>. The IVUS VH data were stored on a CD/DVD and sent to the imaging core lab for offline analysis (Cardialysis BV, Rotterdam, The Netherlands). Data acquisition was ECG-gated and recorded during the automated withdrawal of the catheter using a mechanical pullback device (Boston Scientific, Santa Clara, USA or Volcano Therapeutics, Rancho Cordova, CA) at a pullback speed of 0.5 mm/s. Cine runs, before and during contrast injection, were performed to define the position of the IVUS catheter before the pullback was started.

IVUS B-mode images were reconstructed from the RF data by customized software (Version 4.3 IVUSLab). Longitudinal and cross-sectional views were used to determine the contours. Manual contour detection of both the lumen and the media-adventitia interface was performed and the radiofrequency data was normalized using a technique known as “Blind Deconvolution”<sup>16</sup>, an iterative algorithm that deconvolves the catheter transfer function from the backscatter, thus accounting for catheter-to-catheter variability. Geometrical and compositional data were obtained for every slice.

The contours of the external elastic membrane (EEM) and the lumen-intima interface enclosed an area that was defined as the coronary plaque plus media area. Plaque burden was defined as  $[(EEM_{area} - Lumen_{area}) / EEM_{area}] \times 100$ . Plaque eccentricity index was defined as  $(Minimum\ plaque\ thickness / Maximum\ plaque\ thickness)^{17}$ , where 1 indicates concentric

plaque and  $<1$  indicates increasing plaque eccentricity. Direct measurements (lumen and vessel cross-sectional areas - CSA) were also determined.

### **Sub-segment analysis**

First, the most diseased part of the vessel was selected by finding the CSA with the largest plaque burden and the minimum lumen area. Subsequently, its immediate 10 mm proximal (upstream) and distal (downstream) were included in the region of interest (ROI) and only one ROI per vessel was selected for this analysis. Thus, a 20 mm length segment was analyzed per vessel. Finally, the segment was divided in four 5 mm sub-segments, two proximal to the most diseased CSA and two distal (Figure 1 and 2).

In addition, the distribution along the plaque of the CSAs containing more than 5, 10, 15 and 20% of necrotic core within the plaque was analyzed.

### **Statistical analysis**

Three modes of statistical analysis were performed, in order to analyze patient, segment and CSA characteristics. The patient basis database was used to analyze the demographic and clinical characteristics. The segment analysis was performed to describe the IVUS and VH components. Finally, the database per CSA was built to make comparisons and correlations between and within the components of IVUS-VH. Log transformation was performed in the variables with skewed distribution.

Discrete variables are presented as counts and percentages. Continuous variables are presented as means  $\pm$  standard deviation. Correlation analysis and its scatter plot was done using the log transformation of the NC and calcium content.

One-way ANOVA and posthoc test using Bonferroni were performed for mean comparisons.

A two-sided P value  $<0.05$  was required for statistical significance. All analyses were performed using SPSS version 11.5 software (Chicago, Illinois, USA).

## RESULTS

A total of 90 consecutive patients (121 vessels, 4840 CSAs) were included after verification of a properly acquired IVUS. The baseline characteristics of the patient population are depicted in table 1. The mean age was  $57.9 \pm 10.8$  years, most being male patients 68 (75.6 %). Of note, only 7.8% of the population were diabetics.

The vessel of interest was the left anterior descending in 52 (43.0 %), the left circumflex in 31 (25.6 %) and the right coronary artery in 38 (31.4 %) patients. Fifty-three (58.9 %) patients presented with stable angina, 17 (18.9%) with unstable angina/non-ST segment elevation MI, and 20 (22.2 %) with an ST segment elevation acute myocardial infarction.

### IVUS-VH geometrical findings

The mean eccentricity plaque index was  $0.20 \pm 0.12$ , (median 0.16, IQR 0.06-0.29). The tapering of the vessel in the analyzed segment showed small changes from proximal to distal in vessel and luminal CSA; the vessel CSA in the sub-segment 1 was  $15.7 \pm 5.2 \text{mm}^2$  and the sub-segment 4 was  $13.5 \pm 5 \text{mm}^2$ , and the luminal CSA were larger in sub-segment one and four, 8.9 and  $7.8 \text{mm}^2$  respectively, compared to the mid sub-segments, being  $7.2 \text{mm}^2$  in two and  $7.0 \text{mm}^2$  in three respectively. (Figure 1 and table 2).

Furthermore, the plaque burden had the following distribution,  $43 \pm 14\%$ ,  $51.8 \pm 14.1\%$ ,  $50.3 \pm 13.5\%$  and  $41.9 \pm 12.7\%$  from proximal to distal (sub-segment 1 through sub-segment 4) ( $p < 0.001$ )(Table 2).

### IVUS-VH morphological findings

The mean relative necrotic core content was larger in the two upstream sub-segments than in the downstream sub-segment of the plaque, being  $11.6 \pm 10\%$  in sub-segment 1 (compared to

sub-segment 4 the mean difference was 1.4, 95%CI [0.29, 2.42],  $p=0.004$ ); the content of necrotic core in sub-segment 2 was  $11.7\pm 9.7\%$  (compared to sub-segment 4 the mean difference was 1.5, 95%CI [0.40, 2.56],  $p=0.002$ ), whereas in the sub-segment 4 the necrotic core was  $10.2\pm 9.9\%$ . Irrespective of the cut off used for the content of NC per CSA (5, 10, 15 or 20%) the number of CSAs with NC  $>5\%$  were higher in the upstream part of the plaque. If only CSAs with more than 10% of NC content are considered for the analysis - threshold that was previously used as part of the definition of IVUS-derived thin cap fibroatheroma (IDTFCA)-<sup>18</sup>, the topographic distribution was as follows: the sub-segment 1 had a total of 574 CSAs; 585 CSAs in the sub-segment 2; 541 CSAs in the sub-segment 3, and in the most distal 522 CSAs (sub-segment 4) were found,  $p=0.014$ . (Figure 1 and Table 2)

Of note, the calcium content had the same distribution as the necrotic core, being larger in the sub-segment 2 ( $6.5\pm 9.7\%$ ) than in sub-segment 4 ( $5.4\pm 9.5\%$ ,  $p=0.03$ ). In addition, the per CSA analysis showed that there was a positive correlation between necrotic core and calcium with a Pearson correlation coefficient of 0.74,  $p<0.001$  (Figure 3).

Interestingly, fibrous tissue was larger in downstream sub-segments. Indeed, the largest amount of fibrous tissue was found in segment 3 with  $63.8\pm 9\%$ ; when compared with the other three subsegments the difference was statistically significant,  $p=0.008$ . (Table 2).

As an exploratory analysis, the total population was split into two groups: stable angina vs. acute coronary syndrome, and the plaque composition was then evaluated. Interestingly, the overall content of NC was larger in patients with ACS  $13.7\pm 8.2\%$  than patients with stable angina  $8.1\pm 6.4\%$ ,  $p=0.001$ . Conversely, the fibrous tissue was larger in patients with stable angina  $66.9\pm 13.8$  vs.  $58.8\pm 13.6$ ,  $p=0.006$ . (Table 3). However, irrespective of the clinical presentation the distribution of CSAs with NC  $>10\%$  followed the same distribution as in the overall analysis, being more frequent in the upstream part of the plaque. Thus, stable patients in the upstream part of the plaque had 523 CSAs and in the downstream part 454, whereas in

the patients with acute coronary syndrome the upstream part had 636 CSAs and the downstream part 609.

## DISCUSSION

The main findings of this study were the following: the necrotic core was predominantly distributed in the proximal segments of the coronary plaque. The upstream sub-segments presented significantly larger content of necrotic core (one and two) than the downstream sub-segments, specifically, the most distal one. Likewise, the calcium distribution followed the same pattern as the necrotic core. Conversely, the fibrous tissue was the predominant component in the downstream sub-segments. Moreover, and in line with our previous report, we have confirmed the finding that the plaque composition is different in patients with acute coronary syndromes and stable angina; the content of NC was larger in the first group, whereas the fibrous tissue was predominant in the second group<sup>9</sup>.

To the best of our knowledge, this is the first *in vivo* study showing marked topographic differences in tissue composition within atherosclerotic plaques.

It is known that in regions with endothelial dysfunction, which coincide with low shear stress, nitric oxide (NO) bioavailability is decreased<sup>19,20</sup>, leading to a pro-atherosclerotic state. As a result, atherothrombosis had a peculiar geometric distribution along the vascular system<sup>21</sup>.

Supporting the hypothesis that shear stress might influence plaque composition. Our group has previously investigated the plaque composition of acknowledged regions of low shear stress such as the opposite wall to the flow divider at the ostium of the left anterior descending in comparison with the distal part of the left main that has a flow laminar velocity pattern<sup>22</sup>. The plaque burden was larger in the ostium of the left anterior descending than in distal left main (45.5±10.2 vs. 36.4±10.8 %, p<0.0001). In addition, in the ostium the plaques presented more calcified (4.13±5.1 vs. 1.28±2.0 %, p<0.0001) and necrotic core (12.36±9.2 vs. 7.90±8.6 %, p<0.0001) content<sup>22</sup>. Of note, the aforementioned analysis was done

considering the radial distribution of the plaque and in a very limited number of CSAs (n=6 mm).

Acute coronary syndromes are due to non-obstructive plaques in the majority of the cases<sup>23,24</sup>, and previous pathological and *in vivo* studies have suggested that necrotic-core rich plaques are more likely to cause ACS than fibrotic plaques<sup>9,25,26</sup>. Hence, the early identification of the rupture-prone plaques might have a great impact in the current approach of the coronary artery disease. Indeed, another interesting feature of the focal atherosclerotic coronary plaque - documented in this *in vivo* study - is that necrotic core is an unevenly distributed component along the same plaque, being larger proximal to the minimal lumen site. Likewise, previous reports have shown that ruptured plaques associated with acute coronary syndromes are mostly located proximal to the most diseased part of the plaque<sup>27</sup>, where it has been also suggested that the plaque rupture-healing process that could cause plaque growth takes place. Moreover, in that area prevails high SS, which has been hypothesized to cause increment in nitric oxide bioavailability from the endothelium resulting in the thinning of the fibrous cap<sup>8</sup>. Why all this complex process is happening in the upstream part of the plaque is not obvious<sup>8</sup>. However, it has been also hypothesized that the plasmin, which is produced by the endothelium at high SS, is a strong activator of metalloproteinase secreted by macrophages<sup>28</sup>, which could be an important factor to the breakdown of the collagenous cap.

The predominantly proximal distribution of necrotic core was not an isolated finding, since concomitantly the fibrous component was found to be the most prevalent tissue at downstream sites, where the SMCs are predominant and their synthesis of extracellular matrix is not offset by macrophages<sup>12</sup>. Indeed, when low SS prevails (as in those areas), the SMCs produce the matrix, which provides the mechanical strength of the plaque cap<sup>25,29</sup>.

Equally important, the calcium was found to be located in the same region of the necrotic core at the proximal part of the plaque. As for vascular calcification, several proteins have been

shown to be involved in this also intriguing process, such as bone morphogenic protein, osteoprotegerin, matrix Gla protein, and osteopontin<sup>30</sup>. The macrophages, which are mainly located on upstream sites, express osteopontin<sup>31</sup> a protein that has been identified by immunohistochemistry in atherosclerotic plaques<sup>32</sup>.

The longitudinal heterogeneity in plaque composition documented in this study might help us to better understand the participation of shear stress in the plaque growth and instability processes.

### **Limitations of the study**

There are a number of limitations associated with the present study. The studied population was relatively small and some variables are underrepresented such as female and diabetic patients; only non-flow limiting, eccentric and non-severely calcified plaques were considered. Hence, small changes in the plaque composition, although significant, were documented. A study with obstructive plaques might show bigger differences.

An arbitrary region of interest (20 mm) subdivided in sub-segments of 5 mm was used as a template for the analysis in our study. This segmental analysis only permits a rudimentary assessment of the relationship between shear stress and vessel wall composition. A more accurate assessment would imply a continuous point-to-point comparison of the two techniques, but this is currently not possible due to the fact that two different catheters must be used for the acquisition and spatial differences in matching is unavoidable.

In the near future, IVUS-VH and palpography will be acquired in a single pull back, making the analysis of morphological, compositional and mechanical properties of the plaque more reliable.

Undoubtedly, histopathology remains the gold standard to typify tissue but this IVUS-VH has the potential to provide real-time accurate information regarding tissue characterization and plaque morphology.

## **CONCLUSIONS**

The necrotic core and calcium content were larger in the upstream part of the coronary plaque. Furthermore, the fibrous tissue prevailed in the downstream section of the plaque.

## **ACKNOWLEDGEMENTS**

Authors would like to thank you Maria de Lourdes Heredia Garcia (MD) for help with data acquisition and Evelyn Regar (MD, PhD) for her invaluable support reviewing the paper.

## REFERENCES

1. Zarins CK, Bomberger RA, Glagov S. Local effects of stenoses: increased flow velocity inhibits atherogenesis. *Circulation*. 1981;64:II221-7.
2. Krams R, Verheye S, van Damme LC, Tempel D, Gourabi BM, Boersma E, Kockx MM, Knaapen MW, Strijder C, van Langenhove G, Pasterkamp G, van der Steen AF, Serruys PW. In vivo temperature heterogeneity is associated with plaque regions of increased MMP-9 activity. *Eur Heart J*. 2005;26:2200-5.
3. Dirksen MT, van der Wal AC, van den Berg FM, van der Loos CM, Becker AE. Distribution of inflammatory cells in atherosclerotic plaques relates to the direction of flow. *Circulation*. 1998;98:2000-3.
4. Sukhova GK, Schonbeck U, Rabkin E, Schoen FJ, Poole AR, Billingham RC, Libby P. Evidence for increased collagenolysis by interstitial collagenases-1 and -3 in vulnerable human atheromatous plaques. *Circulation*. 1999;99:2503-9.
5. Galis ZS, Khatri JJ. Matrix metalloproteinases in vascular remodeling and atherogenesis: the good, the bad, and the ugly. *Circ Res*. 2002;90:251-62.
6. van der Wal AC, Becker AE, van der Loos CM, Das PK. Site of intimal rupture or erosion of thrombosed coronary atherosclerotic plaques is characterized by an inflammatory process irrespective of the dominant plaque morphology. *Circulation*. 1994;89:36-44.
7. Libby P. Molecular bases of the acute coronary syndromes. *Circulation*. 1995;91:2844-50.
8. Slager CJ, Wentzel JJ, Gijsen FJ, Schuurbijs JC, van der Wal AC, van der Steen AF, Serruys PW. The role of shear stress in the generation of rupture-prone vulnerable plaques. *Nat Clin Pract Cardiovasc Med*. 2005;2:401-7.
9. Rodriguez-Granillo GA ME, Valgimigli M, van Mieghem CAG, Regar E, de Feyter PJ, Serruys PW. Coronary plaque composition of non-culprit lesions assessed by in vivo intracoronary ultrasound radio frequency data analysis, is related to clinical presentation. *Am Heart J*. 2005;In press.
10. Moreno PR, Falk E, Palacios IF, Newell JB, Fuster V, Fallon JT. Macrophage infiltration in acute coronary syndromes. Implications for plaque rupture. *Circulation*. 1994;90:775-8.
11. van der Wal AC, Becker AE, Koch KT, Piek JJ, Teeling P, van der Loos CM, David GK. Clinically stable angina pectoris is not necessarily associated with histologically stable atherosclerotic plaques. *Heart*. 1996;76:312-6.
12. Slager CJ, Wentzel JJ, Gijsen FJ, Thury A, van der Wal AC, Schaar JA, Serruys PW. The role of shear stress in the destabilization of vulnerable plaques and related therapeutic implications. *Nat Clin Pract Cardiovasc Med*. 2005;2:456-64.
13. Nair A, Kuban BD, Tuzcu EM, Schoenhagen P, Nissen SE, Vince DG. Coronary plaque classification with intravascular ultrasound radiofrequency data analysis. *Circulation*. 2002;106:2200-6.
14. Rodriguez-Granillo GA, Bruining N, Mc Fadden E, Ligthart JM, Aoki J, Regar E, de Feyter P, Serruys PW. Geometrical validation of intravascular ultrasound radiofrequency data analysis (Virtual Histology) acquired with a 30 MHz boston scientific corporation imaging catheter. *Catheter Cardiovasc Interv*. 2005;66:514-8.
15. Bruining N, Hamers R, Teo TJ, de Feijter PJ, Serruys PW, Roelandt JR. Adjustment method for mechanical Boston scientific corporation 30 MHz intravascular ultrasound catheters connected to a Clearview console. Mechanical 30 MHz IVUS catheter adjustment. *Int J Cardiovasc Imaging*. 2004;20:83-91.
16. Karsen KF BE. Blind deconvolution of ultrasonic traces accounting for pulse variance. *IEEE Trans Ultrason Ferroelectr Freq Control*. 1999;46:564-573.
17. Di Mario C, Gorge G, Peters R, Kearney P, Pinto F, Hausmann D, von Birgelen C, Colombo A, Mudra H, Roelandt J, Erbel R. Clinical application and image interpretation in intracoronary ultrasound. Study Group on Intracoronary Imaging of the Working Group of Coronary Circulation and of the Subgroup on Intravascular Ultrasound of the Working Group of Echocardiography of the European Society of Cardiology. *Eur Heart J*. 1998;19:207-29.
18. Rodriguez-Granillo Gaston A M, Garcia-García Héctor M., MD, Mc Fadden Eugene P, MD, FRCPI, Valgimigli Marco, MD, Aoki Jiro, MD, de Feyter Pim, MD, PhD, Serruys Patrick W, MD, PhD. In vivo intravascular ultrasound-derived thin-cap fibroatheroma detection using ultrasound radio frequency data analysis. *J Am Coll Cardiol*. 2005;46.

19. Ignarro LJ, Napoli C. Novel features of nitric oxide, endothelial nitric oxide synthase, and atherosclerosis. *Curr Atheroscler Rep.* 2004;6:281-7.
20. Voetsch B, Jin RC, Loscalzo J. Nitric oxide insufficiency and atherothrombosis. *Histochem Cell Biol.* 2004;122:353-67.
21. Malek AM, Alper SL, Izumo S. Hemodynamic shear stress and its role in atherosclerosis. *Jama.* 1999;282:2035-42.
22. Rodriguez-Granillo GA G-GH, Wentzel J, Valgimigli M, Tsuchida K, van der Gissen W, de Jaegere P, Regar E, de Feyter P, Serruys PW. Plaque composition and its relationship with acknowledged shear stress patterns in coronary arteries. *J Am Coll Cardiol.* 2005;In press.
23. Kannel WB, Doyle JT, McNamara PM, Quickenon P, Gordon T. Precursors of sudden coronary death. Factors related to the incidence of sudden death. *Circulation.* 1975;51:606-13.
24. Falk E, Shah PK, Fuster V. Coronary plaque disruption. *Circulation.* 1995;92:657-71.
25. Davies MJ, Richardson PD, Woolf N, Katz DR, Mann J. Risk of thrombosis in human atherosclerotic plaques: role of extracellular lipid, macrophage, and smooth muscle cell content. *Br Heart J.* 1993;69:377-81.
26. Kragel AH, Reddy SG, Wittes JT, Roberts WC. Morphometric analysis of the composition of atherosclerotic plaques in the four major epicardial coronary arteries in acute myocardial infarction and in sudden coronary death. *Circulation.* 1989;80:1747-56.
27. Fujii K, Kobayashi Y, Mintz GS, Takebayashi H, Dangas G, Moussa I, Mehran R, Lansky AJ, Kreps E, Collins M, Colombo A, Stone GW, Leon MB, Moses JW. Intravascular ultrasound assessment of ulcerated ruptured plaques: a comparison of culprit and nonculprit lesions of patients with acute coronary syndromes and lesions in patients without acute coronary syndromes. *Circulation.* 2003;108:2473-8.
28. Lijnen HR. Plasmin and matrix metalloproteinases in vascular remodeling. *Thromb Haemost.* 2001;86:324-33.
29. Burleigh MC, Briggs AD, Lendon CL, Davies MJ, Born GV, Richardson PD. Collagen types I and III, collagen content, GAGs and mechanical strength of human atherosclerotic plaque caps: span-wise variations. *Atherosclerosis.* 1992;96:71-81.
30. Fuster V, Moreno PR, Fayad ZA, Corti R, Badimon JJ. Atherothrombosis and high-risk plaque part I: evolving concepts. *J Am Coll Cardiol.* 2005;46:937-54.
31. Ikeda T, Shirasawa T, Esaki Y, Yoshiki S, Hirokawa K. Osteopontin mRNA is expressed by smooth muscle-derived foam cells in human atherosclerotic lesions of the aorta. *J Clin Invest.* 1993;92:2814-20.
32. O'Brien ER, Garvin MR, Stewart DK, Hinohara T, Simpson JB, Schwartz SM, Giachelli CM. Osteopontin is synthesized by macrophage, smooth muscle, and endothelial cells in primary and restenotic human coronary atherosclerotic plaques. *Arterioscler Thromb.* 1994;14:1648-56.

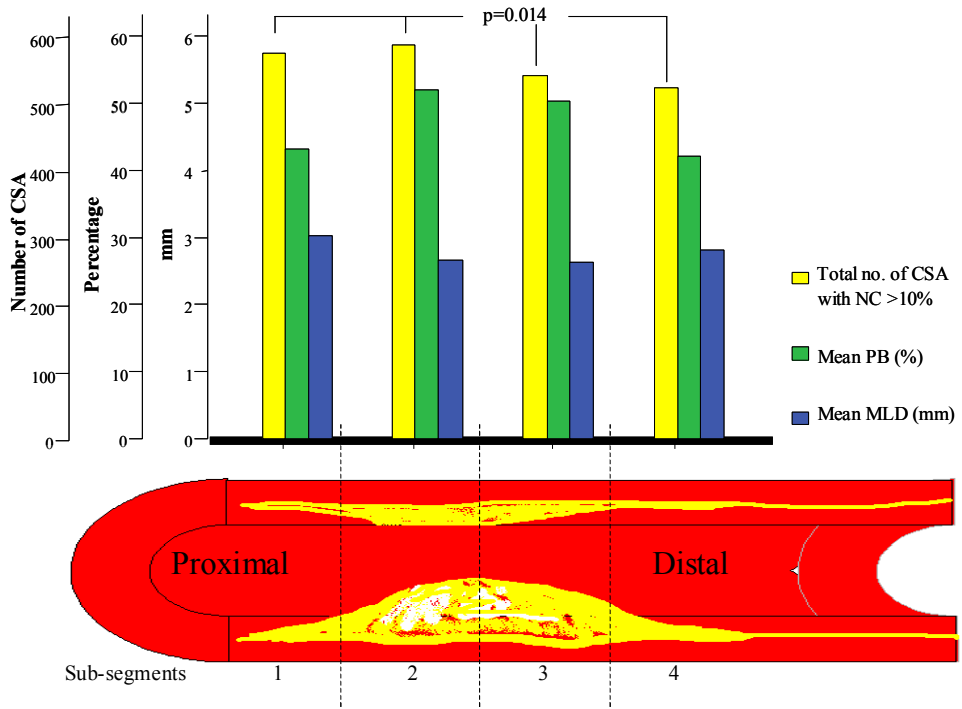


Figure 1.

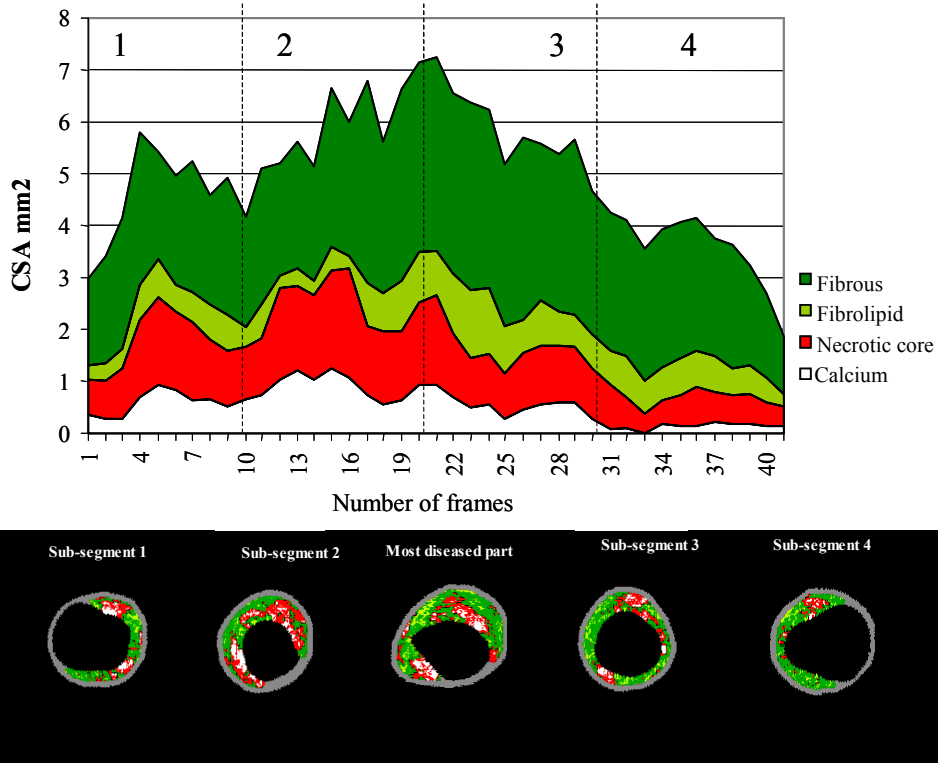


Figure 2

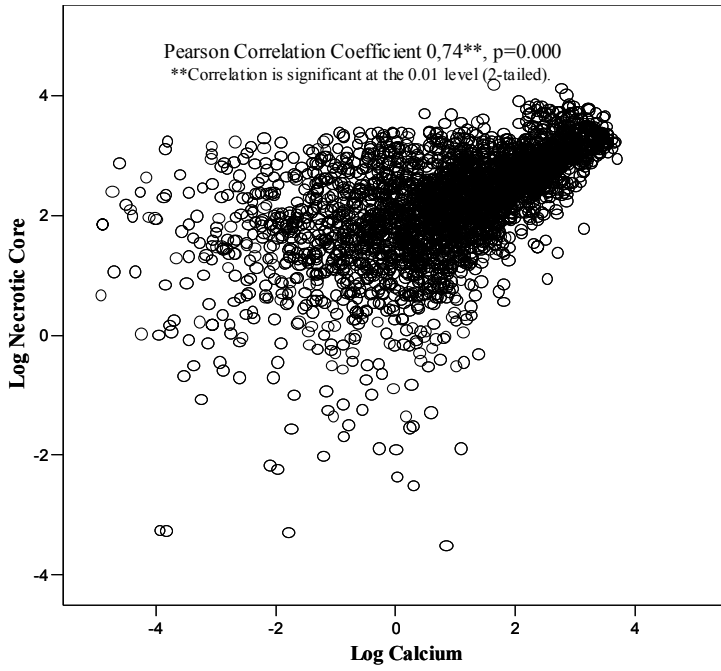


Figure 3.

**Table 1: Demographic characteristics, n=90**

Variables	
Age yrs±SD	57.9±10.8
BMI Kg/m <sup>2</sup>	26.3±2.8
Male (%)	68 (75.6)
Diabetes (%)	7 (7.8)
Hyperlipidemia (%)	69 (76.6)
Hypertension (%)	40 (44.4)
Current smoking (%)	23 (25.5)
Prior ACS (%)	12 (13.3)
Prior PCI (%)	26 (28.9)
<u>Clinical presentation</u>	
Stable angina (%)	53 (58.9)
Unstable angina (%)	17 (18.9)
Acute myocardial infarction (%)	20 (22.2)
<u>Vessel treated, n=121</u>	
Left anterior descending (%)	52 (43.0)
Left circumflex (%)	31 (25.6)
Right coronary artery (%)	38 (31.4)

**Table 2: Geometrical and Composition IVUS -Virtual Histology Results**

	Proximal		Distal		
	Sub-segments				
	1	2	3	4	p
<b>IVUS-VH geometrical findings</b>					
Vessel CSA (mm <sup>2</sup> )	15.7±5.2	15±5	14.2±5	13.5±5	<0.001
Luminal CSA (mm <sup>2</sup> )	8.9±3.8	7.2±3.4	7.05±3.3	7.82±3.4	<0.001
MLD (mm)	3±0.7	2.7±0.7	2.6±0.6	2.8±0.6	<0.001
Plaque burden (%)	43±14	51.8±14.1	50.3±13.5	41.9±12.7	<0.001
<b>IVUS-VH compositional findings</b>					
Necrotic Core (%)	11.6±10.5*	11.7±9.7**	10.9±9.5	10.2±9.9	0.001
Calcium (%)	5.9±9.9	6.5±9.7§	6.3±9.4	5.4±9.5	0.031
Fibrous (%)	61.5±20.8	62.9±17.6	63.8±17.6†‡	61.4±22.7	0.008
Fibrolipid (%)	17.1±12.8	18.1±12.5	18.3±12.1	17.3±13.7	0.05
CSAs NC >5%	850	828	819	721	<0.001
CSAs NC >10%	574	585	541	522	0.014

---

CSAs NC >15%	390	373	343	320	0.018
CSAs NC >20%	242	218	194	185	0.026

---

---

\* p = 0.004 compare to sub-segment four

\*\* p = 0.002 compare to sub-segment four

§ p = 0.03 compare to sub-segment four

† p=0.037 compare to sub-segment one

‡ p=0.019 compare to sub-segment four

**Table 3: Clinical Presentation and Virtual Histology Analysis**

	Stable n=53	ACS n=37	p
Necrotic core (%)	8.1±6.4	13.7±8.2	0.001
Calcium (%)	4.0±7.2	6.9±8.1	0.09
Fibrous (%)	66.9±13.8	58.8±13.6	0.006
Fibrolipid (%)	9.6±9.9	18.4±9.8	0.55

**Legends of the figures and tables**

**Figure 1.** The drawing shows a coronary plaque divided in four segments; from proximal to distal four 5 mm sub-segments were considered for the analysis. In the cluster bar graph, three variables are represented. The yellow bar is showing the total number of cross sectional areas (CSA) with a necrotic core (NC) larger than 10% in each sub-segment. The green bar is representing the plaque burden (PB). The blue bar represents the minimum lumen diameter (MLD).

**Figure 2.** In this example case, the cumulative curve is showing the different components of the plaque per mm<sup>2</sup> in every CSA (cross-sectional area). On the bottom, the IVUS-VH images are a representative CSA of each sub-segment and most diseased part.

**Figure 3.** Scatter plot showing the positive correlation between the content of calcium and necrotic core.

**Table 1.** ACS refers to acute coronary syndrome and PCI refers to percutaneous coronary intervention,

**Table 2.** CSA, cross sectional area; MLD, minimum luminal diameter; NC, necrotic core; ACS, acute coronary syndrome

**Table 3.** ACS, acute coronary syndrome.





**Chapter 5. Tissue characterization of non-target atherosclerotic coronary plaques. Relationship with demographical data.**

**5.1) Coronary plaque composition of non-culprit lesions by in vivo intravascular ultrasound radiofrequency data analysis is related to clinical presentation.**

**Am Heart Journal. 2006 May;151(5):1027-31.**

**Rodriguez Granillo GA, McFadden EP, Valgimigli M, et al.**



# Coronary plaque composition of nonculprit lesions, assessed by in vivo intracoronary ultrasound radio frequency data analysis, is related to clinical presentation

Gastón A. Rodríguez-Granillo, MD, Eugène P. Mc Fadden, MD, FRCPI, Marco Valgimigli, MD, Carlos A. G. van Mieghem, MD, Evelyn Regar, MD, PhD, Pim J. de Feyter, MD, PhD, and Patrick W. Serruys, MD, PhD *Rotterdam, The Netherlands*

**Background** Identification of subclinical high-risk plaques is potentially important because they may have greater likelihood of rupture and subsequent thrombosis. The purpose of this study was to assess the relationship between plaque composition determined by intravascular ultrasound (IVUS) radio frequency (RF) data analysis and clinical presentation.

**Methods** In 55 patients, a nonculprit vessel with <50% diameter stenosis was studied with IVUS. Tissue maps were reconstructed from RF data using IVUS-Virtual Histology software.

**Results** Mean percentage of the different plaque components were  $0.99\% \pm 0.9\%$ , calcium;  $68.04\% \pm 9.8\%$ , fibrous;  $19.31\% \pm 7.3\%$ , fibrolipidic; and  $9.43\% \pm 6.6\%$ , lipid core. Mean lipid core percentage was significantly larger in patients with acute coronary syndrome (ACS) when compared with stable patients ( $12.26\% \pm 7.0\%$  vs  $7.40\% \pm 5.5\%$ ,  $P = .006$ ). In addition, stable patients showed more fibrotic vessels ( $70.97\% \pm 9.3\%$  vs  $63.96\% \pm 9.1\%$ ,  $P = .007$ ). There was no significant difference for either mean calcium ( $1.20\% \pm 1.1\%$  vs  $0.83\% \pm 0.7\%$ ,  $P = .124$ ) or fibrolipidic ( $20.57\% \pm 6.9\%$  vs  $18.40\% \pm 7.6\%$ ,  $P = .281$ ) percentages in ACS and stable patients, respectively. Vessel area obstruction did not differ between groups ( $46.49\% \pm 10.9\%$  vs  $42.83\% \pm 11.8\%$ ,  $P = .221$ ).

There was a significant, albeit weak, positive correlation between lipid core percentage and stenosis severity as determined by vessel area obstruction ( $r = 0.34$ ,  $P = .015$ ).

**Conclusions** In this study, plaque characterization of nonculprit vessels using spectral analysis of IVUS RF data analysis was significantly related to clinical presentation. Percentage of lipid core, a feature related to acute coronary events and worse prognosis, was significantly larger in patients with ACS. Conversely, stable patients showed more fibrotic content. (*Am Heart J* 2006;151:1027-31.)

Unheralded sudden death and acute myocardial infarction (AMI) are common presentations of coronary atherosclerosis.<sup>1,2</sup> Most such events are related to thrombotic occlusion at the site of non-flow limiting atherosclerotic plaques in epicardial coronary arteries. The identification of subclinical high-risk plaques is potentially important because they may not only have a greater likelihood of rupture and subsequent thrombosis<sup>3</sup> but also may be important contributor in the pathophysiology of plaque progression.<sup>4,5</sup>

Histologic studies suggest that plaque composition plays a central role in the pathogenesis and clinical consequences of epicardial occlusion, independent of the severity of the underlying stenosis.<sup>6</sup> In the carotid and coronary circulation, plaque echogenicity, measured noninvasively, has been related to the histologic components of plaque.<sup>7-10</sup> Furthermore, carotid plaque echolucency (low echogenicity) was associated with future neurologic events.<sup>11-13</sup> Intravascular ultrasound (IVUS)-based plaque characterization in the coronary circulation requires invasive assessment and has been less extensively studied. A recent study showed that treatment with atorvastatin resulted in quantifiable changes in coronary plaque echogenicity, compatible with changes in plaque composition.<sup>14</sup> These findings offered a potential explanation for the clinical efficacy of statins despite only modest effects on plaque volume.<sup>15,16</sup>

From the Erasmus Medical Center, Thoraxcenter, Rotterdam, The Netherlands.

Submitted February 28, 2005; accepted June 15, 2005.

Reprint requests: Patrick W. Serruys, MD, PhD, Thoraxcenter, Bd406, Erasmus MC, Dr Molewaterplein 40, 3015-GD Rotterdam, The Netherlands.

E-mail: p.w.j.c.serruys@erasmusmc.nl

0002-8703/\$ - see front matter

© 2006, Mosby, Inc. All rights reserved.

doi:10.1016/j.ahj.2005.06.040

Although grayscale ultrasound is of limited value for identification of specific plaque components, spectral analysis of IVUS radio frequency (RF) data (IVUS–Virtual Histology [IVUS-VH]; Volcano Therapeutics, Rancho Cordova, CA) has demonstrated potential to provide detailed quantitative information on plaque composition, as implicated by validation studies of explanted human coronary segments.<sup>17–19</sup>

The purpose of this study was to assess potential relations of plaque composition determined by IVUS RF data analysis to clinical presentation in patients with ischemic heart disease.

## Methods

In 55 patients, a nonculprit, de novo, angiographically nonobstructive (<50%) lesion was investigated with IVUS-VH. The region of interest (ROI) was determined by identifiable anatomic landmarks (side branch or the ostium of the vessel). Major exclusion criteria were anatomic criteria that precluded safe IVUS examination of a >30-mm-long ROI. All patients gave written informed consent.

### Intravascular ultrasound–Virtual Histology

Extensive detail regarding the validation of IVUS-VH on explanted human coronary segments has previously been reported. Briefly, IVUS-VH uses spectral analysis of IVUS RF data to construct tissue maps that classify plaque into 4 major components. In an ex vivo validation study, 4 histologic plaque components (fibrous, fibrolipid, lipid core, and calcium) were correlated with a specific spectrum of the RF signal.<sup>17</sup> These different plaque components were assigned color codes. Calcified, fibrous, fibrolipidic, and lipid core regions were labeled white, green, greenish yellow, and red, respectively. In addition to compositional data, IVUS-VH software provides geometric data of the vessel. Intravascular ultrasound–Virtual Histology data were acquired, during a continuous pullback (0.5 mm/s) with a commercially available mechanical sector scanner (Ultracross 30-MHz catheter; Boston Scientific, Santa Clara, CA), by a dedicated IVUS-VH console (Volcano Therapeutics). The IVUS-VH data were stored on a CD-ROM and sent to the imaging core laboratory (Cardialysis, Rotterdam, The Netherlands) for off-line analysis. Intravascular ultrasound B-mode images were reconstructed from the RF data by custom software (IVUSLab, Volcano Therapeutics). Subsequently, manual contour detection of both the lumen and the media-adventitia interface was performed. To account for catheter-to-catheter variability, the acquired RF data were normalized using a technique known as “blind deconvolution.” Blind deconvolution is an iterative algorithm that deconvolves the catheter transfer function from the backscatter, thus enabling automated data normalization.<sup>20,21</sup> Compositional and geometric data were expressed as mean percentages for the ROI. To assess the stenosis severity of the lesions, we report the mean external elastic membrane (EEM) area obstruction  $\{[(EEM_{area} - Lumen_{area})/EEM_{areal}] \times 100\}$ .

As an exploratory analysis, we evaluated the prevalence of angiographically “complex” (irregular or scalloped borders, ulceration or filling defects) or “smooth” (absence of complex features) lesions. In addition, we assessed the prevalence of

**Table I.** Demographics (N = 55)

Male sex	44 (80.0)
Age (y) (mean ± SD)	57.6 ± 9.5
Diabetes	5 (9.1)
Hypertension*	20 (36.4)
Hypercholesterolemia†	46 (83.6)
Current smoking	15 (27.3)
Previous smoking	14 (25.5)
Family history of CAD	30 (54.5)
Clinical presentation	
Stable angina	32 (58.2)
ACS	23 (41.8)

Values are presented as n (%), unless otherwise indicated. CAD, Coronary artery disease.

\* Blood pressure of  $\geq 160/95$  mm Hg or treatment of hypertension.

† Total cholesterol of  $\geq 215$  mg/dL or treatment of hypercholesterolemia.

plaque rupture by IVUS, defined as plaque ulceration with a tear detected in the fibrous cap.

### Statistical analysis

Discrete variables are presented as counts and percentages. Continuous variables are presented as mean ± SD. We looked for correlations between the percentages of the 4 different plaque components and the EEM area obstruction using univariate Pearson correlation coefficients. Differences in means among groups were analyzed by 2-sample *t* test or by 1-way analysis of variance. A *P* value of <.05 (2-sided) was considered to indicate statistical significance. Statistical analyses were performed with use of SPSS software version 11.5 (SPSS Inc., Chicago, IL).

## Results

Patient characteristics are presented in Table I. The mean age was  $57.6 \pm 9.5$  years. Forty-four (80%) patients were male. There was a low prevalence (9.1%) of diabetes. The study vessel was the left anterior descending in 23 patients (41.8%), the right coronary artery in 22 patients (40.0%), and the left circumflex in 10 patients (18.2%). The mean length of the ROI was  $35 \pm 13$  mm.

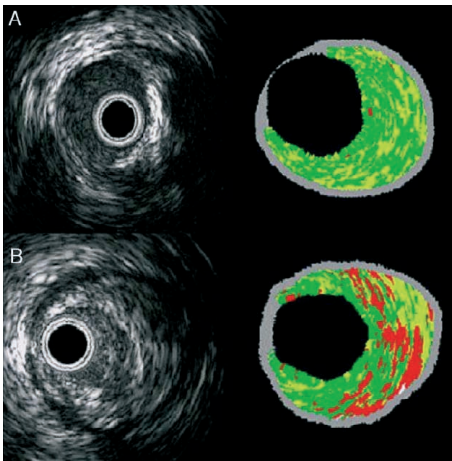
Five (9.1%) of the nonsignificant lesions evaluated showed complex characteristics. Of these, 2 were present in patients with acute coronary syndrome (ACS) and 3 in stable patients (*P* = .93). Plaque rupture was identified by IVUS in 10 (18.2%) lesions (3 in patients with ACS and 7 in stable patients, *P* = .41).

The population was prospectively divided in 2 groups, stable patients (*n* = 32) and patients presenting with ACSs (defined as unstable angina, non–ST-segment elevation myocardial infarction, or ST-segment elevation myocardial infarction; *n* = 23). C-reactive protein (CRP) measurements were available in 41 (74.5%) patients. C-reactive protein levels did not differ significantly between patients with ACS (*n* = 15) and stable (*n* = 26) patients ( $2.0 \pm 1.5$  vs  $1.7 \pm 0.9$ , *P* = .49).

Overall relative values of plaque composition are presented in Table II. The predominant (68%) plaque component was fibrous tissue (Figure 1).

**Table II.** Overall plaque composition of the study population

	Plaque component (%)
Lipid core	9.43 ± 6.6
Calcium	0.99 ± 0.9
Fibrous	68.04 ± 9.8
Fibrolipidic	19.31 ± 7.3

**Figure 1**

Examples of fibrotic (A) and lipid core-rich (B) cross-sectional areas of coronary arteries. Grayscale IVUS is displayed on the left panel, whereas the right panel shows the reconstructed IVUS-VH where calcified, fibrous, fibrolipidic and lipid core regions are labeled white, green, greenish yellow, and red, respectively.

## Colour figures on pages 441-449

Mean lipid core percentage was significantly larger in patients with ACS when compared with stable patients ( $12.26\% \pm 7.0\%$  vs  $7.40\% \pm 5.5\%$ ,  $P = .006$ ). Conversely, stable patients showed more fibrotic vessels than patients with ACS ( $70.97\% \pm 9.3\%$  vs  $63.96\% \pm 9.1\%$ ,  $P = .007$ ). There was no significant difference for either mean calcium ( $1.20\% \pm 1.1\%$  vs  $0.83\% \pm 0.7\%$ ,  $P = .124$ ) and fibrolipidic ( $20.57\% \pm 6.9\%$  vs  $18.40\% \pm 7.6\%$ ,  $P = .281$ ) percentages in patients with ACS and stable patients, respectively (Table III).

Relative lipid core content was significantly correlated to CRP levels ( $r = 0.45$ ,  $P = .003$ ). The relationship between CRP levels and relative plaque composition is depicted in Table IV.

**Table III.** Geometric and compositional data assessed by IVUS RF data analysis (N = 55)

	Stable (n = 32)	ACS (n = 23)	P
Lipid core	7.40 ± 5.5	12.26 ± 7.0	.006
Calcium	0.83 ± 0.7	1.20 ± 1.1	.124
Fibrous	70.97 ± 9.3	63.96 ± 9.1	.007
Fibrolipidic	18.40 ± 7.6	20.57 ± 6.9	.281
EEM area obstruction	42.83 ± 11.8	46.49 ± 10.9	.221

Values are percentages. External elastic membrane area obstruction defined as  $[(EEM_{area} - Lumen_{area})/EEM_{area}] \times 100$ .

**Table IV.** Relationship between CRP levels and relative plaque composition

	CRP levels	P
Lipid core	0.45	.003
Calcium	-0.05	.78
Fibrous	-0.24	.14
Fibrolipidic	-0.12	.46

There was a significant, albeit weak, positive correlation between lipid core percentage and stenosis severity as determined by percentage of EEM area obstruction ( $r = 0.34$ ,  $P = .015$ ).

No significant difference was found in lipid core (percentage) between left anterior descending ( $10.19\% \pm 6.2\%$ ), right coronary artery ( $8.05\% \pm 5.8\%$ ), and left circumflex ( $10.73\% \pm 8.9\%$ ) ( $P = .443$ ).

## Discussion

The major findings of this study were first that, in nonculprit lesions, there were significant differences in plaque composition between patients who presented with ACSs and those who presented with stable angina. In those with ACS, percentage of lipid core was significantly greater than in stable patients, whereas a converse trend was observed for fibrotic content. Secondly, in the overall patient population, stenosis severity on IVUS-VH was positively correlated with percent lipid core.

Coronary occlusion and AMI commonly arise from intermediate lesions.<sup>6,22</sup> This had led investigators to suggest that mild to moderate lesions are more lipid-rich and thus prone to rupture.<sup>6,23</sup> However, it has been established that moderate lesions cause more occlusions because of their greater incidence throughout the coronary tree.<sup>24</sup>

Pathological studies showed that lipid-rich plaques are more prone to rupture than fibrotic plaques.<sup>3</sup> Kragel et al<sup>25</sup> showed that the percentage of “pultaceous debris” (an alternative term for lipid core, defined as amorphous debris containing cholesterol clefts rich in extracellular lipid) was of 16% in the AMI group and of 7% in the sudden coronary death group. These postmortem results are in line with the *in vivo* results of the present study.

To date, there is no validated technique capable of identifying and quantifying the lipid core *in vivo*. Intravascular ultrasound-Virtual Histology extends the ability of grayscale IVUS to aid the assessment of plaque composition, thus having the potential to identify high-risk plaques before the rupture has occurred and prospectively follow their natural history. In addition, it allows a morphologic evaluation of atherosclerotic plaques by quantifying its different components and determining its location in relation to the lumen.

An angiographic study demonstrated that patients with ACS frequently have additional complex non-culprit coronary plaques and that such findings were independent predictors of future clinical events.<sup>26</sup> More recently, IVUS and angioscopic studies extended these findings, and it is now generally accepted that multifocal instability is common in ACS.<sup>27,28</sup> Rioufol et al<sup>27</sup> found at least 1 plaque rupture remote from the culprit lesion in 80% of patients, remote from the culprit artery in 71% of patients, and in both nonculprit arteries in 12.5% of patients. The significantly higher lipid core burden found in nonculprit lesions of patients with ACS potentially supports the theory that ACS is a multifocal process.<sup>29</sup>

In the present study, we found a significant, albeit weak, positive correlation between mean lipid core percentage and vessel area obstruction determined by IVUS-VH, suggesting that lipid core increases linearly with further increase in the degree of stenosis. However, the relative importance of this relationship must be further explored in large prospective, natural history studies.

It is noteworthy that the sclerotic component of the vessel wall (fibrous tissue) accounted for almost 70% of the overall plaque area composition. This observation is concordant with previously reported morphometric data from postmortem studies,<sup>25</sup> thus providing indirect evidence for the validity of the technique.

The identification of high-risk plaques is potentially important because they may not only have a greater likelihood of rupture and subsequent thrombosis<sup>3</sup> but also may be an important contributor in the pathophysiology of plaque progression.<sup>4,5</sup>

Finally, these observations raise the possibility that plaque characterization with IVUS-VH could have an additive value in refining risk stratification of subclinical atherosclerosis by providing means to identify high-risk plaques in prospective, natural history studies.

## Limitations

The present was a pilot, observational study that included a small population. Accordingly, a potential selection bias cannot be disregarded. Only a short segment of the coronary tree was evaluated, therefore this may not be representative of the whole coronary tree. Because our investigation aimed a local assessment of a nonculprit vessel and levels of systemic inflammatory markers such as CRP are influenced by many factors, we did not systematically analyze CRP levels in this population. Therefore, cautious interpretation of the correlation reported must be undertaken. Although histopathology remains the gold standard, this technique has the potential to provide real-time accurate information regarding tissue characterization and plaque morphology.

## Conclusions

In this pilot study, plaque characterization of non-culprit vessels using spectral analysis of IVUS RF data analysis was significantly related to clinical presentation. Percentage of lipid core, a feature related to acute coronary events and worse prognosis, was significantly larger in patients with ACS. Conversely, stable patients showed more fibrotic content. This technique could have an additive value in refining risk stratification of subclinical atherosclerosis by providing means to identify high-risk plaques in prospective, natural history studies.

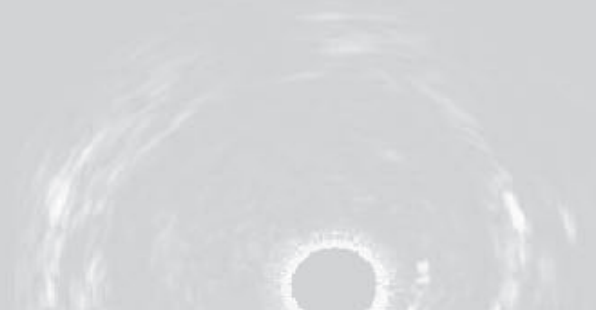
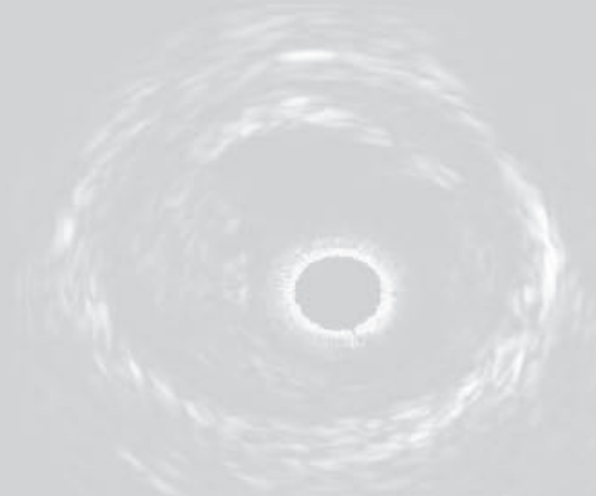
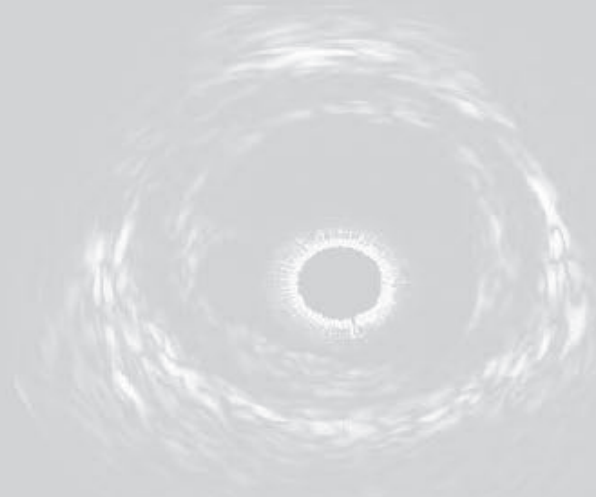
## References

1. Kannel WB, Doyle JT, McNamara PM, et al. Precursors of sudden coronary death. Factors related to the incidence of sudden death. *Circulation* 1975;51:606-13.
2. Falk E, Shah PK, Fuster V. Coronary plaque disruption. *Circulation* 1995;92:657-71.
3. Davies MJ, Richardson PD, Woolf N, et al. Risk of thrombosis in human atherosclerotic plaques: role of extracellular lipid, macrophage, and smooth muscle cell content. *Br Heart J* 1993;69:377-81.
4. Burke AP, Kolodgie FD, Farb A, et al. Healed plaque ruptures and sudden coronary death: evidence that subclinical rupture has a role in plaque progression. *Circulation* 2001;103:934-40.
5. Kaski JC, Chen L, Crook R, et al. Coronary stenosis progression differs in patients with stable angina pectoris with and without a previous history of unstable angina. *Eur Heart J* 1996;17:1488-94.
6. Little WC, Constantinescu M, Applegate RJ, et al. Can coronary angiography predict the site of a subsequent myocardial infarction in patients with mild-to-moderate coronary artery disease? *Circulation* 1988;78(5 Pt 1):1157-66.
7. El-Barghouty NM, Levine T, Ladva S, et al. Histological verification of computerised carotid plaque characterisation. *Eur J Vasc Endovasc Surg* 1996;11:414-6.
8. Granholdt ML, Nordstgaard BG, Wiebe BM, et al. Echo-lucency of computerized ultrasound images of carotid atherosclerotic plaques are associated with increased levels of triglyceride-rich lipoproteins as well as increased plaque lipid content. *Circulation* 1998;97:34-40.

9. Rasheed Q, Dhawale PJ, Anderson J, et al. Intracoronary ultrasound-defined plaque composition: computer-aided plaque characterization and correlation with histologic samples obtained during directional coronary atherectomy. *Am Heart J* 1995;129:631-7.
10. Prati F, Arbustini E, Labellarte A, et al. Correlation between high frequency intravascular ultrasound and histomorphology in human coronary arteries. *Heart* 2001;85:567-70.
11. Polak JF, Shemanski L, O'Leary DH, et al. Hypoechoic plaque at US of the carotid artery: an independent risk factor for incident stroke in adults aged 65 years or older. *Cardiovascular Health Study. Radiology* 1998;208:649-54.
12. Gronholdt ML, Nordestgaard BG, Schroeder TV, et al. Ultrasonic echolucent carotid plaques predict future strokes. *Circulation* 2001;104:68-73.
13. Mathiesen EB, Bonaa KH, Joakimsen O. Echolucent plaques are associated with high risk of ischemic cerebrovascular events in carotid stenosis: the tromso study. *Circulation* 2001;103:2171-5.
14. Scharf M, Bocksch W, Koschyk DH, et al. Use of intravascular ultrasound to compare effects of different strategies of lipid-lowering therapy on plaque volume and composition in patients with coronary artery disease. *Circulation* 2001;104:387-92.
15. Cannon CP, Braunwald E, McCabe CH, et al. Intensive versus moderate lipid lowering with statins after acute coronary syndromes. *N Engl J Med* 2004;350:1495-504.
16. Nissen SE, Tuzcu EM, Schoenhagen P, et al. Effect of intensive compared with moderate lipid-lowering therapy on progression of coronary atherosclerosis: a randomized controlled trial. *JAMA* 2004;291:1071-80.
17. Nair A, Kuban BD, Tuzcu EM, et al. Coronary plaque classification with intravascular ultrasound radiofrequency data analysis. *Circulation* 2002;106:2200-6.
18. Moore MP, Spencer T, Salter DM, et al. Characterisation of coronary atherosclerotic morphology by spectral analysis of radio-frequency signal: in vitro intravascular ultrasound study with histological and radiological validation. *Heart* 1998;79:459-67.
19. Watson RJ, McLean CC, Moore MP, et al. Classification of arterial plaque by spectral analysis of in vitro radio frequency intravascular ultrasound data. *Ultrasound Med Biol* 2000;26:73-80.
20. Kåresen K. Deconvolution of sparse spike trains by iterated window maximization. *IEEE Trans Signal Process* 1997;45:1173-83.
21. Kåresen KF, Bølviken E. Blind deconvolution of ultrasonic traces accounting for pulse variance. *IEEE Trans Ultrason Ferroelectr Freq Control* 1999;46:564-73.
22. Ambrose JA, Tannenbaum MA, Alexopoulos D, et al. Angiographic progression of coronary artery disease and the development of myocardial infarction. *J Am Coll Cardiol* 1988;12:56-62.
23. Nobuyoshi M, Tanaka M, Nosaka H, et al. Progression of coronary atherosclerosis: is coronary spasm related to progression? *J Am Coll Cardiol* 1991;18:904-10.
24. Alderman EL, Corley SD, Fisher LD, et al. Five-year angiographic follow-up of factors associated with progression of coronary artery disease in the Coronary Artery Surgery Study (CASS). CASS Participating Investigators and Staff. *J Am Coll Cardiol* 1993;22:1141-54.
25. Kragel AH, Reddy SG, Wittes JT, et al. Morphometric analysis of the composition of atherosclerotic plaques in the four major epicardial coronary arteries in acute myocardial infarction and in sudden coronary death. *Circulation* 1989;80:1747-56.
26. Goldstein JA, Demetriou D, Grines CL, et al. Multiple complex coronary plaques in patients with acute myocardial infarction. *N Engl J Med* 2000;343:915-22.
27. Rioufal G, Finet G, Ginon I, et al. Multiple atherosclerotic plaque rupture in acute coronary syndrome: a three-vessel intravascular ultrasound study. *Circulation* 2002;106:804-8.
28. Asakura M, Ueda Y, Yamaguchi O, et al. Extensive development of vulnerable plaques as a pan-coronary process in patients with myocardial infarction: an angioscopic study. *J Am Coll Cardiol* 2001;37:1284-8.
29. Buffon A, Biasucci LM, Liuzzo G, et al. Widespread coronary inflammation in unstable angina. *N Engl J Med* 2002;347:5-12.



**PART III: EXPLORING HISTOLOGICAL SURROGATES AND  
PLAQUE VULNERABILITY CRITERIA USING INTRAVASCULAR  
ULTRASOUND RADIOFREQUENCY DATA ANALYSIS.**





## **Chapter 6. Plaque rupture**

### **6.1) Global characterization of coronary plaque rupture phenotype using 3- vessel intravascular ultrasound radiofrequency data analysis.**

**Eur Heart J. Accepted.**

**Rodriguez Granillo GA, García-García HM, Valgimigli M, et al.**



**Global characterization of coronary plaque rupture  
phenotype using 3-vessel intravascular ultrasound  
radiofrequency data analysis**

**Gastón A. Rodríguez-Granillo MD, Héctor M. García-García MD, Marco Valgimigli MD, Sophia Vaina MD, Carlos van Mieghem MD, Robert J. van Geuns MD PhD, Maarten van der Ent MD PhD, Evelyn Regar MD PhD, Peter de Jaegere MD PhD, Willem van der Giessen MD PhD, Pim de Feyter MD PhD, Patrick W. Serruys MD, PhD**

From the Department of Cardiology of the Thoraxcenter, Erasmus MC, Rotterdam, The Netherlands.

**ABSTRACT**

**Aims:** To compare the global characteristics of patients with and without evidence of plaque rupture (PR) in their coronary tree, and to evaluate the phenotype of ruptured plaques using IVUS radiofrequency data analysis (IVUS-VH).

**Methods and results:** Forty patients underwent 3-vessel IVUS-VH interrogation. 28 PRs were diagnosed in 26 vessels (25.7 % of the vessels studied) of 20 patients (50 % of the population). Ruptures located in the LAD were clustered in the proximal part of the vessel, whereas ruptures located in the RCA were more distally located,  $p= 0.02$ . Patients with at least one PR presented larger body mass index (BMI) ( $28.4\pm 3.7$  kg/m<sup>2</sup> vs.  $25.8\pm 2.6$  kg/m<sup>2</sup>,  $p= 0.01$ ) and plaque burden ( $40.7\pm 7.6$  % vs.  $33.7\pm 8.4$  %,  $p= 0.01$ ) than patients without rupture, despite showing similar lumen CSA ( $9.6\pm 3.3$  mm<sup>2</sup> vs.  $9.2\pm 2.3$  mm<sup>2</sup>,  $p=0.60$ ). Among current smokers, 66.7 % presented a PR in their coronary tree. Finally, PR sites showed a higher content of necrotic core compared to minimum lumen area (MLA) sites ( $17.48\pm 10.8$  % vs.  $13.10\pm 6.5$  %,  $p= 0.03$ ) and a trend towards higher calcified component.

**Conclusions:** Patients with at least one PR in their coronary tree presented larger BMI and worse IVUS-derived characteristics compared to patients without PR.

**Keywords:** plaque rupture, ultrasonography, atherosclerosis, vulnerable plaque

## INTRODUCTION

It has been established that coronary plaque rupture is the cause of death in a large proportion of sudden coronary death patients<sup>1</sup>. Despite its preconceived dire prognosis, retrospective studies have determined that plaque rupture is a common finding in both coronary and non-coronary sudden death patients<sup>1,2</sup>. In addition, clinically silent plaque rupture has been identified as a cause of plaque progression<sup>3,4</sup>. The fate of a given atherosclerotic plaque is thus linked not only to its severity but also to its histological composition, and the presence of a rich necrotic core has been consistently related to plaque fissuring<sup>5,6</sup>.

Intravascular ultrasound (IVUS) has been largely demonstrated to be an accurate diagnostic tool able to provide a high resolution, real-time, tomographic view of the coronary arteries. As such, several studies have portrayed the prevalence of plaque rupture in living patients by means of IVUS<sup>7,8</sup>. IVUS has though a suboptimal predictive value to estimate the composition of coronary arteries, particularly of lipid deposits<sup>9</sup>. In turn, spectral analysis of IVUS radiofrequency data has demonstrated improved accuracy for tissue characterization<sup>10</sup>. Besides, to date, no study has reported the global burden of the disease and its relationship with plaque rupture by means of IVUS.

The purpose of our study was two-fold: first, to compare the global characteristics of patients with and without evidence of plaque rupture (PR) in their coronary tree; and secondly, to evaluate the phenotype of ruptured against non-ruptured plaques using IVUS radiofrequency data analysis (IVUS-VH).

## **METHODS**

### **Patients**

In this single-center, investigators-driven, observational, prospective study; patients referred to our institution for elective or urgent PCI with absence of extensive calcification, severe vessel tortuosity and haemodynamic instability and with suitable anatomy underwent IVUS interrogation of the 3 main epicardial coronary arteries. The patients included in this study, are part of published (IBIS-1) <sup>11</sup> and unpublished (LICO, BETAX) mono-center studies conducted at our center.

Patients with stable angina, unstable angina and acute myocardial infarction were included. Myocardial infarction (MI) was diagnosed by an increase in the creatine kinase MB level to more than two-fold the normal limit. Acute coronary syndrome (ACS) patients encompassed patients presenting with unstable angina, non-ST segment elevation MI, or ST segment elevation MI. The institution's ethics committee approved the study protocol, which complies with the Declaration of Helsinki, and written informed consent was obtained from all patients.

### **Intravascular ultrasound**

#### **IVUS acquisition**

The IVUS catheters used were commercially available mechanical and electronical catheters (Ultracross<sup>TM</sup> 30 MHz catheter, Boston Scientific, Santa Clara, USA; Eagle Eye<sup>TM</sup> 20 MHz catheter, Volcano Corporation, Rancho Cordova, USA). After administration of intracoronary nitrates, the IVUS catheter was introduced up to the distal coronary bed of the 3 coronary vessels. IVUS was aimed to be performed prior to any intervention. Using an automated pullback device, the transducer was withdrawn at a continuous speed of 0.5 mm/s until the ostium was seen. Cine runs, before and during contrast injection, were performed to define the position of the IVUS catheter before the pullback was started. IVUS-VH (Volcano

Corporation, Rancho Cordova, USA) acquisition was ECG-gated using a dedicated console (Volcano Corporation, Rancho Cordova, USA). IVUS-VH data were stored on CD-ROM / DVD and sent to the imaging core lab for offline analysis.

### **IVUS-VH analysis**

IVUS B-mode images were reconstructed from the RF data by customized software and contour detection was performed using cross-sectional views with a semi-automatic contour detection software to provide geometrical and compositional output (IvusLab 3.0 for 30 MHz acquisitions and IvusLab 4.4 for 20 MHz acquisitions respectively; Volcano Corporation, Rancho Cordova, USA). The RF data was normalized using a technique known as “Blind Deconvolution”, an iterative algorithm that deconvolves the catheter transfer function from the backscatter, thus accounting for catheter-to-catheter variability <sup>11</sup>.

Details regarding the validation of IVUS-VH on explanted human coronary segments have previously been reported <sup>10</sup>. Briefly, IVUS-VH uses spectral analysis of IVUS radiofrequency data to construct tissue maps that classify plaque into four major components. In preliminary *in vitro* studies, four histological plaque components (fibrous, fibrolipidic, necrotic core and calcium) were correlated with a specific spectrum of the radiofrequency signal <sup>10</sup>. These different plaque components were assigned color codes. Calcified, fibrous, fibrolipidic and necrotic core regions were labeled white, green, greenish-yellow and red respectively.

The contours of the external elastic membrane (EEM) and the lumen-intima interface enclosed an area that was defined as the coronary plaque plus media area. Plaque burden was calculated as  $[(EEM_{\text{area}} - \text{Lumen}_{\text{area}}) / EEM_{\text{area}}] \times 100$ . Following a previously reported classification, plaque rupture was defined as a ruptured capsule with an underlying cavity (figure 1), or plaque excavation by atheromatous extrusion with no visible capsule <sup>7,8</sup>. Rupture sites separated by at least 5 mm length of rupture-free vessel were considered as different

ruptures. Screening for diagnosis of a plaque rupture required the independent review and agreement between two experienced IVUS observers (G.A.R.G. and H.M.G.G.), who had no knowledge about demographical data of the patients. Disagreement was solved by consensus between the observers. Lumen contour detection at the rupture site was performed following the intima-lumen interface, excluding the rupture cavity from the plaque plaque CSA calculation. Absolute geometrical data and absolute and relative compositional data were obtained for each cross-sectional area (CSA) and an average was calculated for each coronary and for the total coronary tree. Finally, measurements were calculated in CSAs meeting criteria of plaque rupture and at the site of the minimum lumen area (MLA).

As pre-specified sub-analysis, we compared the different geometrical and compositional characteristics of the 3 main epicardial coronaries. In addition, the difference between culprit/target and non-culprit/non-target vessels was assessed.

### **Statistical analysis**

Discrete variables are presented as counts and percentages. Continuous variables are presented as means  $\pm$  SD or medians (25<sup>th</sup>, 75<sup>th</sup> percentile) when indicated. Based on previous histopathological findings showing that ruptured plaques presented 34 % of necrotic core, 10 % more than non-ruptured plaques<sup>14</sup>, we calculated a sample size of 36 subjects to achieve a power of 80 % to detect a true difference in population means, considering a type I error of 0.05 (two-sided) and a within group standard deviation of 15.

Comparisons between groups were performed using paired and independent student's *t* test, or  $\chi^2$  tests as indicated. For variables with a non-normal distribution we used Kruskal-Wallis or Wilcoxon signed ranks tests as indicated. A two-sided *p* value of less than 0.05 indicated statistical significance. Statistical analyses were performed with use of SPSS software, version 13.0 (Chicago, Illinois, USA).

## RESULTS

### Patients

Forty-six patients were included in the study protocol. Subsequently, six patients were excluded from the final analysis due to the absence of coronary plaque outside the stented segment in one patient, and bad quality acquisition owed to non-continuous pullback in five patients. Accordingly, 40 non-consecutive patients were prospectively included in the study. IVUS interrogation of the 3 main coronaries was attempted in all patients. Two-vessel IVUS interrogation was achieved in all patients and 3-vessel IVUS imaging was achieved in 31 (77.5 %) cases. Five vessels were excluded from the analysis due to the lack of a diseased non-stented segment. Patient characteristics are provided in table 1. The mean age was  $55.7 \pm 11.0$  years. 29 (72.5%) patients were male. There was a low prevalence (10.0 %) of diabetes. Thirteen (32.5 %) patients presented with stable angina, 12 (30.0 %) presented with unstable angina, and 15 (37.5 %) with AMI. The global geometrical and compositional characteristics of the coronary tree are presented in table 1.

### Plaque rupture: Prevalence and location

Twenty-eight plaque ruptures were diagnosed in 26 vessels (25.7 % of the vessels studied) of 20 patients (50 % of the population). Sixteen (59.3 %) ACS patients presented at least one plaque rupture in their coronary tree, whereas such finding was observed in 4 (30.8%) stable patients. The tear was located in the shoulder of the plaque in 18 (64.3 %) cases and in the centre of the plaque on 10 (35.7 %) cases.

Ruptures were located in the left anterior descending (LAD) artery in 13 cases (34.2 %), in the left circumflex (LCx) in 7 cases (21.2 %) and in the right coronary artery (RCA) in 8 cases (24.2 %). Ruptures located in the LAD were clustered in the proximal part of the vessel [(median mms from the ostium (interquartile range, IQR): 14.16 (8.5-26.5)], whereas ruptures located in the LCx were widely distributed [(median (IQR): 21.9 (5.7-35.5)] and ruptures in

the RCA were more distally located [(median (IQR): 38.8 (28.8-60.0)]. Plaque ruptures were located at the MLA in 6 cases (21.4 %), proximal to the MLA in 9 cases (32.1 %) and distal to the MLA in 11 cases (39.3 %). The MLA could not be identified accurately in 2 (7.1 %) cases due to the presence of diffuse disease. Six (28.6 %) of the culprit vessels of ACS contained a plaque rupture, whereas such finding was present in 16 (31.4 %) of non-culprit vessels.

Multiple plaque rupture was present in 6 ACS patients (22 % of all ACS patients). No multiple plaque rupture was identified in stable patients. Two patients presented 2 different ruptures in the same vessel.

### **Plaque rupture: Demographical and IVUS-derived characteristics**

Table 2 depicts the demographical characteristics and the IVUS-VH measurements of patients with and without the presence of plaque rupture in their coronary tree. Body mass index was significantly higher in patients with rupture ( $28.4 \pm 3.7$  kg/m<sup>2</sup> vs.  $25.8 \pm 2.6$  kg/m<sup>2</sup>,  $p = 0.01$ ). Of note, 66.7 % of current smokers presented a ruptured plaque in their coronary tree.

Patients with ruptured plaques in their coronary tree had globally more severe disease (plaque burden  $40.7 \pm 7.6$  % vs.  $33.7 \pm 8.4$  %,  $p = 0.01$ ; table 2).

Finally, plaque rupture sites showed a higher relative content of necrotic core compared to MLA sites ( $16.7$ ;  $7.9$ - $26.5$  % vs.  $11.8$ ;  $8.4$ - $17.1$  %,  $p = 0.03$ )(table 3).

### **Differences between coronaries and culprit vs. non-culprit lesions**

The LAD presented more severe plaques [plaque burden; LAD  $42.2 \pm 9.9$  % vs. LCx  $33.17 \pm 9.2$  % vs. RCA  $33.96 \pm 10.3$ ], more calcified plaques (LAD  $3.15$ ;  $1.74$ - $4.91$  % vs. LCx  $2.10$ ;  $1.17$ - $3.79$  % vs. RCA  $1.49$ ;  $0.39$ - $2.53$  %) and showed larger necrotic core content (LAD  $11.68$ ;  $5.3$ - $15.8$  % vs. LCx  $7.71$ ;  $4.15$ - $13.6$  % vs. RCA  $9.18$ ;  $3.87$ - $13.3$  %) of plaques compared to the LCx and the RCA respectively (table 4).

There were no significant differences in IVUS-VH measurements between stable angina ( $n = 13$ ) and ACS ( $n = 27$ ) patients. IVUS-VH parameters other than mean plaque burden

( $40.62 \pm 10.7$  % vs.  $35.26 \pm 10.2$  %,  $p=0.02$ ) did not differ significantly between culprit/target and non-culprit/non-target vessels. Furthermore, in ACS patients, geometrical and compositional characteristics did not differ significantly between culprit and non-culprit vessels, only showing trends for larger plaque burden ( $39.39 \pm 10.0$  % vs.  $34.60 \pm 10.0$  %,  $p=0.07$ ) and relative necrotic core content ( $12.16$ ;  $5.4$ - $16.6$  % vs.  $9.66$ ;  $5.2$ - $13.8$  %,  $p=0.17$ ) in culprit vessels.

## DISCUSSION

Several histopathological and, more recently, IVUS studies have described the distinctive morphological features present in plaque rupture sites. Nevertheless, none has prospectively compared the clinical and IVUS-derived characteristics of patients with and without the presence of plaque rupture in their coronary tree.

In the present prospective 3-vessel IVUS study, patients with at least one plaque rupture in their coronary tree presented larger body mass index and overall worse IVUS-derived (geometrical and compositional) characteristics compared to patients without evidence of plaque rupture. In addition, plaque rupture sites had a worse phenotype than the MLA sites of the same vessels.

Coronary plaque rupture is the ultimate consequence of the progressive accumulation of lipid-rich atheroma and fibrous cap thinning, commonly involving haemodynamically non-significant lesions<sup>13</sup>. For decades, the corollary of such event has been deemed an acute occlusion of the corresponding artery with the subsequent ACS and its inherent dire prognosis. Ex-vivo studies have challenged such concept by providing evidence that subclinical rupture is not rare in sudden death patients<sup>2,4</sup>. Furthermore, recent IVUS studies have reported a prevalence of plaque rupture of 20 to 30 % in stable angina (SA) patients<sup>7,14,15</sup>. In agreement with such previous reports, we identified plaque rupture in 30.8 % of SA patients, whereas 59.3 % of the ACS patients presented plaque rupture.

Patients with at least one plaque rupture in their coronary tree (50 % of the population) showed a larger body mass index, and were more likely current smokers. These findings have a physiopathological basis since both high body weight<sup>16</sup> and smoking<sup>17</sup> are associated with an increase in the expression of matrix-metalloproteinases, enzymes involved in the collagen breakdown of fibrous caps<sup>18</sup>. Patients with plaque rupture also showed more severe burden of

the disease and larger calcium, fibrous and necrotic content of plaques than patients without rupture.

Several studies showed increased inflammatory marker levels, larger lipid cores and pronounced medial thinning in positive remodeled vessels<sup>19-21</sup>.

Our study extends those earlier findings and establishes a link between plaque rupture and coronary remodelling. Despite larger mean plaque CSAs, patients with the presence of at least one plaque rupture in their coronary tree showed similar lumen CSAs. The lack of lumen encroachment despite a significant increase in plaque burden was probably driven by a positive remodeling phenomenon, clearly shown as a significant increase in vessel CSA.

At site-specific locations, ruptured sites showed an overall worse phenotype than MLA sites. In particular, ruptured sites showed a higher necrotic core content (16.7; 7.9-26.5 % vs. 11.8; 8.4-17.1 %,  $p=0.03$ ). These results were in line with histopathological findings supporting the role of the atheromatous core as the most thrombogenic component of atherosclerotic plaques<sup>22</sup>. Of interest, and in agreement with Farb *et al* who frequently found calcium in ruptured plaques<sup>23</sup>, ruptured sites showed a larger calcium content than the MLA sites and than the overall population.

It is noteworthy yet confirmatory of a previous ex-vivo study<sup>24</sup> that there was no significant difference in plaque composition between culprit and non-culprit vessels, supporting the validity of the interrogation of a single vessel to estimate the global burden of the disease<sup>25</sup>. Nevertheless, several differences were detected between the 3 major epicardial arteries. Interestingly, the LAD showed more severe lesions and a worse phenotype than the LCx and RCA. In addition, ruptures located in the LAD were clustered in the proximal part of the vessel, whereas ruptures located in the RCA were more distally located, and ruptures in the LCx showed no apparent site-specificity. A recent IVUS study found a similar distribution throughout the coronary tree<sup>26</sup>. Overall, these findings might potentially explain the higher

restenosis rates seen in the LAD, particularly in the proximal LAD, compared to the LCx and RCA respectively <sup>27</sup>.

Clinical and ex-vivo studies have conclusively established that there is commonly a delay between the rupture of a plaque and its clinical consequence, if any <sup>15,28,29</sup>. Indeed, Rittersma et al have recently studied thrombectomy material of STEMI patients and found that 51 % of the patients had day to weeks old thrombotic material <sup>29</sup>. Thrombotic occlusion of a vessel seems to be an episodic event <sup>4</sup> and the underlying prevailing composition of the cavity (figure 1) might potentially have a prognostic value in identifying plaques at higher risk of occlusion. Large prospective studies using IVUS-VH might shed light into this question.

**Limitations**

All analyses and comparisons performed in the present manuscript beyond the assessment of the necrotic core content in ruptured versus non-ruptured plaques should be regarded as exploratory and hypothesis-generating since we cannot rule out the possibility that inflation of type I error due to multiple comparisons may have confounded our results. The relatively small population included may limit this study. Small ruptures, ruptures masked by overlying thrombus and the lack of assessment of minor branches may lead to an underestimation of the prevalence of such finding. Finally, prioritizing patient's safety, the decision to perform pre-intervention and 3-vessel IVUS was at the discretion of the operator, potentially inducing a selection bias.

**Conclusions**

The present study extends earlier findings about the prevalence, distribution and morphology of plaque rupture in the coronary tree. In this prospective 3-vessel IVUS study, patients with at least one plaque rupture in their coronary tree had larger body mass index and overall worse IVUS-derived characteristics compared to patients without evidence of plaque rupture. In addition, plaque rupture sites had a worse phenotype than the MLA sites of the same vessels.

**Acknowledgements**

We thank Mrs. Inés Dávalos Michel for her generous contribution to the study. We declare that Dr. G.A. Rodriguez-Granillo has received a research grant from Volcano Corp.

## References

1. Virmani R, Kolodgie FD, Burke AP, Farb A, Schwartz SM. Lessons from sudden coronary death: a comprehensive morphological classification scheme for atherosclerotic lesions. *Arterioscler Thromb Vasc Biol.* 2000;20:1262-75.
2. Arbustini E, Grasso M, Diegoli M, Morbini P, Aguzzi A, Fasani R, Specchia G. Coronary thrombosis in non-cardiac death. *Coron Artery Dis.* 1993;4:751-9.
3. Mann J, Davies MJ. Mechanisms of progression in native coronary artery disease: role of healed plaque disruption. *Heart.* 1999;82:265-8.
4. Burke AP, Kolodgie FD, Farb A, Weber DK, Malcom GT, Smialek J, Virmani R. Healed plaque ruptures and sudden coronary death: evidence that subclinical rupture has a role in plaque progression. *Circulation.* 2001;103:934-40.
5. Davies MJ, Richardson PD, Woolf N, Katz DR, Mann J. Risk of thrombosis in human atherosclerotic plaques: role of extracellular lipid, macrophage, and smooth muscle cell content. *Br Heart J.* 1993;69:377-81.
6. Gertz SD, Roberts WC. Hemodynamic shear force in rupture of coronary arterial atherosclerotic plaques. *Am J Cardiol.* 1990;66:1368-72.
7. Ge J, Chirillo F, Schwedtmann J, Gorge G, Haude M, Baumgart D, Shah V, von Birgelen C, Sack S, Boudoulas H, Erbel R. Screening of ruptured plaques in patients with coronary artery disease by intravascular ultrasound. *Heart.* 1999;81:621-7.
8. Rioufol G, Finet G, Ginon I, Andre-Fouet X, Rossi R, Vialle E, Desjoyaux E, Convert G, Huret JF, Tabib A. Multiple atherosclerotic plaque rupture in acute coronary syndrome: a three-vessel intravascular ultrasound study. *Circulation.* 2002;106:804-8.
9. Peters RJ, Kok WE, Havenith MG, Rijsterborgh H, van der Wal AC, Visser CA. Histopathologic validation of intracoronary ultrasound imaging. *J Am Soc Echocardiogr.* 1994;7:230-41.

10. Nair A, Kuban BD, Tuzcu EM, Schoenhagen P, Nissen SE, Vince DG. Coronary plaque classification with intravascular ultrasound radiofrequency data analysis. *Circulation*. 2002;106:2200-6.
11. Van Mieghem CAG, McFadden EP, de Feyter PJ, Bruining N, Schaar JA, Mollet NR, Cademartiri F, Goedhart D, de Winter S, Rodriguez Granillo GA, Valgimigli M, Mastik F, van der Steen AF, van der Giessen WJ, Sianos G, Backx B, Morel MA, van Es GA, Kaplow J, Zaleski A, Serruys PW. Non-invasive Detection of Subclinical Coronary Atherosclerosis Coupled With Assessment, Using Novel Invasive Imaging Modalities, of Changes in Plaque Characteristics Over Time: The IBIS Study (Integrated Biomarker and Imaging Study). *J Am Coll Cardiol*. 2006 Mar 21; 47(6):1134-42. Epub Feb 23.
12. Kåresen K. Deconvolution of sparse spike trains by iterated window maximization. *IEEE Trans Signal Process*. 1997;45:1173-1183.
13. Falk E, Shah PK, Fuster V. Coronary plaque disruption. *Circulation*. 1995;92:657-71.
14. Hong MK, Mintz GS, Lee CW, Kim YH, Lee SW, Song JM, Han KH, Kang DH, Song JK, Kim JJ, Park SW, Park SJ. Comparison of coronary plaque rupture between stable angina and acute myocardial infarction: a three-vessel intravascular ultrasound study in 235 patients. *Circulation*. 2004;110:928-33.
15. Maehara A, Mintz GS, Bui AB, Walter OR, Castagna MT, Canos D, Pichard AD, Satler LF, Waksman R, Suddath WO, Laird JR, Jr., Kent KM, Weissman NJ. Morphologic and angiographic features of coronary plaque rupture detected by intravascular ultrasound. *J Am Coll Cardiol*. 2002;40:904-10.
16. Laimer M, Kaser S, Kranebitter M, Sandhofer A, Muhlmann G, Schwelberger H, Weiss H, Patsch JR, Ebenbichler CF. Effect of pronounced weight loss on the

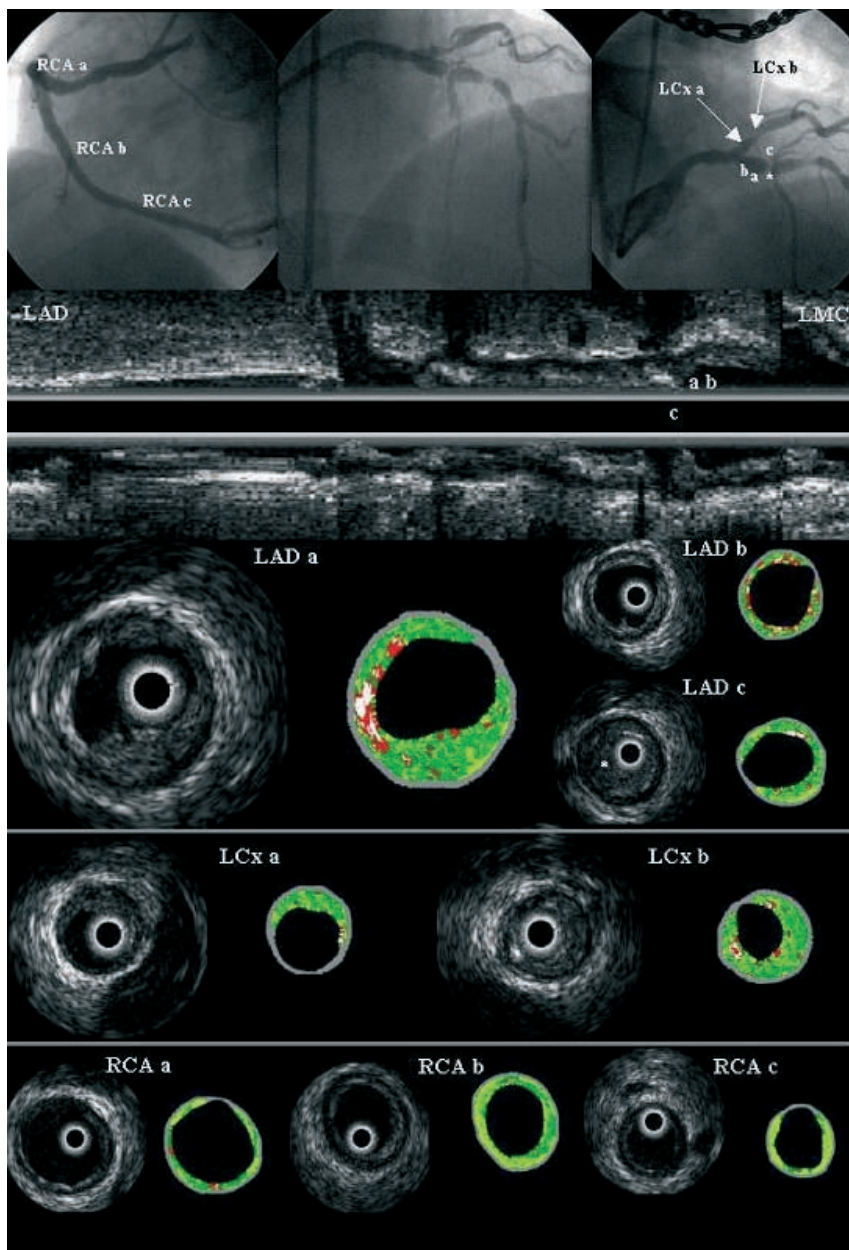
- nontraditional cardiovascular risk marker matrix metalloproteinase-9 in middle-aged morbidly obese women. *Int J Obes (Lond)*. 2005;29:498-501.
17. Kangavari S, Matetzky S, Shah PK, Yano J, Chyu KY, Fishbein MC, Cercek B. Smoking increases inflammation and metalloproteinase expression in human carotid atherosclerotic plaques. *J Cardiovasc Pharmacol Ther*. 2004;9:291-8.
  18. Shah PK, Falk E, Badimon JJ, Fernandez-Ortiz A, Mailhac A, Villareal-Levy G, Fallon JT, Regnstrom J, Fuster V. Human monocyte-derived macrophages induce collagen breakdown in fibrous caps of atherosclerotic plaques. Potential role of matrix-degrading metalloproteinases and implications for plaque rupture. *Circulation*. 1995;92:1565-9.
  19. Pasterkamp G, Schoneveld AH, van der Wal AC, Haudenschild CC, Clarijs RJ, Becker AE, Hillen B, Borst C. Relation of arterial geometry to luminal narrowing and histologic markers for plaque vulnerability: the remodeling paradox. *J Am Coll Cardiol*. 1998;32:655-62.
  20. Varnava AM, Mills PG, Davies MJ. Relationship between coronary artery remodeling and plaque vulnerability. *Circulation*. 2002;105:939-43.
  21. Burke AP, Kolodgie FD, Farb A, Weber D, Virmani R. Morphological predictors of arterial remodeling in coronary atherosclerosis. *Circulation*. 2002;105:297-303.
  22. Fernandez-Ortiz A, Badimon JJ, Falk E, Fuster V, Meyer B, Mailhac A, Weng D, Shah PK, Badimon L. Characterization of the relative thrombogenicity of atherosclerotic plaque components: implications for consequences of plaque rupture. *J Am Coll Cardiol*. 1994;23:1562-9.
  23. Farb A, Burke AP, Tang AL, Liang TY, Mannan P, Smialek J, Virmani R. Coronary plaque erosion without rupture into a lipid core. A frequent cause of coronary thrombosis in sudden coronary death. *Circulation*. 1996;93:1354-63.

24. Kragel AH, Reddy SG, Wittes JT, Roberts WC. Morphometric analysis of the composition of atherosclerotic plaques in the four major epicardial coronary arteries in acute myocardial infarction and in sudden coronary death. *Circulation*. 1989;80:1747-56.
25. Rodriguez-Granillo GA, McFadden E, Valgimigli M, van Mieghem CAG, Regar E, de Feyter PJ, Serruys PW. Coronary plaque composition of non-culprit lesions assessed by in vivo intracoronary ultrasound radio frequency data analysis, is related to clinical presentation. *Am Heart J*. 2005;In press.
26. Hong MK, Mintz GS, Lee CW, Lee BK, Yang TH, Kim YH, Song JM, Han KH, Kang DH, Cheong SS, Song JK, Kim JJ, Park SW, Park SJ. The site of plaque rupture in native coronary arteries: a three-vessel intravascular ultrasound analysis. *J Am Coll Cardiol*. 2005;46:261-5.
27. Ashby DT, Dangas G, Mehran R, Lansky AJ, Narasimaiah R, Iakovou I, Polena S, Satler LF, Pichard AD, Kent KM, Stone GW, Leon MB. Comparison of clinical outcomes using stents versus no stents after percutaneous coronary intervention for proximal left anterior descending versus proximal right and left circumflex coronary arteries. *Am J Cardiol*. 2002;89:1162-6.
28. Ojio S, Takatsu H, Tanaka T, Ueno K, Yokoya K, Matsubara T, Suzuki T, Watanabe S, Morita N, Kawasaki M, Nagano T, Nishio I, Sakai K, Nishigaki K, Takemura G, Noda T, Minatoguchi S, Fujiwara H. Considerable time from the onset of plaque rupture and/or thrombi until the onset of acute myocardial infarction in humans: coronary angiographic findings within 1 week before the onset of infarction. *Circulation*. 2000;102:2063-9.
29. Rittersma SZ, van der Wal AC, Koch KT, Piek JJ, Henriques JP, Mulder KJ, Ploegmakers JP, Meesterman M, de Winter RJ. Plaque instability frequently occurs

days or weeks before occlusive coronary thrombosis: a pathological thrombectomy study in primary percutaneous coronary intervention. *Circulation*. 2005;111:1160-5.

**Figure legend**

LAD refers to left anterior descending, LCx refers to left circumflex and RCA to right coronary artery. Three-vessel imaging using IVUS-VH (where calcified tissue is labelled as white, fibrous as green, fibrolipidic tissue as greenish-yellow and necrotic core as red) in a 57 year-old male presenting with unstable angina. Plaque rupture in the ostial LAD (LAD a). The underlying substrate of the cavity is rich in necrotic-core (red) and calcium (white), whereas the thrombus has migrated distally (LAD c, \*).



Colour figures on pages 441-449

## TABLES

**Table 1** Baseline characteristics and average IVUS parameters (n= 40)

	<b>n (%)</b>
Age (years±SD)	55.7±11.0
Male sex	29 (72.5)
Diabetes	4 (10.0)
Hypertension	17 (42.5)
Current smoking	15 (37.5)
Previous smoking	6 (15.0)
Hypercholesterolemia	20 (50.0)
Family history of coronary disease	19 (47.5)
Height (cm±SD)	174.5±9.2
Weight (kg±SD)	82.8±14.0
Body mass index (kg/m <sup>2</sup> ±SD)	27.1±3.4
LDL (mmol/L±SD)	2.70±0.7
HDL (mmol/L±SD)	1.20±0.5
<b>Clinical Presentation</b>	
Stable angina	13 (32.5)
Unstable angina	12 (30.0)
Acute myocardial infarction	15 (37.5)
<b>IVUS-VH measurements:</b>	
Analyzed length (mm)*	46.9;33.9-59.8
<b>Geometrical parameters</b>	
Lumen CSA (mm <sup>2</sup> ±SD)	9.4±2.8
Vessel CSA (mm <sup>2</sup> ±SD)	15.1±4.8
Plaque CSA (mm <sup>2</sup> ±SD)	5.8±2.7
Plaque max. thickness (mm±SD)	0.9±0.2
Plaque burden (%±SD)	37.2±8.7
<b>Compositional parameters</b>	
Calcium CSA (mm <sup>2</sup> ±SD)	0.07; 0.03-0.14
Calcium (%±SD)	2.50; 1.45-3.53
Fibrous CSA (mm <sup>2</sup> ±SD)	1.53; 0.81-2.11
Fibrous (%±SD)	57.84; 52.3-64.5
Fibrolipidic CSA (mm <sup>2</sup> ±SD)	0.48; 0.26-0.77
Fibrolipidic (%±SD)	17.96; 13.9-21.9
Necrotic core CSA (mm <sup>2</sup> ±SD)	0.26; 0.15-0.42
Necrotic core (%±SD)	10.13; 6.2-12.6

Discrete variables are presented as counts and percentages. Continuous variables are presented as means ± SD or medians (25<sup>th</sup>, 75<sup>th</sup> percentile) when indicated. CSA refers to cross-sectional area. \* refers to the average analyzed length per coronary.

**Table 2. Demographical characteristics and IVUS-derived of patients with and without the presence of plaque rupture**

	<b>Rupture (n=20)</b>	<b>No rupture (n=20)</b>	<b>p value</b>
Age (years±SD)	53.0±11.4	58.5±10.1	0.12
Body mass index (kg/m <sup>2</sup> ±SD)	28.4±3.7	25.8±2.6	0.01
<u>Sex</u>			0.08
Male (% within RF)	17 (58.6)	12 (41.4)	
Female sex (% within RF)	3 (27.3)	8 (72.7)	0.99
Diabetes (% within RF)	2 (50.0)	2 (50.0)	0.34
Hypertension (% within RF)	10 (58.8)	7 (41.2)	0.09
Current smoking (% within RF)	10 (66.7)	5 (33.3)	0.53
Hypercholesterolemia (% within RF)	11 (55.0)	9 (45.0)	0.34
Family history of coronary disease (% within RF)	8 (42.1)	11 (57.9)	0.92
LDL (mmol/L±SD)	2.72±0.5	2.69±0.9	0.91
HDL (mmol/L±SD)	1.19±0.6	1.21±0.3	0.09*
<u>Clinical Presentation</u>			
Stable angina	4 (30.8)	9 (69.2)	
Acute coronary syndrome	16 (59.3)	11 (40.7)	
<b><u>IVUS-VH measurements:</u></b>			
<b>Geometrical parameters</b>			
Lumen CSA (mm <sup>2</sup> )	9.6±3.3	9.2±2.3	0.60
Vessel CSA (mm <sup>2</sup> )	16.5±6.0	13.8±2.7	0.08
Plaque CSA (mm <sup>2</sup> )	6.9±3.3	4.6±1.4	0.01
Plaque max. thickness (mm)	1.0±0.2	0.8±0.2	0.02
Plaque burden (%)	40.7±7.6	33.7±8.4	0.01
<b>Compositional parameters</b>			

Calcium CSA (mm <sup>2</sup> )	0.09; 0.06-0.16	0.04; 0.02-0.11	0.01
Calcium (%)	2.53; 2.09-3.53	2.06; 0.67-3.58	0.14
Fibrous CSA (mm <sup>2</sup> )	1.94; 1.31-3.49	1.00; 0.70-1.68	0.003
Fibrous (%)	62.3; 55.9-64.8	54.2; 47.0-63.8	0.04
Fibrolipidic CSA (mm <sup>2</sup> )	0.58; 0.34-1.08	0.34; 0.22-0.55	0.03
Fibrolipidic (%)	17.8; 15.0-22.5	18.9; 12.8-21.9	0.95
Necrotic core CSA (mm <sup>2</sup> )	0.30; 0.22-0.51	0.22; 0.06-0.37	0.02
Necrotic core (%)	10.74; 7.7-12.5	9.22; 4.1-13.02	0.26

Values are expressed in means  $\pm$ SD. CSA refers to cross-sectional area. \*Across groups. Comparisons between groups were performed using independent student's *t* test,  $\chi^2$  or Kruskal-Wallis test as indicated.

**Table 3. Focal characteristics of ruptured plaques and minimal lumen area (MLA) controls (n= 28)**

	<b>Rupture site</b>	<b>MLA site</b>	<b>p value</b>
<b>Geometrical parameters</b>			
Lumen CSA (mm <sup>2</sup> )	9.47±6.3	6.76±4.2	<0.001
Vessel CSA (mm <sup>2</sup> )	19.09±9.3	19.15±9.8	0.95
Plaque CSA (mm <sup>2</sup> )	9.63±4.2	12.38±6.9	0.01
Plaque max. thickness (mm)	1.38±0.3	1.71±0.5	0.002
Plaque burden (%)	51.32±10.6	64.06±10.1	<0.001
<b>Compositional parameters*</b>			
Calcium CSA (mm <sup>2</sup> )	0.25; 0.05-0.55	0.27; 0.05-0.49	0.50
Calcium (%)	4.75; 1.22-7.83	2.97; 0.87-7.18	0.14
Fibrous CSA (mm <sup>2</sup> )	3.65; 1.67-5.67	4.09; 3.18-6.89	0.008
Fibrous (%)	60.3; 50.1-67.9	58.3; 55.6-66.2	0.53
Fibrolipidic CSA (mm <sup>2</sup> )	0.94; 0.40-1.82	1.40; 0.93-3.25	0.001
Fibrolipidic (%)	15.4; 10.9-22.6	20.5; 13.5-28.6	0.005
Necrotic core CSA (mm <sup>2</sup> )	0.83; 0.41-1.52	0.92; 0.54-1.64	0.35
Necrotic core (%)	16.7; 7.9-26.5	11.8; 8.4-17.1	0.03

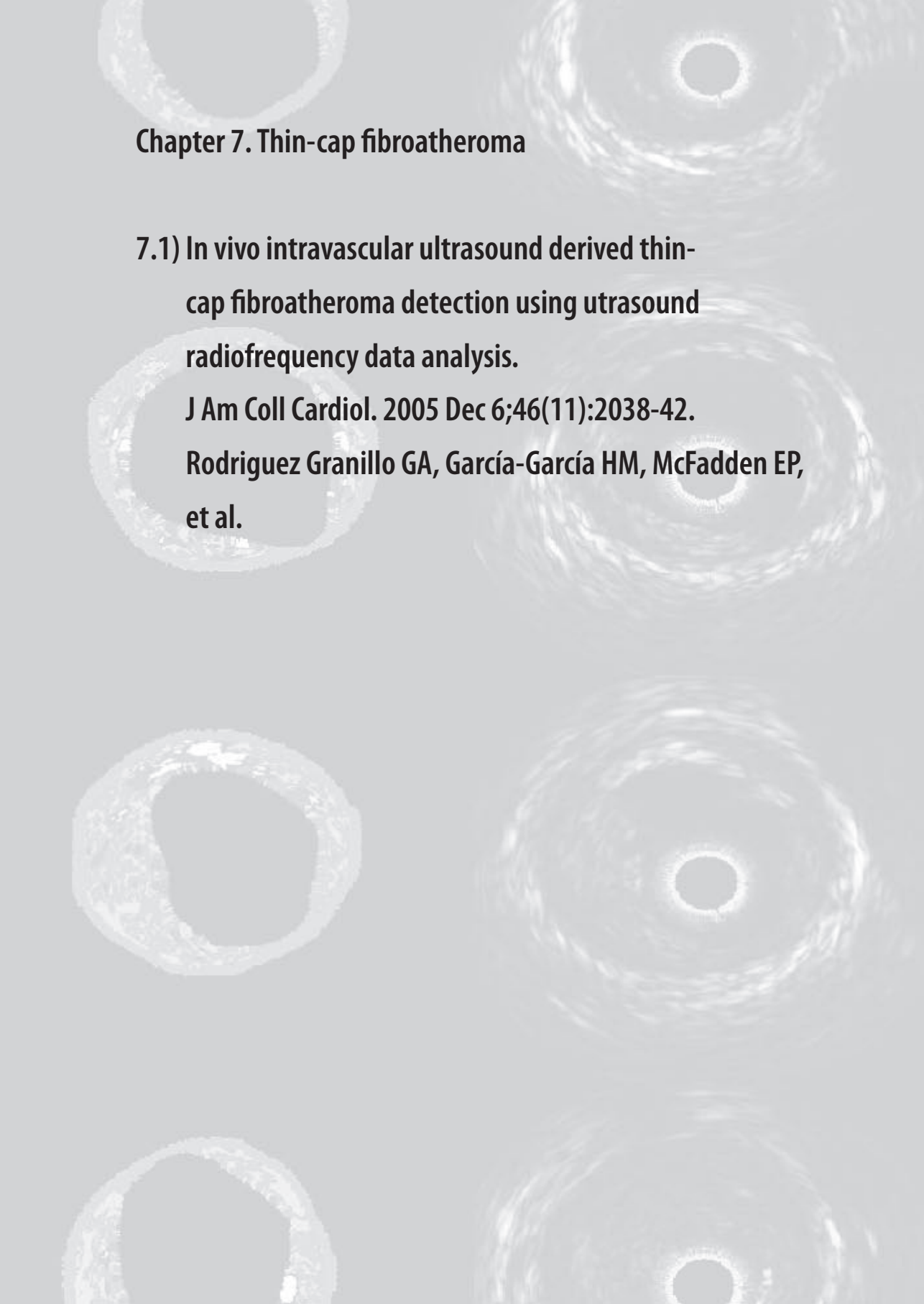
Values are expressed in means ±SD or median (interquartile range) as indicated. CSA refers to cross-sectional area. Comparisons between groups were performed using paired student's *t* test and Wilcoxon signed ranks test

**Table 4. Differences between the coronaries (n= 101)**

	<b>LAD (n= 37)</b>	<b>LCx (n= 32)</b>	<b>RCA (n=32)</b>
Analyzed length (mm±SD)	42.37±17.7	48.85±20.9	51.76±16.6
<b>Geometrical parameters</b>			
Lumen CSA (mm <sup>2</sup> )	8.53±2.6	9.26±3.2	11.07±4.6
Vessel CSA (mm <sup>2</sup> )	14.94±4.6	14.18±5.6	16.81±6.8
Plaque CSA (mm <sup>2</sup> )	6.43±2.8	4.92±3.3	5.74±3.0
Plaque max. thickness (mm)	1.05±0.3	0.84±0.3	0.85±0.3
Plaque burden (%)	42.2±9.9	33.17±9.2	33.96±10.3
<b>Compositional parameters</b>			
Calcium CSA (mm <sup>2</sup> )	0.11; 0.04-0.22	0.05; 0.02-0.14	0.04; 0.01-0.09
Calcium (%)	3.15; 1.74-4.91	2.10; 1.17-3.79	1.49; 0.39-2.53
Fibrous CSA (mm <sup>2</sup> )	1.82; 1.12-3.13	0.90; 0.59-1.55	1.12; 0.68-2.52
Fibrous (%)	62.1; 54.0-68.2	56.5; 42.5-66.0	59.5; 52.2-68.0
Fibrolipidic CSA (mm <sup>2</sup> )	0.52; 0.30-1.01	0.31; 0.16-0.49	0.34; 0.18-0.83
Fibrolipidic (%)	17.6; 12.8-23.0	15.2; 12.7-21.0	18.6; 13.5-23.6
Necrotic core CSA (mm <sup>2</sup> )	0.28; 0.19-0.57	0.14; 0.07-0.30	0.21; 0.05-0.38
Necrotic core (%)	11.68; 5.3-15.8	7.71; 4.15-13.6	9.18; 3.87-13.3

Values are expressed in means ±SD or median (interquartile range) as indicated. LAD, LCx and RCA refer to left anterior descending, left circumflex and right coronary arteries, respectively. CSA refers to cross-sectional area.





## **Chapter 7. Thin-cap fibroatheroma**

### **7.1) In vivo intravascular ultrasound derived thin-cap fibroatheroma detection using ultrasound radiofrequency data analysis.**

**J Am Coll Cardiol. 2005 Dec 6;46(11):2038-42.**

**Rodriguez Granillo GA, García-García HM, McFadden EP,  
et al.**



# In Vivo Intravascular Ultrasound-Derived Thin-Cap Fibroatheroma Detection Using Ultrasound Radiofrequency Data Analysis

Gastón A. Rodríguez-Granillo, MD, Héctor M. García-García, MD, Eugène P. Mc Fadden, MD, FRCPI, Marco Valgimigli, MD, Jiro Aoki, MD, Pim de Feyter, MD, PhD, Patrick W. Serruys, MD, PhD  
Rotterdam, the Netherlands

<b>OBJECTIVES</b>	The purpose of this study was to assess the prevalence of intravascular ultrasound (IVUS)-derived thin-cap fibroatheroma (IDTCFA) and its relationship with the clinical presentation using spectral analysis of IVUS radiofrequency data (IVUS-Virtual Histology [IVUS-VH]).
<b>BACKGROUND METHODS</b>	Thin-cap fibroatheroma lesions are the most prevalent substrate of plaque rupture. In 55 patients, a non-culprit, non-obstructive (<50%) lesion was investigated with IVUS-VH. We classified IDTCFA lesions as focal, necrotic core-rich ( $\geq 10\%$ of the cross-sectional area) plaques being in contact with the lumen; IDTCFA definition required a percent atheroma volume (PAV) $\geq 40\%$ .
<b>RESULTS</b>	Acute coronary syndrome (ACS) (n = 23) patients presented a significantly higher prevalence of IDTCFA than stable (n = 32) patients (3.0 [interquartile range (IQR) 0.0 to 5.0] vs. 1.0 [IQR 0.0 to 2.8], p = 0.018). No relation was found between patient's characteristics such as gender (p = 0.917), diabetes (p = 0.217), smoking (p = 0.904), hypercholesterolemia (p = 0.663), hypertension (p = 0.251), or family history of coronary heart disease (p = 0.136) and the presence of IDTCFA. A clear clustering pattern was seen along the coronaries, with 35 (35.4%), 31 (31.3%), 19 (19.2%), and 14 (14.1%) IDTCFAs in the first 10 mm, 11 to 20 mm, 21 to 30 mm, and $\geq 31$ mm segments, respectively, p = 0.008. Finally, we compared the severity (mean PAV $56.9 \pm 7.4$ vs. $54.8 \pm 6.0$ , p = 0.343) and the composition (mean percent necrotic core $19.7 \pm 4.1$ vs. $18.1 \pm 3.0$ , p = 0.205) of IDTCFAs between stable and ACS patients, and no significant differences were found.
<b>CONCLUSIONS</b>	In this in vivo study, IVUS-VH identified IDTCFA as a more prevalent finding in ACS than in stable angina patients. (J Am Coll Cardiol 2005;46:2038–42) © 2005 by the American College of Cardiology Foundation

Sudden cardiac death or unheralded acute coronary syndromes (ACS) are common initial manifestations of coronary atherosclerosis, and most such events occur at sites of non-flow limiting coronary atherosclerosis (1,2). Autopsy data suggest that plaque composition is a key determinant of the propensity of atherosclerotic lesions to provoke clinical events. Thin-cap fibroatheroma (TCFA) plaques with large avascular, hypocellular lipid cores seem particularly prone to rupture and result in epicardial occlusion (3–5).

Careful systematic evaluation, in a large series of victims of sudden cardiac death, suggested that ruptured TCFA was the precipitating factor for 60% of acute coronary thrombi. Furthermore, 70% of those patients had other TCFA that had not ruptured (5).

Intravascular ultrasound (IVUS) is the gold standard for evaluation of coronary plaque, lumen, and vessel dimensions (6,7). However, although visual interpretation of gray-scale IVUS can identify calcification within plaques, it cannot reliably differentiate lipid-rich from fibrous plaque (7). Recently, spectral analysis of IVUS radiofrequency data (IVUS-Virtual Histology [IVUS-VH]) has demonstrated potential to provide detailed quantitative information on

plaque composition and morphology and has been validated in studies of explanted human coronary segments (8).

In the present study, we evaluated the prevalence of IVUS-derived TCFA (IDTCFA) in coronary artery segments with non-significant lesions on angiography using IVUS-VH.

## METHODS

In 55 patients, a non-culprit, de novo, angiographically non-obstructive (<50%) lesion was investigated with IVUS-VH. Written informed consent was obtained from all patients.

**IVUS-VH acquisition and analysis.** Details regarding the validation of the technique on explanted human coronary segments have previously been reported (8). Briefly, IVUS-VH uses spectral analysis of IVUS radiofrequency data to construct tissue maps that classify plaque into four major components (fibrous [labeled green], fibrolipidic [labeled greenish-yellow], necrotic core [labeled red], and calcium [labeled white]) which were correlated with a specific spectrum of the radiofrequency signal and assigned color codes (8).

Intravascular Ultrasound-Virtual Histology data were acquired after intracoronary administration of nitrates using a continuous pullback (Ultracross 2.9-F 30-MHz catheter, Boston Scientific, Santa Clara, California), by a dedicated

From the Erasmus Medical Center, Thoraxcenter, Rotterdam, the Netherlands.  
Manuscript received May 25, 2005; revised manuscript received June 24, 2005,  
accepted July 25, 2005.

**Abbreviations and Acronyms**

ACS	= acute coronary syndrome
IDTCFA	= intravascular ultrasound-derived thin-cap fibroatheroma
IQR	= interquartile range
IVUS	= intravascular ultrasound
IVUS-VH	= Intravascular Ultrasound-Virtual Histology
LAD	= left anterior descending coronary artery
LCX	= left circumflex artery
PAV	= percent atheroma
RCA	= right coronary artery
ROI	= region of interest
TCFA	= thin-cap fibroatheroma

IVUS-VH console (Volcano Therapeutics, Rancho Cordova, California). The IVUS-VH data were stored on a CD-ROM and sent to the imaging core lab for offline analysis. Intravascular ultrasound B-mode images were reconstructed from the radiofrequency data by customized software (IVUSLab, Volcano Therapeutics, Rancho Cordova, California). Manual contour detection of both the lumen and the media-adventitia interface was performed, and the radiofrequency data were normalized using a technique known as “blind deconvolution,” an iterative algorithm that deconvolves the catheter transfer function from the backscatter, thus accounting for catheter-to-catheter variability (9). Geometric and compositional data were obtained for every slice and expressed as mean percent for each component. The plaque eccentricity index (EI) was calculated by dividing the minimum plaque thickness by the maximum plaque thickness. Percent atheroma volume (PAV) was defined as:  $EEM_{area} - lumen_{area} / EEM_{area} \times 100$ , where EEM refers to external elastic membrane.

Subsequently, we evaluated the presence of IDTCFA lesions along the interrogated vessels, and their incidence and characteristics were determined. Finally, the spatial distribution of IDTCFA along the coronaries was evaluated

starting from the ostium and dividing the vessel in 10-mm segments, evaluating a minimal length of 30 mm.

**Definition of IDTCFA.** Two experienced, independent IVUS analysts defined IDTCFA as a lesion fulfilling the following criteria in at least three consecutive frames: 1) necrotic core  $\geq 10\%$  without evident overlying fibrous tissue (Fig. 1); and 2) PAV  $\geq 40\%$ .

We selected this cutoff value because TCFA lesions are very unlikely present in segments with  $<40\%$  occlusion (10). Cross sections with non-uniform rotational distortion artifact were excluded from the analysis.

**Statistical analysis.** Discrete variables are presented as counts and percentages. Continuous variables are presented as medians (25th, 75th percentile) or mean values  $\pm$  SD when indicated. Pearson’s chi-square or Fisher exact test, Student *t* test, and Wilcoxon rank-sum tests were performed, as indicated. A two-sided *p* value of  $<0.05$  indicated statistical significance. Logistic regression analysis was performed to identify potential predictors of the presence of IDTCFA. Statistical analyses were performed with use of 11.5 SPSS software (SPSS Inc., Chicago, Illinois).

**RESULTS**

The baseline characteristics of the patients ( $n = 55$ ) studied are presented in Table 1. Thirty-four (61.8%) patients had at least one IDTCFA in the region of interest (ROI).

The population was prospectively divided into two groups, stable patients and patients presenting with ACS (defined as unstable angina, non-ST-segment elevation myocardial infarction, or ST-segment elevation myocardial infarction).

**IDTCFA incidence and predictors.** Acute coronary syndrome patients had a significantly higher incidence of IDTCFA than stable patients (3.0 [interquartile range (IQR) 0.0 to 5.0] vs. 1.0 [IQR 0.0 to 2.8],  $p = 0.018$ ). When corrected for the length of the ROI, the density of

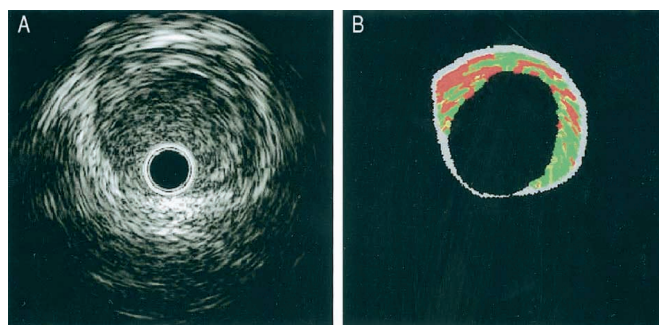


**Figure 1.** Left anterior descending artery depicted by Intravascular Ultrasound-Virtual Histology, where calcified, fibrous, fibrolipidic, and necrotic core regions are labeled white, green, greenish-yellow, and red, respectively. **Panel A** shows an intravascular ultrasound cross-sectional area reconstructed from backscattered signals. **Panel B** shows the corresponding tissue map depicting a necrotic core-rich plaque with necrotic core tissue in contact with the lumen.

Colour figures on pages 441-449

**Table 1.** Baseline Characteristics (n = 55)

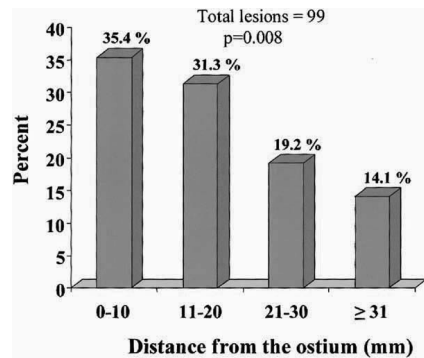
	n (%)
Age (yrs ± SD)	57.6 ± 9.5
Male gender	44 (80.0)
Diabetes	5 (9.1)
Hypertension	20 (36.4)
Current smoking	15 (27.3)
Previous smoking	14 (25.5)
Hypercholesterolemia	46 (83.6)
Family history of coronary disease	30 (54.5)
Vessel	
Right coronary artery	22 (40.0)
Left anterior descending	23 (41.8)
Left circumflex	10 (18.2)
Clinical presentation	
Stable	32 (58.2)
Acute coronary syndrome	23 (41.8)

IDTCFA remained statistically significant (0.7 [IQR 0.0 to 1.3] IDTCFA/cm vs. 0.2 [IQR 0.0 to 0.7] IDTCFA/cm,  $p = 0.031$ ) (Table 2).

No relation was found between patient's characteristics such as gender ( $p = 0.917$ ), diabetes ( $p = 0.217$ ), smoking ( $p = 0.904$ ), hypercholesterolemia ( $p = 0.663$ ), hypertension ( $p = 0.251$ ), or family history of coronary heart disease ( $p = 0.136$ ) and the presence of IDTCFA.

**Characteristics and location.** We compared the severity (mean PAV  $56.9 \pm 7.4\%$  vs.  $54.8 \pm 6.0\%$ ,  $p = 0.343$ ) and the composition (mean percent necrotic core  $19.7 \pm 4.1\%$  vs.  $18.1 \pm 3.0\%$ ,  $p = 0.205$ ) of IDTCFAs between ACS and stable patients, and no significant differences were found. Although not significantly, the left anterior descending coronary artery (LAD) (73.9% of the LADs,  $n = 23$ ) was the most frequent location, followed by the left circumflex artery (LCX) (60.0% of the LCXs,  $n = 10$ ) and the right coronary artery (RCA) (50.0% of the RCAs,  $n = 22$ ,  $p = 0.254$ ).

Four patients were excluded from the spatial distribution subanalysis, three because the IVUS assessment of the ROI was shorter than 30 mm and the last one because the pullback did not reach the ostium. A total of 99 IDTCFA were present in vessels that met the aforementioned criteria. A clear clustering pattern was seen along the coronaries, with 35 (35.4%), 31 (31.3%), 19 (19.2%), and 14 (14.1%) IDTCFAs in the first 10 mm, 11 to 20 mm, 21 to 30 mm, and  $\geq 31$  mm segments, respectively,  $p = 0.008$  (Fig. 2). The results showed a clear clustering pattern of the lesions along the coronaries, with 66 (66.7%) IDTCFA located in


**Figure 2.** Bar graphs illustrating the frequency of intravascular ultrasound-derived thin-cap fibroatheroma (IDTCFA) starting from the ostium.

the first 20 mm, whereas further along the vessels the incidence was significantly lower (33, 33.3%,  $p = 0.008$ ).

## DISCUSSION

Post-mortem observations have documented several characteristic histological patterns that are substrates for sudden death related to epicardial coronary occlusion, of which the most common is TCFA (5,11,12). The same studies have demonstrated that plaque rupture at TCFA may also occur without clinical consequences. The ability to identify TCFA in patients would both help clarify the natural history of TCFA and provide the means to assess the effects of pharmacological, or other, intervention.

Until recently, no technique could identify TCFA *in vivo*. However, spectral analysis of IVUS radiofrequency (IVUS-VH) data has demonstrated potential to provide detailed quantitative information both on overall plaque composition and on the anatomic relation of specific plaque components to the lumen of the vessel, and it has been validated in studies of explanted human coronary segments (8).

**IDTCFA definition.** It is well established that tissue shrinkage occurs during tissue fixation (13). Shrinkage of up to 60%, 15%, and 80% can occur during critical-point drying, free drying, and air drying, respectively (14). Furthermore, postmortem contraction of arteries is an additional confounding factor (15).

Although the most accepted threshold to define a cap as "thin" has been set at  $65 \mu\text{m}$  (16), a number of important

**Table 2.** Incidence and Characteristics of IDTCFA Lesions in Stable and ACS Patients

	Length of ROI	IDTCFA	IDTCFA/cm	% PAV	% NC	EI
Stable (n = 32)	35.41 ± 11.6	1.0 (0.0, 2.8)	0.2 (0.0, 0.7)	54.8 ± 6.0	18.1 ± 3.0	0.23 ± 0.1
ACS (n = 23)	33.90 ± 15.0	3.0 (0.0, 5.0)	0.7 (0.0, 1.3)	56.8 ± 7.4	19.7 ± 4.1	0.27 ± 0.2
p value	0.684	0.018	0.031	0.343	0.205	0.35

Continuous variables are presented as medians (25th, 75th percentile) or mean values ± SD when indicated.

ACS = acute coronary syndrome; EI = plaque eccentricity index (defined as minimum plaque thickness divided by maximum plaque thickness); IDTCFA = intravascular ultrasound-derived thin-cap fibroatheroma; % PAV = percent atheroma volume (defined as  $EEM_{\text{area}} - lumen_{\text{area}}/EEM_{\text{area}} \times 100$ , where EEM refers to external elastic membrane); ROI = region of interest; % NC = percent necrotic core of the cross-sectional area.

ex vivo studies have used higher ( $>200 \mu\text{m}$ ) thresholds (4,17,18). Indeed, one of these studies identified a mean cap thickness of 260 and 360  $\mu\text{m}$  for “vulnerable” and “non-vulnerable” plaques, respectively (18). Because the axial resolution of IVUS-VH is between 100 to 150  $\mu\text{m}$ , we assumed that the absence of visible fibrous tissue overlying a necrotic core suggested a cap thickness of below 100 to 150  $\mu\text{m}$  and used the absence of such tissue to define a thin fibrous cap (19). Figure 1 depicts a typical example of IDTCFA.

**Incidence, characteristics, and distribution of IDTCFA.** The major findings of our study were first that IVUS-VH findings, compatible with IDTCFA, were common in non-culprit lesions of patients undergoing percutaneous intervention in another vessel. Second, the prevalence of IDTCFA was significantly higher in patients who presented with ACS compared to stable patients. In addition, the distribution of IDTCFA lesions along the coronary vessels was clearly clustered. Finally, we found no significant correlation between the presence of conventional risk factors and the occurrence of IDTCFA.

In vivo studies established that a multifocal instability process is present in ACS (20,21). Rioufol et al. (20) found at least one plaque rupture remote from the culprit lesion in 80% of patients and from the culprit artery in 71% of patients (20). The significantly higher prevalence of IDTCFA in non-culprit coronaries of patients presenting with an ACS supports the theory that holds ACS as multifocal processes.

The distribution of the IDTCFA in the coronaries was in line with previous ex vivo and clinical studies, with a clear clustering pattern from the ostium, thus supporting the non-uniform distribution of vulnerable plaques along the coronary tree (22,23). Of note, the mean PAV and the mean necrotic core percentage of the IDTCFAs detected by IVUS-VH were also similar to previously reported histopathological data (55.9% vs. 59.6% and 19% vs. 23%, respectively) (10).

The large number of high-risk plaques found throughout the coronary tree by means of angiography, angioscopy, IVUS, and palpography, in addition to the unpredictability of the natural history of such lesions and the uncertainty about whether vulnerable plaque characteristics will subsequently lead to fatal or non-fatal ischemic events, suggests that potential local preventive strategies could not be cost-effective (12,20,21,24,25). On the contrary, a systemic “plaque stabilization” approach including statins and angiotensin-converting enzyme inhibitors could be capable of “cooling-down” the inflammatory burden.

To our knowledge, this is the first study to detect in vivo the presence of an IVUS surrogate of TCFA. This novel intravascular diagnostic tool could potentially aid the assessment of the effect of antiatherosclerotic drugs, and allow a more comprehensive pathophysiologic approach towards natural history studies.

**Study limitations.** The present was an observational study where we evaluated only one coronary artery per patient.

The inferior axial resolution of IVUS-VH in comparison to histology could influence our results. This study does not directly assess the incremental value of IVUS-VH over visual identification of plaque characterization. The main finding of the study (IDTCFA) is only a surrogate of a histopathological finding. Besides, the lack of a direct comparison between IVUS-VH and histopathology renders our observation to some extent only exploratory. Accordingly, interpretation of our findings must be cautious. Prospective studies are needed in order to evaluate the prognostic value and natural history of such finding. The seemingly high prevalence of IDTCFA in comparison with histopathological studies is mainly driven by the sampling limitation of such studies and has previously been acknowledged (26).

**Conclusions.** In this in vivo study, IVUS-VH identified IDTCFA as a more prevalent finding in ACS than in stable angina patients. Prospective studies are needed in order to evaluate the prognostic value of such finding in natural history studies.

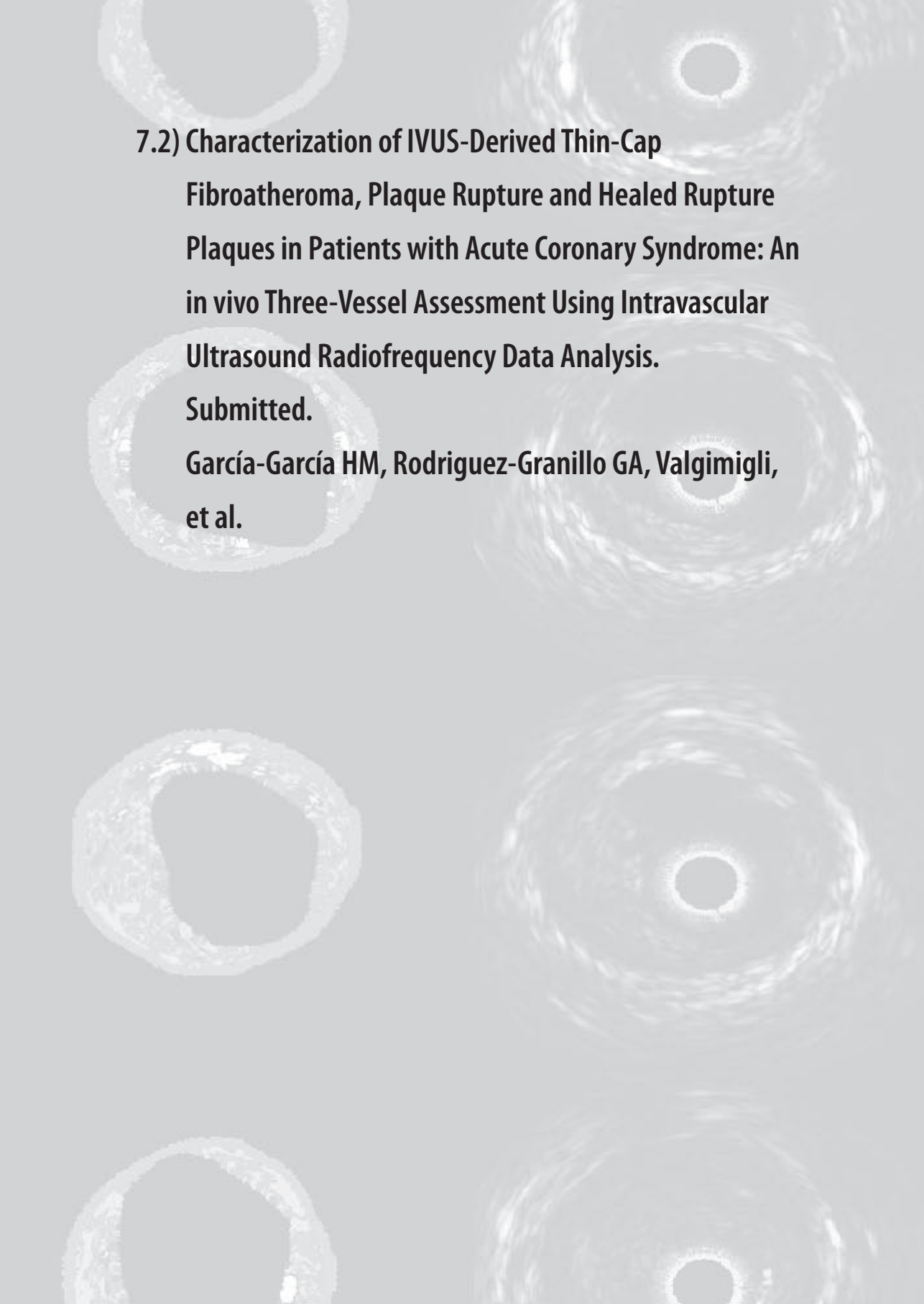
**Reprint requests and correspondence:** Dr. Patrick W. Serruys, Thoraxcenter, Bd406, Dr. Molewaterplein 40, 3015-GD Rotterdam, the Netherlands. E-mail: p.w.j.c.serruys@erasmusmc.nl.

## REFERENCES

- Ambrose JA, Tannenbaum MA, Alexopoulos D, et al. Angiographic progression of coronary artery disease and the development of myocardial infarction. *J Am Coll Cardiol* 1988;12:56–62.
- Little WC, Constantinescu M, Applegate RJ, et al. Can coronary angiography predict the site of a subsequent myocardial infarction in patients with mild-to-moderate coronary artery disease? *Circulation* 1988;78:1157–66.
- Davies MJ, Richardson PD, Woolf N, Katz DR, Mann J. Risk of thrombosis in human atherosclerotic plaques: role of extracellular lipid, macrophage, and smooth muscle cell content. *Br Heart J* 1993;69:377–81.
- Felton CV, Crook D, Davies MJ, Oliver MF. Relation of plaque lipid composition and morphology to the stability of human aortic plaques. *Arterioscler Thromb Vasc Biol* 1997;17:1337–45.
- Virmani R, Kolodgie FD, Burke AP, Farb A, Schwartz SM. Lessons from sudden coronary death: a comprehensive morphological classification scheme for atherosclerotic lesions. *Arterioscler Thromb Vasc Biol* 2000;20:1262–75.
- Nishimura RA, Edwards WD, Warnes CA, et al. Intravascular ultrasound imaging: in vitro validation and pathologic correlation. *J Am Coll Cardiol* 1990;16:145–54.
- Peters RJ, Kok WE, Havenith MG, Rijsterborgh H, van der Wal AC, Visser CA. Histopathologic validation of intracoronary ultrasound imaging. *J Am Soc Echocardiogr* 1994;7:230–41.
- Nair A, Kuban BD, Tuzcu EM, Schoenhagen P, Nissen SE, Vince DG. Coronary plaque classification with intravascular ultrasound radiofrequency data analysis. *Circulation* 2002;106:2200–6.
- Kåresen KF, Bølviken E. Blind deconvolution of ultrasonic traces accounting for pulse variance. *IEEE Trans Ultrason Ferroelectr Freq Control* 1999;46:564–73.
- Virmani R, Burke AP, Kolodgie FD, Farb A. Vulnerable plaque: the pathology of unstable coronary lesions. *J Interv Cardiol* 2002; 15:439–46.
- Davies MJ, Thomas A. Thrombosis and acute coronary-artery lesions in sudden cardiac ischemic death. *N Engl J Med* 1984;310:1137–40.
- Burke AP, Kolodgie FD, Farb A, et al. Healed plaque ruptures and sudden coronary death: evidence that subclinical rupture has a role in plaque progression. *Circulation* 2001;103:934–40.

13. Lee RM. A critical appraisal of the effects of fixation, dehydration and embedding of cell volume. In: Revel JP, Barnard T, Haggis GH, editors. *The Science of Biological Specimen Preparation for Microscopy and Microanalysis*. Scanning Electron Microscopy. Chicago, IL: AMF O'Hare, 1984:61–70.
14. Boyde A, Jones SJ, Tamarin A. Dimensional changes during specimen preparation for scanning electron microscopy. *Scan Electron Microsc* 1977;1:507–18.
15. Fishbein MC, Siegel RJ. How big are coronary atherosclerotic plaques that rupture? *Circulation* 1996;94:2662–6.
16. Burke AP, Farb A, Malcom GT, Liang YH, Smialek J, Virmani R. Coronary risk factors and plaque morphology in men with coronary disease who died suddenly. *N Engl J Med* 1997;336:1276–82.
17. Mann JM, Davies MJ. Vulnerable plaque. Relation of characteristics to degree of stenosis in human coronary arteries. *Circulation* 1996;94: 928–31.
18. Schaar JA, De Korte CL, Mastik F, et al. Characterizing vulnerable plaque features with intravascular elastography. *Circulation* 2003;108: 2636–41.
19. Nair ACD, Vince DG. Regularized autoregressive analysis of intravascular ultrasound data: improvement in spatial accuracy of plaque tissue maps. *IEEE Trans Ultrason Ferroelectr Freq Control* 2004;51: 420–31.
20. Rioufol G, Finet G, Ginon I, et al. Multiple atherosclerotic plaque rupture in acute coronary syndrome: a three-vessel intravascular ultrasound study. *Circulation* 2002;106:804–8.
21. Asakura M, Ueda Y, Yamaguchi O, et al. Extensive development of vulnerable plaques as a pan-coronary process in patients with myocardial infarction: an angioscopic study. *J Am Coll Cardiol* 2001;37: 1284–8.
22. Kolodgie FD, Burke AP, Farb A, et al. The thin-cap fibroatheroma: a type of vulnerable plaque: the major precursor lesion to acute coronary syndromes. *Curr Opin Cardiol* 2001;16:285–92.
23. Wang JC, Normand SL, Mauri L, Kuntz RE. Coronary artery spatial distribution of acute myocardial infarction occlusions. *Circulation* 2004;110:278–84.
24. Goldstein JA, Demetriou D, Grines CL, Pica M, Shoukfeh M, O'Neill WW. Multiple complex coronary plaques in patients with acute myocardial infarction. *N Engl J Med* 2000;343:915–22.
25. Schaar JA, Regar E, Mastik F, et al. Incidence of high-strain patterns in human coronary arteries: assessment with three-dimensional intravascular palpography and correlation with clinical presentation. *Circulation* 2004;109:2716–9.
26. Farb A, Tang AL, Burke AP, Sessums L, Liang Y, Virmani R. Sudden coronary death. Frequency of active coronary lesions, inactive coronary lesions, and myocardial infarction. *Circulation* 1995;92:1701–9.



The background of the slide features a grid of eight circular cross-sections of arteries, likely generated from Intravascular Ultrasound (IVUS) data. These images show the internal structure of the vessel walls, including the lumen and the surrounding tissue layers. The images are arranged in two columns and four rows, with the text overlaid on the left side.

**7.2) Characterization of IVUS-Derived Thin-Cap  
Fibroatheroma, Plaque Rupture and Healed Rupture  
Plaques in Patients with Acute Coronary Syndrome: An  
in vivo Three-Vessel Assessment Using Intravascular  
Ultrasound Radiofrequency Data Analysis.**

**Submitted.**

**García-García HM, Rodríguez-Granillo GA, Valgimigli,  
et al.**



**Characterization of IVUS-Derived Thin-Cap Fibroatheroma,  
Plaque Rupture and Healed Rupture Plaques in Patients with  
Acute Coronary Syndrome: An *in vivo* Three-Vessel Assessment  
Using Intravascular Ultrasound Radiofrequency Data Analysis**

**Héctor M. García-García MD; Gastón A. Rodríguez-Granillo MD; Marco Valgimigli MD; Neville Kukreja MRCP; Masato Otsuka MD; Dick Goedhart PhD<sup>1</sup>; Marco Bressers MSc<sup>1</sup>; Marie-angele M. Morel BSc<sup>1</sup>; Gerrit-Ann van Es PhD<sup>1</sup>; Pim J. de Feyter MD, PhD; Patrick W. Serruys MD, PhD.**

Thoraxcenter, Erasmus MC, Rotterdam, The Netherlands

<sup>1</sup> Cardialysis BV, Rotterdam, The Netherlands

**Abbreviations list**

ACS- Acute coronary syndrome

CSA – Cross sectional area

EEM- External elastic membrane

IVUS- Intravascular ultrasound

IDHR- IVUS-derived healed rupture

IDTCFA- IVUS-derived thin-cap fibroatheroma

PB- Plaque burden

PR- Plaque rupture

STEMI – ST segment elevation myocardial infarction

NSTEMI – Non-ST segment elevation myocardial infarction

UA – Unstable angina

VH- Virtual Histology

**ABSTRACT**

**Background:** The morphologic features of the different atherosclerotic plaques have been derived from lesions studied in post-mortem studies. We therefore characterized *in vivo* IVUS-derived (ID) thin-cap fibroatheroma (IDTCFA), plaque rupture (PR) and ID-healed rupture (IDHR) plaques in patients with acute coronary syndrome using three vessel IVUS-radiofrequency data.

**Methods and results:** Thirty-five patients were studied. A total of 183 IDTCFAs, 19 PR (ratio 9.6 IDTCFAs/1 PR) and 35 IDHR plaques (ratio 5.2 IDTCFAs/1 IDHR plaque) were identified. Nine IDHR were found together with either IDTCFA (6) or PR (3). Ninety five (52.2%) IDTCFAs, 11 (57.9%) PR and 20 (57.1%) IDHR plaques were located within the first 3 cm of the main coronary arteries. The necrotic core content was  $22.2\pm 9.3\%$  in the IDTCFA,  $13.0\pm 7.8\%$  in PR and  $20.2\pm 7.1$  in the IDHR plaques,  $p<0.001$ . The vessel CSA in IDTCFAs was  $16.2\pm 6.1$  mm<sup>2</sup>, in PR  $19.0\pm 9.3$  mm<sup>2</sup> and in IDHR plaques was  $20.8\pm 6.5$  mm<sup>2</sup>,  $p=0.164$ . Plaque burden was significantly different, in IDTCFAs was  $47.6\pm 8.1\%$ , in PR  $45.0\pm 9.2\%$  and in IDHR plaque was  $56.2\pm 9.7\%$ ,  $p<0.001$ .

**Conclusions:** In patients with acute coronary syndromes IDTCFA, plaque ruptures and IDHR plaques had a higher prevalence in the first three centimetres in the main epicardial vessels. Furthermore, there was a gradient in plaque size and plaque composition between the different plaque morphologies.

**Key words:** Atherosclerosis, imaging, coronary disease

**Introduction**

Unheralded cardiovascular events such as acute coronary syndromes (ACS) are commonly triggered by atherothrombotic phenomena occurring at sites of either non-flow limiting atherosclerosis<sup>1,2</sup> or significant coronary artery disease<sup>3-5</sup>. Mostly the formation of thrombi is due to plaque disruption<sup>6,7</sup>. Plaques underlying a coronary thrombus have peculiar morphologic, compositional and mechanical characteristics such as high content of necrotic-core<sup>8,9</sup>, thin fibrous cap, scarcity of smooth muscle cells, intense inflammatory infiltration of the fibrous cap<sup>10-12</sup> and high degree of mechanical strain expressed by the plaque<sup>13</sup>. These morphological features of the so-called “vulnerable plaques” or thin-cap fibroatheroma (TCFA) have been derived from lesions observed in post-mortem studies. Recently, our group has published the *in vivo* assessment of such plaques using IVUS- radiofrequency data (Virtual Histology-VH), confirming a higher prevalence of IVUS-derived thin-cap fibroatheroma (IDTCFA) in patients with ACS as compared to stable angina<sup>14</sup>.

When TCFA ruptures, different stages of the healing reaction can be identified microscopically<sup>15</sup>. This process of thinning of the fibrous cap, followed by its rupture, thrombosis and healing can promote atherosclerotic plaque growing. Therefore an analysis of these different atherosclerotic plaque morphologies *in vivo* would be of critical importance in the understanding the stages of the disease process.

We thus sought to comprehensively characterize *in vivo* by means of IVUS-VH the morphological phases of vulnerable plaque transition, including the detection of plaque rupture and IVUS-derived healed rupture (IDHR) plaques together with the previously described IDTCFA in patients with acute coronary syndrome undergoing three vessel IVUS investigation.

## Methods

### Patient selection

From January to May 2005, all patients with acute coronary syndromes admitted for coronary catheterization and subsequent intervention were eligible if all three coronary vessels were suitable for IVUS interrogation (absence of extensive angiographic calcification and/or severe vessel tortuosity). Acute coronary syndrome encompasses unstable angina (UA) according to the Braunwald classification, non-ST-segment elevation myocardial infarction (NSTEMI), and ST-segment elevation myocardial infarction (STEMI). Percutaneous treatment of the culprit lesion before any imaging acquisition was mandatory in all patients. The three-vessel IVUS-VH acquisition timing was as follows: in patients with UA/NSTEMI acquisition was performed just after the interventional treatment and in patients suffering from STEMI was done when the patient was symptoms free, without ECG changes and hemodynamically stable, which was defined as systolic blood pressure >90 mmHg without vasopressor or inotropic support and heart rate between 60 and 100 bpm. Informed written consent was obtained from all patients. Our local Ethics Committee approved the protocol.

### Definitions used in this study

*Necrotic core tissue in contact with the lumen*, defined as the presence of necrotic core tissue in direct contact with the luminal space and with no detectable overlying fibrous tissue, reported as a binary variable irrespective of the amount of necrotic core.

*Plaque burden (PB)*, defined as  $EEM_{\text{area}} - \text{Lumen}_{\text{area}} / EEM_{\text{area}} \times 100$ , where EEM refers to external elastic membrane.

*IVUS-derived TCFA<sup>14</sup>*, is defined as a lesion fulfilling the following criteria in at least 3 consecutive CSAs : 1) plaque burden  $\geq 40\%$ ; 2) necrotic core  $\geq 10\%$ <sup>16</sup> in direct contact with

the lumen in the investigated CSA (**figure 1A**); All consecutive CSAs having the same morphologic characteristics were considered as part of the same IDTCFA lesion.

*Plaque rupture* was defined as a ruptured capsule with an underlying cavity (**figure 1B**), or plaque excavation by atheromatous extrusion with no visible capsule<sup>17,18</sup>. Rupture sites separated by at least 5 mm length of rupture-free vessel were considered as different ruptures.

*IVUS-derived healed rupture (IDHR)*, consists of a pool of necrotic core buried by a layer of fibrous tissue. Repetition of the same pattern creates a multilayered appearance as described by histopathology<sup>10</sup>(**figure 1C**).

Screening for diagnosis of an IDTCFA, plaque rupture and IDHR required the independent review and agreement between two experienced IVUS observers (H.M.G.G and G.A.R.G.), who had no knowledge about demographical data of the patients. Disagreement was solved by consensus between the observers, when needed a third expert was consulted.

## IVUS-VH Acquisition and Analysis

Details regarding the validation of the technique, on explanted human coronary segments, have previously been reported<sup>19</sup>. Briefly, IVUS-VH uses spectral analysis of IVUS radiofrequency data to build tissue maps that are correlated with a specific spectrum of the radiofrequency signal and assigned colour codes [fibrous (labelled green), fibrolipidic (labelled greenish-yellow), necrotic core (labelled red) and calcium (labelled white)]<sup>19</sup>.

IVUS-VH data was acquired using a continuous pullback (Eagle-Eye™ 20 MHz Volcano Therapeutics, Rancho Cordova, CA), by a dedicated IVUS-VH console (Volcano Therapeutics, Rancho Cordova, CA). The IVUS-VH data were stored on a DVD and sent to the imaging core lab for offline analysis (Cardialysis BV, Rotterdam, The Netherlands). Data acquisition was ECG-gated and recorded during the automated withdrawal of the catheter using a mechanical pullback device (Volcano Therapeutics, Rancho Cordova, CA) at a pullback speed of 0.5 mm/s. Cine runs, before and during contrast injection, were performed to define the position of the IVUS catheter before the pullback was started.

The IVUS-VH sampling rate during pullback is gated to peak R-wave and is therefore dependent on heart rate. For instance, during constant heart rate of 60 bpm, then data will be collected every 0.5 mm.

IVUS B-mode images were reconstructed from the RF data by customized software (4.4 IVUSLab, Volcano Therapeutics, Rancho Cordova, CA). Longitudinal and cross-sectional views were used to determine the contours; if poor quality of the IVUS was observed, which was defined as uncertainty of the luminal border and presence of artifacts, the vessel was not included in this analysis. Manual contour detection of both the lumen and the media-adventitia interface was performed and the radiofrequency data was normalized using a technique known as “Blind Deconvolution”<sup>20</sup>, an iterative algorithm that deconvolves the

catheter transfer function from the backscatter, thus accounting for catheter-to-catheter variability. Geometrical and compositional data were obtained for every slice.

### **Objective**

To investigate the prevalence, composition and distribution of different plaque morphologies (IDTCFA, plaque ruptures and IDHR plaques) in the three vessels of patients with ACS.

## Statistical analysis

Discrete variables are presented as counts and percentages. Continuous variables are presented as means  $\pm$  SD. A two-sided p value of less than 0.05 indicated statistical significance. Assumptions for normality were checked after transformation based on a p-value  $>0.20$  at Kolmogorov-Smirnov test and on visual assessment of Q-Q plots of residuals. Accordingly, log transformation was performed on the variables with skewed distribution. To determine the distribution of the IDTCFAs, plaque rupture and IDHR plaques along the vessels, the vessel was divided into 10-mm length segments. The frequency of such lesions was assessed as a function of the distance from the ostium of the artery. When a plaque extended through more than one 10-mm segment, the plaque was counted in the starting segment.

IVUS-VH CSAs were analyzed for their attribute of belonging to an IDTCFA or not. (By definition these IDTCFAs have a length of at least three consecutive CSA). Summary statistics was used to count the number of frames containing or not an IDTCFA in order to obtain the raw-Odds, by vessel (LAD, LCX and RCA). Finally, in a General Estimating Equations model, with binomial distribution and a logit link function, cases were regarded as a random factor and we allowed for an autoregressive correlation structure<sup>21,22</sup>. Vessel was a fixed factor in the model. For the pair wise comparisons between vessels an Odds Ratio was calculated together with its 95% two-sided confidence interval and a p-value to express the probability of that confidence interval to contain the value 1 with  $\alpha=0.05$ .

Within each patient we calculated the mean for each plaque morphology (i.e., IDTCFA, plaque rupture, IDHR, IDHR with IDTCFA and IDHR with plaque rupture) class as a summary statistic for calcified area, fibrous area, fibrolipid area and necrotic core area. This statistic then was analyzed in a general linear model, using patient and morphology class as

independent predictors. Comparisons between morphology classes were made taking into account the specific patient level for a given patient.

Statistical analyses were performed with use of SPSS software, version 11.5 and SAS V8.02.

## Results

Thirty five patients (95 vessels) were consecutively enrolled in this study. In ten patients one of the three vessels was not suitable for IVUS-VH analysis, 5 vessels due to full metal jacket and 5 vessels had IVUS-VH of poor quality (EEM out of the frame and irregular pullback). The baseline characteristics are depicted in **table 1**. The mean age was  $52.4 \pm 9.4$  years. Mostly being male patients 82.9%, while only 11.1% were diabetic. Fifty seven percent had STEMI. The culprit vessel was identified in the entire population; the left anterior descending (LAD) was the culprit vessel in 19 (52.8%) cases, and the left circumflex (LCX) and the right coronary artery (RCA) in 8 (22.2%) and 9 (25.0%) cases, respectively. In one patient suffering from unstable angina two culprit vessels were detected.

In total, 10146 CSAs were studied. Three main plaque morphologies were identified: IDTCFA (1146 CSAs, 177 lesions), plaque rupture (71 CSAs, 16 lesions) and ID healed rupture (284 CSAs, 26 lesions). In addition, we have found some IDHR with IDTCFA (124 CSAs, 6 lesions) and IDHR with plaque rupture (9 CSAs, 3 lesions) (**Table 2**). Eighty five percent of CSAs (8635/10146) did not fulfill criteria for any of the IVUS derived plaque morphologies mentioned previously.

### Prevalence and distribution of the IDTCFA

A total of 183 IDTCFAs were found, 69 (37.7%) in the LAD, 55 (30.0%) in the LCX and 59 (32.2%) in the RCA. The overall distribution along the vessels from ostial to distal segments is shown in (**figure 2**). Half of these IDTCFAs (95 IDTCFAs – 52.2%) were located within the first 3 cm of the arteries. However, when this analysis was performed for each vessel, the distribution of the IDTCFAs was different, being more proximally located in the LAD and LCX, whereas in the RCA they were more distally located (**figure 3**). The left anterior descending had higher probability to contain CSAs belonging to an IDTCFA compared to the

left circumflex (OR 2.96, 95%CI [1.65,5.32],  $p=0.0006$ ) and compared to the right coronary artery (OR 1.99, 95%CI [1.06,3.71],  $p=0.032$ ).

The mean of IDTCFA/cm in the culprit vessel of 0.7, while in the non-culprit vessel was 0.4,  $p=0.04$ .

### **Prevalence and distribution of plaque rupture and IVUS-derived healed rupture plaques**

There were a total of 19 plaque ruptures (ratio 9.6 IDTCFAs/1 plaque rupture) and 35 IDHR (ratio 5.2 IDTCFAs/1 IDHR plaque) in the studied population. Nine IDHR were found together with either IDTCFA (6) or PR (3).

The distribution of the plaque rupture followed the same pattern as the IDTCFA distribution, being more frequent in the proximal three centimeter of the coronary tree 11/19 (57.9%) (**Figure 2**). Ruptures were located in the LAD artery in 8 cases (42.1 %), in the LCx in 4 cases (21.0 %) and in the RCA in 7 cases (36.8 %).

The prevalence of IDHR plaques, as in the two previous plaque types was more frequent in the proximal 3 cm of the coronary arteries 20/35 (57.1%) (**Figure 2**). IDHR plaques were located in the LAD artery in 14 cases (40.0 %), in the LCx in 9 cases (25.7 %) and in the RCA in 12 cases (34.3 %).

### **Comparison of the composition and geometrical analysis of the IDTCFA, plaque rupture and IDHR plaques**

Although by definition the IDTCFA CSAs had to have plaque burden  $>40\%$  and NC  $>10\%$  an analysis of the overall composition of the CSAs (1146) with characteristics of IDTCFA was performed.

The necrotic core content was  $22.2\pm 9.3\%$  in the IDTCFA,  $13.0\pm 7.8\%$  in plaque ruptures and  $20.2\pm 7.1\%$  in the IDHR plaques,  $p<0.001$ . Whereas the calcified tissue content was as follows:  $6.5\pm 5.5\%$  in the IDTCFA,  $5.4\pm 6.4\%$  in plaque ruptures and  $9.1\pm 6.5\%$  in the IDHR plaques.  $P<0.001$ .

The vessel CSA in IDTCFAs was  $16.2\pm 6.1$  mm<sup>2</sup>, in plaque rupture  $19.0\pm 9.3$  mm<sup>2</sup> and in IDHR plaques was  $20.8\pm 6.5$  mm<sup>2</sup>,  $p=0.164$ . However, considering those CSAs with non-specific plaque morphology as reference (vessel CSA  $16.6\pm 6.9$  mm<sup>2</sup>), there was a significant increase in the vessel CSA in plaque ruptures,  $p=0.05$ . Lumen CSA was  $8.5\pm 3.9$  mm<sup>2</sup>,  $10.5\pm 6.5$  mm<sup>2</sup> and  $9.1\pm 3.7$  mm<sup>2</sup>, respectively,  $p<0.001$ . With respect to plaque CSA in IDTCFAs was  $7.6\pm 3.0$  mm<sup>2</sup>, in plaque rupture  $8.4\pm 4.0$  mm<sup>2</sup> and in IDHR plaques  $11.7\pm 4.2$  mm<sup>2</sup>  $p<0.001$ . Finally, plaque burden was significantly different, in IDTCFAs was  $47.6\pm 8.1\%$ , in plaque ruptures  $45.0\pm 9.2\%$  and in IDHR plaque was  $56.2\pm 9.7\%$ ,  $p<0.001$ .

**Figure 4.**

**Discussion**

The main findings of the present study can be summarized as follows: 1. In 35 patients (95 vessels and 10146 CSAs) 183 IDTCFAs, 19 plaque ruptures and 35 IDHR plaques were detected. The half of the IDTCFAs, plaque ruptures and IDHR plaques were located within the first 3 cm of the main coronary arteries. 2. There was similar content of necrotic core in CSAs belonging to the IDTCFA and to IDHR, but the content in these two was larger than in plaque ruptures. In this study the necrotic core in IDTCFAs 22.2% is in line with a recently published data by Virmani et al who reported 24% of necrotic core in TCFA<sup>23</sup>. 3. There was a gradient of disease among the identified plaque morphologies, with positive remodelling in the ones with larger amount of necrotic core.

**Rationale for IDTCFA definition.**

Vulnerable plaques have particular plaque morphology, which consists in a thin fibrous cap overlying a necrotic rich core; this is the current paradigm, however there is a myriad of limitations in detecting these morphologic characteristics *in vivo*.

First, at what point is a fibrous cap considered thin? Mann and Davies<sup>5</sup> reported in 1996 a study of 160 coronary plaques obtained from 31 subjects who died of sudden cardiac death and reported a mean cap thickness of 250 $\mu$ m (range 20 – 1140 $\mu$ m) in plaques that were types IV and V. Another pioneering study is by Burke et al<sup>4</sup>; they sectioned the coronary arteries every 3-mm intervals and only CSA with more than 50% of narrowing were analyzed in 41 plaque ruptures; these plaques had a mean fibrous cap thickness of 23 $\pm$ 19 $\mu$ m, and they also reported that 95% of the ruptures plaques have cap thickness <65 $\mu$ m. This value of cap thickness in plaque rupture has been used –maybe inappropriately- to define the thickness of the cap in thin-cap fibroatheroma<sup>16,23</sup>, even when TCFA have less necrotic core, less number of cholesterol clefts and less macrophage infiltration of the fibrous cap compared to ruptured

plaque described in these pathologic studies<sup>23</sup>. Pathologists may examine the pathological substrate at the advent of the clinical event responsible for it, but their technique faces the following technical issues: Tissue shrinkage occurs during tissue fixation<sup>24</sup>. Shrinkage of up to 60%, 15%, and 80% can occur during critical-point drying, free drying, and air drying, respectively. Furthermore, postmortem contraction of arteries is an additional confounding factor<sup>25</sup>.

On the other hand, *ex vivo* studies have used a higher cap thickness to consider vulnerability ( $> 200 \mu\text{m}$ )<sup>5,26,27</sup>. Indeed, our group identified – using the elastography technique in *ex-vivo*, pressurized fresh tissue human coronary arteries analyzed by histology subsequently - a mean cap thickness of 259  $\mu\text{m}$  and 363  $\mu\text{m}$  for “vulnerable” and “non-vulnerable” plaques respectively<sup>26</sup>. Considering that the axial resolution of IVUS-VH is 246  $\mu\text{m}$ , in this study we assumed that the absence of visible fibrous tissue overlying a necrotic core corresponded to a cap thickness of below 246  $\mu\text{m}$  and therefore used this absence of a visible fibrous cap on IVUS to define a fibrous cap as thin<sup>28</sup>.

Among the clinicians and the pathologists there is not yet a consensus about the critical threshold of cap thickness, which would reliably predict and herald an imminent plaque rupture. To some extent this is due to the absence of an *in vivo* technique able to provide an accurate and precise anatomical and histochemical assessment of the fibrous cap combined with the lack of natural history of such plaques. With this respect, optical coherence tomography (OCT) imaging might be an option in the near future. OCT allows high-resolution (axial resolution of 10  $\mu\text{m}$  and lateral resolution of 20  $\mu\text{m}$ ) imaging in biological systems. Accordingly, OCT is the technique with the highest capacity to allow *in-vivo*, real time visualization and measurement of a thin fibrous cap. On top of its reliability as a tool to measure the thickness of the cap *in vivo*, recent both post- mortem and *in vivo* studies have

shown that OCT is capable of evaluating the macrophage content of infiltrated fibrous caps<sup>29,30</sup>.

### **The potential for multi-focal instability process in patients with ACS**

Overall, in this study the first three centimeters in the coronary tree contained more than half of the IDTCFA, plaque ruptures and IDHR, which is in line with previous reports<sup>15,31</sup>. The mean of IDTCFA/cm in the culprit vessel was 0.7, while in the non-culprit vessel was 0.4,  $p=0.04$ ; most of the ruptures 13 (68.4%) were found in the non-culprit vessel, possibly due to the fact that the culprit lesion was stented before the imaging acquisition; the ratio of IDTCFA/plaque rupture was 9.6:1. In the same way, previous *in vivo* studies have established that a multifocal instability process is present in ACS<sup>18,32</sup>. Rioufol et al found at least one plaque rupture remote from the culprit lesion in 80 % of patients and from the culprit artery in 71 % of patients<sup>18</sup>. In addition, a high prevalence of rupture-prone lesions has been found throughout the coronary tree by means of angiography<sup>33</sup>, angioscopy<sup>32</sup>, IVUS<sup>18</sup> and palpography<sup>34</sup>.

### **Understanding the atherosclerosis process**

The present technique that assesses simultaneously plaque size and composition confirm the progressive degree and extension of tissue alteration in the different types of identifiable plaques by IVUS-VH: Non predefined plaque morphology (Intimal pathological thickening and fibroatheroma), IDTCFA, plaque rupture and IDHR, **figure 4**. The vessel CSA increases from 16.6 mm<sup>2</sup> in non predefined plaque morphology CSAs to 19.09 mm<sup>2</sup> in plaque ruptures and to 20.86 mm<sup>2</sup> in IDHR, suggesting a different degree of positive remodeling, which is also accompanied by a proportional increase in necrotic core in IDHR (**see figure 4**). This increase in necrotic core is putatively not seen in plaque rupture mainly because the content

of the cavity in a plaque rupture has been expelled from the plaque with subsequent embolization in to distal segment of the vessel.

The IVUS-derived healed ruptures had the largest content of calcified tissue among the different plaque morphologies, and similar content of necrotic core to IDTCFAs, but larger plaque CSA and plaque burden than IDTCFA. IDHR are chronic plaques that have undergone many rupturing events, which might have contributed to an increase in plaque burden and also in the content of calcified tissue<sup>15</sup>. Another interesting finding in IDHR is the colocalization of IDTCFA and plaque ruptures, which supports the paradigm that there is a continuous process of thinning, rupturing and healing in these plaques, which may be clinically silent. However, its appearance by IVUS-VH, although peculiar and of similar gross appearance to histological images, is not conclusively diagnostic of healed rupture, as it is by histology. Histology is able to fully characterize such plaques and provide detailed information of the different types of matrix in the fibrous cap either proteoglycan or collagen making possible to discriminate between old and new rupture sites.

This analysis makes us think that there exist a gradient of disease between the different types of plaques, which is feasible to follow over time. In other words, the natural history of the atherosclerotic plaques might be determined *in vivo*, if serial IVUS-VH analyses of specific region of interest are performed in longitudinal clinical studies.

### **Do we have any accurate imaging technique to assess plaque tissue composition?**

The optimal design for assessing the accuracy of a diagnostic tool has to be a prospective blind comparison between the new test and the reference test in a group of patients covering the spectrum of disease that is likely to be encountered in the use of the diagnostic test<sup>35</sup>. This has been done for IVUS-VH by Nair et al<sup>19</sup>. This validation of the intravascular ultrasound radiofrequency data analysis to predict coronary plaque composition was performed in 88

plaques in 51 LAD arteries, which were imaged *ex-vivo* using 30-MHz IVUS transducers, with accuracies ranging from 89.5 to 92.8% among the four tissue components. A second validation has been performed to test the current classification tree using the Eagle eye 20-MHz IVUS catheter with better results.

The second step using IVUS-VH is, then, to detect *in vivo* the pathological characteristics of atherosclerotic plaques<sup>14</sup>. In other words, the phenomenological description of *in vivo* anatomy has to ascertain that the description of IVUS-VH corresponds and at least does not negate what the pathologists have reported in the past.

Several studies are ongoing using this diagnostic tool to evaluate either the temporal change of such plaques over time in order to unravel their natural history or detect the treatment effect of some drugs. The former is the primary end point of the PROSPECT study and SPECIAL study and the latter is the IBIS-2 study primary end point.

## Limitations

As stated in our previous report<sup>14</sup>, the main findings of the study, IDTCFA and IDHR are only surrogates of the true histopathological findings and the lack of a direct comparison between IVUS-VH and histopathology of our “*in vivo*” patients render our observations to some extent only exploratory. The inferior axial resolution of IVUS-VH in comparison to histology remains a major handicap, but is partially compensated by the higher sampling rate of the ultrasonic approach when compared to the pathologic.

Some cases in the present study had extensive stenting of the culprit vessel, so that the vessel was not included in the analysis; in general, the more severe diseased part of the vessel was stented before IVUS acquisition eliminating potentially the analysis of the most pathological region of interest.

The length of the IVUS acquisition was different between the major coronary vessels. In particular, distal segments were less studied. Although an appropriate statistical analysis was performed to adjust for the differences in the number of CSAs studied along the vessels, the studied length could have affected the prevalence of the plaque morphologies.

## Conclusions

In patients with acute coronary syndromes IVUS-derived TCFA, plaque rupture and IDHR plaques had a higher prevalence in the first three centimeters in the main epicardial vessels. Furthermore, there is a gradient in plaque size and plaque composition between the different plaque morphologies.

### **Acknowledgements**

We thank Ma. De Lourdes Heredia García (MD) for her generous contribution to the study, and to Jurgen Ligthart for his support in IVUS analysis. Also to Evelyn Regar (MD, PhD) for critical review of the manuscript.

## References

1. Giroud D, Li JM, Urban P, Meier B, Rutishauer W. Relation of the site of acute myocardial infarction to the most severe coronary arterial stenosis at prior angiography. *Am J Cardiol.* 1992;69:729-32.
2. Little WC, Constantinescu M, Applegate RJ, Kutcher MA, Burrows MT, Kahl FR, Santamore WP. Can coronary angiography predict the site of a subsequent myocardial infarction in patients with mild-to-moderate coronary artery disease? *Circulation.* 1988;78:1157-66.
3. Spaulding CM, Joly LM, Rosenberg A, Monchi M, Weber SN, Dhainaut JF, Carli P. Immediate coronary angiography in survivors of out-of-hospital cardiac arrest. *N Engl J Med.* 1997;336:1629-33.
4. Burke AP, Farb A, Malcom GT, Liang YH, Smialek J, Virmani R. Coronary risk factors and plaque morphology in men with coronary disease who died suddenly. *N Engl J Med.* 1997;336:1276-82.
5. Mann JM, Davies MJ. Vulnerable plaque. Relation of characteristics to degree of stenosis in human coronary arteries. *Circulation.* 1996;94:928-31.
6. Falk E. Plaque rupture with severe pre-existing stenosis precipitating coronary thrombosis. Characteristics of coronary atherosclerotic plaques underlying fatal occlusive thrombi. *Br Heart J.* 1983;50:127-34.
7. Davies MJ, Thomas A. Thrombosis and acute coronary-artery lesions in sudden cardiac ischemic death. *N Engl J Med.* 1984;310:1137-40.
8. Kragel AH, Reddy SG, Wittes JT, Roberts WC. Morphometric analysis of the composition of atherosclerotic plaques in the four major epicardial coronary arteries in acute myocardial infarction and in sudden coronary death. *Circulation.* 1989;80:1747-56.
9. Rodriguez-Granillo GA ME, Valgimigli M, van Mieghem CAG, Regar E, de Feyter PJ, Serruys PW. Coronary plaque composition of non-culprit lesions assessed by in vivo intracoronary ultrasound radio frequency data analysis, is related to clinical presentation. *Am Heart J.* 2005;In press.
10. Virmani R, Kolodgie FD, Burke AP, Farb A, Schwartz SM. Lessons from sudden coronary death: a comprehensive morphological classification scheme for atherosclerotic lesions. *Arterioscler Thromb Vasc Biol.* 2000;20:1262-75.
11. Davies MJ, Richardson PD, Woolf N, Katz DR, Mann J. Risk of thrombosis in human atherosclerotic plaques: role of extracellular lipid, macrophage, and smooth muscle cell content. *Br Heart J.* 1993;69:377-81.
12. Schaar JA, Muller JE, Falk E, Virmani R, Fuster V, Serruys PW, Colombo A, Stefanadis C, Ward Casscells S, Moreno PR, Maseri A, van der Steen AF. Terminology for high-risk and vulnerable coronary artery plaques. Report of a meeting on the vulnerable plaque, June 17 and 18, 2003, Santorini, Greece. *Eur Heart J.* 2004;25:1077-82.
13. Loree HM, Kamm RD, Stringfellow RG, Lee RT. Effects of fibrous cap thickness on peak circumferential stress in model atherosclerotic vessels. *Circ Res.* 1992;71:850-8.
14. Rodriguez-Granillo GA, Garcia-Garcia HM, Mc Fadden EP, Valgimigli M, Aoki J, de Feyter P, Serruys PW. In vivo intravascular ultrasound-derived thin-cap fibroatheroma detection using ultrasound radiofrequency data analysis. *J Am Coll Cardiol.* 2005;46:2038-42.

15. Burke AP, Kolodgie FD, Farb A, Weber DK, Malcom GT, Smialek J, Virmani R. Healed plaque ruptures and sudden coronary death: evidence that subclinical rupture has a role in plaque progression. *Circulation*. 2001;103:934-40.
16. Virmani R, Burke AP, Kolodgie FD, Farb A. Vulnerable plaque: the pathology of unstable coronary lesions. *J Interv Cardiol*. 2002;15:439-46.
17. Ge J, Chirillo F, Schwedtmann J, Gorge G, Haude M, Baumgart D, Shah V, von Birgelen C, Sack S, Boudoulas H, Erbel R. Screening of ruptured plaques in patients with coronary artery disease by intravascular ultrasound. *Heart*. 1999;81:621-7.
18. Rioufol G, Finet G, Ginon I, Andre-Fouet X, Rossi R, Vialle E, Desjoyaux E, Convert G, Huret JF, Tabib A. Multiple atherosclerotic plaque rupture in acute coronary syndrome: a three-vessel intravascular ultrasound study. *Circulation*. 2002;106:804-8.
19. Nair A, Kuban BD, Tuzcu EM, Schoenhagen P, Nissen SE, Vince DG. Coronary plaque classification with intravascular ultrasound radiofrequency data analysis. *Circulation*. 2002;106:2200-6.
20. Karsen KF BE. Blind deconvolution of ultrasonic traces accounting for pulse variance. *IEEE Trans Ultrason Ferroelectr Freq Control*. 1999;46:564-573.
21. Zeger SL, Liang KY, Albert PS. Models for longitudinal data: a generalized estimating equation approach. *Biometrics*. 1988;44:1049-60.
22. Zeger SL, Liang KY. An overview of methods for the analysis of longitudinal data. *Stat Med*. 1992;11:1825-39.
23. Virmani R, Kolodgie FD, Burke AP, Finn AV, Gold HK, Tulenko TN, Wrenn SP, Narula J. Atherosclerotic plaque progression and vulnerability to rupture: angiogenesis as a source of intraplaque hemorrhage. *Arterioscler Thromb Vasc Biol*. 2005;25:2054-61.
24. MKW L. A critical appraisal of the effects of fixation, dehydration and embedding of cell volume. In: *The Science of Biological Specimen Preparation for Microscopy and Microanalysis*. Revel JP, Barnard T, Haggis GH (eds). *Scanning Electron Microscopy, AMF O'Hare*,. 1984;IL 60666:pp.61-70.
25. Fishbein MC, Siegel RJ. How big are coronary atherosclerotic plaques that rupture? *Circulation*. 1996;94:2662-6.
26. Schaar JA, De Korte CL, Mastik F, Strijder C, Pasterkamp G, Boersma E, Serruys PW, Van Der Steen AF. Characterizing vulnerable plaque features with intravascular elastography. *Circulation*. 2003;108:2636-41.
27. Felton CV, Crook D, Davies MJ, Oliver MF. Relation of plaque lipid composition and morphology to the stability of human aortic plaques. *Arterioscler Thromb Vasc Biol*. 1997;17:1337-45.
28. Nair A CD, Vince DG. Regularized Autoregressive Analysis of Intravascular Ultrasound Data: Improvement in Spatial Accuracy of Plaque Tissue Maps. *IEEE Transactions on Ultrasonics, Ferroelectrics, and Frequency Control*. 2004;51:420-431.
29. Tearney GJ, Yabushita H, Houser SL, Aretz HT, Jang IK, Schlendorf KH, Kauffman CR, Shishkov M, Halpern EF, Bouma BE. Quantification of macrophage content in atherosclerotic plaques by optical coherence tomography. *Circulation*. 2003;107:113-9.
30. MacNeill BD, Jang IK, Bouma BE, Iftimia N, Takano M, Yabushita H, Shishkov M, Kauffman CR, Houser SL, Aretz HT, DeJoseph D, Halpern EF, Tearney GJ. Focal and multi-focal plaque macrophage distributions in patients with acute and stable presentations of coronary artery disease. *J Am Coll Cardiol*. 2004;44:972-9.
31. von Birgelen C, Klinkhart W, Mintz GS, Papatheodorou A, Herrmann J, Baumgart D, Haude M, Wieneke H, Ge J, Erbel R. Plaque distribution and vascular remodeling of

- ruptured and nonruptured coronary plaques in the same vessel: an intravascular ultrasound study in vivo. *J Am Coll Cardiol.* 2001;37:1864-70.
32. Asakura M, Ueda Y, Yamaguchi O, Adachi T, Hirayama A, Hori M, Kodama K. Extensive development of vulnerable plaques as a pan-coronary process in patients with myocardial infarction: an angioscopic study. *J Am Coll Cardiol.* 2001;37:1284-8.
  33. Goldstein JA, Demetriou D, Grines CL, Pica M, Shoukfeh M, O'Neill WW. Multiple complex coronary plaques in patients with acute myocardial infarction. *N Engl J Med.* 2000;343:915-22.
  34. Schaar JA, Regar E, Mastik F, McFadden EP, Saia F, Disco C, de Korte CL, de Feyter PJ, van der Steen AF, Serruys PW. Incidence of high-strain patterns in human coronary arteries: assessment with three-dimensional intravascular palpography and correlation with clinical presentation. *Circulation.* 2004;109:2716-9.
  35. Lijmer JG, Mol BW, Heisterkamp S, Bossel GJ, Prins MH, van der Meulen JH, Bossuyt PM. Empirical evidence of design-related bias in studies of diagnostic tests. *Jama.* 1999;282:1061-6.

**Tables:**

<b>Table 1. Baseline characteristics, n=35</b>	
Age, yrs	52.4±9.4
Male %	82.9
Body mass index, kg/m <sup>2</sup>	27.6±4.1
Diabetes mellitus %	11.1
Hypertension %	30.6
Family history of CHD %	41.7
Current smoking %	66.7
Hypercholesterolemia %	41.7
Previous ACS %	17.1
Previous PCI %	5.7
<u>Clinical presentation %</u>	
Unstable angina/Non-ST-segment elevation MI	42.9
Acute MI	57.1
<u>Culprit vessel %, n=36</u>	
Left anterior descending	52.8
Left circumflex	22.2
Right coronary artery	25.0
<u>Study vessel %, n= 95</u>	
Left anterior descending	85.7
Left circumflex	97.1
Right coronary artery	88.6

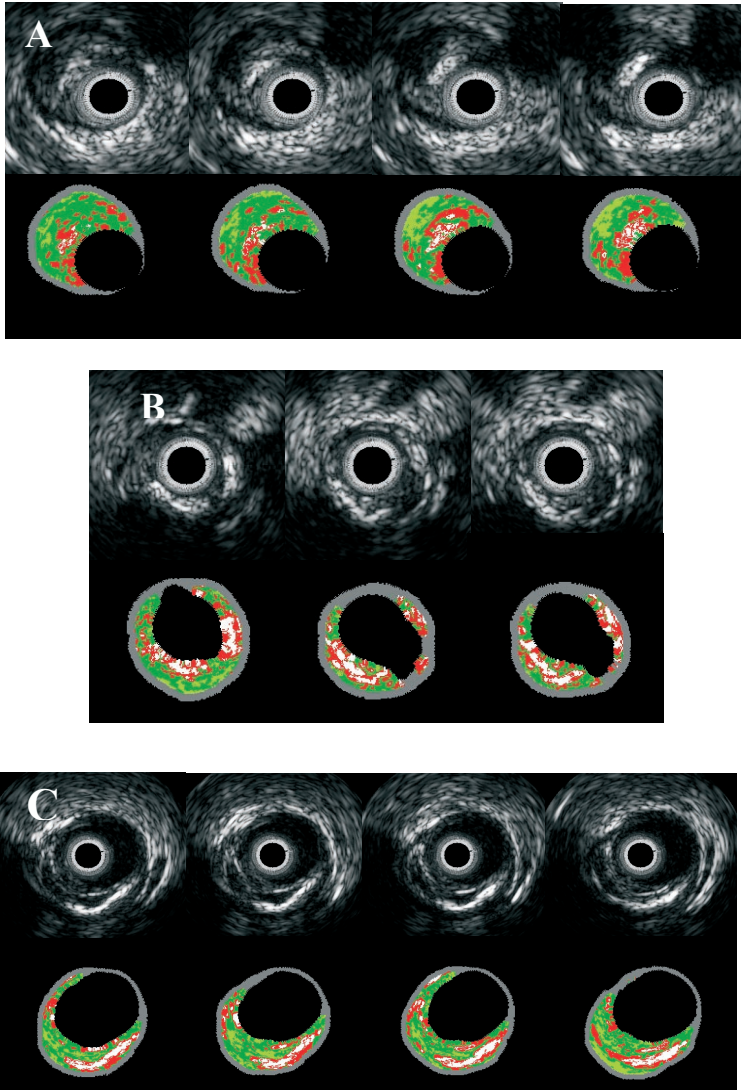
Table 2. Plaque composition and geometrical analysis in the different plaque morphologies												
	I. Non-predefined morphology, n=183 (10146 CSAs)		2. IDTCFA, n=183 (1146 CSAs)		3. Plaque rupture, n=19 (71CSAs)		4. IDHR, n=26 (284 CSAs)		5. IDHR with IDTCFA, n=6 (124 CSAs)		6. IDHR with plaque rupture, n=3 (9 CSAs)	
	Mean±SD	Mean±SD	Mean±SD	Mean±SD	Mean±SD	Mean±SD	Mean±SD	p value 4 vs.2,3	Mean±SD	Mean±SD	Mean±SD	p value*
<b>Compositional analysis</b>												
Calcium (mm2)	0.2±0.3	0.1±0.3	0.3±0.3	0.3±0.4	0.3±0.4	0.8±0.7	0.8±0.7	<0.001, <0.001	0.7±0.6	0.7±0.4	0.7±0.4	<0.001
Calcified (%)	3.6±5.8	2.5±5.3	6.5±5.5	5.4±6.4	5.4±6.4	9.1±6.5	9.1±6.5	0.02, 0.03	8.5±5.4	9.9±4.0	9.9±4.0	<0.001
Fibrous (mm2)	2.1±1.8	1.6±1.7	2.6±1.4	3.2±1.9	3.2±1.9	4.7±2.3	4.7±2.3	0.02, 0.02	4.1±2.1	3.5±0.8	3.5±0.8	0.008
Fibrous (%)	64.5±13.1	56.9±25.6	58.0±10.6	64.1±12.4	64.1±12.4	58.9±9.1	58.9±9.1	0.65, 0.49	54.6±8.8	52.3±6.1	52.3±6.1	0.545
Fibroliplid (mm2)	0.6±0.7	0.5±0.7	0.6±0.6	1.0±1.1	1.0±1.1	0.9±0.7	0.9±0.7	0.27, 0.27	0.8±0.6	1.0±0.4	1.0±0.4	0.272
Fibroliplid (%)	19.9±13.4	18.4±14.8	13.3±8.2	17.5±9.7	17.5±9.7	11.9±6.8	11.9±6.8	0.60, 0.20	11.0±6.7	14.0±4.3	14.0±4.3	<0.001
Necrotic core (mm2)	0.4±0.6	0.3±0.5	1.0±0.7	0.6±0.5	0.6±0.5	1.6±0.9	1.6±0.9	<0.001, <0.001	2.0±1.2	1.7±0.5	1.7±0.5	<0.001
Necrotic core (%)	12.0±10.8	8.7±9.9	22.2±9.3	13.0±7.8	13.0±7.8	20.2±7.1	20.2±7.1	0.89, 0.007	25.8±7.0	23.8±1.6	23.8±1.6	<0.001
<b>Geometrical analysis</b>												
Vessel CSA (mm2)	17.1±6.9	16.6±6.9	16.2±6.1	19.0±9.3	19.0±9.3	20.8±6.5	20.8±6.5	0.89, 0.21	19.5±6.5	20.4±4.2	20.4±4.2	0.164
Lumen CSA (mm2)	10.6±5.0	11.0±5.0	8.5±3.9	10.5±6.5	10.5±6.5	9.1±3.7	9.1±3.7	<0.001, <0.001	8.6±3.1	9.9±2.3	9.9±2.3	<0.001

Plaque CSA (mm <sup>2</sup> )	6.5±3.4	5.6±3.3	7.6±3.0	8.4±4.0	11.7±4.2	0.001,0.001	11.0±4.2	10.5±2.3	<0.001
Plaque Maximum Thickness (mm <sup>2</sup> )	1.0±0.3	0.8±0.4	1.2±0.3	1.2±0.4	1.5±0.3	<0.001,0.004	1.5±0.2	1.6±0.3	<0.001
Plaque Minimum Thickness (mm <sup>2</sup> )	0.1±0.2	0.1±0.1	0.2±0.2	0.2±0.2	0.4±0.3	0.24,0.52	0.3±0.2	0.2±0.2	0.012
Plaque Eccentricity (Min/Max)	0.1±0.1	0.1±0.1	0.2±0.2	0.1±0.1	0.2±0.2	0.50,0.94	0.2±0.2	0.1±0.1	0.362
Plaque burden (%)	38.3±12.4	33.5±12.9	47.6±8.1	45.0±9.2	56.2±9.7	<0.001, 0.009	56.0±9.1	51.8±6.7	<0.001

SD, standard deviation; CSA, cross sectional area; n, refers total number of lesions; IDTCFA, IVUS-derived thin cap fibroatheroma; PR, plaque rupture; IDHR, IVUS-derived healed rupture

\*Comparison between 1,2,3,4 and 5 plaque morphologies

Figure 1



Colour figures on pages 441-449

Figure 2.

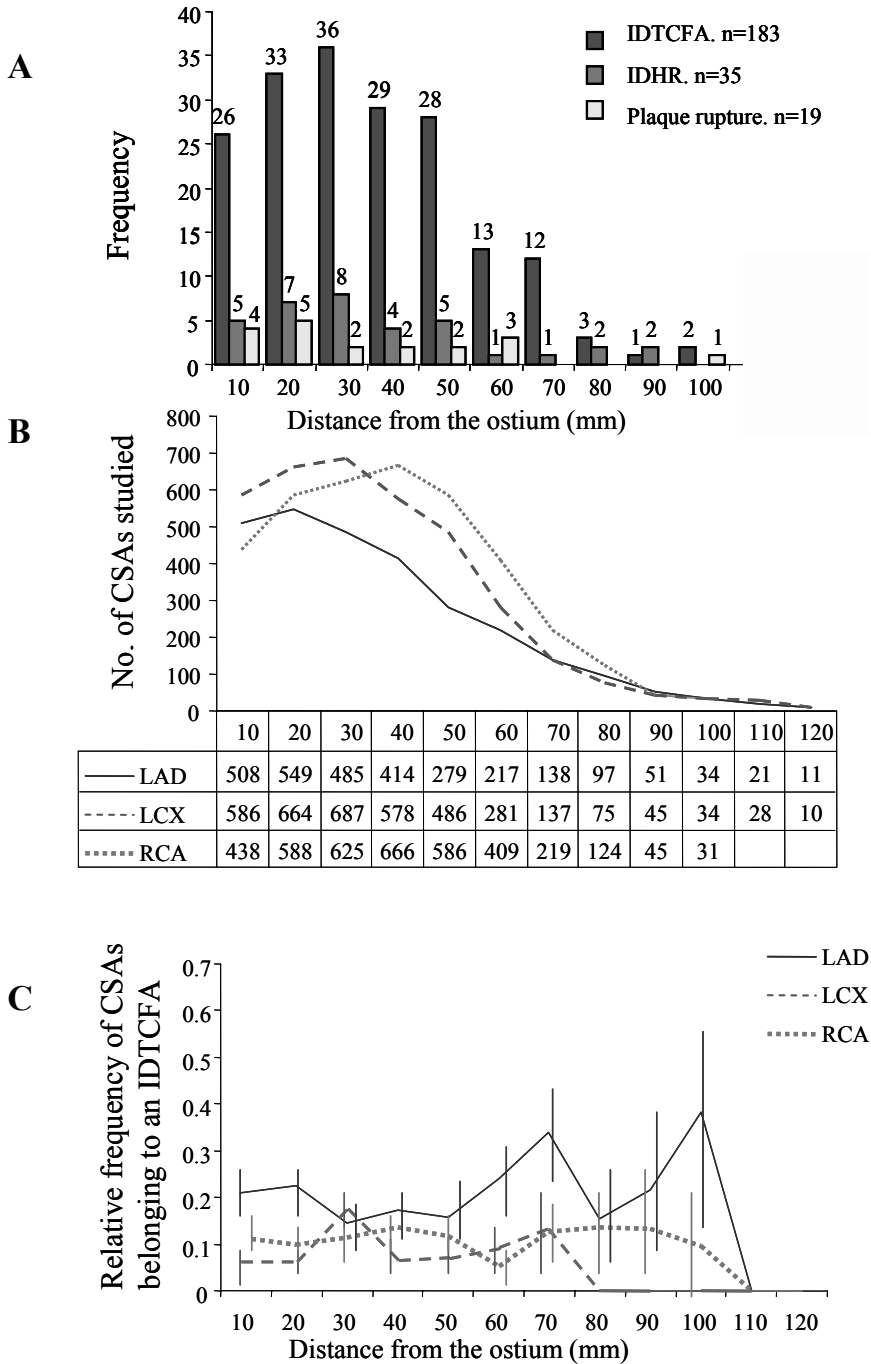
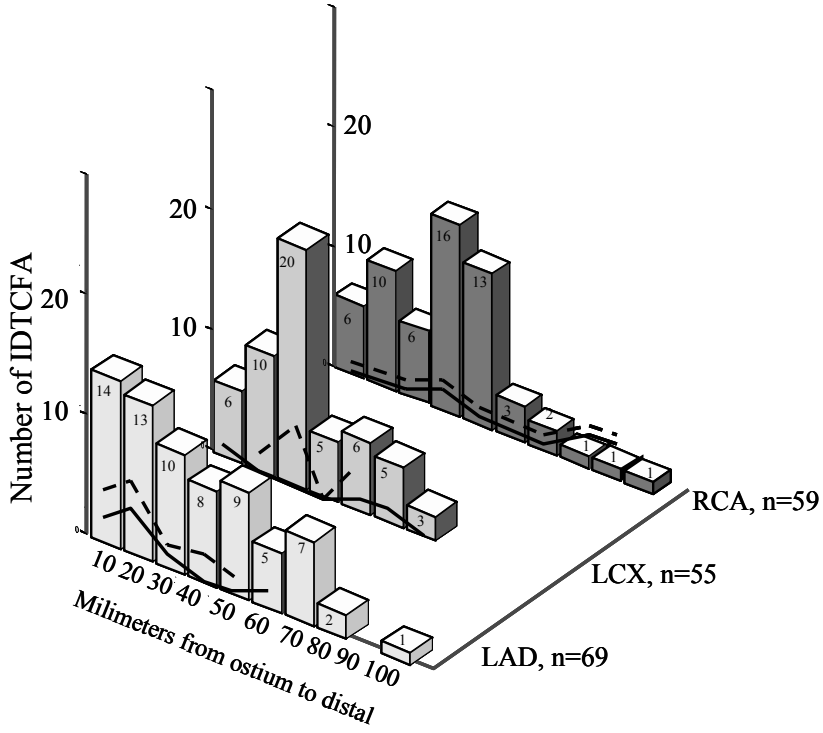
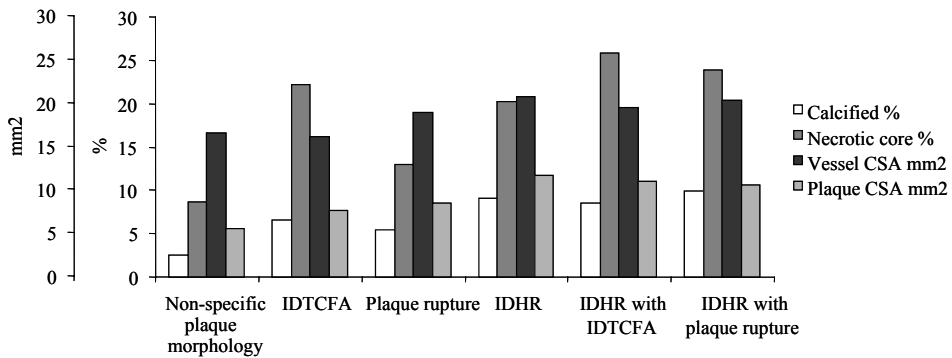


Figure 3.



**Figure 4**



## Figure legend

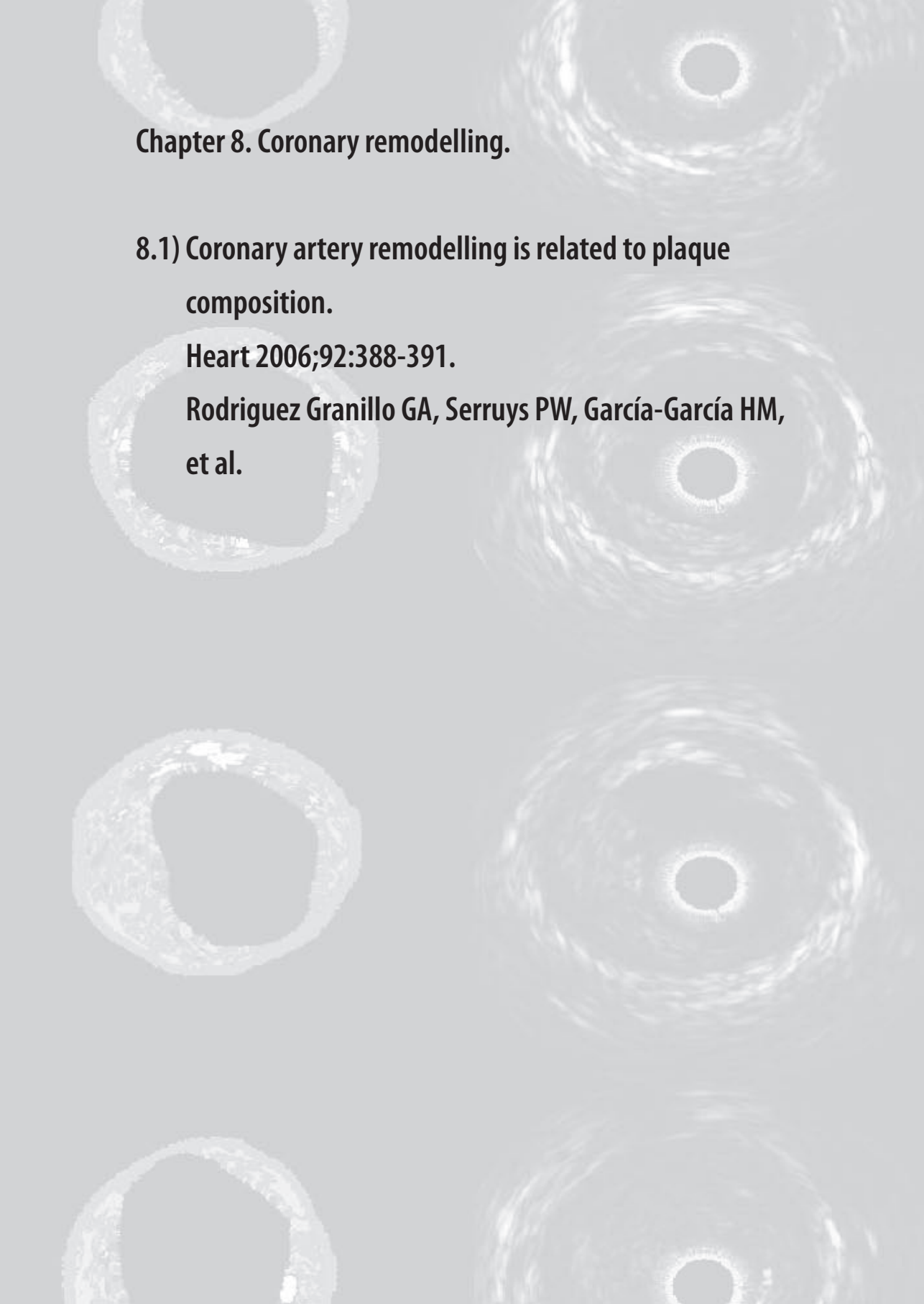
Figure 1. Panel A. an example of IVUS-derived thin cap fibroatheroma with its three components is shown: 1) plaque burden more than 40%. 2) necrotic core in direct contact with the lumen and 3) the % necrotic core in the cross sectional area is larger than 10%, all these characteristics are present in more than three consecutive frames. Panel B. a plaque rupture is seen between 3 and 5 o'clock. Lastly, panel C is showing an IVUS-derived healed rupture plaque, a multilayering appearance in the IVUS gray scale image is observed, which is characterized in different tissues in the corresponding IVUS-VH images.

Figure 2. In panel A, the distribution of IVUS-derived thin cap fibroatheroma (IDTCFA - blue bar), IVUS-derived healed rupture plaque (red bar) and plaque rupture (yellow bar) is depicted. Panel B represents the number of CSA (cross sectional area) studied in each segment. Lastly, panel C shows the density of CSAs belonging to an IDTCFA as a function from the distance to the ostium. IDHR, IVUS-derived healed rupture; LAD, left anterior descending; LCX, left circumflex; RCA, right coronary artery.

Figure 3. The 3-D bar graph depicts the IVUS-derived thin cap fibroatheroma (IDTCFA) distribution with respect to the vessel studied. The continuous line indicates the frequency of plaque rupture and the dashed line is to indicate the frequency of IVUS-derived healed rupture plaques. LAD, left anterior descending; LCX, left circumflex; RCA, right coronary artery.

Figure 4. This figure shows that there is a gradient of disease between the different plaque morphologies. The expansive vessel wall remodeling is greater when the necrotic core increases. CSA, cross sectional area; IDTCFA, IVUS-derived thin cap fibroatheroma; IDHR, IVUS-derived healed rupture.





**Chapter 8. Coronary remodelling.**

**8.1) Coronary artery remodelling is related to plaque composition.**

**Heart 2006;92:388-391.**

**Rodriguez Granillo GA, Serruys PW, García-García HM, et al.**



## BASIC RESEARCH

## Coronary artery remodelling is related to plaque composition

G A Rodriguez-Granillo, P W Serruys, H M Garcia-Garcia, J Aoki, M Valgimigli, C A G van Mieghem, E McFadden, P P T de Jaegere, P de Feyter



Heart 2006;92:388–391. doi: 10.1136/hrt.2004.057810

See end of article for authors' affiliations

Correspondence to:  
Professor  
Patrick W Serruys,  
Thoraxcentrum, Bd-406,  
Dr Malewaterplein 40,  
3015-GD Rotterdam,  
Netherlands; p.w.j.c.  
serruys@erasmusmc.nl

Accepted 13 June 2005  
Published Online First  
17 June 2005

**Objective:** To assess the potential relation between plaque composition and vascular remodelling by using spectral analysis of intravascular ultrasound (IVUS) radiofrequency data.

**Methods and results:** 41 coronary vessels with non-significant (< 50% diameter stenosis by angiography),  $\leq 20$  mm, non-ostial lesions located in non-culprit vessels underwent IVUS interrogation. IVUS radiofrequency data obtained with a 30 MHz catheter, were analysed with IVUS virtual histology software. A remodelling index (RI) was calculated and divided into three groups. Lesions with  $RI \geq 1.05$  were considered to have positive remodelling and lesions with  $RI \leq 0.95$  were considered to have negative remodelling. Lesions with  $RI \geq 1.05$  had a significantly larger lipid core than lesions with  $RI 0.96\text{--}1.04$  and  $RI \leq 0.95$  ( $22.1$  (6.3) v  $15.1$  (7.6) v  $6.6$  (6.9),  $p < 0.0001$ ). A positive correlation between lipid core and  $RI$  ( $r = 0.83$ ,  $p < 0.0001$ ) and an inverse correlation between fibrous tissue and  $RI$  ( $r = -0.45$ ,  $p = 0.003$ ) were also significant. All of the positively remodelled lesions were thin cap fibroatheroma or fibroatheromatous lesions, whereas negatively remodelled lesions had a more stable phenotype, with 64% having pathological intimal thickening, 29% being fibrocalcific lesions, and only 7% fibroatheromatous lesions ( $p < 0.0001$ ).

**Conclusions:** In this study, *in vivo* plaque composition and morphology assessed by spectral analysis of IVUS radiofrequency data were related to coronary artery remodelling.

Glagov *et al*<sup>1</sup> described vascular remodelling as a compensatory enlargement of the coronary arteries in response to an increase in plaque area. This concept has further evolved into a dynamic theory whereby vessels may also shrink in response to plaque growth.<sup>2</sup> This remodelling modality has been related to a more stable phenotype and clinical presentation,<sup>3–6</sup> whereas several studies showed an increase in inflammatory marker concentrations, larger lipid cores, and pronounced medial thinning in positively remodelled vessels.<sup>3–7</sup>

Recently, retrospective pathological studies have identified morphological and compositional features characteristic of plaque rupture.<sup>8–9</sup> This has led to a new classification of coronary lesions that more comprehensively illustrates plaque progression.<sup>9</sup>

Grey scale intravascular ultrasound (IVUS) is of limited value for identification of specific plaque components.<sup>10</sup> However, spectral analysis of IVUS radiofrequency data (IVUS virtual histology (VH)) has the potential to provide detailed quantitative information on plaque composition and has been validated in explanted human coronary segments.<sup>11</sup>

In this study, we sought to evaluate *in vivo* the relation between plaque composition and coronary artery remodelling by using ultrasound radiofrequency data analysis. In addition, we classified lesions with respect to their morphology and evaluated the potential relation between lesion type and coronary remodelling.<sup>9</sup>

## METHODS

## Patients

Forty one consecutive patients were retrospectively selected after screening a 54 patient database where non-culprit, angiographically non-obstructive (<50%),  $\leq 20$  mm, non-ostial lesions were investigated with IVUS. Patients were excluded if they had diffusely diseased vessels or lacked a

lesion occluding  $\geq 40\%$  of the cross sectional area (CSA). Lesions located in proximal and mid segments of a coronary artery were included in the study.

Major exclusion criteria were coronary anatomy that precluded safe IVUS examination of a suitable region of interest. Informed, written consent was obtained from all the patients.

## IVUS-VH acquisition and analysis

Details regarding the validation of the technique on explanted human coronary segments have previously been reported.<sup>11</sup> Briefly, IVUS-VH uses spectral analysis of IVUS radiofrequency data to construct tissue maps that classify plaque into four major components. In preliminary *in vitro* studies, four histological plaque components (fibrous, fibrolipidic, lipid core, and calcified) were correlated with a specific spectrum of the radiofrequency signal.<sup>11</sup> These plaque components were assigned colour codes. Calcified, fibrous, fibrolipidic, and lipid core regions were labelled white, green, greenish yellow, and red, respectively.

IVUS-VH data were acquired after intracoronary administration of nitrates by means of a continuous pullback (0.5 mm/s) with a commercially available mechanical sector scanner (Ultracross 2.9 French, 30 MHz catheter; Boston Scientific, Santa Clara, California, USA) by a dedicated IVUS-VH console (Volcano Therapeutics, Rancho Cordova, California, USA). The IVUS-VH data were stored on a CD ROM and sent to the imaging core laboratory for offline analysis. IVUS B mode images were reconstructed from the radiofrequency data by customised software (IVUSLab, Volcano Therapeutics). Subsequently, contours of both the lumen and the media-adventitia interface were detected

**Abbreviations:** CSA, cross sectional area; IVUS, intravascular ultrasound; MLA, minimum lumen area; RI, remodelling index; VH, virtual histology

manually. To account for catheter to catheter variability the acquired radiofrequency data were normalised by a technique known as “blind deconvolution”. Blind deconvolution is an iterative algorithm that deconvolves the catheter transfer function from the backscatter, thus enabling automated data normalisation.<sup>12,13</sup> Compositional data of the minimum lumen area (MLA) were expressed as percentage of the plaque CSA corresponding to each plaque component.

The MLA site and a reference site  $\leq 10$  mm proximal to the lesion were selected. There were no major side branches between the MLA and reference sites.

Remodelling was assessed by means of the remodelling index (RI), expressed as the external elastic membrane CSA (MLA site) divided by the reference external elastic membrane CSA as previously described.<sup>6,14,15</sup>

We defined positive remodelling as  $RI \geq 1.05$  and negative remodelling as  $RI \leq 0.95$ . Values in between were considered neutral (no remodelling). Percentage stenosis of the MLA site was defined as:

$$\text{vessel}_{\text{area}}^{\text{MLA}} - \text{lumen}_{\text{area}}^{\text{MLA}} / \text{vessel}_{\text{area}}^{\text{MLA}} \times 100.$$

In accordance with previously reported data, we classified lesions as pathological intimal thickening (mainly fibrotic-fibro-lipidic tissue, with the lipid core constituting 0% to  $\leq 3\%$  of the CSA), fibrocalcific lesions (featuring mainly fibrotic plaques, with some calcification and a lipid core occupying between 3–10% of the CSA), fibrous cap atheroma (lipid rich ( $> 10\%$  CSA) plaques with overlying fibrous tissue), and thin cap fibroatheroma (lipid-rich ( $> 10\%$  CSA) plaques with no overlying fibrous tissue). Figure 1 depicts examples of this classification. To classify lesions, these criteria had to be met in the MLA site plus the immediate distal and proximal cross sections. Since the axial resolution of this technique is between 100–150  $\mu\text{m}$ , we assumed that the absence of fibrous tissue overlying a lipid core suggested a cap thickness of below 100–150  $\mu\text{m}$ .<sup>16</sup>

### Statistical analysis

Discrete variables are presented as counts and percentages. Continuous variables are presented as mean (SD). We looked for correlations between the RI and both plaque components and percentage stenosis MLA by using Pearson correlation coefficients. Differences in means between groups were analysed by a two sided *t* test or by one way analysis of variance. We compared frequencies by means of the  $\chi^2$  test. A probability value of  $p < 0.05$  indicated significance. Data were statistically analysed with SPSS software version 11.5 (SPSS Inc, Chicago, Illinois, USA).

### RESULTS

Table 1 shows patient characteristics. Mean age was 55.9 (10.9). Most patients were men (83%) with a low prevalence of diabetes (7.3%). The study vessel was the right coronary artery in 19 patients (46.3%), the left anterior descending in 16 patients (39.0%), and the left circumflex in six patients (14.6%).

Lesions with positive remodelling had significantly larger lipid core percentages than lesions with no remodelling or negative remodelling (22.1 (6.3)% *v* 15.1 (7.6)% *v* 6.6 (6.9)%,

**Table 1** Baseline characteristics (n = 41)

Age (years)	55.9 (10.9)
Men	19 (83%)
Diabetes	3 (7.3%)
Hypertension*	12 (29.3%)
Current smoking	8 (19.5%)
Previous smoking	15 (36.6%)
Hypercholesterolaemia†	32 (78%)
Family history of coronary disease	19 (46.3%)
Previous myocardial infarction	6 (14.6%)
Artery	
Right coronary	19 (46.3%)
Left anterior descending	16 (39%)
Left circumflex	6 (14.6%)
Clinical presentation	
No angina‡	11 (26.8%)
Stable angina	14 (34.1%)
Unstable angina	6 (14.6%)
Myocardial infarction	10 (24.4%)

Data are mean (SD) or number (%).

\*Blood pressure  $\geq 160/95$  mm Hg or treatment for hypertension; †total cholesterol  $>5.57$  mmol/l or treatment for hypercholesterolemia; ‡these patients were studied at scheduled follow up angiography.

**Table 2** Geometrical and compositional data of the minimum lumen area (MLA) site

	Remodelling index			p Value
	$\leq 0.95$	0.96–1.04	$\geq 1.05$	
Number	29 (70.7%)	3 (7.3%)	9 (22%)	
Stenosis (%)	63.1 (7.5)	69.1 (8.6)	59.9 (9.9)	0.24
Calcific CSA (%)	1.38 (2.7)	2.07 (3.2)	1.67 (1.6)	0.88
Fibrous CSA (%)	68.6 (13.7)	62.9 (9.5)	58.1 (12.9)	0.13
Fibro-lipidic CSA (%)	23.5 (9.9)	19.9 (6.9)	18.1 (12.6)	0.39
Lipid core CSA (%)	6.6 (6.9)	15.1 (7.6)	22.1 (6.3)	$<0.0001$

Data are mean (SD).

Percentage stenosis of the MLA site is calculated as  $\text{vessel}_{\text{area}}^{\text{MLA}} - \text{lumen}_{\text{area}}^{\text{MLA}} / \text{vessel}_{\text{area}}^{\text{MLA}} \times 100$ . Remodelling index (RI) is defined as MLA of the external elastic membrane (EEM) cross sectional area (CSA)/reference EEM CSA.

respectively,  $p < 0.0001$ ). Negative remodelling lesions tended to have larger fibrous tissue percentages than lesions with no remodelling and positive remodelling (68.6 (13.7)% *v* 62.9 (9.5)% *v* 58.1 (12.9)%,  $p = 0.13$ ). Table 2 shows these results.

Table 3 presents Pearson correlation coefficients between the RI and both plaque components and percentage stenosis MLA. The positive correlation between the lipid core and the RI was significant ( $r = 0.83$ ,  $p < 0.0001$ ) (fig 2). Moreover, fibrous tissue was inversely correlated with the RI ( $r = -0.45$ ,  $p = 0.003$ ) (fig 3). Lastly, the percentage stenosis of the MLA and the RI were non-significantly inversely related ( $r = -0.27$ ,  $p = 0.09$ ).

With regard to lesion type, thin cap fibroatheroma and fibroatheromatous lesions comprised 100% of the positively

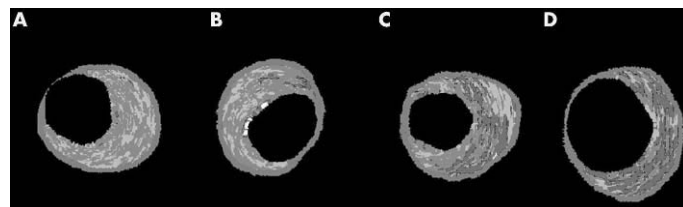


**Figure 1** Minimum lumen area (MLA) sites depicting the progression of atherosclerotic disease. The plaque components were assigned colour codes. Calcified, fibrous, fibro-lipidic, and lipid core regions were labelled white, green, greenish yellow, and red, respectively. MLA sites feature (A) pathological intimal thickening and (B) fibrocalcific, (C) fibroatheromatous, and (D) thin cap fibroatheromatous lesions.

**Table 3** Relations between remodelling index (RI), percentage stenosis of the MLA, and plaque composition of the MLA site

	RI	p Value
Lipid core CSA (%)	0.83	<0.0001
Fibrous CSA (%)	-0.45	0.003
Percentage stenosis MLA	-0.27	0.09
Calcific CSA (%)	0.12	0.47
Fibrolipidic CSA (%)	-0.17	0.28

Data are Pearson correlation coefficients.

remodelled lesions, whereas negative remodelling lesions had a more stable phenotype: 64% had pathological intimal thickening, 29% were fibrocalcific, and only 7% were fibroatheromatous lesions ( $p < 0.0001$ ) (fig 4).

## DISCUSSION

Recently, the relation between vascular remodelling and plaque composition was assessed by IVUS.<sup>17-20</sup> This catheter based diagnostic tool provides an accurate tomographic view of the coronary arteries and in vitro validation studies have shown a high correlation with histological samples.<sup>21-23</sup> Nevertheless, accurate plaque characterisation with visual interpretation of grey scale IVUS, particularly of lipid rich plaques, remains unresolved.<sup>22</sup> On the contrary, spectral analysis of IVUS radiofrequency data (IVUS-VH) has the potential to provide detailed quantitative information on plaque composition and has been validated in studies of explanted human coronary segments.<sup>11</sup>

The results of the present study confirm in vivo the relation between plaque composition and coronary remodelling. Lipid core size was significantly larger in positively remodelled coronary lesions than in those with vessel shrinkage. Furthermore, the fibrotic burden of the plaque was significantly and inversely correlated with the RI.

Lastly, positively remodelled lesions had a higher risk phenotype, with 56% of them being classified as thin cap fibroatheroma, the lesion type most likely to rupture.<sup>24</sup> On the contrary, negative remodelling was associated with a more stable phenotype: 64% had pathological intimal thickening and no evidence of thin cap fibroatheroma. Fibrocalcific lesions, a potential hallmark of the end stage of atheromatous plaque rupture or erosion with healing and calcification, were found in 29% of negatively remodelled lesions.<sup>9</sup>

Overall, these findings support the importance of the histological composition of atherosclerotic plaque as a major contributor to its fate as described by Davies *et al*,<sup>8</sup> who

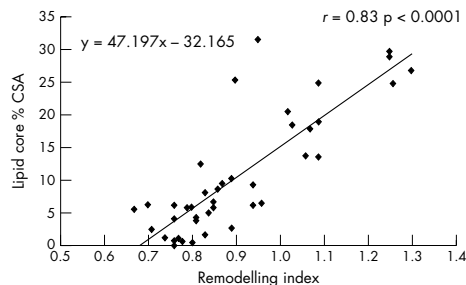


**Figure 2** Linear regression plot showing positive correlation between lipid core and remodelling. CSA, cross sectional area. Remodelling index is defined as MLA of the external elastic membrane (EEM) CSA/reference EEM CSA.

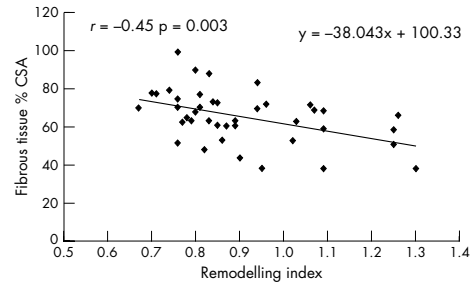


**Figure 3** Linear regression plot showing an inverse relation between fibrous tissue and remodelling.

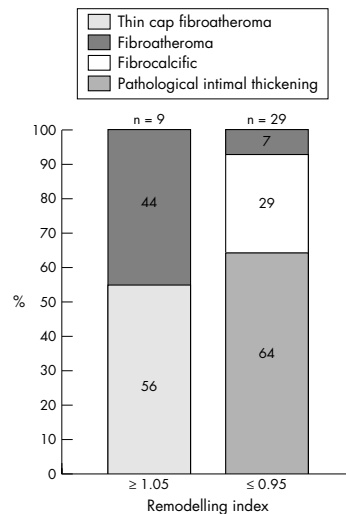


**Figure 4** Bar graphs illustrating the lesion type frequencies according to remodelling modality. All of the high risk plaques had positive remodelling (56% were thin cap fibroatheroma and 44% fibroatheromatous lesions). Negatively remodelled lesions had a more stable phenotype, with 93% being low risk lesions and only 7% fibroatheromatous lesions.

showed that plaques with a large lipid core harbour a higher risk of rupture and subsequent thrombosis. The lipid core is a source of metalloproteinases, a group of proteolytic enzymes that have an important function in vascular remodelling mechanisms and whose most common locations are foam cell accumulation areas and shoulder regions.<sup>25, 26</sup>

Conversely, negatively remodelled vessels consisted predominantly of fibrotic plaques. In addition, in line with previously reported data, negatively remodelled lesions had a higher degree of stenosis.<sup>2, 17, 27</sup> The findings of this study are consistent with previous pathological findings in patients after sudden death.<sup>5</sup> However, such postmortem studies do not have implications in the natural history of high risk plaques and thus in the clinical outcome of patients. On the contrary, we strongly believe that the identification of these high risk plaques in vivo may provide more insights into the prognosis and natural history of such lesions and into the

effect of conventional and emerging anti-atherosclerotic pharmacological interventions.

### Limitations

Since this was a cross sectional study and atherosclerosis is usually a diffuse disease, finding a fully non-diseased reference site is not guaranteed. Therefore, we cannot rule out the early presence of remodelling in the reference site. In addition, this was a pilot study that needs further confirmation in a larger population. Moreover, classifying lesion types by this technique lacks the accuracy of histopathological classification, since resolution is inferior. Nevertheless, a significant relation was found by using this arbitrary classification. Although histopathological classification remains the ideal, spectral analysis of IVUS radiofrequency data has the potential to provide real time accurate information regarding tissue characterisation and plaque morphology.

### Conclusions

In this small clinical study, in vivo plaque composition and morphology assessed by spectral analysis of IVUS radiofrequency data were related to coronary artery remodelling, supporting the role of plaque composition in the mechanisms of vessel remodelling. Lipid core size was significantly larger in positively remodelled coronary lesions than in those with vessel shrinkage. Furthermore, the fibrotic burden of the plaque was significantly and inversely correlated with the RI. The findings of this study are consistent with previous pathological findings. However, postmortem studies do not have the potential to provide prospective information about the natural history of high risk plaques. On the contrary, we strongly believe that the identification of these high risk plaques in vivo may provide more insights into the prognosis and natural history of such lesions and into the effect of conventional and emerging anti-atherosclerotic pharmacological interventions.

### Authors' affiliations

G A Rodriguez-Granillo, P W Serruys, H M Garcia-Garcia, J Aoki, M Valgimigli, C A G van Mieghem, E McFadden, P P T de Jaegere, P de Feyter, Thoraxcentre, Erasmus Medical Centre, Rotterdam, the Netherlands

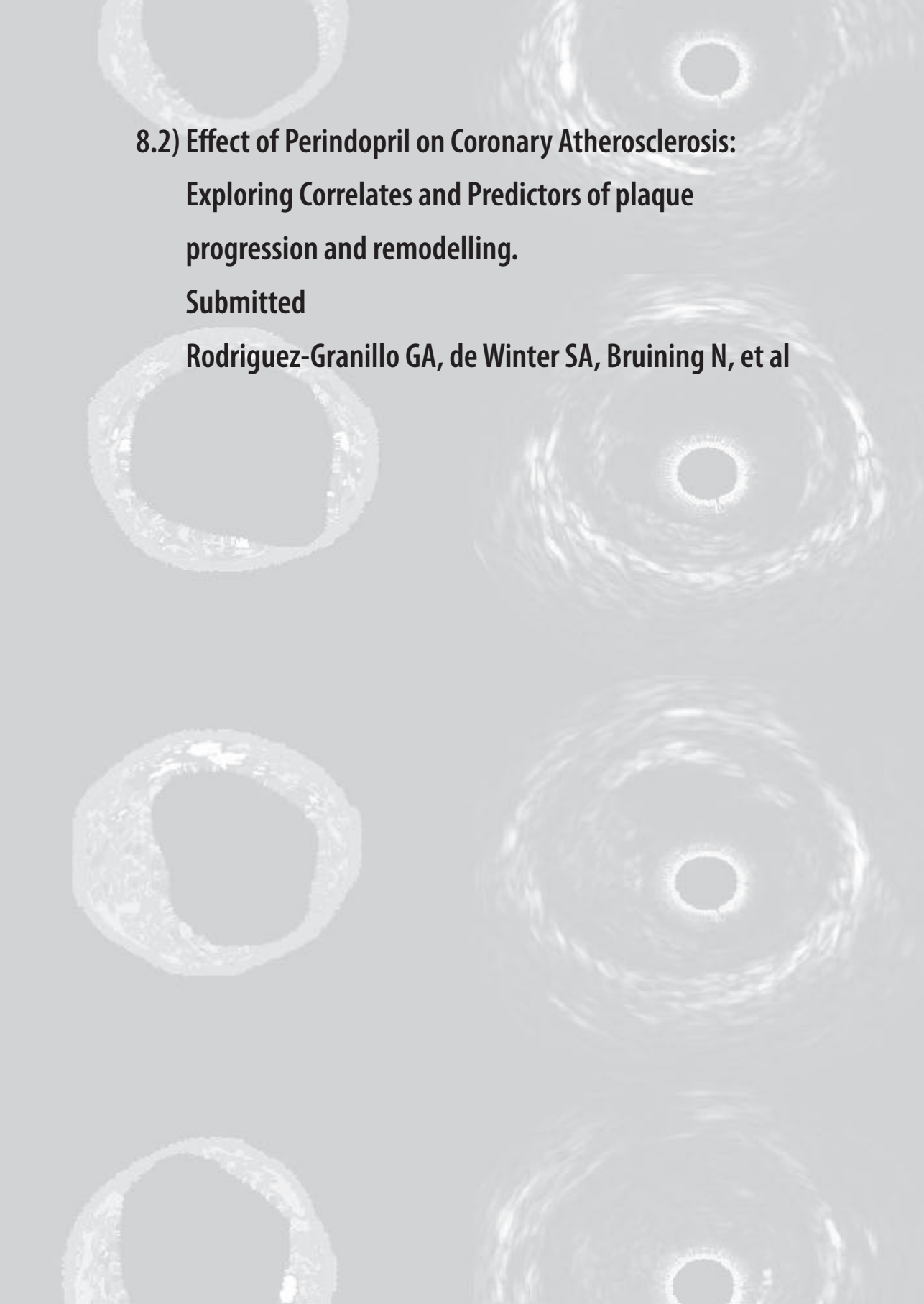
No author has any conflict of interest.

All authors have approved the final manuscript, which has not been published and is not under consideration elsewhere.

### REFERENCES

- Glagov S, Weisenberg E, Zarins CK, et al. Compensatory enlargement of human atherosclerotic coronary arteries. *N Engl J Med* 1987;**316**:1371–5.
- Pasterkamp G, Wensing PJ, Post MJ, et al. Paradoxical arterial wall shrinkage may contribute to luminal narrowing of human atherosclerotic femoral arteries. *Circulation* 1995;**91**:1444–9.

- Smits PC, Pasterkamp G, Quarles van Ufford MA, et al. Coronary artery disease: arterial remodelling and clinical presentation. *Heart* 1999;**82**:461–4.
- Pasterkamp G, Schoneveld AH, van der Wal AC, et al. Relation of arterial geometry to luminal narrowing and histologic markers for plaque vulnerability: the remodeling paradox. *J Am Coll Cardiol* 1998;**32**:655–62.
- Varnava AM, Mills PG, Davies MJ. Relationship between coronary artery remodeling and plaque vulnerability. *Circulation* 2002;**105**:939–43.
- Nakamura M, Nishikawa H, Mukai S, et al. Impact of coronary artery remodeling on clinical presentation of coronary artery disease: an intravascular ultrasound study. *J Am Coll Cardiol* 2001;**37**:63–9.
- Burke AP, Kolodgie FD, Farb A, et al. Morphological predictors of arterial remodeling in coronary atherosclerosis. *Circulation* 2002;**105**:297–303.
- Davies MJ, Richardson PD, Woolf N, et al. Risk of thrombosis in human atherosclerotic plaques: role of extracellular lipid, macrophage, and smooth muscle cell content. *Br Heart J* 1993;**69**:377–81.
- Virmani R, Kolodgie FD, Burke AP, et al. Lessons from sudden coronary death: a comprehensive morphological classification scheme for atherosclerotic lesions. *Arterioscler Thromb Vasc Biol* 2000;**20**:1262–75.
- Peters RJ, Kok WE, Havenith MG, et al. Histopathologic validation of intracoronary ultrasound imaging. *J Am Soc Echocardiogr* 1994;**7**:230–41.
- Nair A, Kuban BD, Tuzcu EM, et al. Coronary plaque classification with intravascular ultrasound radiofrequency data analysis. *Circulation* 2002;**106**:2200–6.
- Käresen K. Deconvolution of sparse spike trains by iterated window maximization. *IEEE Trans Signal Process* 1997;**45**:1173–83.
- Käresen KF, Bøvikken E. Blind deconvolution of ultrasonic traces accounting for pulse variance. *IEEE Trans Ultrason Ferroelectr Freq Control* 1999;**46**:564–73.
- Schoenhagen P, Ziada KM, Kapadia SR, et al. Extent and direction of arterial remodeling in stable versus unstable coronary syndromes: an intravascular ultrasound study. *Circulation* 2000;**101**:598–603.
- Gussenhoven EJ, Gesselschop JH, van Lankeven W, et al. Remodeling of atherosclerotic coronary arteries assessed with intravascular ultrasound in vitro. *Am J Cardiol* 1997;**79**:699–702.
- Nair A, Calvetti D, Vince DG. Regularized autoregressive analysis of intravascular ultrasound data: improvement in spatial accuracy of plaque tissue maps. *IEEE Trans Ultrason, Ferroelectr Freq Control* 2004;**51**:420–31.
- Mintz GS, Kent KM, Pichard AD, et al. Contribution of inadequate arterial remodeling to the development of focal coronary artery stenoses: an intravascular ultrasound study. *Circulation* 1997;**95**:1791–8.
- Tauth J, Pinnow E, Sullebarger JT, et al. Predictors of coronary arterial remodeling patterns in patients with myocardial ischemia. *Am J Cardiol* 1997;**80**:1352–5.
- Sabate M, Kay IP, de Feyter PJ, et al. Remodeling of atherosclerotic coronary arteries varies in relation to location and composition of plaque. *Am J Cardiol* 1999;**84**:135–40.
- Fuessl RT, Kranenberg E, Kiausch U, et al. Vascular remodeling in atherosclerotic coronary arteries is affected by plaque composition. *Coron Artery Dis* 2001;**12**:91–7.
- Tobis JM, Mallory JA, Gessert J, et al. Intravascular ultrasound cross-sectional arterial imaging before and after balloon angioplasty in vitro. *Circulation* 1989;**80**:873–82.
- Potkin BN, Bartorelli AL, Gessert JM, et al. Coronary artery imaging with intravascular high-frequency ultrasound. *Circulation* 1990;**81**:1575–85.
- Nishimura RA, Edwards WD, Warnes CA, et al. Intravascular ultrasound imaging: in vitro validation and pathologic correlation. *J Am Coll Cardiol* 1990;**16**:145–54.
- Farb A, Tang AL, Burke AP, et al. Sudden coronary death: frequency of active coronary lesions, inactive coronary lesions, and myocardial infarction. *Circulation* 1995;**92**:1701–9.
- Galis ZS, Khatri JJ. Matrix metalloproteinases in vascular remodeling and atherogenesis: the good, the bad, and the ugly. *Circ Res* 2002;**90**:251–62.
- Galis ZS, Sukhova GK, Lark MW, et al. Increased expression of matrix metalloproteinases and matrix degrading activity in vulnerable regions of human atherosclerotic plaques. *J Clin Invest* 1994;**94**:2493–503.
- Pasterkamp G, Wensing PJ, Hillen B, et al. Impact of local atherosclerotic remodeling on the calculation of percent luminal narrowing. *Am J Cardiol* 1997;**79**:402–5.



**8.2) Effect of Perindopril on Coronary Atherosclerosis:  
Exploring Correlates and Predictors of plaque  
progression and remodelling.**

**Submitted**

**Rodriguez-Granillo GA, de Winter SA, Bruining N, et al**



**Protective Effect of Perindopril on Coronary Remodelling:  
Insights from a multicenter, randomized study.**

**Gastón A. Rodríguez-Granillo MD, Sebastiaan de Winter BSc, Nico Bruining PhD,  
Jurgen M.R. Ligthart BSc, Héctor M. García-García MD, Marco Valgimigli MD, Pim  
J. De Feyter MD, PhD**

From the Department of interventional Cardiology, Thoraxcenter, Erasmus MC, Rotterdam,  
The Netherlands.

**Objective:** This study sought to evaluate the effect of perindopril in coronary remodelling.

**Background:** ACE-inhibitors have shown to be effective in reversing vascular remodelling in the peripheral circulation.

**Methods:** In this double-blind, multicenter trial patients without clinical evidence of heart failure were randomized to perindopril 8mg/d for at least 3 years and IVUS investigation was performed at both time-points. Positive and negative remodelling was defined as an increase (positive remodelling) or decrease (negative remodelling) decrease in mean vessel cross-sectional area (CSA) > 2 standard deviation of the mean intra-observer difference

**Results:** A total of 118 matched evaluable IVUS (711 matched 5 mm segments) were available at follow-up. After a median follow-up of 3.0 (interquartile range 1.9, 4.1) years, there was no significant difference in the change of plaque cross-sectional area (CSA) between perindopril (360 segments) and placebo (351 segments) groups,  $p=0.27$ . Conversely, the change in vessel CSA was significantly different between groups (perindopril  $-0.18\pm 2.4$  mm<sup>2</sup> vs. placebo  $0.19\pm 2.4$ ,  $p=0.04$ ). Negative remodelling, defined as occurred more frequently in the perindopril than in the placebo group [124 (34.4) vs. 86 (24.5),  $p=0.01$ ], and the placebo group showed a larger mean remodelling index than the perindopril group ( $1.03\pm 0.2$  vs.  $1.00\pm 0.2$ ,  $p=0.06$ ). The temporal change in vessel dimensions assessed by the remodelling index was significantly correlated with the change in plaque dimensions ( $r=0.48$ ,  $p<0.0001$ ).

**Conclusion:** In this study, long-term administration of perindopril was associated with a better vascular remodelling profile without affecting the lumen.

## Introduction

By preventing encroachment of the lumen and hence coronary flow, outward (positive) remodelling of coronary vessels was initially regarded as beneficial<sup>1</sup>. Notwithstanding, several studies have shown increased levels of inflammatory markers, larger lipid cores and pronounced medial thinning in positive remodelled vessels; being all factors related to the tendency of plaques to undergo rupture<sup>2-5</sup>. In addition, a number of landmark studies have established that most atherothrombotic events have non-flow limiting lesions as substrate<sup>6,7</sup>. Angiotensin-converting enzyme (ACE) inhibitors have demonstrated their efficacy in reducing mortality in both high and low risk patients<sup>8,9</sup>. In parallel, ACE-inhibitors inhibit progressive left ventricular remodelling, a critical factor that determines life expectancy<sup>10,11</sup>. More recently, ACE-inhibitors have shown to be effective in reversing vascular remodelling in the peripheral circulation<sup>12,13</sup>.

Atherosclerosis is a highly dynamic and multifocal disease, and coronary remodelling occurs diffusely within a vessel, even in seemingly healthy references<sup>14,15</sup>. Accordingly, longitudinal studies have been recognized as the gold-standard for remodelling assessment<sup>15,16</sup>.

The PERindopril's Prospective Effect on Coronary aTherosclerosis by IntraVascular ultrasound Evaluation (PERSPECTIVE) trial evaluated the effect of long-term administration of perindopril on coronary plaque progression as assessed by angiography and intravascular ultrasound (IVUS) and demonstrated that the clinical benefit of ACE inhibitors cannot be attributed to their effect on plaque size. We performed a post-hoc analysis of the PERSPECTIVE study to assess the effect of perindopril in coronary remodelling based on the hypothesis that ACE-inhibitors' effect on vascular remodelling might partially explain the clinical benefit obtained despite the lack of effect on lumen and plaque size. In addition, we evaluated the effect of perindopril on a surrogate of plaque composition.

## Methods

The EUROPA was a multicenter, randomized, double-blind, placebo-controlled study that evaluated the effect of perindopril on prevention of cardiovascular events in patients with coronary artery disease on 12,218 patients. PERSPECTIVE was a sub-study of the EUROPA trial that sought to explore the effect of perindopril on atherosclerosis progression/regression using coronary angiography and intravascular ultrasound (IVUS).

The methodology of the EUROPA trial have been extensively described elsewhere <sup>9</sup>. In brief, patients were eligible if they were aged  $\geq 18$  years, without clinical evidence of heart failure and with evidence of coronary heart disease documented by previous myocardial infarction ( $>3$  months before screening), percutaneous or surgical coronary revascularization ( $> 6$  months before screening), or angiographic evidence of at least 70% narrowing of one or more major coronary arteries.

In addition, for the IVUS sub-analysis patients required anatomically suitable vessels for the angiography/IVUS sub-study.

In a run-in period, enrolled patients received 4 mg/d oral perindopril for 2 weeks in addition to their normal medication, followed by 8 mg/d for 2 weeks if the initial dose was tolerated. At the end of the run-in period, patients were randomly assigned to perindopril 8mg/d or placebo for at least 3 years.

The institutional ethics committees of all participating centers approved the study protocol and informed written consent was obtained from all patients.

### **Intravascular Ultrasound acquisition**

IVUS was acquired using 20, 30 and 40 MHz imaging catheters following coronary angiography. The catheter was advanced distal to an anatomically identifiable landmark, allowing the evaluation of a segment of at least 30 mm. Cine runs, before and during contrast injection, were performed to define the position of the IVUS catheter before the pullback was

started. Using an automated pullback device, the transducer was withdrawn at a continuous speed of 0.5 mm/s until the ostium. IVUS data was acquired after the intracoronary administration of nitroglycerin and stored on S-VHS videotape. The videotapes were digitized on a computer system, transformed into the DICOM medical image standard and stored on an IVUS Picture Archiving and Communications System (PACS). After a 3-year follow-up period, patients underwent repeat catheterization and IVUS examination of the same region of interest (ROI) using an identical frequency IVUS imaging catheter.

### **Intravascular Ultrasound analysis**

Quantitative coronary ultrasound (QCU) analysis was performed by an independent core laboratory (Cardialysis BV, Rotterdam, The Netherlands) using validated semi-automatic contour detection software (Curad, version 3.1, Wijk bij Duurstede, The Netherlands). The IntelliGate™ image-based gating method was applied to eliminate catheter-induced image artefacts, by retrospectively selecting end-diastolic frames<sup>17</sup>.

In order to avoid the significant impact of interobserver variability<sup>18</sup>, contour detection was performed by a single experienced IVUS analyst who was blinded for the randomization allocation and time-point of the study. Longitudinal and cross-sectional views were used to determine the contours.

The contours of the external elastic membrane (EEM) and the lumen-intima interface enclosed an area that was defined as the coronary plaque plus media area. Plaque burden (PB) was defined as  $[(EEM_{\text{area}} - \text{Lumen}_{\text{area}}) / EEM_{\text{area}}] \times 100$ . Direct measurements (lumen and vessel CSA) were also determined. In the baseline IVUS study, a region of interest (ROI) was identified using landmarks such as side-branches and the coronary ostium. At 3-year follow-up, the same matched ROI was identified using the original landmarks to determine the lumen and vessel dimensional changes over time and consequently to calculate the impact on plaque

changes. In order to accurately assess the remodelling pattern within a vessel, the ROIs were subsequently also subdivided in matched 5 mm sub-segments independent of the length of the pullback in the original IVUS study. Segments with a PB <10% were excluded.

Coronary remodelling was assessed using continuous and categorical variables. The remodelling index (RI) was defined as  $EEM_{\text{area}}$  at follow-up divided by the  $EEM_{\text{area}}$  at baseline.

Finally, we evaluated the number of segments presenting positive remodelling (defined as a relative increase in vessel CSA larger than two standard deviations from the mean relative intra-observer difference) and negative remodelling (defined as a relative temporal decrease larger than two standard deviations from the mean relative intra-observer difference).

### **IVUS tissue characterization**

We used a computer-aided, in-house developed gray-scale value analysis program for plaque characterization<sup>19</sup>. Using the mean gray level of the adventitia as a threshold, plaque was classified as more (hyperechogenic) or less (hypoechoic) bright in relation to the adventitia. Upper and calcified tissue was defined as tissue that has a mean gray value higher than the mean adventitial intensity plus two times its standard deviation. The echogenicity software calculated the distribution of the gray-values present in the adventitia layer. When this distribution was not normal (severely calcified vessels), the data was excluded for IVUS analysis since the acoustic shadowing obscures the media-adventitia interface thus introducing serious inaccuracy in the contour detection.

### **Statistical analysis**

Discrete variables are presented as counts and percentages. Continuous variables are presented as means  $\pm$  standard deviation or medians (interquartile range) as indicated. Pearson correlation coefficients were performed in order to estimate correlations between

Differences between groups were assessed by paired and unpaired Student's *t* test when applicable. Fisher's exact test was used for categorical variables. A two-sided P value <0.05 was required for statistical significance. All analyses were performed using SPSS version 11.5 software (Chicago, Illinois, USA).

## Results

### Study population

A total of 118 patients who had completed IVUS investigation at baseline and follow-up were included in the study. Populations were well matched (Table 1). The mean age was  $56.6 \pm 8.9$ , 100 (83.3 %) were male, 11 (9.2 %) had diabetes mellitus, 59 (49.2 %) had history of prior myocardial infarction and 30 (25.0 %) had hypertension. With regards to concomitant baseline medication, 115 (95.8 %) were on aspirin, 67 (55.8 %) were receiving beta-blockers, 32 (26.7 %) were receiving nitrates, 46 (38.3 %) were on calcium channel blocker therapy and 91 (75.8 %) were on lipid-lowering therapy. Coronary risk factors and baseline blood pressure were well balanced between groups (table 1).

At a median follow-up of 3.0 (range 1.9, 4.1) years, the rate of adverse events was minimal. Coronary revascularization [2 (3.3%) vs. 4 (6.9 %),  $p= 0.38$ ] and acute myocardial infarction [1 (1.7 %) vs. 3 (5.2 %),  $p= 0.30$ ] rates were not statistically significant between perindopril and placebo groups. No deaths, strokes or admissions for heart failure were reported.

### IVUS intra-observer variability

Fifteen cases (678 frames) were re-analyzed by the same observer yielding minor differences between the 2 measurements. Relative differences for lumen, vessel and plaque CSA were  $1.43 \pm 4.2$  %,  $1.01 \pm 3.4$  % and  $3.50 \pm 8.5$  % respectively. In addition, lumen ( $r^2= 0.99$ ,  $p < 0.0001$ ), vessel ( $r^2= 0.99$ ,  $p < 0.0001$ ) and plaque ( $r^2= 0.87$ ,  $p < 0.0001$ ) CSA measurements were highly correlated.

### Intravascular Ultrasound measurements

due to sub-optimal IVUS quality (due to severely calcified vessels, severe artefacts or absence of clear anatomical landmarks). Quantitative IVUS results are shown in table 2.

In the perindopril group, the temporal change in mean plaque CSA compared with baseline was  $-0.15 \pm 1.7 \text{ mm}^2$  ( $p = 0.11$ ). For the placebo group, the change was  $-0.01 \pm 1.7 \text{ mm}^2$  ( $p = 0.95$ ), with a  $p$  value of 0.27 between groups. The temporal change in mean vessel CSA was  $-0.18 \pm 2.4 \text{ mm}^2$  in the perindopril group and  $0.19 \pm 2.4 \text{ mm}^2$  in the placebo group, with a  $p$  value of 0.04 between groups. With regards to plaque hypoechogenicity, no significant difference was present between groups (perindopril  $-0.30 \pm 1.7 \text{ mm}^2$  vs. placebo  $-0.11 \pm 1.7 \text{ mm}^2$ ,  $p = 0.12$ ). Both groups showed a highly heterogeneous remodelling pattern along the coronary segments (figure 1). Nevertheless, the placebo group showed a larger mean RI than the perindopril group ( $1.03 \pm 0.2$  vs.  $1.00 \pm 0.2$ ,  $p = 0.06$ ). Of interest, negative remodelling was present in 124 (34.4 %) segments in the perindopril group and in 86 (24.5 %) segments in the placebo group. Conversely, positive remodelling was observed in 102 (28.3 %) segments in the perindopril group and in 110 (31.3 %) segments in the placebo group, with a significant (chi-square) difference between groups ( $p = 0.02$ ). These changes are depicted in table 3.

### **Linear regression analysis**

The temporal change in vessel dimensions assessed by the RI was significantly correlated with the change in plaque dimensions ( $r = 0.48$ ,  $p < 0.0001$ ). The degree of such correlation was higher in the perindopril group than in the placebo group ( $r = 0.58$ ,  $p < 0.0001$  vs.  $r = 0.36$ ,  $p < 0.0001$ ). As expected, the change in hypoechogenic content was highly related to the change in plaque ( $r = 0.95$ ,  $p < 0.001$ ) and vessel ( $r = 0.45$ ,  $p < 0.001$ ) CSA.

A strong relationship was found between changes in plaque and changes in vessel size (perindopril  $r = 0.62$ ,  $p < 0.0001$ ; and placebo  $r = 0.35$ ,  $p < 0.0001$ ). Such relation became stronger with increasing levels of PB at baseline (figure 2 a). In parallel, the placebo group

showed a significant inverse relationship between the change in plaque and lumen CSA that was stronger at earlier stages of the disease (figure 2 b).

## Discussion

The importance of coronary remodelling as a factor that has a major impact in the maintenance of lumen dimensions has been undoubtedly established<sup>1</sup>. Recently, several investigators have linked this originally deemed protective compensatory response of the vessel to the presence of a more unstable phenotype and plaque rupture<sup>2-5, 20</sup>. Conversely, a paradoxical negative remodelling pattern has been associated with a more stable clinical presentation and lesion phenotype<sup>2,21</sup>. To date, most studies have assessed coronary remodelling at a single time-point and focally within the vessel, using proximal and distal references as surrogates of vessel size before it becomes diseased. However, coronary atherosclerosis is commonly a diffuse disease and finding a healthy reference is hard to attain. Moreover, such diffuse pattern implies a heterogeneous behaviour of atherosclerotic disease within a single vessel. Yet, although the assessment of coronary remodelling using serial determinations is highly required it has been scarcely exploited<sup>14,22</sup>.

The findings of the present longitudinal *in-vivo* study offer several insights towards the better understanding of the long-term effect that ACE-inhibitors have on coronary atherosclerosis.

Overall, no significant differences regarding the temporal changes in plaque and lumen size were present between patients assigned to perindopril and placebo. Nevertheless, there was a significant difference between groups regarding the change in vessel size.

Negative remodelling occurred more frequently in the perindopril group than the placebo group. It is noteworthy though, that as a result of a parallel non-significant plaque regression effect, this slight constrictive effect had no impact on the lumen size. Similarly, the placebo group showed a larger mean remodelling index than the perindopril group and a trend towards an enlargement of the coronaries with no change in plaque size, resulting in a non-significant increase of the lumen area.

The observed effect of perindopril on vessel remodelling might potentially be owed to the reduction in metalloproteinase levels induced by ACE-inhibitors<sup>23</sup>, since these enzymes have a central role in the physiopathology of vessel remodelling<sup>15</sup>.

### **Contrasts with histopathology**

Coronary remodelling has been long believed a vessel response to accommodate increasing burden of plaque without affecting the lumen patency<sup>1</sup>. In his study, Glagov made a static assessment of the correlation between plaque and vessel size in explanted left main coronary arteries. Our results are in line with the study of Glagov with respect to the fact that coronary remodelling is a phenomenon that occurs since very early stages of the disease and is mainly driven by the progressive accumulation of plaque within the vessel wall. Nevertheless, in our study, the strenghtness of the relationship between changes in plaque CSA and changes in lumen CSA decreased with increasing levels of stenosis at baseline (figure 1). Conversely, Glagov established that the positive correlation between vessel size and plaque size was stronger in sections with stenoses  $\leq 20\%$  and that an abrupt drop in lumen area was evident only after the obstruction reached 30 to 40%<sup>1</sup>. In brief, our results contradict Glagov's in the sense that the control group showed higher remodelling capacity (and lumen maintenance) when the baseline severity of the disease was higher. It is noteworthy, however, that Glagov's seminal investigation was performed in the left main coronary artery, a coronary segment with a more benign plaque composition<sup>24</sup>, while it has previously been shown that the remodelling pattern of plaques is highly related to the underlying composition of plaques<sup>5</sup>. Finally, it is worth mentioning that, although there was no significant difference between groups regarding the change of hypoechogenic tissue, the administration of perindopril induced a significant beneficial shift in the echogenicity of plaques compared to baseline.

The findings of the present study confirm that coronary atherosclerosis is a highly dynamic disease. Moreover, the constrictive, yet lumen-preserving, effect shown has previously been

associated with a more stable phenotype of lesions and better clinical presentation thus our results might contribute to explain the clinical-atheroclerotic burden divergent outcomes observed with ACE-inhibitors.

### **Study limitations**

A substantial number of vessels were excluded from the analysis due to sub-optimal image quality, principally due to the presence of severely calcified vessels. Nevertheless, we want to emphasize that this was essential to have a highly accurate assessment of the vessel contours. Larger studies in higher risk patients using IVUS as primary endpoint might conclusively determine the role of ACE inhibitors in atherosclerosis natural history. Only a single coronary artery was assessed by IVUS potentially being not representative of the entire coronary tree. Moreover, different IVUS catheters and consoles were used over a 3-year period, potentially influencing the results. Nevertheless, individual serial assessments were performed using identical IVUS catheters. To correct for any dimensional discrepancies, the results of the 30 MHz catheter were adjusted using a previously reported mathematical algorithm<sup>25</sup>.

### **Conclusion**

Our findings enforce the relationship between plaque progression and coronary remodelling. In this study, perindopril was related to a better vascular remodelling profile. Overall, our results might partially explain the discordance between the clinical benefit obtained with perindopril inhibitors and the absence of significant impact in plaque size.

## References

1. Glagov S, Weisenberg E, Zarins CK, Stankunavicius R, Kolettis GJ. Compensatory enlargement of human atherosclerotic coronary arteries. *N Engl J Med* 1987;316:1371-5.
2. Pasterkamp G, Schoneveld AH, van der Wal AC, Haudenschild CC, Clarijs RJ, Becker AE, Hillen B, Borst C. Relation of arterial geometry to luminal narrowing and histologic markers for plaque vulnerability: the remodeling paradox. *J Am Coll Cardiol* 1998;32:655-62.
3. Varnava AM, Mills PG, Davies MJ. Relationship between coronary artery remodeling and plaque vulnerability. *Circulation* 2002;105:939-43.
4. Burke AP, Kolodgie FD, Farb A, Weber D, Virmani R. Morphological predictors of arterial remodeling in coronary atherosclerosis. *Circulation* 2002;105:297-303.
5. Rodriguez-Granillo GA, Serruys PW, Garcia-Garcia HM, Aoki J, Valgimigli M, van Mieghem CA, Mc Fadden E, de Jaegere PP, de Feyter P. Coronary artery remodelling is related to plaque composition. *Heart* 2005.
6. Ambrose JA, Tannenbaum MA, Alexopoulos D, Hjemdahl-Monsen CE, Leavy J, Weiss M, Borrico S, Gorlin R, Fuster V. Angiographic progression of coronary artery disease and the development of myocardial infarction. *J Am Coll Cardiol* 1988;12:56-62.
7. Little WC, Constantinescu M, Applegate RJ, Kutcher MA, Burrows MT, Kahl FR, Santamore WP. Can coronary angiography predict the site of a subsequent myocardial infarction in patients with mild-to-moderate coronary artery disease? *Circulation* 1988;78:1157-66.
8. Yusuf S, Sleight P, Pogue J, Bosch J, Davies R, Dagenais G. Effects of an angiotensin-converting-enzyme inhibitor, ramipril, on cardiovascular events in high-risk patients. The Heart Outcomes Prevention Evaluation Study Investigators. *N Engl J Med* 2000;342:145-53.
9. Fox KM. Efficacy of perindopril in reduction of cardiovascular events among patients with stable coronary artery disease: randomised, double-blind, placebo-controlled, multicentre trial (the EUROPA study). *Lancet* 2003;362:782-8.
10. Effects of enalapril on mortality in severe congestive heart failure. Results of the Cooperative North Scandinavian Enalapril Survival Study (CONSENSUS). The CONSENSUS Trial Study Group. *N Engl J Med* 1987;316:1429-35.
11. Effect of enalapril on survival in patients with reduced left ventricular ejection fractions and congestive heart failure. The SOLVD Investigators. *N Engl J Med* 1991;325:293-302.
12. De Ciuceis C, Amiri F, Brassard P, Endemann DH, Touyz RM, Schiffrin EL. Reduced vascular remodeling, endothelial dysfunction, and oxidative stress in resistance arteries of angiotensin II-infused macrophage colony-stimulating factor-deficient mice: evidence for a role in inflammation in angiotensin-induced vascular injury. *Arterioscler Thromb Vasc Biol* 2005;25:2106-13.
13. Dupuis F, Atkinson J, Liminana P, Chillon JM. Comparative effects of the angiotensin II receptor blocker, telmisartan, and the angiotensin-converting enzyme inhibitor, ramipril, on cerebrovascular structure in spontaneously hypertensive rats. *J Hypertens* 2005;23:1061-6.
14. Hibi K, Ward MR, Honda Y, Suzuki T, Jeremias A, Okura H, Hassan AH, Maehara A, Yeung AC, Pasterkamp G, Fitzgerald PJ, Yock PG. Impact of different definitions on the interpretation of coronary remodeling determined by intravascular ultrasound. *Catheter Cardiovasc Interv* 2005;65:233-239.
15. Ward MR, Pasterkamp G, Yeung AC, Borst C. Arterial remodeling. Mechanisms and clinical implications. *Circulation* 2000;102:1186-91.
16. Hibi K, Ward MR, Honda Y, Suzuki T, Jeremias A, Okura H, Hassan AH, Maehara A, Yeung AC, Pasterkamp G, Fitzgerald PJ, Yock PG. Impact of different definitions on the interpretation of coronary remodeling determined by intravascular ultrasound. *Catheter Cardiovasc Interv* 2005.

17. De Winter SA, Hamers R, Degertekin M, Tanabe K, Lemos PA, Serruys PW, Roelandt JR, Bruining N. Retrospective image-based gating of intracoronary ultrasound images for improved quantitative analysis: the intelligate method. *Catheter Cardiovasc Interv* 2004;61:84-94.
18. Hausmann D, Lundkvist AJ, Friedrich GJ, Mullen WL, Fitzgerald PJ, Yock PG. Intracoronary ultrasound imaging: intraobserver and interobserver variability of morphometric measurements. *Am Heart J* 1994;128:674-80.
19. de Winter SA, Heller I, Hamers R, de Feyter PJ, Serruys PWC, Roelandt JR, Bruining N. Computer assisted three-dimensional plaque characterization in ultracoronary ultrasound studies. *Computers in Cardiology* 2003;30:73-76.
20. von Birgelen C, Klinkhart W, Mintz GS, Papatheodorou A, Herrmann J, Baumgart D, Haude M, Wieneke H, Ge J, Erbel R. Plaque distribution and vascular remodeling of ruptured and nonruptured coronary plaques in the same vessel: an intravascular ultrasound study in vivo. *J Am Coll Cardiol* 2001;37:1864-70.
21. Smits PC, Pasterkamp G, Quarles van Ufford MA, Eefting FD, Stella PR, de Jaegere PP, Borst C. Coronary artery disease: arterial remodelling and clinical presentation. *Heart* 1999;82:461-4.
22. Von Birgelen C, Hartmann M, Mintz GS, Bose D, Eggebrecht H, Gossel M, Neumann T, Baumgart D, Wieneke H, Schmermund A, Haude M, Erbel R. Spectrum of remodeling behavior observed with serial long-term ( $\geq 12$  months) follow-up intravascular ultrasound studies in left main coronary arteries. *Am J Cardiol* 2004;93:1107-13.
23. Schieffer B, Bunte C, Witte J, Hoepfer K, Boger RH, Schwedhelm E, Drexler H. Comparative effects of AT1-antagonism and angiotensin-converting enzyme inhibition on markers of inflammation and platelet aggregation in patients with coronary artery disease. *J Am Coll Cardiol* 2004;44:362-8.
24. Valgimigli M, Rodriguez-Granillo GA, Garcia-Garcia HM, Vaina S, De Jaegere P, De Feyter P, Serruys PW. Plaque composition in the left main stem mimics the distal but not the proximal tract of the left coronary artery: influence of clinical presentation, length of the left main trunk, lipid profile and systemic levels of C-reactive protein. *J Am Coll Cardiol*. In press.
25. Bruining N, Hamers R, Teo TJ, de Feijter PJ, Serruys PW, Roelandt JR. Adjustment method for mechanical Boston scientific corporation 30 MHz intravascular ultrasound catheters connected to a Clearview console. Mechanical 30 MHz IVUS catheter adjustment. *Int J Cardiovasc Imaging* 2004;20:83-91.

**Table 1:** Study population

	Perindopril (n= 60)	Placebo (n=58)	p value
<b>Baseline characteristics</b>			
Age (yrs±SD)	57.9±9.2	55.2±8.5	0.09
Male sex	50 (83.3)	50 (86.2)	0.67
Diabetes	4 (6.7)	7 (12.1)	0.32
Hypertension*	12 (20.0)	18 (31.0)	0.17
Smoking	15 (25.0)	11 (19.0)	0.43
Hypercholesterolemia	51 (85.0)	47 (81.0)	0.57
Family history of CHD	16 (26.7)	17 (29.3)	0.75
Previous MI	32 (53.3)	27 (46.6)	0.47
Previous PTCA	53 (88.3)	57 (98.3)	0.03
Previous CABG	1 (1.7)	0 (0.0)	0.33
Systolic BP	130.6±14.2	132.4±13.6	0.48
Diastolic BP	78.9±6.9	79.2±7.5	0.78
BMI	26.5±2.6	27.4±3.1	0.91
Heart rate	68.5±10.1	65.7±7.1	0.09
<b>Anginal status</b>			
CCS I	50 (83.3)	45 (77.6)	0.44
CCS II	8 (13.3)	12 (20.7)	0.29
CCS III	2 (3.3)	1 (1.7)	0.58
CCS IV	0 (0.0)	0 (0.0)	NA
<b>Other medications</b>			
Platelet inhibitors	58 (96.7)	57 (98.3)	0.58
Beta-blockers	32 (53.3)	35 (60.3)	0.45
Nitrates	20 (33.3)	12 (20.7)	0.13
Ca-channel blockers	26 (43.3)	20 (34.5)	0.33
Lipid lowering agents	46 (76.7)	45 (77.6)	0.91
<b>At 3-year follow-up</b>			
Systolic BP	130.2±16.5	131.1±14.1	0.66
Diastolic BP	76.5±8.5	79.0±8.4	0.12
<b>Other medications</b>			
Platelet inhibitors	53 (88.3)	52 (89.7)	0.82
Beta-blockers	37 (61.7)	36 (62.1)	0.97
Nitrates	12 (20.0)	11 (19.0)	0.89
Ca-channel blockers	20 (33.3)	21 (36.2)	0.75
Lipid lowering agents	52 (86.7)	47 (81.0)	0.41

Hypercholesterolemia defined as cholesterol >6.5 mmol/L or on lipid-lowering therapy.

Blood pressure (BP) >160/95 mmHg or receiving antihypertensive treatment.

CCS refers to Canadian Cardiovascular Society.

**Table 2.** Intravascular ultrasound quantitative analysis

Mean cross-sectional area (mm <sup>2</sup> )	Treatment (n=360)	Placebo (n=351)	p value
<b>Vessel</b>			
Baseline	15.60±5.0	15.82±5.1	0.57
Follow-up	15.42±4.8	16.01±4.9	
Nominal change	-0.18±2.4	0.19±2.4	0.04
Relative change	-1.18±17.0	1.20±15.7	
P value compared with baseline	0.15	0.13	
<b>Lumen</b>			
Baseline	9.21±3.9	9.76±4.1	0.07
Follow-up	9.17±3.9	9.96±4.4	
Nominal change	-0.04±1.9	0.20±2.4	0.14
Relative change	-0.42±23.4	2.03±26.6	
P value compared with baseline	0.70	0.12	
<b>Plaque</b>			
Baseline	6.39±2.8	6.06±2.6	0.10
Follow-up	6.25±2.7	6.05±2.8	
Nominal change	-0.15±1.7	-0.01±1.7	0.27
Relative change	-2.28±28.2	-0.09±32.6	
P value compared with baseline	0.11	0.95	
<b>Plaque burden (%)</b>			
Baseline	41.29±13.1	39.01±12.8	0.02
Follow-up	40.81±13.4	38.55±14.3	
Nominal change	-0.48±8.1	-0.47±9.5	0.98
Relative change	-1.16±22.9	-1.20±29.9	
P value compared with baseline	0.26	0.36	
<b>Hyoechoogenicity</b>			
Baseline	5.87±2.6	5.66±2.4	0.29
Follow-up	5.56±2.4	5.56±2.5	
Nominal change	-0.30±1.7	-0.11±1.7	0.12
Relative change	-5.19±32.2	-1.90±34.5	
P value compared with baseline	0.001	0.23	

**Table 3.** Frequency of 5 mm segments with different remodelling patterns with perindopril and placebo respectively.

	Perindopril, n (%) (n= 360)	Placebo, n (%) (n=351)	p value ( $\chi^2$ across group)
<b>Neutral</b>	134 (37.2)	155 (44.2)	0.01
<b>Positive remodelling</b>	102 (28.3)	110 (31.3)	
<b>Negative remodelling</b>	124 (34.4)	86 (24.5)	

### **Figure legends**

Figure 1. Linear regression scatter plot between the remodelling index and the difference in plaque cross-sectional area (CSA).

Figure 2. Bar graphs illustrating: A) the relationship between  $\Delta$  plaque size and  $\Delta$  vessel size and B) the relationship between  $\Delta$  plaque size and  $\Delta$  lumen size.

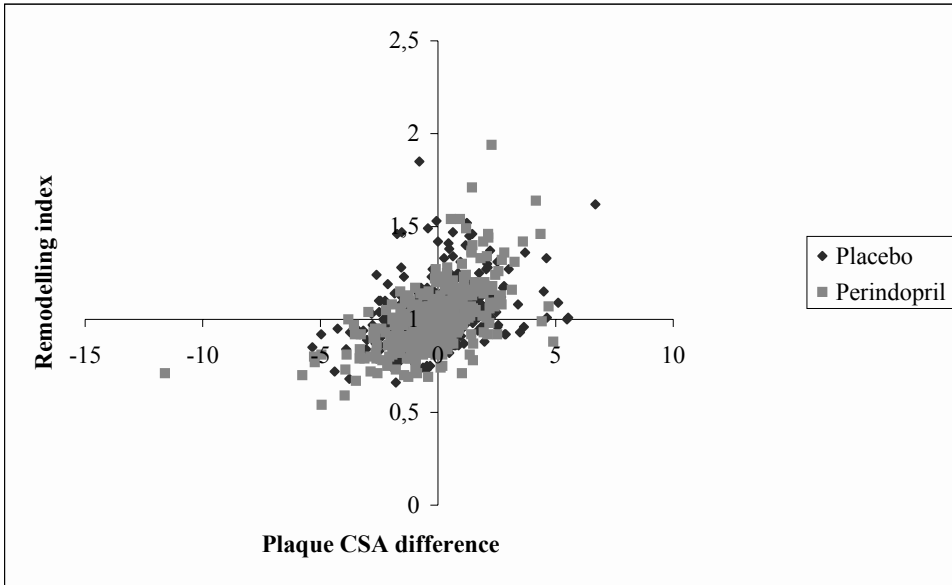
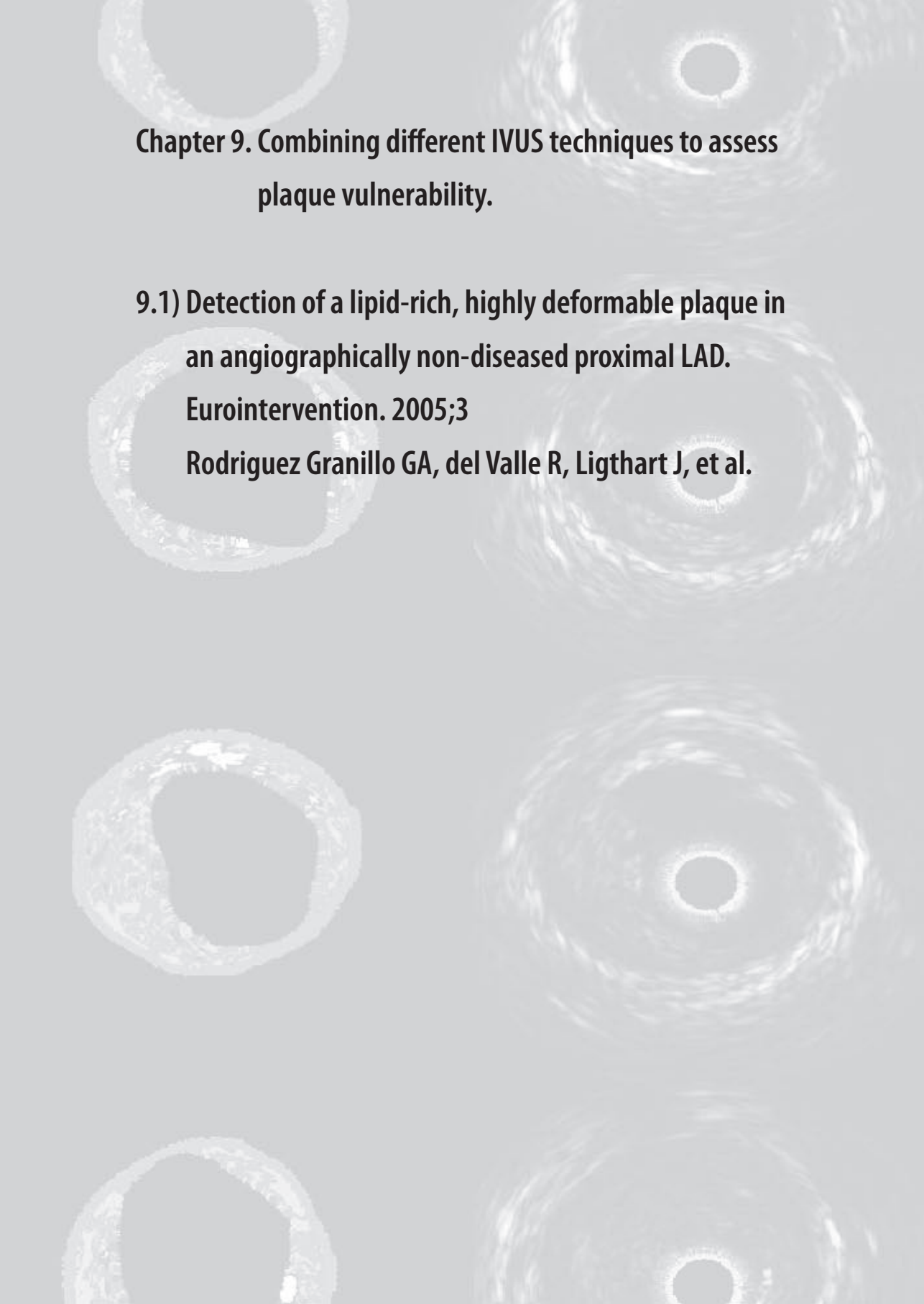


Figure 1



The background of the slide features a grid of six grayscale IVUS (Intravascular Ultrasound) cross-sectional images of arteries. The images are arranged in two columns and three rows. The left column shows the vessel wall with varying degrees of plaque accumulation, while the right column shows the lumen. The overall appearance is that of a medical or scientific presentation.

**Chapter 9. Combining different IVUS techniques to assess plaque vulnerability.**

**9.1) Detection of a lipid-rich, highly deformable plaque in an angiographically non-diseased proximal LAD.**

**Eurointervention. 2005;3**

**Rodriguez Granillo GA, del Valle R, Ligthart J, et al.**



## Detection of a necrotic core-rich, highly deformable plaque in an angiographically non-diseased proximal LAD

Gastón A. Rodríguez-Granillo, MD; Raquel del Valle, MD; Jurgen Ligthart, BSc; Patrick W. Serruys\*, MD, PhD

Thin-cap fibro atheroma (TCFA) lesions, the most prevalent precursor of plaque rupture, are composed of a lipid-rich necrotic core, a thin-fibrous cap with macrophage and lymphocyte infiltration, decreased smooth muscle cell content and expansive remodeling. Virtual Histology™ uses spectral analysis of intravascular ultrasound (IVUS) radiofrequency data to construct tissue maps that classify plaque into four major components; calcified, fibrous, fibrolipidic and necrotic core regions that are labeled white, green, greenish-yellow and red respectively. Palpography™ evaluates *in vivo* the mechanical properties of plaque tissue. The local strain is calculated from the radiofrequency traces using cross-correlation analysis and displayed, colour coded, from blue (for 0% strain) through yellow (for 2% strain) via red (Figure 1).

At a defined pressure, soft tissue (lipid-rich) components will deform more than hard (fibrous-calcified) components. Both techniques have been previously validated<sup>1,2</sup>.

Figure 1a shows an angiographically non-diseased proximal left anterior descending (LAD) artery. IVUS longitudinal reconstruction (Figure 1b) shows diffuse LAD disease. An eccentric mixed plaque that did not compromise the lumen was detected in the proximal LAD

(Figure 1c). This segment was further analyzed with Palpography (20 MHz Eagle Eye, Volcano Therapeutics) and Virtual Histology™ (30 MHz Ultracross, Boston Scientific Corp) (Figures 1d and 1e). Despite its innocuous appearance on gray-scale IVUS, highly deformable shoulders with an underlying necrotic core-rich substrate were detected with the aid of strain and compositional imaging.

Although compatible with the presence of a vulnerable plaque, the prognostic value of these findings is currently unknown and needs to be established in large prospective randomized trials. Thus, the patient was discharged on intensive systemic therapy including lipid-lowering agents.

### References

1. Nair A, Kuban BD, Tuzcu EM, Schoenhagen P, Nissen SE, Vince DG. Coronary plaque classification with intravascular ultrasound radiofrequency data analysis. *Circulation*. Oct 22 2002;106(17):2200-2206.
2. Schaar JA, Regar E, Mastik F, McFadden EP, Saia F, Disco C, de Korte CL, de Feyter PJ, van der Steen AF, Serruys PW. Incidence of high-strain patterns in human coronary arteries: assessment with three-dimensional intravascular palpography and correlation with clinical presentation. *Circulation*. Jun 8 2004;109(22):2716-2719.

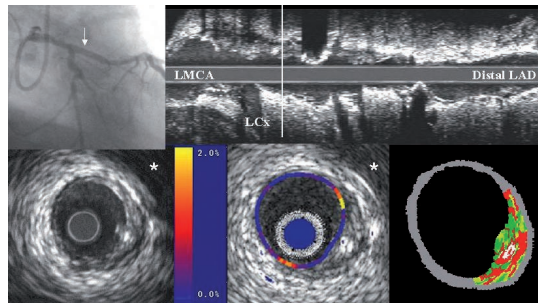


Figure 1. LAD= left anterior descending coronary artery. LCx= Left circumflex coronary artery. LMCA= Left main coronary artery. \* Pericardium.

Colour figures on pages 441-449



**9.2) In vivo relationship between compositional and mechanical imaging of coronary arteries: insights from intravascular ultrasound radiofrequency data analysis.**

**Am Heart Journal. 2006 May;151(5):1032-6.**

**Rodriguez Granillo GA, García-García HM, Valgimigli M, et al.**





# In vivo relationship between compositional and mechanical imaging of coronary arteries: Insights from intravascular ultrasound radiofrequency data analysis

Gastón A. Rodríguez-Granillo, MD,<sup>a</sup> Héctor M. García-García, MD,<sup>a</sup> Marco Valgimigli, MD,<sup>a</sup> Johannes A. Schaar, MD, PhD,<sup>a</sup> Ravindra Pawar,<sup>b</sup> William J. van der Giessen, MD, PhD,<sup>a</sup> Evelyn Regar, MD, PhD,<sup>a</sup> Antonius F.W. van der Steen, PhD,<sup>a</sup> Pim J. de Feyter, MD, PhD,<sup>a</sup> and Patrick W. Serruys, MD, PhD<sup>a</sup> *Rotterdam, The Netherlands*

**Objective** We sought to explore in vivo the relation between mechanical and compositional properties of matched cross sections (CSs) using novel catheter-based techniques.

**Background** Intravascular ultrasound (IVUS) palpography allows the assessment of local mechanical tissue properties. Spectral analysis of IVUS radiofrequency data (IVUS-VH) is a tool to assess plaque morphology and composition.

**Methods and Results** Palpography analysis defined high- and low-strain regions. One hundred twenty-three CSs (27 vessels) were colocalized. The mean strain value was higher in CSs with necrotic core (NC) in contact with the lumen than in CSs with no NC contact with the lumen ( $1.03 \pm 0.5$  vs  $0.86 \pm 0.4$ ,  $P = .06$ ).

Mean relative calcium ( $1.61 \pm 2.5\%$  vs  $0.25 \pm 0.7\%$ ,  $P = .001$ ) and NC ( $15.64 \pm 10.6\%$  vs  $2.8 \pm 3.9\%$ ,  $P < .001$ ) content were significantly higher in the CSs with NC in contact with the lumen, whereas the inverse was seen for the fibrotic component of the plaque ( $64.16 \pm 11.6\%$  vs  $75.75 \pm 13.7$ ,  $P < .001$ ). The sensitivity, specificity, positive predictive value, and negative predictive value of IVUS-VH to detect high strain were 75.0%, 44.4%, 56.3%, and 65.1%, respectively. A significant inverse relationship was present between calcium and strain levels ( $r = -0.20$ ,  $P = .03$ ). After adjusting for univariate predictors, the contact of NC with the lumen was identified as the only independent predictor of high strain (OR 5.0, 95% CI 1.7-14.1,  $P = .003$ ).

**Conclusion** In the present study, IVUS-VH showed an acceptable sensitivity to detect high strain. In turn, the specificity was low. Of interest, a significant inverse relationship was present between calcium and strain levels. (Am Heart J 2006;151:1032.e1-1032.e6.)

Several studies have established that no association exists between the stenosis severity at previous angiogram and the subsequent occurrence of site-related vessel closure.<sup>1-3</sup> It is also well known that a large number of people die suddenly, lacking previous history of coronary artery disease.<sup>4</sup>

In spite of significant improvement in prevention strategies, coronary plaque rupture is still a frequent and unpredictable event that has a major impact in the global burden of cardiovascular disease.<sup>5</sup> In response to that, intensive research efforts have been made throughout the

past decade to attain the early identification of atherosclerotic plaques that might eventually rupture. Initially, different histopathological lines of investigation have led to the identification of morphological and compositional features related to plaque rupture, such as thin fibrous cap, paucity of smooth muscle cells, heavy inflammatory infiltration of the cap, and large necrotic cores.<sup>6-8</sup> In parallel, the degree of mechanical stress suffered by the plaque was found a predictor of the thickness of the cap.<sup>9</sup>

More recently, several catheter-based techniques have been developed to identify the aforementioned features in vivo.<sup>10-14</sup>

Intravascular ultrasound (IVUS) palpography is a technique that allows the assessment of local mechanical tissue properties.<sup>13,15</sup> This technique has shown a high sensitivity and specificity to detect vulnerable plaques in vitro.<sup>13</sup> Indeed, and in agreement with previous findings in a finite element model, a strong inverse relation was found between cap thickness and strain.<sup>9,13</sup> Separately, spectral analysis of the IVUS radiofrequency data (IVUS-VH) is emerging as a tool to

From the <sup>a</sup>Thoraxcenter, Erasmus MC, Rotterdam, The Netherlands, and <sup>b</sup>Cardialysis BV, Rotterdam, The Netherlands.

All authors have approved the final manuscript, which has not been published and is not under consideration elsewhere. We declare that there is no conflict of interest for any author.

Submitted June 29, 2005; accepted December 6, 2005.

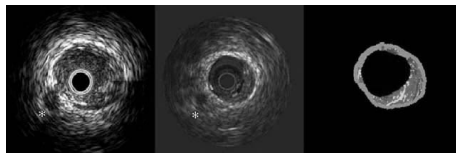
Reprint requests: Patrick W. Serruys, MD, PhD, Thoraxcenter, Bld406, Dr. Molewaterplein 40, 3015-GD Rotterdam, The Netherlands.

E-mail: p.w.j.c.serruys@erasmusmc.nl

0002-8703/\$ - see front matter

© 2006, Mosby, Inc. All rights reserved.

doi:10.1016/j.ahj.2005.12.018

**Figure 1**

Colocalization of the CS with IVUS-VH and palpography. At the 7-o'clock position, a side branch induces an artificial high-strain spot. Two high-strain spots were detected at the 2- and 6 o'clock positions. Virtual Histology analysis showed a mainly fibrotic plaque with necrotic core in contact with the lumen at the 2- and 6-o'clock positions.

assess plaque morphology and composition.<sup>10</sup> The relationship between mechanical and compositional properties of coronary atherosclerosis has not been fully elucidated. We thus sought to explore *in vivo* the relation between mechanical (palpography) and compositional (IVUS-VH) properties of matched cross-sectional areas using novel catheter-based techniques.

## Methods

This investigator-driven prospective study sought to explore the relation between 2 catheter-based techniques (IVUS-VH and palpography) with regard to the detection of compositional and mechanical properties of subclinical atherosclerosis. Patients admitted for coronary catheterization and subsequent intervention were eligible if a nontarget vessel was suitable for IVUS interrogation (absence of diameter stenosis  $\geq 50\%$ , extensive calcification, and/or severe vessel tortuosity) of at least 30 mm of length. In addition, hemodynamically unstable patients were excluded. Informed consent was obtained from all patients.

### Intravascular ultrasound palpography acquisition and analysis

Intravascular ultrasound palpography is a technique that allows the assessment of local mechanical tissue properties. At a defined pressure difference, soft tissue (eg, lipid-rich) components will deform more than hard tissue components (eg, fibrous-calcified).<sup>13,15</sup> In coronaries, the tissue of interest is the vessel wall, whereas the blood pressure with its physiological changes during the heart cycle is used as the excitation force. Radiofrequency data obtained at different pressure levels are compared to determine the local tissue deformation.

Each palpogram represents the strain information for a certain cross section (CS) over the full cardiac cycle. The longitudinal resolution of the acquisitions depends on heart rate and pullback speed. With a heart rate of 60 beat/min and a pullback speed of 1.0 mm/s, the longitudinal resolution is 1.0 mm. Palpograms were acquired using a 20-MHz phased-array IVUS catheter (Avanar, Volcano Therapeutics, Rancho Cordova, CA). Cine runs, before and during contrast injection, were performed to define the position of the IVUS catheter

$\geq 10$  mm distal to an anatomical identifiable landmark. Digital radiofrequency data were acquired using a custom-designed workstation.

During the recordings, data were continuously acquired at a pullback speed of 1.0 mm/s using an automated pullback device (Track Back II, Volcano Therapeutics) with simultaneous recording of the electrocardiogram and the aortic pressure. The data were stored on a DVD and sent to the imaging core laboratory for offline analysis (Cardialysis BV, Rotterdam, The Netherlands).

The local strain was calculated from the gated radiofrequency traces using cross-correlation analysis and displayed and color-coded from blue (for 0% strain) through yellow (for 2% strain) via red (Figure 1), as described before.<sup>16</sup> This color-coded information was superimposed on the lumen vessel boundary of the cross-sectional IVUS image.

Using previously described methodology, plaque strain values were assigned a Rotterdam classification (ROC) score ranging from 1 to 4 (ROC I, 0-0.5%; ROC II, 0.6-0.9%; ROC III, 0.9-1.2%; ROC IV, >1.2%).<sup>17</sup> A region was defined as a high-strain spot when it had high strain (ROC III-IV) that spanned an arc of at least  $12^\circ$  at the surface of a plaque (identified on the IVUS recording) adjacent to low-strain regions (<0.5%). The highest value of strain in the CS was taken as the strain level of the spot.

### Intravascular ultrasound radiofrequency data acquisition and analysis

Details regarding the validation of the technique on explanted human coronary segments have previously been reported.<sup>10</sup> Briefly, IVUS-VH uses spectral analysis of IVUS radiofrequency data to construct tissue maps that were correlated with a specific spectrum of the radiofrequency signal and assigned color codes (fibrous [labeled green], fibrolipidic [labeled greenish yellow], necrotic core [labeled red], and calcium [labeled white]).<sup>10</sup>

After the palpography acquisition, IVUS-VH data were acquired using a continuous pullback (Ultracross 30-MHz catheter, Boston Scientific, Santa Clara, CA), by a dedicated IVUS-VH console (Volcano Therapeutics). The IVUS-VH data were stored on a CD-ROM and sent to the imaging core laboratory for offline analysis (Cardialysis BV, Rotterdam, The Netherlands). Data acquisition was electrocardiogram-gated and recorded during the automated withdrawal of the catheter using a mechanical pullback device (Boston Scientific) at a pullback speed of 0.5 mm/s.

Intravascular ultrasound B-mode images were reconstructed from the radio frequency data by customized software (IVUSLab, Volcano Therapeutics). Semiautomated contour detection of both the lumen and the media-adventitia interface was performed, and the radio frequency data were normalized using a technique known as "blind deconvolution," an iterative algorithm that deconvolves the catheter transfer function from the backscatter, thus accounting for catheter-to-catheter variability.<sup>18,19</sup> Compositional data were obtained for every slice and expressed as mean percent for each component.

### Cross-correlation of techniques

An independent experienced palpography analyst (RP) blinded for any patient's information regarding clinical or

**Table I.** Baseline characteristics (n = 27)

Age	59.2 ± 10.1
Male	21 (77.8%)
Body mass index	26.5 ± 3.2
Diabetes mellitus	5 (18.5%)
Hypertension	10 (37.0%)
Family history of CHD	18 (66.7%)
Current smoking	8 (29.6%)
Previous smoking	10 (37.0%)
Hypercholesterolemia	24 (88.9%)
Clinical presentation	
Stable angina	18 (66.7%)
ACS	9 (33.3%)
Study vessel	
Left anterior descending	9 (33.3%)
Left circumflex	4 (14.8%)
Right coronary artery	14 (51.9%)
Baseline medication	
Statin	22 (81.5%)
β-Blocker	15 (55.6%)
ACE inhibitor	16 (59.3%)

Acute coronary syndromes were defined as unstable angina, non-ST-segment elevation myocardial infarction, or ST-segment elevation myocardial infarction. CHD, Coronary heart disease; ACE, angiotensin-converting enzyme.

IVUS-VH data randomly selected CSs with high-and/or low-strain spots within the pullback analysis. Intentionally, and to avoid bias owing to the knowledge that the prevalence of high-strain spots is significantly lower than the prevalence of low-strain spots, such random selection was performed after randomly assigning 2 batches of balanced high- and low-strain spots.<sup>15</sup> Subsequently, a color-blinded side-by-side view (Palpography and IVUS-VH) was undertaken to facilitate the identification of the same matched region with both techniques. Using longitudinal as well as cross-sectional views and with the aid of anatomical landmarks such as side-branches, veins, calcified spots, and pericardium, 2 experienced IVUS analysts (GARG and HMG) blinded for the palpography results identified the given CSs (Figure 1).

Area (plaque burden [PB]), defined as  $EEM_{area} - lumen_{area} / EEM_{area} \times 100$ , where EEM refers to external elastic membrane; and plaque eccentricity index [EI], defined as minimum plaque thickness divided by maximum plaque thickness) and compositional (percent calcified, fibrous, fibrolipidic, and necrotic core tissues) outputs were calculated for every matched CS. In addition, the presence of direct contact between necrotic core tissue and the lumen with no overlying fibrous tissue (suggesting the presence of a thin cap) was determined as a visual binary assessment, irrespective of the amount of necrotic core.

### Statistical analysis

Discrete variables are presented as counts and percentages. Continuous variables are presented as means ± SD. A 2-sided *P* value of <.05 indicated statistical significance. The sensitivity (proportion of high-strain spots where NC contact with the lumen is present), specificity (proportion of low-strain spots where no NC contact with the lumen is present), positive predictive value (proportion of spots with NC contact with the lumen is present where high strain is present), and negative predictive value (proportion of spots with no NC contact with the lumen where no high strain is present) of the presence of

**Table II.** Relationship between strain levels and relative plaque composition**Pearson correlation coefficient between strain levels (%) and relative plaque composition (n = 123)**

	Strain level	<i>P</i>
Necrotic core (%)	0.11	.25
Calcium (%)	-0.20	.03
Fibrous (%)	0.06	.55
Fibrolipidic (%)	-0.13	.15

NC in contact with the lumen (IVUS-VH finding) to detect high strain (palpography finding) was evaluated. Pearson correlation coefficient was used to assess the relationship between strain values (%) and relative plaque composition.

Logistic regression analysis was performed using the forward Wald method to identify potential predictors of the presence of high strain (ROC III-IV) spots among all IVUS-VH-derived variables (calcified content, fibrous content, fibrolipidic content, necrotic core content, EI, plaque burden, and contact of necrotic core with the lumen). Statistical analyses were performed with use of SPSS software, version 11.5 (SPSS Inc, Chicago, IL).

## Results

Thirty-three consecutive patients were prospectively enrolled in this study. In 6 cases, matching was unsuccessful because of nonuniform rotational distortion or motion artifacts. The baseline characteristics of the patient population (n = 27) are depicted in Table I. The mean age was 59.2 ± 10.1 years and most patients were men (n = 21, 77.8%). The study vessel was the left anterior descending in 9 (33.3%), the left circumflex in 4 (14.8%), and the right coronary artery in 14 (51.9%) patients. Eighteen (66.7%) patients presented with stable angina, and 9 (33.3%), with an acute coronary syndrome (ACS).

As aforementioned, the prevalence of high- and low-strain spots was balanced (n = 60 and 63, respectively). In turn, IVUS-VH identified necrotic core in contact with lumen more frequently (n = 80 and 43, respectively). Pearson correlation coefficients between strain values and relative plaque composition are depicted in Table II. No significant correlation was present between necrotic core (%) and strain levels (*r* = 0.11, *P* = .25). Nevertheless, a significant (albeit weak) inverse relationship was present between calcium (%) and strain levels (*r* = -0.20, *P* = .03).

The mean strain value was higher, although not significant, in CSs with necrotic core in contact with the lumen than in CSs with no contact with the lumen (1.03 ± 0.5% vs 0.86 ± 0.4%, *P* = .06).

Plaque composition of the CS with necrotic core in contact with the lumen differed considerably from CS with overlying fibrous tissue (Table III). Calcium (1.61 ±

**Table III.** Mean plaque composition and conventional intravascular ultrasound output in CSs with and without necrotic core contact with the lumen

Percent	Necrotic core relation with the lumen		P
	No contact (n = 43)	Contact (n = 80)	
Calcium	0.25 ± 0.7	1.61 ± 2.5	.001
Fibrous	75.75 ± 13.7	64.16 ± 11.6	<.001
Fibrolipidic	21.17 ± 13.7	18.57 ± 9.2	.21
Necrotic core	2.8 ± 3.9	15.64 ± 10.6	<.001
PB (%)	48.8 ± 9.4	50.63 ± 11.3	.38
EI	0.15 ± 0.1	0.23 ± 0.1	.01

2.5% vs 0.25 ± 0.7%,  $P = .001$ ) and necrotic core (15.64 ± 10.6% vs 2.8 ± 3.9%,  $P < .001$ ) content were significantly larger in the CSs with contact with the lumen, whereas the inverse was seen for the fibrotic component of the plaque (64.16 ± 11.6% vs 75.75 ± 13.7,  $P < .001$ ).

Conversely, plaque composition did not differ significantly between high- and low-strain CSs (Table IV).

The sensitivity, specificity, positive predictive value, and negative predictive value of IVUS-VH to detect high strain as assessed by palpography were 75.0%, 44.4%, 56.3%, 65.1%, respectively.

## Discussion

Currently, there are several intravascular diagnostic tools capable of locally evaluating determinants of plaque vulnerability, such as the size of the necrotic core, thickness of the fibrous cap, inflammation within the cap, and positive remodeling<sup>10,11,13,14,20</sup>. Nevertheless, to date, the natural history of lesions with such characteristics remains unknown, and the limited knowledge about their eventual prognosis is provided by retrospective histopathological studies.

The predictive accuracy of palpography to detect vulnerability features has been previously demonstrated in vitro.<sup>13</sup> Nevertheless, this technique does not provide quantitative information regarding important determinants of plaque vulnerability such as necrotic core content and remodeling pattern of the plaque.

In turn, spectral analysis of IVUS-VH has been validated as a tool to quantitatively assess the 4 different components of coronary atherosclerotic plaques.<sup>10</sup> In addition, it can provide data regarding coronary remodeling.<sup>21</sup>

In the present study, we have evaluated the mechanical strain and the composition of the same region by combining the use of palpography and subsequent IVUS-VH. Intravascular ultrasound radiofrequency data showed an acceptable sensitivity to detect high strain, as assessed by palpography. In turn, the specificity was low, reflecting a high number of false positives.

**Table IV.** Mean plaque composition and conventional intravascular ultrasound output in CSs with low (ROC III) and high (ROC III-IV) mechanical strain

Percent	ROC		P
	ROC I-II (n = 63)	ROC III-IV (n = 60)	
Calcium	1.46 ± 2.6	0.80 ± 1.5	.09
Fibrous	67.54 ± 13.2	68.90 ± 13.8	.58
Fibrolipidic	20.23 ± 11.4	18.68 ± 10.6	.44
Necrotic core	10.74 ± 11.5	11.61 ± 10.0	.65
PB (%)	49.80 ± 10.9	50.22 ± 10.6	.83
EI	0.21 ± 0.1	0.19 ± 0.1	.41

Of interest, and consistent with a previous in vitro study who established that calcified tissue has highly static mechanical properties, a significant (albeit weak) inverse relationship was present between calcium and strain levels.<sup>22</sup>

The rationale for the hypothesis that the contact of the necrotic core with the lumen is a predictor of an overlying thin cap was based on several facts. It has been established that tissue shrinkage occurs during fixation processes.<sup>23</sup> Shrinkage of up to 60%, 15%, and 80% can occur during critical-point drying, free drying, and air drying, respectively.<sup>24</sup> Furthermore, postmortem contraction of arteries is an additional confounding factor.<sup>25</sup>

Although the most customary threshold to define a cap as “thin” has been set at 65 μm,<sup>26</sup> several important ex vivo studies have used a higher (>200 μm) threshold.<sup>13,27,28</sup> Indeed, one of these studies identified a mean cap thickness of 260 μm and 360 μm for “vulnerable” and “nonvulnerable” plaques, respectively.<sup>13</sup> Because the axial resolution of IVUS-VH is between 100 and 150 μm, we assumed that the absence of visible fibrous tissue overlying a necrotic core suggested a cap thickness of below 100 to 150 μm and used the absence of such tissue to define a thin fibrous cap.<sup>29</sup>

In the present study, logistic regression analysis identified the contact of necrotic core tissue with the lumen as the only predictor of the presence of high-strain spots (OR 5.0, CI 95% 1.7-14.1,  $P = .003$ ), whereas the necrotic core size had no relation with the presence of such spots. These exploratory results were in line with previous histopathological findings, where no correlation has been found between the size of the necrotic lipid core and the thickness of the cap.<sup>27</sup> In addition, it has been previously established by our group that there is an inverse significant relation between strain (measured by palpography) and cap thickness, whereas no significant correlation between strain and necrotic core content was investigated.<sup>13</sup>

Both the size of the necrotic core and the degree of coronary artery calcification are known to correlate with plaque progression.<sup>30,31</sup> These plaque components have also been associated to an increase in coronary

events.<sup>7,32</sup> It is therefore not unexpected that regions with necrotic core in contact with the lumen had higher concentrations of calcium.

In vivo studies established that a multifocal instability process is present in ACS.<sup>11,33</sup> Rioufol et al.<sup>33</sup> found at least 1 plaque rupture remote from the culprit lesion in 80% of patients and from the culprit artery in 71% of patients. A high prevalence of “high-risk” lesions has been found throughout the coronary tree by means of angiography,<sup>34</sup> angiography,<sup>11</sup> IVUS,<sup>35</sup> and palpography.<sup>15</sup> Furthermore, the unpredictability of the natural history of such lesions and the uncertainty of whether vulnerable plaque characteristics might subsequently lead to fatal or nonfatal ischemic events suggest that potential local preventive strategies could not be cost-effective. Until large randomized trials determine any potential benefit provided by local pacification strategies, we definitively do not advocate the local treatment of such alleged “high risk” plaques.

Nevertheless, the development of an accurate diagnostic tool with the capability of simultaneously assessing more than one of the different acknowledged features of high-risk plaques could potentially enhance the prognostic value of the invasive detection of vulnerable plaque.

Because IVUS-VH and palpography use the same source data (radiofrequency data analysis), information regarding both techniques might be obtained using the same pullback, potentially increasing the prognostic value of certain seemingly pejorative plaque characteristics assessed in prospective natural history studies. The present study, therefore, has value in determining a line of investigation for future studies using an improved methodological approach that will be provided by simultaneous recording of mechanical and compositional data and by quantitatively measuring the amount of necrotic core in contact with the lumen.

Although our results show a link between both techniques, the present hypothesis-generating study should be regarded as exploratory and not as proof of principle. Prospective studies are required to investigate the prognostic value of these findings.

### Limitations

The present study compared 2 techniques, which have been validated *ex vivo*.<sup>10,13</sup> However, the predictive value of these techniques to detect high-risk spots is currently unknown and needs to be explored in prospective natural history studies. Selection bias cannot be disregarded in the present population. The small size of the population included might have potentially induced a selection bias. Nevertheless, the conductance of large prospective studies will confirm or contradict these preliminary observations.

The inferior axial resolution of IVUS-VH in comparison with histology could influence our results. In addition, because of the use of different pullbacks and gating method, a slight mismatch in the colocalization of the same CS could not be disregarded. However, the longitudinal resolution of palpography is ~1 mm, and to classify a region as high or low strain, the characteristics should be present for at least 1 cardiac cycle. The interpretation of the screening tests performed has to be cautious because of the lack of a gold standard to compare with. Finally, because IVUS-VH analysis software currently does not have a tool to assess quantitatively the amount of contact of necrotic core with the lumen, its predictive accuracy to detect high-strain spots might be influenced.

### Conclusions

In the present study, IVUS-VH showed an acceptable sensitivity to detect high strain as assessed by palpography. In turn, the specificity was low, reflecting a high number of false positives. Of interest, a significant inverse relationship was present between calcium and strain levels. As an exploratory analysis, the contact of necrotic core tissue with the lumen was found the only predictor of the detection of high strain.

### References

1. Ambrose JA, Tannenbaum MA, Alexopoulos D, et al. Angiographic progression of coronary artery disease and the development of myocardial infarction. *J Am Coll Cardiol* 1988;12:56-62.
2. Little WC, Constantinescu M, Applegate RJ, et al. Can coronary angiography predict the site of a subsequent myocardial infarction in patients with mild-to-moderate coronary artery disease? *Circulation* 1988;78(5 Pt 1):1157-66.
3. Giroud D, Li JM, Urban P, et al. Relation of the site of acute myocardial infarction to the most severe coronary arterial stenosis at prior angiography. *Am J Cardiol* 1992;69:729-32.
4. Kannel WB, Doyle JT, McNamara PM, et al. Precursors of sudden coronary death. Factors related to the incidence of sudden death. *Circulation* 1975;51:606-13.
5. Burke AP, Kolodgie FD, Farb A, et al. Healed plaque ruptures and sudden coronary death: evidence that subclinical rupture has a role in plaque progression. *Circulation* 2001;103:934-40.
6. Virmani R, Kolodgie FD, Burke AP, et al. Lessons from sudden coronary death: a comprehensive morphological classification scheme for atherosclerotic lesions. *Arterioscler Thromb Vasc Biol* 2000;20:1262-75.
7. Davies MJ, Richardson PD, Woolf N, et al. Risk of thrombosis in human atherosclerotic plaques: role of extracellular lipid, macrophage, and smooth muscle cell content. *Br Heart J* 1993;69:377-81.
8. Schaar JA, Muller JE, Falk E, et al. Terminology for high-risk and vulnerable coronary artery plaques. Report of a meeting on the vulnerable plaque, June 17 and 18, 2003, Santorini, Greece. *Eur Heart J* 2004;25:1077-82.
9. Loree HM, Kamm RD, Stringfellow RG, et al. Effects of fibrous cap thickness on peak circumferential stress in model atherosclerotic vessels. *Circ Res* 1992;71:850-8.

10. Nair A, Kuban BD, Tuzcu EM, et al. Coronary plaque classification with intravascular ultrasound radiofrequency data analysis. *Circulation* 2002;106:2200-6.
11. Asakura M, Ueda Y, Yamaguchi O, et al. Extensive development of vulnerable plaques as a pan-coronary process in patients with myocardial infarction: an angioscopic study. *J Am Coll Cardiol* 2001;37:1284-8.
12. Stefanadis C, Diamantopoulos L, Vlachopoulos C, et al. Thermal heterogeneity within human atherosclerotic coronary arteries detected in vivo: a new method of detection by application of a special thermography catheter. *Circulation* 1999;99:1965-71.
13. Schaar JA, De Korte CL, Mastik F, et al. Characterizing vulnerable plaque features with intravascular elastography. *Circulation* 2003;108:2636-41.
14. Jang IK, Tearney GJ, MacNeill B, et al. In vivo characterization of coronary atherosclerotic plaque by use of optical coherence tomography. *Circulation* 2005;111:1551-5.
15. Schaar JA, Regar E, Mastik F, et al. Incidence of high-strain patterns in human coronary arteries: assessment with three-dimensional intravascular palpography and correlation with clinical presentation. *Circulation* 2004;109:2716-9.
16. de Korte CL, Carlier SG, Mastik F, et al. Morphological and mechanical information of coronary arteries obtained with intravascular elastography: feasibility study in vivo. *Eur Heart J* 2002;23:405-13.
17. Mieghem CA, Bruining N, Schaar JA, et al. Rationale and methods of the integrated biomarker and imaging study (IBIS): combining invasive and noninvasive imaging with biomarkers to detect subclinical atherosclerosis and assess coronary lesion biology. *Int J Cardiovasc Imaging* 2005;21:425-41.
18. Kåresen KF, Bølviken E. Blind deconvolution of ultrasonic traces accounting for pulse variance. *IEEE Trans Ultrason Ferroelectr Freq Control* 1999;46:564-73.
19. Nair A, Vince DG. "Blind" data calibration of intravascular ultrasound data for automated tissue characterization. *IEEE Ultrason Symp* 2004;1126-9.
20. Romer TJ, Brennan III JF, Fitzmaurice M, et al. Histopathology of human coronary atherosclerosis by quantifying its chemical composition with Raman spectroscopy. *Circulation* 1998;97:878-85.
21. Rodriguez-Granillo GA, Serruys PW, Garcia-Garcia HM, et al. Coronary artery remodelling is related to plaque composition. *Heart* 2005 [Jun 17. Epub ahead of press].
22. Lee RT, Richardson SG, Loree HM, et al. Prediction of mechanical properties of human atherosclerotic tissue by high-frequency intravascular ultrasound imaging. An in vitro study. *Arterioscler Thromb* 1992;12:1-5.
23. Lee MKW. A critical appraisal of the effects of fixation, dehydration and embedding of cell volume. In: Revel JP, Barnard T, Haggis GH, editors. *The science of biological specimen preparation for microscopy and microanalysis*. Illinois: Scanning Electron Microscopy, AMF O'Hare; 1984. p. 61-70.
24. Boyde A, Jones SJ, Tamarin A. Dimensional changes during specimen preparation for scanning electron microscopy. *Scan Electron Microsc*;1977;507-18.
25. Fishbein MC, Siegel RJ. How big are coronary atherosclerotic plaques that rupture? *Circulation* 1996;94:2662-6.
26. Burke AP, Farb A, Malcom GT, et al. Coronary risk factors and plaque morphology in men with coronary disease who died suddenly. *N Engl J Med* 1997;336:1276-82.
27. Mann JM, Davies MJ. Vulnerable plaque. Relation of characteristics to degree of stenosis in human coronary arteries. *Circulation* 1996;94:928-31.
28. Felton CV, Crook D, Davies MJ, et al. Relation of plaque lipid composition and morphology to the stability of human aortic plaques. *Arterioscler Thromb Vasc Biol* 1997;17:1337-45.
29. Nair A, Calvetti D, Vince DG. Regularized autoregressive analysis of intravascular ultrasound data: improvement in spatial accuracy of plaque tissue maps. *IEEE Trans Ultrason Ferroelectr Freq Control* 2004;51:420-31.
30. Takaya N, Yuan C, Chu B, et al. Presence of intraplaque hemorrhage stimulates progression of carotid atherosclerotic plaques: a high-resolution magnetic resonance imaging study. *Circulation* 2005;111:2768-75.
31. Sangiorgi G, Rumberger JA, Severson A, et al. Arterial calcification and not lumen stenosis is highly correlated with atherosclerotic plaque burden in humans: a histologic study of 723 coronary artery segments using nondecalfying methodology. *J Am Coll Cardiol* 1998;31:126-33.
32. Budoff MJ, Yu D, Nasir K, et al. Diabetes and progression of coronary calcium under the influence of statin therapy. *Am Heart J* 2005;149:695-700.
33. Rioufol G, Finet G, Giron I, et al. Multiple atherosclerotic plaque rupture in acute coronary syndrome: a three-vessel intravascular ultrasound study. *Circulation* 2002;106:804-8.
34. Goldstein JA, Demetriou D, Grines CL, et al. Multiple complex coronary plaques in patients with acute myocardial infarction. *N Engl J Med* 2000;343:915-22.

**9.3) In vivo, cardiac-cycle related intimal displacement of coronary plaques assessed by 3-D ECG-gated intravascular ultrasound: exploring its correlate with tissue deformability identified by palpography.**

**Int J Cardiovasc Imaging. 2006 Apr;22(2):147-52.**

**Rodriguez Granillo GA, Agostoni P, García-García HM, et al.**



## ***In-vivo*, cardiac-cycle related intimal displacement of coronary plaques assessed by 3-D ECG-gated intravascular ultrasound: exploring its correlate with tissue deformability identified by palpography**

Gastón A. Rodríguez-Granillo, Pierfrancesco Agostoni, Héctor M. García-García, Pim de Feyter & Patrick W. Serruys

*Erasmus Medical Center, Thoraxcenter, Rotterdam, The Netherlands*

Received 20 May 2005; accepted in revised form 7 June 2005

*Key words:* atherosclerosis, imaging, mechanical strain, ultrasonography

### **Abstract**

*Background:* ECG-gated image acquisition of intravascular ultrasound (IVUS) has been shown to provide more accurate measurements at different phases of the cardiac cycle. *Objective:* We sought to explore the ability dynamic assessment of ECG-gated 3-D IVUS to identify deformable regions of coronary plaques, by testing the hypothesis that at a given pressure and region, a faster displacement of the intima would correspond to high strain (soft tissue) regions assessed by palpography. *Methods:* ECG-gated 3-D IVUS and palpograms were acquired using 30 and 20 MHz IVUS imaging catheters respectively. Frames with high and/or low strain spots identified by palpography were randomly selected and the spots were assigned to a respective quadrant within the cross section. A color-blinded side-by-side view was performed to enable the co-localization of the same region. Subsequently, the pressure driven displacement of the intima was established for each quadrant and a binary score (significant displacement or no displacement) was decided. *Results:* One hundred and twenty-four quadrants were studied and the prevalence of highly deformable quadrants was low ( $n=7$ , 5.6% of the total). The sensitivity, specificity, positive predictive value and negative predictive value of 3-D ECG-gated IVUS to detect deformable quadrants as assessed by palpography were 42.9, 87.2, 16.7, and 96.2% respectively. *Conclusion:* In this pilot *in vivo* study, the intimal displacement velocity in the radial direction assessed by gray-scale 3-D ECG-gated IVUS failed to correlate with highly deformable regions. However, these preliminary findings suggest that the absence of significant displacement of the intima might be accurate to predict the absence of deformable tissue.

### **Introduction**

Despite major improvements in the management and diagnosis of patients with coronary artery disease, a large number of victims who are apparently healthy die suddenly without prior symptom [1, 2]. Intensive efforts are currently being made to detect *in vivo* vulnerability features of coronary atherosclerotic plaques. Several catheter-based

techniques have been developed with the aim of characterizing and eventually evaluating the effect of conventional and novel therapeutic intervention of such non-flow-limiting lesions [3–5].

An important patho-morphologic feature of vulnerable plaques is the eccentric accumulation of a lipid-rich necrotic core within the vessel wall, separated from the lumen by a thin fibrous cap. This observation led to the hypothesis that vulnerable

lesions might have mechanical properties that differ from those of chronic stable lesions. Indeed, both plaque rupture and increased inflammatory markers have been reported to occur more frequently in regions with increased mechanical stress [3, 6, 7].

Intravascular Ultrasound (IVUS) is an invasive diagnostic tool that provides a real-time, high-resolution, tomographic view of coronary arteries. It thereby enables the assessment of morphology, severity and extension of coronary plaque. By reducing motion artifacts caused by the displacement of the catheter relative to the vessel wall during a pullback, ECG-gated image acquisition of IVUS has been shown to provide more accurate measurements with lower intra and interobserver variability [8–10]. In addition, it allows measurements at different phases of the cardiac cycle [8].

A recent study established that the luminal, pressure driven displacement of low echogenic (soft) plaques is faster than the one present in calcified lesions [11].

In this study, we sought to explore the ability of ECG-gated 3-D IVUS to identify deformable regions of coronary plaques, by testing the hypothesis that at a given pressure and region, a faster displacement of the intima would correspond to high strain regions as assessed by palpography, which represent soft (highly deformable) tissue.

## Methods

Patients were eligible if they had a *de novo*, non-significant (angiographically <50%) stenosis in a native coronary artery. Patients were excluded from the study if any of the following conditions were present: (1) severe vessel tortuosity (2) severely calcified vessels. Written informed consent was obtained from all patients.

### *Intravascular ultrasound acquisition*

IVUS was performed after intracoronary administration of nitrates using a single-element, 30 MHz rotating transducer (3.2 F Ultracross™, Boston Scientific Corp.). Cine runs, before and during contrast injection, were performed to define

the position of the IVUS catheter  $\geq 10$  mm distal to a clear anatomical landmark. The ECG-gated image acquisition and digitization were performed by a 3-D image acquisition workstation (EchoScan, TomTec, Munich, Germany), which received the video signal input from the IVUS console and the ECG-signal from the patient. This system steered the ECG-gated stepping pullback device to withdraw the imaging transducer. The workstation considered the heart rate variability and only acquired images from cycles meeting a predetermined range. Premature beats were rejected.

If an R–R interval failed to meet the preset range, the catheter remained at the same site until a cardiac cycle met the predetermined R–R range. Subsequently, the transducer was withdrawn 0.2 mm and images were recorded. Image acquisition required on average 1 min per cm.

### *Palpography acquisition*

Palpograms were acquired using a 20-MHz phased-array IVUS catheter (Volcano Therapeutics, Rancho Cordova, USA). Cine runs, before and during contrast injection, were performed to define the position of the IVUS catheter  $\geq 10$  mm distal to the same landmark used for the 30 MHz catheter. Digital radiofrequency data were acquired using a custom-designed workstation.

Intravascular ultrasound palpography is a technique that allows the assessment of local mechanical tissue properties [3, 12]. At a defined pressure, soft tissue (lipid-rich) components will deform more than hard tissue components (fibrous-calcified) [13]. In coronaries, the tissue of interest is the vessel wall, whereas the blood pressure with its physiologic, systolic and diastolic changes during the heart cycle is used as the excitation force. Images obtained at different pressure levels are compared to determine the local tissue deformation.

Each palpogram represents the strain information for a certain cross section over the full cardiac cycle. The longitudinal resolution of the acquisitions depends on heart rate and pullback speed. With a heart rate of 60 bpm and a pullback speed of 1.0 mm/s, the longitudinal resolution is 1.0 mm. For palpography, catheter displacement is the main

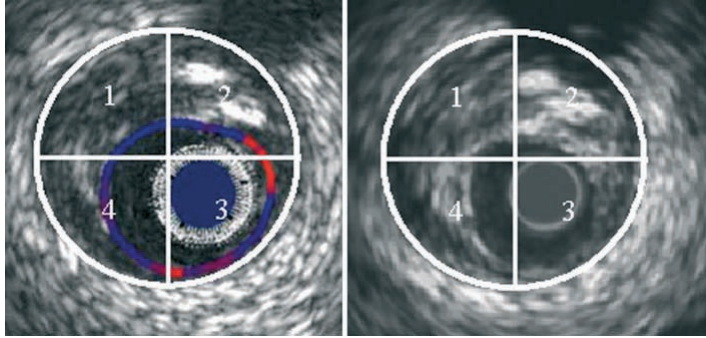


Figure 1. Matched cross-section imaged with palpography (left) and 3-D ECG-gated (right) intravascular ultrasound. A highly deformable plaque and significant intimal radial displacement is present in quadrant 3.

source of signal decorrelation and thus a source of error in strain estimation [14]. During the recordings, data were continuously acquired at a pullback speed of 1.0 mm/s using a mechanical pullback device (Track Back II, Volcano Therapeutics) with simultaneous recording of the ECG and the aortic pressure. The data set is subdivided into heart cycles by use of the R wave of the ECG signal.

#### Palpography analysis

The local strain was calculated from the gated radiofrequency traces using cross-correlation analysis and displayed, color-coded, from blue (for 0% strain) through yellow (for 2% strain) via red. This color-coded circumferential image was superimposed on the cross-sectional IVUS image (Figure 1).

A region was defined as a high-strain spot when it had high strain ( $\geq 0.9\%$  at 4 mm Hg pressure difference) that spanned an arc of at least  $12^\circ$  at the surface of a plaque (identified on the IVUS recording) adjacent to low-strain regions ( $< 0.5\%$  at 4 mm Hg pressure difference). The highest value of strain was taken as the strain level of the spot. An independent experienced analyst randomly selected frames with high and/or low strain spots within the pullback analysis and positioned the spots in a respective quadrant according to the spatial location within the cross section (Figure 1).

#### Qualitative IVUS analysis

A color-blinded side-by-side view (gray-scale IVUS and Palpography) was undertaken to facilitate the identification of the same region with both techniques. Using longitudinal as well as cross-sectional views and with the aid of anatomical landmarks such as side-branches, veins, calcified spots and pericardium, three experienced IVUS analysts blinded for the palpography results identified the given frames. Images were rotated with the purpose of matching the orientation of the images provided in the palpogram. With the aid of dynamic evaluation of both longitudinal and cross-sectional views, the longitudinal movement of the catheter at the current frame was estimated qualitatively.

Subsequently, and provided that the longitudinal movement was not significant (determined by cyclic entrance/exit of identifiable anatomical landmarks), the pressure driven displacement of the intima was established for each quadrant and a binary score (significant displacement or no displacement) was decided by consensus of the three analysts.

#### Statistical analysis

Continuous variables are presented as mean  $\pm$  SD. The sensitivity (proportion of deformable quadrants

where significant displacement of the intima is present), specificity (proportion of non-deformable quadrants where no displacement of the intima is present), positive predictive value (proportion of quadrants with significant displacement of the intima where deformable tissue is present) and negative predictive value (proportion of quadrants with no displacement of the intima where no deformable tissue is present) of the 3-D ECG-gated IVUS to detect deformable regions of the coronaries was evaluated.

## Results

We studied 9 male patients with a mean age  $59 \pm 9.3$ . The study vessel was the left anterior descending artery in 3 (33.3%), the left circumflex artery in 2 (22.2%) and the right coronary artery in 4 (44.4%) patients.

Thirty-seven frames were selected for paired analysis and 6 were excluded due to significant longitudinal movement of the catheter, which was assessed using longitudinal and cross-sectional views.

As aforementioned, 4 quadrants per frame were individually assessed leading to a total of 124 quadrants.

Overall, the number of highly deformable quadrants was low ( $n=7$ , 5.6% of the total). Conversely, the number of quadrants where significant displacement of the intima was present was slightly higher ( $n=18$ , 14.5%).

The sensitivity, specificity, positive predictive value and negative predictive value of 3-D ECG-gated IVUS to detect deformable quadrants as assessed by palpography were 42.9, 87.2, 16.7, and 96.2% respectively.

## Discussion

The sensitivity and specificity of palpography to detect vulnerable plaques has recently been assessed in post-mortem human coronary arteries where vulnerable plaques were detected with a sensitivity of 88% and a specificity of 89% [12]. In addition to *ex-vivo* studies, this technique has also been tested *in-vivo*, where palpography detected a

high incidence of deformable plaques in ACS patients. Furthermore, the number of highly deformable lesions was correlated to the clinical presentation and levels of C-reactive protein [3].

The detection of vulnerable plaques by IVUS is mainly based on a series of case reports [15–18]. These reports describe morphologic features of already ruptured plaques but not the prospective detection of rupture-prone plaques. Nevertheless, one prospective study showed that large eccentric plaques containing an echolucent zone by IVUS were found to be at increased risk of instability even though the lumen area was preserved at the time of initial study [19].

Conventional gray-scale IVUS studies commonly evaluate the static character of the tissue. As the vessel wall is always subject to shear and wall stress, understanding the dynamic characteristics of coronary atherosclerosis by analyzing the intimal displacement velocity in the radial direction could provide an additive value to gray-scale IVUS [11].

In the current report, we evaluated the sensitivity and specificity of 3-D ECG-gated IVUS to detect deformable (high strain) plaques assessed by palpography. The sensitivity was low and the specificity was high. It is noteworthy that only a low percent (5.6%) of the analyzed frames presented a high strain. 3-D ECG-gated IVUS seems thus poorly sensitive to detect deformable spots. However, these preliminary findings may suggest that the absence of significant displacement of the intima appear to be highly accurate to predict the absence of underlying deformable tissue.

In coronary arteries, the natural motion of the catheter, related to blood flow pattern during systole and diastole and to the contraction of the heart, is inevitable. During systole, blood flow is low, the heart is contracting, and the catheter moves toward the ostium. Conversely, during the diastolic phase, blood flow increases, the heart relaxes, and the catheter moves distally away from the ostium [20]. It has been reported that ECG-gating the IVUS acquisition can significantly reduce the motion artifacts [8, 20]. However, in the present study all vessels presented some longitudinal movement artifact that could have ultimately influenced the interpretation of the images.

### Limitations

This study included a small number of patients. Nevertheless, the conductance of large *in vivo* studies of this type is difficult due to obvious ethical issues. The small prevalence of deformable (high-strain) quadrants could influence the results. Accordingly, interpretation of these results should be cautious and regarded as preliminary. Despite the ECG-gating, motion artifacts seem to be inevitable and could potentially have created misinterpretation of the images. The present is a comparison between quantitative and qualitative techniques. The lack of a quantitative definition of both significant intimal displacement and longitudinal movement could potentially influence the results. However, characterization of such definitions was performed by 3 experienced IVUS analysts. On the other hand, the “gold standard” for sensitivity analysis was an only recently validated technique. However it has shown a high sensitivity and specificity to identify vulnerable plaques [12].

### Conclusion

In this pilot *in vivo* study, the intimal displacement velocity in the radial direction assessed by gray-scale 3-D ECG-gated IVUS failed to correlate with highly deformable regions. The sensitivity was low and the specificity was high. Dynamic assessment of 3-D ECG-gated IVUS seems thus poorly sensitive to detect deformable spots. However, these preliminary findings suggest that the absence of significant displacement of the intima might potentially predict the absence of underlying deformable tissue. Larger studies using a both qualitative and quantitative approach are needed to further investigate the value of these findings.

### References

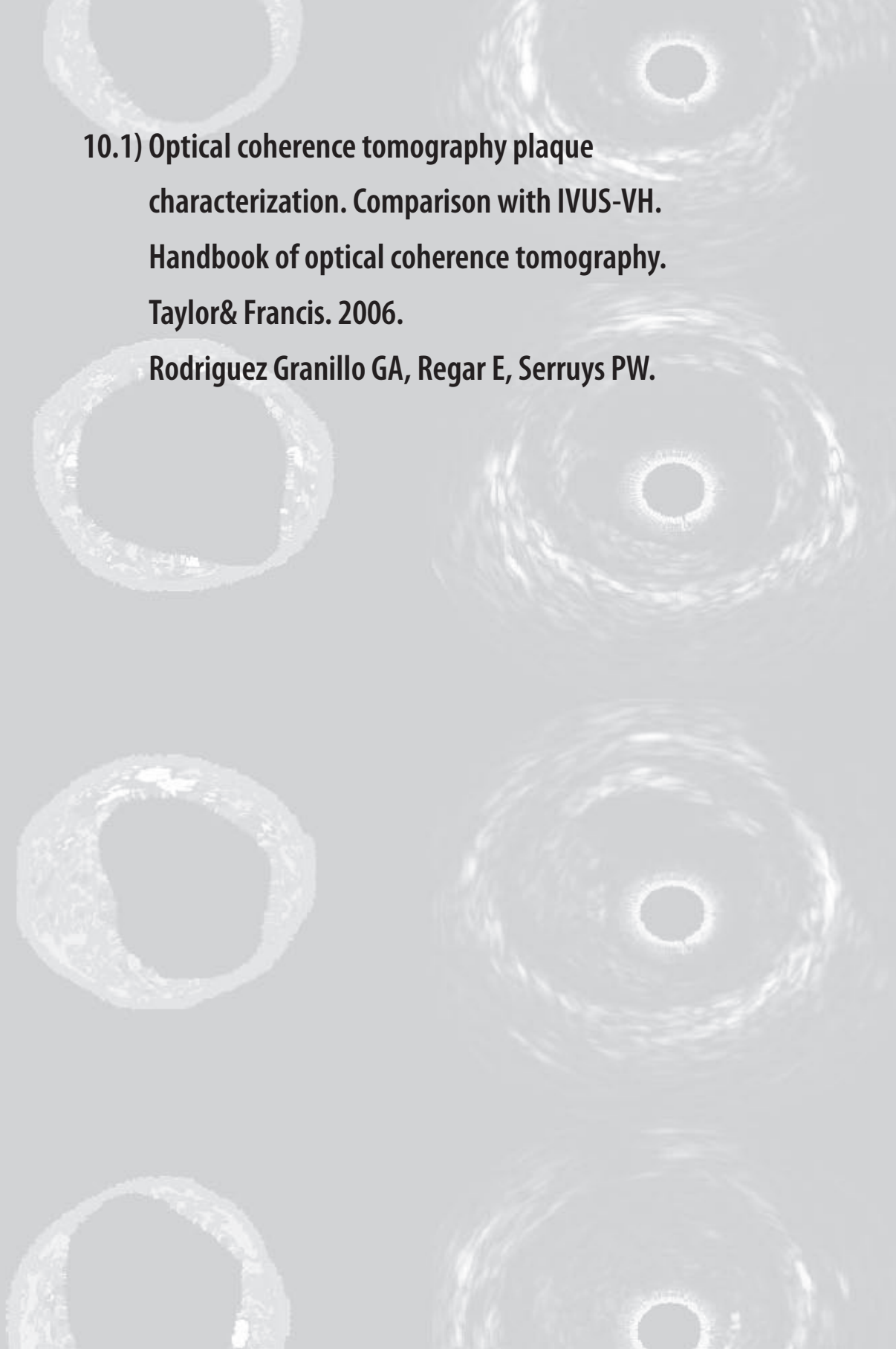
- Kannel WB, Doyle JT, McNamara PM, Quickenton P, Gordon T. Precursors of sudden coronary death. Factors related to the incidence of sudden death. *Circulation* 1975; 51: 606–613.
- Falk E, Shah PK, Fuster V. Coronary plaque disruption. *Circulation* 1995; 92: 657–671.
- Schaar JA, Regar E, Mastik F, et al. Incidence of high-strain patterns in human coronary arteries: assessment with three-dimensional intravascular palpography and correlation with clinical presentation. *Circulation* 2004; 109: 2716–2719.
- Regar E, Schaar J, van der Giessen W, van der Steen AF, Serruys PW. Real-time, in-vivo optical coherence tomography of human coronary arteries using a dedicated imaging wire. *Am J Cardiol* 2002; 90: 129H.
- Asakura M, Ueda Y, Yamaguchi O, et al. Extensive development of vulnerable plaques as a pan-coronary process in patients with myocardial infarction: an angiographic study. *J Am Coll Cardiol* 2001; 37: 1284–1288.
- Burleigh MC, Briggs AD, Lendon CL, Davies MJ, Born GV, Richardson PD. Collagen types I and III, collagen content, GAGs and mechanical strength of human atherosclerotic plaque caps: span-wise variations. *Atherosclerosis* 1992; 96: 71–81.
- Loree HM, Kamm RD, Stringfellow RG, Lee RT. Effects of fibrous cap thickness on peak circumferential stress in model atherosclerotic vessels. *Circ Res* 1992; 71: 850–858.
- Bruining N, von Birgelen C, de Feyter PJ, et al. ECG-gated versus nongated three-dimensional intracoronary ultrasound analysis: implications for volumetric measurements. *Cathet Cardiovasc Diagn* 1998; 43: 254–260.
- von Birgelen C, de Vrey EA, Mintz GS, et al. ECG-gated three-dimensional intravascular ultrasound: feasibility and reproducibility of the automated analysis of coronary lumen and atherosclerotic plaque dimensions in humans. *Circulation* 1997; 96: 2944–2952.
- von Birgelen C, de Feyter PJ, de Vrey EA, et al. Simpson's rule for the volumetric ultrasound assessment of atherosclerotic coronary arteries: a study with ECG-gated three-dimensional intravascular ultrasound. *Coron Artery Dis* 1997; 8: 363–369.
- Saijo Y, Tanaka A, Owada N, Akino Y, Nitta S. Tissue velocity imaging of coronary artery by rotating-type intravascular ultrasound. *Ultrasonics* 2004; 42: 753–757.
- Schaar JA, De Korte CL, Mastik F, et al. Characterizing vulnerable plaque features with intravascular elastography. *Circulation* 2003; 108: 2636–2641.
- de Korte CL, van der Steen AF, Cespedes EI, Pasterkamp G. Intravascular ultrasound elastography in human arteries: initial experience *in vitro*. *Ultrasound Med Biol* 1998; 24: 401–408.
- Konofagou E, Ophir J. A new elastographic method for estimation and imaging of lateral displacements, lateral strains, corrected axial strains and Poisson's ratios in tissues. *Ultrasound Med Biol* 1998; 24: 1183–1199.
- Ge J, Haude M, Gorge G, Liu F, Erbel R. Silent healing of spontaneous plaque disruption demonstrated by intracoronary ultrasound. *Eur Heart J* 1995; 16: 1149–1151.
- Jeremias A, Ge J, Erbel R. New insight into plaque healing after plaque rupture with subsequent thrombus formation detected by intravascular ultrasound. *Heart* 1997; 77: 293.
- Ge J, Chirillo F, Schwedtmann J, et al. Screening of ruptured plaques in patients with coronary artery disease by intravascular ultrasound. *Heart* 1999; 81: 621–627.
- Rioufol G, Finet G, Ginon I, et al. Multiple atherosclerotic plaque rupture in acute coronary syndrome: a three-vessel

- intravascular ultrasound study. *Circulation* 2002; 106: 804–808.
19. Yamagishi M, Terashima M, Awano K, et al. Morphology of vulnerable coronary plaque: insights from follow-up of patients examined by intravascular ultrasound before an acute coronary syndrome. *J Am Coll Cardiol* 2000; 35: 106–111.
20. Arbab-Zadeh A, DeMaria AN, Penny WF, Russo RJ, Kimura BJ, Bhargava V. Axial movement of the intravascular ultrasound probe during the cardiac cycle: implications for three-dimensional reconstruction and measurements of coronary dimensions. *Am Heart J* 1999; 138: 865–872.

*Address for correspondence:* Prof. P.W. Serruys, Thoraxcenter, Bd 406, Dr. Molewaterplein 40, 3015-GD Rotterdam, The Netherlands  
Tel.: +31-10-4635260; Fax: +31-10-4369154  
E-mail: p.w.j.c.serruys@erasmusmc.nl

**10.1) Optical coherence tomography plaque  
characterization. Comparison with IVUS-VH.  
Handbook of optical coherence tomography.  
Taylor& Francis. 2006.**

**Rodriguez Granillo GA, Regar E, Serruys PW.**





## **OCT plaque characterization – comparison to IVUS VH**

Gastón A. Rodriguez-Granillo MD

Evelyn Regar MD, PhD

Patrick W. Serruys MD, PhD

From the Erasmus Medical Center, Rotterdam, The Netherlands

Angiography has been for decades the gold standard to assess the morphology and severity of atherosclerotic lesions in the coronary tree. Nevertheless, quantitative angiographic measurements can be deceptive since this technique only allows the assessment of the shape of the lumen <sup>1</sup>. In turn, atherosclerosis is a disease of the vessel wall and, due to the compensatory expansive remodelling effect, the lumen area remains unaffected until final stages of the disease <sup>2</sup>.

It has been established that unheralded acute coronary syndromes are common initial manifestations of coronary atherosclerosis and that most such events arise from sites with non-flow limiting coronary atherosclerosis <sup>3,4</sup>. Post-mortem studies suggested that plaque composition is a crucial determinant of the propensity of atherosclerotic lesions to rupture. Recently, a study including a large series of victims of sudden cardiac death suggested that ruptured thin-cap fibroatheroma (TCFA) lesions were the precipitating factor of 60 % of acute coronary thrombi. Furthermore, 70 % of those patients had other TCFA in their coronary tree that had not ruptured <sup>5</sup>. A large (avascular, hypocellular, lipid-rich) necrotic core, a thin fibrous cap with inflammatory infiltration and paucity of smooth muscle cells, and the presence of expansive (positive) remodeling have been identified as the major criteria to define TCFA lesions <sup>6,7-10</sup>.

Detection of these non-obstructive, lipid rich, high-risk plaques may have an important impact on the prevention of acute myocardial infarction and sudden death.

Currently, there are several intravascular tools capable of locally evaluating the aforementioned determinants of plaque vulnerability.

We will focus the chapter on the current status of optical coherence tomography (OCT) and spectral analysis of the radiofrequency data (IVUS-VH) and the potential of combining these intravascular diagnostic tools to enhance the prognostic value of invasive plaque characterization and vulnerable plaque imaging.

## Technical aspects of the techniques

### IVUS-VH

Intravascular ultrasound (IVUS) is the gold standard for evaluation of coronary plaque, lumen, and vessel dimensions; providing an accurate, reproducible, real-time, tomographic assessment of the vessel wall<sup>11-13</sup>. However, although visual interpretation of gray-scale IVUS can identify calcification within plaques, it cannot reliably differentiate lipid-rich from fibrous plaque<sup>12</sup>.

IVUS gray-scale imaging is formed by the envelope (amplitude) of the radiofrequency (RF) signal, discarding considerable amount of information lying beneath and between the peaks of the RF signal. The amplitude of the RF data might sometimes be similar between different tissues, leading to misinterpretation of gray-scale imaging. Nevertheless, the frequency and power of the RF signal commonly differs between tissues, regardless eventual similarities on the amplitude (Figure 1). Spectral analysis of the RF data (IVUS-VH, Volcano Corp., Rancho Cordoba, USA) evaluates different spectral parameters of the RF data (Y-intercept, minimum power, maximum power, mid-band power, frequency at minimum power, frequency at maximum power, slope, etc.) to construct tissue maps that classify plaque into four major components. In preliminary *in vitro* studies, four histological plaque components (fibrous, fibrolipidic, necrotic core and calcium) were correlated with a specific spectrum of the radiofrequency signal<sup>14</sup>. These different plaque components were assigned color codes. Calcified, fibrous, fibrolipidic and necrotic core regions were labeled white, green, greenish-yellow and red respectively (figure 2). This approach has led to a significant increase in the sensitivity and specificity of IVUS to characterize plaque, particularly of lipid deposits.

Indeed, the sensitivity of gray-scale to detect lipid deposits was reported as low as 46 %, whereas the predictive accuracy of IVUS to detect necrotic core areas is 86 %<sup>14,15</sup>.

Furthermore, recent improvements in the classification tree have led to a further enhancement in the accuracy of the technique and has been demonstrated using atherectomy samples, reaching a sensitivity and specificity higher than 90 % for detecting necrotic core<sup>16</sup>.

This technology has an axial, spatial and longitudinal resolution of 100, 240 and 300  $\mu\text{m}$  respectively.

IVUS-VH data is currently acquired using a commercially available phased-array (64 elements) catheter (Eagle Eye<sup>TM</sup> 20 MHz catheter, Volcano Corporation, Rancho Cordova, USA). Using an automated pullback device, the transducer is withdrawn at a continuous speed of 0.5 mm/s until the ostium. Cine runs, before and during contrast injection, are performed to define the position of the IVUS catheter before the pullback is started. IVUS-VH acquisition is ECG-gated at the R-tops using a dedicated console (Volcano Corporation, Rancho Cordova, USA).

### ***IVUS-VH analysis***

IVUS B-mode images are reconstructed from the RF data by customized software and contour detection is performed using cross-sectional views with a semi-automatic contour detection software to provide a quantitative geometrical and compositional output (IvusLab 4.4, Volcano Corporation, Rancho Cordova, USA). Due to the unreliability of manual calibration<sup>17</sup>, the RF data is normalized using a technique known as “Blind Deconvolution”, an iterative algorithm that deconvolves the catheter transfer function from the backscatter, thus accounting for catheter-to-catheter variability<sup>18</sup>.

## **Optical coherence tomography (OCT)**

In brief, Optical coherence tomography (OCT) imaging is based on low coherence near infrared light that is emitted by a superluminescent diode. A center wave length around 1300 nm is used since it minimizes the energy absorption in the light beam caused by protein, water, haemoglobin, and lipids. The light waves are reflected by the internal microstructures within biological tissues as a result of their differing optical indices.

OCT allows high-resolution (axial resolution of 10  $\mu\text{m}$  and lateral resolution of 20  $\mu\text{m}$ ) imaging in biological systems<sup>19</sup>. Accordingly, OCT is the technique with the highest capacity to allow *in-vivo*, real time visualization and measurement of a thin fibrous cap. The relative shallow penetration depth that hampers imaging of the entire vessel wall in medium and large vessels limits OCT imaging, however.

We have recently demonstrated that, in addition to high resolution qualitative analyses, highly reproducible OCT quantitative measurements can be achieved using an automated continuous pullback<sup>20</sup>. Nevertheless, the need to clear the artery from blood during imaging precludes interrogation of long and proximal segments of the coronary tree.

## **Plaque characterization and vulnerable plaque detection with OCT and IVUS-VH**

### **Qualitative and quantitative detection of necrotic core-rich plaques**

A recent *ex vivo* study has shown that OCT can discriminate 3 plaque types (fibrous, fibrocalcific and lipid-rich) with a sensitivity and specificity ranging between 71 and 98 %<sup>21</sup>. In this study, Yabushita et al. found that histologically confirmed fibrous plaques exhibited homogeneous, highly backscattering (signal-rich) plaques devoid of OCT signal-poor regions (figure 3, A). Similarly, fibrocalcific plaques were characteristically signal-poor with sharply delineated upper and/or lower borders (figure 3, B) whereas histologically confirmed lipid-rich plaques revealed diffusely bordered, signal-poor regions (figure 3, C).

Although OCT has demonstrated a high accuracy to characterize coronary plaques, imaging of the entire external elastic membrane is rarely achieved due to the shallow penetration of the technique (2 mm), precluding the quantitative analysis of each of the different plaque components. This limitation became manifest in a more recent *in vivo* study that showed no difference in lipid-rich plaques defined by OCT criteria between ACS and stable angina patients<sup>22</sup>. Since the risk of rupture and subsequent thrombosis is highly related to the relative lipid content, this limitation portrays a major shortcoming of OCT towards vulnerable plaque imaging<sup>7</sup>.

IVUS-VH capacity of identifying four different tissue components has been validated *ex vivo* with predictive accuracies 79.7%, 81.2%, 92.8%, and 85.5% for detecting fibrous tissue (areas of densely packed collagen), fibrolipidic tissue (areas with significant lipid interspersed in collagen), calcified tissue (areas with dense calcium deposits without adjacent necrosis) and necrotic core tissue (areas comprising cholesterol clefts, foam cells, and microcalcifications). Aside from the *ex vivo* validation study, we have performed the first clinical experiences and found indirect evidence about the *in vivo* validation of the technique. In particular, we sought to study sub-clinical atherosclerosis by evaluating the composition of non-culprit coronaries patients with IVUS-VH. In this study, we found that in non-culprit lesions, there were significant differences in plaque composition between patients who presented with acute coronary syndromes (ACS) and those who presented with stable angina (SA). In those with ACS, percent necrotic core was significantly greater than in stable patients, whereas a converse trend was observed for fibrotic content. In addition, we found a significant relationship between the necrotic core percentage and vessel area obstruction, suggesting that the necrotic core increases linearly with further increase in the degree of stenosis. Finally, we found a significant, albeit weak, relationship between relative necrotic core content and CRP levels<sup>23</sup>.

### Thin fibrous cap detection

As a result of its extremely high axial resolution (10  $\mu\text{m}$ ), there is no doubt that OCT is the *in vivo* gold standard for identifying and measuring the thickness of the fibrous cap<sup>22</sup>. In his study, Jang et al. identified a significant difference in minimal cap thickness between acute myocardial infarction (AMI) and SA patients, with median (interquartile range) values of 47.0 (25.3-184.3)  $\mu\text{m}$  and 102.6 (22.0-291.1)  $\mu\text{m}$  in AMI and SA patients respectively ( $p=0.02$ ).

On top of its reliability as a tool to measure the thickness of the cap *in vivo*, recent both post-mortem and *in vivo* studies have shown that OCT is capable of evaluating the macrophage content of infiltrated fibrous caps<sup>24,25</sup>.

We recently evaluated the incidence of IVUS-derived thin-cap fibroatheroma (IDTCFA) in coronary artery segments with non-significant lesions on angiography using IVUS-VH<sup>26</sup>. In this study, 2 experienced, independent IVUS analysts defined IDTCFA as a lesion fulfilling the following criteria in at least 3 consecutive cross-sectional areas: 1) necrotic core  $\geq 10\%$  without evident overlying fibrous tissue; 2) percent obstruction  $\geq 40\%$ . In this study, sixty-two percent of patients had at least one IDTCFA in the interrogated vessels. ACS patients had a significantly higher incidence of IDTCFA than stable patients [3.0 (interquartile range 0.0, 5.0) IDTCFA/coronary vs. 1.0 (interquartile range 0.0, 2.8) IDTCFA/coronary,  $p=0.018$ ]. Of note, no relation was found between patient's characteristics and the presence of IDTCFA. Finally, a clear clustering pattern was seen along the coronaries, with 66 (66.7%) IDTCFA located in the first 20 mm whereas further along the vessels the incidence was significantly lower (33, 33.3%,  $p=0.008$ )<sup>26</sup>. Such distribution of the IDTCFA in the coronaries was in line with previous *ex vivo* and clinical studies, with a clear clustering pattern from the ostium, thus supporting the non-uniform distribution of vulnerable plaques along the coronary tree<sup>27,28</sup>.

The significantly higher prevalence of IDTCFA in non-culprit coronaries of patients presenting with an ACS supports the theory that holds ACS as multifocal processes. Of note, the mean PAV and the mean necrotic core areas of the IDTCFAs detected by IVUS-VH were also similar to previously reported histopathological data (55.9 % vs. 59.6 % and 19 % vs. 23 % respectively)<sup>29</sup>.

It is worth mentioning that, although the most accepted threshold to define a cap as “thin” has previously been set at <65  $\mu\text{m}$ , this was based on post mortem studies<sup>30</sup>. Extrapolation of such criteria to *in vivo* studies requires caution. It is well established that tissue shrinkage occurs during tissue fixation<sup>31</sup>. Shrinkage (particularly of collagen tissue, the main component of fibrous caps) of up to 60 %, 15 % and 80% can occur during critical-point-drying, free-drying, and air-drying respectively<sup>32</sup>. Furthermore, post-mortem contraction of arteries is an additional confounding factor<sup>33</sup>. It is likely therefore, that the threshold used to define a thin cap *in vivo* should be higher than 65  $\mu\text{m}$ . Since the axial resolution of IVUS-VH is 100-150  $\mu\text{m}$ , we assumed that the absence of visible fibrous tissue overlying a necrotic core suggested a cap thickness of below 100-150  $\mu\text{m}$  and used the absence of such tissue to define a thin fibrous cap<sup>34</sup>. Finally, it is noteworthy that a number of important *ex vivo* studies have used a higher (> 200  $\mu\text{m}$ ) threshold<sup>9,35,36</sup>. Indeed, one of these studies identified a mean cap thickness of 260  $\mu\text{m}$  and 360 for “vulnerable” and “non-vulnerable” plaques respectively<sup>36</sup>. For all the aforementioned reasons, we believe that IVUS-VH is able to detect thin caps.

### **Positive remodelling detection**

Expansive remodelling of coronary vessels was originally deemed a beneficial compensatory effect that counterbalanced the axial progressive growth of the vessel wall to preserve the lumen dimensions<sup>2</sup>. However, several studies have shown increased levels of inflammatory markers, larger necrotic cores and pronounced medial thinning in positive remodelled vessels;

all factors related to the tendency of plaques to undergo rupture<sup>37-40</sup>. Overall, this has led the experts to confer positive remodelling a major importance in the vulnerability triad<sup>6</sup>.

Precise contour detection of the external elastic membrane (vessel area) is pivotal to estimate the presence and pattern of remodelling. Due to the high penetration of 20 MHz catheters, IVUS-VH can accurately assess vessel size and therefore, provided that plaque are not heavily calcified, estimate the degree and type of remodelling. This was recently demonstrated *in vivo*, where we found a significant positive relationship between relative necrotic core content and the remodelling index ( $r= 0.83$ ,  $p<0.0001$ ). Moreover, fibrous tissue was inversely correlated to the remodelling index ( $r= -0.45$ ,  $p=0.003$ , figure 3)<sup>40</sup>.

Likewise, lesions with positive remodelling presented significantly larger necrotic core percentages than lesions with no remodelling or negative remodelling ( $22.1\pm 6.3$  vs.  $15.1\pm 7.6$  vs.  $6.6\pm 6.9$  %,  $p<0.0001$ ). Conversely, negative remodelling lesions tend to show larger fibrous tissue percentages than lesions with no remodelling and positive remodelling ( $68.6\pm 13.7$  vs.  $62.9\pm 9.5$  vs.  $58.1\pm 12.9$  %,  $p=0.13$ ).

In contrast, and as aforementioned, OCT imaging of the entire media-adventitia interface is rarely achieved, precluding the use of OCT to assess the remodelling pattern of coronaries.

### **Combining OCT and IVUS-VH**

Throughout the chapter, we have discussed in detail the advantages and disadvantages of OCT and IVUS-VH for imaging coronary atherosclerotic plaques *in vivo* (tables 1 and 2). It is clear that the finest tool to assess the presence of the major criteria that define TCFA would be a tool that combines the optimal axial resolution of OCT with the accurate plaque characterization and deep penetration of IVUS-VH. Unfortunately, such tool has not yet been developed. Instead, intensive efforts are being made to overcome the weaknesses of both techniques. In the meantime, we are currently assessing *in vivo* the agreement between both

techniques to characterize plaques. Using side-branches as landmarks and with the aid of longitudinal and cross-sectional views, matching of cross-sections is feasible (figure 4). Our preliminary experience shows a high agreement between techniques towards the detection of fibrous, fibrocalcific and necrotic core regions (figures 5, 6 and 7).

Despite major advances in the management and diagnosis of patients with coronary artery disease, a large number of victims who are apparently healthy die suddenly without prior symptom<sup>41,42</sup>. Most of these events are related to plaque rupture and subsequent thrombotic occlusion at the site of non-flow limiting atherosclerotic lesions in epicardial coronary arteries.<sup>3,4</sup> In addition, silent plaque rupture and its subsequent wound healing accelerate plaque growth and are a more frequent feature in arteries with less severe luminal narrowing<sup>43</sup>. The prospective detection of TCFA lesions may have a major impact on the prevention of acute myocardial infarction and sudden death. Both OCT and IVUS-VH have demonstrated the ability to identify in vivo surrogates of TCFA. Nevertheless, prospective studies are needed in order to evaluate the prognostic value of such findings in natural history studies.

**References**

1. Topol EJ, Nissen SE. Our preoccupation with coronary luminology. The dissociation between clinical and angiographic findings in ischemic heart disease. *Circulation* 1995;92:2333-42.
2. Glagov S, Weisenberg E, Zarins CK, Stankunavicius R, Kolettis GJ. Compensatory enlargement of human atherosclerotic coronary arteries. *N Engl J Med* 1987;316:1371-5.
3. Ambrose JA, Tannenbaum MA, Alexopoulos D, Hjemdahl-Monsen CE, Leavy J, Weiss M, Borrico S, Gorlin R, Fuster V. Angiographic progression of coronary artery disease and the development of myocardial infarction. *J Am Coll Cardiol* 1988;12:56-62.
4. Little WC, Constantinescu M, Applegate RJ, Kutcher MA, Burrows MT, Kahl FR, Santamore WP. Can coronary angiography predict the site of a subsequent myocardial infarction in patients with mild-to-moderate coronary artery disease? *Circulation* 1988;78:1157-66.
5. Farb A, Burke AP, Tang AL, Liang TY, Mannan P, Smialek J, Virmani R. Coronary plaque erosion without rupture into a lipid core. A frequent cause of coronary thrombosis in sudden coronary death. *Circulation* 1996;93:1354-63.
6. Schaar JA, Muller JE, Falk E, Virmani R, Fuster V, Serruys PW, Colombo A, Stefanadis C, Ward Casscells S, Moreno PR, Maseri A, van der Steen AF. Terminology for high-risk and vulnerable coronary artery plaques. Report of a meeting on the vulnerable plaque, June 17 and 18, 2003, Santorini, Greece. *Eur Heart J* 2004;25:1077-82.
7. Davies MJ, Richardson PD, Woolf N, Katz DR, Mann J. Risk of thrombosis in human atherosclerotic plaques: role of extracellular lipid, macrophage, and smooth muscle cell content. *Br Heart J* 1993;69:377-81.
8. Gertz SD, Roberts WC. Hemodynamic shear force in rupture of coronary arterial atherosclerotic plaques. *Am J Cardiol* 1990;66:1368-72.

9. Felton CV, Crook D, Davies MJ, Oliver MF. Relation of plaque lipid composition and morphology to the stability of human aortic plaques. *Arterioscler Thromb Vasc Biol* 1997;17:1337-45.
10. Virmani R, Kolodgie FD, Burke AP, Farb A, Schwartz SM. Lessons from sudden coronary death: a comprehensive morphological classification scheme for atherosclerotic lesions. *Arterioscler Thromb Vasc Biol* 2000;20:1262-75.
11. Tobis JM, Mallery JA, Gessert J, Griffith J, Mahon D, Bessen M, Moriuchi M, McLeay L, McRae M, Henry WL. Intravascular ultrasound cross-sectional arterial imaging before and after balloon angioplasty in vitro. *Circulation* 1989;80:873-82.
12. Potkin BN, Bartorelli AL, Gessert JM, Neville RF, Almagor Y, Roberts WC, Leon MB. Coronary artery imaging with intravascular high-frequency ultrasound. *Circulation* 1990;81:1575-85.
13. Nishimura RA, Edwards WD, Warnes CA, Reeder GS, Holmes DR, Jr., Tajik AJ, Yock PG. Intravascular ultrasound imaging: in vitro validation and pathologic correlation. *J Am Coll Cardiol* 1990;16:145-54.
14. Nair A, Kuban BD, Tuzcu EM, Schoenhagen P, Nissen SE, Vince DG. Coronary plaque classification with intravascular ultrasound radiofrequency data analysis. *Circulation* 2002;106:2200-6.
15. Peters RJ, Kok WE, Havenith MG, Rijsterborgh H, van der Wal AC, Visser CA. Histopathologic validation of intracoronary ultrasound imaging. *J Am Soc Echocardiogr* 1994;7:230-41.
16. Nasu K TE, Katoh O, Margolis P, Vince DG, Virmani R, Takeda Y, Suzuki T. Correlation of in vivo intravascular ultrasound radiofrequency data analysis with in vitro histopathology in human coronary atherosclerotic plaques (VH-DCA Japan trial). *European Society of Cardiology, Stockholm* 2005.

17. Rodriguez-Granillo GA, Aoki J, Ong AT, Valgimigli M, Van Mieghem CA, Regar E, McFadden E, De Feyter P, Serruys PW. Methodological considerations and approach to cross-technique comparisons using in vivo coronary plaque characterization based on intravascular ultrasound radiofrequency data analysis: insights from the Integrated Biomarker and Imaging Study (IBIS). *Int J Cardiovasc Intervent* 2005;7:52-8.
18. Kåresen K. Deconvolution of sparse spike trains by iterated window maximization. *IEEE Trans Signal Process* 1997;45:1173-1183.
19. Hrynchak P, Simpson T. Optical coherence tomography: an introduction to the technique and its use. *Optom Vis Sci* 2000;77:347-56.
20. Regar E, Rodriguez-Granillo G, Bruining N, de Winter S, Hamers R, van Langenhove G, Verheye S, Serruys PW. Intracoronary Optical Coherence Tomography (OCT) - A Novel Approach for Three-Dimensional Quantitative Analysis. *German Society of Cardiology, Mannheim* 2004.
21. Yabushita H, Bouma BE, Houser SL, Aretz HT, Jang IK, Schlendorf KH, Kauffman CR, Shishkov M, Kang DH, Halpern EF, Tearney GJ. Characterization of human atherosclerosis by optical coherence tomography. *Circulation* 2002;106:1640-5.
22. Jang IK, Tearney GJ, MacNeill B, Takano M, Moselewski F, Iftima N, Shishkov M, Houser S, Aretz HT, Halpern EF, Bouma BE. In vivo characterization of coronary atherosclerotic plaque by use of optical coherence tomography. *Circulation* 2005;111:1551-5.
23. Rodriguez-Granillo GA, McFadden E, Valgimigli M, van Mieghem CAG, Regar E, de Feyter PJ, Serruys PW. Coronary plaque composition of non-culprit lesions assessed by in vivo intracoronary ultrasound radio frequency data analysis, is related to clinical presentation. *Am Heart J* 2005;Accepted.

- 24.** Tearney GJ, Yabushita H, Houser SL, Aretz HT, Jang IK, Schlendorf KH, Kauffman CR, Shishkov M, Halpern EF, Bouma BE. Quantification of macrophage content in atherosclerotic plaques by optical coherence tomography. *Circulation* 2003;107:113-9.
- 25.** MacNeill BD, Jang IK, Bouma BE, Iftimia N, Takano M, Yabushita H, Shishkov M, Kauffman CR, Houser SL, Aretz HT, DeJoseph D, Halpern EF, Tearney GJ. Focal and multifocal plaque macrophage distributions in patients with acute and stable presentations of coronary artery disease. *J Am Coll Cardiol* 2004;44:972-9.
- 26.** Rodriguez Granillo GA, Garcia-Garcia HM, Mc Fadden E, Valgimigli M, Aoki J, de Feyter P, Serruys PW. In Vivo Intravascular Ultrasound-Derived Thin-Cap Fibroatheroma Detection Using Ultrasound Radiofrequency Data Analysis. *J Am Coll Cardiol* 2005;46. In press.
- 27.** Kolodgie FD, Burke AP, Farb A, Gold HK, Yuan J, Narula J, Finn AV, Virmani R. The thin-cap fibroatheroma: a type of vulnerable plaque: the major precursor lesion to acute coronary syndromes. *Curr Opin Cardiol* 2001;16:285-92.
- 28.** Wang JC, Normand SL, Mauri L, Kuntz RE. Coronary artery spatial distribution of acute myocardial infarction occlusions. *Circulation* 2004;110:278-84.
- 29.** Virmani R, Burke AP, Kolodgie FD, Farb A. Vulnerable plaque: the pathology of unstable coronary lesions. *J Interv Cardiol* 2002;15:439-46.
- 30.** Burke AP, Farb A, Malcom GT, Liang YH, Smialek J, Virmani R. Coronary risk factors and plaque morphology in men with coronary disease who died suddenly. *N Engl J Med* 1997;336:1276-82.
- 31.** Lee RM. A critical appraisal of the effects of fixation, dehydration and embedding of cell volume. In: *The Science of Biological Specimen Preparation for Microscopy and Microanalysis*. Revel JP, Barnard T, Haggis GH (eds). *Scanning Electron Microscopy, AMF O'Hare*, 1984: pp.61-70.

32. Boyde A JS, Tamarin A. Dimensional changes during specimen preparation for scanning electron microscopy. *Scanning Electron Microscopy* 1977;507-518.
33. Fishbein MC, Siegel RJ. How big are coronary atherosclerotic plaques that rupture? *Circulation* 1996;94:2662-6.
34. Nair A CD, Vince DG. Regularized Autoregressive Analysis of Intravascular Ultrasound Data: Improvement in Spatial Accuracy of Plaque Tissue Maps. *IEEE Transactions on Ultrasonics, Ferroelectrics, and Frequency Control* 2004;51:420-431.
35. Mann JM, Davies MJ. Vulnerable plaque. Relation of characteristics to degree of stenosis in human coronary arteries. *Circulation* 1996;94:928-31.
36. Schaar JA, De Korte CL, Mastik F, Strijder C, Pasterkamp G, Boersma E, Serruys PW, Van Der Steen AF. Characterizing vulnerable plaque features with intravascular elastography. *Circulation* 2003;108:2636-41.
37. Pasterkamp G, Schoneveld AH, van der Wal AC, Haudenschild CC, Clarijs RJ, Becker AE, Hillen B, Borst C. Relation of arterial geometry to luminal narrowing and histologic markers for plaque vulnerability: the remodeling paradox. *J Am Coll Cardiol* 1998;32:655-62.
38. Varnava AM, Mills PG, Davies MJ. Relationship between coronary artery remodeling and plaque vulnerability. *Circulation* 2002;105:939-43.
39. Burke AP, Kolodgie FD, Farb A, Weber D, Virmani R. Morphological predictors of arterial remodeling in coronary atherosclerosis. *Circulation* 2002;105:297-303.
40. Rodriguez-Granillo GA, Serruys PW, Garcia-Garcia HM, Aoki J, Valgimigli M, van Mieghem CA, Mc Fadden E, de Jaegere PP, de Feyter P. Coronary artery remodelling is related to plaque composition. *Heart* 2005.
41. Kannel WB, Doyle JT, McNamara PM, Quickenton P, Gordon T. Precursors of sudden coronary death. Factors related to the incidence of sudden death. *Circulation* 1975;51:606-13.
42. Falk E, Shah PK, Fuster V. Coronary plaque disruption. *Circulation* 1995;92:657-71.

**43.** Burke AP, Kolodgie FD, Farb A, Weber DK, Malcom GT, Smialek J, Virmani R. Healed plaque ruptures and sudden coronary death: evidence that subclinical rupture has a role in plaque progression. *Circulation* 2001;103:934-40.

## TABLES

Table 1 Technical specifications of OCT and IVUS-VH

	Axial resolution	Penetration	Requires flushing/occlusion	Guiding catheter
<b>OCT</b>	10 $\mu\text{m}$	$\sim 2$ mm	yes	8F
<b>IVUS-VH</b>	100-150 $\mu\text{m}$	$\sim 10$ mm	no	5F

OCT refers to optical coherence tomography. IVUS-VH refers to spectral analysis of intravascular ultrasound radiofrequency data.

**Table 2** Ability to detect the major criteria of vulnerability<sup>6</sup>

	Thickness of the cap	Macrophages	Quantification of necrotic core	Remodelling
<b>OCT</b>	+++	+++	+	NA
<b>IVUS-VH</b>	++	NA	+++	++

OCT refers to optical coherence tomography. IVUS-VH refers to spectral analysis of intravascular ultrasound radiofrequency data.

**Legends**

- Figure 1. IVUS gray-scale imaging is formed by the envelope (amplitude) of the radiofrequency (RF) signal, discarding considerable amount of information lying beneath and between the peaks of the RF signal. The frequency of a tissue may differ despite having the same amplitude.
- Figure 2. The left panel shows an IVUS cross-sectional area reconstructed from backscattered signals. The right panel shows the corresponding tissue map depicting where the different plaque components are assigned color codes. Calcified, fibrous, fibrolipidic and necrotic core regions are labeled white, green, greenish-yellow and red respectively.
- Figure 3. Examples of OCT cross-sections of: fibrous concentric intimal thickening exhibiting a homogeneous, highly backscattering (signal-rich) intima (i) devoid of OCT signal-poor regions (panel A); a calcified (c) plaque (panel B, signal-poor with sharply delineated borders) with overlying fibrous cap; and a lipid-rich (l) plaque depicting diffusely bordered, signal-poor regions (panel C). M refers to media.
- Figure 4. Matching of OCT and IVUS-VH is feasible using side-branches as landmarks and longitudinal and cross-sectional views.
- Figure 5. Matched imaging immediately distal to a stent showing an eccentric fibrotic plaque with both techniques.

Figure 6. Matched imaging distal to sidebranch (\*) showing fibrotic tissue at 12 o'clock and 7 o'clock, whereas a heterogeneous, signal-poor region is located at 9 o'clock and correlated well with a necrotic-core-rich region with IVUS-VH.

Figure 7. From left to right: IVUS cross-sectional area reconstructed from backscattered signals showing a small calcified region at 6 o'clock. IVUS-VH shows a necrotic core-rich tissue with underlying calcified tissue. A lipid-rich region with underlying calcified tissue can be appreciated with OCT imaging.

**FIGURES**

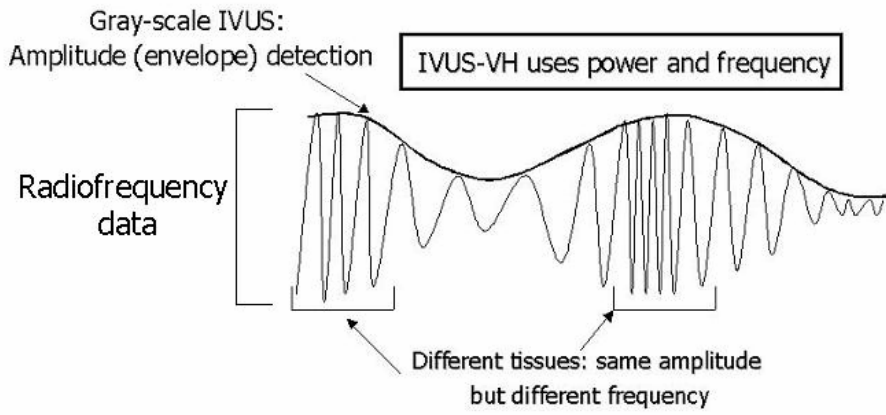


Figure 1

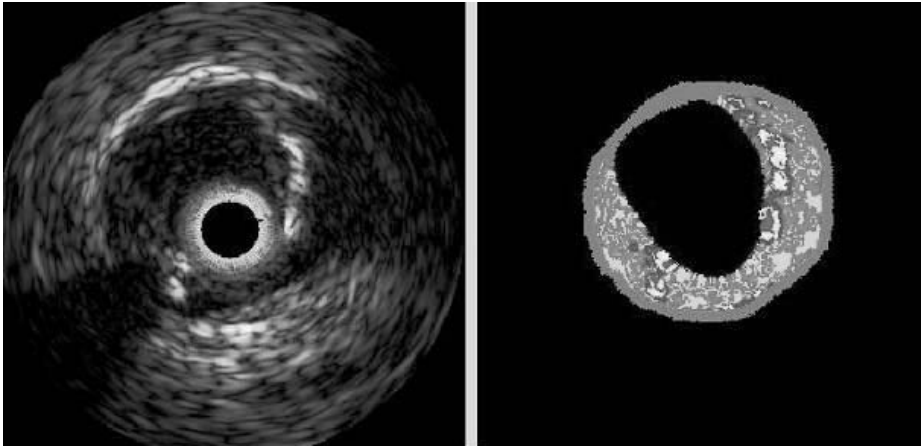


Figure 2

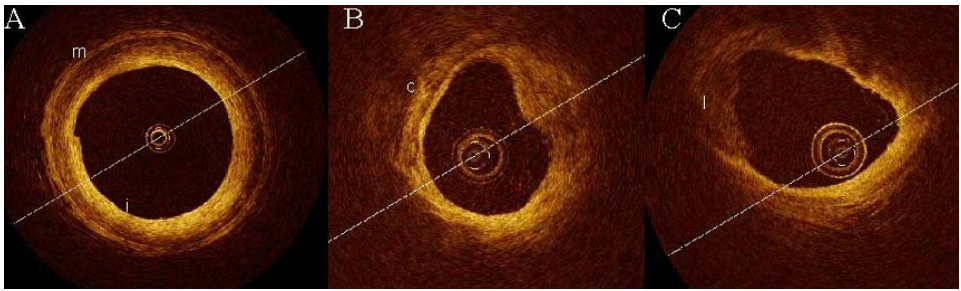


Figure 3

Colour figures on pages 441-449

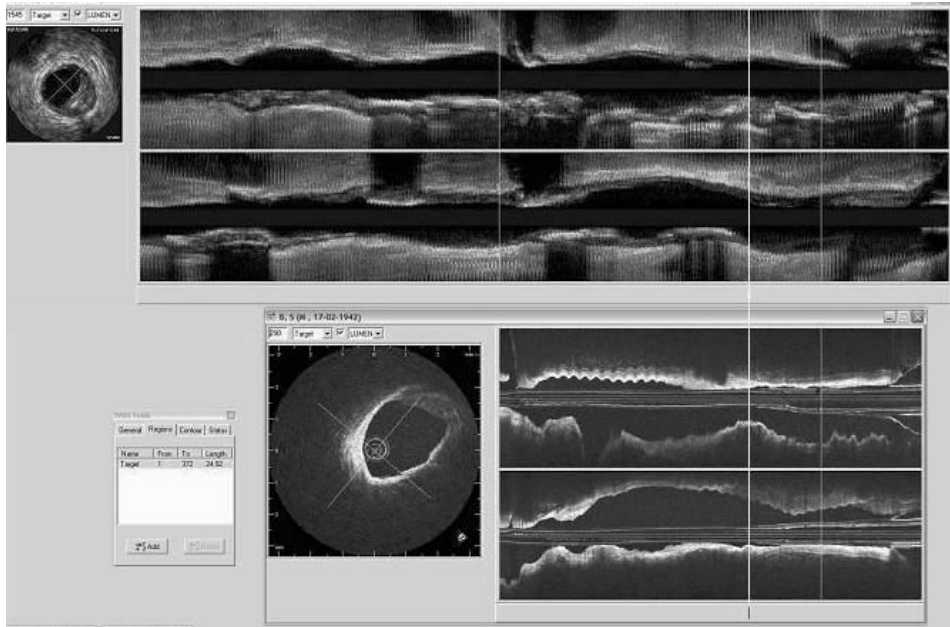


Figure 4

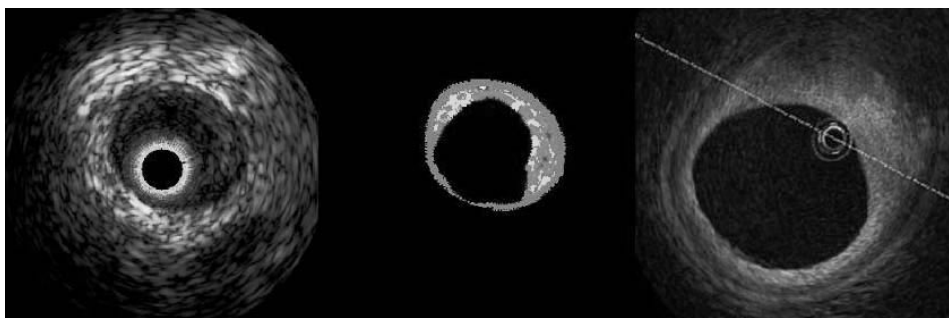


Figure 5

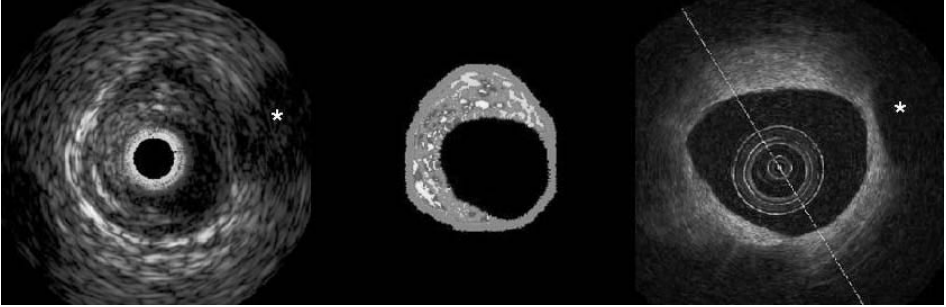


Figure 6

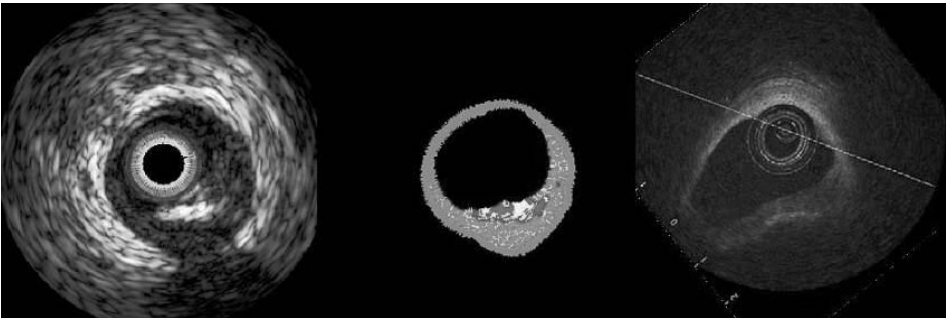
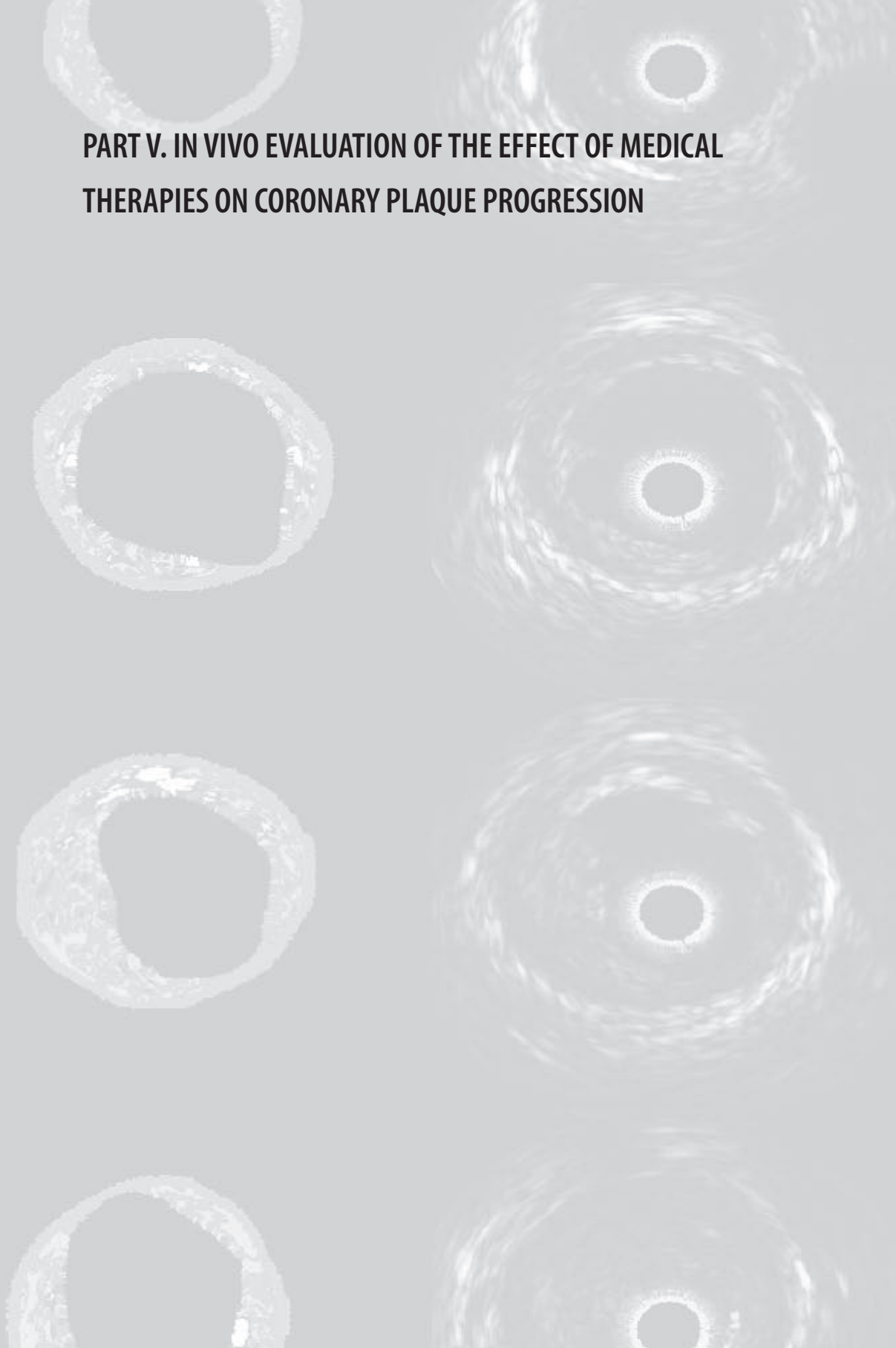


Figure 7



**PART V. IN VIVO EVALUATION OF THE EFFECT OF MEDICAL  
THERAPIES ON CORONARY PLAQUE PROGRESSION**







**11.1) Statin therapy promotes plaque regression: a meta-analysis of the studies assessing temporal changes in coronary plaque volume using intravascular ultrasound.**

**Submitted**

**Rodríguez Granillo GA, Agostoni P, García-García HM et al.**



## **Statin therapy promotes plaque regression in coronary artery segments:**

### **A meta-analysis of the studies assessing temporal changes in coronary plaque volume using intra-vascular ultrasound.**

Gastón A. Rodriguez-Granillo MD<sup>1,2</sup>

Pierfrancesco Agostoni MD<sup>3</sup>

Héctor M. Garcia-Garcia MD<sup>1</sup>

Giuseppe G. L. Biondi-Zoccai, MD<sup>4</sup>

Eugène Mc Fadden MD, FRCPI<sup>1</sup>

Giovanni Amoroso MD, PhD<sup>5</sup>

Peter de Jaegere MD, PhD<sup>1</sup>

Nico Bruining PhD<sup>1</sup>

Pim de Feyter MD, PhD<sup>1</sup>

Patrick W. Serruys MD, PhD<sup>1</sup>

<sup>1</sup> Department of Cardiology, Thoraxcenter, Erasmus Medical Center, Rotterdam, The Netherlands

<sup>2</sup> Department of Cardiovascular Imaging, Otamendi Hospital, Buenos Aires, Argentina

<sup>3</sup> Antwerp Cardiovascular Center Middelheim, AZ Middelheim, Antwerp, Belgium

<sup>4</sup> Hemodynamics and Cardiovascular Radiology Service, Policlinico San Donato, Milan, Italy

<sup>5</sup> Onze Lieve Vrouw Gasthuis, Amsterdam, The Netherlands



**Abstract**

**Aims:** To assess the temporal effect of statin therapy on coronary atherosclerotic plaque volume as measured by intravascular ultrasound (IVUS).

**Methods and results:** We searched PubMed for eligible studies published between 1990 and January 2006. Inclusion criteria for retrieved studies were: 1) IVUS volume analysis at baseline and follow-up 2) statin therapy in at least one group of patients. Nine studies including 985 patients (with 11 statin treatment arms) were selected. After a mean follow-up of  $9.8 \pm 4.9$  months, we found a significant reduction in coronary plaque volume [WMD  $-5.77 \text{ mm}^3$  (95%CI  $-10.36, -1.17$ ,  $p=0.01$ )], with no significant heterogeneity between studies ( $p= 0.47$ ). Pre-specified subgroup analyses showed similar trends. Studies where the achieved LDL-cholesterol level was lower than 100 mg/dl showed a trend for plaque regression [WMD  $-7.88 \text{ mm}^3$  (95%CI  $-16.31, 0.55$ ,  $p=0.07$ )] whereas studies where the achieved LDL-C was  $\geq 100$  mg/dl the trend was less evident [WMD  $-4.22 \text{ mm}^3$  (95%CI  $-10.27, 1.82$ ,  $p=0.17$ )]. Plaque volume remained substantially unchanged in patients not treated with statins [WMD  $0.13 \text{ mm}^3$  (95%CI  $-4.42, 4.68$ ,  $p=0.96$ )].

**Conclusions:** Statin therapy, in particular when achieving the target LDL level, appears to promote a significant regression of coronary plaque volume as measured by IVUS.

**Key Words:** statins; atherosclerosis; ultrasonography; plaque progression

**Introduction**

Lipid lowering therapies have been shown to strikingly improve clinical outcomes of patients with coronary artery disease, both in the primary and secondary prevention realms.<sup>1,2</sup> In addition, statin therapy is currently regarded as an effective strategy to reduce coronary atherosclerosis progression, evaluated with angiography.<sup>3</sup> Nonetheless, angiographic measurements can be misleading since they only allow the evaluation of the silhouette of the lumen, while atherosclerosis is commonly a diffuse disease of the vessel wall. Moreover, the evaluation of the remodeling phenomenon often present in coronary arteries is essential for the interpretation of the treatment effect but cannot be assessed by angiography, yielding to poor *ex vivo* correlation.<sup>4</sup>

In order to assess more accurately plaque size and distribution, intravascular ultrasound (IVUS) has evolved as a precise invasive tool that is being increasingly used to quantitatively determine the extent, spatial distribution, and morphology of the atherosclerotic disease.

A significant statin-induced regression of atherosclerotic plaque burden was recently reported in peripheral arteries.<sup>5-7</sup> However, despite several studies evaluated the effect of statins in coronary arteries, plaque regression has not been conclusively demonstrated.

We thus performed a meta-analysis of all clinical studies that assessed IVUS-based progression/regression of coronary atherosclerosis to evaluate whether the treatment with statins can promote coronary plaque regression over time.

## **Methods**

### **Search strategy**

Two trained investigators (G.A.R.G. and P.A.) searched PubMed for eligible studies published in peer review journals between January 1990 and January 2006. Search key words included: “(reduc\* OR regres\* OR progress\*) AND (ivus OR intravascular ultrasound)”, where \* denotes a wildcard, which is a symbol used to search all the words beginning with the written root. PubMed was searched using the method described by Biondi-Zoccai et al.<sup>8</sup> No language restriction was used. Cross-references were checked and experts were contacted to identify other relevant trials.

### **Selection strategy**

Citations initially selected by systematic search were first retrieved as title and/or abstract and screened independently by two reviewers (G.A.R.G. and P.A.). Potentially relevant reports were then retrieved as complete manuscripts and assessed for compliance to inclusion and exclusion criteria.

Inclusion criteria for retrieved studies were: 1) IVUS volume analysis in native coronary arteries at baseline and follow-up 2) statin therapy in at least one group of patients.

Exclusion criteria were: 1) no volumetric output (only cross-sectional area analysis), 2) studies in vessels different from coronary arteries.

### **Data extraction and end-point definitions**

All the data of interest were abstracted in pre-specified structured collection forms.

Every study used the same IVUS imaging catheter both at baseline and follow-up. All IVUS investigations were performed after intracoronary administration of nitrates. Cine runs, before and during contrast injection, were performed to define the position of the

catheter distal to an identifiable side-branch. Using an automated pullback device, the transducer was withdrawn at a continuous speed of 0.5 mm/s and IVUS data was stored on super-VHS for subsequent analysis. Our primary end-point of interest was the progression/regression of coronary atherosclerotic burden evaluated by IVUS volumetric analysis. According to the different studies included in the analysis, plaque volume was calculated as:  $\sum_{m=1}^n (\text{Vessel}_{\text{area}} - \text{Lumen}_{\text{area}}) * d$ ; where n refers to number of images, m to image and d to distance between images. In case this data were not provided in the published manuscript, the authors were contacted to obtain the aforementioned values.

We compared baseline vs. follow-up plaque volume in the patients receiving statins and in the control group (when present). In addition, as sensitivity analyses, we stratified the studies according to achieved LDL-C levels and time to follow-up seeking an enlightenment of the results.

### **Data analysis**

Statistical analysis was performed using the Review Manager 4.2 freeware package.<sup>9</sup> Continuous variables are reported as mean  $\pm$  standard deviation unless otherwise specified. Random-effect weighted mean difference (WMD) with 95% confidence intervals (CI), was used as summary statistics for the comparison of continuous variables; this analysis is utilized when the unit of measure of the variable under analysis remains constant across the different studies.<sup>10</sup> The currently recommended inverse variance-weighting method, according to Dersimonian and Laird, was used for random-effect comparison.<sup>10</sup> Reported values were two-tailed and results were considered statistically significant at p value  $<0.05$ . Statistical heterogeneity (i.e. the between-study discrepancy in effect size estimates) was assessed with the Cochran Q test. This test strongly suggests underlying statistical heterogeneity for p values  $<0.10$ ,

even if other causes of heterogeneity (such as clinical differences between treatment, follow-up duration, or patient population should not be dismissed). The appraisal of statistical heterogeneity is pivotal to meta-analysis as some authorities advocate the statistical pooling of different trials only in the presence of statistical homogeneity <sup>10</sup>. Finally, to assess the risk of small study bias (including publication bias), we built a funnel plot by graphically showing the relationship between effect size and statistical weight for each individual study. A symmetrical and funnel-shaped plot supports the lack of significant small study bias, while a strongly asymmetric plot suggests the underlying presence of small study or publication bias (i.e. where smaller studies reporting positive outcomes were more likely to be published than equally small studies reporting negative or non-significant results). Publication bias, if not recognized and acknowledged, can lead to meta-analyses with biased and overly optimistic findings, and should thus be actively investigated and appraised <sup>10</sup>.

## Results

PubMed queries permitted the retrieval of 977 citations. The majority of the papers were excluded because they were editorials, reviews or studies addressing the role of IVUS as an adjunctive tool to percutaneous coronary interventions. Finally, 18 papers were assessed for compliance to inclusion and exclusion criteria, leading to further exclusion of 9 studies. One study was not included since only area measurements and not volume analyses were reported<sup>11</sup>. One study did not include a treatment arm<sup>12</sup>. Three other studies were excluded because they evaluated IVUS in femoral arteries and transplant-associated arteriosclerosis<sup>13-15</sup>. One study used antihypertensive agents and three others used lipid lowering therapies different from statins<sup>16-19</sup>. Nine published studies were finally selected<sup>17,20-27</sup>.

The 9 studies included 985 patients. The majority of the studies were randomized comparisons of a statin vs. placebo, aside from the study of Jensen et al. that was a single arm observational study. In the randomized REVERSAL trial both arms received statins, but different molecules, and in the study by Kawasaki et al., there were three groups: two receiving 2 different statins and one receiving placebo. Thus, overall 784 patients were allocated to statin treatment in 11 different groups (table 1).

All studies used the absolute change in plaque volume in a matched region of interest evaluated at the longest available follow-up as an imaging endpoint, apart from the study by Petronio et al., that reported the change in plaque volume adjusted for analyzed vessel length. We contacted the authors to obtain the absolute change in plaque volume.

In the GAIN study, patients were allocated to atorvastatin in an increasing dose to achieve a LDL-cholesterol level < 100 mg/dL or placebo.<sup>21</sup> For the ESTABLISH study, 20 mg/d of atorvastatin vs. placebo were administrated.<sup>20</sup> In contrast, the REVERSAL

investigators compared an intensive lipid lowering therapy with a moderate one (atorvastatin 80 mg/day vs. pravastatin 40 mg/day).<sup>28</sup> Kawasaki et al. compared 20 mg/day of atorvastatin vs. 20 mg/day of pravastatin vs. placebo.<sup>26</sup> Petronio et al. compared 20 mg/day of simvastatin vs. placebo.<sup>24</sup> The study of Yokoyama et al. compared 10 mg/day of atorvastatin vs. placebo control.<sup>25</sup> Nishioka et al. compared the administration of different statin regimens (pravastatin 10 mg/day, atorvastatin 10 mg/day, simvastatin 5 mg/day or fluvastatin 20 mg/day) vs. placebo control.<sup>23</sup> Tani et al compared pravastatin 10 mg/d in patients whose LDL-C level was < 140 mg/dl or 20 mg/d in patients whose LDL-C level was > 140 mg/dl vs. control.<sup>27</sup> Finally, patients in the observational study of Jensen et al. received increasing doses of simvastatin to reach an LDL-cholesterol level <3.0 mmol/L.<sup>22</sup>

Except from 2 studies<sup>20,23</sup>, all investigation excluded patients presenting with an acute coronary syndrome.

### ***Effect on coronary plaque volume***

Figure 1 shows the WMD in plaque volume between follow-up and baseline with respective 95% CI at a mean follow-up of 9.8±4.9 months. There was a significant reduction in coronary plaque volume over time [WMD -5.77 mm<sup>3</sup> (95%CI -10.36, -1.17, p=0.01)], with no significant heterogeneity between studies (p=0.47).

According to pre-specified subgroup analyses evaluating the studies according to the length of the follow-up (table 2), similar trends were noted either in studies with a 6-month follow-up [158 patients, WMD -5.07 mm<sup>3</sup> (95%CI -10.67, 0.53, p=0.08)], or in studies with longer follow-up [626 patients, WMD -6.67 mm<sup>3</sup> (95%CI -19.62, 6.28, p=0.31)], albeit significant plaque regression did not occur, possibly due to a smaller sample size. No significant heterogeneity (p=1.00) between studies was found for the

former subgroup analysis, whereas a significant heterogeneity between studies was present for the later analysis ( $p=0.06$ ).

Studies where the achieved LDL-C level was lower than 100 mg/dl showed a strong trend for plaque regression [443 patients, [WMD  $-7.88 \text{ mm}^3$  (95%CI  $-16.31, 0.55$ ,  $p=0.07$ )]. Conversely, studies where the LDL-cholesterol achieved was higher than 100 mg/dl showed that the trend toward plaque regression (table 3) was less evident [341 patients, WMD  $-4.22 \text{ mm}^3$  (95%CI  $-10.27, 1.82$ ,  $p=0.17$ )]. Also in these subgroup analyses, no significant heterogeneity between studies (respectively  $p=0.23$  and  $p=0.76$ ) was noted.

After a mean follow-up of  $7.7\pm 2.9$  months, plaque volume remained substantially unchanged when evaluating the control groups not receiving statin therapy (7 groups, 206 patients [WMD  $0.13 \text{ mm}^3$  (95%CI  $-4.42, 4.68$ ,  $p=0.96$ )], with no heterogeneity between studies ( $p=0.83$ ).

Figures 2 and 3 show the WMD between follow-up and baseline in lumen and in vessel volume respectively, in patients receiving statin therapy. There was no significant change in coronary lumen volume over time [WMD  $1.20 \text{ mm}^3$  (95%CI  $-3.48, 5.88$ ,  $p=0.61$ )], with no significant heterogeneity between studies ( $p=0.99$ ). There was also no significant change in vessel volume over time [WMD  $-1.48 \text{ mm}^3$  (95%CI  $-10.06, 7.09$ ,  $p=0.73$ )], with no significant heterogeneity between studies ( $p=1.00$ ).

Finally, the funnel plot showed no evidence of publication bias (figure 4).

## Discussion

In the present systematic overview, statins were found to promote significant coronary plaque regression as assessed by IVUS. Nine studies and 11 statin arms were included in this meta-analysis where after a follow-up of around 10 months a significant regression of coronary atherosclerotic plaque volume was evident. Our data are further supported by the substantial statistical homogeneity between the included studies.

Atherosclerosis is a dynamic disease. The presence of cardiovascular risk factors has been related to endothelial dysfunction<sup>29</sup> and such impairment was found to lead to increased permeability, extracellular accumulation of lipids, smooth muscle cell proliferation and ultimately linear progression of plaque.<sup>30</sup> On the other hand, it has been clearly established that plaque rupture and its subsequent healing can cause rapid progression.<sup>31,32</sup> Hence, the natural history of atherosclerotic plaque is unpredictable, lacking a constant growth pattern.

Atherosclerotic plaque regression after the onset of an intensive statin therapy strategy has been previously reported in the peripheral circulation.<sup>5-7,33</sup> The mechanisms involved in such process are still not fully elucidated, being so far ascribed to changes in LDL-C and HDL-C.<sup>5,18,34</sup> It has been suggested that, by decreasing the lipid content of plaques and promoting a shift towards a more stable phenotype, statins may induce a “plaque stabilization” effect. Indeed, 3 of the studies included in the present meta-analysis found significant differences in surrogates of plaque composition despite no significant changes in plaque volume.<sup>21,25,26</sup> Furthermore, statins have shown to reduce the inflammatory burden of plaques as well as to improve the endothelial function.<sup>35-37</sup>

It is likely therefore that the antiatherosclerotic effect of statins is pleomorphic and effective against the two major mechanisms of atherosclerotic plaque progression.

Aside from the aforementioned unpredictability of the disease, differences in the baseline atherosclerotic burden, in the intensity of the installed therapies and in patient demographics make the time-to biological effect hard to determine. Former clinical studies suggested that statin-induced plaque regression was only attainable after at least one-year of therapy.<sup>11,33</sup> In turn, and in line with histopathological studies that demonstrated an early stabilizing and reductive effect of statins on atherosclerotic plaque,<sup>5,38</sup> we did not identify a major difference in the outcome of studies with short and long-term follow-up (table 2). Separately and interestingly, studies in which the achieved LDL-C level was <100 mg/dl, showed a strong trend towards regression (table 3), supporting the association between the changes LDL-C and plaque volume.<sup>28</sup> This finding was in line with a recent non-invasive imaging study that identified a greater regression in patients who reached an LDL-C level < 100 mg/dl.<sup>6</sup> Finally, it is noteworthy that the reduction in plaque volume did not imply a significant increase in lumen volume, confirming the lack of sensitivity of conventional angiography to detect the effect of statins on the change in lumen size.

Overall, our data endorses the LDL-C target level proposed by the NCEP Adult Treatment Panel-III guidelines and should add evidence to further encourage physicians to enhance their attempt to reach such goal.

The results of our meta-analysis are indirectly further reinforced by the lack of regression in patients assigned to placebo. In these patients no substantial modification of plaque volume was noted over time.

Although IVUS is a highly accurate tool to measure changes in the vessel wall, factors such as intra- and inter-observer variability, severely calcified vessels and artifacts can impair the reproducibility of serial measurements.<sup>39,40,41</sup> It is therefore important to

establish new standards regarding the acquisition, analysis and reporting of IVUS clinical studies.

The present meta-analysis demonstrates that a significant reduction in coronary plaque volume, measured invasively, can be achieved using statin therapy. Still, the discordance between the clinical effects of statins and their effects on plaque volume remains striking. An adjunctive significant effect on plaque composition may potentially explain such difference and is currently the subject of intensive research efforts.<sup>21,25,26</sup>

### **Limitations**

This meta-analysis was not based on individual data. Furthermore, only one vessel was interrogated with IVUS, potentially not being representative of the total burden of the entire coronary tree. Although no significant heterogeneity was present between studies, bias adjudicated to small trials cannot be fully disregarded. Furthermore, minor differences regarding IVUS methodology could potentially influence our findings.

### **Conclusions**

Statin therapy, in particular when achieving the target LDL-C < 100 mg/dl level, appears to promote a significant regression of plaque volume in coronary artery segments as measured by IVUS.

## References

1. Randomised trial of cholesterol lowering in 4444 patients with coronary heart disease: the Scandinavian Simvastatin Survival Study (4S). *Lancet*. 1994;344:1383-9.
2. Downs JR, Clearfield M, Weis S, Whitney E, Shapiro DR, Beere PA, Langendorfer A, Stein EA, Kruyer W, Gotto AM, Jr. Primary prevention of acute coronary events with lovastatin in men and women with average cholesterol levels: results of AFCAPS/TexCAPS. Air Force/Texas Coronary Atherosclerosis Prevention Study. *Jama*. 1998;279:1615-22.
3. Balk EM, Karas RH, Jordan HS, Kupelnick B, Chew P, Lau J. Effects of statins on vascular structure and function: A systematic review. *Am J Med*. 2004;117:775-90.
4. Grodin CM, DI, Pastgernac A, et al. Discrepancies between cineangiographic and post-mortem findings in patients with coronary artery disease and recent myocardial revascularization. *Circulation*. 1974;49:703-709.
5. Lima JA, Desai MY, Steen H, Warren WP, Gautam S, Lai S. Statin-induced cholesterol lowering and plaque regression after 6 months of magnetic resonance imaging-monitored therapy. *Circulation*. 2004;110:2336-41.
6. Corti R, Fuster V, Fayad ZA, Worthley SG, Helft G, Chaplin WF, Muntwyler J, Viles-Gonzalez JF, Weinberger J, Smith DA, Mizsei G, Badimon JJ. Effects of aggressive versus conventional lipid-lowering therapy by simvastatin on human atherosclerotic lesions: a prospective, randomized, double-blind trial with high-resolution magnetic resonance imaging. *J Am Coll Cardiol*. 2005;46:106-12.

7. Yonemura A, Momiyama Y, Fayad ZA, Ayaori M, Ohmori R, Higashi K, Kihara T, Sawada S, Iwamoto N, Ogura M, Taniguchi H, Kusuhara M, Nagata M, Nakamura H, Tamai S, Ohsuzu F. Effect of lipid-lowering therapy with atorvastatin on atherosclerotic aortic plaques detected by noninvasive magnetic resonance imaging. *J Am Coll Cardiol.* 2005;45:733-42.
8. Biondi-Zoccai GG, Agostoni P, Abbate A, Testa L, Burzotta F. A simple hint to improve Robinson and Dickersin's highly sensitive PubMed search strategy for controlled clinical trials. *Int J Epidemiol.* 2005;34:224-5; author reply 225.
9. 4.2. Review Manager. Available from The Cochrane Collaboration at <http://www.cochrane.org>. Accessed: November 29, 2004.).
10. Clarke M OA. Cochrane reviewer's Handbook 4.2.0 [Updated March 2003]. In: *The Cochrane Library, Issue 2, 2003. Oxford, UK: Update Software.*
11. Takagi T, Yoshida K, Akasaka T, Hozumi T, Morioka S, Yoshikawa J. Intravascular ultrasound analysis of reduction in progression of coronary narrowing by treatment with pravastatin. *Am J Cardiol.* 1997;79:1673-6.
12. von Birgelen C, Hartmann M, Mintz GS, Baumgart D, Schmermund A, Erbel R. Relation between progression and regression of atherosclerotic left main coronary artery disease and serum cholesterol levels as assessed with serial long-term (> or =12 months) follow-up intravascular ultrasound. *Circulation.* 2003;108:2757-62.
13. Hagenshaars T, Gussenhoven EJ, Kranendonk SE, Blankensteijn JD, Honkoop J, van der Linden E, van der Lugt A. Early experience with intravascular ultrasound in evaluating the effect of statins on femoropopliteal arterial disease: hypothesis-generating observations in humans. *Cardiovasc Drugs Ther.* 2000;14:635-41.

14. Fang JC, Kinlay S, Beltrame J, Hikiti H, Wainstein M, Behrendt D, Suh J, Frei B, Mudge GH, Selwyn AP, Ganz P. Effect of vitamins C and E on progression of transplant-associated arteriosclerosis: a randomised trial. *Lancet*. 2002;359:1108-13.
15. Kapadia SR, Nissen SE, Ziada KM, Rincon G, Crowe TD, Boparai N, Young JB, Tuzcu EM. Impact of lipid abnormalities in development and progression of transplant coronary disease: a serial intravascular ultrasound study. *J Am Coll Cardiol*. 2001;38:206-13.
16. Matsuzaki M, Hiramori K, Imaizumi T, Kitabatake A, Hishida H, Nomura M, Fujii T, Sakuma I, Fukami K, Honda T, Ogawa H, Yamagishi M. Intravascular ultrasound evaluation of coronary plaque regression by low density lipoprotein-apheresis in familial hypercholesterolemia: the Low Density Lipoprotein-Apheresis Coronary Morphology and Reserve Trial (LACMART). *J Am Coll Cardiol*. 2002;40:220-7.
17. Nissen SE, Tuzcu EM, Libby P, Thompson PD, Ghali M, Garza D, Berman L, Shi H, Buebendorf E, Topol EJ. Effect of antihypertensive agents on cardiovascular events in patients with coronary disease and normal blood pressure: the CAMELOT study: a randomized controlled trial. *Jama*. 2004;292:2217-25.
18. Nissen SE, Tsunoda T, Tuzcu EM, Schoenhagen P, Cooper CJ, Yasin M, Eaton GM, Lauer MA, Sheldon WS, Grines CL, Halpern S, Crowe T, Blankenship JC, Kerensky R. Effect of recombinant ApoA-I Milano on coronary atherosclerosis in patients with acute coronary syndromes: a randomized controlled trial. *Jama*. 2003;290:2292-300.

19. Tardif JC, Gregoire J, L'Allier PL, Anderson TJ, Bertrand O, Reeves F, Title LM, Alfonso F, Schampaert E, Hassan A, McLain R, Pressler ML, Ibrahim R, Lesperance J, Blue J, Heinonen T, Rodes-Cabau J. Effects of the acyl coenzyme A:cholesterol acyltransferase inhibitor avasimibe on human atherosclerotic lesions. *Circulation*. 2004;110:3372-7.
20. Okazaki S, Yokoyama T, Miyauchi K, Shimada K, Kurata T, Sato H, Daida H. Early statin treatment in patients with acute coronary syndrome: demonstration of the beneficial effect on atherosclerotic lesions by serial volumetric intravascular ultrasound analysis during half a year after coronary event: the ESTABLISH Study. *Circulation*. 2004;110:1061-8.
21. Scharfl M, Bocksch W, Koschyk DH, Voelker W, Karsch KR, Kreuzer J, Hausmann D, Beckmann S, Gross M. Use of intravascular ultrasound to compare effects of different strategies of lipid-lowering therapy on plaque volume and composition in patients with coronary artery disease. *Circulation*. 2001;104:387-92.
22. Jensen LO, Thayssen P, Pedersen KE, Stender S, Haghfelt T. Regression of coronary atherosclerosis by simvastatin: a serial intravascular ultrasound study. *Circulation*. 2004;110:265-70.
23. Nishioka H, Shimada K, Kataoka T, Hirose M, Asawa K, Hasegawa T, Yamashita H, Ehara S, Kamimori K, Sakamoto T, Kobayashi Y, Yoshimura T, Yoshiyama M, Takeuchi K, Yoshikawa J. Impact of HMG-CoA reductase inhibitors for non-treated coronary segments. *Osaka City Med J*. 2004;50:61-8.
24. Petronio AS, Amoroso G, Limbruno U, Papini B, De Carlo M, Micheli A, Ciabatti N, Mariani M. Simvastatin does not inhibit intimal hyperplasia and restenosis but promotes plaque regression in normocholesterolemic patients

- undergoing coronary stenting: a randomized study with intravascular ultrasound. *Am Heart J.* 2005;149:520-6.
25. Yokoyama M, Komiyama N, Courtney BK, Nakayama T, Namikawa S, Kuriyama N, Koizumi T, Nameki M, Fitzgerald PJ, Komuro I. Plasma low-density lipoprotein reduction and structural effects on coronary atherosclerotic plaques by atorvastatin as clinically assessed with intravascular ultrasound radio-frequency signal analysis: a randomized prospective study. *Am Heart J.* 2005;150:287.
  26. Kawasaki M, Sano K, Okubo M, Yokoyama H, Ito Y, Murata I, Tsuchiya K, Minatoguchi S, Zhou X, Fujita H, Fujiwara H. Volumetric quantitative analysis of tissue characteristics of coronary plaques after statin therapy using three-dimensional integrated backscatter intravascular ultrasound. *J Am Coll Cardiol.* 2005;45:1946-53.
  27. Tani S, Watanabe I, Anazawa T, Kawamata H, Tachibana E, Furukawa K, Sato Y, Nagao K, Kanmatsuse K, Kushiro T; Surugadai Atherosclerosis Regression Investigators. Effect of pravastatin on malondialdehyde-modified low-density lipoprotein levels and coronary plaque regression as determined by three-dimensional intravascular ultrasound. *Am J Cardiol.* 2005;96:1089-94.
  28. Nissen SE, Tuzcu EM, Schoenhagen P, Brown BG, Ganz P, Vogel RA, Crowe T, Howard G, Cooper CJ, Brodie B, Grines CL, DeMaria AN. Effect of intensive compared with moderate lipid-lowering therapy on progression of coronary atherosclerosis: a randomized controlled trial. *Jama.* 2004;291:1071-80.

29. Davies MJ, Thomas AC. Plaque fissuring--the cause of acute myocardial infarction, sudden ischaemic death, and crescendo angina. *Br Heart J*. 1985;53:363-73.
30. Zaman AG, Helft G, Worthley SG, Badimon JJ. The role of plaque rupture and thrombosis in coronary artery disease. *Atherosclerosis*. 2000;149:251-66.
31. Ambrose JA, Tannenbaum MA, Alexopoulos D, Hjemdahl-Monsen CE, Leavy J, Weiss M, Borricco S, Gorlin R, Fuster V. Angiographic progression of coronary artery disease and the development of myocardial infarction. *J Am Coll Cardiol*. 1988;12:56-62.
32. Little WC, Constantinescu M, Applegate RJ, Kutcher MA, Burrows MT, Kahl FR, Santamore WP. Can coronary angiography predict the site of a subsequent myocardial infarction in patients with mild-to-moderate coronary artery disease? *Circulation*. 1988;78:1157-66.
33. Nolting PR, de Groot E, Zwinderman AH, Buirma RJ, Trip MD, Kastelein JJ. Regression of carotid and femoral artery intima-media thickness in familial hypercholesterolemia: treatment with simvastatin. *Arch Intern Med*. 2003;163:1837-41.
34. Amarenco P, Labreuche J, Lavallee P, Touboul PJ. Statins in stroke prevention and carotid atherosclerosis: systematic review and up-to-date meta-analysis. *Stroke*. 2004;35:2902-9.
35. Toutouzas K, Vaina S, Tsiamis E, Vavuranakis M, Mitropoulos J, Bosinakou E, Toutouzas P, Stefanadis C. Detection of increased temperature of the culprit lesion after recent myocardial infarction: the favorable effect of statins. *Am Heart J*. 2004;148:783-8.

36. Furman C, Copin C, Kandoussi M, Davidson R, Moreau M, McTaggart F, Chapman MJ, Fruchart JC, Rouis M. Rosuvastatin reduces MMP-7 secretion by human monocyte-derived macrophages: potential relevance to atherosclerotic plaque stability. *Atherosclerosis*. 2004;174:93-8.
37. Landmesser U, Bahlmann F, Mueller M, Spiekermann S, Kirchhoff N, Schulz S, Manes C, Fischer D, de Groot K, Fliser D, Fauler G, Marz W, Drexler H. Simvastatin versus ezetimibe: pleiotropic and lipid-lowering effects on endothelial function in humans. *Circulation*. 2005;111:2356-63.
38. Crisby M, Nordin-Fredriksson G, Shah PK, Yano J, Zhu J, Nilsson J. Pravastatin treatment increases collagen content and decreases lipid content, inflammation, metalloproteinases, and cell death in human carotid plaques: implications for plaque stabilization. *Circulation*. 2001;103:926-33.
39. Hagens T, Gussenhoven EJ, van Essen JA, Seelen J, Honkoop J, van der Lugt A. Reproducibility of volumetric quantification in intravascular ultrasound images. *Ultrasound Med Biol*. 2000;26:367-74.
40. Gaster AL, Korsholm L, Thayssen P, Pedersen KE, Haghfelt TH. Reproducibility of intravascular ultrasound and intracoronary Doppler measurements. *Catheter Cardiovasc Interv*. 2001;53:449-58.
41. Bekerredjian R, Hardt S, Just A, Hansen A, Kuecherer H. Influence of Catheter Position and Equipment-Related Factors on the Accuracy of Intravascular Ultrasound Measurements. *J Invasive Cardiol*. 1999;11:207-212.

## FIGURE LEGENDS

**Figure 1.** Weighted mean difference (WMD) with 95% confidence interval (CI) of difference in plaque volume between follow-up and baseline in the statin arm of the included studies.

**Figure 2.** Weighted mean difference (WMD) with 95% confidence interval (CI) of difference in lumen volume between follow-up and baseline in the statin arm of the included studies.

**Figure 3.** Weighted mean difference (WMD) with 95% confidence interval (CI) of difference in vessel volume between follow-up and baseline in the statin arm of the included studies.

**Figure 4.** The funnel plot shows no asymmetry therefore no publication bias present in the meta-analysis.

## TABLES

Table 1 Characteristics of the studies included in the meta-analysis

Study	Year	Design	n†	Treatment	Follow-up Mean (%)	Age	Male	LDL-fu mg/dl
<b>GAIN</b> <sup>21</sup>	2001	MC	48	atorvastatin	12 months	61	85	86±30
<b>ESTABLISH</b> <sup>20</sup>	2004	SC	24	atorvastatin	6 months	61	86	70±25
<b>REVERSAL</b> <sup>28</sup>	2004	MC	253	atorvastatin	18 months	56	71	79±30
<b>REVERSAL</b>	2004	MC	249	pravastatin	18 months	57	73	110±26
<b>Petronio et al</b> <sup>24</sup>	2005	SC	36	simvastatin	12 months	63	72	94±9
<b>Kawasaki et al</b> <sup>26</sup>	2005	SC	17	atorvastatin	6 months	66	71	95±15
<b>Kawasaki et al</b> <sup>26</sup>	2005	SC	18	pravastatin	6 months	67	72	102±13
<b>Nishioka et al</b> <sup>23</sup>	2005	SC	22	statin	6 months	66	77	106±20
<b>Jensen et al</b> <sup>22</sup>	2004	SC	40	simvastatin	12 months	58	100	40±10
<b>Yokoyama et al</b> <sup>25</sup>	2005	SC	25	atorvastatin	6 months	62	90	87±29
<b>Tani et al</b> <sup>27</sup>	2005	SC	52	pravastatin	6 months	63	75	104±20

† Number of patients in the treatment arm. MC refers to multi-center. SC refers to single-center. LDL-fu indicates LDL obtained at follow-up.

**Table 2 Stratification of the change in plaque volume according to the length of the follow-up.**

	<u>Follow-up 6 months (n= 158)</u>		<u>Follow-up &gt; 6 months (n= 626)</u>	
<b>Study</b>	<b>WMD (95% CI)</b>	<b>Study</b>	<b>WMD (95% CI)</b>	
<b>ESTABLISH</b>	-8.20 (-34.79, 18.39)	<b>GAIN</b>	1.20 (-31.45, 33.85)	
<b>Nishioka et al.</b>	-4.60 (-13.01, 3.81)	<b>Jensen et al.</b>	-3.70 (-16.63, 9.23)	
<b>Kawasaki (atorva) et al.</b>	-3.80 (-24.84, 17.24)	<b>REVERSAL (atorva)</b>	-0.50 (-20.07, 19.07)	
<b>Kawasaki (prava) et al.</b>	-1.60 (-23.18, 19.98)	<b>REVERSAL (prava)</b>	5.10 (-14.85, 25.05)	
<b>Tani et al.</b>	-7.00 (-17.82, 3.82)	<b>Petronio et al.</b>	-30.00 (-47.18, -12.82)	
<b>Yokohama et al.</b>	-3.90 (-21.18, 13.38)			
Total	-5.07 (-10.67, 0.53)	Total	-6.67 (-19.62, 6.28)	
p value	0.08	p value	0.31	

**WMD refers to weighted mean difference**

Table 3 Stratification of the change in plaque volume according to LDL-C levels at follow-up.

Study	Follow-up LDL-C levels < 100 mg/dl (n= 443)		Follow-up LDL-C levels $\geq$ 100 mg/dl (n= 341)	
	WMD (95% CI)	Study	WMD (95% CI)	Study
<b>GAIN</b>	1.20 (-31.45, 33.85)	Nishioka et al.	-4.60 (-13.01, 3.81)	
<b>ESTABLISH</b>	-8.20 (-34.79, 18.39)	Kawasaki et al. (prava)	-1.60 (-23.18, 19.98)	
Jensen et al.	-3.70 (-16.63, 9.23)	<b>REVERSAL (prava)</b>	5.10 (-14.85, 25.05)	
<b>REVERSAL (atorva)</b>	-0.50 (-20.07, 19.07)	Tani et al.	-7.00 (-17.82, 3.82)	
Kawasaki et al. (atorva)	-3.80 (-24.84, 17.24)	Total	-4.22 (-10.27, 1.82)	
Petronio et al.	-30.00 (-47.18, -12.82)	p value	0.17	
Yokohama et al.	-3.90 (-21.18, 13.38)			
Total	-7.88 (-16.31, 0.55)			
p value	0.07			

WMD refers to weighted mean difference

Figures

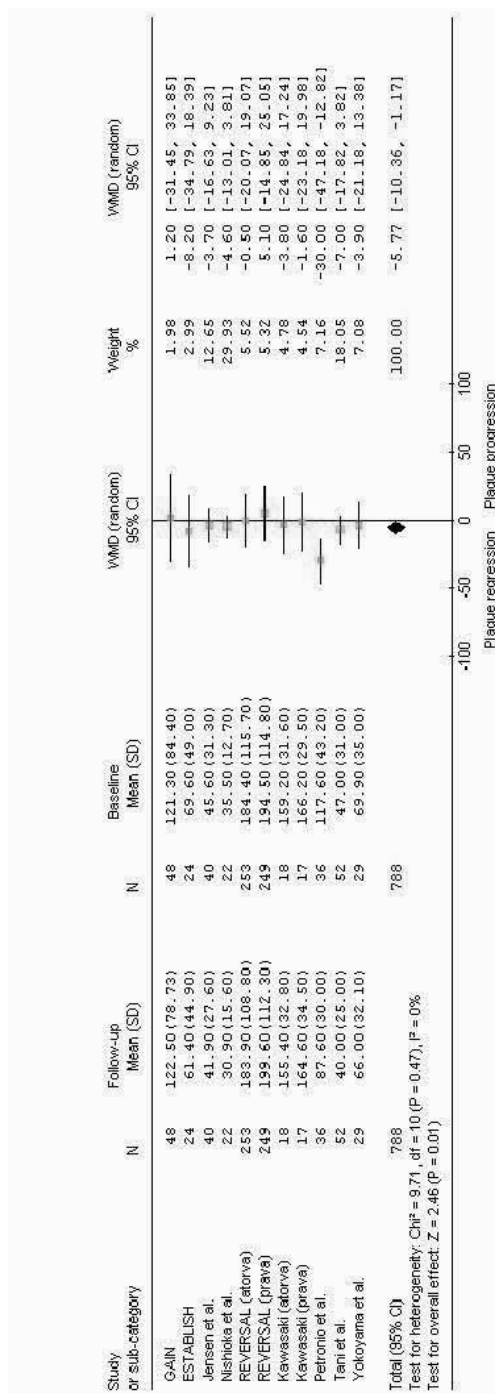


Figure 1

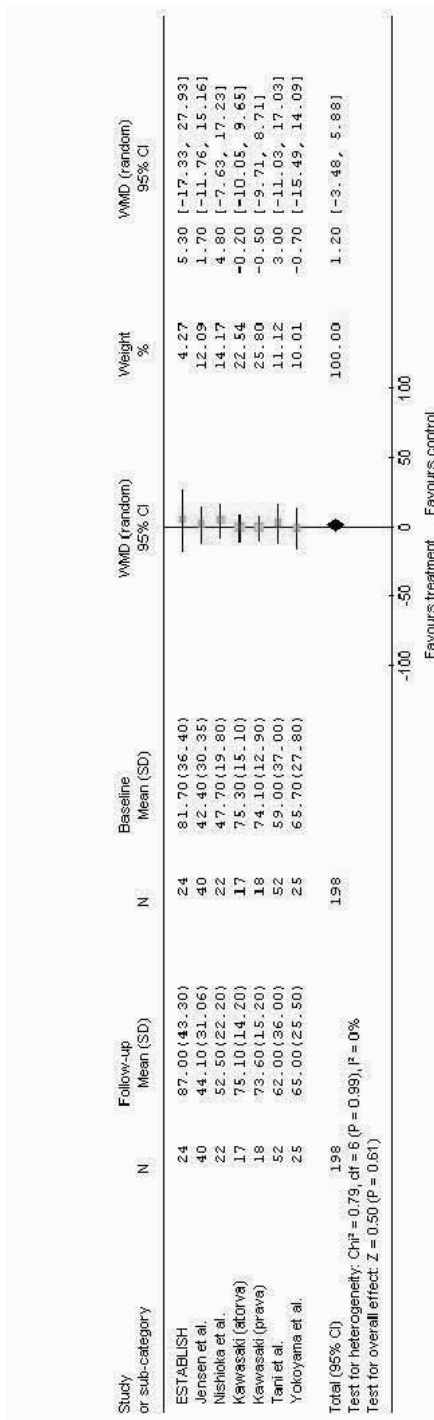


Figure 2

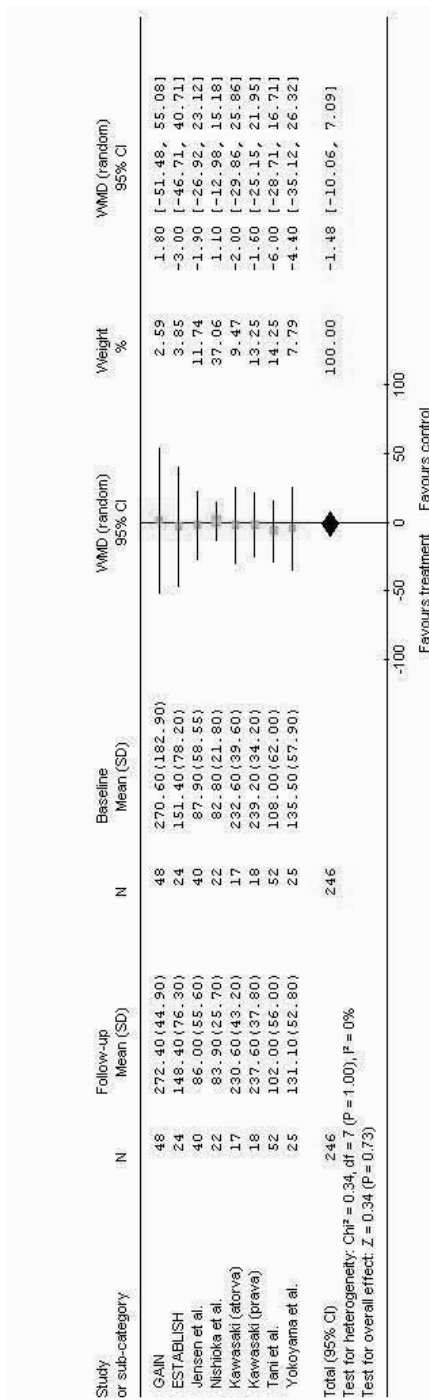


Figure 3

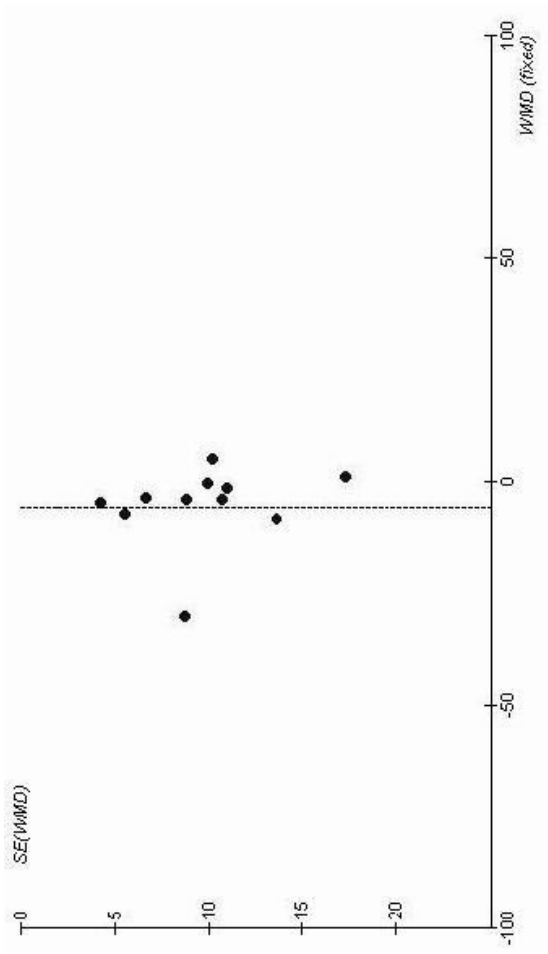
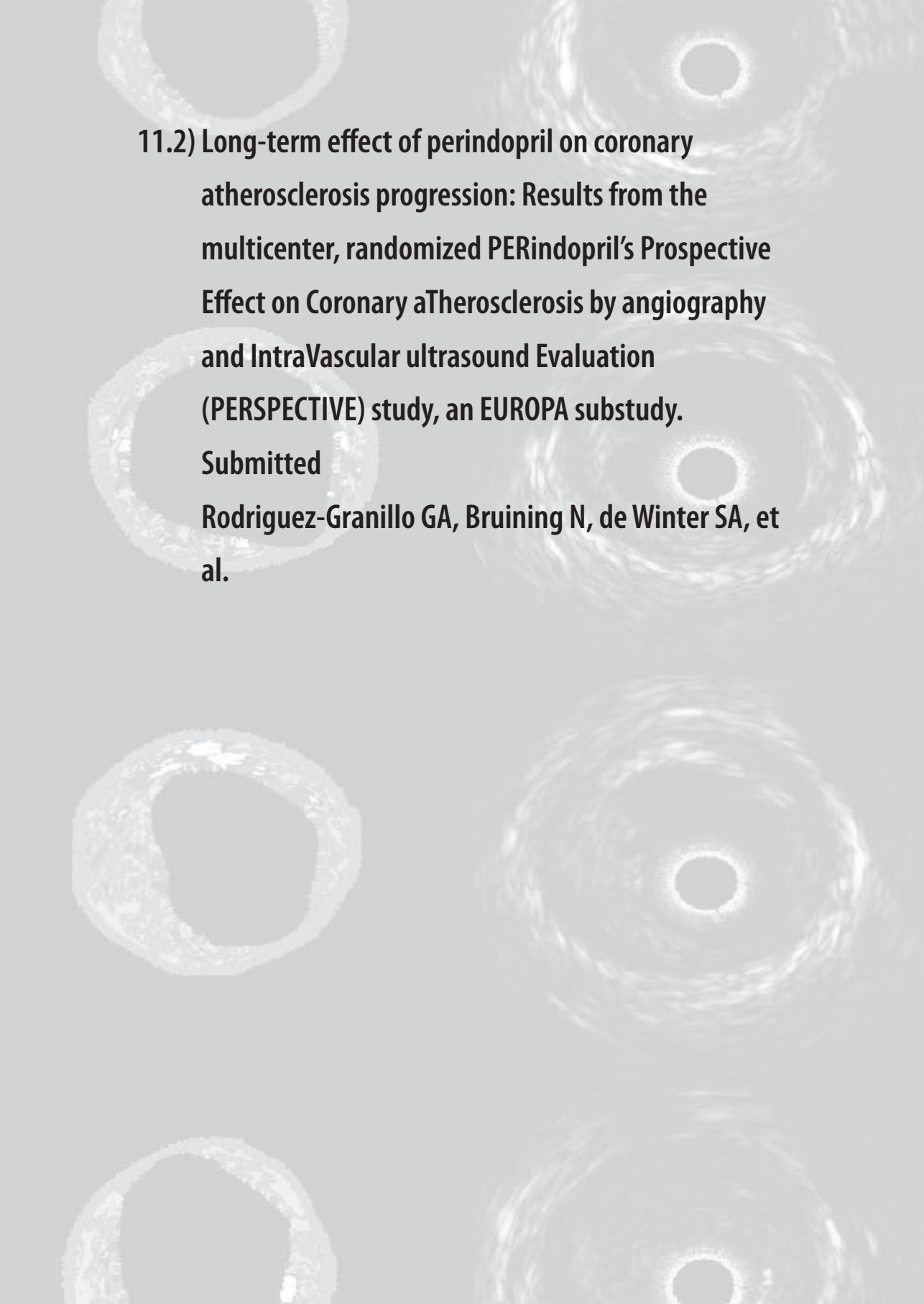


Figure 4





**11.2) Long-term effect of perindopril on coronary atherosclerosis progression: Results from the multicenter, randomized PERindopril's Prospective Effect on Coronary aTherosclerosis by angiography and IntraVascular ultrasound Evaluation (PERSPECTIVE) study, an EUROPA substudy.**

**Submitted**

**Rodriguez-Granillo GA, Bruining N, de Winter SA, et al.**



## **Long-Term Effect of Perindopril on Coronary Atherosclerosis**

### **Progression:**

**Results from the multicenter, randomized PERindopril's Prospective Effect on Coronary aTherosclerosis by angiography and IntraVascular ultrasound Evaluation (PERSPECTIVE) study, an EUROPA substudy.**

**Gastón A. Rodriguez-Granillo MD**

**Nico Bruining PhD**

**Sebastiaan de Winter BSc**

**Jeroen Vos MD**

**Jurgen M.R. Ligthart BSc**

**Jaap Deckers J.W. MD, PhD**

**Maarten L. Simoons MD, PhD**

**Kim M. Fox FRCP<sup>1</sup>**

**Pim J. De Feyter MD, PhD**

From the Department of Cardiology, Thoraxcenter, Erasmus MC, Rotterdam, Netherlands.

<sup>1</sup> Cardiology Department, National Heart and Lung Institute and Royal Brompton Hospital, London, United Kingdom

## ABSTRACT

**Background:** The EUROPA trial, a double-blind, multicenter trial in 12,218 patients has shown that the long-term administration of 8 mg/day of perindopril induces a significant reduction in adverse clinical events in patients with established CHD.

**Objective:** The Perspective study, a substudy of the Europa Trial, was designed to evaluate the effect of long-term administration of perindopril on coronary plaque progression as assessed by quantitative angiography (QCA) and intravascular ultrasound (IVUS).

**Methods:** The Perspective study evaluated 244 patients (mean age 57 yrs, 81 % male). Evaluable QCA was obtained from 194 patients, 96 patients randomized to perindopril and 98 patients to placebo. Concomitant treatment at baseline consisted of aspirin (90%) lipid-lowering agents (70%) and  $\beta$ -blockers (60%) The primary endpoint was the difference of minimum ( $M^{\text{in}}\text{LD}$ ) and mean ( $M^{\text{can}}\text{LD}$ ) lumen diameter (QCA) measured at baseline and 3-year follow-up between the perindopril and placebo groups. The difference of mean plaque cross-sectional area (PCSA) between groups (IVUS) was a pre-specified secondary endpoint.

**Results:** After a median follow-up of 3.0 (range 1.9, 4.1) years, no statistically significant differences in QCA measurements were detected between perindopril and placebo groups [ $M^{\text{in}}\text{LD}$  (-0.07 $\pm$ 0.4 mm vs. -0.02 $\pm$ 0.4 mm,  $p=0.34$ ) and of  $M^{\text{can}}\text{LD}$  (-0.05 $\pm$ 0.2 mm vs -0.05 $\pm$ 0.3 mm,  $p=0.89$ )]. The mean absolute reduction in PCSA was not significantly different between perindopril and placebo groups (-0.18 $\pm$ 1.2 mm<sup>2</sup> vs. -0.02 $\pm$ 1.2 mm<sup>2</sup>,  $p=0.48$ ).

**Conclusion:** Long-term administration of perindopril had no significant effect on progression of CAD as assessed by QCA and IVUS in patients on concomitant intensive medical treatment.

**Keywords:** atherosclerosis, progression/regression, ultrasonography, ace-inhibitor

## **Introduction**

Angiotensin-converting enzyme (ACE) inhibitors were shown to be effective in reducing coronary adverse events in high risk patients and in patients with stable angina without overt heart failure although they provided no benefit in a low risk population (1,2).

Animal studies have established that ACE inhibitors exert an anti-atherosclerotic effect, stabilizing plaque progression and even altering plaque composition, thus potentially offering a mechanistic explanation for the reduction in clinical events (3-6).

More recently, human studies of carotid arteries demonstrated that ACE inhibitors had a beneficial effect on atherosclerosis progression (7,8). Yet, no data are available on the efficacy of these agents on the progression of atherosclerosis in the coronary tree.

The EUROPA trial, a prospective, double-blinded, randomized controlled trial; demonstrated that 8 mg/day of perindopril during 4 years induced a 20% relative risk reduction of cardiovascular adverse events in patients with stable coronary artery disease (9).

The PERindopril's Prospective Effect on Coronary aTherosclerosis by IntraVascular ultrasound Evaluation (PERSPECTIVE) was a substudy of EUROPA trial that evaluated the effect of long-term administration of perindopril on coronary plaque size as assessed by angiography and intra-coronary ultrasound (IVUS).

## Methods

The EUROPA trial evaluated the effect of an ACE-inhibitor perindopril on prevention of cardiovascular events in 12,218 patients with stable coronary artery disease. The PERSPECTIVE was a sub-study of the EUROPA trial that sought to explore the effect of perindopril on atherosclerosis progression/regression using coronary angiography and IVUS.

The methodology of the EUROPA trial has been extensively described elsewhere (9). In the run-in period, enrolled patients received 4 mg/d oral perindopril for 2 weeks in addition to their normal medication, followed by 8 mg/d for 2 weeks if the initial dose was tolerated. At the end of the run-in period, patients were randomly assigned to perindopril 8mg/d or placebo for at least 3 years. The efficacy outcome, was the rate of major adverse cardiac events (MACE), defined as cardiovascular mortality, non-fatal MI and cardiac arrest with successful resuscitation.

Patients included in the main EUROPA trial in which a coronary angiogram was indicated were eligible for the study. In addition to EUROPA's inclusion and exclusion criteria, anatomically suitable vessels for the QCA / IVUS sub-study were required.

The institutional ethics committees of all participating centers approved the study protocol and informed written consent was obtained from all patients.

### Angiographic acquisition

Coronary angiograms were obtained at baseline before medication was started and at follow-up after at least 3 years. A minimum of 3 orthogonal projections of the region of interest were filmed at baseline, and the same projections were used at follow-up. Quantitative coronary angiographic (QCA) analysis was performed by an independent core laboratory (Cardialysis BV, Rotterdam, The Netherlands) as previously described

with a validated computer-based edge-detection system (CAAS II; Pie Medical, Maastricht, The Netherlands) (10). The catheter tip was cleared of contrast for accurate calibration. Interpolated reference diameter, minimal luminal diameter, mean lumen diameter, and diameter stenosis were measured at both time points using the “worst” view of an end-diastolic frame.

### **Intravascular Ultrasound acquisition**

IVUS was acquired using 20, 30 and 40 MHz imaging catheters following coronary angiography. The catheter was advanced distal to an anatomically identifiable landmark, allowing the evaluation of a segment of at least 30 mm. Cine runs, before and during contrast injection, were performed to define the position of the IVUS catheter before the pullback was started. Using an automated pullback device, the transducer was withdrawn at a continuous speed of 0.5 mm/s until the ostium. IVUS data was acquired after the intracoronary administration of nitroglycerin and stored on S-VHS videotape. The videotapes were digitized on a computer system, transformed into the DICOM medical image standard and stored on an IVUS Picture Archiving and Communications System (PACS). After a 3-4 year follow-up period, patients underwent repeat catheterization and IVUS examination of the same region of interest (ROI) using an identical IVUS imaging catheter.

### **Intravascular Ultrasound analysis**

Quantitative coronary ultrasound (QCU) analysis was performed by an independent core laboratory (Cardialysis BV, Rotterdam, The Netherlands) using validated semi-automatic contour detection software (Curad, version 3.1, Wijk bij Duurstede, The Netherlands). The IntelliGate™ image-based gating method was applied to eliminate motion artifacts by retrospectively selecting end-diastolic frames (11).

The cross-sectional areas (CSA) of both the lumen and vessel (defined as the external elastic membrane EEM) were calculated for each cross-sectional image. The contours of the EEM and the lumen-intima interface enclosed an area that was defined as the coronary plaque plus media area.

In the baseline IVUS study a region of interest (ROI) was identified using landmarks such as side-branches and the coronary ostium. At 3-year follow-up, the same matched ROI was identified using the same landmarks.

### **Study endpoints**

The primary endpoint was the difference of minimum and mean lumen diameter (QCA) measured at baseline and 3-year follow-up between the perindopril and placebo groups.

Pre-specified secondary endpoints were the difference of mean plaque CSA (mm<sup>2</sup>) and in plaque volume (mm<sup>3</sup>) as measured by IVUS at baseline and at 3-year follow-up between groups.

The development of new lesions ( $\geq 20$  % decrease in minimum lumen diameter measured by QCA) was another pre-specified secondary endpoint.

### **Statistical analysis**

Discrete variables were presented as counts and percentages or median (interquartile range) when indicated. Continuous variables were presented as means  $\pm$  standard deviation.

Based on a previous QCA progression/ regression trial, we calculated a sample size of 99 paired subjects to achieve a power of 80 %, considering an type I error probability of 0.05 (two-sided), a difference (between groups) in minimum lumen diameter of 0.08 and a within group standard deviation of 0.20 (12). In this calculation a drop-out rate of 15 % non-analyzable patients was included. Differences between groups were assessed

by paired and unpaired Student's  $t$  test when applicable. For the comparison between categorical variables the  $\chi^2$  test was used. A two-sided  $p$  value  $<0.05$  was required for statistical significance. All analyses were performed using SAS 6.12 software (SAS Institute Inc.).

## Results

Out of 244 patients who were randomized, 194 had complete matched baseline and follow-up angiograms. The reasons for incomplete angiographic follow-up are depicted in figure 1.

The baseline demographics of the study population are presented in table 1. Coronary risk factors and baseline blood pressure were well balanced, showing no statistical differences between groups. At baseline and during the study period, more than 70 % of patients received lipid-lowering treatment more than 90 % platelet-inhibitors and about 60% were on  $\beta$ -blocker treatment.

At a median follow-up (intention to treat) of 3.4 (range 1.5, 4.3) years, the rate of adverse events (defined as cardiac death, myocardial infarction and cardiac resuscitation) was not statistically different between the perindopril and placebo groups [6 (4.7%) vs. 7 (6.0%), RR -3.6, 95% CI (-21.1, 13.9)] and slightly lower than the event rate reported in the EUROPA trial (8 % vs. 10 %).

### QCA measurements

Follow-up angiography was performed after a median of 3.0 (range 1.9, 4.1) years. The effects of perindopril on the angiographic findings are shown in table 2. The difference of minimum lumen diameter and mean lumen diameter between baseline and follow-up in the perindopril group did not differ from that observed in the placebo group (-0.07 $\pm$ 0.4 mm vs. -0.02 $\pm$ 0.4 mm,  $p=0.34$ ; and -0.05 $\pm$ 0.2 mm vs. -0.05 $\pm$ 0.3 mm,  $p=0.89$ , respectively). Twelve (12.5 %) new lesions developed in the perindopril group, and 7 (7.1 %) in the placebo group ( $p=0.30$ ).

### IVUS analyses

A total of 144 matched evaluable IVUS were available at follow-up. 32 patients were excluded due to sub-optimal IVUS quality (caused by severely calcified vessels, severe image artifacts or absence of clear anatomical landmarks). The QCU results are shown in table 3. There was no significant differences in IVUS measurements between groups. In the perindopril group, the serial absolute change in mean plaque CSA compared with baseline was  $-0.20 \pm 1.6 \text{ mm}^2$  and for the placebo the change was  $-0.09 \pm 1.2 \text{ mm}^2$ , ( $p=0.63$ ). The absolute change in plaque volume did not differ between groups ( $-2.55 \pm 44.6 \text{ mm}^3$  in the perindopril group versus  $-3.74 \pm 36.3 \text{ mm}^3$  in the placebo group,  $p=0.86$ ).

## Discussion

The PERSPECTIVE sub-study was designed to demonstrate whether an effect of perindopril on plaque size would explain the beneficial clinical effect observed in the main EUROPA study. A mechanistic explanation was supported by the fact that, the reduction in cardiovascular events in the main trial was larger than that expected for the observed reduction in blood pressure (9). This was further enforced by the observations of the SECURE study (7), a sub-study of the HOPE trial (1) that identified a significant beneficial effect of ACE inhibitors on carotid atherosclerosis progression at 4.5 years of follow-up.

The present study demonstrated that in patients with established CAD, stable angina and without overt heart failure the administration of perindopril on top of concomitant intensive medical treatment has no significant effect on progression of atherosclerosis as assessed by QCA and IVUS.

These findings suggest that the clinical benefit obtained in the EUROPA trial cannot be attributed to their effect on plaque size or on the development of new lesions (9).

There are several hypotheses for the lack of effect of perindopril on plaque size in our sub-study in coronary arteries.

First, the duration of the follow-up was longer in the EUROPA trial (~4 vs. ~3 years). In addition, the event rate was higher in the EUROPA trial than in its present substudy.

Second, in the Perspective substudy both the treated group and placebo group were intensively treated with aspirin and lipid-lowering agents during the study period. The latter have demonstrated to be effective agents to reduce coronary plaque progression and might therefore have obscured potential anti-atherosclerotic effects of perindopril (13). Indeed, both placebo and treatment group showed no evidence of plaque

progression, contrary to the observation that atherosclerosis progresses in coronary patients not on statin treatment (14).

Third, it may be possible that perindopril has no effect on plaque size, and that its beneficial clinical effect is related to an improvement in the endothelial function or to a shift in the histological composition of plaques (3,6). Whether a significant improvement in the endothelial function is induced by long-term treatment with perindopril will be addressed by another EUROPA substudy (15). Fourth, only a single coronary artery segment was interrogated, thus potential coronary artery disease progression in other segments of the coronary tree could have been missed. Finally, it may be speculated that perindopril has no effect of coronary plaques, as opposed to a beneficial effect of ACE-inhibitors on carotid plaques shown in the SECURE study (8). However, other reasons may also explain the difference in outcome between the 2 studies. A shorter follow-up period, a lower risk population (adverse events rate of 6 % vs. 14 %), and a higher frequency of standard medical therapy of the patients in the PERSPECTIVE study compared to the patients in the SECURE study might explain the difference in outcome between the two studies. In particular, 73 % versus 35 % of the patients were under lipid lowering therapy in the PERSPECTIVE and SECURE studies respectively, while aspirin (~97 % vs. ~85 %) and beta-blockers (~60 % vs. ~42 %) therapy were also more frequently administered in our study (7).

## **Limitations**

The present study has a number of limitations. A substantial number of patients were excluded from the IVUS analysis due to sub-optimal image quality and severe calcification precluding accurate plaque size assessment. This has resulted in a rather small study sample size and larger studies may be required, using IVUS as primary endpoint, to conclusively determine the efficacy of ACE inhibitors on progression of atherosclerosis. Finally, different IVUS catheters with different specifications were used over a 3-year period which may have induced small variations in measurements and thus may have obscured potential subtle changes in plaque measurements, even though the measurements obtained with the various 30 MHz catheters were adjusted according to a previously reported mathematical algorithm (16).

### **Conclusions**

The results of the present study suggest that in patients with established CAD, stable angina and without overt heart failure the clinical benefit obtained with perindopril treatment during a period of 3 year cannot be attributed to an effect on coronary plaque size.

### **Acknowledgements**

This study was supported by Servier, France. The sponsor was not involved in the data collection and data analysis.

**References**

1. Yusuf S, Sleight P, Pogue J, Bosch J, Davies R, Dagenais G. Effects of an angiotensin-converting-enzyme inhibitor, ramipril, on cardiovascular events in high-risk patients. The Heart Outcomes Prevention Evaluation Study Investigators. *N Engl J Med* 2000;342:145-53.
2. Braunwald E, Domanski MJ, Fowler SE, et al. Angiotensin-converting-enzyme inhibition in stable coronary artery disease. *N Engl J Med* 2004;351:2058-68.
3. Hornig B, Kohler C, Drexler H. Role of bradykinin in mediating vascular effects of angiotensin-converting enzyme inhibitors in humans. *Circulation* 1997;95:1115-8.
4. Candido R, Jandeleit-Dahm KA, Cao Z, et al. Prevention of accelerated atherosclerosis by angiotensin-converting enzyme inhibition in diabetic apolipoprotein E-deficient mice. *Circulation* 2002;106:246-53.
5. Powell JS, Clozel JP, Muller RK, et al. Inhibitors of angiotensin-converting enzyme prevent myointimal proliferation after vascular injury. *Science* 1989;245:186-8.
6. Hayek T, Hamoud S, Keidar S, et al. Omapatrilat decreased macrophage oxidative status and atherosclerosis progression in atherosclerotic apolipoprotein E-deficient mice. *J Cardiovasc Pharmacol* 2004;43:140-7.
7. Lonn E, Yusuf S, Dzavik V, et al. Effects of ramipril and vitamin E on atherosclerosis: the study to evaluate carotid ultrasound changes in patients treated with ramipril and vitamin E (SECURE). *Circulation* 2001;103:919-25.
8. Hosomi N, Mizushige K, Ohyama H, et al. Angiotensin-converting enzyme inhibition with enalapril slows progressive intima-media thickening of the common carotid artery in patients with non-insulin-dependent diabetes mellitus. *Stroke* 2001;32:1539-45.
9. Fox KM. Efficacy of perindopril in reduction of cardiovascular events among patients with stable coronary artery disease: randomised, double-blind, placebo-controlled, multicentre trial (the EUROPA study). *Lancet* 2003;362:782-8.

10. Reiber JH, Serruys PW, Kooijman CJ, et al. Assessment of short-, medium-, and long-term variations in arterial dimensions from computer-assisted quantitation of coronary cineangiograms. *Circulation* 1985;71:280-8.
11. De Winter SA, Hamers R, Degertekin M, et al. Retrospective image-based gating of intracoronary ultrasound images for improved quantitative analysis: the intelligate method. *Catheter Cardiovasc Interv* 2004;61:84-94.
12. Bestehorn HP, Rensing UF, Roskamm H, et al. The effect of simvastatin on progression of coronary artery disease. The Multicenter coronary Intervention Study (CIS). *Eur Heart J* 1997;18:226-34.
13. Nissen SE, Tuzcu EM, Schoenhagen P, et al. Effect of intensive compared with moderate lipid-lowering therapy on progression of coronary atherosclerosis: a randomized controlled trial. *Jama* 2004;291:1071-80.
14. Balk EM, Karas RH, Jordan HS, Kupelnick B, Chew P, Lau J. Effects of statins on vascular structure and function: A systematic review. *Am J Med* 2004;117:775-90.
15. PERTINENT--perindopril-thrombosis, inflammation, endothelial dysfunction and neurohormonal activation trial: a sub-study of the EUROPA study. *Cardiovasc Drugs Ther* 2003;17:83-91.
16. Bruining N, Hamers R, Teo TJ, de Feijter PJ, Serruys PW, Roelandt JR. Adjustment method for mechanical Boston scientific corporation 30 MHz intravascular ultrasound catheters connected to a Clearview console. Mechanical 30 MHz IVUS catheter adjustment. *Int J Cardiovasc Imaging* 2004;20:83-91.

## TABLES

Table 1: Study population

	Perindopril (n= 96)	Placebo (n=98)	difference	95% CI	EUROPA (overall) (n= 12,218)
<b>Baseline characteristics</b>					
Age (yrs±SD)	57.5±9.3	56.1±9.0	1.3	-1.3, 3.9	60±9
Male sex	77 (80.2)	80 (81.6)	-1.4	-12.5, 9.6	10,439 (85.4)
Diabetes	8 (8.3)	8 (8.2)	0.2	-7.6, 7.9	1502 (12.3)
Hypertension*	19 (19.8)	24 (24.5)	-4.7	-16.4, 7.0	3312 (27.1)
Smoking	24 (25.0)	22 (22.4)	2.6	-9.4, 14.5	1869 (15.3)
Hypercholesterolemia	75 (78.1)	79 (80.6)	-2.5	-13.9, 8.9	7737 (63.0)
PVD	2 (2.1)	4 (4.1)	-2.0	-6.8, 2.9	883 (7.2)
Previous MI	44 (45.8)	53 (54.1)	-8.2	-22.3, 5.8	7910 (64.7)
Previous PTCA	83 (86.5)	92 (93.9)	-7.4	-15.7, 0.9	3573 (29.2)
Previous CABG	1 (1.0)	0 (0.0)	1.0	-1.0, 3.1	3587 (29.4)
Systolic BP (mmHg)	132.7±16.0	131.2±14.2	1.5	-2.7, 5.8	137 (15)
Diastolic BP (mmHg)	80.0±7.6	78.2±7.6	1.8	-0.3, 4.0	82 (8)
Weight (kg)	78.3±11.4	80.8±12.1	-2.6	-5.9, 0.8	81.5 (12)
Heart rate	69.3±11.1	66.3±7.8	3	0.4, 5.8	68 (10)
<b>Anginal status</b>					
CCS I	82 (85.4)	81 (82.7)	2.8	-7.5, 13.1	NA (81)
CCS II	12 (12.5)	15 (15.3)	-2.8	-12.5, 6.9	NA (17)
CCS III	2 (2.1)	2 (2.0)	0.0	-4.0, 4.0	NA (2)
CCS IV	0 (0.0)	0 (0.0)	0.0	0.0, 0.0	
<b>Other medications</b>					
Platelet inhibitors	92 (95.8)	96 (98.0)	-2.1	-7.0, 2.8	11,278 (92.3)
Beta-blockers	55 (57.3)	62 (63.3)	-6.0	-19.7, 7.8	7535 (61.6)
Nitrates	39 (30.7)	20 (17.1)	14.9	3.3, 26.5	5242 (42.9)
Ca-channel blockers	52 (40.9)	41 (35.0)	6.9	-6.6, 20.4	3826 (31.3)
Lipid lowering agents	93 (73.2)	86 (73.5)	-5.7	-17.9, 6.5	7033 (57.6)

**At follow-up**

Systolic BP	131.0±17.9	133.7±15.1	-2.7	-7.3, 1.9	NA
Change in SP	-1.9±17.7	2.8±14.4	-4.7	-9.2, 0.3	NA
Diastolic BP	76.0±8.1	77.9±8.5	-1.9	-4.2, 0.4	NA
Change in DP	-3.4±9.2	-0.3±9.2	-3.2	-5.7, 0.6	NA

Hypercholesterolemia defined as cholesterol >6.5 mmol/L or on lipid-lowering therapy. Blood pressure (BP) > 160/95 mmHg or receiving antihypertensive treatment. PVD refers to peripheral vascular disease. CCS refers to Canadian Cardiovascular Society. NA refers to non-available.

Table 2. Quantitative coronary angiography results

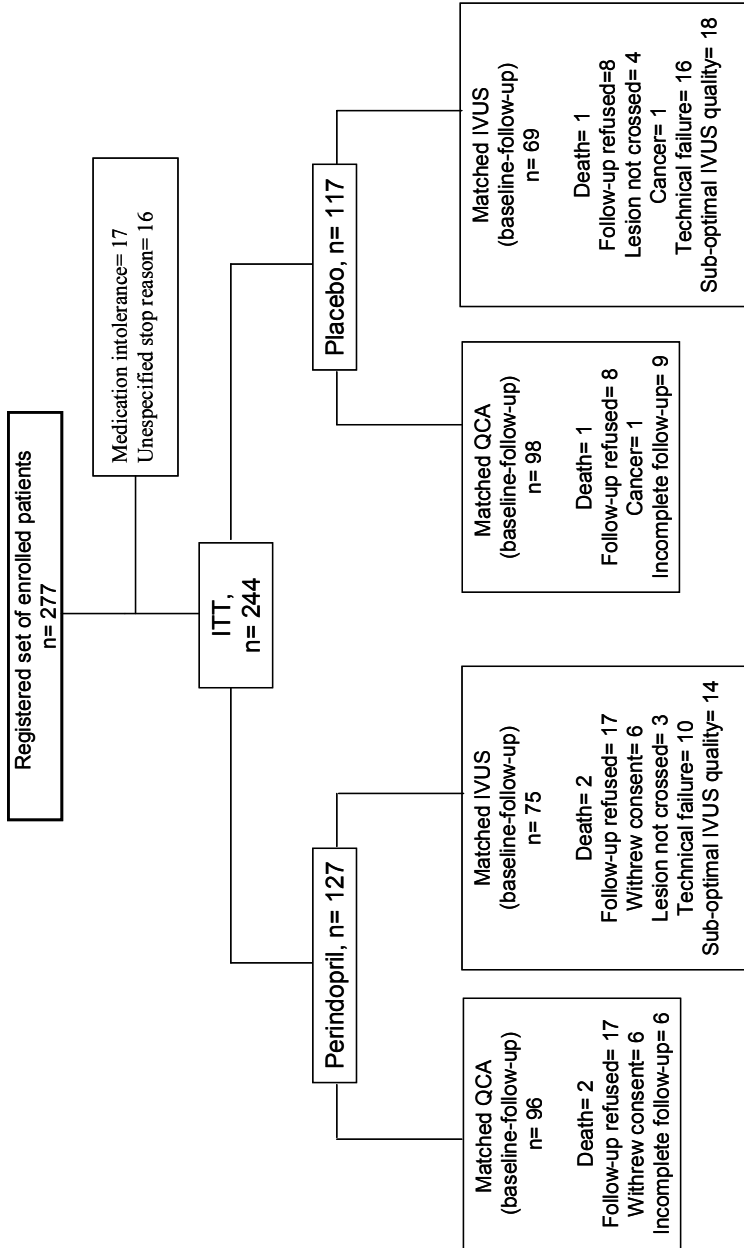
	Perindopril (n= 96)	Placebo (n= 98)	p value
<b>Length</b>			
Baseline	32 ± 17	32 ± 15	
Follow-up	31 ± 16	31 ± 14	
Nominal change	-0.72 ± 3	-0.36 ± 3	0.41
<b>Reference diameter</b>			
Baseline	3.09 ± 0.6	2.96 ± 0.6	
Follow-up	3.04 ± 0.7	2.93 ± 0.6	
Nominal change	-0.05 ± 0.4	-0.03 ± 0.3	0.74
<b>Minimal lumen diameter</b>			
Baseline	2.19 ± 0.5	2.14 ± 0.7	
Follow-up	2.11 ± 0.6	2.13 ± 0.6	
Nominal change	-0.07 ± 0.4	-0.02 ± 0.4	0.34
<b>Mean lumen diameter</b>			
Baseline	2.92 ± 0.5	2.88 ± 0.6	
Follow-up	2.87 ± 0.5	2.83 ± 0.6	
Nominal change	-0.05 ± 0.2	-0.05 ± 0.3	0.89
<b>Diameter stenosis</b>			
Baseline	29 ± 13	28 ± 15	
Follow-up	29 ± 17	27 ± 15	
Nominal change	0.42 ± 12	-0.56 ± 13	0.58
<b>Development of new lesions (%)*</b>	12 (12.5)	7 (7.1)	0.30

\* (&gt;=20 % decrease in minimal lumen diameter)

Table 3: Intra-vascular ultrasound results

Mean cross-sectional area (mm <sup>2</sup> )	Perindopril (n=75)	Placebo (n=69)	p value
<b>Length</b>			
Baseline	30.47±13.7	31.10±15.2	0.79
Follow-up	30.68±13.5	30.79±14.7	0.96
<b>Vessel</b>			
Baseline	15.45±4.5	15.79±4.7	
Follow-up	15.30±4.4	15.86±4.6	
Nominal change	-0.15±2.0	0.06±1.7	0.49
<b>Lumen</b>			
Baseline	9.05±3.3	9.60±3.9	
Follow-up	9.10±3.3	9.75±4.1	
Nominal change	0.05±1.5	0.15±1.7	0.71
<b>Plaque</b>			
Baseline	6.40±2.7	6.19±2.3	
Follow-up	6.20±2.6	6.10±2.5	
Nominal change	-0.20±1.6	-0.09±1.2	0.63
<b>Plaque volume (mm<sup>3</sup>)</b>			
Baseline	192.06±115.2	189.74±107.5	
Follow-up	189.51±114.1	186.01±104.9	
Nominal change	-2.55±44.6	-3.74±36.3	0.86

**Figure 1.** Study flow chart.





**11.3) First-In-Man Prospective Evaluation of Temporal Changes in Coronary Plaque Composition By In Vivo Ultrasound Radio Frequency Data Analysis: An Integrated Biomarker and Imaging Study (IBIS) Substudy.**

**Eurointervention. 2005;3:282-288.**

**Rodriguez Granillo GA, Serruys PW, McFadden, et al.**



# First-in-man prospective evaluation of temporal changes in coronary plaque composition by *in vivo* intravascular ultrasound radiofrequency data analysis: an Integrated Biomarker and Imaging Study (IBIS) substudy

Gastón A. Rodriguez-Granillo<sup>1</sup>, MD; Patrick W. Serruys<sup>\*1</sup>, MD, PhD, FACC; Eugène P. McFadden<sup>1</sup>, MD, FRCPI, FACC; Carlos A.G. van Mieghem<sup>1</sup>, MD; Dick Goedhart<sup>2</sup>; Nico Bruining<sup>1</sup>, PhD; Antonius F.W. van der Steen<sup>1</sup>, PhD; Willem J. van der Giessen<sup>1</sup>, MD, PhD; Peter de Jaegere<sup>1</sup>, MD, PhD; D. Geoffrey Vince<sup>3</sup>, PhD; George Sianos<sup>1</sup>, MD, PhD; June Kaplow<sup>4</sup>, PhD; Andrew Zalewski<sup>4,5</sup>, MD, PhD; Pim J. de Feyter<sup>1</sup>, MD, PhD, FACC

1. Erasmus Medical Center, Thoraxcenter, Rotterdam, The Netherlands - 2. Cardialysis, Rotterdam, The Netherlands - 3. Cleveland Clinic Foundation, Ohio, USA - 4. GlaxoSmithKline, Philadelphia, PA, USA - 5. Thomas Jefferson University, PA, USA

This study was supported by unrestricted education grant from GlaxoSmithKline.

## KEYWORDS

Ultrasonography,  
Atherosclerosis,  
Coronary disease.

## Abstract

**Background:** The composition of atherosclerotic coronary plaque is a major determinant of future clinical events. Spectral analysis of IVUS radiofrequency data has demonstrated potential to provide detailed quantitative information on plaque composition. We prospectively assessed plaque composition in matched coronary segments at a six-month interval and sought to explore correlations between temporal changes in plaque composition and circulating biomarkers.

**Methods and results:** Twenty coronary segments (mean baseline length, 29.9±14.1mm) with non-significant angiographic (<50 % diameter) stenosis, in non-culprit vessels of patients (n=20) referred for percutaneous intervention, were studied at baseline and six-month follow-up. Spectral analysis of IVUS radiofrequency data, obtained with a 30 MHz catheter in segments matched on predefined anatomic landmarks, was performed with IVUS-Virtual Histology™ software. After 6 months, an overall decrease in the level of different biomarkers of instability was present. There were no significant changes in absolute values (mm<sup>2</sup>) of plaque components; calcium (0.036±0.05 vs. 0.033±0.04), fibrous (2.68±1.5 vs. 2.90±1.5), fibrolipidic (0.77±0.4 vs. 0.73±0.4), and lipid core (0.42±0.4 vs. 0.52±0.5), between baseline and six-months. Nor did any conventional IVUS variable (lumen, vessel, or plaque cross-sectional area, or percent area stenosis). Change in lipid core area (r=0.51, p=0.024), fibrous area (r=0.49, p=0.033) and calcium area (r=0.63, p=0.004), were significantly correlated with change in Lp-PLA<sub>2</sub> activity.

**Conclusions:** Routine medical care does not result in significant overall changes in IVUS-derived plaque size or composition over a 6-month period. This study provides indication of quantifiable boundaries beyond which modifications in tissue composition might be interpreted as statistically significant.

## Abbreviations

**IVUS** = Intravascular ultrasound

## Introduction

Despite significant advances in diagnosis and therapy, coronary atherosclerosis remains a major cause of death in developed countries<sup>1</sup>. Pathological studies have related specific coronary plaque characteristics to fatal ischemic events but conventional imaging techniques cannot reliably identify them prospectively. Coronary angiography is the standard invasive technique to evaluate the presence and extent of coronary atherosclerosis. However, due to the phenomenon of positive vessel remodelling advanced atherosclerotic disease is often present despite only minimal lumen encroachment on angiography<sup>2-4</sup>. Most future atherothrombotic events will occur at the site of these non-obstructive plaques<sup>5</sup>. The histological composition of atherosclerotic plaque has been linked to the fate of the plaque as described by Davies *et al.*, who showed that plaques with  $\geq 40\%$  of lipid core harbor a higher risk of undergoing rupture and subsequent thrombosis<sup>6</sup>. Thus far, although different lipid-lowering strategies have demonstrated a clear clinical benefit, changes in local plaque burden are modest, ranging from no changes to slower progression or at most halting progression of coronary atheroma<sup>7-10</sup>. Accordingly, a beneficial change in composition might be present and yet remain unnoticed. This hypothesis is supported by experimental, and other *in vivo* observations<sup>9,11</sup>.

Plaque characterization through visual interpretation of gray scale IVUS is imprecise, specially when assessing heterogeneous, lipid-rich plaques<sup>12</sup>. In contrast, spectral analysis of IVUS radiofrequency data has demonstrated potential to provide detailed quantitative information on plaque composition and has been validated in studies of explanted human coronary segments<sup>13</sup>.

Circulating biomarker levels have been shown to predict clinical events in seemingly healthy subjects and in large cohorts of patients with coronary disease<sup>14</sup>. The combination of novel imaging techniques and the assessment of circulating biomarkers could have a potential role in refining the risk stratification in patients and eventually aid further development of novel drug therapies.

This pilot study evaluated for the first time, human coronary atherosclerotic plaque composition at two timepoints six months apart with ultrasound radiofrequency data analysis. In addition, we explored the correlation between different plaque components and circulating biomarker levels.

## Methods

### Patients

The Integrated Biomarker and Imaging Study (IBIS) was a prospective, single center, non-controlled observational study. In this study 84 patients underwent repeated invasive and non-invasive imaging (angiography, IVUS, palpography, multislice computed tomography) at baseline and at 6-month follow-up in the same matched Region Of Interest (ROI). The ROI was determined using identifiable anatomic landmarks (side branch or the ostium of the vessel).

Concomitantly, multiple biomarkers were assessed. IVUS-Virtual Histology™ (IVUS-VH) only became available late in the enrollment period and the 20 patients undergoing serial IVUS-VH constituted the present study population.

In the IBIS trial, patients were eligible if they were referred for percutaneous coronary intervention (PCI) and had a non-significant (< 50 %) lesion, within a ROI in a non-intervened vessel that could be safely interrogated with IVUS. Major relevant exclusion criteria were renal dysfunction (creatinine > 2 mg/dl), life expectancy less than one year, or factors that made follow-up difficult. The Medical Ethics Committee of the Erasmus Medical Center approved the study protocol and all patients gave written informed consent. All imaging techniques were analyzed independently. All patients underwent repeat IVUS-VH imaging at 6 month follow-up, in the same matched ROI as illustrated in Figure 1.

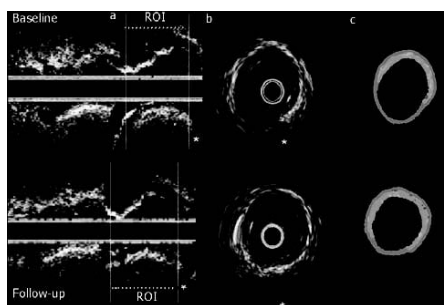


**Figure 1.** (a) The use of identifiable side-branches as anatomic landmarks ensures that the same region of interest (ROI) is analysed at baseline (above) and follow-up (below). (b) Cross-sectional areas, at the two timepoints, can also be matched using side-branches (star) and other identifiable anatomical landmarks. (c) Virtual Histology™ reconstruction of b, depicting essentially unchanged plaque composition.

## IVUS-VH acquisition and analysis

Details regarding the validation of the technique, on explanted human coronary segments, have previously been reported<sup>13,15,16</sup>. Briefly, IVUS-VH uses spectral analysis of IVUS radiofrequency data to construct tissue maps that classify plaque into four major components. In preliminary *in vitro* studies, four histological plaque components (fibrous, fibrolipid, lipid core and calcium) were correlated with a specific spectrum of the radiofrequency signal<sup>13</sup>. These different plaque components were assigned color codes. Calcified, fibrous, fibrolipidic and lipid core regions were labeled white, green, greenish-yellow and red respectively.

IVUS-VH data were acquired, during a continuous pullback (0.5 mm per second) with a commercially available mechanical sector scanner (Ultracross™, 30 MHz catheter, Boston Scientific, Santa Clara, CA, USA), by a dedicated IVUS-VH console (Volcano Therapeutics, Rancho Cordova, CA, USA). The IVUS VH data were stored on a CD-ROM and sent to the imaging core lab for offline analysis (Cardialys, Rotterdam, the Netherlands). IVUS B-mode images were recon-

structured from the RF data by custom software (IVUSLab, Volcano Therapeutics, Rancho Cordova, CA, USA). Subsequently, semi-automatic contour detection of both the lumen and the media-adventitia interface was performed. To account for catheter-to-catheter variability the acquired RF data was normalized using a technique known as "Blind Deconvolution". Blind deconvolution is an iterative algorithm that deconvolves the catheter transfer function from the backscatter, thus enabling automated data normalization<sup>17,18</sup>. Compositional and geometrical data were expressed as mean cross sectional areas (CSA, mm<sup>2</sup>). Plaque area was defined as  $Vessel_{area} - Lumen_{area}$  and percent area stenosis was defined as  $[(Vessel_{area} - Lumen_{area})/Vessel_{area}] \times 100$ . For describing geometrical data plaque was defined as plaque plus media whereas for plaque compositional data the media was not included.

## Biomarkers

Blood for biomarker analysis was centrifuged within 30 minutes and stored at -70°C. Serum C-reactive protein (Diagnostic Systems Laboratories), plasma interleukin 6 and tumor necrosis factor- $\alpha$  (R&D Systems), were measured in the Human Biomarker Center (GlaxoSmithKline, PA) with use of protocols provided by the manufacturer. Lipoprotein-associated phospholipase A<sub>2</sub> activity assay measures the proportional release of aqueous <sup>3</sup>H acetate resulting from the enzymatic cleavage of the <sup>3</sup>H acetyl-platelet activating factor substrate (100  $\mu$ M). N-terminal pro brain natriuretic peptide was measured with use of a two-site electrochemiluminescent assay. The limits of quantification were 0.0048 mg/L for C-reactive protein, 0.057 pg/mL for interleukin-6, 3.92 nmol/min/mL for lipoprotein phospholipase A<sub>2</sub> activity, 10 pg/ml for N-terminal pro brain natriuretic peptide, 0.88 pg/mL for tumor necrosis factor- $\alpha$ , 0.062 ng/mL for sCD40L and 0.13 ng/mL for active MMP-9. Since Lp-PLA<sub>2</sub> is known to be associated with LDL in plasma, we also measured LDL cholesterol<sup>19,20</sup>.

## Statistical analysis

Discrete variables are presented as counts and percentages. Continuous variables are presented as means  $\pm$  standard deviations (SD). Differences in means among groups were analyzed by a two-tailed sample t-test. A P value of less than 0.05 was considered to indicate statistical significance.

Bland Altman analysis plots were used to assess changes between baseline and follow-up<sup>21</sup>. The limits of agreement were determined by the mean difference between both techniques  $\pm$  2 SD.

Comparisons between quantitative outcomes were performed with use of scatterplots and linear regression analysis (regression coefficient). Biomarkers were not normally distributed except for lipoprotein-associated phospholipase A<sub>2</sub> activity. Thus, where appropriate, analyses were performed after natural logarithmic transformation. We looked for correlations between imaging endpoints and circulating biomarkers and calculated the univariate Pearson correlation coefficients. Statistical analyses were performed with use of SAS Version 8 (SAS Institute, Cary, NC).

## Results

Baseline patient (n=20) characteristics are presented in Table 1. The population was relatively young, with a low (10%) prevalence of diabetes; and 65% of the patients were receiving statin therapy

at baseline. The mean values of the conventional IVUS variables, at baseline and follow-up, are presented in Table 2. Of note, the length of region of interest was the same during serial studies (29.9 $\pm$ 14.1 mm vs. 29.3 $\pm$ 13.8 mm, NS). After 6 months, there were no significant changes in LDL-cholesterol ( $\Delta$  0.07 $\pm$ 0.3 nMol/L, p=0.36) and HDL-cholesterol ( $\Delta$  -0.09 $\pm$ 0.2 nMol/L, p=0.09) levels. Although there were no significant changes in mean vessel or lumen cross-sectional areas, there were non-significant trends towards an increase in absolute plaque area and percent area obstruction (Table 2).

**Table 1. Patient's demographical characteristics (n: 20)**

Male sex (%)	18 (90)
Age (yr $\pm$ SD)	56.3 $\pm$ 13.3
Diabetes (%)	2 (10)
Hypertension (%)*	7 (35)
Hypercholesterolemia (%)#	16 (80)
Current smoking (%)	3 (15)
Previous smoking (%)	11 (55)
Family history of coronary disease (%)	10 (50)
Previous myocardial infarction (%)	9 (45)
<b>Medications at baseline</b>	
Statins (%)	13 (65)
Beta-blockers (%)	11 (55)
Angiotensin converting enzyme inhibitors (%)	4 (20)
Angiotensin II antagonist (%)	4 (20)
<b>Clinical presentation</b>	
Stable angina (%)	7 (35%)
Unstable angina (%)	6 (30%)
Myocardial infarction (%)	7 (35%)

\*Blood pressure  $\geq$  160/95 mmHg or treatment for hypertension, # total cholesterol > 215 mg/dl or treatment for hypercholesterolemia

**Table 2. Intravascular ultrasound derived dimensions of vessel, lumen, and plaque area and mean plaque burden at baseline and six month follow-up.**

Mean cross-sectional area (mm <sup>2</sup> ) $\pm$ SD	Baseline	6 months	p value
Lumen	8.5 $\pm$ 3.1	8.3 $\pm$ 2.7	0.4866
Vessel	15.0 $\pm$ 3.8	15.0 $\pm$ 3.5	0.9369
Plaque	6.5 $\pm$ 2.1	6.8 $\pm$ 2.0	0.0742
Percent area stenosis (%)	44.2 $\pm$ 10.7	45.7 $\pm$ 9.8	0.0999

Plaque area refers to  $Vessel_{area} - Lumen_{area}$ . Percent area stenosis refers to  $[(Vessel_{area} - Lumen_{area})/Vessel_{area}] \times 100$ .

## Plaque characterization using IVUS-VH

Absolute values for major plaque components (calcium, fibrous, fibrolipidic and lipid core), at baseline and follow-up, are presented in Table 3. Overall, there were no significant changes over time. These results are illustrated in graphic form in Figure 2.

Bland Altman plots for conventional IVUS variables (Figure 3) and for individual plaque components on IVUS-VH (Figure 4) show that there were no systematic differences, for any variable, between baseline and follow-up. The predominant components were fibrous (68%) and fibrolipidic (20%) plaque. Typical examples of baseline and follow-up findings are presented in Figures 1 and 5.

**Table 3. Plaque composition at baseline and six month follow-up.**

Mean cross-sectional area (mm <sup>2</sup> )±SD	Baseline	6 month	p value
Calcium	0.036±0.05	0.033±0.04	0.7031
Fibrous	2.68±1.5	2.90±1.5	0.1412
Fibrolipidic	0.77±0.4	0.73±0.4	0.7118
Lipid core	0.42±0.4	0.52±0.5	0.2643

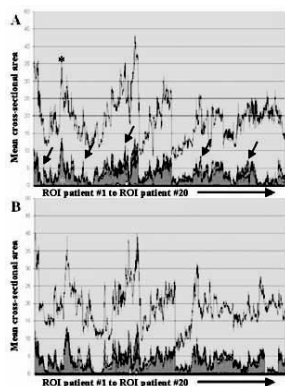


Figure 2. Plaque composition in all 20 patients is plotted sequentially on the x axis (A. Baseline, B. Follow-up). The y axis shows the total percent area stenosis (colored peaks), the composition (calcium: white, fibrous: green, fibrolipidic: greenish-yellow and lipid core: red) and the external elastic membrane (EEM, gray line). After 6 months, no major overall changes in coronary atherosclerosis regarding plaque areas and compositional components are evident in all available cross-sections.

### Changes in IVUS-VH vs. changes in biomarkers

Temporal changes of biomarker levels are depicted in Table 4. There was a significant decrease in Lp-PLA<sub>2</sub> ( $p < 0.0001$ ), CRP ( $p = 0.02$ ), IL-6 ( $p = 0.004$ ) and NT-pro-BNP ( $p = 0.02$ ). Active MMP-9 levels increased ( $p = 0.002$ ). Among the seven biomarkers tested in the IBIS trial, Lp-PLA<sub>2</sub> activity emerged repeatedly as being significantly correlated to the change in plaque composition observed by IVUS-VH analysis. As shown in Figure 6, change in lipid core area ( $r = 0.51$ ,  $p = 0.024$ ), fibrous area ( $r = 0.49$ ,  $p = 0.033$ ) and calcium area ( $r = 0.63$ ,  $p = 0.004$ ), were significantly correlated with change in Lp-PLA<sub>2</sub>. In parallel, the change in LDL cholesterol was also significantly correlated with the change in lipid core area ( $r = 0.61$ ,  $p = 0.016$ , Figure 6D). In contrast, there were only non-significant trends between changes in CRP or active MMP-9 and change in lipid core area ( $r = 0.45$ ,  $p = 0.061$  and  $r = 0.44$ ,  $p = 0.061$ , respectively).

**Table 4. Levels of biomarkers at baseline and follow-up**

	Baseline	Follow-up	P value
Lp-PLA <sub>2</sub>	124.2±35.1	87.4±28.2	<0.0001
CRP	2.0±1.1	1.1±0.8	0.02
Active MMP-9	4.4±0.7	5.4±0.8	0.002
IL-6	1.9±1.4	0.9±1.1	0.004
sCD40L	0.7±0.6	0.9±0.7	0.51
NT-proBNP	5.3±1.3	4.6±0.9	0.02
TNF-α	0.7±0.3	0.7±0.8	0.97

Lp-PLA<sub>2</sub>: lipoprotein-associated phospholipase A<sub>2</sub>;  
 CRP: high sensitivity C-reactive protein, active;  
 MMP-9: active metalloproteinase 9;  
 IL-6: interleukin 6;  
 sCD40L: soluble CD40 ligand;  
 NT-proBNP: N-terminal pro brain natriuretic peptide;  
 TNF-α: tumor necrosis factor alpha.

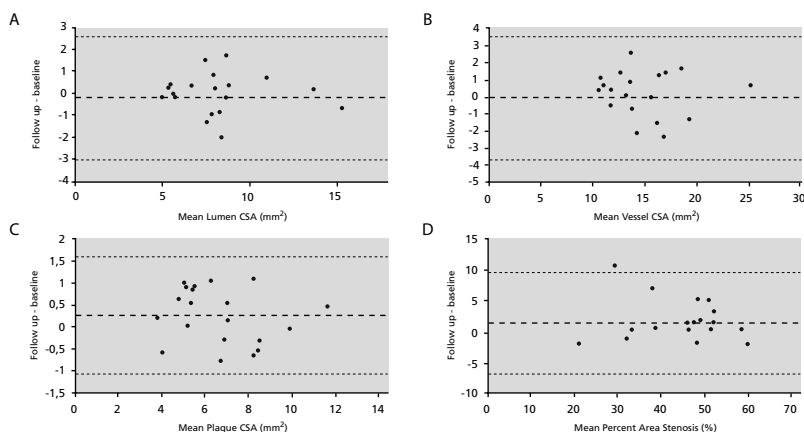


Figure 3. This Bland-Altman plot demonstrates that there is no systematic change in any conventional intravascular ultrasonography parameter (A: lumen cross-sectional area (CSA), B: vessel CSA, C: plaque CSA and D: percent area stenosis) over the 6 month observation period.

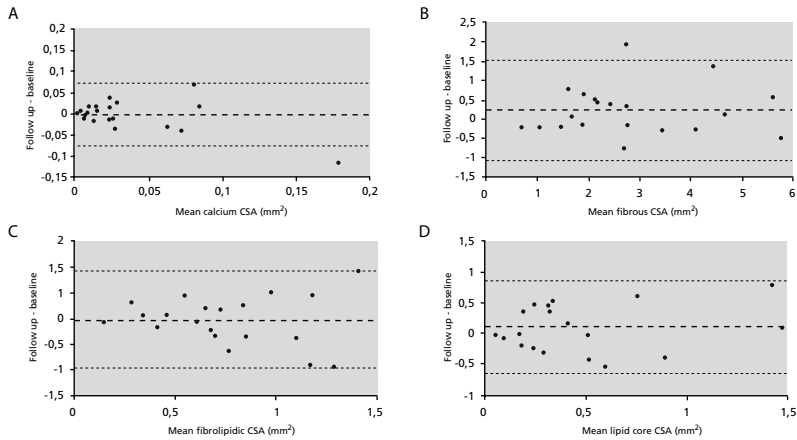


Figure 4. Panels a, b, c and d show Bland-Altman plots demonstrating that there is no systematic change in plaque composition over the 6 month observation period.

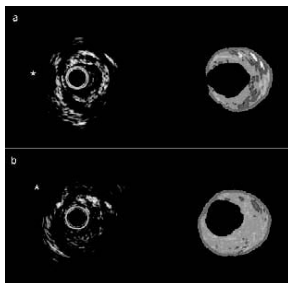


Figure 5. Matched baseline and follow-up IVUS-VH cross-sections from a patient who presented with an unheralded ST elevation myocardial infarction and had no previous medical history of note. There was a predominantly fibrous plaque (green) with islands of lipid core (red), as illustrated in a cross-sectional image (Panel A) from the baseline pullback. At six-months follow-up (Panel B), a matched cross-section (the anatomic landmark was a side-branch, indicated by the asterisk) shows a mainly fibrotic plaque with an apparent reduction in lipid core area.

## Discussion

Although pathological studies have demonstrated that the potential of atherosclerotic coronary plaque to precipitate clinical events is strongly influenced by plaque composition, no imaging techniques in clinical use can reliably assess plaque composition<sup>11</sup>. In the IBIS trial, we have prospectively evaluated non-flow limiting atherosclerotic plaques with conventional and novel imaging techniques over a 6-month observational period in order to establish the background changes in the imaging parameters that reflect the variability and reproducibility of the measurements in a contemporary patient pop-

ulation treated with conventional medications such as statins, angiotensin-converting enzyme inhibitors and antiplatelet drugs. The major finding of this study was that, over this relatively short observational period, there were no significant changes in the mean values of either classic IVUS parameters (vessel, lumen, or plaque area, or percent area obstruction) or of novel IVUS-VH parameters. Most IVUS studies on plaque progression have mandated follow-up at a time-point between 12 and 18 months<sup>7-10,22</sup>. The absence of significant changes on classic IVUS parameters, in the present study, is therefore not unexpected. As this is the first prospective study to assess serially plaque composition, using IVUS-VH technique, these findings must be interpreted as preliminary. The lack of significant change in plaque composition, over a short time-period suggests that the technique is reproducible *in vivo*. Although there were no significant changes in either mean values of classic IVUS parameters or individual plaque components on IVUS-VH, there was a trend towards an increase in plaque area, reflecting a non-significant increase in lipid core area. This observation is consistent with histopathological studies showing that the atheromatous component of plaque enlarges in a linear fashion with increasing degrees of cross-sectional narrowing and with the fact that the lipid core is the most active component of the plaque<sup>23,24</sup>. In that respect, it is remarkable to note that the majority of the relationships between the biomarkers and the compositional nature of the plaque concern the lipid core and among the biomarkers analyzed Lp-PLA<sub>2</sub> exhibits the most active role. This enzyme plays a key role in mediating the hydrolysis of oxidatively modified phosphatidylcholines in LDL, thus generating lysophosphatidylcholine and oxidized fatty acids, molecules that are implicated in several detrimental effects in the vessel wall<sup>25-28</sup>. To what extent the observed changes in plaque composition are mediated by Lp-PLA<sub>2</sub> or its carrier, LDL cholesterol, can be only addressed in the future larger studies with potent Lp-PLA<sub>2</sub> inhibitors. It is noteworthy, however, that the change in levels of LDL

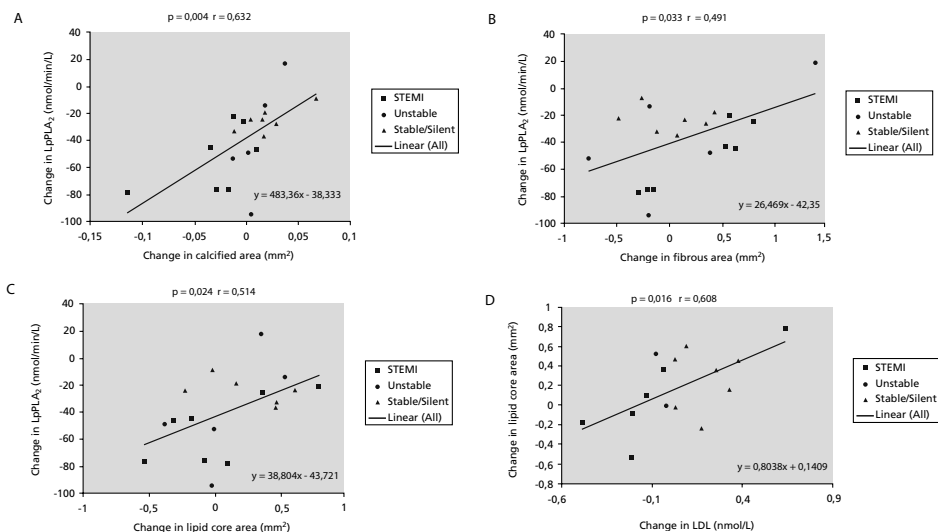


Figure 6. Significant correlations were noted between temporal changes in Lp-PLA<sub>2</sub> activity and the changes in lipid core (panel A) fibrous component (panel B), and calcium (panel C) in mean cross sectional areas (CSA). Panel D shows the significant correlation between changes in lipid core and LDL-cholesterol. Lp-PLA<sub>2</sub> refers to lipoprotein-associated phospholipase A<sub>2</sub>.

was also positively correlated with changes in lipid core areas. These findings make the observed association between imaging-derived assessment of lipid core and both LDL (i.e., atherogenic substrate) as well as Lp-PLA<sub>2</sub> activity (i.e., enzyme responsible for LDL-derived inflammatory mediators) more consistent. Aside from the lipid core and the calcified components, the sclerotic component of the vessel wall (fibrous tissue) accounted for almost 70% of plaque area composition. This observation is concordant with previously reported morphometric data from postmortem studies<sup>23</sup>, thus providing indirect evidence for the validity of the technique. Plaque characterization *in vivo* has the potential to allow the assessment of the effects of pharmacological therapies on the coronary arteries, thereby enabling a better understanding of the disease and further development of new pharmacologic interventions. Using a slightly different approach, spectral analysis of radiofrequency data has recently shown that statins can promote detectable changes in plaque composition despite lacking a significant shift in plaque burden<sup>29</sup>. This pilot clinical study provides some indication on the boundaries of change beyond which modifications in tissue composition might be interpreted as statistically significant change in a contemporary population of patients with CAD that are treated with routine medical therapy following PCI.

### Limitations

The IBIS study was an observational, non-controlled, single center study where plaque composition was re-assessed after a short time (6 months). Only a relatively short vessel segment was interrogated by IVUS (~30 mm) that may not be representative of plaque com-

position within the entire coronary tree. We also wish to underscore that the results of the present study are derived from a small subset of patients and will require further confirmation. Finally, the patient population included in the IBIS study was intentionally heterogeneous and most had a high level of background medication. Whether novel IVUS-based plaque imaging could refine risk stratification in patients undergoing clinically mandated cardiac catheterization will require long-term natural history studies, nonetheless, information regarding plaque composition is obtained during a standard IVUS pullback without the need for additional instrumentation of the coronary artery.

### Conclusions

After a 6-month observational period, no significant changes were detected in plaque burden or composition. These results were expected, since no new therapeutic intervention was tested and all patients received routine medical care following PCI. This pilot clinical study provides some indication on the boundaries of change beyond which modifications in tissue composition might be interpreted as statistically significant. IVUS-VH may provide insights into pathophysiology in studies of the natural history of coronary plaque. Furthermore, it may provide surrogate endpoints and offers the potential to allow the assessment of emerging pharmacologic interventions with novel mechanisms of action.

### Acknowledgements

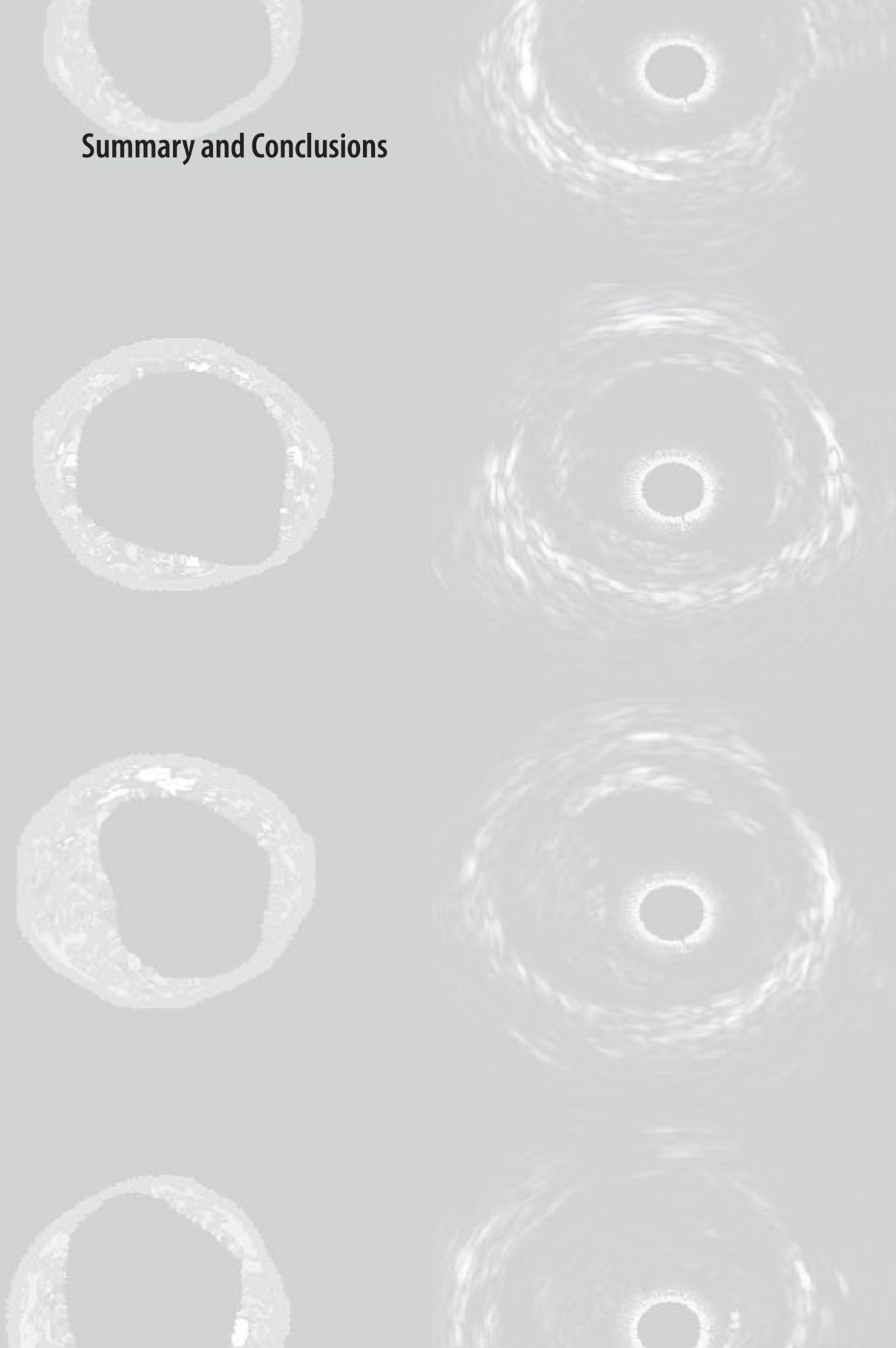
This study was supported by unrestricted education grant from GlaxoSmithKline.

## References

1. Yusuf S, Reddy S, Ounpuu S, Anand S. Global burden of cardiovascular diseases: part I: general considerations, the epidemiologic transition, risk factors, and impact of urbanization. *Circulation*. 2001;104:2746-53.
2. Pasterkamp G, Schoneveld AH, van der Wal AC, Haudenschild CC, Clarijs RJ, Becker AE, Hillen B, Borst C. Relation of arterial geometry to luminal narrowing and histologic markers for plaque vulnerability: the remodeling paradox. *J Am Coll Cardiol*. 1998;32:655-62.
3. Smits PC, Pasterkamp G, Quarles van Ufford MA, Eefting FD, Stella PR, de Jaegere PP, Borst C. Coronary artery disease: arterial remodeling and clinical presentation. *Heart*. 1999;82:461-4.
4. Schoenhagen P, Ziada KM, Kapadia SR, Crowe TD, Nissen SE, Tuzcu EM. Extent and direction of arterial remodeling in stable versus unstable coronary syndromes: an intravascular ultrasound study. *Circulation*. 2000;101:598-603.
5. Burke AP, Koldogje FD, Farb A, Weber DK, Malcom GT, Smialek J, Virmani R. Healed plaque ruptures and sudden coronary death: evidence that subclinical rupture has a role in plaque progression. *Circulation*. 2001;103:934-40.
6. Davies MJ, Richardson PD, Woolf N, Katz DR, Mann J. Risk of thrombosis in human atherosclerotic plaques: role of extracellular lipid, macrophage, and smooth muscle cell content. *Br Heart J*. 1993;69:377-81.
7. Nissen SE, Tuzcu EM, Schoenhagen P, Brown BG, Ganz P, Vogel RA, Crowe T, Howard G, Cooper CJ, Brodie B, Grines CL, DeMaria AN. Effect of intensive compared with moderate lipid-lowering therapy on progression of coronary atherosclerosis: a randomized controlled trial. *Jama*. 2004;291:1071-80.
8. Jensen LO, Thyssen P, Pedersen KE, Stender S, Haghfelt T. Regression of coronary atherosclerosis by simvastatin: a serial intravascular ultrasound study. *Circulation*. 2004;110:265-70.
9. Scharf M, Bocksch W, Koschyk DH, Voelker W, Karsch KR, Kreuzer J, Hausmann D, Beckmann S, Gross M. Use of intravascular ultrasound to compare effects of different strategies of lipid-lowering therapy on plaque volume and composition in patients with coronary artery disease. *Circulation*. 2001;104:387-92.
10. Takagi T, Yoshida K, Akasaka T, Hozumi T, Morioka S, Yoshikawa J. Intravascular ultrasound analysis of reduction in progression of coronary narrowing by treatment with pravastatin. *Am J Cardiol*. 1997;79:1673-6.
11. Helft G, Worthley SG, Fuster V, Fayad ZA, Zaman AG, Corti R, Fallon JT, Badimon JJ. Progression and regression of atherosclerotic lesions: monitoring with serial noninvasive magnetic resonance imaging. *Circulation*. 2002;105:993-8.
12. Gussenhoven EJ, Essed CE, Lancee CT, Mastik F, Fritman P, van Egmond FC, Reiber J, Bosch H, van Urk H, Roelandt J, et al. Arterial wall characteristics determined by intravascular ultrasound imaging: an in vitro study. *J Am Coll Cardiol*. 1989;14:947-52.
13. Nair A, Kuban BD, Tuzcu EM, Schoenhagen P, Nissen SE, Vince DG. Coronary plaque classification with intravascular ultrasound radiofrequency data analysis. *Circulation*. 2002;106:2200-6.
14. Ridker PM. Clinical application of C-reactive protein for cardiovascular disease detection and prevention. *Circulation*. 2003;107:363-9.
15. Nair A, Kuban BD, Obuchowski N, Vince DG. Assessing spectral algorithms to predict atherosclerotic plaque composition with normalized and raw intravascular ultrasound data. *Ultrasound Med Biol*. 2001;27:1319-31.
16. Nair A, Calvetti D, Vince DG. Regularized autoregressive analysis of intravascular ultrasound backscatter: improvement in spatial accuracy of tissue maps. *IEEE Trans Ultrason Ferroelectr Freq Control*. 2004;51:420-31.
17. Káresen K. Deconvolution of sparse spike trains by iterated window maximization. *IEEE Trans Signal Process*. 1997;45:1173-1183.
18. Káresen K, Bølviiken E. Blind deconvolution of ultrasonic traces accounting for pulse variance. *IEEE Trans Ultrason Ferroelectr Freq Control*. 1999;46:564-573.
19. Stafforini DM, Prescott SM, McIntyre TM. Human plasma platelet-activating factor acetylhydrolase. Purification and properties. *J Biol Chem*. 1987;262:4223-30.
20. Tsoukatos DC, Arborati M, Liapikos T, Clay KL, Murphy RC, Chapman MJ, Ninio E. Copper-catalyzed oxidation mediates PAF formation in human LDL subspecies. Protective role of PAF:acetylhydrolase in dense LDL. *Arterioscler Thromb Vasc Biol*. 1997;17:3505-12.
21. Bland JM, Altman DG. Statistical methods for assessing agreement between two methods of clinical measurement. *Lancet*. 1986;1:307-10.
22. von Birgelen C, Hartmann M, Mintz GS, Baumgart D, Schmermund A, Erbel R. Relation between progression and regression of atherosclerotic left main coronary artery disease and serum cholesterol levels as assessed with serial long-term (> or =12 months) follow-up intravascular ultrasound. *Circulation*. 2003;108:2757-62.
23. Kragel AH, Reddy SG, Wittes JT, Roberts WC. Morphometric analysis of the composition of atherosclerotic plaques in the four major epicardial coronary arteries in acute myocardial infarction and in sudden coronary death. *Circulation*. 1989;80:1747-56.
24. Wilcox JN, Smith KM, Schwartz SM, Gordon D. Localization of tissue factor in the normal vessel wall and in the atherosclerotic plaque. *Proc Natl Acad Sci U S A*. 1989;86:2839-43.
25. Parthasarathy S, Steinbrecher UP, Barnett J, Witztum JL, Steinberg D. Essential role of phospholipase A2 activity in endothelial cell-induced modification of low density lipoprotein. *Proc Natl Acad Sci U S A*. 1985;82:3000-4.
26. Hakkinen T, Luoma JS, Hiitunen MO, Macphee CH, Milliner KJ, Patel L, Rice SQ, Tew DG, Karkola K, Yla-Herttuala S. Lipoprotein-associated phospholipase A(2), platelet-activating factor acetylhydrolase, is expressed by macrophages in human and rabbit atherosclerotic lesions. *Arterioscler Thromb Vasc Biol*. 1999;19:2909-17.
27. Quinn MT, Parthasarathy S, Steinberg D. Lysophosphatidylcholine: a chemotactic factor for human monocytes and its potential role in atherogenesis. *Proc Natl Acad Sci U S A*. 1988;85:2805-9.
28. Carpenter KL, Challis IR, Arends MJ. Mildly oxidised LDL induces more macrophage death than moderately oxidised LDL: roles of peroxidation, lipoprotein-associated phospholipase A2 and PPARgamma. *FEBS Lett*. 2003;553:145-50.
29. Kawasaki M, Sano K, Okubo M, Yokoyama H, Ito Y, Murata I, Tsuchiya K, Minatoguchi S, Zhou X, Fujita H, Fujiwara H. Volumetric quantitative analysis of tissue characteristics of coronary plaques after statin therapy using three-dimensional integrated backscatter intravascular ultrasound. *J Am Coll Cardiol*. 2005;45:1946-53.



## Summary and Conclusions



## **Summary and Conclusions**

Intravascular ultrasound (IVUS) has emerged as a highly accurate tool for the serial assessment of the natural history of coronary atherosclerosis and to evaluate the effect of different conventional and emerging drug therapies on the progression of atherosclerosis. The contemporary and future application of IVUS is linked to the study of different applications of the analysis of radiofrequency data, both for the improvement of plaque characterization and for the assessment of mechanical properties of plaques. Overall, such insightful analysis of the radiofrequency data might potentially aid the detection of plaques with allegedly high-risk characteristics and monitor their natural history in prospective natural history studies.

This thesis provides important data regarding the internal and external validation of spectral analysis of radiofrequency data for the assessment of plaque composition *in vivo*.

### **Technical issues**

From a technical standpoint, we have learned from this thesis that manual calibration leads to high variability and therefore an algorithm correcting for the inter-catheter variability is essential for the reproducibility of the technique (chapter 2.4).

The reproducibility of IVUS-VH was initially evaluated in an indirect fashion (chapter 11.3) and later using an appropriate methodology (chapter 2.3). The latter study demonstrated that the geometrical and compositional output of IVUS-VH is acceptably reproducible. Finally, non-uniform pullbacks, particularly present when using phased array

catheters devoid of covering sheath, remain an issue of concern and should be taken into account for the conductance of longitudinal studies (chapter 2.3).

### **Clustering of plaque composition along coronary arteries.**

Local factors seem to play a role in determining plaque progression and stability throughout the coronary tree. This has been demonstrated both in pathological studies and in clinical studies using angiography and IVUS (to detect plaque rupture in the latter). This thesis has extensively addressed the non-uniformity of plaque composition along the coronary tree (chapters 3.1, 3.2, 7.1 and 7.2).

In particular, we determined that plaque composition is not uniformly distributed along the left coronary artery with a progressive increase in necrotic core starting from the proximal half of the left main coronary artery to the most proximal segment of the left anterior descending or circumflex artery, followed by a steady decline towards those segments which are more distally located along the vessel.

### **Influence of shear stress on atherosclerosis**

In chapter 4.1, we found that atherosclerotic plaques located at the ostium of the left anterior descending artery presented larger plaque burden, eccentricity and maximum plaque thickness than distal left main plaques. In addition, a larger calcified and necrotic core content was found distal to the circumflex take-off. Lesions were predominantly located in the outer wall of the carina and such location was associated with larger necrotic core content. Overall, these results confirm the key role of flow dynamics in the genesis and progression of atherosclerosis.

## **Vulnerable plaque**

In chapter 6.1, a prospective 3-vessel IVUS study, patients with at least one plaque rupture in their coronary tree had larger body mass index and overall worse IVUS-derived characteristics compared to patients without evidence of plaque rupture. In addition, plaque rupture sites had a worse phenotype than the most diseased sites of the same vessels.

It has been established that thin-cap fibroatheroma (TCFA) lesions with large avascular, hypocellular, lipid cores, are the most prevalent substrate of plaque rupture. A large series of victims of sudden cardiac death suggested that ruptured TCFA was the precipitating factor for 60 % of acute coronary thrombi. The same study demonstrated that plaque rupture at TCFA may also occur without clinical consequences. The ability to identify TCFA in patients would both help clarify the natural history of these lesions and provide the means to assess the effects of pharmacological or other interventions.

In chapter 7.1, we found that IVUS-VH findings, compatible with IVUS-derived TCFA (IDTCFA), were common in non-culprit lesions of patients undergoing percutaneous intervention in another vessel. In addition, the prevalence of IDTCFA was significantly higher in patients who presented with ACS compared to stable patients and the distribution of IDTCFA lesions along the coronary vessels was clearly clustered. These findings were further confirmed in a 3-vessel population (chapter 7.2).

In chapter 8.1, we verified *in vivo* the relationship between plaque composition and coronary remodeling. Necrotic core size was significantly larger in coronary lesions that demonstrated positive remodelling than in those that experienced vessel shrinkage.

Furthermore, the fibrotic burden of the plaque was significantly and inversely correlated to the remodeling index.

### **Combining different invasive imaging techniques**

Intravascular ultrasound palpography is a technique that allows the assessment of local mechanical tissue properties. This technique has shown a high sensitivity and specificity to detect vulnerable plaques *in vitro*. The relationship between mechanical and compositional properties of coronary atherosclerosis has not been fully elucidated. In chapter 9.2, we sought to explore *in vivo* the relation between mechanical (palpography) and compositional (IVUS-VH) properties of matched cross-sectional areas using novel catheter-based techniques. IVUS-VH showed an acceptable sensitivity to detect high strain as assessed by palpography. In turn, the specificity was low, reflecting a high number of false positives. Of interest, a significant inverse relationship was present between calcium and strain levels and the contact of necrotic core tissue with the lumen was found the only predictor of the detection of high strain.

In chapter 9.3, we evaluated the sensitivity and specificity of 3-D ECG-gated IVUS to detect deformable (high strain) plaques assessed by palpography. The sensitivity was low and the specificity was high. Nevertheless, it should be mentioned that this small study suffered from several limitations.

### **Plaque progression/regression**

IVUS has become the gold standard to assess *in vivo* the effect of conventional and novel medical therapies on plaque size and composition. In this respect, we have evaluated the geometrical and compositional agreement between mechanical and rotational catheters

(chapter 2.1). A significant variability in direct measurements and plaque echogenicity was identified confirming the importance of the use of a single IVUS catheter for longitudinal measurements.

Chapter 11.1 is a meta-analysis of all clinical studies that assessed IVUS-based progression/regression of coronary atherosclerosis to evaluate whether the treatment with statins can promote coronary plaque regression over time. In this study, we found that statin therapy, in particular when achieving the target LDL-C < 100 mg/dl level, appears to promote a significant regression of plaque volume in coronary artery segments as measured by IVUS.

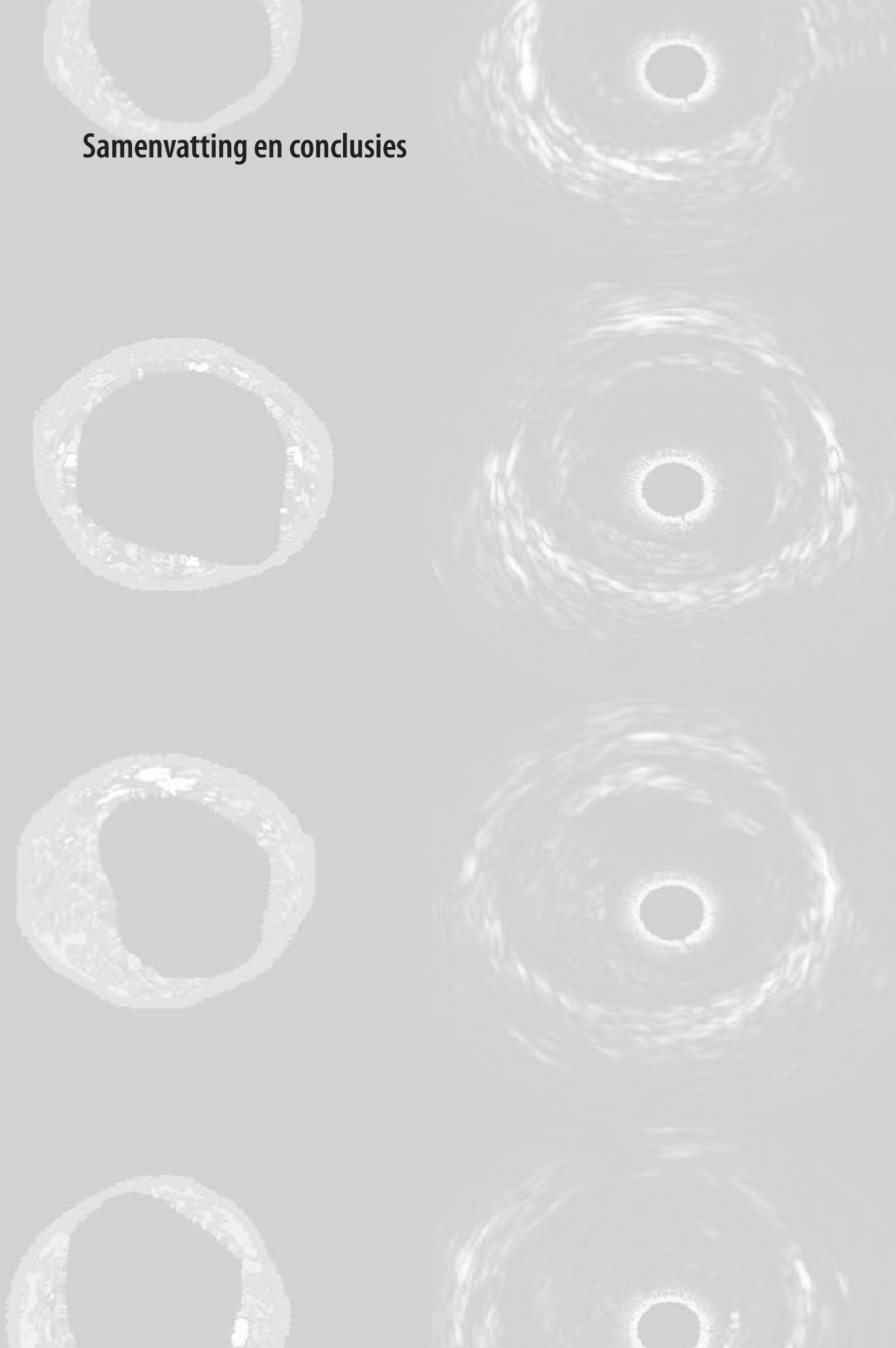
Additionally, we evaluated the effect of ACE-inhibitors on coronary atherosclerosis and our results suggest that in patients with established CAD, stable angina and without overt heart failure, the clinical benefit obtained with perindopril treatment during a period of 3 year cannot be attributed to an effect on coronary plaque size.

## **Conclusion**

We believe that the work presented in this thesis is of value to better understand the extent, distribution, morphology and composition of atherosclerosis in living patients.

We have provided important data regarding the accuracy of an in vivo tissue characterization technique (IVUS-VH). Among our findings, we have identified a potential in vivo surrogate of thin cap fibroatheroma, the most prevalent predecessor of plaque rupture. Nevertheless, interpretation of our findings must be cautious until conclusive data supplied by prospective natural history studies is released.

## Samenvatting en conclusies



## **Samenvatting en conclusies**

Intravasculaire echo (IVUS) is uitgegroeid tot een accurate methode voor het bestuderen van de ontstaanswijze van atherosclerose en IVUS is effectieve techniek gebleken in het beoordelen van het effect van verschillende conventionele en nieuwe farmacologische behandelingen op het gebied van atherosclerose. De toepassingen van IVUS zijn gekoppeld aan de verschillende toepassingen van de analyse van radiofrequency data, zowel ter verbetering van plaque karakterisering als voor de beoordelingen van de mechanische eigenschappen van de plaque. Inzicht in de analyse van radiofrequency data kan voordeel bieden in de opsporing, beoordeling en monitoring van potentiële “hoog risico” plaques in een verscheidenheid aan prospectieve studies.

Dit proefschrift verschaft belangrijke gegevens betreffende de interne en externe validiteit van de analyse van radiofrequency data ter beoordeling van plaque samenstelling in vivo.

### ***Technische zaken***

Vanuit een technisch oogpunt hebben we uit dit proefschrift geleerd dat manuele calibratie leidt tot een hoge variabiliteit en daarom is een algoritme dat corrigeert voor de inter-katheter variabiliteit essentieel voor de reproduceerbaarheid van de techniek (hoofdstuk 2.4).

De reproduceerbaarheid van IVUS Virtuele Histologie (IVUS-VH) werd aanvankelijk geëvalueerd op een indirecte manier (hoofdstuk 11.3) en later op een gestructureerde manier (hoofdstuk 2.3). De laatstgenoemde studie toonde aan dat de geometrie en samenstelling van de plaque, verworven door IVUS-VH, acceptabel en reproduceerbaar was. Uiteindelijk presenteren niet gelijkvormige pullbacks zich met name wanneer “phased array katheters” verstoken raken van de omhullende sheath. Dit blijft een rede tot bezorgdheid en moet in overweging worden genomen bij het oprichten van longitudinale studies (hoofdstuk 2.3).

## ***Clustering van plaque samenstelling in de coronairarteriën***

Lokale factoren lijken een rol te spelen in de beoordeling van plaque progressie en stabiliteit doorheen het coronaire stelsel. Dit is zowel in pathologische als klinische studies aangetoond, middels het gebruik van angiografie en IVUS (om scheuring van de plaque op te sporen). Dit proefschrift heeft uitgebreid aandacht besteed aan de niet uniforme plaque samenstelling doorheen de coronairarteriën (hoofdstuk 3.1, 3.2, 7.1 en 7.2).

Meer specifiek hebben we aangetoond dat de samenstelling van de plaque niet uniform verdeeld is in de linker coronairarterie met een progressieve toename in de hoeveelheid van de grootte van de necrotische kern, vanaf de hoofdstam tot aan het meest proximale segment van de linker coronairarterie of circumflex, gevolgd door een geleidelijke toename richting de meer distale segmenten.

## ***De invloed van shear stress op atherosclerose***

In hoofdstuk 4.1 hebben we gevonden dat atherosclerotische plaques in het ostium van de linker coronairarterie meer plaque belasting ondervinden, meer excentrisch zijn en een grotere maximale plaque dikte hebben dan plaques meer distaal in de hoofdstam. Daarbij, meer calcificatie en hoeveelheid necrotische kern werd gevonden distaal van het ostium van de circumflex. De laesies waren met name gelokaliseerd in de buitenwand van de carina, resulterend in grotere hoeveelheden necrotische kern. Deze resultaten bevestigen de sleutelrol van de stroomdynamiek in het ontstaan en de progressie van atherosclerose.

## ***Vulnerable plaque***

In hoofdstuk 6.1, een prospectieve 3-vats IVUS studie, bleken patiënten met ten minste 1 plaquescheur in hun coronairen een grotere body mass index te hebben en globaal slechtere door IVUS verkregen prognose te hebben in vergelijking tot patiënten zonder aanwijzingen

voor plaque scheuring. Plaatsen waarop scheuring van de plaque plaatsvond hadden een ongunstiger phenotype dan de meest zieke gedeelten van dezelfde vaten.

Het is vastgesteld dat fibroatheromas met een dunne kap (TCFA) laesies met grote avasculaire en hypocellulaire vetkernen, de meest voorkomende substraten zijn voor plaquescheuring. Een grote serie van slachtoffers van plotse cardiale dood suggereerde dat gescheurde TCFAs de aanleiding waren voor 60% van acute coronaire thrombi. Dezelfde studies hebben aangetoond dat plaque scheuring bij TCFA's ook zonder klinische consequenties kan verlopen. De mogelijkheid tot het identificeren van TCFA's in patiënten kan leiden tot het beter in kaart brengen van ontstaanswijze van deze laesies en een mogelijkheid bieden tot het beoordelen van het effect van farmacologische of andere interventies.

In hoofdstuk 7.1 vonden we dat IVUS-VH bevindingen als met IVUS verkregen TCFAs (IDTCFA), veel voorkwamen in non-culprit laesies en in patiënten die percutane interventies in andere vaten ondergingen. Daarbij kwamen IDTCFAs significant vaker voor in patiënten die zich presenteerden met acuut coronair syndroom in vergelijking tot patiënten met stabiele angina pectoris en de verdeling van IDTCFA laesies doorheen de coronairen was duidelijk geclusterd. Deze bevindingen werden bevestigd in een 3-vats populatie (hoofdstuk 7.2).

In hoofdstuk 8.1 bestudeerden we in vivo de relatie tussen plaque samenstelling en coronaire vervorming. De grootte van de necrotische kern was significant groter in coronaire laesies die positieve vervorming vertoonden in vergelijking tot coronaire laesies die vessel krimping vertoonden. De fibrotische belasting van de plaque was significant en reversibel gecorreleerd met de index van vervorming.

## ***Combineren van verschillende invasieve beeldvormende technieken***

Intravasculaire geluidsgolf palpografie is een techniek die het toelaat de lokale mechanische weefseleigenschappen te beoordelen. Deze techniek heeft bewezen een hoge sensitiviteit en specificiteit te hebben voor het detecteren van de gevoelige plaque in vitro. De relatie tussen de mechanische eigenschappen van coronaire atherosclerose en de samenstelling hiervan is momenteel nog niet bekend. In hoofdstuk 9.2 hebben we in vivo de relatie tussen mechanische eigenschappen (palpografie) en samenstelling van de plaque (IVUS-VH) van gematchte dwars doorsneden middels een nieuwe katheter gebaseerde techniek. IVUS-VH toonde een acceptabele sensitiviteit om hoge spanning te detecteren middels palpografie. Anderzijds bleek de specificiteit laag te zijn, resulterend in een hoog aantal vals positieven. Opmerkelijk was dat er een significante omgekeerde relatie was tussen calcium en spanningswaarden en het contact van necrotische kern weefsel met het lumen was de enige voorspeller voor het aantonen van hoge spanning.

In hoofdstuk 9.3 evalueerden we de sensitiviteit en specificiteit van 3-D ECG gated IVUS voor het detecteren van vervormbare (hoge spanning) plaques beoordeeld middels palpografie. De sensitiviteit was laag en de specificiteit was hoog. Er moet echter wel gezegd worden dat deze kleine studie meerdere beperkingen had.

## ***Plaque progressie/regressie***

IVUS is de gouden standaard geworden voor de in vivo beoordeling van het effect van conventionele en nieuwe medische therapieën op het gebied van plaque samenstelling en grootte. In dit opzicht hebben we gekeken naar de overeenkomsten in geometrie en samenstelling zoals bepaald met mechanische en draaiende katheters (hoofdstuk 2.1). Een

significante variabiliteit in de directe metingen en plaque echogeniciteit werd aangetoond, wat het belang aantoonde van een enkele IVUS katheter voor longitudinale metingen.

Hoofdstuk 11.1 is een meta-analyse van alle klinische studies die IVUS gebaseerde progressie/regressie van coronair arterie sclerose beoordeelden om te kijken of de behandeling met statines plaque regressie kan veroorzaken. In deze studie, met op IVUS gebaseerde eindpunten, vonden we dat behandeling met statines, met name wanneer er een LDL-C gehalte  $< 100\text{mg/dl}$  werd behaald, significante plaque regressie kan veroorzaken.

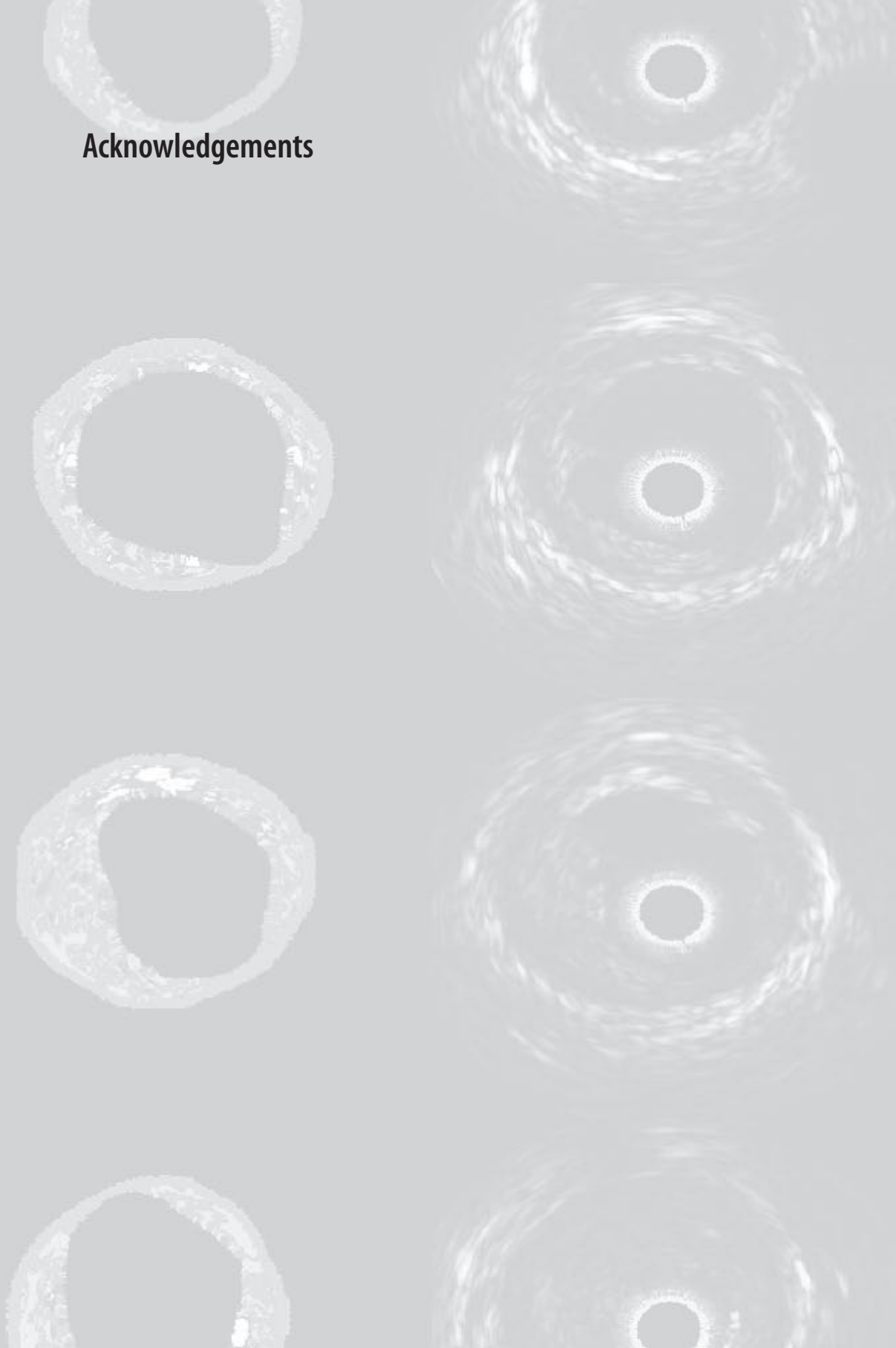
Aanvullend beoordeelden we het effect van ACE-remmers op coronaire atherosclerose. In patiënten met aangetoond coronairlijden en stabiele angina pectoris zonder duidelijk hartfalen, waren de klinische voordelen behaald met perindopril behandeling gedurende 3 jaar niet toe te schrijven aan een effect van de coronaire plaque grootte.

## **Conclusie**

Wij zijn van mening dat het werk gepresenteerd in dit proefschrift van aanzienlijke waarde is op het gebied van het begrijpen van de uitgebreidheid van coronairlijden, haar verdeling, morfologie en samenstelling in levende patiënten.

We hebben belangrijke gegevens gepubliceerd met betrekking tot de accuraatheid van een techniek voor in vivo weefsel beoordeling (IVUS-VH). We hebben een potentieel in vivo surrogaat gevonden (TCFA) als meest voorkomende precursor van plaque scheuring. Onze bevindingen moeten echter met enige voorzichtigheid geïnterpreteerd worden gezien er nog geen duidelijk beeld is over de precieze natuurlijke ontstaanswijze van de plaque.

## Acknowledgements



I have reached now probably the most important part of the thesis, where I truly and gratefully acknowledge all the people that stood beside me during this journey.

First of all (as in red wine, first always comes the most gifted one), I would like to thank my wife, the wonderful Inés. She left all behind, her city, family, friends and job to join me in Rotterdam. She even had to struggle for 2 years to obtain a residence permit that never came about, but she still was always my main motivation and support with her unique smile, energy and positiveness. Painting our small apartment in Den Haag, biking to Scheveningen, drinking a beer at “The Plein”, eating “dubbel vla” while watching a movie, biking to the laundry with 7 kgs of clothes under unprecedented temperatures... Ine, de todos los recuerdos que nos llevamos a Buenos Aires lo mejor fue haber compartido todo eso con vos. Gracias por todo lo que me diste en tantos años, esta tesis es tuya, como lo soy yo desde que te conocí.

I would like to thank in second place Professor Serruys. Prof., you have taught me so many things. I have never seen such a hard working person like you; even a Japanese fellow looks lazy beside you. It is incredible how you never loose your passion for what you do. It was an honor to work with you and I am extremely grateful for the time I have spent watching and listening how you set the path for the present and future interventional cardiology.

Professor de Feyter, thank you for teaching me without words that in research we have to be cautious and patient. I enjoyed very much the time that you approached me during a break in a meeting in Taormina and you told me about the wonders of the mountains of Italy.

I would like to thank the generous participation of the prestigious PhD Committee Members; Anton van der Steen, Rob Krams, Don Poldermans, Allard van der Wal, Gerard Pasterkamp and William Wijns.

The Z guys, in order of appearance. Jiro Aoki (Jiro-san), my dear Japanese friend. I cannot fully tell you how great was meeting you. You made my life less miserable during my first months in Rotterdam, when I was all alone living in an unfurnished, unconnected (no tv, no telephone, no internet) tiny apartment. We spent so many great moments together; Inés and I really miss you and the great Asato. It is not by chance that we are organizing the thesis defense on the same date.

Dr. Vijay Maniyal from Cochin, India. We had so much fun with Jiro and Vijay that we couldn't stop laughing, specially that day when you said you didn't know Elvis or The Beatles, but that you knew perfectly well the Spice Girls! Vijay, you are a fantastic, loveable person, I hope yourself, Prya and Vishnu are happy back in Cochin.

Marco Valgimigli, Marquino, finally you did it, I told you from the beginning! You are an extremely gifted and hard working italian. I have learned a lot about research with you. You are certainly what Prof. would call a future, or better yet present, "trialist". Those 10 days in Sardegna were wonderful, as was the last month I spent with you and Paty in your apartment. I really hope the best for you and Paty. Malagutona, I miss our talks and your spaghetti aglio olio pepperoncino!!! I'll see you in Buenos Aires for some crispy parotids!!

Héctor García<sup>2</sup>, Que hubo Guey, deja de quejarte ya....My dear friend, my SPSS advisor, for moments almost a psychologist...We made a great team, the only bad consequence was that you made me increase at least 8 kilos during our IVUS analyses in Cardialysis eating nachos, cookies, coke, etc, etc...Even while I was back in Buenos Aires we continued working together quite a lot and I will miss such a prolific partnership. I am very glad that

Lulu is working now and I hope both of you together with Andrés can achieve your personal goals.

Pierfrancesco Agostoni, another gifted Italian who, as well as Marco, knows how to enjoy life aside from flow charts and catheters. Ago, I miss the great evenings either at our place or in Rotterdam. Those were really good moments. You should come to visit us in Buenos Aires, the city that never sleeps. I am completely sure that you will soon become a great interventional cardiologist.

Andrew Ong, the living GPS. If you want to know where to, how to, when to, etc... just ask Andrew. Thanks for encouraging me in the initial moments and “veel success” in Australia. Carlos van Mieghem, an authentic gentleman. Carlos, you are a serious, hard working, honest man and I appreciate that. I hope the best for you and your family wherever the future finds you.

The “former” fellows, Pedro Lemos, Angela Hoye and Francesco Saia. Thank you very much for your kind advice and support. You are already demonstrating your skills in the “real world”. Pedrinho, I apologize on beforehand for eliminating you from the World Cup. Try next time.

The other Japanese fellows, Keiichi and Shuzou. Keiichi-san, the fastest eater in the world; is also a dedicated father, and both a gifted writer and (this comes from the X files) dancer. Thank you for all the help and I wish you the best for your family.

Shuzou, the most “western” Japanese. A rocket can go off beside him and he will still smile and be positive. I really admire that kind of attitude. Sophia Vaina, a very kind, ambitious and hard working Greek fellow. Sophia, it was great meeting you, thank you for your kindness and I hope you can go back soon to Greece and meet your husband. Joost, the

only dutch fellow, who was very kind to translate the conclusions. Thanks a lot Joost, it's a pity we share so little time at the Thorax.

I would like to give special thanks to Eugene Mc Fadden, a real model to follow, both personally and from a working standpoint. Eugene, it was wonderful meeting you and having time to know you a bit. Next time you come to Argentina call me in advance so you don't get stuck in Iguazu for a week!!

Anya, Professor's right hand and a key person for every fellow, thanks a lot for your kindness. Evelyn Regar, thanks for involving me in the fascinating world of OCT. Nico Bruining, beste Nico, you taught me that dutch people also enjoy dark humour and I loved that. We worked together quite a lot and I really hope that we will work together again in the future. Sebastiaan de Winter, expert software programmer. We also shared everlasting months working in the PERSPECTIVE and other projects. I am indebted with you for all your efforts. Jurgen Ligthart, a trademark of the Thoraxcenter, thanks for introducing me in the fantastic world of IVUS. We spent endless our analyzing cases, eating stroopwafels and drinking tons of coffee. Thanks Jurg, the Thorax would not be the same without you.

Thanks to Paul Cummins and Arno Ruiter for the help in study management and constant smile. Thanks to Annet Louw for her great assistance for the thesis preparation.

I would like to thank all the staff of the Thorax; the interventional cardiologists Wim van der Giessen, Peter de Jaegere, Maarten van Ent, Eric Duckers, Robert J. van Geuns and George Sianos; and the technicians Gio, Elko, Emil, John, Max, Maaïke, Anne-Marie....

I would like to sincerely thank all the people in Cardialysis. I have spent almost half of my time in Rotterdam doing IVUS analyses there. In particular I would like to thank Marie-Angele Morel, an extremely kind, capable and efficient person; Gerrit-Anne van Es, Ravindhra Pawar, Ally, Jamal, Dick...Thanks to all of you. Also to Yvonne van Lint, who

speaks in perfect Spanish but strangely (I believe she has never been there) with a Cuban accent, what I find quite funny. Gracias por toda tu ayuda, espero verte en Buenos Aires!

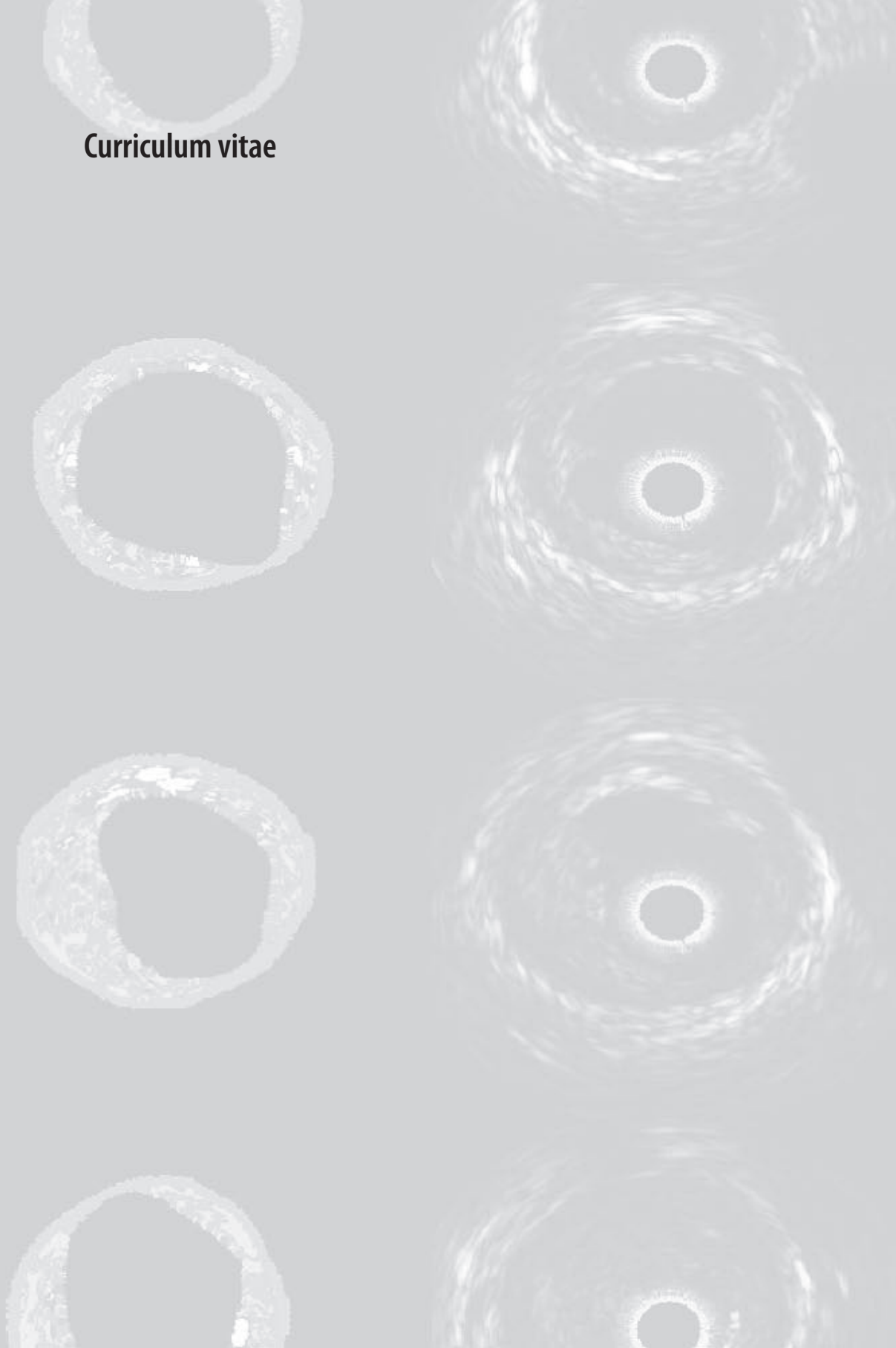
Very special thanks to the friends that we made in Den Haag, with whom we built up a little Argentina in The Netherlands. Tano y Vicky (con Isa y Franchu), Nico y Sofí (con Viole y Olivia), Felix y Ana, Bastiaan y Paty (con Max), y la trotamundos Dieuwke, gracias a todos por su apoyo tanto en los malos como en los buenos momentos. Se extrañan los asados, las charlas, las críticas, las risas, los gritos, todo.

Thanks a lot to Isa Usandivaras (@design), who designed the thesis cover.

My co-workers in Buenos Aires, Miguel Rosales, Elina Degrossi and Milu Durbano, and all the Interventional Cardiology Department of the Otamendi Hospital; gracias por el apoyo. My in laws Pepe, Susy and brother and sister in law Panchín and Mary, gracias por estar siempre ahí. Finally, I would like to thank my family. My father Alfredo, for reflecting always an image of hard work, for having generated my curiosity for research and for encouraging me to come to Rotterdam. My mother Delia, for educating me as a person and setting most of the values I have. My brothers and sisters: Matías, Tomás, Agustina and Clara; gracias chicos por el apoyo incondicional. I would also like to thank my grandmother Beba and grandfather Alfredo, an example to follow, both in life and in work, gracias abuelo!.

I hope my words were clear, our experience in The Netherlands was globally (from a cultural, social, academic, and sentimental point of view) incredible. Muchas Gracias!!

# Curriculum vitae



Gastón A. Rodríguez Granillo, son of Alfredo E. Rodríguez and Delia M. Granillo Casas was born in Buenos Aires, Argentina on January 13th, 1979. He married Inés Dávalos Michel on December 6<sup>th</sup>, 2003.

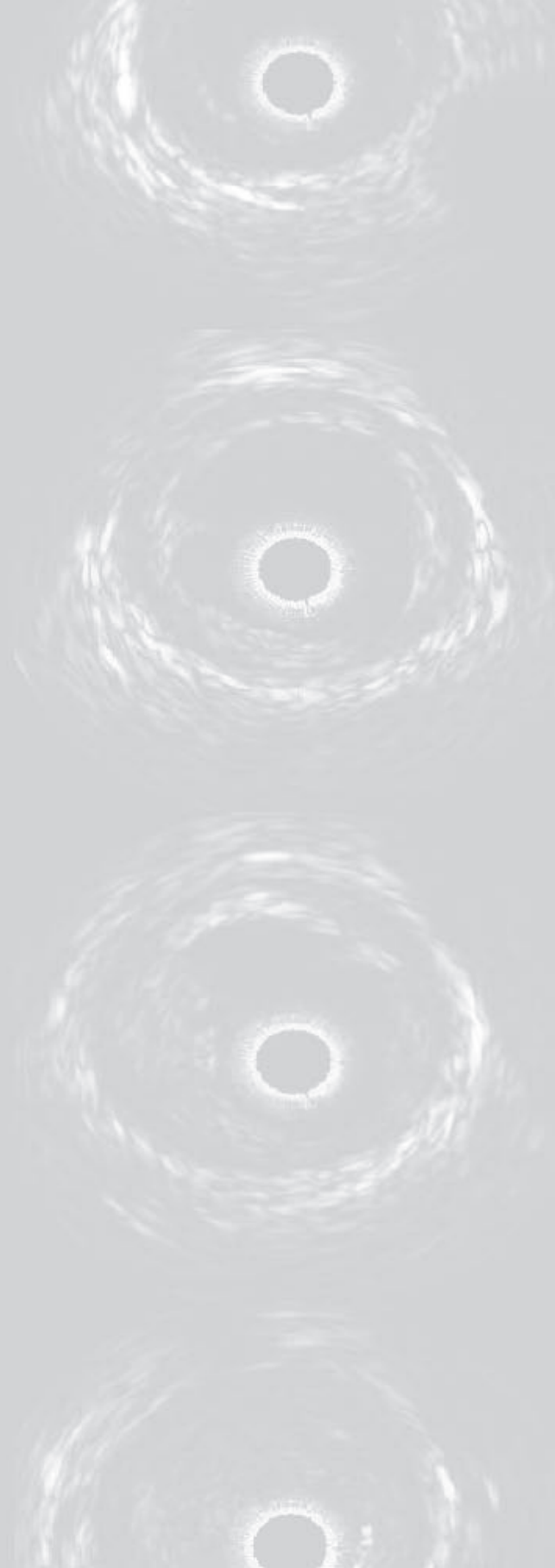
He carried out his undergraduate studies at the “Colegio Champagnat”, located in Buenos Aires and graduated in 1996.

He obtained his medical degree in 2002 at the “Universidad Austral”, located in Buenos Aires.

Work experience:

- Emergency Department, (2000-2002). Hospital Municipal Sanguinetti, Pilar, Argentina.
- Department of Cardiology (2002-2003). Sanatorio Otamendi, Buenos Aires, Argentina.
- Interventional Cardiology Department (2003-2005). Erasmus Medical Center, Rotterdam, The Netherlands.
- Cardiovascular Imaging Department (November 2005- ). Sanatorio Otamendi, Buenos Aires, Argentina.

## Publications



## Publications

1. **Rodriguez Granillo GA**, Aoki J, Ong ATL, Valgimigli M, van Mieghem C, Regar E, McFadden E, de Feyter P, Serruys PW. Methodological Considerations and Approach to Cross-Technique Comparisons using In Vivo Coronary Plaque Characterization Based on Intravascular Ultrasound Radiofrequency Data Analysis: Insights From the Integrated Biomarker and Imaging Study (IBIS). *International Journal of Cardiovascular Interventions*. 2005;7(1):52-8.
2. **Rodriguez Granillo GA**, Bruining N, McFadden E, Ligthart J, Aoki J, Regar E, de Feyter P, Serruys PW. Geometrical validation of intravascular ultrasound radiofrequency data analysis (Virtual Histology™) acquired with a 30 MHz Boston Scientific Corporation imaging catheter. *Catheterization and Cardiovascular Interventions* 66:514–518 (2005).
3. **Rodriguez Granillo GA**, Serruys PW, García-García HM, Aoki J, Valgimigli M, van Mieghem C, McFadden E, de Jaegere P, de Feyter P. Coronary artery remodelling is related to plaque composition. *Heart* 2006;92:388-391.
4. **Rodriguez Granillo GA**, Schaar J, Regar E, Serruys PW. New insights towards catheter-based identification of vulnerable plaque. *Rev Esp Cardiol* 2005; 58: 1197 - 1206.
5. **Rodriguez Granillo GA**, Serruys PW, McFadden EP, van Mieghem C, Goedhart D, Bruining N, Sianos G, van der Steen A, Margolis P, Vince DG, Kaplow J, Zalewski A, de Feyter P. First in man prospective evaluation of temporal changes in coronary plaque composition by in vivo intravascular ultrasound radiofrequency

- data analysis: an integrated biomarker and imaging study (IBIS) substudy. *EuroInterv* 2005;3:282-288.
6. **Rodriguez Granillo GA**, García-García HM, McFadden EP, Valgimigli M, Aoki J, de Feyter P, Serruys PW. In vivo intravascular ultrasound derived thin-cap fibroatheroma detection using ultrasound radiofrequency data analysis. *J Am Coll Cardiol*. 2005 Dec 6;46(11):2038-42.
  7. **Rodriguez Granillo GA**, McFadden EP, Aoki J, van Mieghem C, Regar E, Bruining N, Serruys PW. In vivo variability in quantitative coronary ultrasound and tissue characterization with mechanical and phased-array catheters. *Int J Cardiovasc Imaging*. 2006 Feb;22(1):47-53.
  8. **Rodriguez Granillo GA**, McFadden EP, Valgimigli M, van Mieghem C, Regar E, de Feyter P, Serruys PW. Coronary plaque composition of non-culprit lesions by in vivo intravascular ultrasound radiofrequency data analysis is related to clinical presentation. *Am Heart Journal*. 2006 May;151(5):1027-31.
  9. **Rodriguez Granillo GA**, Agostoni P, García-García HM, de Feyter P, Serruys PW. In vivo, cardiac-cycle related intimal displacement of coronary plaques assessed by 3-D ECG-gated intravascular ultrasound: exploring its correlate with tissue deformability identified by palpography. *Int J Cardiovasc Imaging*. 2006 Apr;22(2):147-52.
  10. **Rodriguez Granillo GA**, García-García HM, Valgimigli M, Pawar R, van der Steen A, de Feyter P, Serruys PW. In vivo relationship between compositional and mechanical imaging of coronary arteries: insights from intravascular ultrasound radiofrequency data analysis. *Am Heart Journal*. 2006 May;151(5):1032-6.

11. **Rodriguez Granillo GA**, del Valle R, Ligthart J, Serruys PW. Detection of a lipid-rich, highly deformable plaque in an angiographically non-diseased proximal LAD. *EuroInterv*. 2005;1:367.
12. **Rodriguez Granillo GA**, García-García HM, Wentzel JJ, Valgimigli M, Regar E, van der Giessen W, de Jaegere P, de Feyter P, Serruys PW. Plaque composition and its relationship with acknowledged shear stress patterns in coronary arteries. *J Am Coll Cardiol*. 2006 Feb 21;47(4):884-5.
13. **Rodriguez Granillo GA**, García-García HM, Valgimigli M, Vaina S, van Mieghem CAG, Regar E, de Jaegere P, van der Ent M, van Geuns RJ, de Feyter P, Serruys PW. Global characterization of coronary plaque rupture phenotype using 3-vessel intravascular ultrasound radiofrequency data analysis. *Eur Heart J*. Accepted.
14. **Rodriguez Granillo GA**, Vaina S, García-García HM, Valgimigli M, Duckers E, van Geuns RJ, Regar E, van der Giessen WJ, Bressers M, Goedhart D, Morel MA, de Feyter P, Serruys PW. Reproducibility of intravascular ultrasound radiofrequency data analysis: implications for the design of longitudinal studies. *Int J Cardiovasc Imag*. 2006 Mar 31; (Epub ahead of print).
15. **Rodriguez Granillo GA**, van Dijk LC, McFadden EP, Serruys PW. Percutaneous radial intervention for complex bilateral renal artery stenosis using paclitaxel eluting stents. *Catheter Cardiovasc Interv*. 2005 Jan;64(1):23-7.
16. **Rodriguez Granillo GA**, Valgimigli M, Ong ATL, Aoki J, van Mieghem C, Hoye A, Tsuchida K, McFadden EP, de Feyter P, Serruys PW. Paclitaxel eluting stents for the treatment of angiographically non-significant atherosclerotic lesions. *International Journal of Cardiovascular Interventions*. *Int J Cardiovasc Intervent*. 2005;7(2):68-71.

17. **Rodriguez Granillo GA**, Valgimigli M, Garcia-Garcia HM, Ong ATL, Aoki J, van Mieghem C, Tsuchida K, McFadden EP, van der Giessen W, de Feyter P, Serruys PW. One year clinical outcome after coronary stenting of very small vessels using 2.25 mm sirolimus and paclitaxel eluting stents: a comparison between the RESEARCH and T-SEARCH registries. *J Invasive Cardiol* 2005;17:409-412.
18. **Rodriguez Granillo GA**, Rosales M, Rodríguez A. Application of Multislice Computed Tomography Coronary Angiography for the Diagnostic Work-up of Acute Coronary Syndromes. *Int J Cardiol*. In press.
19. **Rodriguez Granillo GA**, Agostoni P, García-García HM, Biondi-Zoccai GG, McFadden EP, Bruining N, de Jaegere P, de Feyter P, Serruys PW. Statin therapy promotes plaque regression: a meta-analysis of the studies assessing temporal changes in coronary plaque volume using intravascular ultrasound. Submitted.
20. **Rodriguez Granillo GA**, Bruining N, de Winter S, Vos J, Ligthart J, García-García HM, Valgimigli M, Simoons ML, Fox KM, de Feyter PJ. Long term effect of perindopril on coronary atherosclerosis: results from a multicenter, randomized, double-blind trial. Submitted.
21. **Rodriguez Granillo GA**, Rosales M, Rodríguez A. Multislice CT coronary angiography findings meeting criteria of vulnerability in the left anterior descending artery. *EuroInterv*. In press.
22. Valgimigli M, **Rodriguez-Granillo GA**, Garcia-Garcia HM, Malagutti P, Regar E, De Jaegere P, Van der Giessen WJ, De Feyter P, Serruys PW. Distance from the Ostium as an Independent Determinant of Coronary Plaque Composition In Vivo An Intravascular Ultrasound Study Based Radiofrequency Data Analysis In Humans. *Eur Heart J*. 2006 Mar; 27(6):655-63. Epub 2006 Jan 13.

23. Valgimigli M, **Rodriguez-Granillo GA**, Garcia-Garcia HM, Malagutti P, Regar E, De Jaegere P, Van der Giessen WJ, De Feyter P, Serruys PW. Plaque composition in the left main stem mimics the distal but not the proximal tract of the left coronary artery: Influence of clinical presentation, length of the left main trunk, lipid profile and systemic inflammatory status. *J Am Coll Cardiol*. In press.
24. García-García HM, **Rodriguez Granillo GA**, Valgimigli M, Wentzel J, Gijssen F, Schuurbiens JCH, Krams R, de Feyter P, Serruys PW. Distribution of necrotic core in human coronary arteries is related to blood flow: An in vivo assessment by intravascular ultrasound radiofrequency data analysis. Submitted.
25. Valgimigli M, **Rodriguez Granillo GA**, Agostoni F, Serruys PW. The enduring challenge of vulnerable plaque detection in the cardiac catheterization laboratory. *Dialogues Cardiovasc Med*. 2005; 10:141-150.
26. Garcia-Garcia HM, **Rodriguez-Granillo GA**, Valgimigli M, Regar E, Morel MA, van Es GA, de Feyter PJ, Serruys PW. Distribution of IVUS-Derived Thin-Cap Fibroatheroma in Patients with Acute Coronary Syndrome: An in vivo Three-Vessel Assessment Using Intravascular Ultrasound Radiofrequency Data Analysis. Submitted.
27. Vijayakumar M, **Rodriguez Granillo GA**, Lemos PA, Aoki J, Ong AT, McFadden E, Sianos G, Hofma SH, Smits PC, van der Giessen W, de Feyter P, van Domburg RT, Serruys PW. Sirolimus-eluting Stents for the Treatment of Atherosclerotic Ostial Lesions. *J Invasive Cardiol*. 2005 Jan;17(1):10-2.
28. Aoki J, **Rodriguez Granillo GA**, Serruys PW. Emergent strategies in the interventional cardiology. *Rev Esp Cardiol*. 2005 Aug;58(8):962-973.

29. Valgimigli M, van Mieghem CAG, Ong ATL, Aoki J, **Rodriguez Granillo GA**, McFadden EP, Kappetein A, de Feyter P, Smits PC, Regar E, van der Giessen WJ, Sianos G, de Jaegere P, van Domburg RT, Serruys PW. Short- and Long-term Clinical Outcome after Drug-Eluting Stent Implantation for the Percutaneous Treatment of Left Main Coronary Artery Disease. Insights from the Rapamycin Eluting- and Taxus-Stent Evaluated At Rotterdam Cardiology Hospital Registries (RESEARCH and T-SEARCH). *Circulation*, Mar 2005; 111: 1383 - 1389.
30. Valgimigli M, Malagutti P, **Rodriguez-Granillo G**, Garcia Garcia H, Polad J, Tsuchida K, Regar E, van der Giessen W, de Jaegere P, de Feyter P, Serruys PW. Distal Left Main Coronary Disease Is a Major Predictor of Outcome in Patients Undergoing Percutaneous Intervention in the Drug-Eluting Stent Era: An Integrated Clinical and Angiographic Analysis Based on the Rapamycin-Eluting Stent Evaluated At Rotterdam Cardiology Hospital (RESEARCH) and Taxus-Stent Evaluated At Rotterdam Cardiology Hospital (T-SEARCH) Registries. *J Am Coll Cardiol* 2006 47: 1530-1537.
31. Aoki J, Ong ATL, **Rodriguez Granillo GA**, van Mieghem CAG, Valgimigli M, Tsuchida K, Garcia-Garcia HM, McFadden E, van Domburg RT, de Feyter P, Serruys PW. Full Metal Jacket (stented length  $\geq$  64 mm) Using Drug-Eluting Stents for De Novo Coronary Lesions. *Am Heart J*. 2005 Nov;150(5):994-9.
32. Aoki J, Ong AT, **Rodriguez Granillo GA**, van Mieghem CA, Daemen J, Sonnenschein K, McFadden EP, Sianos G, van der Giessen WJ, de Feyter PJ, van Domburg RT, Serruys PW. The Efficacy of Sirolimus-Eluting Stents versus Bare Metal Stents for Diabetic Patients Undergoing Elective Percutaneous Coronary Intervention. *J Invasive Cardiol*. 2005 Jul;17(7):344-8.

33. Van Mieghem CAG, Bruining N, Schaar JA, McFadden EP, Mollet NR, Cademartiri F, Mastik F, Ligthart JMR, **Rodriguez Granillo GA**, Valgimigli M, Sianos G, van der Giessen WJ, Backx B, Morel MA, van Es GA, Kaplow J, Zalewski A, van der Steen AF, de Feyter PJ, Serruys PW. Rationale and methods of the Integrated Biomarker and Imaging Study (IBIS): combining invasive and non-invasive imaging with biomarkers to detect subclinical atherosclerosis and assess coronary lesion biology. *International Journal of Cardiovascular Imaging*. 2005 Aug;21(4):425-41.
34. Van Mieghem CAG, McFadden EP, de Feyter PJ, Bruining N, Schaar JA, Mollet NR, Cademartiri F, Goedhart D, de Winter S, **Rodriguez Granillo GA**, Valgimigli M, Mastik F, van der Steen AF, van der Giessen WJ, Sianos G, Backx B, Morel MA, van Es GA, Kaplow J, Zalewski A, Serruys PW. Non-invasive Detection of Subclinical Coronary Atherosclerosis Coupled With Assessment, Using Novel Invasive Imaging Modalities, of Changes in Plaque Characteristics Over Time: The IBIS Study (Integrated Biomarker and Imaging Study). *J Am Coll Cardiol*. 2006 Mar 21; 47(6):1134-42.
35. Mansour S, van der Heyden M, de Bruyne B, Vandekerckhove B, Delrue L, van Haute I, Heyndrickx GR, Carlier S, **Rodriguez Granillo GA**, Wijns W, Bartunek J. Intracoronary delivery of hematopoietic bone marrow stem cells and luminal loss of the infarct-related artery in patients with recent myocardial infarction. *J Am Coll Cardiol* 2006 47: 1727-1730.
36. Saia F, Schaar J, Regar E, **Rodriguez-Granillo GA**, de Feyter P, Mastik F, Marzocchi A, Marrozzini C, Ortolani P, Palmerini T, Branzi A, van der Steen AFW, Serruys PW. Clinical imaging of the vulnerable plaque in the coronary arteries: new

- intracoronary diagnostic methods. *J Cardiovasc Med (Hagerstown)*. 2006 Jan;7(1):21-28.
37. Agostoni P, Valgimigli M, Van Mieghem CA, **Rodriguez-Granillo GA**, Aoki J, Ong AT, Tsuchida K, McFadden EP, Ligthart JM, Smits PC, de Jaegere P, Sianos G, Van der Giessen WJ, De Feyter P, Serruys PW. Comparison of early outcome of percutaneous coronary intervention for unprotected left main coronary artery disease in the drug-eluting stent era with versus without intravascular ultrasonic guidance. *Am J Cardiol*. 2005 Mar 1;95(5):644-7.
38. Aoki J, Ong AT, Arampatzis CA, Vijayakumar M, **Rodriguez Granillo GA**, Disco CM, Serruys PW. Comparison of three-year outcomes after coronary stenting versus coronary artery bypass grafting in patients with multivessel coronary disease, including involvement of the left anterior descending coronary artery proximally (a subanalysis of the arterial revascularization therapies study trial). *Am J Cardiol*. 2004 Sep 1;94(5):627-31.
39. Ong A, Serruys PW Aoki J, Hoyer A, van Mieghem C, **Rodriguez Granillo G**, Valgimigli M, Sonnenschein K, Regar E, van der Ent M, de Jaegere P, McFadden EP, Sianos G, van der Giessen W, de Feyter P, van Domburg R,. The unrestricted use of paclitaxel versus sirolimus-eluting stents for coronary artery disease in an unselected population. One Year Results of The Taxus-Stent Evaluated At Rotterdam Cardiology Hospital (T-SEARCH) Registry. *J Am Coll Cardiol*. 2005 Apr 5;45(7):1135-41.
40. Ong A, Hoyer A, Aoki J, van Mieghem C, **Rodriguez Granillo G**, Sonnenschein K, Regar E, McFadden EP, Sianos G, van der Giessen W, de Feyter P, van Domburg R, Serruys PW. 30-Day Incidence and 6-Month Clinical Outcome of Thrombotic

- Stent Occlusion Following Bare Metal, Sirolimus or Paclitaxel Stent Implantation. *J Am Coll Cardiol*. 2005 Mar 15;45(6):947-53.
41. Valgimigli M, Malagutti P, Aoki J, Garcia-Garcia HM, **Rodriguez-Granillo G**, van Mieghem C, Ligthart JM, Ong AT, Sianos G, Regar E, van Domburg RT, de Feyter P, de Jaegere P, Serruys PW. Sirolimus-eluting versus paclitaxel-eluting stent implantation for the percutaneous treatment of the left main coronary artery disease: a combined RESEARCH and T-SEARCH long-term analysis. *J Am Coll Cardiol*. 2006 Feb 7;47(3):507-14. Epub 2006 Jan 18.
42. Vijayakumar M, Lemos PA, Hoye A, Ong AT, Aoki J, **Rodriguez Granillo GA**, McFadden E, Sianos G, Hofma SH, Smits PC, van der Giessen W, de Feyter P, van Domburg RT, Cummins PA, Serruys PW. Effectiveness of sirolimus-eluting stent implantation for the treatment of coronary artery disease in octogenarians. *Am J Cardiol*. 2004 Oct 1;94(7):909-13.
43. Ong AT, Aoki J, Hoye A, van Mieghem CA, **Rodriguez Granillo GA**, Valgimigli M, Tsuchida K, Sonnenschein K, Regar E, van der Giessen WJ, de Jaegere PP, Sianos G, McFadden EP, de Feyter PJ, van Domburg RT, Serruys PW. Short and Long Term (1 year) Outcomes of Unrestricted Utilization of Paclitaxel versus Sirolimus-Eluting Stents in 293 Unselected Consecutive Diabetic Patients. *Am J Cardiol* 2005 Aug;96(3):358-62.
44. Hofma SH, Ong AT, Aoki J, van Mieghem CA, **Rodriguez Granillo GA**, Valgimigli M, Regar E, de Jaegere PP, McFadden EP, Sianos G, van der Giessen WJ, de Feyter PJ, van Domburg RT, Serruys PW. One Year clinical follow-up of Paclitaxel-eluting stents for Acute Myocardial Infarction compared to Sirolimus-eluting stents. *Heart*. 2005 May 9;[Epub ahead of print].

45. Tsuchida K, Ong At, Aoki J, van Mieghem CA, **Rodriguez Granillo GA**, Valgimigli M, Sianos G, Regar E, McFadden EP, van der Giessen WJ, de Feyter PJ, de Jaegere PP, van Domburg RT, Serruys PW. Immediate and one-year outcome of percutaneous intervention of saphenous vein graft disease with Paclitaxel-eluting stents. *Am J Cardiol.* 2005 Aug;96(3):395-8.
46. Hoye A, Ong AT, Aoki J, van Mieghem CA, **Rodriguez Granillo GA**, Valgimigli M, Sianos G, McFadden EP, van der Giessen WJ, de Feyter PJ, van Domburg RT, Serruys PW. Drug-Eluting Stent Implantation for Chronic Total Occlusions: Comparison between the Sirolimus- and Paclitaxel-Eluting Stent. *Eurointervention journal.* 2005;1:193-197
47. Hoye A, van Mieghem CA, Ong AT, Aoki J, **Rodriguez Granillo GA**, Valgimigli M, Tsuchida K, Sianos G, McFadden EP, van der Giessen WJ, de Feyter PJ, van Domburg RT, Serruys PW. Percutaneous therapy of bifurcation lesions with drug-eluting stent implantation: the Culotte technique revisited. *Int J Cardiovasc Intervent.* 2005;7(1):36-40.
48. Hoye A, van Mieghem CA, Ong AT, Aoki J, **Rodriguez Granillo GA**, Valgimigli M, Tsuchida K, Sianos G, McFadden EP, van der Giessen WJ, de Feyter PJ, van Domburg RT, Serruys PW. Long-term Outcomes Following Stenting of Bifurcation Lesions Utilizing the “Crush” Technique: Kissing Balloon Post-Dilatation is Mandatory to Reduce Restenosis of the Side Branch. *J Am Coll Cardiol.* In press.
49. Hoye A, van Mieghem CA, Ong AT, Aoki J, **Rodriguez Granillo GA**, Valgimigli M, Tsuchida K, Sianos G, McFadden EP, van der Giessen WJ, de Feyter PJ, van Domburg RT, Serruys PW. Treatment of De Novo Bifurcation Lesions:

Comparison of Sirolimus- and Paclitaxel-Eluting Stents. Eurointervention journal. 2005;1(1):24-30

49. Hoye A, Iakovou I, Lei G, Van Mieghem C, Ong A, Cosgrave J, Sangiorgi GM, Airoidi F, Montorfano M, Michev I, Chieffo A, Carlino M, Corvaja N, Aoki J, **Rodriguez Granillo GA**, Valgimigli M, Sianos G, van der Giessen W, De Feyter P, Van Domburg R, Serruys PW, Colombo A. Long-term outcomes after stenting of bifurcation lesions with the “crush” technique: predictors of an adverse outcome. J Am Coll Cardiol. 2006 May 16;47(10):1949-58.

### **Book chapters**

1. **Rodriguez Granillo GA**, Serruys PW. Intravascular Ultrasound. In “Carotid atheroma” publicado por Cambridge press. In press
2. **Rodriguez Granillo GA**, Regar E. Optical coherence tomography plaque characterization. Comparison with IVUS-VH. In “Handbook of optical coherence tomography”. Taylor& Francis. In press.

**Abstracts**

1. Aoki J, Ong AT, Arampatzis CA, Vijaykumar M, **Rodriguez Granillo GA**, Disco CM, Serruys PW. Comparison of three-year outcomes after coronary stenting versus coronary artery bypass grafting in patients with multivessel coronary disease, including involvement of the left anterior descending coronary artery proximally (a subanalysis of the Arterial Revascularization Therapies Study Trial). European Society of Cardiology. 2004.
2. Aoki J, Ong AT, Hoye A, Lemos PA, **Rodriguez Granillo GA**, van Mieghem CA, Valgimigli M, de Feyter PJ, van Domburg RT, Serruys PW. Comparison of Unrestricted Utilization of Paclitaxel and Sirolimus-Eluting Stents in Consecutive Unselected Diabetic Patients. European Society of Cardiology 2004.
3. Aoki J, Ong AT, **Rodriguez Granillo GA**, van Mieghem CA, Daemen J, Sonnenschein K, McFadden EP, Sianos G, van der Giessen WJ, de Feyter PJ, van Domburg RT, Serruys PW. The Efficacy of Sirolimus-Eluting Stents versus Bare Metal Stents for Diabetic Patients Undergoing Elective Percutaneous Coronary Intervention. American Heart Association 2004.
4. Angela Hoye, Carlos van Mieghem, Andrew TL Ong, Jiro Aoki, **Gaston A. Rodriguez Granillo**, Marco Valgimigli, Keiichi Tsuchida, Georgios Sianos, Eugene McFadden, Willem J. van der Giessen, Pim J. de Feyter, Ron T. van Domburg, Patrick W. Serruys. Percutaneous Coronary Intervention of De Novo Bifurcation Lesions: Therapy With Sirolimus-Eluting Stents Is Associated With Fewer Major Adverse Cardiac Events and Target Lesion Revascularizations

- Compared With Paclitaxel-Eluting Stent Implantation. American College of Cardiology 2005
5. Jiro Aoki, Andrew T.L. Ong, **Gaston A. Rodriguez Granillo**, Carlos A,G, van Mieghem, Marco Valgimigli, Keiichi Tsuchida, Hector Garcia, Eugene P. McFadden, Ron T. van Domburg, Pim de Feyter, Patrick W. Serruys. Full Metal Jacket for De Novo Coronary Artery Lesions in the Drug-Eluting Stent Era. American College of Cardiology 2005
  6. Carlos Van Mieghem, Eugene McFadden, Pim De Feyter, Patrick Serruys, Johannes Schaar, Nico Bruining, Clemens Disco, Sebastian de Winter, Nico Mollet, Filippo Cademartiri, **Gaston Rodriguez Granillo**, Frits Mastik, Anton van der Steen, Willem van der Giessen, Georgios Sianos, Bianca Backx, Marie-angele Morel, Gerrit-Anne van Es, Jonathon Sawyer, June Kaplow, Andrew Zalewski. Integrating Biomarkers With Invasive and Noninvasive Coronary Plaque Imaging: The IBIS Study (Integrated Biomarker and Imaging Study) American College of Cardiology 2005
  7. Ong AT, Vijayakumar M, Lemos PA, Hoye A, Aoki J, **Rodriguez Granillo GA**, McFadden EP, van der Giessen WJ, de Feyter P, Serruys PW. Sirolimus-eluting Stent Implantation for the Treatment of Coronary Artery Disease in Octogenarians. Presented at the 52<sup>nd</sup> Annual Scientific Meeting of the Cardiac Society of Australia and New Zealand 2004
  8. Ong AT, HoyeA, Aoki J, van Mieghem CA, **Rodriguez Granillo GA**, van der Giessen WJ, de Feyter P, McFadden EP, Serruys PW. Comparative Incidence of Angiographically Proven Early Stent Thrombosis in Unselected Sirolimus and

- Paclitaxel-Eluting Stent Populations. Presented at the 52<sup>nd</sup> Annual Scientific Meeting of the Cardiac Society of Australia and New Zealand 2004
9. Ong AT, Hoye A, Aoki J, van Mieghem CA, **Rodriguez Granillo GA**, van der Giessen WJ, de Feyter P, McFadden EP, Serruys PW. Unrestricted “Real-World” Paclitaxel-Eluting Stent Implantation in a consecutive series of patients. Insights from the Taxus-Stent Evaluated At Rotterdam Cardiology Hospital (T-SEARCH) Registry. Presented at the 52<sup>nd</sup> Annual Scientific Meeting of the Cardiac Society of Australia and New Zealand 2004
  10. Ong AT, Hoye A, Aoki J, van Mieghem CA, **Rodriguez Granillo GA**, Lemos PA, van Domburg RT, Serruys PW. Paclitaxel-Eluting Stent Implantation in an Unselected Consecutive Cohort of Patients with de novo Lesions. Medium Term Results from the Taxus-Stent Evaluated At Rotterdam Cardiology Hospital (T-SEARCH) Registry. Presented at the Annual Scientific Meeting of the European Society of Cardiology 2004
  11. Regar E, **Rodriguez Granillo GA**, Bruining N, de Winter S, Hamers R, van Langenhove G, Verheye S, Serruys PW. Intracoronary optical coherence tomography: a novel approach for three- dimensional quantitative analysis. German Society of Cardiology. Mannheim 2005.
  12. Regar E, Schaar J, Mc Fadden E, van der Giessen W, **Rodriguez Granillo GA**, van Mieghem C, de Feyter P, Serruys PW. Clinical application of real-time, high resolution optical coherence tomography. Can we detect features of vulnerable plaque? German Society of Cardiology. Mannheim 2005
  13. 30-Day Incidence of Thrombotic Stent Occlusion Following Bare Metal, Sirolimus or Paclitaxel Stent Implantation. E. Regar, A.T.L. Ong, A. Hoye, J. Aoki, C. van

- Mieghem, **G.A. Rodriguez Granillo**, K. Sonnenschein, E.P. McFadden, G. Sianos, W.J. van der Giessen, P.P. de Jaegere, P. de Feyter, R.T. van Domburg, P.W. Serruys. German Society of Cardiology. Mannheim 2005
- 14. GA. Rodriguez-Granillo**, HM. Garcia-Garcia, J. Aoki, M. Valgimigli, CAG. Van Mieghem, ATL. Ong, K. Tsuchida, PW. Serruys. Coronary artery remodeling is related to plaque composition. European Society of Cardiology. Stockholm, 2005.
- 15. GA. Rodriguez-Granillo**, M. Valgimigli, E. McFadden, CAG. Van Mieghem, J. Aoki, ATL. Ong, P. De Feyter, PW. Serruys. Coronary plaque composition assessed by in vivo intracoronary ultrasound radiofrequency data analysis, is related to clinical presentation and circulating biomarkers of vulnerability. European Society of Cardiology. Stockholm, 2005.
- 16. GA Rodriguez-Granillo**, P Agostoni, HM Garcia-Garcia, GG Biondi-Zoccai, E Mc Fadden, N Bruining, P de Feyter, PW Serruys. Intravascular ultrasound assessment of the temporal effect of antiatherosclerotic therapies in coronary plaque volume. Insights from a systematic review and meta-analysis of controlled clinical trials. European Society of Cardiology. Stockholm, 2005.
- 17. GA Rodriguez-Granillo**, HM Garcia-Garcia, J Aoki, M Valgimigli, CAG van Mieghem, K Tsuchida, ATL Ong, PW Serruys. Vulnerable plaque detection using ultrasound radio frequency data analysis. European Society of Cardiology. Stockholm, 2005.
- 18. HM Garcia-Garcia, GA Rodriguez-Granillo**, M Valgimigli, J Aoki, CAG van Mieghem, ATL Ong, K Tsuchida, PW Serruys. One year clinical outcome after coronary stenting of very small vessels using 2.25 mm sirolimus and paclitaxel

eluting stents: a comparison between the research and t-search registries. European Society of Cardiology. Stockholm, 2005.

19. Regar E, Schaar J, Mc Fadden E, van der Giessen W, van Mieghem C, **Rodriguez Granillo GA**, de Jaegere PPT, Serruys PW. Real-time, high resolution optical coherence tomography (OCT)- a potential tool to detect features of vulnerable plaque in-vivo? European Society of Cardiology. Stockholm. 2005
20. Pugliese F, Malagutti P, Meijboom WB, Rodriguez G, de Feyter PJ, Krestin GP, Cademartiri F. Vessel wall remodeling with 64-slice CT coronary angiography. Early noninvasive assessment of a parameter for plaque vulnerability with IVUS correlation. European Congress of Radiology. 2005.
21. **GA Rodriguez-Granillo**, HM Garcia-Garcia, M Valgimigli, Pawar R, van der Steen A, de Feyter P, PW Serruys. Sub-internal necrotic core tissue in close contact with the lumen is an independent predictor of the presence of highly deformable regions: Insights from intravascular ultrasound radiofrequency data analysis. TCT 2005. Washington.
22. **GA Rodriguez-Granillo**, HM Garcia-Garcia, S Vaina, E Mc Fadden, M Valgimigli, G Sianos, J Aoki, P de Feyter, PW Serruys. In vivo intravascular ultrasound derived thin-cap fibroatheroma detection using ultrasound radiofrequency data analysis. Athens Interventional Cardiovascular Therapeutics VI. Athens, 2005.
23. **GA Rodriguez-Granillo**, S Vaina, P Agostoni, HM Garcia-Garcia, GG Biondi-Zoccai, G Sianos, Peter de Jaegere, N Bruining, E Mc Fadden, P de Feyter, PW Serruys. Intravascular ultrasound assessment of the temporal effect of antiatherosclerotic therapies in coronary plaque volume. Insights from a systematic

review and meta-analysis of controlled clinical trials. Athens Interventional Cardiovascular Therapeutics VI. Athens, 2005.

24. García-García HM, **Rodríguez Granillo GA**, Valgimigli M, Wentzel J, Gijssen F, Schuurbiens JCH, Krams R, de Feyter P, Serruys PW. Distribution of necrotic core in human coronary arteries is related to blood flow: An in vivo assessment by intravascular ultrasound radiofrequency data analysis. American Heart Association. Atlanta 2006.

Financial support for this thesis was generously provided by:

Volcano Corp.

Pfizer NL

Cardialysis BV

Philips Argentina S.A.

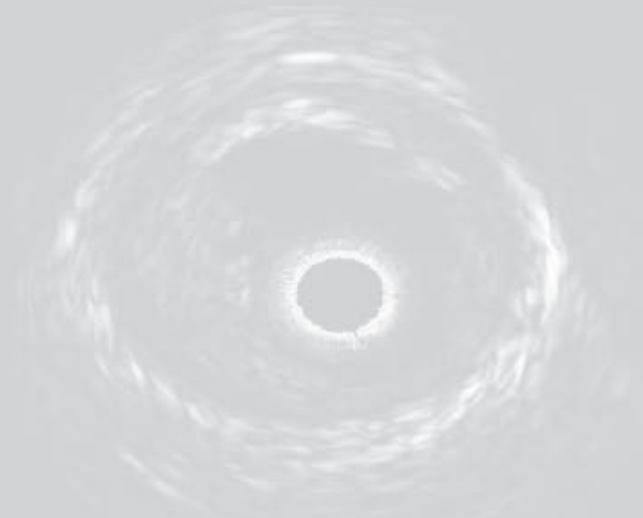
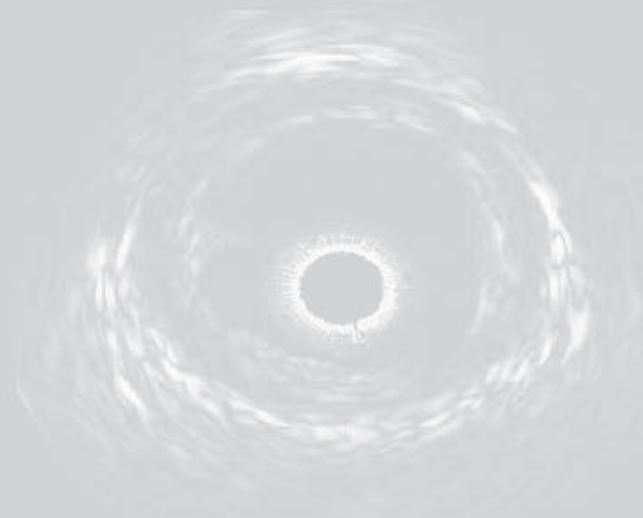
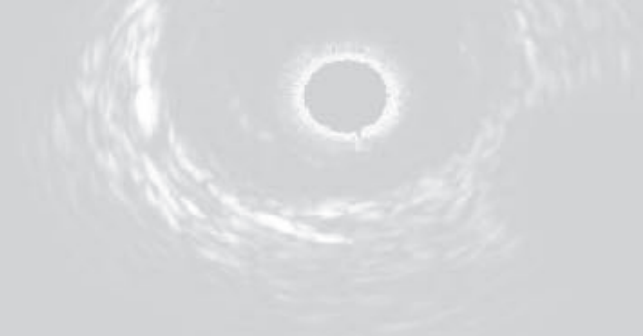
Mallinckrodt Argentina S.A.

Erasmus MC, Rotterdam

Netherlands Heart Foundation



**Color figures**



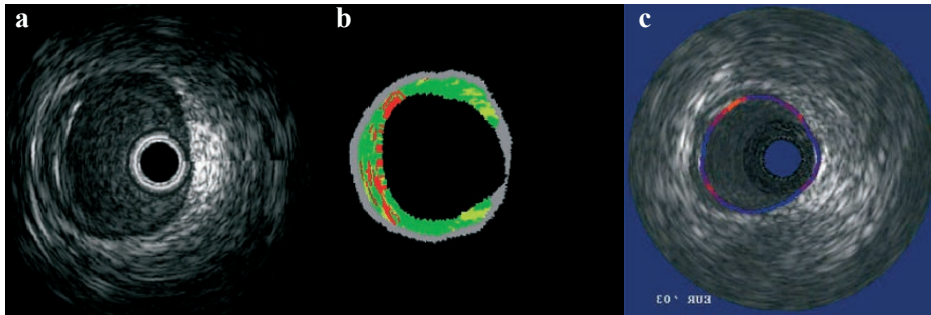


**Figure 1**

Matched cross-section of a left anterior coronary artery imaged by conventional (gray-scale) IVUS (a), IVUS-VH (b) and palpography (c).

IVUS-VH colour-coding labels calcified, fibrous, fibrolipidic and necrotic core regions as white, green, greenish-yellow and red respectively. For palpography, the calculated local strain is also colour-coded, from blue (for 0% strain) through yellow (for 2% strain) via red.

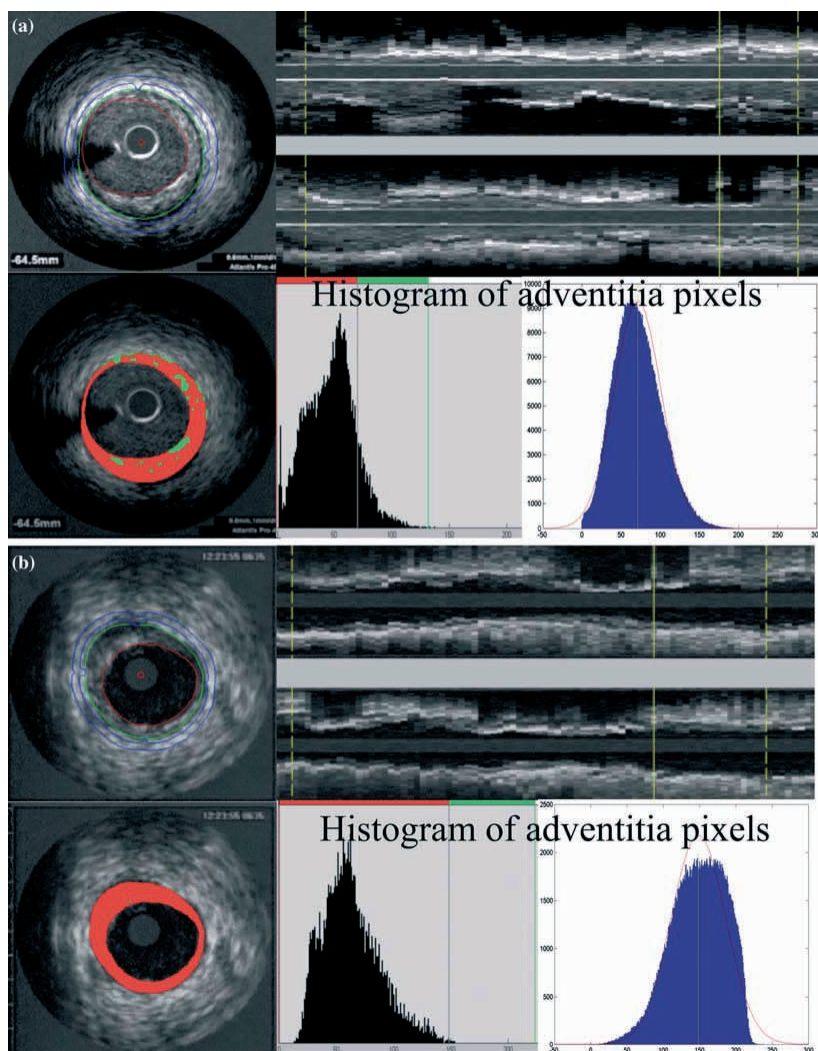


Figure 3. Cross-sectional and longitudinal views of a matched region of interest with 40 (a) and 20 (b) MHz. The adventitia is defined as tissue outside the external elastic membrane. For all non-shadowed adventitia pixels, the mean value and standard deviation are calculated. To observe the suitability, a normal distribution curve based on the same mean and standard deviation histogram is created. Hypochogetic areas are colored red (dark circle) and hyperechogetic areas green (lighter spots).

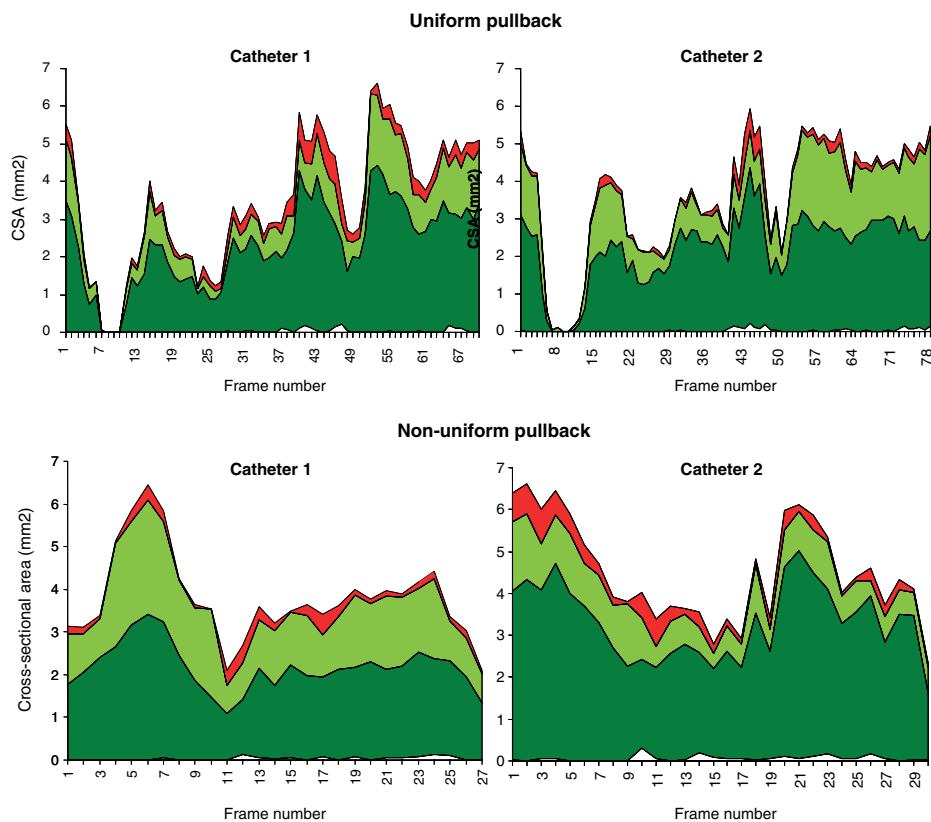


Figure 5. Sequential plotting of a matched ROI interrogated with two catheters. The mean CSA (y axis) of each plaque component is colour-coded (calcium: white; fibrous: green; fibrolipidic: greenish-yellow and necrotic core: red). This figure shows an example of the impact of non-uniform pullbacks on geometrical and compositional measurements.

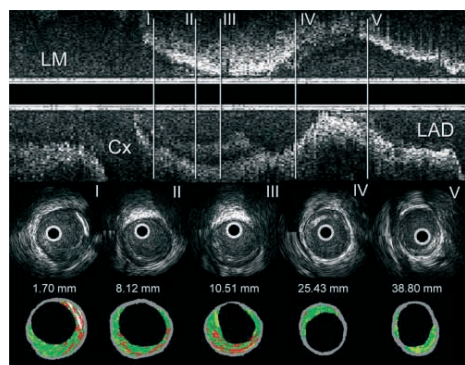
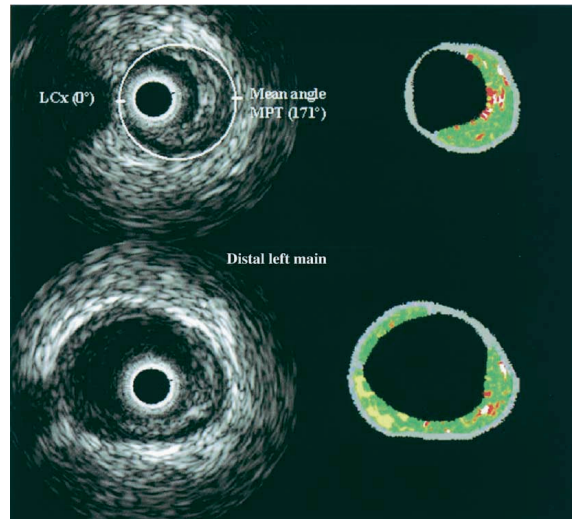
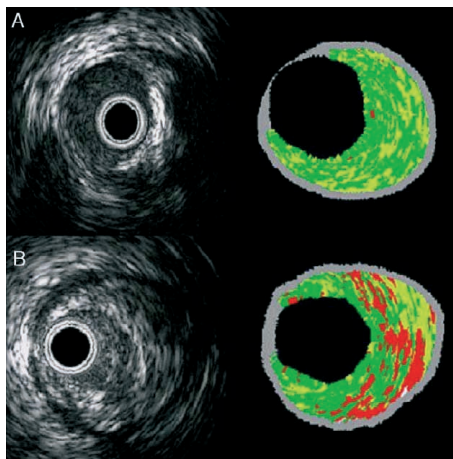


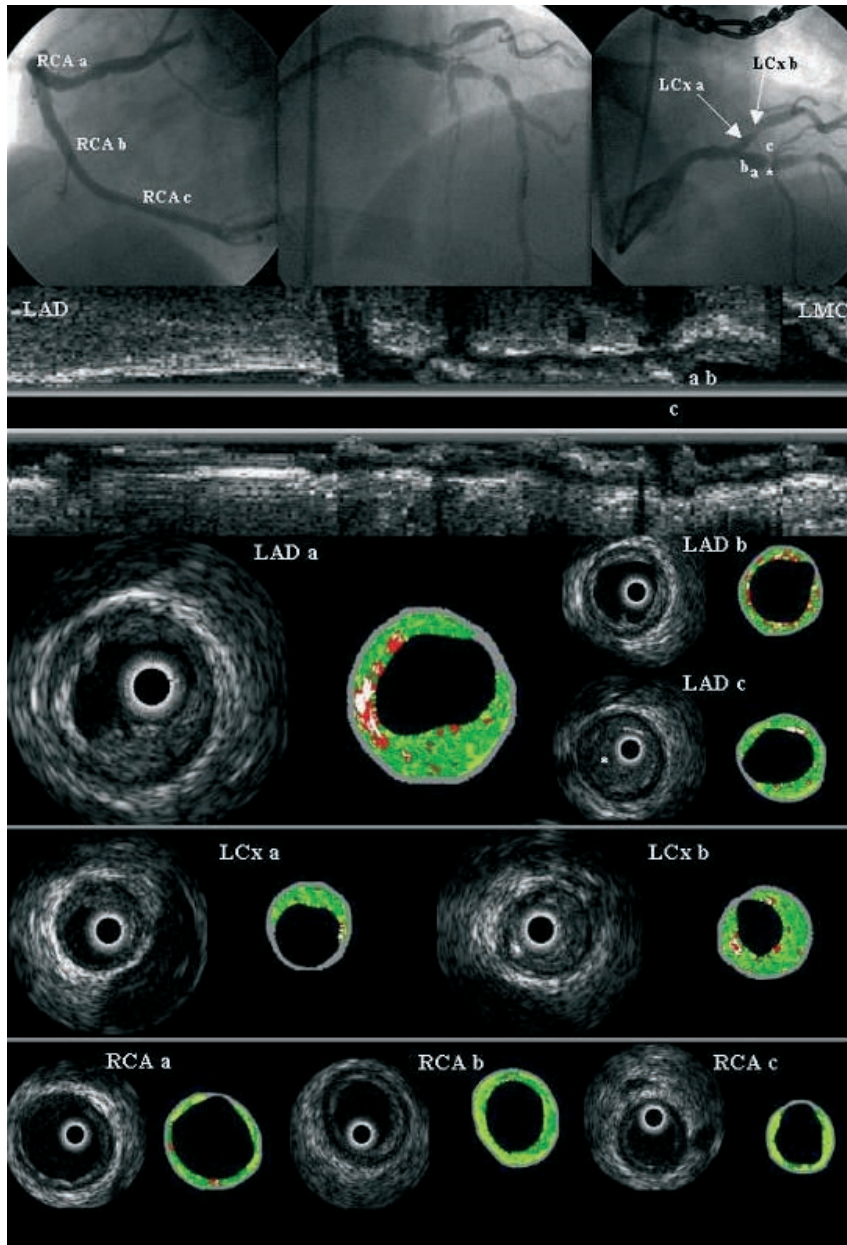
Figure 3. IVUS-VH CSA along a coronary vessel. IVUS-VH cross-sectional areas in a representative patient showing the change in plaque composition (calcium: white; fibrous: green; fibrolipidic: greenish-yellow; and lipid core: red) along the longitudinal axis of the vessel. LM, left main coronary artery; CFX, circumflex artery; LAD, left anterior descending artery. The distance between the cross-sectional area and the ostium of the vessel is reported in millimetres (mm).

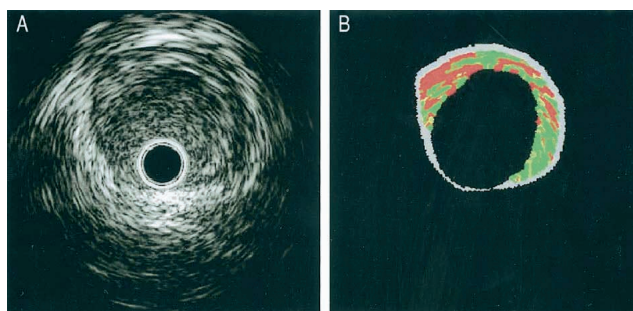


**Figure 1.** Intravascular ultrasound cross-section images from the carina of the left anterior descending coronary artery and of the left main coronary artery. The **left side** shows the reconstructed grayscale, and the **right side** shows the color-coded data (**green** = fibrous; **yellow-green** = fibrolipidic; **red** = necrotic core; **white** = calcium) provided by the IVUS-VH unit (Volcano Therapeutics, Rancho Cordova, California). LCx = left circumflex artery; MPT = maximal plaque thickness.



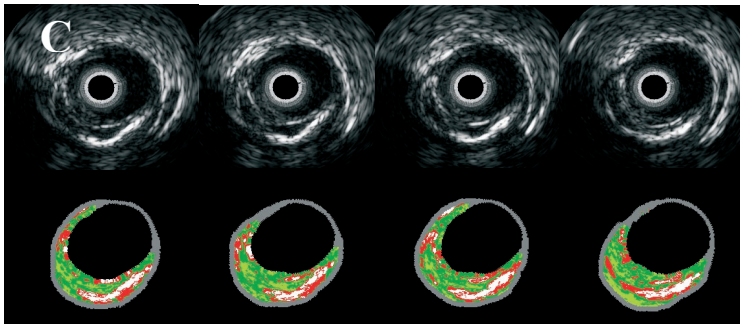
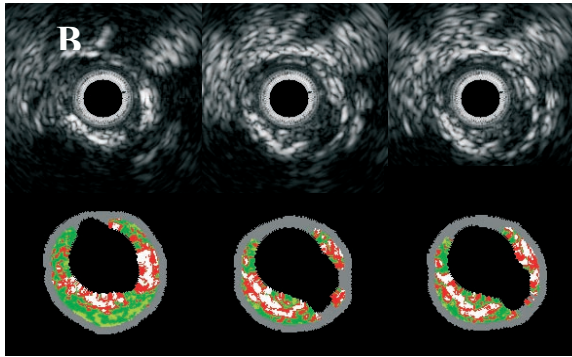
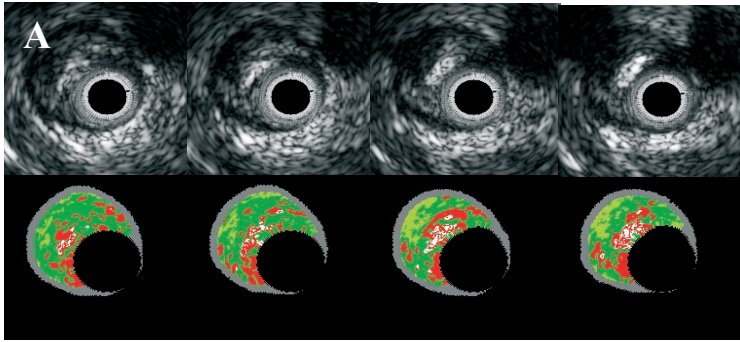
Examples of fibrotic (**A**) and lipid core-rich (**B**) cross-sectional areas of coronary arteries. Grayscale IVUS is displayed on the left panel, whereas the right panel shows the reconstructed IVUS-VH where calcified, fibrous, fibrolipidic and lipid core regions are labeled white, green, greenish yellow, and red, respectively.





**Figure 1.** Left anterior descending artery depicted by Intravascular Ultrasound-Virtual Histology, where calcified, fibrous, fibrolipidic, and necrotic core regions are labeled **white**, **green**, **greenish-yellow**, and **red**, respectively. **Panel A** shows an intravascular ultrasound cross-sectional area reconstructed from backscattered signals. **Panel B** shows the corresponding tissue map depicting a necrotic core-rich plaque with necrotic core tissue in contact with the lumen.

Figure 1



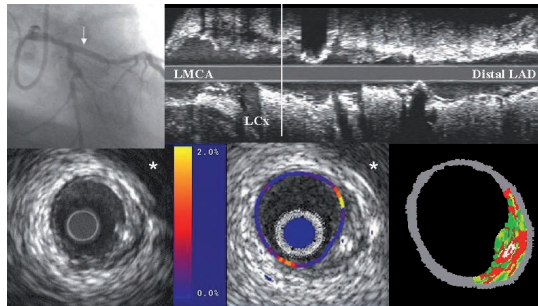


Figure 1. LAD= left anterior descending coronary artery. LCx= Left circumflex coronary artery. LMCA= Left main coronary artery. \* Pericardium.

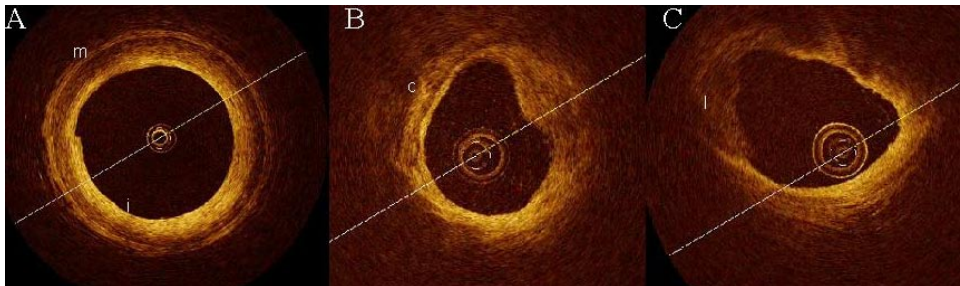


Figure 3